

**ENHANCEMENT OF ONCOLYTIC
COXSACKIEVIRUS A21 WITH CONVENTIONAL
CHEMOTHERAPIES AND IMMUNE
CHECKPOINT INHIBITORS FOR THE
TREATMENT OF MELANOMA**

by

Min Yuan QUAH

B.Biomed Sci (Hons I)

A DISSERTATION SUBMITTED AS FULFILLMENT OF THE REQUIREMENT FOR
THE AWARD OF A DEGREE OF
DOCTOR OF PHILOSOPHY



THE UNIVERSITY OF
NEWCASTLE
AUSTRALIA

School of Biomedical Sciences and Pharmacy,

The University of Newcastle

August 2015

Statement of Originality

The thesis contains no material which has been accepted for the award of any other degree or diploma in any university or other tertiary institution and, to the best of my knowledge and belief, contains no material previously published or written by another person, except where due reference has been made in the text. I give consent to the final version of my thesis being made available worldwide when deposited in the University's Digital Repository**, subject to the provisions of the Copyright Act 1968.

**Unless an Embargo has been approved for a determined period.

Signed: _____

Acknowledgements

I would like to express my appreciation and heartfelt gratitude to the people who supported me during my PhD, because without them I would not have gotten very far. First and foremost, I would like to thank my supervisor, Dr. Gough Au, without whom this project and thesis would not have been possible. Your guidance and unwavering support have consistently been above and beyond all hopes and expectations throughout the entire duration of this journey. Through your guidance, I have gained confidence in my scientific capabilities and judgement, and this has shaped me into the scientist I am now. I will always remember my time as your PhD student with pleasure and I am deeply indebted to you.

I would like to thank my other supervisor A/Prof. Darren Shafren for his thoughtful insights into this project. Years ago in one of our lab meetings, you said that the work we are doing is making a difference in the ‘real’ world. As a young Honours fledgeling, your words were lost on me at the time, but I am proud to say that I now grasp the magnitude of your words and feel truly privileged to have been given the opportunity to undertake a PhD with Viralytics. I cannot thank you enough for your time and invaluable knowledge you have imparted on me.

I would also like to thank the members of the Viralytics team whom I have worked with over the past few years; Prof. Richard Barry, Dr. Roberta Karpathy, Dr. Susanne Johansson, Robert Herd, Bronwyn Davies, Rebecca Ingham, Dr. Camila Salum De Oliveira, Amanda Kelly, Penny Yates, Jack Hockley, Lincoln Smith, Jaclyn Stewart, Erin Green, Ruth Buxton and Dr. Eric Chan. Special thanks to Mr Robert Herd, for reminding me that there is a life outside the PhD. You have taught me so many precious things, always with patience and inspiration for which I cannot thank you enough.

To my family and all of my friends, thank you to each of you for your support throughout these years. Mom and Dad, thank you for always believing in me and your never ending supply of encouragement from thousands of miles away. To my three younger brothers, Min Chern, Min Shern and Min Han, thank you for sounding impressed when I explain my work over Skype. Finally to my loving girlfriend Yvonne, thank you for being my partner in science, crime and in life. For that, you have my utmost thanks, love and appreciation.

To all of the cancer patients,

I hope this work will make a difference...

Contents

List of Figures	xv
List of Tables	xvi
List of Abbreviations	xxv
1 Synopsis	1
2 Introduction and Literature Review	5
2.1 Melanoma	5
2.1.1 Anatomy of normal skin	6
2.1.2 Non-melanoma skin cancer	7
2.1.2.1 Basal cell carcinoma	8
2.1.2.2 Squamous cell carcinoma	8
2.1.3 Malignant melanoma	9
2.1.3.1 Superficial spreading melanoma	10
2.1.3.2 Nodular melanoma	10
2.1.3.3 Lentigo maligna melanoma	11
2.1.3.4 Acral lentiginous melanoma	11
2.1.3.5 Desmoplastic melanoma	11
2.1.3.6 Metastatic melanoma	11
2.1.4 Epidemiology	12
2.1.4.1 Incidence	13
2.1.4.2 Demographics and trends	14
2.1.4.3 Economic impact	17
2.1.5 Risk factors	18
2.1.5.1 Environmental risk factors	19
2.1.5.1.1 Natural ultraviolet radiation exposure	19

2.1.5.1.2	Artificial ultraviolet radiation exposure: tanning beds	20
2.1.5.2	Phenotypic risk factors	21
2.1.5.2.1	Nevi	21
2.1.5.2.2	Pigment	22
2.1.5.3	Genetic risk factors	22
2.1.5.3.1	Personal or family history	22
2.1.5.3.2	Melanoma susceptibility genes	23
2.1.5.4	Additional risk factors	24
2.1.5.4.1	Immunosuppression	25
2.1.5.4.2	Socioeconomic status	25
2.1.6	Pathogenesis	26
2.1.6.1	Ultraviolet-induced melanoma	26
2.1.6.2	Genetic susceptibility in melanoma	31
2.1.6.2.1	Driver mutations arising from ultraviolet mutagenesis	31
2.1.6.2.2	Signalling molecules	31
2.1.6.2.3	Cell cycle regulators	33
2.1.6.3	Immune dysregulation of melanoma	33
2.1.7	Diagnosis	34
2.1.8	Prognosis and staging	35
2.1.9	Treatment	39
2.1.9.1	Surgery	39
2.1.9.2	Cytotoxic chemotherapy	40
2.1.9.2.1	Hydroxyurea	40
2.1.9.2.2	Dacarbazine	41
2.1.9.3	Immunotherapy	41
2.1.9.3.1	Interferon- α 2b (INTRON® A; Merck & Co.)	42
2.1.9.3.2	Interleukin-2 (Proleukin®; Chiron Corp.)	42
2.1.9.3.3	Peginterferon- α -2b (Sylatron™; Merck & Co.)	43
2.1.9.4	Kinase inhibitors	43
2.1.9.4.1	Vemurafenib (Zelboraf®; Roche)	44
2.1.9.4.2	Dabrafenib (Tafinlar®; GlaxoSmithKline)	45
2.1.9.4.3	Trametinib (Mekinist®; GlaxoSmithKline)	45

2.1.9.5	Immune checkpoint inhibitors	46
2.1.9.5.1	Ipilimumab (Yervoy®; Bristol-Myers Squibb) . . .	47
2.1.9.5.2	Pembrolizumab (Keytruda®; Merck & Co.) . . .	48
2.1.9.5.3	Nivolumab (Opdivo®; Bristol-Myers Squibb) . . .	48
2.1.9.6	Oncolytic viruses	49
2.2	Oncolytic virotherapy	51
2.2.1	A brief history of oncolytic virotherapy	51
2.2.2	The ‘renewed’ oncolytic virus paradigm	53
2.2.3	Mechanism of oncolytic virotherapy	54
2.2.3.1	Mechanism of anti-tumour specificity	54
2.2.3.1.1	Tumour-tropism mediated by viral receptors . . .	56
2.2.3.1.2	Attenuation of wild-type viruses through targeted deletion of viral genes	57
2.2.3.1.3	Targeting defective antiviral response pathways . .	59
2.2.3.1.4	Transcriptional targeting	60
2.2.3.1.5	Targeting the hypoxic tumour microenvironment .	61
2.2.3.1.6	Activation through cancer-specific proteases in the tumour microenvironment	62
2.2.3.1.7	MicroRNA regulated tropism	63
2.2.3.2	Mechanisms of anti-tumour efficacy	63
2.2.3.2.1	Direct oncolytic cell death	64
2.2.3.2.2	Induction of ‘bystander cell killing’	64
2.2.3.2.3	Innate anti-angiogenic properties of OV’s	65
2.2.3.2.4	Oncolytic immunotherapy	66
2.2.4	Current clinical status of oncolytic virotherapy in melanoma	67
2.2.4.1	Adenovirus	68
2.2.4.2	Coxsackievirus	68
2.2.4.3	Herpes simplex virus	69
2.2.4.4	Reovirus	70
2.2.4.5	Vaccinia virus	71
2.2.5	Barriers to oncolytic virus monotherapy	76
2.2.5.1	Immunological barriers	76
2.2.5.2	Challenges of intravenous delivery	78
2.2.5.3	Challenges of the tumour microenvironment	79

2.3	Coxsackievirus A21	80
2.3.1	Taxonomy of Coxsackieviruses	80
2.3.2	Virion structure	82
2.3.3	Picornavirus genome	82
2.3.3.1	Genome organisation and processing	83
2.3.3.2	Viral assembly	84
2.3.4	Replication cycle of the Picornaviruses	86
2.3.5	Viral receptors	89
2.3.5.1	Intercellular adhesion molecule (ICAM-1)	89
2.3.5.1.1	Structure of ICAM-1	89
2.3.5.1.2	Function and regulation	91
2.3.5.2	Decay accelerating factor (DAF)	92
2.3.5.2.1	Structure of DAF	92
2.3.5.2.2	Function and regulation	94
2.3.5.3	ICAM-1 and DAF interaction with CVA21	96
2.3.6	Clinical manifestation	100
2.3.7	CVA21 as an oncolytic agent	100
2.4	Study aims and hypothesis	103
3	Materials & Methods	105
3.1	Cell lines	105
3.1.1	Melanoma cells lines	105
3.1.2	Luciferase-expressing cells	105
3.1.3	ICAM-1-transfected murine melanoma cells	106
3.2	Virus and drugs	106
3.2.1	Virus	106
3.2.2	Chemotherapies	106
3.2.3	Vaccine preparation	107
3.3	Antibodies and flow cytometry	107
3.3.1	Antibodies	107
3.3.2	Flow cytometry	108
3.4	Cell viability and synergy assay	108
3.4.1	Viral infectivity assay (TCID ₅₀ assay)	108
3.4.2	Chemosensitivity assay	109
3.4.3	<i>In vitro</i> synergy assay	109

3.4.4	Cell viability assay	110
3.4.5	One-step viral growth curve assay	111
3.4.6	Fluorescence-activated cell scanning analysis of cell cycle distribution	112
3.4.7	Caspase 3/7 analysis by caspase-glo assay	112
3.5	Animals	113
3.5.1	Ethics statement and housing conditions	113
3.5.2	Tumour inoculation	113
3.5.3	Animal monitoring and tumour measurement	113
3.6	<i>In vivo</i> investigations of CVA21 in combination with conventional chemo- therapeutic agents for the treatment of melanoma	114
3.6.1	Immunodeficient mouse melanoma model study design	114
3.6.1.1	Animals and treatment schedule	114
3.6.1.2	<i>In vitro</i> bioluminescent imaging	114
3.6.1.3	Bioluminescent imaging of tumours <i>in vivo</i>	115
3.6.2	Immunocompetent mouse melanoma model study design	115
3.7	Optimisation of the immunocompetent B16-ICAM-1 mouse melanoma model	116
3.7.1	Animals and treatment schedule	116
3.7.2	Histological evaluation of tumours using H&E staining method . . .	116
3.7.3	Tumour cell isolation and primary culture	117
3.8	Animal immunisation with oncolysates and tumour challenge	117
3.9	CVA21 in combination with immune checkpoint inhibitors for the treatment of melanoma <i>in vivo</i>	118
3.9.1	CVA21 and PD-1 blockade in an immunocompetent murine model of melanoma	118
3.9.2	CVA21 and CTLA-4 blockade in an immunocompetent murine model of melanoma	119
3.10	Serum analysis	119
3.10.1	Quantitative RT-PCR detection of CVA21 viral genomes in sera . .	119
3.10.2	Detection of CVA21 viraemia levels	120
3.10.3	Anti-CVA21 neutralising antibody assay	120
3.10.4	Cell viability assay with serum <i>ex vivo</i>	121
3.11	Statistical analysis	121
4	Combination of CVA21 with conventional chemotherapy drugs <i>in vitro</i>	122
4.1	Oncolytic activity of CVA21 in a panel of human melanoma cells	123

4.2	<i>In vitro</i> chemosensitivity assay of DTIC and P + C on a panel of melanoma cell lines	124
4.3	<i>In vitro</i> combination studies with CVA21	132
4.4	Examination of viral replication within cells in the presence of chemotherapy	139
4.5	Cytotoxic activity of CVA21 with DTIC or P + C at clinically relevant concentrations	140
4.6	Effects of CVA21 with DTIC and P + C on the cell cycle	144
4.7	Effects of combination therapy with CVA21 and P + C on caspase-3/7 activation	145
5	<i>In vivo</i> evidence for CVA21 as a monotherapy and in combination with DTIC and P + C for the treatment of melanoma	147
5.1	Immunodeficient xenograft mouse model of melanoma	148
5.1.1	Development of SK-Mel-28 human melanoma cells stably expressing the firefly luciferase gene	148
5.1.2	Establishment of a subcutaneous murine model of melanoma for combination therapy	150
5.1.3	Animal weights throughout the course of study	150
5.1.4	Tumour volume data	153
5.1.5	Bioluminescent imaging <i>in vivo</i>	154
5.1.6	CVA21 viraemia	158
5.2	Development of a syngeneic model of B16-ICAM-1 murine melanoma	160
5.2.1	Establishing B16-ICAM-1 cells for tumour development	160
5.2.2	Assessment of tumour growth and survival analysis	161
5.2.3	Haematoxylin and eosin analysis	163
5.2.4	Isolation and <i>in vitro</i> expansion of murine cells from tumour explants	166
5.3	Combinatory effects of CVA21 and DTIC and P + C on B16-ICAM-1 cells .	168
5.3.1	Dose response of B16-ICAM-1 cells to CVA21 in combination with DTIC and P + C	168
5.3.2	Effects of P + C on CVA21 viral replication in B16-ICAM-1 cells . .	171
5.4	<i>In vivo</i> assessment of combination oncolytic CVA21 and chemotherapy in an immunocompetent mouse model	173
5.4.1	Animal weights throughout the course of study	174
5.4.2	Tumour volume data	175
5.4.3	CVA21 viraemia	178

5.4.4	CVA21 neutralising antibodies	179
6	Combining oncolytic CVA21 with immune checkpoint inhibitors for the treatment of melanoma	180
6.1	Induction of anti-tumour immune response by CVA21 oncolysates	181
6.1.1	Animal weights throughout the course of study	182
6.1.2	Anti-tumour effect of CVA21 oncolysate	182
6.1.3	Survival data of animals treated with CVA21 oncolysate	186
6.2	<i>In vivo</i> assessment of combination oncolytic virotherapy and anti-PD-1 immunotherapy in an immunocompetent mouse model	187
6.2.1	Body weights following treatment with either saline or CVA21 in combination with anti-PD-1 or control antibody	188
6.2.2	Tumour volume data	189
6.2.2.1	Tumour volumes of primary B16-ICAM-1 nodules	190
6.2.2.2	Tumour volumes of secondary B16 nodules	192
6.2.3	Survival in mice treated with CVA21 in combination with anti-PD-1 or a control antibody	193
6.2.4	Serum analysis	195
6.2.4.1	CVA21 viraemia	195
6.2.4.2	CVA21 neutralising antibodies	195
6.3	<i>In vivo</i> assessment of combination oncolytic virotherapy and anti-CTLA-4 immunotherapy in an immunocompetent mouse model	198
6.3.1	Body weights following treatment with either saline or CVA21 in combination with anti-CTLA-4 or control antibody	199
6.3.2	Tumour volume data	200
6.3.2.1	Tumour volumes of primary B16-ICAM-1 nodules	201
6.3.2.2	Tumour volumes of secondary B16 nodules	203
6.3.3	Survival in mice treated with CVA21 in combination with anti-CTLA-4 or a control antibody	205
6.3.4	Serum analysis	207
6.3.4.1	Viraemia analysis	207
6.3.4.2	Neutralising antibodies	207
6.3.4.3	<i>Ex vivo</i> cytotoxicity of serum-mediated cell death	209

7 Discussion and Conclusion	212
7.1 Discussion of research findings	212
7.2 Rationale of combination oncolytic virotherapy	235
7.3 Challenges of combination therapy with OV	237
7.4 Quantifying synergy in drug combination studies	239
7.5 Future directions and conclusion	242
References	247

List of Figures

2.1	Anatomy of normal skin.	7
2.2	Four major subtypes of melanoma.	12
2.3	World age-standardised incidence rates of melanoma, 2012.	15
2.4	Risk factors for melanoma.	18
2.5	Pathogenesis of melanoma.	28
2.6	Molecular steps in UVR-induce melanogenesis.	30
2.7	Clinical significance of dermoscopy.	35
2.8	Timeline of FDA regulatory approval for metastatic melanoma.	39
2.9	The oncolytic virotherapy paradigm.	54
2.10	Mechanism of oncolytic virotherapy.	55
2.11	Barriers to optimal delivery of OV _s to tumours.	77
2.12	Classification of the <i>Picornaviridae</i> family.	81
2.14	The enterovirus genome, polyprotein products and their major function.	84
2.15	Assembly pathway of picornavirus virions.	86
2.16	Replication cycle of the picornavirus.	88
2.17	Structure of the ICAM-1 surface molecule.	91
2.18	Structure of the DAF surface molecule.	94
2.19	Surface cryo-EM reconstruction of coxsackievirus A21.	97
2.20	Surface cryo-EM reconstruction of Echovirus 7.	98
2.21	Interaction between ICAM-1 and DAF.	99
2.13	Virion structure of picornavirus.	101
4.1	Oncolytic effect of CVA21 in melanoma cells.	124
4.2	Cytopathic effects of CVA21 in melanoma cells.	125
4.3	Dose response curve of DTIC in melanoma cells.	127

4.4	Dose response curve of P + C doublet chemotherapy in melanoma cells.	128
4.5	Cytotoxic effect of DTIC on melanoma cells.	130
4.6	Cytotoxic effect of P + C doublet chemotherapy on melanoma cells.	131
4.7	Dose response curves of CVA21 in combination with chemotherapy in SK-Mel-28, Mel-RM, ME4404 and MV3 cells.	133
4.8	Isobolograms showing the interaction between CVA21 and DTIC at EC ₅₀ , EC ₇₅ and EC ₉₀	136
4.9	Isobolograms showing the interaction between CVA21 and P + C at EC ₅₀ , EC ₇₅ and EC ₉₀	137
4.10	Fraction affected (Fa) - combination index (CI) plot.	138
4.11	Effect of DTIC and P + C on CVA21 one step replication kinetics over time.	141
4.12	Dose-dependent cytotoxicity of CVA21 in combination with DTIC and P + C on SK-Mel-28 cells.	142
4.13	Morphological changes in SK-Mel-28 cells observed using crystal violet stain.	143
4.14	Effects of CVA21 and chemotherapy individually and in combination on the cell cycle.	145
4.15	Caspase-3/7 activation in a panel of melanoma cells by caspase-glo assay.	146
5.1	Establishment of SK-Mel-28-luc cells using a lentiviral vector. . . .	149
5.2	Overview of experimental protocol for immunodeficient murine melanoma model.	151
5.3	Mean body weights of mice (g) over time (days).	152
5.4	Combination of chemotherapy and CVA21 virotherapy on SK-Mel-28-luc melanoma xenografts in SCID mice.	154
5.5	Bioluminescent imaging of BALB/c SCID mice transplanted with luciferase expressing SK-Mel-28 cells.	156
5.6	<i>In vivo</i> response monitoring in SK-Mel-28-luc melanoma model with BLI.	157
5.7	Detection of viraemia using one-step qRT-PCR.	159
5.8	Characterisation of B16-ICAM-1 melanoma cells.	161
5.9	Growth of B16 and B16-ICAM-1 flank tumours.	162

5.10	Growth rate and survival analysis for tumour bearing animals. . .	164
5.11	Histological analysis of tumour deposits using H&E staining. . . .	165
5.12	Lytic infection of primary B16 and B16-ICAM-1 culture from <i>in vivo</i> tumour explants.	167
5.13	Cytotoxicity of combination CVA21 and chemotherapy on B16-ICAM-1 murine cell line.	169
5.14	Synergistic activity of CVA21 and chemotherapy in B16-ICAM-1 cells.	170
5.15	Effects of P + C on CVA21 viral production.	172
5.16	Dose-dependent cytotoxicity of CVA21 in combination with P + C on B16-ICAM-1 cells.	172
5.17	Overview of experimental protocol for immunocompetent murine melanoma model.	173
5.18	Mean body weights of mice (g) over time (days).	175
5.19	Combination of chemotherapy and CVA21 virotherapy on B16-ICAM-1 murine flank tumours.	177
5.20	Detection of viraemia following CVA21 oncolytic virotherapy with and without chemotherapy.	178
5.21	Presence of nAbs in serum following treatment with CVA21 and CVA21 in combination with DTIC or P + C.	179
6.1	Overview of experimental protocol for CVA21-oncolysate immunisation murine melanoma model.	182
6.2	Individual body weights of mice (g) over time (days).	183
6.3	B16 tumour growth following immunisation with saline, CVA21, control vaccine, CVA21 + control vaccine, or CVA21 oncolysate. . .	185
6.4	Survival of C57BL/6 mice following immunisation with CVA21 oncolysates.	186
6.5	Treatment scheme of anti-PD-1 combination immune-competent murine melanoma protocol.	188
6.6	Body weights of mice (g) <i>vs</i> time (days).	189
6.7	Tumour volumes following combination anti-PD-1 antibody and CVA21 virotherapy on primary B16-ICAM-1 murine melanoma tumours.	191
6.8	Tumour development of secondary B16 tumour nodules.	193

6.9	Survival of C57BL/6 mice following treatment with saline or CVA21 in combination with the control antibody or anti-PD-1.	194
6.10	Detection of viraemia following CVA21 administration with and without anti-PD-1 immunotherapy.	196
6.11	Detection of CVA21-specific neutralising antibodies following CVA21 administration with and without anti-PD-1 immunotherapy.	197
6.12	Treatment scheme of anti-CTLA-4 combination immune-competent murine melanoma protocol.	198
6.13	Body weights of mice (g) <i>vs</i> time (days).	200
6.14	Tumour volumes following CVA21 virotherapy and CTLA-4 blockade on B16-ICAM-1 primary tumours.	202
6.15	Tumour volumes of secondary B16 murine melanoma tumours.	204
6.16	Analysis of primary and secondary with cure rate.	205
6.17	Kaplan-Meier survival analysis for CVA21 virotherapy with CTLA-4 blockade.	206
6.18	Detection of viraemia following CVA21 administration with and without anti-CTLA-4 immunotherapy.	208
6.19	Serum neutralising antibodies against CVA21 in animals following CVA21 administration with or without anti-CTLA-4 immunotherapy.	210
6.20	<i>Ex vivo</i> cytopathic effects of serum collected from animals treated with anti-CTLA-4.	211

List of Tables

2.1	Comparison of basal cell and squamous cell carcinoma.	9
2.2	Risk factors and relative risk for melanoma.	27
2.3	TNM staging for cutaneous melanoma.	37
2.4	Anatomic stage grouping for cutaneous melanoma with 5- and 10- year survival rates.	38
2.5	The most clinically advanced OVs for the treatment of melanoma.	73
2.6	Common diseases caused by Coxsackieviruses.	101
3.1	Description of the combination index (CI) method.	110
4.1	EC ₅₀ values of CVA21 in four melanoma cell lines.	123
4.2	EC ₅₀ values of DTIC and P + C in four melanoma cell lines. . . .	129
4.3	Combination index (CI) values of each cell line treated with CVA21 and chemotherapy.	134

List of Abbreviations

α	alpha
β	beta
γ	gamma
5-FC	5-fluorocytosine
5-FU	5-fluorouracil
Ab	antibody
ACEC	Animal Care and Ethics Committee
Ad-MMP	adenovirus expressing matrix metalloproteinases
Ad5	serotype 5 adenovirus
ADCC	antibody-dependent cellular cytotoxicity
AIDS	acquired immune deficiency syndrome
AJCC	American Joint Committee on Cancer
ANOVA	analysis of variance
APC	antigen presenting cell
ASIR	age-standardised incidence rate
ATCC	American Type Culture Collection
BCC	basal cell carcinoma
BLI	bioluminescent intensity
cAMP	cyclic adenosine monophosphate
cDNA	complementary DNA
C	carboplatin
CAR	Coxsackievirus and adenovirus receptor
CD	cytosine deaminase
CDC	complement-dependent cytotoxicity
CDK4	cyclindependent kinase 4
CDKN2A	cyclin-dependent kinase inhibitor 2A
CEA	carcinoembryonic antigen

CI	combination index
CO ₂	carbon dioxide
CPA	cyclophosphamide
CPD	cyclobutane pyrimidine dimer
CPE	cytopathic effect
CR	complete response
CRAd	conditionally replicative adenovirus
CT	computed tomography
CTL	cytotoxic T lymphocyte
CTLA-4	cytotoxic T-lymphocyte-associated protein 4
CVA	Coxsackievirus type A serotype
CVA13	Coxsackievirus A13
CVA15	Coxsackievirus A15
CVA18	Coxsackievirus A18
CVA21	Coxsackievirus A21
CVA21-DAFv	a bioselected variant of CVA21 that exclusively utilises DAF as a primary receptor
CVB	Coxsackievirus type B serotype
CVB1	Coxsackievirus B1
CVB3	Coxsackievirus B3
CVB5	Coxsackievirus B5
DAF	decay accelerating factor
DAMP	damage-associated molecular pattern
DEAE-D	Diethylaminoethyl-Dextran
DFS	disease-free survival
DMEM	Dulbecco's Modified Eagle's Medium
DMSO	dimethyl sulphoxide
DNA	deoxyribonucleic acid
DTIC	dacarbazine; 5-(3,3-dimethyl-1-triazenyl)-imidazole-4-carboxamide
e.g.	exempli gratia
eIF-4F	eukaryotic protein synthesis initiation factor 4F
<i>et al.</i>	et alibi
EC ₅₀	effective concentration 50%
ECM	extracellular matrix
ECOG	Eastern Cooperative Oncology Group

EGFR	epidermal growth factor receptor
EORTC	European Organisation for Research and Treatment of Cancer
EV1	Echovirus type 1
FACS	fluorescence-activated cell sorting
FCS	foetal calf serum
FDA	Food and Drug Administration
FITC	fluorescein
GBM	glioblastoma multiforme
GFP	green fluorescent protein
GM-CSF	granulocyte-macrophage colony-stimulating factor
GPI	glycosylphosphatidylinositol
hTERT	human telomerase reverse transcriptase
H	haemagglutinin
H&E	haematoxylin and eosin
HCC	hepatocellular carcinoma
HDACi	histone-deacetylase inhibitors
HEPES	4-(2-Hydroxyethyl)piperazine-1-ethanesulfonic acid
HIF	hypoxia-inducible factor
HR	hazard ratio
HRV	human rhinovirus
HRV2	human rhinovirus type 2
HSP	heat-shock proteins
HSV	herpes simplex virus
HSV1	herpes simplex virus type 1
HSV1-TK	herpes simplex virus type 1 thymidine kinase
HUVEC	human umbilical vein endothelial cell
i.c.	intracranial
i.d.	intradermal
i.m.	intramuscular
i.p.	intraperitoneal
i.t.	intratumoural
i.v.	intravenous
irAE	immune-related adverse event
irPFS	immune-related progression-free survival

Ig	immunoglobulin
IARC	International Agency for Research on Cancer
ICAM-1	intercellular adhesion molecule-1
ICD	immunogenic cell death
ICTV	International Committee for the Taxonomy of Viruses
IFN	interferon
IFN-PEG α -2b	pegylated interferon- α -2b
IHC	immunohistochemical
IL	interleukin
IRES	internal ribosomal entry site
JX-594	pexastimogene devacirepvec
KPMG	Klynveld Peat Marwick Goerdeler
LCMV	lymphocytic choriomeningitis virus
LDH	lactate dehydrogenase
LFA-1	lymphocyte function-associated antigen-1
LPS	lypopolysaccharide
m ⁷ G	monoclonal antibody
mAb	monoclonal antibody
mRNA	messenger ribonucleic acid
miRNA	micro ribonucleic acid
Mac-1	macrophage antigen-1
MAC	membrane attack complex
MAPK	mitogen-activated protein kinase
MC1R	melanocortin 1 receptor
MDSC	myeloid-derived suppressive cell
MHC	major histocompatibility complex
MITF	microphthalmia-associated transcription factor
MMP	matrix metalloproteinase
MOI	multiplicity of infection
MPM	multiple primary melanoma
MRI	magnetic resonance imaging
MRV	mammalian orthoreovirus
MSH	melanocyte stimulating hormone
MTD	maximum tolerated dose

MTIC	methyl-triazeno-imidazole-carboxamide
MTT	methyl thiazolyl tetrazolium
MV	measles virus
MV-CEA	measles virus expressing carcinoembryonic antigen
MV-Edm	Edmonston strain of measles virus
MV-MMP	measles virus expressing matrix metalloproteinases
MV-NIS	measles virus expressing sodium iodide symporter
nAb	neutralising antibody
nt	nucleotide
NDV	Newcastle disease virus
NF- κ B	nuclear factor kappa-light-chain-enhancer of activated B cells
NHS	National Health Service
NIS	sodium-iodide symporter
NK	natural killer
NMSC	non-melanom skin cancer
NSCLC	non-small cell lung cancer
NTC	no tumour control
NTR	non-translated region
NU	neutralizing units
OD	optical density
ORF	open reading frame
ORR	objective response rate
OS	overall survival
OV	oncolytic virus
pfu	plaque-forming unit
poly(A)	polyadenylic acid
pOMC	pro-opiomelanocortin
P	paclitaxel
PAF	population-attributable fraction
PAMP	pathogen-associated molecular pattern
PBMC	peripheral blood mononuclear cell
PBS	phosphate buffered saline
PCR	polymerase chain reaction
PD-1	programmed cell death 1

PDT	photodynamic therapy
PE	phycoerythrin
PFIE	<i>Plasmodium falciparum</i> infected erythrocytes
PFS	progression-free survival
PI	propidium iodide
PI-PLC	phosphatidylinositol-specific phospholipase C
PI3K	phosphatidylinositol-3-kinase
PNP	purine nucleoside phosphorylase
PR	partial response
PSA	prostate-specific antigen
PV	poliovirus
PV1	poliovirus type 1
PV3	poliovirus type 3
PVR	poliovirus receptor
Rb	retinoblastoma
RD	rhabdomyosarcoma
RFS	relapse-free survival
RHC	red hair colour
ROI	regions of interest
ROS	reactive oxygen species
RNA	ribonucleic acid
RdRP	RNA-dependent RNA polymerase
RR	relative risk
RT-PCR	reverse transcription polymerase chain reaction
s.c.	subcutaneous
ss	single-stranded
scFv	single-chain fragment variable
SCC	squamous cell carcinoma
SCID	severe combined immunodeficient
SCR	short consensus repeat
SD	standard deviation
SeV	Sendai virus
SEER	Surveillance Epidemiology and End Results
SEM	standard error mean

SES	socioeconomic status
SFV	Semliki Forest virus
SLAM	signaling lymphocyte activation molecule
SPF	specific-pathogen-free
SR	somatostatin receptor
SVV	Seneca Valley virus
T-Vec	talimogene laherparepvec
TAA	tumour-associated antigen
TCID ₅₀	Tissue culture infectious dose 50%
TCR	T cell receptor
TK	thymidine kinase
TNF	tumour necrosis factor
Toca 511	vocimagene amiretrorepvec
Treg	regulatory T cell
uPA	urokinase plasminogen activator
UICC	Union for International Cancer Control
UK	United Kingdom
USA	United States of America
UTR	untranslated region
UV	ultraviolet
UVR	ultraviolet radiation
<i>vs</i>	versus
VEGF	vascular endothelial growth factor
VGF	vaccinia growth factor
VP	viral protein
VPg	viral protein genome-linked protein
VSV	vesicular stomatitis virus
VV	vaccinia virus
XP	xeroderma pigmentosum

UNITS

Å	angstrom
°C	degrees Celsius
b	base
bp	base pair
d	day
Da	dalton
<i>g</i>	gravitational force
g	gram
h	hour
IU	international unit
L	litre
m	meter
M	Molar
MU	million unit
min	minute
mol	mol
rpm	revolutions per minute
s	second
V	volts
v/v	volume per volume
w/v	weight per volume

NUCLEOTIDES

A	adenine
C	cytosine
G	guanine
T	thymine

PREFIXES

k	kilo	10^3
m	milli	10^{-3}
μ	micro	10^{-6}
n	nano	10^{-9}
p	pico	10^{-12}

Chapter 1

Synopsis

Malignant melanoma is one of the most aggressive and lethal cancers of the skin. Clinical reports have shown patients diagnosed with stage IV of the disease have no longer than five years to live. Depending on the sub-stage of the disease, median survival of patients is between 6 - 18 months. To date, current Food and Drug Administration (FDA) approved anticancer drugs for melanoma have demonstrated limited response rates, few complete remissions and no significant survival benefits. The development of new therapies to effectively eradicate malignant melanoma are desperately in need. Recent growth in the field of oncolytic virotherapy has led to an increased number of clinical trials and acceptance of tumour selective viruses as a promising anticancer strategy. Numerous viruses have emerged as potent oncolytic agents because of their capacity to preferentially infect and destroy cancer cells while leaving normal cells intact. Like most anticancer modalities, it is very likely that oncolytic virotherapy will be used in combination with other existing therapeutics. Numerous groups have begun to explore the possibility of combining oncolytic virotherapy with conventional cancer therapies. The combination of oncolytic virotherapy with other existing cancer therapies may be an effective strategy to overcome the barriers faced by either therapeutic agents when used as monotherapies.

The Kuykendall strain of Coxsackievirus A21 (CVA21) is a naturally occurring common-cold virus that has the inherent capacity to preferentially infect and destroy malignant cells. The oncolytic properties of CVA21 as an anticancer agent have been demonstrated both *in vitro* and *in vivo* studies, against numerous types of cancer, including breast cancer, prostate cancer, glioma, multiple myeloma, non-small cell lung carcinoma, and melanoma. In the clinic, tumour regression was observed in both injectable and distant non-injected lesion without any significant adverse events. Despite CVA21's impressive progress to

date, it is becoming clear the oncolytic viruses (OVs) cannot be viewed as monotherapies. The current trend is for the combination of virotherapy with mainstream therapies. A fundamental requirement for the success of this strategy is that the combination does not interfere with the life cycle of the oncolytic virus from the point of viral entry, to the release of viral progeny.

In **Chapter 4**, we demonstrated that not only does the co-administration of clinically relevant cytotoxic anticancer drugs such as dacarbazine, paclitaxel and carboplatin not interfere with replication cycle of CVA21, enhanced cell destruction of melanoma cells was achieved when both oncolytic agent and chemotherapy were combined. To determine whether actual synergism was present, we subjected our data to the Chou-Talalay median effect equation which provides a robust measurement of drug combination relationships based on combination index values. When the constant drug-ratio design was applied to our combination assays, we discovered that CVA21 does indeed act synergistically with conventional chemotherapy in all melanoma cell lines except SK-Mel-28. However, we anticipate that it is possible to achieve synergistic or additive effects in all cell lines by carefully adjusting the drug concentrations used. Indeed, the combination of CVA21 with either of the chemotherapeutic agents at clinically relevant drug concentrations, resulted in increased cell death in SK-Mel-28 cells. Next, we were interested in identifying the underlying mechanism by which CVA21 is able to synergise with dacarbazine, paclitaxel and carboplatin. No increase in viral replication was observed in any of the test cell lines following combination chemotherapy treatment *vs* virus alone. Cell cycle analysis revealed an increase in the sub-G1/G₀ cell population after treatment with the combination of CVA21 and paclitaxel + carboplatin, but was not associated with the activation of caspase-3/7. Taken together, the combination of CVA21 plus chemotherapy has significant activity in a panel of melanoma cells though the mechanism behind this effect remains to be elucidated.

In **Chapter 5**, we sought to determine whether the synergistic cancer cell death was reproducible *in vivo*. Two melanoma animal models were designed; an immunodeficient melanoma xenograft model and a syngeneic immunocompetent mouse model. Intratumoural injection of infectious CVA21 particles in the presence or absence of cytotoxic chemotherapy mediated complete regression of all injected melanoma xenografts. However, there was no statistical difference between single agent CVA21 and CVA21 in combination

with chemotherapy in our immunodeficient mouse model. Such a result was not unexpected, as the absence of neutralising antibodies in the immunodeficient model allowed the virus to replicate indefinitely until all tumour cells were destroyed. Having proven that cytotoxic chemotherapy failed to interfere with the replication cycle of CVA21 *in vivo*, we developed a syngeneic immunocompetent mouse model and treated the animals with the same combinations as per the immunodeficient study. Overall, we observed an excellent level of treatment tolerability and tumour clearance in both single agent/combination therapy treatment groups. Results from both animal models show that the presence of either chemotherapy does not harm the infectivity or integrity of CVA21 virions *in vivo* and provides a strong rationale for clinical translation.

In **Chapter 6**, we explored the immunotherapeutic potential of oncolytic CVA21. In the first section of this chapter, we examined whether vaccination of immunocompetent animals with cell lysates induced by CVA21 oncolysis (an oncolysate) could initiate the activation of anti-tumour immunity. Following immunisation with the oncolysates, animals were challenged with B16 cells and the development of flank tumours was recorded. Although B16 challenged animals showed reduced tumour growth, it became apparent that viral-mediated lysis of tumour cells alone was insufficient for complete tumour eradication. Thus, based on these observations, the next logical step was to combine oncolytic CVA21 with other immunotherapeutic agents to enhance the activation of anti-tumour immune responses. In the next section, we investigated if the immunomodulatory effects of two T cell regulatory receptors, PD-1 and CTLA-4, together with CVA21 could be harnessed to improve therapeutic efficacy. Animals were treated with intratumoural injections of CVA21 and intraperitoneally with either anti-PD-1 or anti-CTLA-4 antibodies. Animals were rechallenged with B16 cells lacking the CVA21 targeting receptor human ICAM-1 and the development of the secondary flank tumour was used as a measure for the generation of a protective anti-tumour immune response. Remarkably, the combination group displayed a superior anti-tumour response when compared to control animals or either of the agents as monotherapies. We were particularly successful in demonstrating this effect with the CVA21-CTLA-4 combination as indicated by the complete regression of the primary tumour in all treated animals, followed by durable resistance to the secondary tumour challenge in 40% of the animals on study.

The experimental data presented herein highlights the potential of CVA21 as a useful

platform for combination strategies. Using the newly established, fully immunocompetent CVA21-susceptible mouse model of malignant melanoma, we showed that CVA21 in combination with dacarbazine or paclitaxel and carboplatin had significant advantages over either agents as monotherapies. Furthermore, the model was extended to evaluate the protective anti-tumour response generated from CVA21 oncolysis by challenging animals with murine melanoma cells without ICAM-1 surface receptors after the initial treatment. Favourable immune responses and increased therapeutic benefits were observed when CVA21 was administered with the immune checkpoint inhibitors PD-1 and CTLA-4. This study is further proof-of-concept that immunovirotherapy of cancer is achievable with CVA21, leading the way for future clinical trials combining checkpoint modulation with CVA21.

Chapter 2

Introduction and Literature Review

2.1 Melanoma

Cutaneous melanoma, a type of cancer of the skin, is a pre-eminent global public health issue. Despite accounting for only 5% of all skin cancer cases, malignant melanoma is responsible for 75% of all skin cancer-related mortalities. Highly treatable in its early stages, the five-year survival rate of those with localised melanoma is 98%, compared to 62% and 15% for patients with regional and distant metastases respectively. Subsequently, the vast majority of melanoma-related deaths are due to disseminated malignancy, where the median survival of metastatic patients is 6 - 9 months. Only 14% of patients with metastatic melanoma survive for five years.

In the past decade, major advances have been made in the understanding of melanoma. New predisposition genes have been reported, and key somatic mutations in genes such as *BRAF* have directly translated into therapeutic management. Surgery for localised melanoma and regional lymph node metastases is the standard of care. Sentinel-node biopsy provides precise staging but has not been reported to affect survival. The effect of lymph-node dissection on survival is still a topic of investigation. Two distinct approaches have emerged to try to extend survival in patients with metastatic melanoma: immunomodulation checkpoint inhibitor antibodies such as anti-CTLA-4, and targeted therapy with BRAF inhibitors or MEK inhibitors for *BRAF*-mutated melanoma. The combination of BRAF inhibitors and MEK inhibitors might further improve progression-free survival (PFS) and possibly, increase overall survival (OS).

The response patterns of melanoma to immunomodulatory drugs and targeted therapies

can differ substantially. Anti-CTLA-4 immunotherapy can induce long-term responses, but only in a few patients, whereas targeted drugs induce responses in most patients, but nearly all of them relapse because of pre-existing or acquired resistance. Thus, the long-term prognosis of metastatic melanoma remains poor. The anti-PD-1 and anti-PD-L1 antibodies have emerged as breakthrough drugs for melanoma that have high response rates and long durability. Biomarkers that have predictive value remain elusive in melanoma, although emerging data for adjuvant therapy indicates that interferon (IFN) sensitivity is associated with ulceration of primary melanoma. Intense investigation continues for clinical and biological markers that may predict clinical benefit of immunotherapeutic drugs, such as IFN α or anti-CTLA-4 antibodies, and the mechanisms that lead to resistance to targeted drugs.

2.1.1 Anatomy of normal skin

Normal skin can be divided into three layers, the epidermis, dermis and subcutaneous tissue (Figure 2.1). The epidermis or the outer layer consists primarily of keratinocytes and can be further divided into four sublayers. These sublayers represent different stages of maturation of the actively dividing keratinocytes, which occur over a 30-day period [270]. The stratum basale, the deepest sublayer abutting the basement membrane, is composed of keratinocytes that push existing cells to a higher layer. Next are the differentiating cells of the stratum spinosum sublayer, then the stratum granulosum sublayer, where the cells lose their nuclei and secrete lipid into the intercellular spaces. The most superficial of these sublayers is the stratum corneum, which is composed of several laminated and loosely attached keratinised cells. The stratum corneum provides an important barrier function, protecting the underlying layers. Melanocytes reside in the stratum basale and produce the pigment melanin which protects the skin from ultraviolet (UV) radiation.

Underlying the epidermis is the dermis which provides support and nutrients for the epidermis. The dermis is composed of fibres, collagen and elastic tissue throughout the upper papillary layer and the lower reticular layer. Within these layers are some specialised cells including the hair follicles, sebaceous glands (oil glands), apocrine glands (scent glands), and eccrine glands (sweat glands), as well as blood vessels and nerves that allow sensations of touch, temperature, and pain. Fibroblasts in this area produce collagen and elastin. The subcutaneous tissue layer varies in thickness from person to person, contains fat, connective tissue some larger blood vessels, and nerves. It contributes to fat storage

and regulation of temperature of both the skin and body.

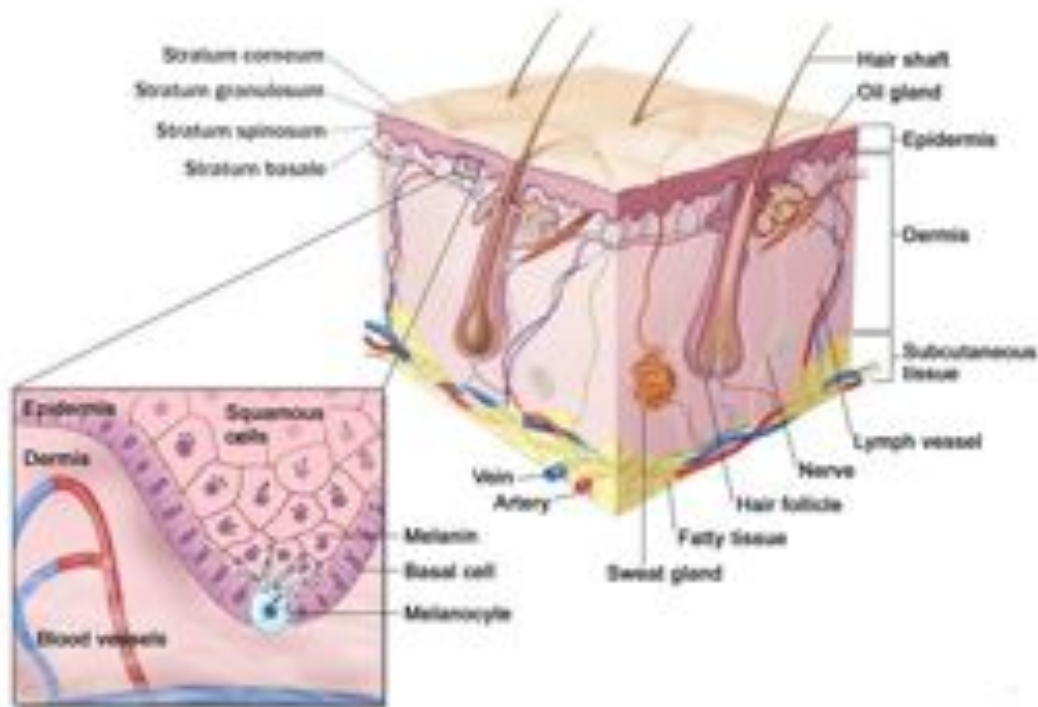


Figure 2.1: Anatomy of the skin, showing the epidermis, dermis, and subcutaneous tissue. Melanocytes are in the layer of basal cells at the base of the epidermis. Source: The National Cancer Institute, available at <http://www.cancer.gov/cancertopics/pdq/genetics/skin/HealthProfessional/page1>.

2.1.2 Non-melanoma skin cancer

Skin cancer is commonly categorised as malignant melanoma and non-melanoma skin cancer (NMSC), the latter encompassing basal cell carcinoma (BCC) and squamous cell carcinoma (SCC) as the major subtypes (other subtypes include cutaneous lymphomas, Merkel-cell carcinomas, and other rare primary cutaneous neoplasms) [474]. Non-melanoma skin cancers are the most common human cancers, and despite growing public awareness of the harmful effects of sun exposure, NMSC incidence continues to rise.

The actual number of NMSC cases is difficult to estimate because BCC and SCC cases are not required to be reported to national cancer registries [36, 351]. However, the overall upward NMSC trend observed in most parts of Canada, Europe, the United States of America (USA), and Australia suggests that the increase in NMSC incidence averages has averaged 3% and 8% annually since 1960 [474]. The majority of NMSC are highly curable, particularly if diagnosed at an early stage. However, malignant melanoma is less predictable and a more lethal form of skin cancer, particularly if diagnosed at an advanced

stage.

2.1.2.1 Basal cell carcinoma

With over 2 million new tumours diagnosed annually and accounting for 80% of all NMSC, BCC is regarded as the most common skin cancer [70]. The mortality is low, but due to its high prevalence, BCC is a significant and costly health problem. The neoplasm is derived from basal cells with 80% of BCC cases occurring on the head and neck of patients [56, 70, 616]. Intermittent UVR exposure and UVR exposure during childhood are cited as predisposing factors to this disease [616, 639]. BCC generally presents as small shiny papules, with pearly borders, prominent engorged vessels on the surface and a central ulcer [270]. Local growth can be highly destructive resulting in recurrent crusting and bleeding, though metastasis is extremely rare with an estimated incidence of 0.0028 - 0.55% [495].

Complete surgical excision is the gold standard treatment because the tumour grows slowly and only rarely metastasise. Radiation therapy is the next option for inoperable tumours or for those where the post-operative defect would be cosmetically disfiguring or functionally disabling [70]. In recent years, new therapeutic approaches have been developed both for locally advanced or metastatic disease (systemic medications) as well as for superficial BCC (topical medications). Topical medications include photodynamic therapy (PDT) [24, 663], imiquimod [24, 464] and 5-fluorouracil [24, 464] while the first agent to be used successfully systemically is the Hedgehog pathway inhibitor, vismodegib (GDC-0449) [663]. These therapeutic options should be considered in the multidisciplinary management of patients with sporadic or hereditary BCC.

2.1.2.2 Squamous cell carcinoma

Squamous cell carcinoma, the second-most common skin cancer, comprises of approximately 15-16% of skin cancer cases [270]. It arises from the malignant proliferation of epidermal keratinocytes and invades the dermis [427]. Cumulative habitual sun exposure has a strong association with the incidence of the disease [229, 639], however, heavy metals (arsenic), chemical carcinogens (tar), sites of scars, chronic trauma, and inflammation have been cited as other contributing factors [8]. Chronically immunosuppressed patients develop very aggressive SCC with a high rate of recurrence and metastatic potential [8, 229]. The clinical presentation of SCC is highly variable but most commonly appears as a firm, smooth, or hyperkeratotic papule or plaque, often with central ulceration [474].

The primary aim of treatment is complete removal of the lesion while achieving a good and acceptable cosmetic outcome as an important secondary goal. Surgical excision, including Mohs micrographic surgery is recommended as first-line treatment for most SCC [528]. Radiotherapy is recommended for high risk tumours, surgically difficult areas and patients greater than 50 years of age. Table 2.1 compares the major differences distinguishing BCC and SCC cases.

Table 2.1: Comparison of basal cell and squamous cell carcinoma.

	Basal cell carcinoma	Squamous cell carcinoma
Characteristics		
UV exposure	Weaker association, exposure in childhood and adolescence more important.	Stronger association, cumulative exposure more important.
Tumour location	Most tumours occur on the head and neck region; one-third occur on areas that receive little or no UV exposure.	More common on the back of the hands, forearms, head and neck, where sun exposure is maximal.
Patient age	Up to 20% of tumours occur in patients younger than 50 years.	Uncommon in patients younger than 50 years.
Treatment		
Surgical	Excision, Mohs micrographic surgery, cyrosurgery, laser ablation, carbon dioxide laser vaporisation, radiotherapy.	
Non-surgical	PDT, imiquimod, 5-fluorouracil, vismodegib.	N/A

Abbreviations: PDT, photodynamic therapy; N/A, not available; UV, ultraviolet.
Source: Adapted from Madan, V., Lear, J. T., and Szeimies, R.-M. (2010). Non-melanoma skin cancer. *Lancet*, 375(9715):673–685.

2.1.3 Malignant melanoma

Malignant melanoma represents only 5% of skin cancer cases, but accounts for 75% of all skin cancer-related mortalities. Malignant melanoma is derived from epidermal melanocytes and can occur in any tissue that contains these cells. Malignant melanoma is induced through multiple mechanisms, including suppression of the immune system of the skin, induction of melanocyte cell division, free radical production, and damage of melanocyte deoxyribonucleic acid (DNA) [252, 510]. Identification of the melanoma susceptibility

gene, *p16*, has elucidated the association between genetics and malignant melanoma [790]. The relationship between *p16* and melanoma has been explained by the observation that UVR can induce p16 expression in human skin [790]. Furthermore, random mutations at the *p16* location are also responsible for many sporadic (non-familial) cases of melanoma.

Most cases of malignant melanoma arise on the skin surface and are therefore detectable by visual examination. Clinical features of malignant melanoma vary greatly. The ABCDE guidelines for evaluating pigmented lesions outlines the clinical presentation and warning signals for most melanomas. ‘A’ stands for asymmetry (one half of the mole does not match the other half); ‘B’ stands for border irregularity (the edges are ragged, notched, or blurred); ‘C’ stands for colour (the pigmentation is not uniform, with variable degrees of tan, brown, or black); ‘D’ stands for diameter greater than 6 mm; and ‘E’ represents evolution, changes in the appearance of the lesion [626]. Many lesions suggestive of melanoma will have some but not all of these characteristics. The following types of malignant melanoma are recognised: superficial spreading melanoma, nodular melanoma, lentigo maligna melanoma, acral lentiginous melanoma and desmoplastic melanoma (See Figure 2.2).

2.1.3.1 Superficial spreading melanoma

Superficial spreading melanoma is the most common type of melanoma in patients with white skin [654]. Although any site can be affected, the commonest sites are the leg in women and the back in men [654]. The lesions are usually flat and variably pigmented. The colour may vary from brown, red to black and range in size from a diameter of less than 5 mm to several centimetres. Lesions may become palpable, indicating invasion and in advanced lesions there may be nodules and ulceration. An amelanotic variant has also been reported and may clinically be mistaken for a banal lesion or vitiligo.

2.1.3.2 Nodular melanoma

Nodular melanoma is more frequent in men than in women and usually presents in the 5th and 6th decades of life [40, 345]. It most commonly arises on the trunk. This type of malignant melanoma grows rapidly and has often invaded deep into the dermis by the time of diagnosis. The clinical presentation is an elevated and dome-shaped nodule that often bleeds and ulcerates [654]. Nodular melanoma may initially be black or deeply pigmented, but often tumours lose pigmentation, causing difficulty with diagnosis.

2.1.3.3 Lentigo maligna melanoma

Lentigo maligna melanoma typically occurs in elderly patients and on sun-damaged skin [37, 415]. Lentigo maligna presents as a flat lesion with variable colour and areas of brown and black and even red or pink [654]. It has an irregular border that expands over many years. Clinically this is apparent as the tumour develops as a single or multiple raised nodules, or plaques within the lesion.

2.1.3.4 Acral lentiginous melanoma

Acral lentiginous melanoma is more common in patients of African and Asian origin [40]. It is more commonly found in elderly males. Acral lentiginous melanoma presents mainly on the sole of the foot, palm of the hand or under the nails. This type of malignant melanoma is characterised by an irregular large, flat, variably pigmented area, from which a raised pigmented and/or ulcerated area may arise [654]. Subungual melanomas may present as longitudinal streaks in the nail and in late stages there may be destruction of the nail.

2.1.3.5 Desmoplastic melanoma

Desmoplastic melanoma is rare and is usually found on the head and neck [654]. The lesions are generally not pigmented and presents as a plaque or nodule, and is often mistaken for a benign tumour or a scar. This subset of melanoma is often recurrent but rarely metastasises to lymph nodes. The lesions are not usually pigmented.

2.1.3.6 Metastatic melanoma

Recurrence and metastases occur in 25% of cases, usually in the first few years, but sometimes decades later [59]. The risk of recurrence is related to the depth of invasion. Local recurrence and metastases do occur, but the majority of metastases occur through lymphatic spread initially. Metastatic disease occurs in areas of high blood flow such as the lung, liver and brain, and less commonly in bone and gastrointestinal tract [13].



Figure 2.2: Four major subtypes of melanoma. (A) Superficial spreading melanoma, characterised by a dark brown plaque with highly irregular, scalloped borders and extensive colour variegation. (B) Nodular melanoma, appears as a relatively symmetric, sharply circumscribed nodule with a blue-grey dermal invasive component. (C) Lentigo maligna melanoma, manifest as an irregular, kidney shaped, thin brown plaque on the face. (D) Acral lentiginous melanoma, appears as a large ulcerative nodule on the plantar surface. Source: Adapted from Gordon, R. (2013). Skin cancer: an overview of epidemiology and risk factors. *Seminars in oncology nursing*, 29(3):160–169. [270].

2.1.4 Epidemiology

A relatively infrequent malignancy in the early 20th century, cutaneous melanoma has evolved to become an increasingly important public health problem worldwide. Although accounting for less than 5% of all skin cancers diagnosed, the disease burden of melanoma is significant, with an estimated 50,000 deaths annually worldwide [351]. Its incidence has steadily increased over the last 50 years in most fair-skinned populations and is predicted to continue increasing for at least two more decades [110, 155, 250, 357, 551, 736]. While mortality rates of melanoma increased in the 1970s and 1980s, these rates have stabilised since the early 1990s in Australian, USA, and certain European countries [48, 179, 173], possibly reflecting the effects of early recognition and the diagnosis of thin melanomas with a more favourable prognosis [108, 251].

On the therapeutic front, several novel agents such as ipilimumab and vemurafenib, have recently been approved for the treatment of metastatic melanoma, opening the era of targeted immune- and mutation-based therapy in advanced disease. Both these agents

have provided promising results with meaningful effects on progression-free and overall survival. The next section of the review discusses the recent trends in melanoma incidence and mortality, economic impact, and demographic trends.

2.1.4.1 Incidence

Melanoma is the 19th most common cancer worldwide with its incidence rising faster than any other solid tumour [351]. The global incidence is approximately 232,130 new cases per year, with 55,489 deaths [351]. Incidence rates are highest in Australia/New Zealand and lowest in South-Central Asia, with around a 135-fold variation in world age-standardised incidence rates (ASIRs) between the regions of the world for males, and around a 150-fold variation for females [351]. Australia has the world's highest ASIR of malignant melanoma (37 per 100,000), which is more than 12 times the average world rate (3 per 100,000) (Figure 2.3) [36, 351]. The Australian Institute of Health and Welfare reported a tremendous increase in ASIR in both males and females from 1991 to 2009, with no signs of it declining. The increase was more marked for males - from 44 per 100,000 in 1991 to 62 per 100,000 in 2009 (an increase of 42%). For females, the ASIR increased by 18%, from 34 per 100,000 to 40 per 100,000 over the same period [36].

In the USA, Siegel *et al.* reports that it is predicted that there will be 73,870 invasive melanomas diagnosed in 2015 and 9,940 people will lose their lives to this disease [682]. Incidence trends released by the Surveillance Epidemiology and End Results (SEER) found rising incidence rates of melanoma for older men, and this trend has worsened for the 10-year period from 2001 to 2011, during which men aged 60 and above experienced a 1.5-fold increase in incidence [332]. Furthermore, between 1992 and 2004, the incidence of melanoma increased for tumours of all histologic subtypes and thicknesses [449]. While this increase may be attributed to higher rates of melanoma screening, the sharpest increase in incidence was evident among low socioeconomic status areas, where individuals are least likely to undergo screening, suggesting that increasing incidence rates are not simply an artefact of screening [449].

In Europe, the estimated ASIR (European standard) of new melanoma cases for 2012 was, 11.4 per 100,000 for males and 11.0 per 100,000 for females [219]. Wide north/south and east/west variations have been reported, ranging from 6 cases for Central and Eastern Europe, 10 cases for Southern Europe, 15 cases for Western Europe, and up to 19 cases

per 100,000 for Northern Europe [219]. Melanoma incidence has been more profoundly raised in Northern Europe, with examples of 10-fold increases in Scandinavian countries between 1953 and 1997 [173]. A recent analysis of the GLOCAN 2012 dataset confirmed that the incidence rate of Central and Eastern Europe is less than half that of Western Europe [351]. Variations among populations in Europe could be explained by differences in skin phenotype as well as in sun-exposure behaviours.

Differing patterns of melanoma incidence have been also noted in relation to age. Despite the reported stabilisation of incidence in younger cohorts in several countries, recent data from the USA have shown an alarming increase in melanoma in young female subjects over the past three decades [602]. An analysis of the SEER data in the 20 - 49 age group showed an increase in the age-adjusted rate from 8.1 in 1975 to 17.1 per 100,000 in 2008 for women, whereas in men the same rate increased from 8.3 to 11.1 per 100,000, respectively [332]. A closer examination of the data revealed that the increase in incidence rates in females peaked in the age group of under 40 years while men exhibited higher incidence rates after the age of 44 years [96]. It is noteworthy that changes in clothing patterns, tanning bed usage and sun seeking behaviour have been evaluated as the most probable cause of the rising melanoma incidence rate in young women [109, 348].

2.1.4.2 Demographics and trends

Some differences in the incidence and anatomic distribution patterns of melanoma are related to race. Melanoma occurs far more common in Caucasians than in persons of other races [156, 250, 551, 357]. A study using data from 38 population-based cancer registries in the USA analysed trends for various racial groups [807]. Overall, Caucasians, African Americans, Asians/Pacific Islanders, and American Indians/Alaskan Natives account for 95%, 0.5%, 0.3%, and 0.2% of the cases reported to SEER in the USA, respectively [807]. Overall, the median age of diagnosis was 59 - 63 years of age for African American and Caucasian patients alike and 52 to 56 years of age in the other racial groups including Hispanics, American Indians, and Asians [807]. In the report, 63% of Caucasian patients were diagnosed with thin melanomas (≤ 1.0 mm in thickness). In African Americans, acral lentiginous melanoma was the most common histologic type, whereas superficial spreading melanoma was most common among the other racial and ethnic groups [807]. The most common anatomic site among Caucasians and American Indians was the trunk, whereas

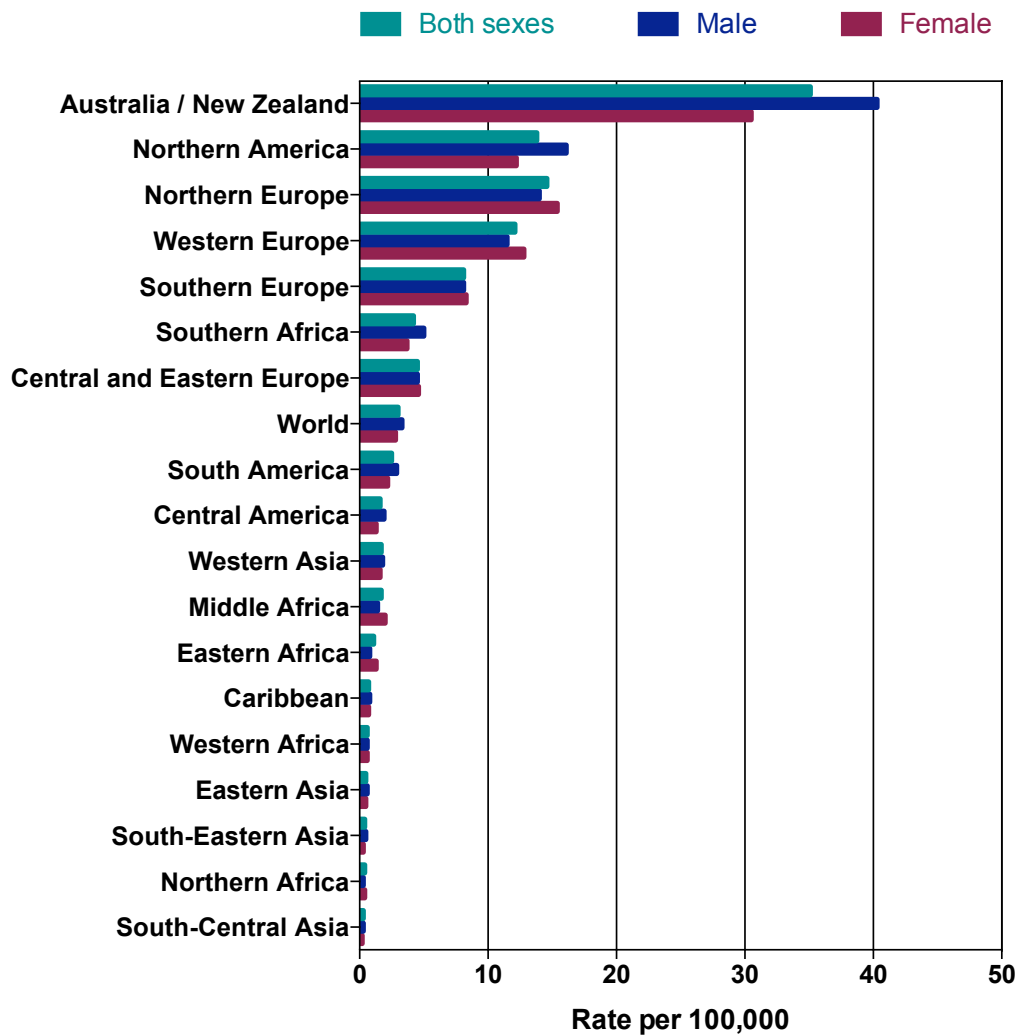


Figure 2.3: Malignant melanoma (C43), World age-standardised incidence rates, world region, 2012 estimates. The main reason for the rise in incidence could be increased exposure of pale white skin to natural UVR. Source: Adapted from J, F. et al. (2013). GLOBOCAN 2012: Estimated Cancer Incidence, Mortality and Prevalence Worldwide in 2012. IARC. Retrieved from http://globocan.iarc.fr/Pages/fact_sheets_population.aspx [351].

in African Americans and Asian Pacific Islanders the most common sites were the lower limbs and hip [807].

Apart from racial differences, melanoma is more common in men than in women, and survival is worse in men [682]. The American Cancer Society estimates that in 2015 approximately 42,670 men and 31,200 women in the USA will be diagnosed with melanoma [682]. In a recent Minnesota review, from 1970 to 2009 there was an 8-fold increase in incidence in young women aged 18 to 39 years, with only a 4-fold increase in young men [615]. The probability of developing melanoma in women younger than 49 years is higher than men, after this age, men experience a sharp increase in incidence and have an overall higher likelihood of developing this malignancy. In males, the most common anatomic sites are the head and neck, whereas in females the extremities and the torso/trunk are most commonly affected.

Interestingly, the male/female ratio of melanoma varies among different countries. A male predominance has been recorded in countries with a high melanoma incidence, such as Australia and the U.S.A. [155, 255]. In Europe, there is a discrepancy concerning sex predominance. The majority of Western and Northern European countries report high incidence rates in females *vs* males, whereas in most Central, Eastern and Southern European countries melanoma predominates in men [219]. In New Zealand, Richardson *et al.* found that the male and female incidence rates were similar but the site of melanoma differed by gender, with the leg being the most common site for females, while the trunk was the most common site for males [625].

With regard to age at diagnosis, generally older melanoma patients have poorer survival in comparison to younger patients [38]. A recent report from the expanded American Joint Committee on Cancer database demonstrated that patients older than 70 years had melanomas with more aggressive prognostic features compared with other age groups [47]. Howlader *et al.* report a similar mortality rate for men and women; however, among those aged 65 years and older, the increase in mortality was higher in men (21.5 per 100,000 in men compared with 7.7 per 100,000 in women) [332]. More specifically, in men and women aged 60 to 69, mortality rates were 2-fold higher in men. Mortality rates also further increased in men older than 70 years, more than 3-fold greater than the trend observed in women in the same age group [332].

2.1.4.3 Economic impact

The rapidly increasing incidence of melanoma has created a major economic burden on the public and private healthcare system globally. In Australia and New Zealand where melanoma incidences are highest in the world, the expenditure on melanoma is staggering. A report prepared by Klynveld Peat Marwick Goerdeler (KPMG) for Melanoma Patients Australia estimates the economic burden on the national healthcare system for advanced melanoma to be AU\$163.9 million in 2014 [414]. Furthermore, the detailed economic study assessing other factors such as loss of productivity, scientific research and informal care, places the estimates at an alarming AU\$422 million in 2014 alone [414]. A retrospective study conducted by Fransen *et al.* estimated that the total cost of NMSC alone was AU\$511.0 million in 2010, and is estimated to increase to AU\$703 million by 2015 [241]. Similarly in New Zealand, O’Dead reports the total cost of skin cancer was NZ\$123.1 million in 2006 and is expected to increase annually [558].

In the USA, the annual direct cost of treating newly diagnosed melanoma has been estimated to be approximately US\$563 million, and the addition of indirect costs could bring the estimate to more than a billion dollars [739]. The most striking finding in the Tsao *et al.* analysis was that 90% of the total annual direct costs account for less than 20% of patients with melanoma disease (stage III and stage IV patients), strongly suggesting that the cost of advanced disease management is exceedingly high [739]. Differentiation by stage revealed that the cost of treating a single stage III or stage IV patient is roughly 40-fold more expensive than the cost of treating one stage I patient [12, 739]. Furthermore, in their analysis of the SEER database from 1991 to 1996, Seidler *et al.* estimates the annual cost of treating melanoma in the population 65 years or older to be a hefty \$390 million [662].

The increase in melanoma incidences has also placed a large financial burden within several European countries. In France, Chevalier *et al.* showed that the annual hospital costs for melanoma care in 2004 was approximately €59 million, 45% of which were from patients with stage IV disease [140]. Vallejo-Torres *et al.* estimate the National Health Service (NHS) cost of skin malignancies in England in 2008 ranged from £106.4 to £112.4 million [750], an increase from the previous estimate of £101.6 million in 2002 [527]. Furthermore, projections estimate the cost to the NHS due to skin cancer to be over £180 million in 2020 [750]. Another research group reported that the total healthcare costs of

skin cancer in Sweden during 2005 were €142.4 million [729], and this increased by €35.2 million 6 years later [213].

2.1.5 Risk factors

Melanoma causation and risk association is complex with genetic and environmental factors affecting individual risk. As noted earlier, Caucasian race, male sex, and older age are also well-recognised factors associated with an increased risk of developing melanoma. In addition to these factors, natural UV exposure, indoor tanning, family history, nevi and several other factors have been identified (Figure 2.4) [270, 471, 600]. Traditionally, these risk factors for melanoma can be categorised as either personal host factors (genetic determinants) or environmental. However, it is likely that this is a false division in that multifactorial genetic features often determine the host's response to environmental events, such as severity of sunburns and the ability to tan. Each of these risk factors corresponds to a genetic predisposition and/or environmental stressor, contributing to the genesis of melanoma. In addition, other factors such as immunosuppression and socioeconomic status may influence melanoma development, all of which are further discussed below. A summary of the relative risk (RR) of each melanoma risk factor is tabulated below (Table 2.2).

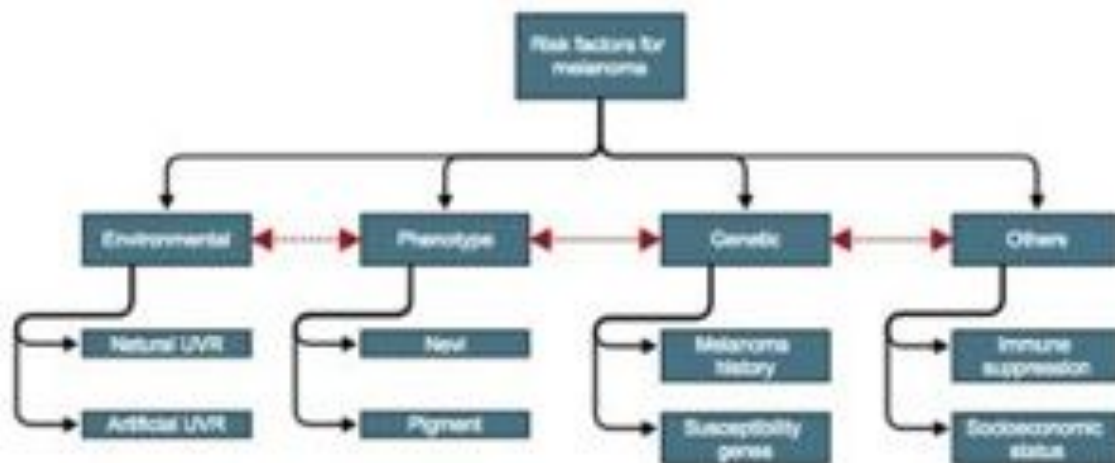


Figure 2.4: Risk factors for melanoma. The major risk factors can be broadly classified into four categories: environmental, phenotype, genetic, and others. The interactions between these factors promote melanogenesis and are currently the subject of ongoing research. Adapted from Azoury, S. C. and Lange, J. R. (2014). Epidemiology, risk factors, prevention, and early detection of melanoma. *The Surgical clinics of North America*, 94(5):945–62– vii [40].

2.1.5.1 Environmental risk factors

The most widely accepted environmental factor contributing to melanoma development is ultraviolet radiation (UVR) [176, 259, 691]. Exposure to UVR, either from sunlight or indoor tanning devices, is the most important, avoidable known risk factor for melanoma.

2.1.5.1.1 Natural ultraviolet radiation exposure

Lifetime exposure to UVR is a well-established risk factor for melanoma development. Ultraviolet radiation has damaging effects on the skin via direct and indirect mechanisms, such as the formation of cyclobutane pyrimidine dimers, gene mutations, immunosuppression and oxidative stress [379]. The role of UVR exposure as a leading environmental cause of melanoma is further supported by a wealth of evidence, including a high prevalence of melanoma in populations that migrated from a low to a high ambient UVR environment [37], a higher incidence in fair-skinned compared with darker-skinned individuals, and a latitude-dependent rise in melanoma rates among white populations with proximity to the equator [111, 520]. Armstrong and Kricger suggest that the amount of average annual UVR exposure correlates with the incidence of melanoma [25]. A more recent meta-analysis conducted by Dennis *et al.*, maintains this notion, reporting an increased risk of melanoma in individuals with an increased number of sunburn episodes [180].

However, examination of the anatomical distribution of cutaneous malignancies suggests a more complex association of melanoma with UVR that does not conform to a straightforward dose-relationship model [209, 248]. A pooled analysis and 7,216 controls at different latitudes showed that different amounts and pattern exposures of UVR exert a differential effect on site-specific melanoma risk [134]. Individuals with melanomas of the head and neck often have had high levels of occupational sun exposure, and therefore develop lesions more frequently on these sun-exposed body areas [134, 785]. Conversely, melanomas occurring on areas that were less frequently exposed such as the trunk tend to occur in people with lower levels of sun exposure and fewer solar keratoses [114, 785].

Molecular studies have given further credibility to the notion that melanoma is a heterogeneous disease comprising distinct biological subtypes possibly arising through different causal pathways [167]. For example, BRAF mutations, which are the principal causal mutation in melanoma are detected in lesions typically arising in anatomical locations of intermittent UVR exposure and in patients with high early-life ambient UV exposure

[72, 204, 725]. In contrast, c-KIT mutations and cyclin D1 gene amplifications are commonly detected in acral and mucosal melanomas or in melanomas related to chronic sun exposure, in which a relative paucity of BRAF mutations is noted [166, 300]. These data suggest important differences between melanomas on a molecular level based on their site, type of sun exposure and genetic factors that are not yet entirely clear.

2.1.5.1.2 Artificial ultraviolet radiation exposure: tanning beds

Over the past 20 years, indoor tanning has become popular among white populations, and particularly in young women [379, 551]. It has been estimated that 70% of the estimated 28 million people in the USA who engage in artificial tanning are women aged 16 to 49 years [423, 716]. To date, there is strong evidence that sun bed users have an increased risk of melanoma development [89, 254, 348, 658]. The Centres for Disease Control and Prevention and the National Cancer Institute reported higher rates of indoor tanning among women, whites and adults aged 18 to 29 years [128]. In a Swedish study, more than half of female subjects 15 to 24 years of age had ‘ever used’ sun bed or sunlamps [783]; and in a survey in England and Wales, 24% of persons 16 to 24 years of age had used these devices [112].

A large case-control study from the Nurses’ Health Study reviewing cancer incidence data over a 20-year span (1989 - 2009) among 73,494 female nurses who used tanning beds prior to the age of 35 years showed a significantly increased risk of melanoma, BCC, and SCC, with multivariable-adjusted hazard ratios of 1.1, 1.5, and 1.5, respectively [823]. This is further supported by the significant increase of trunk-located melanoma in females over the past 20 years, mainly in countries with widespread access to indoor tanning [96, 168, 532]. A recent meta-analysis of 63,942 new cases of cutaneous melanoma diagnosed each year in the 15 countries of the European Community and three more member countries of the European Free Trade Association revealed that 3,438 (5.4%) of these cases were related to sun bed use [89]. Women represented most of this burden with 2,341 cases related to sun bed use; 1,096 cases occurred in men. Boniol *et al.* showed an overall RR of 1.2 (95% CI 1.08 - 1.34) of melanoma development in ‘ever use’ of sun beds and a 1.8% increase of risk for each additional session of sun bed use per year [89]. In addition, a dose dependency underlying this risk association has been also reported, expressed by the length, duration or number of treatment sessions. In a subgroup analysis of subjects who first used sun beds at an age below 35 years, the RR rose to 1.87 (95% CI 1.41 - 2.48) indicating a higher melanoma risk with an early onset of tanning bed exposure [89].

A meta-analysis of 19 other studies conducted by the International Agency for Research on Cancer (IARC) found similar results. The study concluded that ever use of indoor tanning was associated with the development of melanoma with a RR of 1.15; and first use before the age of 35 years significantly increased the RR to 1.75 [348]. On this basis and several other seminal studies, the IARC classified UVR exposure from tanning beds at its highest carcinogenic risk category ('carcinogenic to human') in 2007 [348]. The National Institutes of Health has also concluded that "exposure to sun beds and sunlamps is known to be a carcinogen based on sufficient evidence of carcinogenicity from studies in humans, which indicate a causal relationship between exposure to sun beds, sunlamps and cancer" [540].

2.1.5.2 Phenotypic risk factors

The major constitutional risk factors for melanoma include fair pigmentation, poor tanning ability, multiple nevi, clinically atypical or dysplastic nevi and freckling.

2.1.5.2.1 Nevi

The number of nevi and dysplastic nevi are important markers for melanoma risk. The total number of dysplastic nevi on the whole body is the most important independent risk factor for melanoma, and the risk for melanogenesis increases almost linearly with increased numbers of melanocytic nevi [690, 715]. The common criteria used to diagnose a dysplastic nevi includes two obligate features: size greater than 5 mm in the largest diameter and a prominent flat component; and two of three additional features: asymmetric outline, indistinct borders, and variable pigmentation [745]. The risk conferred by dysplastic nevi are much greater than those conferred by an increased number of common nevi [745]. Studies have demonstrated that dysplastic nevi are reported in up to 34% to 56% of melanoma cases [743, 744].

In their meta-analysis, Gandini *et al.* showed a gradient of risk, proportional to the number of common or dysplastic nevi [247]. The RR for patients with one dysplastic nevi was 1.45 (95% CI 1.31 - 1.60), 3.03 (95% CI 2.23 - 4.06) for patients with three dysplastic nevi, and 6.36 (95% CI 3.80 - 10.33) for those with five dysplastic nevi. Patients with a high number of common nevi (> 100) carried a 7-fold (RR = 6.89; 95% CI 4.63 - 10.25) increased risk for melanoma, compared with those with low numbers (0 - 15 common nevi)

[247]. Furthermore, a joint case-control study conducted by Bataille *et al.* found that dysplastic nevi were three times more frequent in the Australian cohorts (6%) than in the British cohorts (2%), but the prevalence of nevi on non-sun exposed area was the same [58]. In addition, studies have shown that the development of dysplastic nevi can be inhibited by regular use of sunscreen [533, 541]. Taken together, these findings suggest that UVR exposure could lead to the expression of atypical nevi, resulting in an overall increase in melanoma risk.

2.1.5.2.2 Pigment

Apart from nevi counts, the characteristics of an individual's pigment have been consistently associated with an increased likelihood of melanoma development. In a systematic meta-analysis of 60 studies, Gandini *et al.*, concluded that light skin colour (RR 2.06; 95% CI 1.68 - 2.52), poor tanning ability (2.09; 95% CI 1.67 - 2.58), light eyes (1.47; 95% CI 1.28 - 1.69), and hair colour (1.78; 95% CI 1.63 - 1.95) are risk factors for melanoma and are highly correlated [249]. With respect to hair colour, the RR for melanoma of 'light hair colour', consisting of 'blond, red and light brown colour', was 1.87 (95% CI 1.63 - 1.95) compared with the 'medium dark, brown hair colour', with the 'red hair colour' having the highest RR (3.64; 95% CI 2.56 - 5.37). A recent meta-analysis by Olsen *et al.* investigated the contribution of eye and hair colour, skin phototype and the presence of freckling, on melanoma risk [562]. The highest population-attributable fractions (PAFs) were observed for skin phototypes I/II [fair skin, burns easily and poor tanning ability] (0.27), presence of freckling (0.23), and blond hair colour (0.23). The PAF for blue/blue-grey eye colour was higher than for green/grey/hazel eye colour (0.18 *vs* 0.13), while the PAF for red hair colour was 0.10.

2.1.5.3 Genetic risk factors

The genetic basis of melanoma is complex and has both inherited and acquired components. Interactions between the two components plays an important role in melanoma predisposition.

2.1.5.3.1 Personal or family history

A personal history of melanoma is well established as a strong risk factor for melanoma. Several studies have shown that 1 - 8% of patients with prior history of melanoma will develop multiple primary melanomas (MPM) later in life [221, 249, 698]. Once the first

primary melanoma has been diagnosed, Mackie suggests that the RR of a second primary is around 70-fold higher compared with the risk of developing the first primary melanoma [471]. A retrospective analysis of several population studies by Goggins and Tsao identified an increased risk of developing a second melanoma (standardised incidence ratios ranging from 4.5 - 25.6) in patients with a history of a previous primary melanoma [264]. Furthermore, DiFronzo *et al.* calculated the 5- and 10-year risks for developing a second primary melanoma among patients to be 2.8% and 3.6%, respectively [188].

In addition, approximately 8 - 12% of melanoma patients display a familial propensity for the disease [315, 600]. In a combined analysis of 2,952 melanoma patients from eight case-control studies, Ford *et al.* concluded that the risk of cutaneous melanoma was 2-fold higher in patients with a family history of melanoma [237]. Ferrone and colleagues found that 21% of these patients had a positive family history of melanoma compared with only 12% of patients with a single primary melanoma [221]. The risk of these individuals developing multiple melanomas is greatly increased as the genetic factors involved in melanoma pathogenesis can be inherited [237, 268]. These patients should undergo intensive dermatologic screening and should consider genetic testing.

2.1.5.3.2 Melanoma susceptibility genes

Genetic analysis of melanoma related pedigrees has resulted in the identification of two high-penetrance susceptibility genes, the cyclin-dependent kinase inhibitor 2A (*CDKN2A*) on chromosome 19p21 [588] and cyclin-dependent kinase 4 (*CDK4*) on chromosome 12q14 [738, 831]. A recent global study identified that 39% of 385 melanoma-prone families had *CDKN2A* mutations ranging from 20% in Australia, to 45% in North America, to 57% in Europe [266]. Goldstein *et al.* found that the overall cumulative risk of melanoma by the age of 80 among mutation carriers from families with *CDKN2A* mutations was 0.67, but ranged from 0.58 in Europe, to 0.76 in the USA, to 0.91 in Australia [266]. In addition, *CDKN2A* has also been implicated as a nevus susceptibility gene [80]. However, the relationship between *CDKN2A* mutations and the presence of dysplastic nevi is complex, in that not all patients with atypical nevi were carriers of the *CDKN2A* mutation [80]. On the other hand, the frequency of mutations in *CDK4* is much lower and has been reported in less than 15 families worldwide [267, 692, 831]. It is unlikely that *CDK4* has a substantial impact on melanoma risk in the general population, thus, most studies have focused on mutations in *CDKN2A*.

Another well studied genetic variation associated with increased melanoma susceptibility is the presence of certain polymorphisms in the melanocortin 1 receptor (*MC1R*) gene on chromosome 16q24.3 [609, 713]. The *MC1R* gene encodes for melanocyte-stimulating hormone receptor and polymorphisms of this gene are commonly associated with the red hair colour (RHC) phenotype [609]. The RHC phenotype is typical of melanoma patients, characterised by fair pigmentation (fair skin, red or blond hair and freckles), and by sun sensitivity (poor tanning response and solar lentigines) [568, 609, 751]. Interestingly, large independent studies from both Australia and the Netherlands support the notion that certain *MC1R* polymorphisms maybe involved in melanogenesis in two ways, one, as a determinant of the red hair colour (RHC) phenotype, and another as a component in the mitogen-activated protein (MAPK) pathway [703, 753]. In addition, in his seminal paper, Box *et al.* found that when the *MC1R* polymorphism was present, the penetrance of the *CDKN2A* mutations increased from 50% to 84%, and the mean age of disease onset decreased to 37.8 years from 58.1 years [94]. The study provides evidence that variant alleles at the *MC1R* locus significantly increases the penetrance of mutations of *CDKN2A*, exacerbating the disease.

As noted above, although high risk susceptibility genes *CDKN2A* and *CDK4* have been identified, they explain less than half of familial melanoma cases. Rare genetic syndromes such as xeroderma pigmentosum (XP) can also increase an individual's predisposition to the disease. Kraemer *et al.* found that XP patients carry a 1000-fold increase in risk for melanoma above that of the general USA population [415]. Furthermore, these patients are diagnosed with melanoma at a significantly younger age than individuals in the general population; on average, melanoma diagnosis occurs at age 22 years in XP patients *vs* 55 years of age in the general population [97].

2.1.5.4 Additional risk factors

Both environmental and genetic factors are major risk factors in the development of melanoma. However, intense research has unravelled additional factors that may contributed to melanogenesis. These include the immune and socioeconomic status of a patient.

2.1.5.4.1 Immunosuppression

Besides these risk factors, chronic immunosuppression has also been associated with melanoma, especially in those patients with prior cancer (chronic lymphocytic leukemia and non-Hodgkin's lymphoma) [437] or suffering from acquired immune deficiency syndrome (AIDS) [563]. Medically induced immunosuppression, common in organ transplantation recipients is well documented as a significant melanoma risk factor [216, 328, 749]. It accounts for 6.2% of post-transplantation skin cancers in adults and 15% in children [216]. Hollenbeak *et al.* showed that of the 89,786 patients who underwent transplantation, 246 patients developed melanoma, which represented an increase in risk that was 3.6 times greater than the general population [328]. Interestingly, several authors have found that melanocytic nevi, a marker of propensity for melanocytic proliferation, occurs in excess in paediatric and adult transplant recipients [278, 686]. Similarly, excess melanocytic nevi have also been observed in people with HIV infection [278].

2.1.5.4.2 Socioeconomic status

In recent years, there has been an increasing amount of literature describing the influence of socioeconomic status (SES) on cancer survival. There is general agreement that patients from a high SES were more likely to develop melanoma, but were less likely to die from the disease [472, 620, 773]. Reyes-Ortiz and colleague's review of 25 studies in the USA and other countries suggest that high SES groups have greater recreational time and more opportunity for periodic excessive sunlight exposure, thus increasing an individual's exposure to UVR [620]. On the other hand, a population study in the United Kingdom demonstrated that patients from more socially deprived districts were more reluctant to seek advice for a suspicious lesion, resulting in the later diagnosis of the disease and poorer prognosis [208]. Similarly, a review of insurance status using the USA National Cancer Database noted a significantly higher likelihood of uninsured patients (low SES) being diagnosed with advanced-stage melanoma in comparison with privately insured patients (high SES) [293].

A similar relationship between high SES and melanoma incidence has been reported in Europe. In Denmark, Birch-Johansen *et al.* evaluated all 3.22 million Danish residents born between 1925 and 1973 without a previous history of cancer [78]. The population study supports earlier reports that the increased risk for malignant melanoma is associated with higher SES. Similar findings have been found in England where Shack *et al.* reports a

clear correlation between the relative risk of melanoma and the least deprived population (high SES).

Although melanoma incidence parallels SES, more recent studies conducted in the USA suggested that there has also been a marked increase in melanoma incidence in lower SES groups [273, 449]. According to Linos and colleagues, patients living in low SES areas experienced the greatest increase in incidence, and the greatest increases in incidence were among the thickest tumours (2.01 - 4 and \geq 4mm) [449]. Similarly, Greenlee and Howe demonstrated that living at higher poverty levels increased the odds of late-stage melanoma by 2-fold [273]. Both studies draw the conclusion that individuals from lower socioeconomic backgrounds are less likely to have access to medical care or participate in cancer screening programmes than those from more affluent backgrounds.

2.1.6 Pathogenesis

Melanoma originates from malignant transformation of melanocytes, a specialised cell type whose major function is to produce the melanin pigments that determine skin, hair and eye colour, and levels of photo-protection [444]. The traditional Clark model of the progression of melanoma emphasised the stepwise transformation of melanocytes to melanoma, from the formation of nevi to the subsequent development of dysplasia, hyperplasia, invasion and metastasis [513]. However, this ordered stepwise progression from the melanocyte to nevi to melanoma is relatively uncommon. Bevona and colleagues found that only 26% of melanomas arise from nevi, of which 43% arose from dysplastic nevi [73]. This finding would suggest that for the majority of melanomas, the existence of alternative pathways that bypass the nevus as an intermediary step. Evidence from epidemiological studies suggest a more complex model of pathways to melanoma determined by genetic factors, germ-line predisposition and the interplay with environmental factors, most notably UV exposure, and more recently immune dysregulation (Figure 2.5) [40, 57, 177, 459, 649]. This section of the thesis will briefly review aspects of melanoma pathogenesis that are supported by UV induction, the constitutively active MAPK pathway, and immune dysregulation.

2.1.6.1 Ultraviolet-induced melanoma

The role of UVR in inducing melanoma has been well established. When skin is exposed to UVR, UVR gets absorbed by DNA leading to genomic damage [149]. To prevent this from happening, keratinocytes stimulate melanocytes to produce melanin when exposed

Table 2.2: Risk factors and relative risk for melanoma.

Category	Feature	Relative risk (unless indicated otherwise)
Personal history of skin cancer	Melanoma	1 - 8% of melanoma patients will be diagnosed with another melanoma
Family history	Any	1.74
	Parent	2.40
	Sibling	2.98
	Two first-degree relatives	8.92
	Parent with MPMS	61.78
Atypical nevi	0	1.00
	1	1.45
	2	2.10
	3	3.03
	4	4.39
	5	6.36
Common nevi	0 - 15	1.00
	16 - 40	1.47
	41 - 60	2.24
	61 - 80	3.26
	81 - 100	4.74
	101 - 120	6.89
Hair colour	Red <i>vs</i> dark	3.64
	Blond <i>vs</i> dark	1.96
Freckles	High <i>vs</i> low density	2.10
Sun exposure	Intermittent	2.35
	Chronic	0.98
	Sunburn history	2.02
	Tanning salon	1.15
Genotype	CDKN2A	35 - 70 fold
	MC1R	2 - 3.5
	XP	Approximately one in every 5 patients will develop melanoma

Abbreviations: MPM, multiple primary melanomas; CDKN2A, cyclin-dependent kinase inhibitor 2A; MC1R, melanocortin 1 receptor; XP, xeroderma pigmentosum.

Source: Adapted from Psaty, E. L., Scope, A., Halpern, A. C., and Marghoob, A. A. (2010). Defining the patient at high risk for melanoma. *International journal of dermatology*, 49(4):362–376 [600].

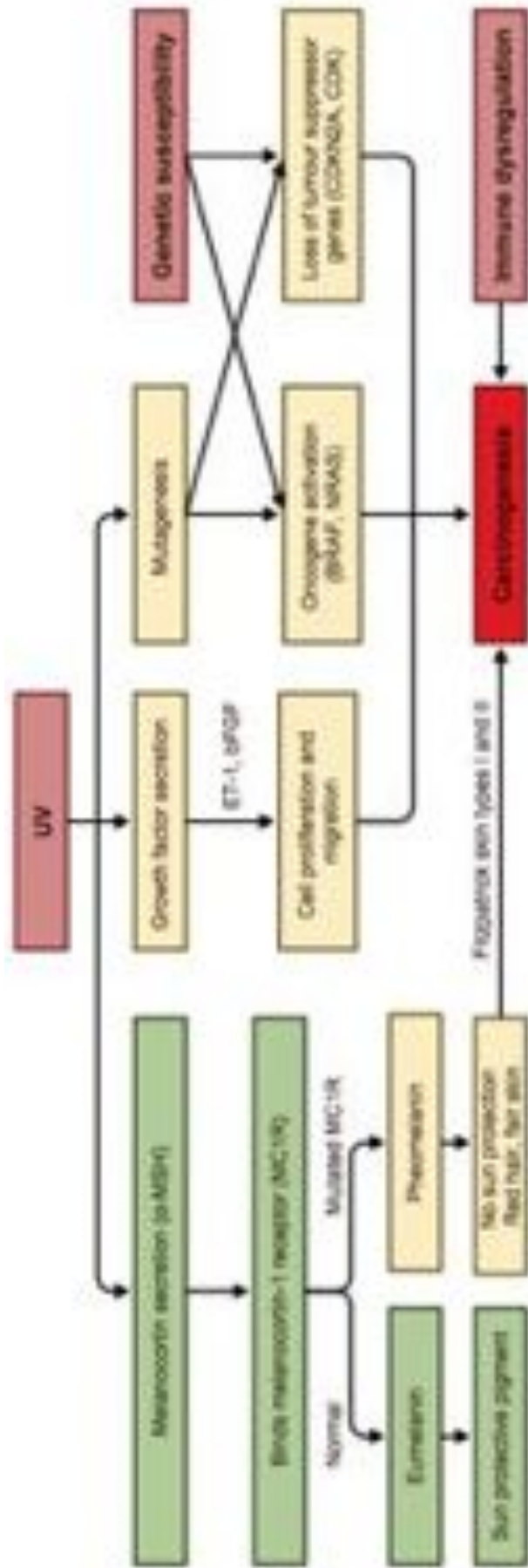


Figure 2.5: Pathogenesis of melanoma. Ultraviolet radiation, genetic susceptibility and immune dysregulation are thought to be the main culprits of melanogenesis. Ultraviolet radiation has direct mutagenic effects on DNA, by stimulating the cellular constituents of the skin to produce growth factors, by reducing cutaneous immune defences, and by promoting the production of harmful reactive oxygen species. Accumulation of genetic mutations in melanocytes leads to activation of oncogenes, inactivation of tumour suppressor genes and impaired DNA repair. Abnormal melanocyte proliferation, blood vessel growth, tumour invasion, evasion of immune response, and metastasis are other key features of melanoma development. Adapted from Thompson, J. F., Scolyer, R. A., and Kefford, R. F. (2005). Cutaneous melanoma. *Lancet*, 365(9460):687–701 [726].

to UVR. Initially, UVR-induced DNA damage induces stabilisation of the p53 tumour suppressor proteins [283]. In turn, p53 transcriptionally activates the expression of pro-opiomelanocortin (pOMC), which is cleaved to produce melanocyte stimulating hormone (MSH) [160]. The release of MSH by keratinocytes acts on melanocytes through the MSH receptor, otherwise known as MC1R. Activation of MC1R leads to elevation of cyclic adenosine monophosphate (cAMP) levels, which subsequently increases transcription of microphthalmia-associated transcription factor (MITF) thus initiating the synthesis of melanin from tyrosine. The synthesised melanin is packaged in melanosomes and transported back to keratinocytes where it localises over the nucleus, thereby protecting the keratinocyte genomic DNA from further damage by UVR (Figure 2.6).

Melanocytes produce two main types of pigment: brown/black eumelanin and yellow/red pheomelanin responsible for the RHC phenotype [252]. The protein MC1R is highly polymorphic and can exist in non-signalling variant forms that are responsible for the production of pheomelanin [751]. Eumelanin is the photo-protective pigment that provides UVR attenuation by transforming UV energy into harmless heat through a chemical process called internal conversion [252, 259]. This photo-protective property enables melanin to dissipate almost all of UVR as heat, thus preventing it from reaching genomic DNA where it can cause damage. Pheomelanin does not exhibit this UV-absorptive activity, and may even contribute to the formation of various reactive oxygen species (ROS) such as cyclobutane pyrimidine dimers (CPDs) and pyrimidine 6-4 pyrimidone [525, 613, 751]. A photochemical reaction that takes place after DNA is exposed to UVB occurring between pyrimidine dimers leads to the formation of these photoproducts [259]. Cyclobutane pyrimidine dimers are formed by the covalent binding of carbon atoms at the C5 and C6 positions of two adjacent pyrimidines, whereas covalent binding between C6 and C4 positions leads to pyrimidine 6-4 pyrimidone photoproducts [613]. Following the formation of these photoproducts, DNA repair enzymes participate in the correction of the damage. Although the DNA repair machinery is able to correct the damage, this is still an error-prone process [324], resulting in the signature $C \rightarrow T$ and $CC \rightarrow TT$ transition mutations [113].

It has also been suggested that UVR can directly activate cell surface growth factor receptors in a ligand-independent manner [358]. The proposed mechanism for this receptor activation is the inhibition of the protein tyrosine phosphatase mediated by oxidative stress

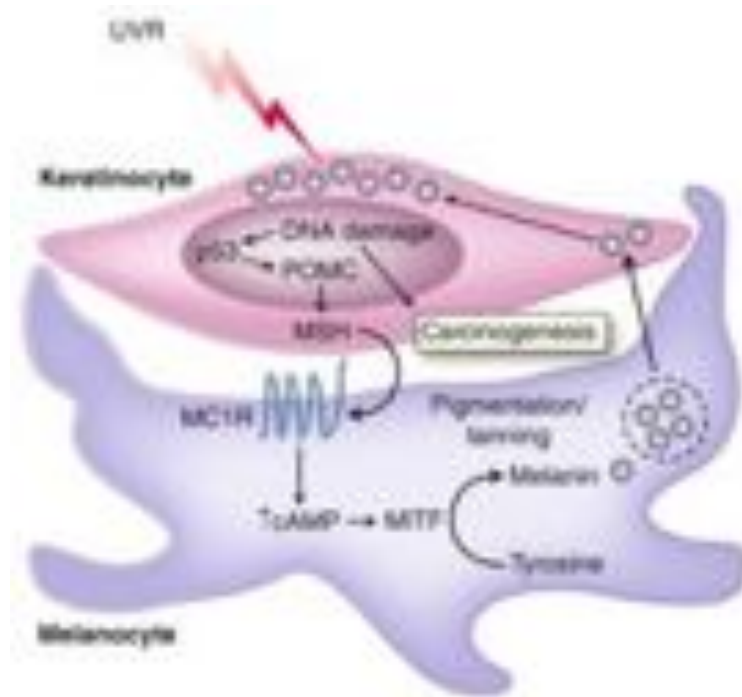


Figure 2.6: Schematic diagram of molecular steps in UVR-induced carcinogenesis pathway. Exposure to UVR leads to tanning and skin cancer development through DNA damage in keratinocytes. DNA damage leads to activation of p53, which leads to expression of pOMC, the precursor of MSH. MSH is secreted by keratinocytes and acts on melanocytes by binding to MC1R, leading to the elevation of cAMP levels. This in turn increases transcription of MITF, which leads to the synthesis of melanin from tyrosine. Melanin is packed in melanosomes and transported to keratinocytes, where it acts to protect the nuclei from further UV exposure. The accumulation of melanin in keratinocytes also leads to the appearance of tanning. Abbreviation: pOMC, pro-opiomelanocortin; MSH, melanocyte stimulating hormone; MC1R, melanocortin-1 receptor; cAMP, cyclic adenosine monophosphate; MITF, microphthalmia-associated transcription factor. Source: Garibyan, L. and Fisher, D. E. (2010). How sunlight causes melanoma. *Current oncology reports*, 12(5):319–326 [252].

[283]. Devary and colleagues detected a proliferative response from the RAS/RAF pathway as a direct result of UV-activated tyrosine kinase receptors [182]. Several other studies have also demonstrated that UV activation of these same receptors could also trigger other tumour-promoting activities, such as the survival through the PI3-kinase/AKT pathway [512, 768]. Furthermore, when epidermal keratinocytes in culture were treated with UV radiation, they synthesised various growth factors such as endothelin-1 (ET-1) and basic fibroblast growth factor (bFGF), stimulating the maturation of melanocytes [22, 717]. These UV-mediated responses are capable of establishing a potent paracrine signalling loop in the skin, facilitating survival and growth of damaged melanocytes, ultimately leading to melanogenesis [1, 358].

2.1.6.2 Genetic susceptibility in melanoma

All cancers, including melanomas, carry somatic mutations. Mutations in important melanoma-associated genes such as *CDKN2A*, *PTEN*, *NRAS*, and *BRAF* are believed to represent the key initiating factors in carcinogenesis [421, 510, 790]. These mutations can arise *de novo* or be transmitted in the germ line from one generation to the next. In the next section, we briefly discuss the impact of UV exposure on the advent of melanoma gene mutations, and the role of cell signalling pathways and cell cycle regulators on melanogenesis.

2.1.6.2.1 Driver mutations arising from ultraviolet mutagenesis

There is an increasing appreciation for the confounding impact of high mutational load due to UV-induced mutagenesis [114, 819]. Somatic alterations arising from these mutations are termed driver mutations, conferring malignant growth advantage. Data presented by Hodis *et al.* using whole-exome sequencing on paired tumour and normal genomic DNA from patient samples found that hotspot-activating mutations in melanoma genes such as *RAC1*, *STK19*, *FBXW7*, and *IDH1* was positively related to direct UVB-mediated damage [323]. These four genes all possessed a relative percentage of C → T mutations that was markedly above the exome-wide-per-sample median. Furthermore, epidemiological and experimental data reviewed by Garibyan and Fisher suggest a causal role for intense UV exposure during development (e.g. blistering sunburns early in life, tanning beds used by young adults) in melanoma pathogenesis [252]. This observation is almost entirely attributable to increased abundance of the C → T or G → A transition, characteristic of a UV-light-induced mutational signature [199, 591]. The collection of these findings provide unequivocal genomic evidence for a direct mutagenic role of UV light in melanoma pathogenesis.

2.1.6.2.2 Signalling molecules

The RAS/RAF/MEK/ERK pathway, also known as the MAPK pathway, is a signal transduction cascade relaying extracellular signals from the plasma membrane to nucleus through a series of consecutive phosphorylation events [494]. In a 2002 genome-wide screen, mutations in *BRAF* were discovered at high frequency in melanomas but at lower frequencies in other malignancies, such as thyroid and colon cancer [169]. This gene encodes a kinase in the MAPK signal transduction pathway and is thus an important regulator of a variety of cellular processes, including growth, survival and migration [494, 711]. On-

cogenic *BRAF* mutations lead to constitutive activation of the kinase activity of BRAF, which provides the cell with continuous growth signals in the absence of extracellular stimuli [479, 767]. Somatic *BRAF* mutations have been found in 50 - 70% of melanomas, with a single substitution (V600E) in exon 15, accounting for > 90% of all *BRAF* mutations [169]. The second most common substitution is V600K where lysine is substituted for valine, occurring in 6 - 29% of BRAF mutant melanomas [644]. Less frequent mutations include V600R (valine to arginine) and K601E (lysine to glutamic acid) [462, 506]. These mutations are distinct from the CC → TT or C → T changes associated with UVR exposure, suggesting a different mechanism of pathogenesis. This is supported by several clinical studies where clinicians have reported that V600E mutant melanoma is associated with young age, a truncal primary melanoma site and a lack of chronic sun damage [462, 506]. Notably, *BRAF* mutations have also been found in up to 80% of benign and dysplastic melanocytic nevi [595, 747], indicating that BRAF activation alone is insufficient for the development of melanoma. This highlights the presence of complex molecular machinery that provides checks and balances which prevent the vast majority of benign nevi from undergoing malignant change.

It is currently unclear if patients with BRAF-mutant melanomas have a poorer prognosis compared with BRAF wild-type disease [462, 500, 524, 536]. However, research has shown that melanomas without *BRAF* mutations usually carry mutations in other components of the MAPK pathway [407]. *NRAS* mutations are commonly found in melanomas of the skin [167, 184, 354], *KIT* mutations are frequent in acral melanomas of the soles, palms and mucosal membranes [166, 118], and *GNAQ* mutations are found in uveal melanomas and blue nevi [754]. Acral and mucosal melanomas have a lower frequency of BRAF mutations, whereas uveal melanomas have not been shown to harbour BRAF mutations [151, 627]. Interestingly, although commonly mutated as somatic events, studies have shown that the *BRAF*, *NRAS*, *PTEN* and *GNAQ* genes are not associated with inherited melanoma susceptibility [127, 310, 425]. While there are several other pathways often abnormally regulated or activated in melanoma, such as the phosphatidylinositol-3-kinase (PI3K), Wnt, and nuclear factor kappa-light-chain-enhancer of activated B cells (NF- κ B) pathway [342, 407, 649], to date most interest has focused on the MAPK pathway.

2.1.6.2.3 Cell cycle regulators

The transformation of melanocytes to melanoma cells is characterised by abnormal proliferation resulting from alterations in cell cycle regulatory mechanisms. Mutations in *CDKN2A* together with *CDK4*, were first identified in clusters of melanoma-prone families in the mid-1990s [589]. Located on chromosome 9p21, the *CDKN2a* locus encodes for two tumour suppressor proteins, p16^{INK4a} and p14^{ARF}. The protein p16^{INK4a} negatively regulates cell growth by arresting cells at G1, while p14^{ARF} enhances apoptosis and blocks oncogenic transformation [172]. Germ-line mutations in *CDK4*, located on chromosome 12q13, have only been identified in a limited number of families to date. When defective, p16^{INK4a} is unable to inactivate CDK4 and CDK6 which initiates the phosphorylation of retinoblastoma tumour suppressor protein (Rb) [66, 172, 311]. When Rb is phosphorylated, it loses its function and releases the transcription factor E2F, leading to uncontrolled DNA replication and cell cycle progression [560]. Another tumour suppressor of interest is the protein product of the *PTEN* (phosphatase with tensin homology) gene, located on chromosome 10. Mutations in *PTEN* are found in 10-20% of primary melanomas [740] and have also been associated with thyroid, breast and endometrial carcinoma [210]. Recent studies have demonstrated that PTEN is a negative regulator of the oncogenic PI3K signalling pathway, which is an important driver of cell proliferation and survival, and inactivation of PTEN by deletion or mutation leads to constitutive activation of this pathway [161].

2.1.6.3 Immune dysregulation of melanoma

The immune recognition of cancer cells typically begins at the cancer site where fragments of dying cancer cells are taken up and processed by professional antigen presenting cells (APCs) such as dendritic cells. This process requires specific APC maturation signals such as damage-associated molecular patterns (DAMPs) [410], without which APCs induce immune tolerance rather than activation [469, 476, 704]. Following activation, APCs migrate to the lymph nodes, displaying a range of peptides including tumour-associated antigens (TAAs) in the context of major histocompatibility complex (MHC) class I and II molecules [93, 760]. This enables antigen recognition by antigen-specific CD4 and CD8 T cells. In addition to the recognition of cognate MHC-peptide complexes, the activation of T cells requires another immunostimulatory signal, which is provided by the activation of a co-stimulatory receptor such as CD28 on the surface of T cells [136]. After successful activation, T cells migrate to tumours through the systemic vasculature by following a chemokine gradient [239, 302]. Adhesion molecules in the tumour endothelium then fa-

facilitate the adherence and extravasation of T cells from the vasculature into the tumour microenvironment [830]. Finally, the recognition of tumour targets proceeds through interaction between the T-cell receptor (TCR) and cognate MHC-peptide complexes on tumour cells that ultimately results in T-cell mediated tumour destruction.

To avoid the recognition and destruction by the immune system, tumours have evolved multiple strategies to attenuate the effectiveness of T-cell mediated responses. This is achieved by interfering with nearly every step required for mounting an effective anti-tumoural immune response, from deregulation of APCs, to establishment of a physical barrier at the vasculature that prevents homing of effector cells, and the suppression of effector lymphocytes [529]. The recognition of these pathways of immunosuppression provides the basis for various immunotherapeutic interventions targeting these mechanisms. In particular, the identification of the co-stimulatory and co-inhibitory receptors regulating T-cell activation provided a rationale for targeting of these proteins for cancer therapy, with significant responses seen in animal models [349, 428]. Since then, antibodies targeting the T cell co-stimulatory and co-inhibitory receptors have been at the forefront of immunotherapy, with profound clinical benefit seen in multiple cancer indications [30, 62, 165, 295, 321, 630, 734, 796].

2.1.7 Diagnosis

The most important factor for the successful management of melanoma is an early diagnosis. Most melanomas can be identified clinically by careful examination with good lighting and magnification. Several characteristics are usually present and recognisable, including asymmetry, border irregularity, colour variation and a diameter greater than 6 mm. These features have been used as the so-called ABCDE system of diagnosis [242, 626]. However, the ABC criteria (asymmetry in shape, border irregularity and colour variegation) become more evident when melanoma is already relatively large in size ($D > 6$ mm) and is evolving [626]. Hand-held instruments for skin surface microscopy (dermoscopy) are now available and have made differentiating between benign and malignant skin lesions more reliable [23]. These instruments all rely on the principle of epiluminescence, using either polarised light or a film of liquid that prevents normal scattering of light at the stratum corneum of the skin and thereby allowing a clear display of the structures beneath it. The advantage of dermoscopy is that equivocal features are often present in very small melanomas, thus increasing detection of suspicious spots even in the context of small and

clinically banal-looking melanomas (Figure 2.7). When clinical diagnosis of a skin lesion is uncertain and melanoma cannot be excluded, the appropriate course of action is to excise the entire lesion for histological examination with a 2-mm clearance margin [726]. This approach allows definitive treatment to be planned appropriately if the diagnosis of melanoma is confirmed. The biopsy will provide details of the thickness of the tumour and any unfavourable features such as ulceration, regression or a high mitotic rate.

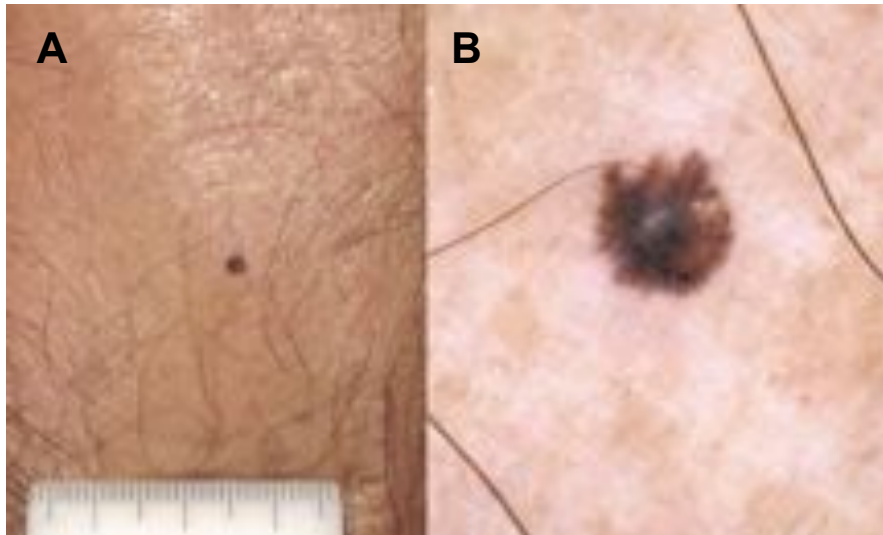


Figure 2.7: Clinical significance of dermoscopy. (A) Melanoma *in situ* on the arm of a 45-year old man. Clinically, the lesion is small and relatively regular in shape, border and colour. (B) Dermoscopically, a combination of melanoma-specific features are clearly evident, including asymmetry of colour and structure, irregular streaks and blue-white structures. Source: Adapted from Argenziano, G. *et al.* (2012). Early diagnosis of melanoma: what is the impact of dermoscopy? *Dermatologic therapy*, 25(5):403–409 [23].

2.1.8 Prognosis and staging

The prognosis for a patient with a newly diagnosed cutaneous melanoma depends mainly on two factors - the thickness of the primary tumour and the presence or absence of metastases to regional lymph nodes [726]. In 2002, the American Joint Committee on Cancer (AJCC) and Union for International Cancer Control (UICC) introduced a new staging system based on the evaluation of the primary tumour, with Breslow's thickness (T) and ulceration as the major prognostic factors; the presence or absence of regional lymphatic metastases (N), with number of involved lymph nodes as secondary factors of major prognostic significance; and distant metastases (M), with metastatic site and serum lactate dehydrogenase (LDH) concentrations as factors of major prognostic significance (Table 2.3) [45].

The staging of melanoma has a significant impact on the course of the disease and dictates the recommendation of treatment. Breslow depth is considered one of the most important prognostic indicators as patients with melanomas measuring less than 1 mm in depth have excellent (90% or greater) 5-year survival while those with tumours measuring greater than 4 mm have a reduced 5-year survival rate (approximately 50%). Stage III disease is defined by lymph node involvement, with stage IIIA being only microscopic involvement of a limited number of lymph nodes and stage IIIC representing involvement of multiple lymph nodes and macroscopic disease [46]. Stage IV disease represents any distant lymph node involvement, as well as lung or any visceral involvement. Table 2.4 shows the survival predictions for patients according to stage.

Since 2002, the melanoma staging system was substantially revised in 2009 for the seventh edition of the AJCC Cancer Staging Manual [46]. It is based on the details of 30,946 patients with stages I, II and III melanoma and 7,972 patients with stage IV melanoma from 17 melanoma treatment centres around the world [46]. For evaluation of the primary tumour, the 2009 AJCC system places heavy emphasis on mitotic activity (measured in mm^2) for the pathological assessment of thin melanoma (≤ 1.00 mm) [727]. Moreover, the 2009 system emphasises the microscopic, rather than macroscopic involvement of sentinel nodes. The use of a synoptic template for histopathological reporting of primary and sentinel nodes using H&E and the addition of immunohistochemical (IHC) staining (diagnosis is based on at least one melanoma associated marker eg: HMB-45, Melan-A/MART 1, S-100) increased diagnostic completeness and quality [559].

Table 2.3: TNM staging for cutaneous melanoma.

T	Thickness (mm)	Ulceration status / Mitosis
Tis	N/A	N/A
T1	≤ 1.00	a: without ulceration and mitosis $< 1/\text{mm}^2$ b: without ulceration and mitosis $\geq 1/\text{mm}^2$
T2	1.01 - 2.00	a: without ulceration b: with ulceration
T3	2.01 - 4.00	a: without ulceration b: with ulceration
T4	> 4.00	a: without ulceration b: with ulceration
N	No. of metastatic nodes	Nodal metastatic burden
N0	0	N/A
N1	1	a: micrometastasis ^a b: micrometastasis ^b
N2	2 - 3	a: micrometastasis ^a b: micrometastasis ^b
N3	4 +	a: micrometastasis ^a b: micrometastasis ^b
M	Site	Serum LDH
M0	No distant metastases	N/A
M1a	Distant skin, subcutaneous, or nodal metastases	Normal
M1b	Lung metastases	Normal
M1c	All other visceral metastases Any distant metastasis	Normal Elevated

Abbreviations: is, *in situ*; N/A, not applicable; LDH, lactate dehydrogenase.

^aMicrometastases are diagnosed after sentinel lymph node biopsy.

^bMacrometastases are defined as clinically detectable nodal metastases confirmed pathologically.

Source: Adapted from Balch, C. M. *et al.* (2009). Final version of 2009 AJCC melanoma staging and classification. *Journal of clinical oncology*, 27(36):6199–6206. [46].

Table 2.4: Anatomic stage grouping for cutaneous melanoma with 5- and 10-year survival rates.

Clinical staging ^a			Pathological staging ^b			Observed survival rate			
T	N	M	T	N	M	5-Year	10-Year		
0	Tis	N0	M0	0	Tis	N0	M0	N/A	N/A
IA	T1a	N0	M0	IA	T1a	N0	M0	97%	95%
IB	T1b	N0	M0	IB	T1b	N0	M0	92%	86%
	T2a	N0	M0		T2a	N0	M0		
IIA	T2b	N0	M0	IIA	T2b	N0	M0	81%	67%
	T3a	N0	M0		T3a	N0	M0		
IIB	T3b	N0	M0	IIB	T3b	N0	M0	70%	57%
	T4a	N0	M0		T4a	N0	M0		
IIC	T4b	N0	M0	IIC	T4b	N0	M0	53%	40%
III	Any T	N > N0	M0	IIIA	T1-4a	N1a	M0	78%	68% [†]
					T1-4a	N2a	M0		
	IIIB	T1-4b	N1a	M0	59%	43%			
		T1-4b	N2a	M0					
		T1-4a	N1b	M0					
		T1-4a	N2b	M0					
		T1-4a	N2c	M0					
	IIIC	T1-4b	N1b	M0	40%	24%			
		T1-4b	N2b	M0					
		T1-4b	N2c	M0					
Any T		N3	M0						
IV	Any T	Any N	M1	IV	Any T	Any N	M1	15 - 20%	10 - 15%

Abbreviations: is, *in situ*; N/A, not applicable.

^a Clinical staging includes microstaging of the primary melanoma and clinical/radiologic evaluation for metastases. By convention, it should be used after complete excision of the primary melanoma with clinical assessment for regional and distant metastases.

^b Pathologic staging includes microstaging of the primary melanoma and pathologic information about the regional lymph nodes after partial (sentinel node biopsy) or complete lymphadenectomy. Pathologic stage 0 or stage IA patients are the exception; they do not require pathologic evaluation of their lymph nodes.

[†] Survival rate is higher for stage IIIA cancers than for some stage II cancers. This is likely because the primary tumour is often less advanced for IIIA cancers.

Source: Adapted from Balch, C. M. *et al.* (2009). Final version of 2009 AJCC melanoma staging and classification. *Journal of clinical oncology*, 27(36):6199–6206 [46].

2.1.9 Treatment

Historically, patients with advanced melanoma have a very poor prognosis with limited treatment options and only until recently has systemic therapy become effective. Prior to 2011, there were four Food and Drug Administration (FDA) approved options for unresectable melanoma. Unfortunately the response rates for hydroxyurea [705] and dacarbazine [206], the first cytotoxic drugs approved for metastatic disease; and interleukin 2 (IL-2) [726], the first immunokine approved, were both poor and unpredictable. Furthermore, interferon- α -2b (IFN α -2b), which was approved in 1995 to treat resectable disease with a high risk of recurrence, has not been shown to reproducibly provide an OS benefit [387]. Since 2011, seven additional therapies have been approved and several more are likely in the near future (Figure 2.8). The following section reviews all therapies approved by the FDA for the treatment of advanced melanoma.

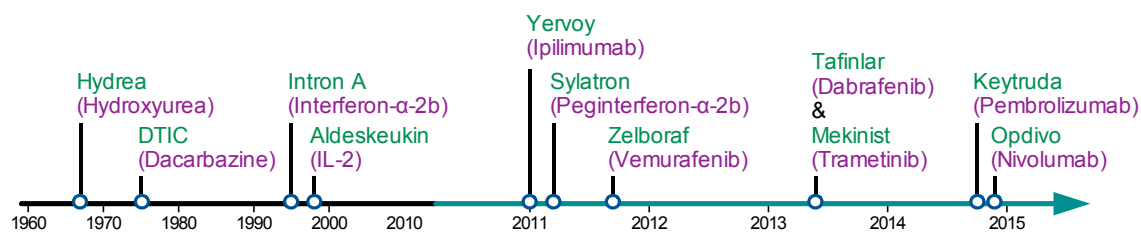


Figure 2.8: Timeline of FDA regulatory approval for the treatment of metastatic melanoma. Between 1967 and 2011, hydroxyurea (1967), dacarbazine (1975), interferon- α -2b (1995) and high dose IL-2 (1998) were the only approved agents for the treatment of advanced melanoma. The number of approved agents has doubled in the past four years with the approvals of ipilimumab, peginterferon- α -2b and vemurafenib in 2011, dabrafenib and trametinib in 2013, pembrolizumab and nivolumab in 2014. Trade names of therapeutics are labelled in green; generic names are labelled in purple.

2.1.9.1 Surgery

The primary treatment method, especially for non-metastatic melanomas is surgical excision. Surgery is an attractive option because patients are rendered ‘disease-free’ with relatively limited associated morbidity while systemically administered therapies require prolonged treatment courses to achieve any noticeable anti-tumour response. The largest study to date reviewed 8,759 patients from a 24-year period and showed that stage IV melanoma patients that underwent a complete metastasectomy of all clinically evident tumours had a 5-year survival rate of 20%, as compared to 7% and 2.1% for those in the palliative surgical and non-surgical groups respectively [561]. More evidence favouring an aggressive surgical approach to resection of metastases was published recently in a retrospective review that evaluated 84 patients who underwent surgical removal of metastatic

disease. Those who had multiple metastasectomies had a statistically significant longer survival than those who underwent a single operative procedure, 62.7 *vs* 42.4 months, respectively [721].

When considering surgical options, excisional biopsy is often the preferred choice, if possible, as it provides an optimal specimen for the evaluation of excision margins for the residual tumour [201, 290, 780]. Incisional biopsies are more difficult to interpret histologically, and carry the risk of not sampling the worst area of the tumour [309]. Excision margins should be determined according to Breslow thickness of the tumour [780]. Standard 1 - 2 cm narrow margins are appropriate for primary skin melanoma [290, 368]. Lentigo maligna melanoma, genital melanoma and lentiginous acral melanomas sometimes require wider safety margins due to the multifocality and poor delineation of the lesion. Facial and acral lesions are often managed with Mohs micrographic surgery for its tissue sparing effect and better cosmetic outcome [784]. Surgery is also helpful in tumour debulking and in palliative therapy of metastases [513].

2.1.9.2 Cytotoxic chemotherapy

If diagnosed at an early stage, surgical excision is curative in most cases. For patients with metastatic melanoma, cytotoxic chemotherapy has been widely used over the last three decades. Hydroxyurea and dacarbazine are the only two chemotherapeutic drugs that have received FDA approval for the treatment of advanced melanoma and will be briefly discussed.

2.1.9.2.1 Hydroxyurea

Hydroxyurea was first synthesised in 1869 in Germany by Dressler and Stein [198]. The precise mechanism by which hydroxyurea produces its anti-neoplastic effects remains unknown. Assays conducted in *Escherichia coli* bacterial systems demonstrate that hydroxyurea causes an immediate inhibition of DNA synthesis by acting as a ribonucleotide reductase inhibitor, without interfering with the normal synthesis of ribonucleic acid (RNA) or protein [416]. In a separate study, Phillips and Tolmach found that treatment of HeLa cells with hydroxyurea immediately after irradiation resulted in a significant decrease in the fraction of surviving cells, but not in non-irradiated cells [586]. They postulated that hydroxyurea may act as a radiation sensitiser by inhibiting the repair of radiation-mediated damaged DNA. In 1967, hydroxyurea became the first drug to be approved by the FDA

for the treatment of advanced melanoma [705]. Despite being well tolerated in patients, hydroxyurea exhibited little efficacy in treating melanoma and was never widely employed [7, 123]. In February 1998, hydroxyurea received a new indication, the treatment of sickle cell disease [497], and its use in melanoma became obsolete.

2.1.9.2.2 Dacarbazine

In 1975, dacarbazine (5-[3,3-dimethyl-1-triazenyl]-imidazole-4-carboxamide, or DTIC) was granted approval by the FDA for the treatment of metastatic melanoma based on objective response rates (ORR). DTIC is one of the triazene derivatives that acts through DNA alkylation, forming crosslinks within and between helices that lead to local denaturation of the DNA strand, interfering with the form and function of cancer cells [206]. A pooled analysis of 23 randomised, controlled trials showed that the ORR for 1,390 patients receiving DTIC monotherapy ranged between 5.3% and 28.0% (average 15.3%) [466]. The majority of these responses were partial with 11.2% partial responses (PR), and 4.2 % complete responses (CR). Evidence-based reviews show that responses are seldom durable, and that these drugs fail to provide any meaningful improvements in patient survival [206]. The primary purpose of dacarbazine therapy for metastatic melanoma is palliation. Dacarbazine is typically administered intravenously at a dose of 150 to 200 mg/m²/d for 5 days or at a single dose of 800 to 1,000 mg/m², with doses repeated every 3 to 4 weeks [206]. The latter schedule is more convenient and is well tolerated by most patients. Common toxicities include mild nausea and vomiting, myelosuppression, and fatigue, and most patients are able to maintain their baseline quality of life [39, 206]. Despite its modest efficacy and lack of data for survival benefit, DTIC continued to be the ‘standard treatment’ of metastatic melanoma for many years.

2.1.9.3 Immunotherapy

As described previously, the benefits of cytotoxic chemotherapy are generally palliative and usually does not lead to durable response or survival benefits. In an effort to develop new treatment modalities, the field of immunotherapy continues to be investigated intensively with the aim of mounting an effective immune response against melanoma. Several immunotherapeutics offering survival benefit have been approved by the FDA for the treatment of melanoma and will be reviewed here.

2.1.9.3.1 Interferon- α 2b (INTRON® A; Merck & Co.)

Interferon- α 2b was the first drug to demonstrate a significant benefit in relapse-free survival (RFS) as well as OS when used at high doses [404, 403]. On the basis of the results of the Eastern Cooperative Oncology Group (ECOG) 1684 trial, IFN- α 2b was approved by the FDA in December 1995 for adjunctive treatment of patients with advanced melanoma (stages IIB, IIC, or stage III) at high risk of recurrence after surgery. The mechanism of action of IFN- α 2b is unclear but it is thought to exert its anti-tumour effects through inhibiting DNA/RNA replication of neoplastic cells, upregulating MHC molecules on APCs [228, 387, 448], as well as stimulating T cells and natural killer (NK) cells [370]. Following the demonstration of IFN activity against malignant cells *in vitro* and *in vivo* [53, 274, 275], several clinical trials of the agent were conducted [404, 402, 403].

The most commonly used treatment protocol employed an induction phase of 20 MU/m², intravenous (i.v.) delivery for 5 days a week for 4 weeks, followed by a maintenance phase at 10 MU/m², s.c., 3 times a week for 48 weeks (total treatment duration of 52 weeks) [387]. The rationale for the initial high-dose i.v. treatment phase was to provide maximal dose intensity and minimise the induction of anti-IFN antibodies. In a randomised clinical trial conducted by the ECOG, ESTG-1684, Kirkwood *et al.* reported a remarkable improvement in RFS and OS in the high-dose IFN arm (RFS 1.72 *vs* 0.98 years, $P = 0.0023$; OS 3.82 *vs* 2.78 years, $P = 0.0237$) [404]. Interestingly, while effects on RFS have been consistently reproduced over multiple independent trials, a systematic review of nine randomised controlled trials confirms the lack of a clear OS benefit as an adjuvant therapy for melanoma [433]. This has led investigators to question whether RFS is a clinically meaningful endpoint and whether IFN- α 2b truly offers any clinical benefits.

2.1.9.3.2 Interleukin-2 (Proleukin®; Chiron Corp.)

The use of high-dose interleukin-2 (IL-2) was approved by the FDA in 1998 on the basis of a phase II study showing durable CRs in patients with metastatic melanoma [32]. IL-2 stimulates T cell and NK cell proliferation, triggering the release of IFN- γ and tumour necrosis factor (TNF), resulting in the destruction of malignant cells [245]. To determine the short- and long-term efficacy of high-dose IL-2 in patients with metastatic melanoma, Atkins *et al.* evaluated 270 patients from 8 clinical trials conducted between 1985 and 1993 [32]. Patients were administered with either 600,000 or 720,000 IU/kg, i.v., every 8 hours for up to 14 consecutive doses over 5 days. A second identical course of treatment was

repeated after six to nine days of rest in stable or responding patients. The overall response rate was 16%, including 17 CRs (6%) and 26 PRs (10%) [32]. The most striking finding of that study was that 12 (28%) of the responding patients remained progression-free. Furthermore, the disease did not progress in any patient responding for more than 30 months. Although the promise of cure with high-dose IL-2 is attractive, its use is still limited due to high toxicity [470]. Unfortunately, treatment with IL-2 is associated with significant toxicity that includes severe hypotension and vascular leak syndrome, resulting in interstitial and pulmonary oedema, renal and hepatic dysfunction, cardiovascular failure, neurological disturbances, nausea, vomiting and thrombocytopenia [661]. This has limited its use to selected patients with good organ function who are treated by experienced clinicians at selected specialised centres.

2.1.9.3.3 Peginterferon- α -2b (SylatronTM; Merck & Co.)

Peginterferon- α -2b (IFN-PEG α -2b) is characterised by the incorporation of a polyethylene glycol molecule (pegylation) to IFN α -2b, which makes it larger and decreases its metabolism. This strategy extended the plasma concentrations of IFN- α -2b in patients, allowing a more convenient treatment regime of only one dose weekly, unlike the non-pegylated formulation, which is administered three times a week [207]. IFN-PEG α -2b was approved by the FDA in 2011 as adjunctive therapy for the treatment of patients with advanced melanoma at high risk of recurrence after surgery based on a randomised phase III clinical trial (18991) conducted by the European Organisation for Research and Treatment of Cancer (EORTC) [207]. The study involved 1,256 patients with stage III melanoma within the post-operative period. Patients received high-dose IFN-PEG α -2b at 6 mg/kg per week for 8 weeks as induction, followed by 3 mg/kg per week for 5 years. Eggermont *et al.* reported a statistically significant improvement in PFS in patients treated with IFN-PEG α -2b compared with the control group (45.6% versus 38.9%), but there was no improvement in OS [207]. In addition, the study showed that 355 of the 608 patients who received treatment (58%) required dose reductions due to toxicity. However, there were no unexpected toxicities associated with IFN-PEG α -2b, and toxicity did not increase with treatment duration.

2.1.9.4 Kinase inhibitors

A major advance in the treatment of melanoma is the identification of activating mutations in the genes of a number of key cell signalling molecules that drive melanoma cell

proliferation and malignant phenotype. A better understanding of the MAPK pathway has led to the development of several new targeted therapies for components of MAPK signalling that are over active in melanoma. Three agents have demonstrated significant clinical benefit and have been approved for use in patients with BRAF mutations: the BRAF inhibitors vemurafenib and dabrafenib; and the MEK inhibitor trametinib.

2.1.9.4.1 Vemurafenib (Zelboraf®; Roche)

Vemurafenib orally administered twice daily was approved by the FDA in August 2011 to treat patients with metastatic or unresectable melanoma containing the V600 mutation. Vemurafenib is designed to selectively inhibit BRAF and is capable of blocking the function of the V600E mutant BRAF protein. The first clinical study of vemurafenib in humans was the phase I clinical trial (BRIM-1) conducted by Flaherty and colleagues [231]. In this trial, vemurafenib (formerly known as PLX4032) given orally twice a day (960 mg per dose) demonstrated an astonishing 81.3% response rate in patients with stage IV melanoma, with two patients achieving aCR. A large phase II trial in 132 patients who completed prior first-line therapy (BRIM-2; NCT00949702) confirmed a high response rate of 52.3% and a median PFS rate of 6.2 months [623]. The results were so promising that almost immediately a phase III clinical trial (BRIM-3; NCT01006980) comparing this drug with DTIC in treatment-naive stage IV melanoma patients was conducted.

In this later BRIM-3 study, a total of 2,107 patients were screened in 104 centres across 12 countries worldwide. Patients were randomised to receive either vemurafenib ($n = 337$, 960 mg orally twice daily) or DTIC ($n = 338$, 1,000 mg/m², i.v., once every 3 weeks). There were no doubts about the superiority of vemurafenib over DTIC. RR were 48% for vemurafenib and 5% for DTIC as well as , improved OS and PFS for vemurafenib with a hazard ratio of 0.37 and 0.26 respectively ($P < 0.001$) [135]. These impressive benefits observed at the time of the first interim analysis led to the recommendation by the data and safety monitoring board to unblind the trial, allowing the crossover of patients in the DTIC group to receive vemurafenib [135].

More recently, McArthur *et al.* presented updated findings on the BRIM-3 trial, showing a significant improvement in OS and PFS for patients receiving vemurafenib (OS 13.6 *vs* 9.7 months, $P = 0.0008$; PFS 6.9 *vs* 1.6 months, $P = 0.0001$) [490]. The toxicity of vemurafenib was well tolerated with adverse events such as alopecia, arthralgia, diarrhoea, fatigue,

nausea, rash, and keratosis of the extremities associated with the drug [135, 231, 490]. Two specific side effects of the BRAF inhibitors observed were the appearance of squamous cell tumours, none of them with malignant potential, and photosensitivity. Both symptoms were not therapy-limiting, and were managed with the excision of benign tumours and with the application of sunscreen, respectively [92, 135]. However, the curve of disease-free survival (DFS), although it separates rapidly from the DTIC curve, falls after 5 - 6 months, indicating an acquired resistance to vemurafenib in melanoma.

2.1.9.4.2 Dabrafenib (Tafinlar®; GlaxoSmithKline)

Dabrafenib is another potent BRAF kinase inhibitor that has demonstrated significant activity in patients with advanced melanoma compared with DTIC. Dabrafenib was approved by the FDA in May 2013 for the treatment of patients with advanced melanoma that harbour the V600E mutation. In the pivotal phase III trial (BREAK-3), 250 patients with unresectable stage III or stage IV melanoma were randomly assigned in a 3:1 ratio to either dabrafenib (150 mg orally twice a day) or DTIC (1000 mg/m², i.v. every three weeks) [307]. Similar to vemurafenib, patients were allowed to cross over to the alternative treatment upon the development of progressive disease. The administration of dabrafenib significantly increased PFS compared with DTIC (median PFS 5.1 *vs* 2.7 months, $P < 0.0001$) [307]. In addition, the PFS as estimated by independent review confirmed the investigator-assessed results, with a median for dabrafenib of 6.7 months *vs* 2.9 months for DTIC (HR 0.35, 95% CI 0.20 - 0.61) [307]. Confirmed objective responses were seen in 93 of 187 patients treated with dabrafenib (49.7%), and only 4 of 63 patients treated with DTIC (6.3%). Overall survival was updated at the 2013 ASCO meeting with the OS favouring patients treated with dabrafenib (OS 18 *vs* 15 months, $P > 0.05$), but was not statistically significant [308]. However, 36 of 63 patients (57%) originally treated with DTIC crossed over to dabrafenib, potentially obscuring an OS benefit from initial dabrafenib therapy. Treatment with dabrafenib was generally well tolerated. The most common side effects were the development of squamous cell carcinomas, arthralgia, fever, fatigue, and headache [307].

2.1.9.4.3 Trametinib (Mekinist®; GlaxoSmithKline)

Trametinib is a potent, highly specific inhibitor of the signalling molecules MEK1/MEK2 in the MAPK pathway. Trametinib was originally approved for the treatment of patients who had previously been treated with a BRAF inhibitor for advanced melanoma that

contained a BRAF V600E or V600K mutation. This approval was based upon a pivotal phase III trial (METRIC) showing prolongation of OS using trametinib as a single agent (2 mg orally once daily) in patients who had not received prior treatment with a BRAF inhibitor [232]. Flaherty *et al.* reported an increase in PFS and OS with trametinib when compared to the chemotherapy arm (median PFS 4.8 *vs* 1.5 months, $P = 0.001$; 6-month survival rate 81% *vs* 67%, $P = 0.01$) [232]. Common toxic effects include rash, diarrhoea and peripheral oedema.

More recently, trametinib has been combined with dabrafenib in an effort to delay the development of resistance to treatment and reduce toxicities directly associated with BRAF inhibition. In the phase III trial (COMBI-d), 423 patients were randomly assigned to either dabrafenib (150 mg orally twice daily) plus trametinib (2 mg orally once daily) or to dabrafenib plus placebo [463]. The primary endpoint of the trial which was PFS was significantly prolonged with the combination compared to dabrafenib alone (median 9.3 *vs* 8.8 months, $P = 0.03$) [463]. In another phase III trial (COMBI-v), 704 patients with previously untreated metastatic melanoma were randomly assigned to either dabrafenib (150 mg orally twice daily) plus trametinib (2 mg orally once daily) or vemurafenib (960 mg orally twice daily) [628]. Remarkably, both OS and median PFS was significantly increased with the dabrafenib plus trametinib combination (one-year survival rate 72% *vs* 65%, $P = 0.005$; median PFS 11.4 *vs* 7.3 months, $P < 0.001$). Notably, the median duration of response in the combination therapy group was almost twice as long as that in the vemurafenib group (13.8 months *vs* 7.5 months). Furthermore, the incidence of cutaneous SCC and keratoacanthoma occurred only in 1% of patients in the combination group and 18% of those in the vemurafenib group [628].

2.1.9.5 Immune checkpoint inhibitors

The field of immunotherapy in melanoma has long been appreciated, with reports of spontaneous melanoma regression first published more than 50 years ago [152]. Several early immunotherapies have shown durable remissions in small subsets of patients but have low response rates and are often limited by high toxicity. The most successful immunotherapy approach to date has been immune checkpoint inhibition, where the tumouricidal activity of T cells is directed towards malignant cells. Clinical results with these agents have been remarkable, leading to the accelerated FDA approval of several of these agents.

2.1.9.5.1 Ipilimumab (Yervoy®; Bristol-Myers Squibb)

Cytotoxic T-lymphocyte-associated protein 4 (CTLA-4) is an inhibitory receptor expressed on the surface of T cells after activation [9]. CTLA-4 competes with a positive receptor, CD28, for ligands B7.1 (CD80) and B7.2 (CD86) located on the surface of APCs [304, 420, 434]. CTLA-4 has a greater affinity for its ligands than its counterpart, CD28 and delivers a negative signal upon ligand binding [434]. Therefore, its activity results in downregulation of T cell activation and impaired cellular immune function. Blocking CTLA-4 with anti-CTLA-4 mAbs is thought to prevent downregulation of T cell activation, thus sustaining immune responses such as those against tumour antigens. Work on targeting the receptors regulating the state of T cell activation for cancer therapy was pioneered by James Allison and colleagues in 1996 [428]. In their seminal paper, Leach *et al.* demonstrated regression of tumours in different animal tumour models after blocking CTLA-4 [428].

Following these studies, human CTLA-4 blocking antibodies, ipilimumab (IgG1) and tremelimumab (IgG2), have been evaluated in multiple clinical trials, and both agents demonstrated durable responses in phase I and II clinical studies in advanced melanoma with a similar toxicity profile [116, 557, 630, 797]. An improvement in OS was only seen with ipilimumab in phase III evaluation [321, 630], which led to the drug's approval by the FDA in 2011. The clinical trial showed that four treatments with ipilimumab at 3 mg/kg were associated with a median OS of 10.1 months *vs* 6.4 months in patients receiving gp100 peptide vaccine alone [321], while tremelimumab failed to show any clinical benefit over standard-of-care chemotherapy [622]. A possible explanation for this might be that human IgG2 exist as a dimetric tetravalent, resulting in the problematic tendency of forming covalent dimers [651]. In this regard, IgG2 dimerisation may aggregate in the serum resulting in lower T-cell binding affinity.

Furthermore, a follow-up phase III study by Robert *et al.* showed that ipilimumab in combination with DTIC was more effective at prolonging survival than DTIC alone (11.2 months *vs* 9.1 months) [630]. As expected, adverse effects of ipilimumab are consistent with the hypothesis that CTLA-4 blockade breaks immune tolerance. The adverse events associated have been designated as 'immune-related adverse events' (irAEs), with inflammatory conditions occurring in the gastrointestinal tract (diarrhoea and colitis), skin (rash and pruritis) and liver (hepatitis) [321, 630, 777].

2.1.9.5.2 Pembrolizumab (Keytruda®; Merck & Co.)

Pembrolizumab is an anti-programmed cell death 1 (PD-1) monoclonal antibody that has been extensively evaluated in both ipilimumab naive and previously treated patients. The PD-1 molecule, expressed by T cells, has two primary ligands; PD-L1, found on cancer cells; and PD-L2, found on APCs [99, 734]. When bound to PD-L1, PD-1 acts as a negative regulator of T cells. Similar to anti-CTLA-4 therapy, antibodies against both PD-L1 and PD-1 have been developed to inhibit this down-regulatory pathway, allowing for unopposed T-cell activation. This leads to activation of tumour-specific T cells that can contribute to the anticancer response [193, 349]. Pembrolizumab was awarded an accelerated FDA approval in September 2014 following data from an international multi-centre, randomised dose-comparative phase I study involving 173 patients with unresectable or metastatic melanoma whose disease had progressed after at least two ipilimumab doses [629]. All patients were treated with pembrolizumab, either at 2 mg/kg or 10 mg/kg i.v. once every 3 weeks. The study reports an ORR of 26% at both doses, suggesting that pembrolizumab could be an effective treatment option for patients with ipilimumab-refractory advanced melanoma.

Pembrolizumab's safety was evaluated in a large phase I trial (KEYNOTE-001; NCT01295827) where 411 patients suffering from advanced melanoma were treated with one of the three dose schedules (10 mg/kg every two weeks, 10 mg/kg every three weeks, or 2 mg/kg every three weeks) [621]. Using multivariate analysis of the entire study population, Ribas *et al.* found no significant differences in outcomes between the three dose schedules [621]. The study resulted in an ORR of 34%, a PFS of 5.5 months, and an OS of 69% at one year and 62% at 18 months. In addition, the study included a cohort of patients who were randomly assigned to either 2 or 10 mg/kg of pembrolizumab administered every three weeks [296]. Similarly, Hamid *et al.* did not find a significant difference in ORRs between patients treated with either 2 or 10 mg/kg every three weeks [296]. Adverse effects included arthralgia, fatigue, rash, diarrhoea and pruritus, all of which were manageable and not treatment-limiting [621]. Success in these phase I studies has led to on-going phase II (KEYNOTE-002; NCT01704287) and III (KEYNOTE-006; NCT01866319) trials.

2.1.9.5.3 Nivolumab (Opdivo®; Bristol-Myers Squibb)

Nivolumab is another humanised monoclonal antibody that targets the PD-1 protein. On December 2014, the FDA granted accelerated approval to nivolumab for the treatment

of patients with unresectable or metastatic melanoma and disease progression following ipilimumab or BRAF inhibitor treatment (for BRAF V600 positive tumours). The approval was based on the ORR and durability of response in the first 120 patients who were treated with nivolumab and had a minimum 6 months follow-up from an on-going, randomised, open-label phase III trial (CheckMate-037; NCT01721746) [779]. Patients with advanced melanoma who progressed on anti-CTLA-4 therapy and a BRAF inhibitor were randomised (2:1) to receive nivolumab ($n = 268$, 3 mg/kg i.v. every two weeks) or the investigator's choice of chemotherapy ($n = 102$, DTIC, 1000 mg/m² every 3 weeks; or carboplatin, AUC 6 plus paclitaxel, 175 mg/m² every 3 weeks) until disease progression or unacceptable toxicity [779]. Nivolumab consistently achieved higher clinical activity when compared with the investigator's choice of chemotherapy (ORR 32% *vs* 11%, CR 4 *vs* 0, PR 34 *vs* 5), regardless of PD-L1 expression status, BRAF mutation status and prior anti-CTLA-4 benefit [779]. Furthermore, the first interim analysis of the trial confirmed that there were no unexpected irAES, with investigators eagerly anticipating the OS result of nivolumab treated patients [778]. Currently, nivolumab is the only PD-1 antibody that has demonstrated efficacy in a phase III trial [778].

2.1.9.6 Oncolytic viruses

More recently, several studies have explored oncolytic viruses (OVs) as an *in situ* vaccination strategy to potentiate the efficacy of immunomodulatory antibody therapy. The development of OVs as tumour lytic agents to date has been hampered by their poor systemic delivery to metastatic tumour sites and the development of neutralising antibodies. Recently, however, with a better understanding of the interplay between OVs and the immune system, came the recognition that the virus-induced anti-tumour immune responses, rather than direct viral lysis, may be the dominant factor in driving the efficacy of these therapies.

The current leading OV in the field is an oncolytic herpes simplex virus (HSV) encoding granulocyte-macrophage colony-stimulating factor (GM-CSF) (OncoVex^{GM-CSF}), also known as talimogene laherparepvec (T-Vec). Injection of the virus into accessible lesions in patients with advanced melanoma led to responses not only in the injected lesions, but also at distant sites, with improved durable response rate and an OS that approached, but did not meet statistical significance [19, 384, 383]. The phase III trial reported an ORR of 26% in the T-Vec arm and 6% in the control arm [383]. In an analogous study

also performed in patients with advanced melanoma, intralesional injection of another OV, Coxsackievirus A21 (CVA21), similarly led to responses in the virus-injected and distant tumours [20]. The use of OVs is known as oncolytic virotherapy and will be discussed in detail in the following section.

2.2 Oncolytic virotherapy

Oncolytic viruses are live, competent viruses that replicate selectively in tumour cells leading to the destruction of malignancies without causing excessive harm to normal tissues [648]. The selectivity of these viruses for tumours, termed oncotropism, is usually dependent on the expression of surface receptors that allow specific viral binding and entry, as well as, the permissiveness of the tumour cell viral replication. Genetic manipulation of the viral genome is one approach to improve the inherent therapeutic index of OVs by reducing their pathogenicity for non-malignant tissue but enhancing their capacity for targeted tumour killing [31]. In addition to this direct oncolytic activity, OVs are also very effective at inducing immune responses to themselves and to the infected tumour cells, stimulating both anti-viral and anti-tumoural immune responses. Taken together, OVs offer appealing advantages over conventional cancer therapy and are a promising new approach for the treatment of human cancer. The intention of this section of the review is to provide a brief history and highlight the mechanisms of oncolytic virotherapy, discuss the main challenges of oncolytic virotherapy; and lastly, summarise the key clinical oncolytic virotherapy experience to date.

2.2.1 A brief history of oncolytic virotherapy

The notion that naturally occurring viruses may be used as a therapeutic modality against cancer has existed for more than 100 years [389]. Since the mid-1900s, there have been sporadic reports of patients achieving tumour regression in association with concurrent viral infection, caused by agents such as hepatitis virus [461, 781], influenza [192], measles [86, 719], mumps virus [29], smallpox [301], and varicella [76]. One of the earliest cases of tumour regression associated with viral infection was in 1904, where a woman with leukaemia dramatically improved following an episode of presumed, but not clinically proven, influenza [192]. In a paper published in 1912, the Italian physician Nicola DePace presented findings that a female patient suffering from cervical carcinoma had undergone a complete spontaneous remission after receiving an inoculation of the live attenuated Pasteur-Roux rabies virus vaccine. She was receiving treatment after being bitten by a stray dog [181].

In another independent case, in 1951, a four year old boy was admitted into the Laboratory of Experimental Oncology, Switzerland, and was diagnosed with lymphatic leukaemia [76]. His white blood cell count was grossly elevated at 175,000 cells/mm³ [normal range

is between 4,300 - 10,800 cells/mm³], bone-marrow aspirate revealing that 98.5% of which were lymphocytes. He also had a greatly enlarged liver, spleen and cervical lymph nodes. During his stay in the hospital, he developed varicella. Onset of the disease led to a drastic drop in his white blood cell count, 7,500 cells/mm³ [falling within the normal range], and both his liver and spleen receded in size. However, the therapeutic phase was only transient as the patient succumbed to the disease 6 months later.

Observations of these spontaneous remission cases sparked the interest of using live viruses as a treatment for various cancers, and led to the initiation of experimental human trials [122, 330, 331, 339, 338]. In 1949, 21 patients suffering from Hodgkin's lymphoma received a total of 37 inoculations of serum and tissue extract containing infectious hepatitis viral agents [331]. Following treatment, thirteen displayed clinical evidence of the development of viral hepatitis infection, however only seven among them showed amelioration of Hodgkin's lymphoma. In a separate study in 1956, and perhaps one of the most notable human trials of oncolytic virotherapy, a group of clinicians at the National Cancer Institute, USA, led by Smith R.R. injected different serotypes of adenoidal-pharyngeal-conjunctival virus [currently known as adenovirus], into 40 patients suffering from cervical carcinoma [338]. Twenty-six (65%) of the forty patients responded to the viral treatment. A localised area of necrosis limited only to the carcinoma and formation of cavities in the central portion of the tumours were reported between the fourth and tenth day. However, despite continuous inoculation of the virus, rapid tumour regrowth in all patients soon followed after the initial tumour regression.

From studying these reports, we can ascertain the following: (i) naturally occurring replicating competent viruses are able to eradicate tumour cells under the right circumstances; (ii) successful tumour regression following viral infection was mostly observed in children with immune systems that were not fully mature or in adult patients who were immune compromised, suffering from lymphoma or leukemia; (iii) tumour remissions were generally temporary and transient; and (iv) these early trials were most often uncontrolled and used crude virus preparations with uncharacterised potencies. Consequently, clinicians abandoned the idea of using viruses as cancer therapies, partly due to the early success of chemotherapies and radiation therapies. It was only decades later, in the 1990s, with the advent of molecular biology and gene therapy that the concept of viruses as anti-neoplastic agents was rekindled. Genetic engineering enabled a broad range of potentially pathogenic

viruses to be manipulated for safety and targeting.

2.2.2 The ‘renewed’ oncolytic virus paradigm

Oncolytic virotherapy is the use of viruses that are naturally occurring or have been engineered to selectively replicate in tumours and kill malignant cells without harming healthy host cells. Traditionally, the aim of this approach was to harness the self-amplifying lytic replication cycle of OVs to cause direct oncolysis of cancerous cells, leading to regression of the bulk of the tumour [170, 759]. It has become increasingly clear that OVs also utilise other anticancer mechanisms to eradicate tumours. Oncolytic viruses such as vaccinia virus (VV) and vesicular stomatitis virus (VSV), for example, interfere with tumour vasculature, thereby compromising the growth of tumours [21]. However, the most relevant systemic mechanism of action of OVs is likely the virus-induced engagement of the immune system to recognise tumour antigens that were previously either unrecognised or had been subject to immune tolerance [141, 442, 597, 598]. Replicating virus within tumour cells can attract immune cells into the tumour environment, leading to cross-priming of TAAs for the activation of an effective anticancer immune responses. For instance, T-Vec showed a potent anti-melanoma immune response after local intratumoural injection in patients with metastatic malignant melanoma in phase II/III clinical trials [384].

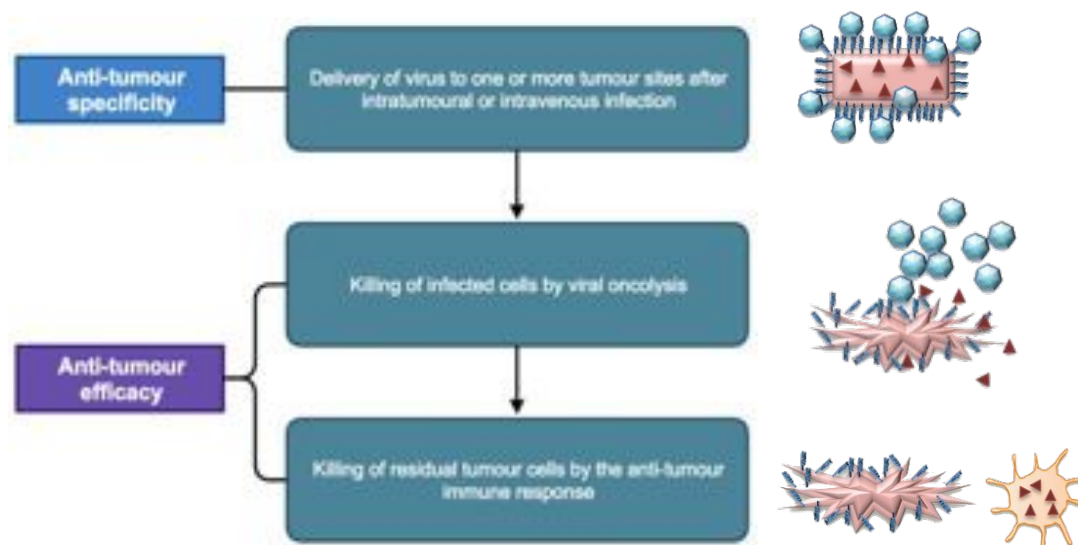


Figure 2.9: The oncolytic virotherapy paradigm. Oncolytic viruses selectively target tumour cells by exploiting differences between tumour and normal cells. It has become apparent that there are two driving forces behind OV anti-tumour efficacy. Aside from direct cytopathic effects and oncolysis of tumour cells, interactions of OV with the immune system can trigger systemic anti-tumour immunity through the release of tumour-associated antigens. In the diagram on the right, virus particles preferentially infects tumours cells expressing high levels of viral entry receptors. The OV replicates, rupturing the tumour cell, releasing progeny virions and TAAs into the tumour microenvironment. Dendritic cells process and present tumour antigens to mediate an anti-tumour specific immune response. Adapted from Russell, S. J., Peng, K.-W., and Bell, J. C. (2012). Oncolytic virotherapy. *Gene Therapy*, 30(7):658– 670 [648].

2.2.3 Mechanism of oncolytic virotherapy

Oncolytic virotherapy offers several appealing advantages over the use of conventional cancer therapies, including improved anti-tumour selectivity and efficacy. Many viruses show intrinsic selectivity for replication in cancer cells, and selectivity can be further augmented if required by using a range of strategies such as introducing essential virus genes that are under the transcriptional control of tumour-associated transcription factors. The potency of oncolytic virotherapy arises from the ability of the lytic virus to replicate itself within tumour cells before spreading to infect adjacent cells. The mechanism of oncolytic virotherapy can be divided into anti-tumour specificity and anti-tumour efficacy (Figure 2.10), which will be further discussed below.

2.2.3.1 Mechanism of anti-tumour specificity

Specificity for cancer cells at the cell-entry level or during the viral replication process is an essential trait of OVs to allow therapy without harming normal tissue. Over the centuries, viruses have developed many different mechanisms by which they can successfully infect

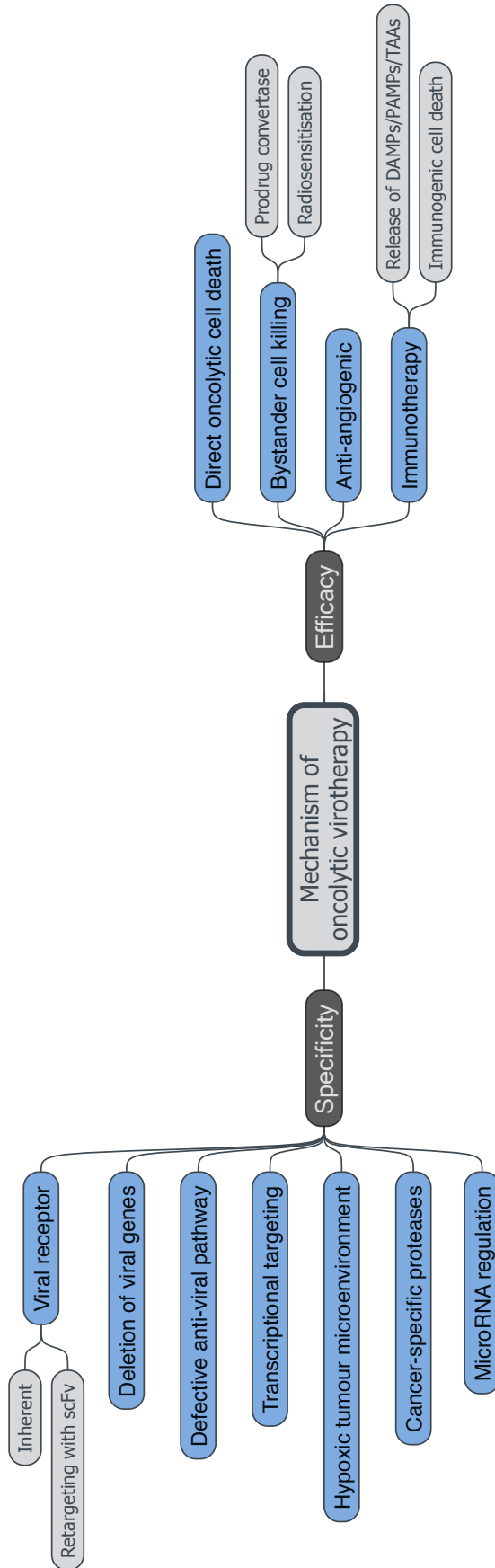


Figure 2.10: Mechanism of oncolytic virotherapy. Oncolytic viruses are replication-competent viruses that have the capacity to selectively infect tumour cells without harming normal host cells. Oncolytic viruses also have the ability to recognise malignant cells and kill these cells via a number of mechanisms, including direct lysis, expression of cytotoxic and anti-angiogenic proteins, as well as the induction of anti-tumoural immunity. Adapted from Russell, S. J. and Peng, K.-W. (2007). Viruses as anticancer drugs. *Trends in Pharmaceutical Sciences*, 28(7):326–333 [647].

a host cell to maximise their replication. The hallmark changes of malignancies such as self-sufficiency in growth signals, resistance to programmed cell death, immune evasion, limitless replicative potential, sustained angiogenic capacity, tissue invasion, and metastasis [299], bears a striking resemblance to the cellular changes caused by viral infection. Hence, it is not surprising that many viruses have taken advantage of this dynamic environment, preferentially replicating within tumour cells. Furthermore, the next generation of OVs have been genetically modified to improve tumour-tropism. Engineered viruses may be placed under the transcriptional control of tumour cell-specific promoters or under cell-specific translational control. Generally, seven main approaches have been employed by OVs to maintain their oncotropism.

2.2.3.1.1 Tumour-tropism mediated by viral receptors

Many of the cancer-specific mutations result in the over-expression of molecules on the cell surface, which are expressed at relatively lower levels, or absent, on corresponding normal cells. Shafren *et al.* have identified a collection of picornaviruses that have the inherent capacity to preferentially infect tumour cells based on their over-expression of virus cell-entry receptors. For example, echovirus type 1 (EV1) normally infects cells through the $\alpha_2\beta_1$ integrin, which is often over-expressed on ovarian [675] and gastric cancer cell lines [291]. Several serotypes of the Coxsackievirus species A (CVA) bind to intercellular adhesion molecule-1 (ICAM-1) or decay accelerating factor (DAF), two proteins that are often found in abundance on the surface of melanoma cells [33, 35, 670].

In a similar fashion, a recombinant type 1 poliovirus (PV1) with reduced neuropathogenicity targets the poliovirus receptor (PVR, CD155) often over-expressed on glioma cells [282, 555]. In contrast to wild-type measles virus (MV), the Edmonston vaccine lineage of measles virus (MV-Edm) enters cells more efficiently through the membrane cofactor protein (MCP; also known as CD46) [195], which coincidentally is expressed at high density on several cancer indications [14, 284, 579, 580]. More recently, the selectivity of Seneca Valley virus (SVV) is also believed to be via targeting of over-expressed cell-surface receptors, although the host receptor has not yet been identified [757]. The Sindbis virus is an OV that gains preferential access to tumour cells as a result of over-expression of the 67 kDa high affinity laminin receptor in ovarian cancers [741, 769].

A further extension of this feature is that OVs can be engineered to target antigens

or receptors expressed exclusively on the tumour cell surface. This approach is most suitable for larger sized viruses and thus, has been extensively validated using recombinant MV and adenoviruses [489, 539, 758]. Wild-type MV is an enveloped virus (100 - 200 nm in diameter) that is highly contagious, responsible for millions of deaths worldwide [799]. Measles-related mortality has been attributed mostly to severe immune suppression as a result of the virus binding to its primary receptor, signalling lymphocyte activation molecule (SLAM; also known as CD150) [185, 720], which is expressed on activated T and B cells, dendritic cells, and macrophages [150, 333, 514].

To engineer a safer oncolytic MV, the first step was to introduce specific mutations into the SLAM- or CD46-dependent fusion domains, ablating cognate receptor recognition, thus generating a ‘blind’ recombinant MV [761]. The next step was to redirect virion binding to tumour-associated receptors or ligands using single-chain fragment variable (scFv) antibodies. Specific scFv antibodies can be generated against any human proteins of interest and are relatively easy to produce [124]. The envelope of oncolytic MVs can then be tailored to bind to the protein of interest. Nakamura *et al.* were the first group to demonstrate oncolytic efficacy after completely ablating the productive interactions of the MV-Edm to its native receptor, retargeting the virus to CD38 and epidermal growth factor receptor (EGFR) using scFv antibodies [538]. These retargeted viruses replicated within and killed cancer cells that expressed CD38 and EGFR, but were unable to infect cells that expressed SLAM or CD46 [538]. In summary, receptor retargeting allows for more virulent viruses to be used in a safe manner, thus increasing its therapeutic index.

2.2.3.1.2 Attenuation of wild-type viruses through targeted deletion of viral genes

The most potent OVs are arguably wild-type viruses. However, these viruses may kill normal cells and cause dose-limiting toxicities. Ideally, OVs should be highly attenuated in normal cells, but retain their normal replicative abilities within cancer cells. Efforts have therefore been made to reduce the toxicity of most OVs by the deletion of key viral genes whose function can be reconstituted within cancer cells only. The leading example highlighting this mechanism of tumour-tropism is the oncolytic adenovirus *dl1520/ONYX-015*. Developed by Onyx Pharmaceuticals, ONYX-015 is a mutant adenovirus that lacks the gene *E1B-55K* [313, 314, 392]. Normally, the viral protein E1B55K binds and inactivates the tumour suppressor p53 to allow viral replication to take place [380, 816]. Another key

fact is that genetic studies have shown that the p53 tumour suppressor pathway is inactivated in nearly all human tumours, highlighting the potential of ONYX-015 in treating p53-deficient tumours [133, 676].

Taken together, Bischoff *et al.* published the first paper in which they employed a conditionally replicative adenovirus (CRAd) deficient in the *E1B-55K* early gene to accomplish tumour-specific oncolysis of p53-deficient human tumour cells [79]. The targeted deletion of *E1B-55K* resulted in impeded adenoviral replication in cells with normal p53 function but yielded a virus that was capable of destroying tumour cells carrying mutations of the p53 tumour suppressor [79, 430]. Other adenoviral genes that have been targeted include the introduction of specific mutations in the *E1A* gene to block its binding to the Rb protein [243, 362, 788]. The E1B protein has been shown to bind to p53 to help immortalise cells such that adenovirus replication can continue. Furthermore, Kim *et al.* have shown that a deletion in the Rb-binding sites of *E1A* together with E1B 19kDa and E1B 55kDa deletions generated a novel Ad that was more cancer-cell-specific than the single-mutant viruses [394].

This approach has been extended to other OV's such as HSV, VV and more recently poliovirus (PV). The first genetically attenuated HSV type 1 (HSV1) mutant (also known as *dlsptk*) contained a deletion of the thymidine kinase (*TK*) gene and was described for the treatment of malignant gliomas [486]. The TK deficient HSV1 mutant effectively lysed glioma cell lines *in vitro* and prolonged survival of mice bearing intracranial (i.c.) tumours [486]. However, the *TK* gene deletion rendered *dlsptk* resistant to anti-herpetic drugs, such as acyclovir and ganciclovir, thus, preventing the advancement of this virus into human trials due to safety concerns [121, 386]. Since then, numerous HSV1 genes, including γ 34.5 [378, 516, 611], ICP6 [5, 269, 515], ICP47 [265], UL24 [67, 504], UL39 [516, 577], and US3 [382], have been deleted/mutated to generate oncolytic prototypes. Furthermore, several of these oncolytic HSV1 mutants (G207, 1716, OncoVex^{GM-CSF}, NV1020, HF10, G47 Δ) are being clinically tested in a range of cancer indications [385, 454, 756]. In a similar way, McCart *et al.* was successful in further improving the specificity of VV for replication in tumours by mutating the vaccinia growth factor (*VGF*) gene in parallel with the *TK* gene [492].

In addition to the three OV's described above, there has been recent interest in the use

of a recombinant PV for the treatment of glioma [263, 262]. Gromeier *et al.* demonstrated that the neuropathogenicity of PV could be attenuated by mutations within the internal ribosomal entry site (IRES) sequence located in the 5' untranslated region of its RNA genome [279]. Remarkably, substitution of the PV1 (Mahoney strain) IRES sequence with the IRES sequence from human rhinovirus type 2 (HRV2) severely attenuated the virus in normal cells while maintaining its ability to replicate in glioma cells [279]. This mutant, referred to as PV1(RIPO), was demonstrated to be safe for intracranial administration in mice and *Cynomolgus* monkeys [280].

Recombinants of PV such as PV1(RIPO) and PV3(RIPO) (a chimera of wild-type Leon/37 PV3 carrying the HRV2 IRES) are naturally tropic for glioblastoma multiforme (GBM) due to expression of the PVR CD155 on these tumours [279, 282, 507]. Subsequently, these chimeric phenotypes have led to intense efforts to develop a derivative of PV1(RIPO), called PVS-RIPO (a virus in which the IRES of the Sabin 1 vaccine virus has been exchanged with the HRV2 IRES, not the wild-type PV1 Mahoney strain) [555]. The virus PVS-RIPO was shown to be genetically stable after *in vivo* passage in GBM xenografts while still retaining excellent cytotoxic properties in malignant cells [191]. Furthermore, PVS-RIPO is incapable of causing poliomyelitis or encephalitis in non-human primates even after high-dose intracerebral inoculation, alleviating concerns regarding its phenotypic stability in the context of its replication in malignant glioma [281]. Taken together, these findings validate the continuation of PVS-RIPO research into clinical trials for patients with recurrent GBM. In summary, recombinant OVs have demonstrated marked attenuation *in vivo* while still preserving the ability to replicate efficiently in the tumour environment.

2.2.3.1.3 Targeting defective antiviral response pathways

For viruses which utilise receptors that are also abundant on normal cells, the mechanisms that govern the natural preferential replication in cancer cells are generally intracellular. An important intracellular pathway frequently altered during the transformation of a normal cell to a malignant cell is the IFN-mediated response pathway [75, 448, 718]. Interferons have a diverse range of biological functions; they inhibit cell proliferation by causing cell cycle arrest at G₁ [27, 655], induce apoptosis [137, 695], and promote the maturation of various lymphocytes [214, 228]. As these activities oppose the establishment of uncontrolled growth, it is not surprising to find that this pathway is often dysfunctional in cancer cells

[75, 614, 718]. Interferon is also a key mediator of a host's antiviral response and thus, tumour cells which acquire mutations allowing them to escape the IFN-mediated growth control program, will simultaneously compromise their antiviral response. This is the major mechanism of selectivity for Newcastle disease virus (NDV) [418], and VSV, [708, 709] which are both exquisitely sensitive to the antiviral effects of IFN.

Despite NDV [617] and mumps virus [534] using sialic acid as their receptor and alphaviruses using heparan sulphate or ICAM-1, all of which are abundantly expressed on many normal cells, these viruses show high cancer cell selectivity. In these cases their preference to cancer cells stems from the fact that many, if not most, tumour cells display an impaired antiviral response due to failure of critical components of the IFN response system [708]. In fact, one strategy to enhance the tumour cell specificity of OVs is to mutate them to induce a more potent IFN response. While this reduces the replication of such viruses in normal cells, cancer cells remain permissive to the viruses because they are unable to launch an antiviral response due to deficient IFN signalling.

2.2.3.1.4 Transcriptional targeting

An alternative approach to create tumour-selective OVs is through the use of tumour-specific gene promoters to drive the expression of viral genes essential for viral replication. OVs derived from this method have limited replication capabilities in normal cells, but can replicate unperturbed in malignant cells. Reprogramming the replication function of OVs is better suited to DNA viruses with large genome-packaging capacities, and thus, has been predominantly explored for adenoviruses [143, 406, 489]. There are two types of tumour-specific gene promoters. The first type of promoters are those that are very active in many different tumour types (tissue-specific), with little or no activity in normal cells. For instance, the promoter of human telomerase reverse transcriptase (hTERT) [397, 424] and survivin [811, 812] are highly active in most tumour and immortal cell lines, but inactive in normal somatic cell types. Both the hTERT [336, 794] and the human survivin gene promoter [375, 827] are often utilised to control the expression of several essential early genes (*E1A*, *E1B* and *E4*) in oncolytic adenoviruses, displaying high selectivity and therapeutic potential in pre-clinical models. The second type of promoters that are in use are exclusive for particular tumour types (tumour-specific), such as alphafetoprotein for hepatocellular carcinoma (HCC) [292, 590], IAI.3B for ovarian cancer [294], estrogen-response element for breast cancer [319], musashi-1 for glioma [377], and prostate-specific

antigen (PSA) for prostate cancer [631].

In 1997, Rodriguez *et al.* were the first group to publish the use of the PSA promoter to restrict adenovirus replication [631]. They placed the essential adenoviral gene *E1A* under the transcriptional control of the PSA promoter. Experiments in cell culture systems demonstrated selective *E1A* expression and adenovirus replication only in PSA-positive LNCaP prostate cancer cells, but not in the PSA-negative DU145 cancer cells. Furthermore, Rodriguez *et al.* were also successful in showing the therapeutic effects of the PSA promoter-driven adenovirus in LNCaP tumour xenografts [631]. In the same year, Miyataken *et al.* retargeted the replication of HSV1 to albumin-expressing liver cells using the albumin promoter [518]. Since then, several other groups have published work on HSV1 retargeting using other promoters including carcinoembryonic antigen (CEA) [619], musashi-1 [377, 376], and nestin [374]. An extensive review on the various promoters and viral genes exploited for reprogramming virus replication for oncolysis has been published by Dorer & Nettelbeck [194].

2.2.3.1.5 Targeting the hypoxic tumour microenvironment

As tumours grow rapidly at an uncontrolled rate, tumour cells must adapt to the hypoxic microenvironment by stimulating angiogenesis. The tumour selectivity of OV's might be further improved by the incorporation of hypoxia-responsive elements into tumour-specific promoters to exploit the relatively hypoxic conditions within tumours. The first study harnessing the hypoxic environment for tumour selectivity was an oncolytic adenovirus that incorporated an *E1A* gene controlled by a minimal dual-specificity promoter that responded to hypoxia as well as estrogens for the treatment of breast cancer [318]. Subsequent studies made specific modifications such that the viruses were totally dependent on hypoxia-inducible factor (HIF) for viral replication [142, 596]. A dual regulated oncolytic Ad CNHK500 was developed where the *E1B* gene was controlled by a hypoxia responsive promoter and the *E1A* gene was controlled by a hTERT promoter. *In vitro*, this virus showed improved specificity and i.v. delivery of the virus demonstrated significant anti-tumour efficacy in a xenograft model of HCC [824].

In addition, Connor and colleagues have shown that wild-type VSV is capable of replication under hypoxic conditions, demonstrating that VSV had an inherent capacity for infecting and killing hypoxic cancer cells [154]. In a similar fashion, Sgubin *et al.* showed

for the first time that the HSV G47 Δ could replicate and kill hypoxic human glioma stem cells and that i.t. injection of the OV in orthotopic human glioma stem cell xenografts led to successful infection and replication in hypoxic areas of the tumours *in vivo* [667]. More recently, Gupta-Saraf *et al.* found that the oncolytic mammalian orthoreovirus (MRV) could infect prostate tumours cells under hypoxic conditions and these cells showed reduced levels of HIF-1a, the master transcriptional regulator of hypoxia [288]. Together, these findings provide evidence of OVs being a viable therapeutic option for selectively targeting hypoxic cells.

2.2.3.1.6 Activation through cancer-specific proteases in the tumour microenvironment

The replication and pathogenesis of almost every virus is dependent on interactions with host cell proteases. Enveloped viruses, such as paramyxoviruses, influenza and HIV-1, require protease cleavage of viral glycoproteins for productive cell entry following receptor recognition. Interestingly, many cancer cells express proteases that can be exploited to enhance viral specificity. Desirable protease targets for OVs that require activation are those that are expressed preferentially and/or at high levels by malignant cells. Notably, matrix metalloproteinases (MMPs) are endopeptidases that are over-expressed in nearly every malignancy [205]. For example, the protease cleavage specificity of the fusion protein from MV and Sendai virus (SeV) was changed from being dependent on the ubiquitous protease furin or the respiratory airway tryptase Clara, respectively, to being dependent on MMPs [400, 697]. Recombinant MV that expressed the modified fusion protein (MV-MMP) was unable to propagate or produce cytopathic effects (CPE) unless it was added to cells that expressed MMPs [697]. In mice, MV-MMP retained full oncolytic activity when inoculated into MMP-positive s.c. cancers, but unlike wild-type MV, MV-MMP did not infect and kill susceptible mice after i.c. inoculation, which proved the safety of the virus had been enhanced [697].

More recently, this approach has been tested in adenovirus, with the replication-competent MMP-dependent adenovirus (Ad-MMP) showing increased anti-tumour activity compared to the wild-type adenovirus in an orthotopic model of pancreatic cancer [372]. Moreover, no signs of pancreatic toxicity were detected. Another protease that is commonly upregulated with other MMPs in the tumour microenvironment is the urokinase-type plasminogen activator (uPA) [16, 17]. Several groups in Japan have developed and optimised

the design of a protease-specific oncolytic recombinant SeV that demonstrates catalytic activity against MMPs and uPAs [399, 400, 526]. These new vectors showed dramatically enhanced anti-tumour activity *in vitro* and *in vivo*. In summary, this retargeting strategy could potentially be adopted by large enveloped viruses such as HSV and NDV that are currently being trialled clinically to further enhance tumour selectivity.

2.2.3.1.7 MicroRNA regulated tropism

Given the potential off-target effects of transcriptional control and the significant risk of reversion to wild-type, other tropism-modifying strategies are of interest. A relatively new mechanism by which OV tumour-cell selectivity may be regulated is through viral encoded targets for microRNA (miRNA). miRNAs are short (~22 nt) regulatory RNAs that act post-transcriptionally to influence cell proliferation, cell differentiation, apoptosis and tumourigenesis. Through complementary base pairing with short sequences, usually located within the 3' untranslated region (UTR) in cellular mRNA, miRNAs act to suppress mRNA translation, and depending on the degree of complementarity, completely degrade mRNA.

Currently, this targeting strategy has been shown to be successful in a broad range of OVs, including PV [51], HSV [439], VSV [203, 391], VV [320], MV [44, 429], Semliki Forest virus (SFV) [818] and adenovirus serotype 5 (Ad5) [126, 817]. For instance, Edge *et al.* developed a tumour-specific VSV by inserting three copies of the miRNA-let-7 target elements in the 3' UTR of the VSV RNA genome [203]. Similarly, by inserting four copies of muscle-specific miRNA target elements into the CVA21 genome, Kelly *et al.* prevented myositis from developing in severe combined immunodeficient (SCID) mice infected with miRNA-targeted CVA21 without compromising the potency of the virus [390]. Taken together, these reports show that miRNA-mediated attenuation of OVs is a feasible and promising strategy for generating safer oncolytic virotherapy agents.

2.2.3.2 Mechanisms of anti-tumour efficacy

Several mechanisms used by OVs to exert their anti-tumour effects have been proposed. The first mechanism describes the capability of viruses to directly lyse infected cells as a result of viral replication. The second strategy describes cell death in uninfected cells through the anti-angiogenesis and anti-vasculature properties of certain OVs, a mechanism termed 'bystander cell killing'. Lastly, is the stimulation of the host's immune response to

recognise and engage tumour antigens that were previously either unrecognised or subject to immune tolerance.

2.2.3.2.1 Direct oncolytic cell death

Many naturally occurring OV_s have a preferential tropism for malignant cells while others can be genetically engineered to change their cellular tropism toward cancer [648]. The altered tumour microenvironment provides favourable conditions for OV_s to replicate effectively, leading to direct oncolysis of the infected cells. The life cycle of viruses consists of three stages; infection, replication, and finally, release. In a suitable environment, viral replication cycle is continuously repeated, creating infectious viral progeny which can infect adjacent tumour cells and destroy them through replication. This feature of replication-competent viruses provides an exponential amplification of the initial viral dose, which continues until the complete destruction of susceptible cells or inhibition by the immune system. In addition to viruses causing direct oncolysis, some also exert cytotoxicity via production of proteins that induce necrotic or apoptotic cellular destruction. For instance, adenoviruses express E3-11.6K death protein [731, 732, 733] and E4ORF4 [681] late in the cell cycle triggering cell death and viral release through cell lysis.

2.2.3.2.2 Induction of ‘bystander cell killing’

OV_s must infect and kill tumour cells to achieve efficacy, and despite *in situ* replication, accessing and infecting all malignant cells within a tumour remains a major clinical challenge, one that is difficult to achieve. Therefore, the therapeutic efficacy of OV_s can be enhanced using strategies that induce ‘bystander cell killing’ in uninfected cells, whereby a protein sensitises both the infected and surrounding uninfected cells to subsequent combination therapies or immune destruction [124, 511]. Prodrug convertases that are expressed from OV_s can enhance the efficacy of chemotherapy by activating prodrugs and ion transport proteins that can promote radiation poisoning of tumours owing to the concentration of radioisotopes. The common goal of these strategies is to reduce systemic toxicity by giving lower doses of minimally toxic chemotherapeutic drugs that are only converted to highly toxic metabolites within the tumour microenvironment.

Prodrug convertases have been extensively studied for the TK, the cytosine deaminase (CD) and, purine nucleoside phosphorylase (PNP) systems. Briefly, the HSV TK phosphorylates ganciclovir to generate ganciclovir triphosphate [508], CD converts chemothera-

peutic 5-fluorocytosine (5-FC) to 5-fluorouracil (5-FU) [337], and PNP converts fludarabine phosphate into 2-fluoroadenine [393]. The CD and PNP systems have been engineered into numerous OV_s including adenovirus [186], MV [746], VV [236], and VSV [436]. The most clinically advanced CD-virus is a replication-competent retrovirus known as vocimagene amiretrorepvec (Toca 511) [581]. Toca 511 is currently being tested in combination with 5-FC in phase I and II clinical trials using i.t. administration in patients with grade 4 GBM (NCT01156584).

In addition, OV_s have also been used induce ‘bystander cell killing’ through radiosensitisation. The normal physiological function of the human sodium-iodide symporter (NIS) is to transport iodide ions into cells [408]. When NIS is expressed from the genome of an OV, infected cells can concentrate radioactive iodide intracellularly, inducing radiation poisoning within the tumour microenvironment [511]. The NIS transgene system has undergone extensive preclinical development in numerous virus families, and radiovirotherapy has consistently achieved synergistic tumour destruction with MV expressing NIS (MV-NIS). Preclinical evaluation of MV-NIS together with radiotherapy has shown success in HCC [83], ovarian carcinoma [306], multiple myeloma [190, 535] and mesothelioma [438]. Phase I clinical trials using MV-NIS have been initiated for ovarian cancer (NCT00408590), multiple myeloma (NCT00450814), mesothelioma (NCT01503177), and head and neck cancer (NCT01846091).

2.2.3.2.3 Innate anti-angiogenic properties of OV_s

The anti-vascular properties of OV_s have been the topic of multiple preclinical and clinical studies. Blood supply within a tumour drives progression and ultimately allows for metastasis. OV_s can infect both developing and established tumour vasculature without harming normal vasculature. Current evidence suggests that there are three inherent mechanism by which OV_s affect tumour vasculature: (i) direct infection of tumour endothelial cells; (ii) induction of virus-mediated immune responses that cause cellular accumulation and decreased tumour perfusion; and (iii) the expression of viral proteins with anti-angiogenic properties [21].

To date, the only OV that has demonstrated anti-vascular properties in humans is the VV expressing GM-CSF, pexastimogene devacirepvec (JX-594). In a phase I/II dose-escalation clinical trial, JX-594 was administered i.t. at 3-week intervals to patients with

primary HCC [456, 574]. Liu *et al.* reported a 43% decrease in tumour perfusion 6 days post-treatment and a significant reduction in circulating vascular endothelial growth factors (VEGFs) [456]. Besides that, in a preclinical three-dimensional reconstruction of VSV infected tumours, Breitbach *et al.* showed that the replication of VSV in tumour vasculature initiated an inflammatory reaction, leading to the recruitment of neutrophils and other immune cells to the tumour bed [101]. Recruitment of these immune cells formed microclots within tumour blood vessels, resulting in loss of perfusion and extensive tumour cell death throughout the core of the tumour [101]. Not all engineered viruses however are anti-angiogenic as studies have shown that the wild-type E1A protein expressed during for the viral replication of adenoviruses, interacts with angiogenic cellular protein p300 to downregulate VEGF [650, 815]. Saito *et al.* demonstrated that cancer cells infected with a mutant adenovirus lacking the p300 binding site in E1A induced a higher level of VEGF expression and that only the wild-type adenovirus could significantly inhibit tumour angiogenesis *in vivo* [650]. This finding may have implications for engineered oncolytic adenoviruses that may be E1A deleted.

2.2.3.2.4 Oncolytic immunotherapy

The traditional paradigm of oncolytic virotherapy is that OVs cause direct lysis of all the resident malignant cells, leading to the regression of the bulk of the tumour [647]. However, it has become increasingly clear that OVs have the additional potential to stimulate both innate and adaptive immune responses against tumours. During an OV infection, TAAs released as a result of direct oncolysis are cross-presented to T cells by endogenous APCs [521]. By recruiting immune cells through the cross-presentation of TAAs, OVs indirectly drive anti-tumour immunity, leading to a more potent anticancer immune response [505, 803]. A number of preclinical studies using HSV [805], reovirus [599] and VSV [187] have successfully demonstrated that anti-tumour immunity plays an important role in the overall efficacy of oncolytic virotherapy.

There is also emerging evidence that OVs are capable of mounting a favourable ‘inflammatory storm’ that redirects the immune response to the normally immunosuppressive tumour microenvironment [505]. Among the many different types of cell death mediated by OVs, some are immunogenic, characterised by the exposure of crucial damage-associated DAMPs, such as calreticulin, heat-shock proteins (HSP) to the cell surface, and/or the release of high-mobility group protein B1 (HMGB1), uric acid, and TAAs all of which ac-

tivate anti-tumour immunity [54, 287, 442]. Additionally, viruses encode structural motifs known as pathogen-associated molecular patterns (PAMPs), that serve as ‘danger’ signals to the host indicating the presence of virus that then triggers host defences [60, 287, 803]. A seminal review by Guo *et al.* provides a discussion on the multiple forms of immunogenic cell death (ICD) induced by various OVs including adenovirus, Coxsackievirus B3 (CVB3), HSV, MV, NDV, parvovirus and VV, and their potential effects on anti-tumour immunity [287]. In general, the inflammatory cascade and ICD induced by OV infection of tumours makes OVs powerful inducers of anti-tumour immunity [54, 442].

Furthermore, the immunotherapeutic potential of OVs can be further enhanced by ‘arming’ OVs with therapeutic transgenes. Some of the most clinically promising OVs are T-Vec and Pexa-Vec, both of which are armed with the human *GM-CSF* gene. Kaufman *et al.* showed that direct injection of melanoma nodules with T-Vec induced local and systemic antigen-specific T-cell responses and decreased CD4⁺FoxP3⁺ regulatory T cells (Treg), CD8⁺FoxP3⁺ suppressor T cells, and myeloid-derived suppressive cells (MDSC) in patients exhibiting therapeutic responses [384]. On the other hand, inflammatory cell infiltration and anti-tumour antibodies mediating complement-dependent cytotoxicity (CDC) were induced after Pexa-Vec treatment of patients with liver tumours [316, 396]. These OVs demonstrated anti-tumour responses in both virus-injected and non-virus-injected lesions. In summary, present studies suggest that the most effective OV treatment regimens will be those that combine potent viral oncolysis with an effective and long-lasting anti-tumour immune response.

2.2.4 Current clinical status of oncolytic virotherapy in melanoma

There has been interest in using viruses to treat cancer for over a century. Partial and even complete cancer remissions were observed in early clinical trials. However, ethical concerns regarding several trials, complications resulting from viral shedding, quality control and production issues of viruses soon led to the decline in enthusiasm for this treatment avenue [389, 426]. The resurgence of oncolytic virotherapy can be attributed to the advent of recombinant DNA technology, strict governance from regulatory bodies, and improved manufacturing standards. Current clinical efforts are driven by significant preclinical results and have focused on the safety of using replication-competent viruses [298]. Recently published clinical trials of oncolytic virotherapy have demonstrated the safety of several viruses after localised and systemic administration [455]. Furthermore, several OVs from

five families have progressed to efficacy trials for the treatment of advanced melanoma (Table 2.5).

2.2.4.1 Adenovirus

Serotype 5 adenoviruses are the most common strains used in adenoviral virotherapy for melanoma. The virus has attracted considerable attention as an anticancer agent because it can be readily engineered and exhibits multiple tumour-targeting mechanisms for enhanced anti-tumour activities [489]. One example is the replication selective Ad-DM-E2F-K- Δ 24RGD (also known as ICOVIR-5). ICOVIR-5 combines five different genetic modifications: (i) deletion of Δ 24; (ii) insertion of E2F-1 promoter; (iii) DM-1 insulator; (iv) the Kozak; and (v) RGD sequence, to achieve a selective and potent anti-tumour effect [120]. Dose response toxicological and efficacy studies performed in pre-clinical mouse models demonstrate the potential of this virus for the treatment of disseminated cancer [120]. ICOVIR-5 dosed at 1×10^{11} virus particles/mouse was able to stop the growth of melanoma xenografts from day 20 after administration. Investigators are currently evaluating the safety of a single endovenous infusion of ICOVIR-5 in locally advanced or metastatic melanoma patients (NCT01864759).

Another oncolytic Ad5, Ad5/3-D24-GM-CSF (also known as ONCOS-102) features a chimeric capsid for enhanced gene delivery to cancer cells, a 24 bp deletion in the RB binding site of E1A for cancer cell restricted replication, and is armed with GM-CSF [412]. A total of 21 patients with advanced solid tumours refractory to standard therapies, including 3 melanoma patients were treated intratumourally and intravenously with ONCOS-102 (up to 3×10^{11} virus particles), combined with low-dose metronomic cyclophosphamide (CPA; 50 mg/day orally) to reduce Tregs [412]. Evidence of biological activity of the virus was seen in 13/21 patients with no severe adverse events documented. Despite these promising clinical results, progression of adenovirus for the treatment of melanoma appears to have halted at phase I clinical trials.

2.2.4.2 Coxsackievirus

The only Coxsackievirus under clinical development is the naturally occurring CVA21 (also known as CAVATAKTM). The phase I safety study involved two doses of CVA21 (up to 1×10^9 TCID₅₀/dose) injected intratumourally into a single cutaneous melanoma deposit of 9 stage IV melanoma patients [668]. The maximum tolerated dose (MTD) of

CVA21 was not reached and no significant toxicities were reported. Following the success of the phase I trial, a phase II trial (CALM; NCT01227551) evaluating the intratumoural efficacy of CVA21 was conducted, recruiting 57 patients with unresectable stage IIIC and stage IV melanoma [20]. Patients received up to 3×10^8 TCID₅₀ of CVA21 on days 1, 3, 5, and 8 and then every three weeks for a further 6 injections. The study achieved an immune-related progression-free survival (irPFS) of 38.6% (22/57) and an ORR of 28.1% (16/57). A major finding of this study was that tumour responses were observed in injected lesions, non-injected non-visceral lesions and in distant non-injected visceral lesions in the absence of circulating infectious CVA21, strongly suggesting the generation of a potent anti-tumour immune response. Currently, the safety and efficacy of CVA21 delivered systemically in patients with solid tumours, including melanoma, lung, prostate, and bladder cancers, in combination with cytotoxic chemotherapy are being evaluated (NCT02043665). Furthermore, combination studies with ipilimumab in patients with stage IIIC and stage IV melanoma are underway (NCT02307149).

2.2.4.3 Herpes simplex virus

There are currently four strains of HSV that have progressed to clinical evaluation for the treatment of melanoma. HF10 is a spontaneously occurring mutant HSV1 (loss of UL56 expression) [748]. Demonstration of pre-clinical efficacy using immunocompetent mouse models led to the phase I clinical investigation of intratumoural HF10 injections (up to 1×10^7 TCID₅₀/dose) in patients with refractory and superficial cancers including melanoma [220, 775]. The treatment regimen was well tolerated with mild-drug related adverse events. Importantly, one patient formed ulcers at both injected and non-injected lesions after a single intralesional injection without affecting normal tissue. Following the success of this trial, a phase II trial evaluating the combination effects of HF10 with ipilimumab is now underway (NCT02272855).

The most clinically advanced HSV is T-Vec, generated from the HSV JS-1 strain. The OV was attenuated by functional deletion of the *ICP34.5* and *ICP47* viral genes, and incorporates the GM-CSF transgene to enhance the host's immune response [450, 383]. In a phase I study, intralesional administration of T-Vec was well tolerated in 26 patients, but no objective responses were observed [334]. However, follow-up biopsies in several patients showed extensive necrosis, T cell infiltration, presence of replicating virus, and the expression of GM-CSF within the tumour [334]. In a subsequent phase II study, 50

patients with unresectable stage IIIC/IV melanoma administered with intralesional T-Vec achieved a ORR of 26% (8CR, 5PR) [665]. Finally, a randomised phase III study comparing intralesional T-Vec to s.c. GM-CSF demonstrated an improvement in durable response rate (16% *vs* 2%) and a trend toward improved OS favouring the T-Vec arm [383]. Currently, T-Vec has completed its international phase III trial and is awaiting regulatory approval.

Similar to T-Vec, key features of the OV HSV^{GM-CSF} (also known as OrienX010) include deletion of both copies of *ICP34.5* and *ICP47* viral genes, insertion of the GM-CSF transgene, and the interruption of the *ICP6* gene [452]. The safety of OrienX010 is currently being evaluated in a phase I trial (NCT01935453). The last HSV strain that is under clinical evaluation for the treatment of melanoma is HSV1716 (also known as Seprehvir[®]), derived from the HSV1(17+) strain with both copies of γ -34.5 genes deleted [569]. The safety and toxicity of HSV1716 administration was first addressed in patients with GBM and anaplastic astrocytoma [305]. This study showed that HSV1716 was well tolerated and no adverse events were observed at high doses of up to 1×10^5 PFU. A pilot study conducted by MacKie *et al.* presented clinical evidence of HSV1716 replication confined to melanoma cells, resulting in the flattening of previously palpable tumour nodules and tumour necrosis of injected lesions [473]. HSV1716 has been applied to treat non-central nervous system solid tumours and malignant melanoma [159, 473].

2.2.4.4 Reovirus

Reovirus serotype-3 Dearing strain has been developed by Oncolytics Biotech[®] under the trade name Reolysin[®]. Reolysin[®] is a wild-type, genetically unaltered virus, and has been tested in numerous clinical trials via both intratumoural injections and intravenous administration, alone and in combination with other anticancer modalities. None of the studies have identified any serious toxicities due to virus treatment [130]. These trials have enrolled patients with haematological malignancies (multiple myeloma) and solid tumours including pancreatic cancer, colorectal cancer, metastatic melanoma, squamous cell carcinoma of the head and neck, non-small cell lung cancer (NSCLC), prostate cancer and malignant gliomas [130].

Recently, Oncolytics Biotech[®] have completed two phase II metastatic melanoma trials. In the first trial, 21 patients received Reolysin[®] (3×10^{10} TCID₅₀) on days 1 - 5 of a 4-week cycle, administered intravenously [246]. Treatment was well tolerated without

any dose reductions needing to be implemented. No disease responses meeting PR or CR criteria were observed, although extensive tumour necrosis (75 - 90%) was documented in the surgical specimen of a patient who had metastatic cutaneous lesions surgically removed. Unfortunately, the trial did not meet the defined efficacy endpoint in order to proceed to the second stage of accrual and further enrolment was closed. On the other hand, preliminary results from the phase II trial of intravenous reovirus (3×10^{10} TCID₅₀, days 1 - 5 of a 3-week cycle) with concurrent paclitaxel (200 mg/m², day 1 of a 3-week cycle) and carboplatin (6 AUC mg/mL, day 1 of a 3-week cycle) chemotherapy has met the first stage primary endpoint (NCT00984464) [564]. The first stage endpoint was met after 3 of 14 patients exhibited a PR, and an additional seven patients had SD for a disease control rate of 71.5%. Given the recent changes in the standard of care for the treatment of metastatic melanoma, investigators are evaluating Reolysin® in combination with B-RAF and PD-1 inhibitors before resuming the second stage of the trial [564].

2.2.4.5 Vaccinia virus

As previously mentioned, oncolytic VV preferentially infects and replicates in tumour cells with a defective IFN pathway. Recombinant VV in which the *VGF* and *TK* genes have been deleted acquire improved tumour selectivity. In humans, clinical results have shown that oncolytic VV was only detected in tumour tissues but not normal tissue, demonstrating its tumour selectivity [100, 316, 340]. In addition, recombinant VVs expressing cytokines or other host immunomodulating genes such as human GM-CSF, anti-angiogenic agents, and extracellular matrix genes have also shown enhanced tumour selectivity and oncolytic effects. For example, Jennerex Biotherapeutics is developing a number of recombinant vaccinia strains including JX-594, JX-929 and JX-963; of these JX-594 is furthest along the clinical pipeline. JX-594 (Wyeth strain) is a replication-competent *TK* gene inactivated oncolytic VV expressing human GM-CSF and *lacZ* transgenes [571]. Early clinical reports of JX-594 began in 1999, with seven melanoma patients receiving escalating doses of the virus (up to 8×10^7 PFU) administered intratumourally [488]. No MTD was documented and regressions of small superficial tumours were reported. In order to confirm and expand upon the early preliminary findings from this trial, Hwang *et al.* performed a low-dose mechanism-of-action-driven clinical trial of JX-594 in patients with metastatic melanoma injected weekly for up to nine total doses (10^8 PFU per dose) [340]. JX-594 was detected in non-injected tumour sites, indicating successful infection at the primary site, spread of JX-594 to distant sites of disease and subsequent productive infection at the

non-injected site.

To further enhance the anti-tumour efficacy of VVs, oncolytic VVs have been genetically engineered to express a variety of transgenes encoding antibodies, cytokines, chemokines, prodrug-converting enzymes, and anti-angiogenic agents. One such oncolytic VV, vvDD-CDSR, is currently under investigation in a phase I clinical trial for a range of solid tumours including melanoma (NCT00574977). vvDD-CDSR is a highly tumour-selective vaccinia virus with an engineered double deletion of the *TK* and *VGF* genes; and incorporation of both CD and somatostatin receptor (SR) genes. Cytosine deaminase converts administered prodrug 5-FC to the antimetabolite 5-FU in cells infected with this virus, leading to effective tumour cytotoxicity, while SR allows anatomical localisation of the virus through the use of ^{111}In -pentetreotide [131, 491]. Finally, another oncolytic VV, GL-ONC1 (GLV-1h68) was constructed by inserting three expression cassettes (encoding *Renilla* luciferase–*Aequorea* green fluorescent protein fusion [GFP], β -galactosidase, and β -glucuronidase) into the F14.5L, J2R (encoding TK) and A56R (encoding haemagglutinin) loci of the viral genome, respectively [825]. Currently, a phase I trial of intratumoural GL-ONC1 in patients with solid tumours including melanoma is ongoing (NCT00794131).

Table 2.5: The most clinically advanced OVs for the treatment of melanoma.

Virus Name of agent	Specification	Combined with	Viral route of delivery	Phase	Status	Sponsor	Clinical trial identifier
Adenovirus							
Ad-DM-E2F-K- Δ 24RGD (ICOVIR-5)	<ul style="list-style-type: none"> • Expression of the E1a-Δ24 • <i>E1a</i> gene under E2F-1 promoter that has been insulated with the myotonic dystrophy locus insulator DM-1 • Kozak sequence inserted before <i>E1a</i> gene • RGD modification of the HI loop 	Sole agent	i.t.	I	Recruiting	Institut Català d'Oncologia	NCT01864759
Ad5/3-D24-GM-CSF (ONCOS-102)	<ul style="list-style-type: none"> • Chimeric 5/3 fibre knob • 24-bp deletion in E1A • GM-CSF inserted in the E3 region 	Combined with low-dose CPA	i.t. + i.v.	I	Completed	Oncos Therapeutics	NCT01598129
Coxsackievirus							
CAVATAK™	<ul style="list-style-type: none"> • Wild-type CVA21, Kuykendall strain 	Sole agent	i.t.	I	Completed	Viralytics	NCT00235482, NCT00438009 NCT02307149
		Combined with ipilimumab	i.t.	I	Recruiting	Viralytics	
		Sole agent	i.t.	II	Recruiting	Viralytics	NCT01227551, NCT01636882
CAVATAK™	<ul style="list-style-type: none"> • Wild-type CVA21, Kuykendall strain 	Sole agent	i.v.	I	Completed	Viralytics	NCT00636558
		Combined with chemotherapy	i.v.	I	Recruiting	Viralytics	NCT02043665
Herpes simplex virus							
HF10	<ul style="list-style-type: none"> • Spontaneous mutant strain of HSV1 (loss of UL56 function) 	Sole agent	i.t.	I	Not yet recruiting	Takara Bio Inc	NCT02428036, NCT01017185
		Combined with ipilimumab	i.t.	II	Recruiting	Takara Bio Inc	NCT02272855

Table 2.5: The most clinically advanced OVs for the treatment of melanoma (*continued*).

Virus Name of agent	Specification	Combined with	Viral route of delivery	Phase	Status	Sponsor	Clinical trial identifier
HSV1716 (Sephrehvir®)	<ul style="list-style-type: none"> • Deletion of both copies of the <i>RL1</i> gene that encodes ICP34.5 	Sole agent	i.t.	I	Recruiting	Nationwide Children's Hospital	NCT00931931
OrienX010	<ul style="list-style-type: none"> • Double deletion of gene encoding ICP34.5 and ICP47 • Interruption of the <i>ICP6</i> gene • Insertion of GM-CSF 	Sole agent	i.t.	I	Recruiting	OrienGene Biotechnology Ltd.	NCT01935453
OncoVEX ^{GM-CSF} (T-Vec)	<ul style="list-style-type: none"> • JS-1 strain with double deletion of gene encoding ICP34.5 and ICP47 • Insertion of GM-CSF 	Sole agent	i.t.	II	Completed	BioVex Limited	NCT00289016
		Sole agent	i.t.	III	Completed	BioVex Limited	NCT00769704, NCT01368276
		Followed by surgical resection	i.t.	II	Recruiting	Amgen	NCT02211131
		Combined with ipilimumab	i.t.	I/II	Recruiting	Amgen	NCT01740297
		Combined with pembrolizumab	i.t.	I/II	Recruiting	Amgen	NCT02263508
Reovirus							
Reolysin®	<ul style="list-style-type: none"> • Wild-type reovirus, reovirus serotype-3 Dearing strain 	Sole agent	i.v.	II	Completed	National Cancer Institute	NCT00651157
		Combined with paclitaxel carboplatin	i.v.	II	Completed	Oncolytics Biotech	NCT00984464

Table 2.5: The most clinically advanced OVs for the treatment of melanoma (*continued*).

Virus Name of agent	Specification	Combined with	Viral route of delivery	Phase	Status	Sponsor	Clinical trial identifier
Vaccinia virus GL-ONC1 (GLV-1h68)	<ul style="list-style-type: none"> • Insertion of <i>Ruc-GFP</i> fusion gene into F14.5L • Insertion of β-galactosidase (<i>lacZ</i>) and β-gluronidase (<i>gusA</i>) reporter gene into J2R (TK) and A56R (HA) loci respectively 	Sole agent	i.t.	I	Recruiting	Genelux Corporation	NCT00794131
JX-594 (Pexa-Vec)	<ul style="list-style-type: none"> • Wyeth strain VV with the deletion of TK • Expressing of <i>lacZ</i> gene • Armed with GM-CSF 	Sole agent	i.t.	I	Completed	Jennerex Biotherapeutics	NCT00625456
vvDD-CDSR	<ul style="list-style-type: none"> • Double deletion of TK and VGF genes • Addition of <i>CD</i> and <i>SR</i> gene 	Sole agent	i.t.	I	Active, not recruiting	David Bartlett	NCT00574977

Abbreviations: CD, cytosine deaminase; GM-CSF, granulocyte-macrophage colony-stimulating factor; H, haemagglutinin; i.t., intratumoural; i.v. intravenous; Ruc-GFP, *Renilla* luciferase and *Aequorea* green fluorescent protein; SR, somatostatin receptor; TK, thymidine kinase; VGF, vaccinia growth factor.

2.2.5 Barriers to oncolytic virus monotherapy

A major assumption in the field of oncolytic virotherapy of tumours is that a small initial dose of a replication-competent OV will amplify through successive rounds of viral replication, resulting in the eventual eradication of the entire tumour mass. This phenomenon can be observed in preclinical studies, but OVs as a standalone therapeutic intervention have not been successful in most clinical trials. Tumours can develop multiple barriers to various anticancer therapies, including oncolytic virotherapy. Several mechanisms have been identified, that may help explain the poor therapeutic efficacy of some OVs in current clinical studies.

2.2.5.1 Immunological barriers

The most significant limitation to oncolytic virotherapy is the activation of the innate immune response to the OV which can occur rapidly after viral infection. Innate immunity provides an initial line of defence that limits the initial viral infection, replication, and spread; signals for the maturation of APCs; and primes the cellular components of the adaptive immune system [285]. Numerous models have shown that the innate immune response (comprising of neutrophils, NK cells, macrophages, and DC cells), when recruited to the site of infection limits viral propagation, with the initial viral titre dramatically reduced over the following days [343, 344, 680]. NK cell mediated lysis of HSV virus infected cells has been shown to prevent viral dissemination to neighbouring cells [49]. Apart from NK cells, macrophages play a critical role in OV clearance by secreting IL-12 to activate NK cells. Recruitment of infiltrating macrophages has been shown to coincide with clearance of over 80% of HSV-derived oncolytic particles [244].

Additionally, viral proteins such as viral capsid particles, early viral protein scaffolding, and transcription factors are processed into viral antigens and are expressed on the surface of the infected cell to attract cytotoxic T lymphocytes (CTLs) [285]. Upon recognition, CTLs will respond to these ‘flagged’ cells by destroying them, eliminating cell populations that are attempting to produce therapeutic OVs. Moreover, recognition of these viral antigens by specific immunoglobulin surface receptors on B lymphocytes can lead to the production of antiviral antibodies, that persists in the circulation, effectively preventing sustained infection and limiting the effectiveness of further viral administration

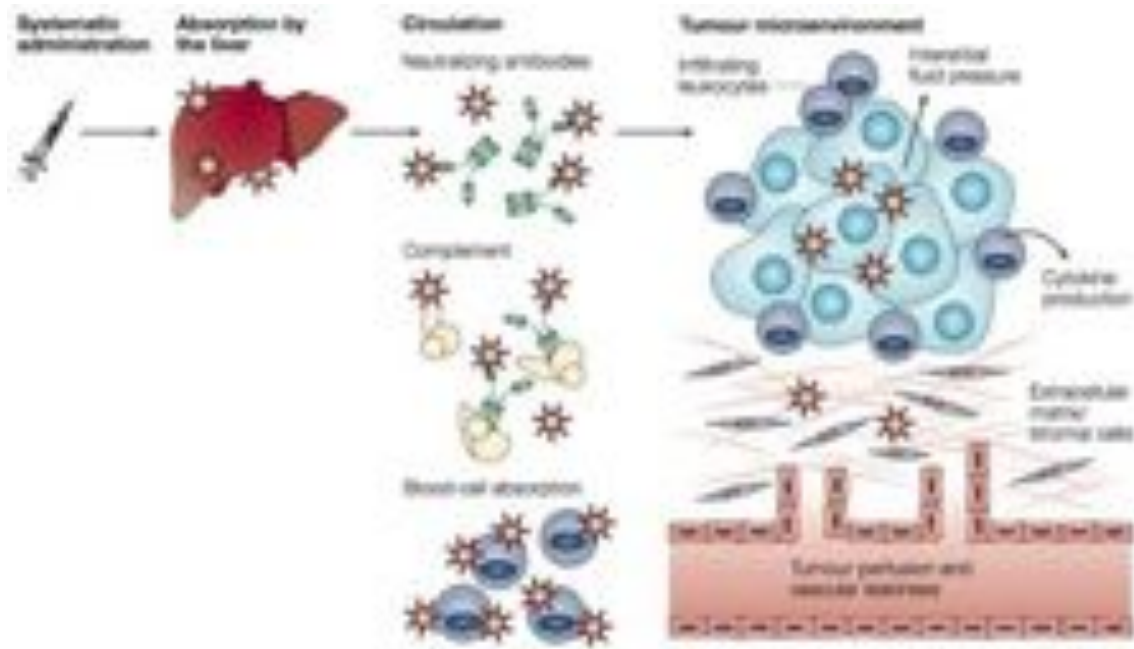


Figure 2.11: Barriers to optimal delivery of OVs to tumours. When an OV is given systemically to a patient (for example, by i.v. injection), there are many barriers that prevent it from reaching the tumour and infecting cancer cells. Within minutes, most of the initial virus inoculum is absorbed by the liver. Virus that escapes this organ can enter the circulation, where it can be quickly neutralised through absorption by blood cells, through the complement cascade or by neutralising antibodies, particularly in instances of pre-existing immunity. For a virion to access the tumour, it must leave the circulation, traversing or leaking through the vascular endothelium against a gradient of interstitial fluid pressure. Additionally, resident or infiltrating leukocytes limit cell–cell spread of the virus, either directly through antiviral activity or indirectly by the release of soluble inflammatory mediators, including IFNs and other cytokines. Source: Parato, K. A. *et al.* (2005). Recent progress in the battle between oncolytic viruses and tumours. *Nature Reviews Cancer*, 5(12):965–976 [572].

[170]. Furthermore, the complement system, composed of soluble factors and cell surface receptors, blocks viral infection by acting on both the innate and adaptive immune responses. These mechanisms include, enhancing humoral immunity regulating antibody effector mechanisms, and modulating T-cell function [706].

2.2.5.2 Challenges of intravenous delivery

Direct injection of OV_s into a primary tumour is still the most effective delivery method, and has produced the most successful anti-tumour effects in animal models. However, many metastatic lesions in humans (common in patients suffering from advanced melanoma) are inaccessible by direct injection and systemic delivery is needed. Systemic delivery remains a significant hurdle for oncolytic virotherapy. The presence of preexisting immunity, whether from previous immunisation, environmental exposure, and/or prior oncolytic virotherapy, is a key barrier [218]. For example, VV, PV, and MV, were candidates in worldwide immunisation programs, thereby contributing to the high level of preexisting immunity to these OV_s in the general population [218, 572]. Reovirus is universally present within the environment and as a result, most people have immunity to it. Several studies have provided evidence that the presence of preexisting neutralising antibodies significantly impairs the effectiveness of i.v. administered virus, thus limiting the ability to give subsequent doses [138, 737].

Blood cells, the complement system, nonspecific uptake by major organs, and the blood brain barrier are some of the factors that pose an impediment to the effective delivery of OV_s via the i.v. route [218]. Preclinical evaluation showed that the activated complement cascade was directly responsible for limiting the initial HSV infection of glioma xenografts established in the brains of rodents [763, 764]. Furthermore, it is well established that many viruses are either filtered or taken up by the lung, liver, or spleen thus reducing systemic availability [218]. Alemany *et al.* found that the rapid clearance (up to 90%) of the Ad5 virus from the bloodstream was due to the uptake by Kupffer cells in the liver [10]. It has also been shown in numerous glioma studies that OV_s are unable to disseminate efficiently into regions of the brain due to the presence of the blood brain barrier resulting in rapid viral clearance by circulating neutralising antibodies [601, 610]. Gromeier *et al.* provides substantial evidence demonstrating successful clearance of subcutaneous xenograft tumours after a single injection of poliovirus, but this did not lead to the clearance of brain metastasis [282].

2.2.5.3 Challenges of the tumour microenvironment

The microenvironment of a solid tumour has several unique characteristics that distinguishes it from normal tissue. The interior of a solid tumour displays high cellular heterogeneity, comprising of both malignant and normal (stromal) cells, various tumour-associated connective tissues, and numerous infiltrating leukocytes [183]. These cells form a complex extracellular matrix (ECM) which modulates tumour growth, progression, vascularisation, and metastasis [386]. While ECM proteins provide structural support to the tumour, it indirectly presents a barrier for efficient dissemination of OV_s. For example, Bilbao *et al.* showed that adenovirus entry into HCC in the livers of immunocompetent mice following i.v. injection was directly related to the thickness of the ECM capsule enveloping the nodules [77]. Further work by McKee *et al.* suggested that passively diffusing OV_s may physically not fit through the strands of the ECM. McKee *et al.* found that due to the size of the OV HSV (which has a diameter of > 100 nm), viral penetration was limited by the fibrillar collagen in the ECM [498]. Melanoma cells in inaccessible regions continued to grow, remaining out of the range of viral infection, and tumour eradication was not achieved [498].

In addition, several studies have demonstrated that the aberrant growth within the tumour microenvironment leads to increased interstitial pressure outwards, preventing diffusion of therapeutics into the tumour [542, 707, 714]. Degradation of the ECM components using MMPs reduces interstitial pressure, leading to enhanced distribution and efficacy of oncolytic HSV [329, 522]. In another study, Grote *et al.* found that oncolytic MV was less efficacious in infecting larger tumours (> 0.4 cm³), suggesting that viral dissemination and efficacy was inversely proportional to tumour size [284]. Moreover, recent work has highlighted the role of tight junctions between tumour cells in barricading tumours from the penetration of therapeutic agents [74]. Strauss *et al.* found that adenoviruses that utilised Coxsackie and adenovirus receptor (CAR) or CD46 as the viral attachment receptors could not infect and lyse ovarian cancer cells of the epithelial phenotype [710]. These receptors were trapped in the tight junctions between cells and therefore not accessible to the virus. In addition, poor vascular permeability, host immune cells, and necrotic areas within an infected tumour can also severely impede the dissemination of OV_s [115, 170, 699, 795].

2.3 Coxsackievirus A21

An emerging OV, CVA21 has shown promise as an anticancer agent in a range of tumour indications. The viral entry receptor of ICAM-1 and DAF are up-regulated on some melanoma cancers when compared to normal tissue. As such, CVA21 has been examined for its capacity to lyse human melanoma cancer cells, and to induce regression of human melanoma xenografts in animal models. The genome and life cycle of CVA21 (a Picornavirus) will be discussed below .

2.3.1 Taxonomy of Coxsackieviruses

Coxsackievirus belongs to the icosahedral shaped family of viruses known as the *Picornaviridae*. Picornaviruses are a family of icosahedral non-enveloped viruses, so named because they are small (typically 28 - 30 nm), ‘pico’, and contain a single-stranded positive sense RNA genome. According to the latest taxonomy report released by the International Committee on Taxonomy of Viruses (ICTV), the *Picornaviridae* family is currently divided into 26 genera: *Aphthovirus*, *Aquamavirus*, *Avihepatovirus*, *Avisivirus*, *Cardiovirus*, *Cosavirus*, *Dicipivirus*, *Enterovirus*, *Erbovirus*, *Gallivirus*, *Hepatovirus*, *Hunnivirus*, *Kobuvirus*, *Megrivirus*, *Mischivirus*, *Mosavirus*, *Oscivirus*, *Parechovirus*, *Passivirus*, *Passerivirus*, *Rosavirus*, *Salivirus*, *Sapelovirus*, *Senecavirus*, *Teschovirus*, and *Tremovirus* [2, 3, 398]. Coxsackievirus belongs to the genus *Enterovirus*, a group of viruses that mostly inhabit, but not limited to the enteric tract of humans. The enterovirus genera can be further sub-categorised into the species of *Enterovirus A*, *B*, *C*, *D*, *E*, *F*, *G*, *H*, and *J*, and *Rhinovirus A*, *B* and *C* (Figure 2.12).

A total of 29 Coxsackievirus serotypes have been discovered to date. Initially, Coxsackieviruses were divided into group A (23 serotypes) and group B (6 serotypes) viruses, based on the differences in the pathogenicity and histopathological lesions observed in suckling mice [258]. Coxsackievirus A-group viruses produce a flaccid paralysis with acute inflammation and necrosis in the fibres of skeletal muscle causing lesions in the limbs [18, 341], while Coxsackievirus B-group viruses causes spastic paralysis, neurodegeneration, affecting the heart, pancreas and liver of newborn mice [341]. Later, following the recommendations from the ICTV based on sequence homology, Coxsackieviruses were reclassified into three enterovirus (EV) clusters, EV-A, EV-B and EV-C [398, 755]. CVA21 belongs to the EV-C cluster, together with poliovirus and several other enteroviruses [102].

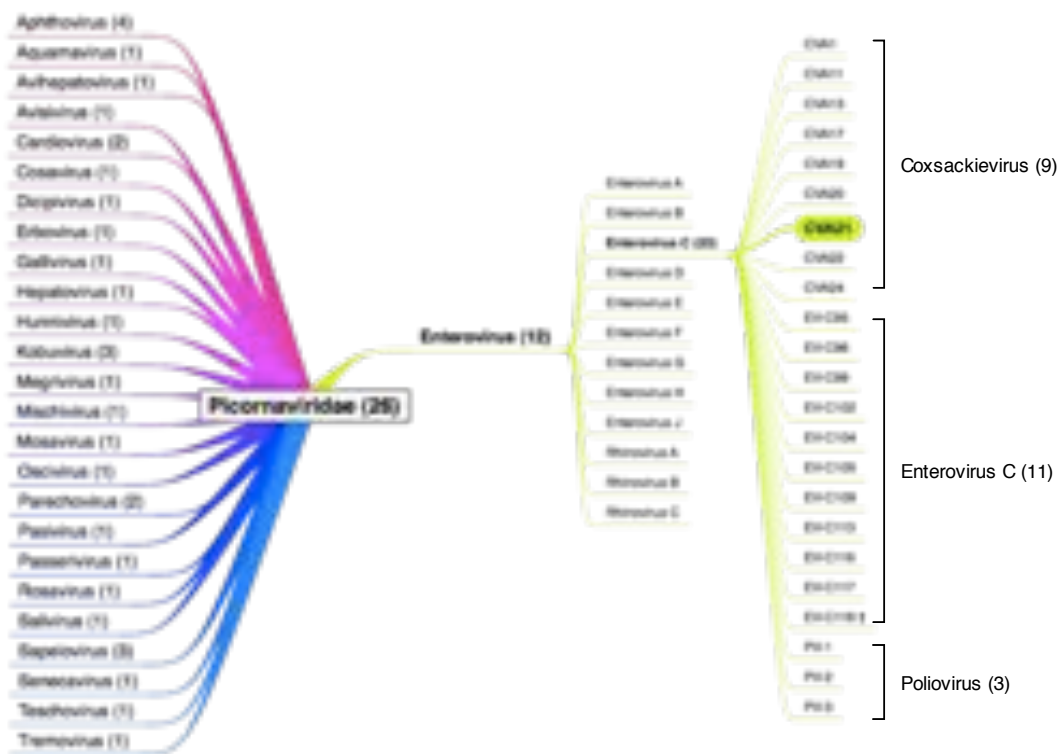


Figure 2.12: Classification of the *Picornaviridae* family. There are currently a total of 26 genera within the *Picornaviridae* family each of which are further divided into numerous species (denoted by the number in brackets). The location of CVA21 within the *Picornaviridae* family is shown coloured in green. † denotes unpublished data (awaiting approval by the ICTV). Abbreviations: CVA, Cocksackievirus A; EV-C, enterovirus C; PV, poliovirus. Source: Adapted from ICTV *Picornaviridae*, available at <http://www.picornastudygroup.com/>.

2.3.2 Virion structure

For all picornaviruses, the single strand of positive-sense RNA is encapsulated in a non-enveloped, icosahedral capsid approximately 28 nm in diameter, with a protein coat made up of 60 protein subunits or protomers [26, 326, 638]. Each protomer is composed of four structural viral proteins (VP1 to VP4). The external surface of the icosahedral shell is formed by VP1, VP2 and VP3, whilst VP4, is located on the internal side of the capsid in close association with the strand of RNA (Figure 2.13A) [638]. The structures of several picornaviruses (including CVA21), have been determined to near atomic resolution, enabling a more detailed characterisation of these viruses [227, 326, 636, 809].

The tertiary structure of all picornaviruses show similar structural patterns in which VP1, VP2 and VP3 have an eight-stranded antiparallel β -barrel type structure which forms the matrix of the shell. Interestingly, Rossmann *et al.* noticed that the organisation of these proteins VP1, VP2 and VP3, interact to form distinct protrusions on the capsid surface [638]. The use of X-ray crystallographic analysis confirmed that the surface of picornavirus virions are corrugated in topography, and includes a star-shaped plateau, or mesa, at the 5-fold axis of symmetry, resulting in the formation of deep surface depressions, otherwise known as ‘canyons’ (Figure 2.13B). The ‘canyons’ are where virus receptors are known to bind with high affinity, although not all picornaviruses have these structures [153, 583, 638, 808]. The interaction between the viral capsid of CVA21 and its binding receptors will be discussed in greater detail in Section 2.3.5.3.

2.3.3 Picornavirus genome

Typical of the picornavirus family, these viruses contain a single molecule of positive stranded RNA as their genome. The RNA is approximately 7,400 nucleotides in length. The unique feature of a positive-sense RNA genome is that the RNA itself is infectious and once inside a permissive cell, is sufficient to be directly translated into new viral proteins [11, 104]. A small 22-amino acid viral-encoded protein, VPg (virion protein genome-linked), is covalently linked to the 5' terminus of the viral genome, while a poly(A) tail is present at the 3' end (Figure 2.14A) [233, 693]. Both termini display UTRs that contain secondary structures necessary for correct genome function. The long 5' UTR makes up approximately 10% of the genome and is involved in the initiation of translation, directing ribosomes to a ‘clover-leaf’ secondary structure known as the IRES [356, 578]. The 3' UTR is shorter, only 70 - 100 nucleotides in length and is used to initiate the synthesis

of negative-stranded RNA [633]. Interestingly, deletion mutants lacking the 3' UTR have been shown to be infectious in cell culture [730].

2.3.3.1 Genome organisation and processing

For RNA translation of the viral genome to occur, the viral protein VPg acts as a primer for the virally-encoded, RNA-dependent, RNA polymerase [576] and the IRES is required for RNA translation [356, 578]. As the picornavirus RNA does not carry any accessory proteins with it except VPg, the first viral action after entry of the RNA into the host cell is viral RNA translation [664]. Once inside a cell, the coding region is translated as a single polyprotein which is cleaved into P1, P2 and P3 proteins by virally-encoded proteases (Figure 2.14B) [327, 353, 645].

Further proteolysis cleaves P3 into 3AB and the 3CD protease. 3CD cleaves P1 into the structural viral proteins VP0, VP1 and VP3, and P2 into 2A and 2BC. Viral proteins undergo further cleavage whereby 2BC cleaves into 2B and 2C, 3AB cleaves to form 3A and 3B, and 3CD cleaves to form 3C and 3D. Early on in the processing of the viral genome, the viral proteinases 2A and 3C are responsible for shutting down cap-dependent host translation, thereby shifting the host cell machinery from cellular to viral processes [215, 417, 458]. The 3D protein is the RNA-dependent RNA polymerase and once released, starts to synthesise negative-sense RNA which is later used as the template for making more of the positive-sense RNA, concentrating viral RNA and proteins in the host cell [63]. The 3' UTR is required for priming the synthesis of negative-sense RNA from the positive-sense RNA strand [633].

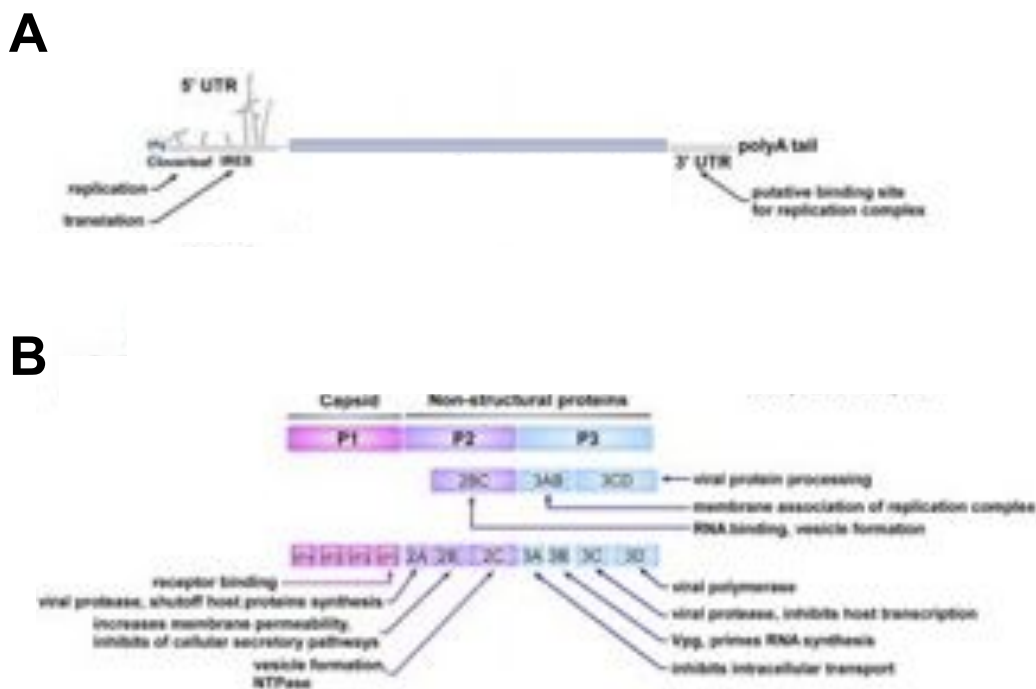


Figure 2.14: Schematic diagram of the enterovirus genome, outlining the polyprotein products and their major functions. (A) Viral genomic RNA has the viral protein VPg at its 5' end instead of a cap structure. The long UTR at the 5' end contains the IRES for translation. The shorter 3' UTR is important in initiating RNA synthesis. (B) The 11 mature polypeptides are shown, together with the three main cleavage intermediates. The P1 region encodes the structural polypeptides while the P2 and P3 regions encode the nonstructural proteins associated with replication. The main biological functions are included for each polypeptide. Source: Lin, J.-Y. *et al.* (2009). Viral and host proteins involved in picornavirus life cycle. *Journal of biomedical science*, 16:103. [443].

2.3.3.2 Viral assembly

Through extensive structural and biochemical studies, the process of picornavirus capsid assembly has been well established [65, 253, 636]. Assembly begins in the cytoplasm where translation of the viral structural polyprotein P1 and subsequent cleavage products allows the formation of 5S protomers consisting of VP0, VP1, and VP3 (Figure 2.15). Five protomers then join together to form a 14S pentameric assembly subunit, twelve of which self-assemble into a naturally occurring empty 80S procapsid [584, 776]. Two distinct assembly pathways have been proposed. In one pathway, twelve pentamers associate around a viral genome, directly forming a provirion (Figure 2.15*i*). In the second pathway, the procapsid is a true intermediate, into which the genome would be packaged by some yet unknown mechanism to form a 160S provirion (Figure 2.15*ii*). Regardless of the pathway used, procapsids are found in all infected cells, and contain 60 copies each of the structural proteins VP0, VP1, and VP3 [55, 164, 451]. After the provirion is formed, interactions

between the structural proteins and the RNA genome cause autocatalytic cleavage of VP0 into VP2 and VP4 [26, 55, 164]. The resultant mature 160S virions are released from infected cells and continue the viral life cycle.

As mentioned above, the encapsidation mechanism of the picornavirus genome is unclear. It is not known whether the RNA genome interacts directly with the structural proteins to form genome-filled capsids [554, 567, 585], or whether they are packaged after the production of empty capsids [256, 604]. Several groups have suggested that the specificity for packaging viral RNA into the capsid is driven by the viral proteins of the RNA replication complex and that the viral RNA itself does not play any role in packaging or assembly [457, 553]. This argument comes from experiments where successful and efficient encapsidation of chimeric genomes was observed when the poliovirus 5' UTR regions were replaced with regions from other picornaviruses such as CVB3 [369] and HRV2 [279]. In contrast, there have been a few studies which gave indirect evidence that there could be regions on the viral RNA genome called packaging signals which make contact with capsid proteins and ensure that the viral genome gets packaged and not cellular RNA [50, 360, 363].

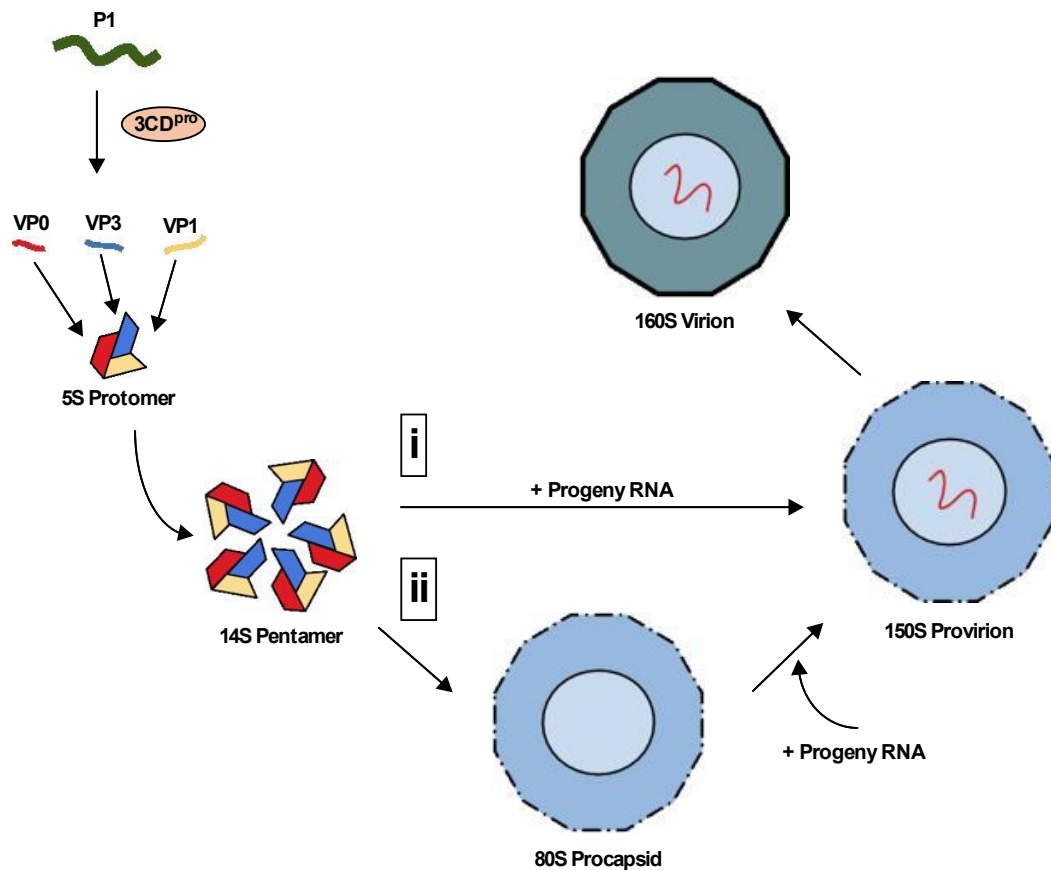


Figure 2.15: Main assembly pathway of picornavirus virions. Processing of P1 capsid proteins and assembly of virion particles first requires the cleavage of the P1 capsid precursor by 3CD^{Pro}. This leads to the formation of VP0, VP1 and VP3, which assembles to form the 5S protomer. These protomers form a 14S pentamer. Twelve 14S pentamers then either assemble around an RNA molecule, or form an 80S procapsid structure into which an RNA molecule is threaded. In either case, the assembly process results in the formation of a short-lived 150S provirion. The mature virion is formed when VP0 is further cleaved into VP4 and VP2 autolytically. Source: Adapted from Cifuentes, J. O. *et al.* (2013). Structures of the procapsid and mature virion of enterovirus 71 strain 1095. *Journal of Virology*, 87(13):7637–7645 [148].

2.3.4 Replication cycle of the Picornaviruses

The general life cycle of picornaviruses occurs entirely within the cytoplasm and is summarised in Figure 2.16 [178, 787]. In order to initiate an infectious cycle, the virus must first attach to its cognate cell surface receptor on a susceptible cell. Following binding to its receptor, the virus undergoes uncoating, and the viral genome is released into the cytoplasm. All picornavirus genomes are positive-sense RNA molecules that encode a single, long open reading frame (ORF) flanked by UTRs at both the 5' and the 3' end of the genome [787]. The positive sense RNA genome is in itself infectious, since it can function as mRNA, thereby coding for the production of viral proteins [607, 624]. The viral proteins

need to be synthesised first to obtain the RNA-dependent RNA polymerase that the cellular machinery lacks. The first 100 nucleotides of the virus 5'-UTR contains a 'cloverleaf' structure that binds viral polypeptide 3C, as well as host protein poly(rC)-binding protein [15]. Formation of this nucleoprotein complex is an absolute requirement for viral RNA replication.

Translation is initiated and is solely driven from the IRES also present in the 5' UTR [356, 578]. The 5' ends of most cellular mRNAs have a 7-methyl guanosine (m^7G) cap structure, which is recognised by the eukaryotic protein synthesis initiation factor 4F (eIF-4F) cap-binding complex as an early event in the translation of cellular proteins. However, this cap is absent from the 5' end of picornavirus RNAs, and therefore cannot undergo cap-dependent translation. The viral genome is translated by a cap-independent mechanism and reliant upon the IRES for initiation of translation. Each member of the family *Picornaviridae* family expresses its viral gene products through the IRES-directed translation of a single ORF that encodes an approximately 200-kDa polyprotein [712]. The complete viral protein coding region is translated as a single polyprotein, which is co-translationally cleaved, by virus-encoded proteases, into three precursor proteins P1, P2 and P3 [405, 793]. The overall arrangement of viral proteins in the polyprotein is highly conserved between members of the same genera, with structural (P1 or capsid) proteins found in the amino-terminal portion of the polypeptide, followed by the non-structural (P2 and P3) proteins [787].

Genome replication takes place in a viral replication complex and depends on the RNA-dependent RNA polymerase (RdRP), $3D^{pol}$, which is the most highly conserved polypeptide among members of the family *Picornaviridae* [787]. Similar to other RdRP, $3D^{pol}$ is error prone and misincorporates $\sim 1 - 2$ nucleotides per genome-copying event [772]. As a result, picornaviruses undergo rapid mutation and evolution in the host. The positive sense RNA genome is copied by $3D^{pol}$ to produce a negative strand RNA intermediate. This is then copied to synthesise new strands of positive sense RNA. Newly synthesised positive sense RNA undergoes morphogenesis with the newly synthesised structural proteins to form a provirion. Following the cleavage of VP0 into VP2 and VP4, an infectious virion is formed, and the progeny virus is released from the cell, often via cell lysis.

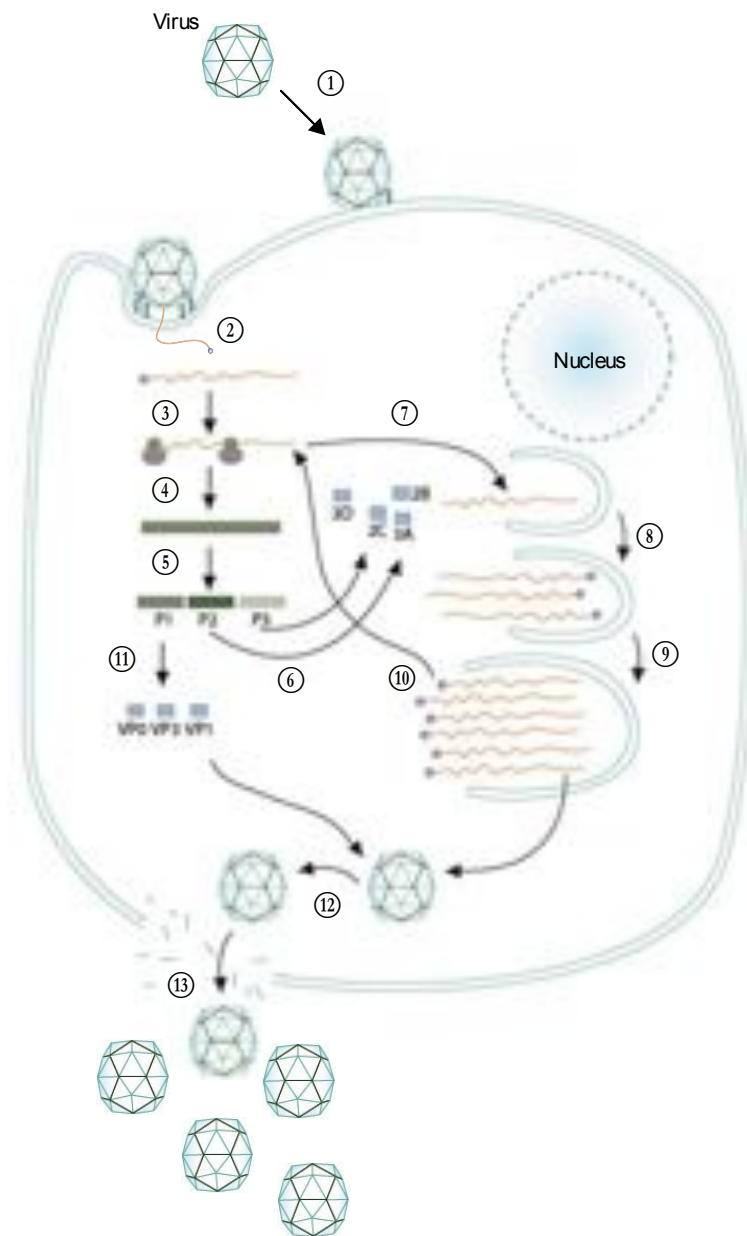


Figure 2.16: Replication cycle of the picornavirus. Step (1) Binding to cognate receptor allowing entry into the cell. (2) The virus undergoes uncoating and the viral genome is released. (3) The VPg protein (small purple circle at 5' end of RNA genome) is removed and the viral RNA associates with ribosomes. (4) Translation is initiated and a polyprotein precursor is synthesised. (5) The polyprotein is cleaved to yield the individual virus proteins. (6) P2 and P3 are involved in polyprotein cleavage and viral RNA synthesis respectively. (7) Proteins involved with RNA synthesis together with the (+) RNA are transported into specific membrane vesicles. (8) The (+) RNA is copied into (-) strands carrying VPg at their 3' ends. (9) These (-) strands serve as templates for the synthesis of (+) strand genomic RNAs. (10) Some of the newly synthesised (+) strand RNA molecules re-enter the translational system after the removal of Vpg. (11) Structural proteins formed by partial cleavage of the P1 precursor. (12) These proteins associate with (+) strand RNA molecules that retain VPg to form progeny virions. (13) Newly synthesised virions are released from the cell by lysis. Source: Adapted from Whitton, J. L., Cornell, C. T., and Feuer, R. (2005). Host and virus determinants of picornavirus pathogenesis and tropism. *Nature Reviews Microbiology*, 3(10):765–776. [787].

2.3.5 Viral receptors

CVA21 has been shown to utilise ICAM-1 and DAF as its cellular receptors [669, 673]. The protein ICAM-1 functions as an internalisation receptor for the prototype strain (Kuykendall), whereas DAF functions as an attachment or co-receptor receptor [673, 674]. The N-terminal domain of ICAM-1 (D1) was found to bind centrally in the canyon on the capsid of CVA21 [637]. On the other hand, CVA21 interacts with the short consensus repeat 1 (SCR1) on DAF [673]. The molecule ICAM-1 is able to induce relatively rapid conformational changes in CVA21 virion structure allowing cell entry, whereas DAF receptor appears to maintain sequestered CVA21 in a conformationally unaltered state [669].

The virus CVA21 can bind to DAF and retain infectivity [544], however, CVA21 can infect a cell using DAF alone only if DAF is cross-linked with a monoclonal antibody against SCR3. The resultant replication is much slower than when ICAM-1 is utilised to enter the cell, suggesting that a different route of entry may be employed. In 2004, our group produced a bioselected variant of CVA21 (CVA21-DAFv) that is capable of lytically infecting cells by utilising DAF alone as an internalisation receptor [364].

2.3.5.1 Intercellular adhesion molecule (ICAM-1)

Intercellular adhesion molecule-1 (ICAM-1; also known as CD54) is an immunoglobulin-like cell adhesion molecule expressed by several cell types, including leukocytes and endothelial cells. It can be induced in a cell-specific manner by several cytokines, for example, TNF- α , IL-1, and IFN- γ , and inhibited by glucocorticoids [202, 594]. Its ligands are the membrane-bound integrin receptors lymphocyte function-associated antigen-1 (LFA-1) [478, 483] and macrophage antigen-1 (Mac-1) on leukocytes [687], sialophorin (CD43) [635], the matrix factor hyaluronan [493] and *Plasmodium falciparum* infected erythrocytes (PFIE) [556]. It also serves as a receptor for multiple enteroviruses, including the major group human rhinoviruses [702] and the human enteroviruses; CVA13, CVA15, CVA18 and CVA21 [543].

2.3.5.1.1 Structure of ICAM-1

The protein ICAM-1 is a transmembrane glycoprotein belonging to the immunoglobulin superfamily [701, 752]. It contains five Ig-like domains (numbered sequentially from the amino end), comprising of 453 amino acids expressed on the extracellular portion of the protein, a hydrophobic transmembrane domain of 24 amino acids, and a charged short cytoplasmic tail of 28 amino acids (Figure 2.17 A) [64, 701, 752]. The endodomain of

ICAM-1 interacts with the cytoskeletal protein, α actinin, determining cell surface distribution [117]. Notably, ICAM-1 is differentially glycosylated depending on the cell type and environment, giving rise to a molecular weight between 55 - 114 kDa [202, 641, 701].

Each Ig-like constant domain consists of seven β -strands ($\beta A - \beta G$), forming two β -sheets arranged in a β -sandwich (Figure 2.17A) [119, 261]. Strands βB and βF are stabilised by disulphide bridges [789]. Crystal structures for the N-terminal of domains 1 and 2 of ICAM-1 suggests that it exists as a dimer on the cell surface [119]. The human *ICAM-1* gene consists of seven exons separated by six introns mapped to chromosome 19, with each Ig-like domain encoded by an individual exon [276, 762].

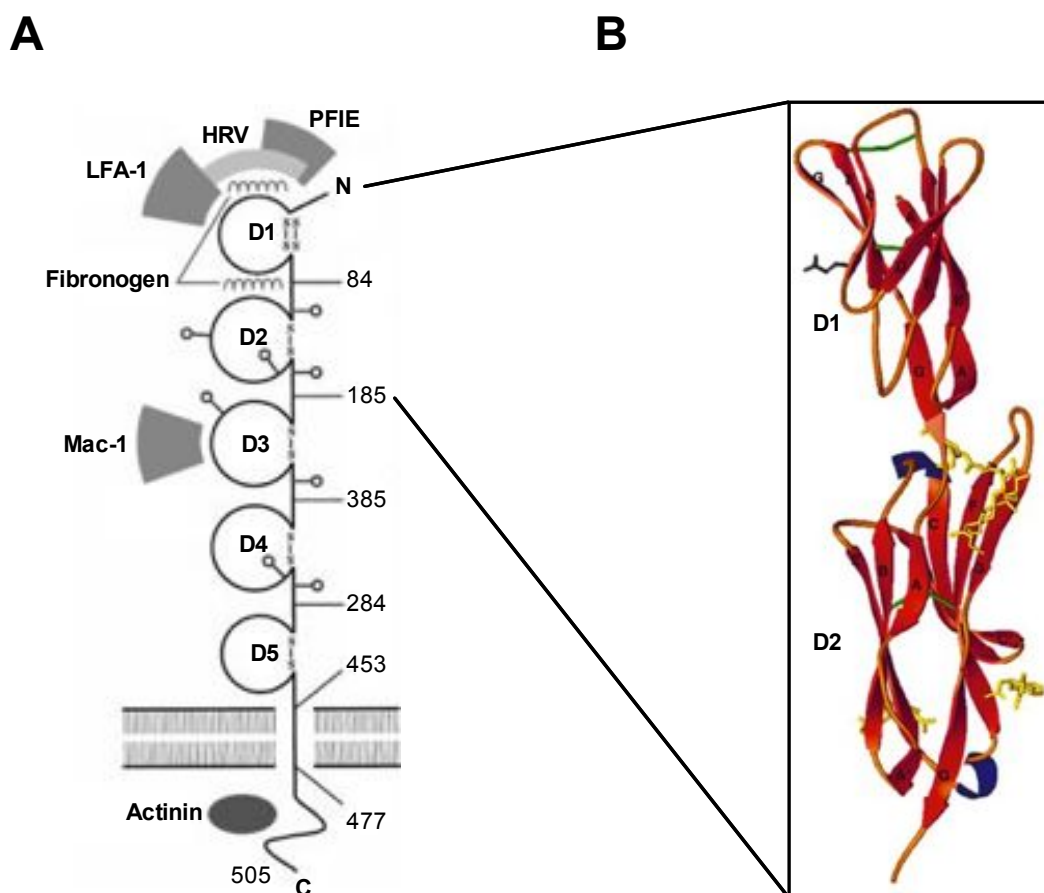


Figure 2.17: Two representations of the structure of ICAM-1. (A) ICAM-1 is made up of a series of five immunoglobulin superfamily domains (D1 - D5), with the carboxyl-terminal sequence anchored in the cellular membrane. Binding sites for HRV, LFA-1, Mac-1, PFIE are highlighted in grey boxes. Disulphide bonds formed between cysteine residues stabilise the immunoglobulin fold. (B) The crystal structure of the N-terminal two domains of ICAM-1. Ribbon diagram with β -strands (β A - β G) in red, α -helix in blue, N-linked sugars in yellow and disulphide bonds in green. Abbreviations: HRV, human rhinovirus; LFA-1, lymphocyte function-associated antigen-1; MAC-1, macrophage antigen-1; PFIE, *Plasmodium falciparum* infected erythrocytes. Source: Adapted from : Casasnovas, J. M. *et al.* (1998). A dimeric crystal structure for the N-terminal two domains of intercellular adhesion molecule-1. *Proceedings of the National Academy of Sciences of the United States of America*, 95(8):4134–4139. [119].

2.3.5.1.2 Function and regulation

The molecule ICAM-1 plays a fundamental role in many immune-related processes. *In situ*, it is constitutively expressed at basal levels on the surface of numerous tissues and cell types, including monocytes, lymphocytes, fibroblasts, and endothelial cells surrounding blood vessels [125, 196, 202, 594, 641]. Its physiological role relates to cell-cell adhesion in immune response biology, and assisting in the migration of leukocytes to sites of inflammation [642]. ICAM-1 is also involved in T-cell activation through interactions with the integrin

molecules LFA-1 and Mac-1 as co-stimulatory ligands [355]. ICAM-1 is also associated with a range of different diseases. For example, ICAM-1 expressed on mucosal epithelial cells function as the receptor for major group rhinoviruses and thus plays a critical role in the pathogenesis of the common-cold [276, 702, 700]. ICAM-1 has also been shown to serve as an antigen by which *Plasmodium falciparum* infected erythrocytes attach to endothelial cells and thus escape removal from the blood stream by the reticuloendothelial system [69]. Additionally, ICAM-1 expression has been associated with cancer development, in particular, it has been positively correlated with the metastatic potential of malignant melanoma [366].

The level of expression of ICAM-1 may be significantly and rapidly modulated by numerous diverse signals, including specific cytokines (IFN- γ , IL-1 and TNF- α), bacterial products (lipopolysaccharide [LPS]), and physical agents such as UVR [202, 419, 552, 594, 800]. Studies have shown that the transcription of the *ICAM-1* gene is regulated by the NF- κ B signalling pathway [632]. Interestingly, the initial reaction of host defences to viruses, which leads to the production of mediators of inflammatory responses, may induce the appearance of more ICAM-1 in nearby cells and thereby enhance subsequent spread of ICAM-1 binding viruses [570, 786].

2.3.5.2 Decay accelerating factor (DAF)

Decay accelerating factor (DAF; also known as CD55), is a complement regulatory protein. DAF, which is expressed on virtually all cell surfaces exposed to serum, acts to protect cells from complement-mediated lysis. DAF binds to and degrades C3/C5 convertases, the central amplification enzymes of the complement cascade [465, 422]. DAF also serves as a primary or accessory receptor molecule for numerous picornaviruses including CVB1, CVB3, CVB5, multiple echoviruses, enterovirus 70 and CVA21 [381, 671, 673].

2.3.5.2.1 Structure of DAF

Most cell surface proteins are anchored in the cell membrane by a hydrophobic transmembrane peptide domain. The protein DAF however, lacks this classic transmembrane domain and has a glycosylphosphatidylinositol (GPI) anchor instead (Figure 2.18A). The GPI-anchor can be cleaved by the enzyme phosphatidylinositol-specific phospholipase C (PI-PLC), which releases DAF from the surface of the cell [171]. Beginning from the N terminus, DAF is composed of four contiguous short consensus repeats (SCRs), a N-

linked glycan located between SCR domains 1 and 2, a serine/threonine/proline-rich region containing *O*-linked glycosylation sites, and the GPI-anchor proximal to the cell surface (Figure 2.18A) [465, 549].

Similar to the structure of ICAM-1, each SCR is about 60 amino acids long and folded into a β -structure stabilised by disulphide bridges [467, 791]. Using X-ray crystallography, the four SCRs form a relatively rigid, ‘bent rod’ structure with dimensions of $160 \times 50 \times 30 \text{ \AA}$ (Figure 2.18B) [467]. An overlay of the eight independent crystal structures generated by Lukacik *et al.* shows minimal variation in the structure of the four SCRs, suggesting that rigidity may be one of the key characteristics of the DAF molecule (Figure 2.18C). In particular, the inflexible domain junctions which give rise to the constant “bent rod” organisation of the SCR2 and SCR3 domain further emphasise the importance of these domains.

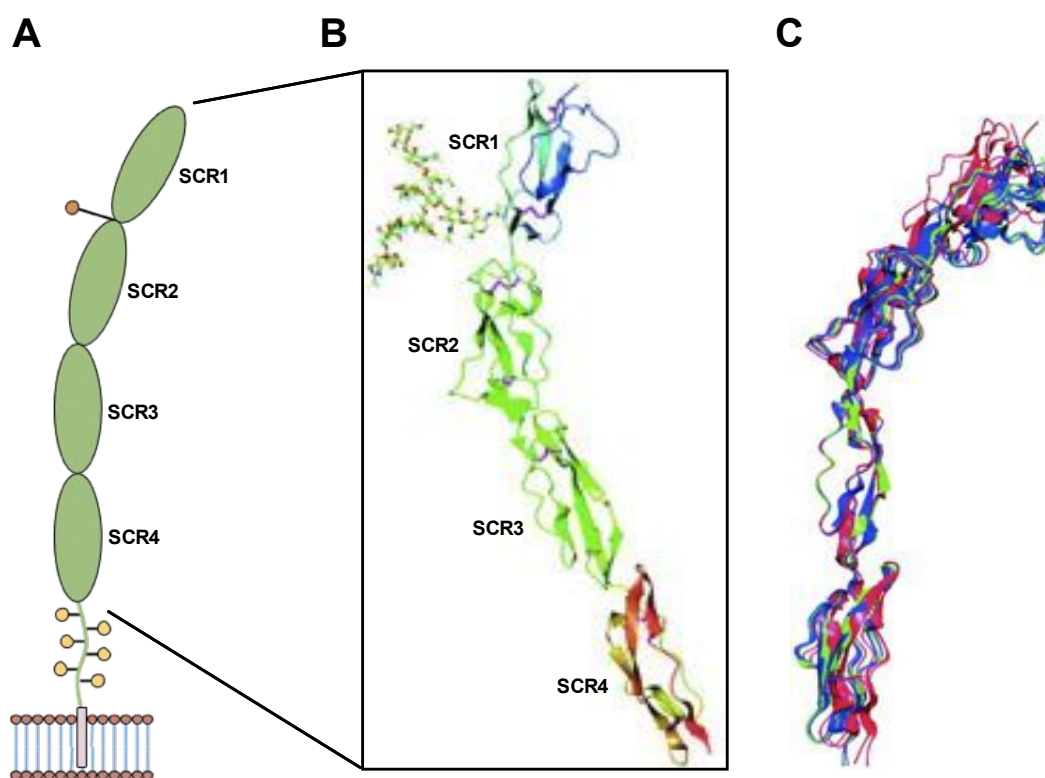


Figure 2.18: Schematic structure of DAF. (A) A representation of the molecule DAF which consists of four SCRs (SCR1 - 4), a serine/threonine-rich region of extensive O-glycosylation (yellow circles) and a GPI anchor attached to the cell membrane, which provides maximum lateral mobility. Orange spheres are N-linked carbohydrate moieties. (B) Crystallographic structure of the four SCR domains with the N-linked glycan between SCR1 and SCR2 (C) Comparison between eight copies of DAF from three different crystal forms. The molecules are coloured so that the two copies from crystal forms A and B are red and green, respectively, and the four copies from crystal form C are blue. Source: Adapted from: Lukacik, P. *et al.* (2004). Complement regulation at the molecular level: the structure of decay-accelerating factor. *Proceedings of the National Academy of Sciences of the United States of America*, 101(5):1279–1284.[467].

2.3.5.2.2 Function and regulation

By binding to C3b or C4b complement fragments, DAF blocks the C3 and C5 convertases of the classical and alternate pathways, inhibiting the downstream assembly of the membrane attack complex (MAC), thus protecting cells from complement-mediated lysis [465]. The molecule DAF prevents formation of cleavage fragments C3a and C5a further inhibiting the amplification of the complement cascade on the surface of host cells. Purified soluble DAF can inhibit complement activation both *in vitro* and *in vivo* [523], however, the anti-complement activity of purified DAF is substantially increased when it is reincorporated in the cell membrane [501, 523]. This suggests that the membrane anchoring of DAF induces favourable changes in its functional conformation. Ab mapping studies have revealed that only Abs directed against DAF SCR3 completely abrogate the complement regulatory

functions of DAF while deletion of SCR1 has no effect on DAF function [158]. More recent studies showed that when bred onto the autoimmune disease-prone MRL/lpr background, $Daf1^{-/-}$ (encodes the murine homologue of human DAF) mice developed exacerbated lymphadenopathy and splenomegaly, raising the possibility that DAF may also function as a negative regulator of adaptive immunity *in vivo* [517]. This was later confirmed by Liu *et al.*, where deficiency in the *Daf1* gene resulted in a significantly enhanced T-cell response via a complement-dependent mechanism, implicating DAF in the regulation of the interplay between complement and T cell immunity [453].

The DAF expression is almost ubiquitous throughout the human body, present on the surface of cells in contact with serum. It is therefore present on all cells that are exposed to complement including red blood cells, leukocytes, endothelial cells and epithelial cells [548]. DAF has also been reported to be expressed in more specialised cells, including human spermatozoa [129], oocytes [722], blastocysts [722], and axons/dendrites [822]. Despite being ubiquitously expressed in normal cells, upregulation of DAF has been reported in several carcinomas [411, 550]. Several groups have found large quantities of DAF in the tumour stroma, suggesting that carcinomas may circumvent complement-mediated tumouricidal activity by releasing soluble forms of DAF into the surrounding extracellular matrix, constituting a novel tumour evasion mechanism [139, 440, 550]. These would form more aggressive tumours as they would be resistant to complement attack.

The expression and regulation of DAF has been extensively studied in human umbilical vein endothelial cells (HUVECs), a cell that has the highest level of surface DAF among human cells that have been studied. Numerous studies have demonstrated upregulation of DAF expression on HUVECs in response to stimulation with phorbol esters [105], wheat germ agglutinin [106], and histamine [742]. In addition, various groups have found that the expression of DAF can be regulated by pro-inflammatory cytokines IL-1 β , IL-4, LPS, and TNF α , all of which cause an increase in surface DAF expression on endothelial cells, though there remains some discrepancy as to the significance of the upregulation [487, 531]. Mason *et al.* provides compelling evidence that pretreatment of endothelial cells with cytokines followed by MAC generation, induced an increase of DAF expression in excess of 3-fold, which was maximal at 24 h post-activation [487]. The major intracellular signal transduction pathways involved in the activation of DAF gene expression at the transcriptional level are similar to those involved in ICAM-1 expression, mainly the MAPK

and NK- κ B signalling cascades [6]. However, despite the fact that several of the same pathways regulate both ICAM-1 and DAF expression, studies examining the co-expression of ICAM-1 and DAF on normal and malignant cells have not been performed.

2.3.5.3 ICAM-1 and DAF interaction with CVA21

A crucial stage in the life cycle of a picornavirus is the attachment of the virus to cell surface receptors. For many picornaviruses, these interactions rely on the highly conserved architecture of the capsid and the use of a cellular receptor that is composed of an Ig-like domain [637]. A distinct feature of the picornavirus capsid is the star-shaped mesa found on each of the 5-fold symmetry axes. X-ray crystallography of the CVA21 capsid reveals a prominent depression surrounding the 5-fold vertex, forming a narrow channel referred to as the ‘canyon’ (Figure 2.19A) [808, 809]. At the base of the ‘canyon’, buried between two β -sheets of the VP1 core, Xiao *et al.* successfully located a hydrophobic ‘pocket’ filled with a lipid moiety and various cofactors known as ‘pocket factors’ [808, 809]. The presence of these molecules are crucial for stabilising the native conformation of virions and an interaction between the viral receptor and the capsid ‘canyon’ instigates the release of these factors, resulting in viral uncoating [226, 689, 771]. Several antiviral compounds have been designed to remove these ‘pocket factors’, thus inhibiting the disassembly of virions [238, 688].

Two cellular receptors have been identified for CVA21, ICAM-1 and DAF. ICAM-1 functions as the main internalisation receptor for CVA21, mediating viral cell entry. The binding site of ICAM-1 within the capsid ‘canyon’ is illustrated below (Figure 2.19B) [808, 809]. Binding of CVA21 to the N-terminal domain of ICAM-1 dislodges the ‘pocket factor’ from the ‘canyon’, and induces conformational changes in the viral capsid architecture that lead to the formation of A-particles and subsequent uncoating of the virion [672]. A-particles are conformationally altered sub-viral proteins that remain after the loss of VP4, sedimenting at 135S (compared to 160S of a native virion) and are believed to be an essential prerequisite for early picornaviral infection [163, 565, 679, 774]. This alteration primes the particle for genome release and RNA translation commences upon entry into the cytoplasm. Furthermore, in an animal study conducted by Dufresne and Gromeier, transgenic mice expressing the human ICAM-1 receptor administered with intramuscular (i.m.) injections of CVA21 developed classic paralytic poliomyelitis, indicative of successful CVA21 infection [200].

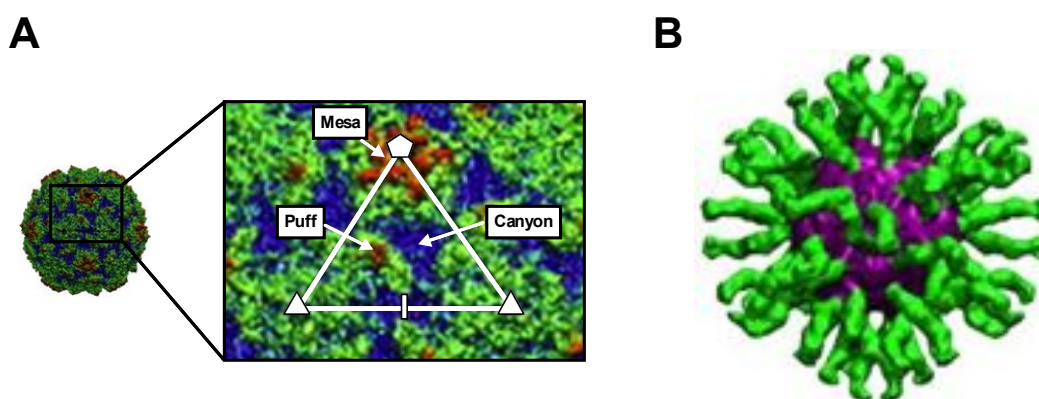


Figure 2.19: Surface cryo-EM reconstruction of CVA21 (Kuykendall) complexed with its receptor ICAM-1. (A) The close-up view of the icosahedral asymmetric unit (indicated by the triangular boundary) of CVA21 shows the topography of the virus surface, including the 5-fold mesa, canyon and puff region. Surface has been coloured from blue to red based on the radial distance to the centre of the virus (B) Surface-rendered cryo-EM reconstruction of CVA21-ICAM-1 complex. View of CVA21 complexed with ICAM-1. CVA21 is shown in purple and ICAM-1 in green. One icosahedral asymmetric unit is outlined in black. Source: Adapted from Xiao, C. *et al.* (2005). The crystal structure of Coxsackievirus A21 and its interaction with ICAM-1. *Structure*, 13(7):1019–1033 [809].

The second component of the CVA21 cellular receptor complex is DAF. In particular, CVA21 binds to the SCR1 of DAF [673]. DAF appears to play a passive role during enteroviral infection, as expression of human DAF alone on murine cells is capable of facilitating cellular binding but not infection by CVB1, CVB3, CVB5, and EV7 [671, 673]. Similarly, binding of CVA21 to DAF alone is not sufficient to initiate a productive infection or the formation of A-particles [673]. In addition, Newcombe *et al.* have showed that the binding of CVA21 with DAF was reversible and that the virion remained infectious for up to 24 h [544]. Furthermore, cryo-EM renderings of the enterovirus echovirus 7 complexed with DAF shows that the DAF molecule appears to binds across the icosahedral two fold axes on the viral surface and not within the capsid altering viral “canyon” (Figure 2.20), which possibly explains why interactions with DAF do not appear to convert native virions to A-particles [312, 593]. Thus, the likely physiological role of DAF during CVA21 infection is to act as a concentration receptor that binds and clusters virus to the cell surface, increasing the opportunity for cell entry via interactions with the main internalisation receptor ICAM-1.

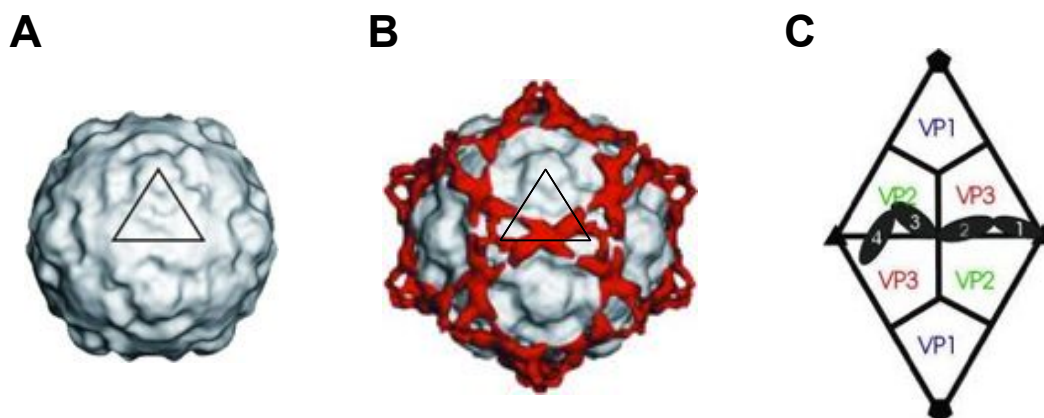


Figure 2.20: Surface cryo-EM reconstruction of Echovirus 7 (Wallace) complexed with its receptor DAF. (A & B) Stereo view of ECHO7 complexed with DAF. ECHO7 is shown in white and DAF in red. One icosahedral asymmetric unit is outlined in black. (C) Top view of two icosahedral asymmetric units of the virus bound with DAF, represented by four SCR domains in black. The positions of fivefold and threefold axes are indicated by pentagons and triangles. Source: Adapted from He, Y. *et al.* Structure of decay-accelerating factor bound to echovirus 7: a virus-receptor complex. *Proceedings of the National Academy of Sciences of the United States of America*, 99(16):10325–10329 [312].

CVA21 is perhaps the only known virus that binds to both ICAM-1 and DAF receptors [672, 673]. The capacity of some viruses to use two or more receptors in a complex suggests that they may use the individual receptor components together in a manner that improves the likelihood of successful infection. An experiment performed by Shafren *et al.* showed that while human rhinovirus-14 (HRV-14) and CVA21 compete for the same epitope on ICAM-1 (D1), monoclonal antibody blockade of this domain protected cells from the HRV-14 infection, but not for CVA21 [674]. This finding raises the interesting possibility that when viral entry mediated by ICAM-1 is impeded, CVA21 may employ an alternate route of cell entry, possibly mediated via cross-linked-DAF [669]. In a separate experiment, Shafren *et al.* showed that cross-linking of DAF with monoclonal antibodies directed against SCR2 and SCR3 induced a lytic infection in rhabdomyosarcoma (RD) cells, without the presence of the ICAM-1 receptor [673]. Taken together, Shafren *et al.* provides evidence that ICAM-1 can effectively cross-link DAF by a mechanism related to the artificial action of cross-linking monoclonal antibodies, thereby allowing cell entry [674]. It is suggested that this interaction is extracellular and is most likely to occur at an epitope located in or proximal to DAF SCR3 [674].

Furthermore, molecular modelling provides additional evidence that there is a spatial association between these two receptors. Analyses by crystallography [119, 813] and elec-

tron microscopy [401, 702] demonstrates that ICAM-1 is bent, and that the bend occurs between domain 3 and 4. As mentioned previously (Section 2.3.5.2.1), DAF has a bent rod structure which exposes the functional domains SCR2 and SCR3. Although no structural modelling of the ICAM-1-DAF complex have been made, the bend at these domains exposes domain 3 on both molecules, further highlighting the possibility of a close spatial interaction between ICAM-1 and DAF at this location (Figure 2.21). In summary, the importance of such a viral receptor complex is that not only does DAF represent an additional site for viral adhesion to the cell surface, the primary entry receptor is in close proximity, improving the chances of a successful infection.

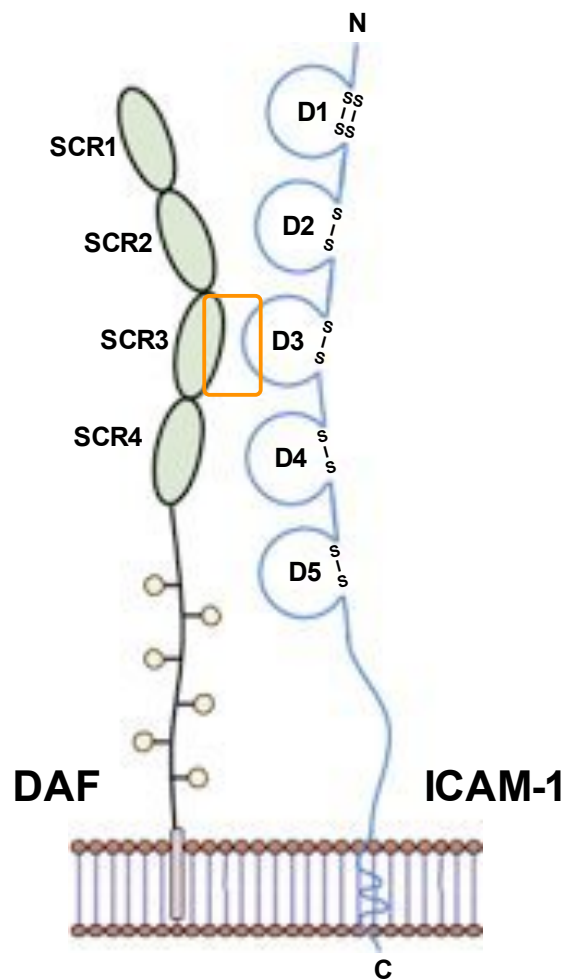


Figure 2.21: Interaction between ICAM-1 and DAF. Schematic representation of the putative extracellular spatial relationship between surfaced-expressed DAF and ICAM-1. The putative site of interaction is boxed in orange. SCR, short consensus repeat; D1 - D5, extracellular domains of ICAM-1. Source: Adapted from Shafren, D. R. *et al.* (2000). Cytoplasmic interactions between decay-accelerating factor and intercellular adhesion molecule-1 are not required for coxsackievirus A21 cell infection. *The Journal of General Virology*, 81(Pt 4):889–894 [674].

2.3.6 Clinical manifestation

Accepted as one of the many causes of the common-cold, the pathogenesis of CVA21 infection has been investigated in a number of studies. The virus, first described by Lennette *et al.* in 1958, was originally isolated from military personnel with febrile cold and was termed the Coe virus [432, 496]. Three years later, Schmidt *et al.* showed that the virus was immunologically identical to prototype CVA21 Kuykendall strain using cross neutralisation and metabolic-inhibition assays [659]. Subsequently, two studies were undertaken in groups of military personnel in which CVA21 was isolated from pharyngeal samples of those displaying signs of upper respiratory illness, whilst the incidence and duration of illness was examined [85, 367]. The authors of both studies noted that the presence of neutralising antibodies conferred protection against CVA21 infection and illness.

Since then, CVA21 has been administered to numerous volunteers to further study the aspects of viral transmission, clinical manifestation, and the host immune response towards the virus [107, 157, 475, 575, 696]. Despite many other Coxsackieviruses being associated with serious diseases including paralysis, aseptic meningitis, hand-foot-and-mouth disease, hepatitis, herpangina, myocarditis, and pneumonia, CVA21 possesses relatively low pathogenicity, limited to acute respiratory illnesses and diarrhoea (Table 2.6) [52, 640]. This is clearly a highly desirable attribute for an OV.

2.3.7 CVA21 as an oncolytic agent

As mentioned earlier, CVA21 can use ICAM-1 and/or DAF for attachment and infection. ICAM-1 and DAF are often abundant on the cell surface of many tumour lines, making these cells more sensitive to CVA21 infection. The same molecules contribute to tumour malignancy, since high expression of DAF protects tumour cells from cytotoxic complement action [694], while ICAM-1 promotes tumour dissemination and its metastatic potential [366, 634]. The oncolytic activity of CVA21 was demonstrated in different types of tumours both *in vitro* and in animal models. CVA21 was effective against melanoma [35, 670], lung cancer [801, 802], multiple myeloma [34], breast cancer [684, 685], prostate cancer [71], and glioma (unpublished data). As discussed in Section 2.2.4.2, CVA21 is currently under clinical evaluation under the trade name CAVATAK™.

In 2004, Shafren *et al.* established that the upregulation of ICAM-1 in melanoma could be exploited for CVA21 virotherapy [670]. CVA21 infection produced extensive lytic cell

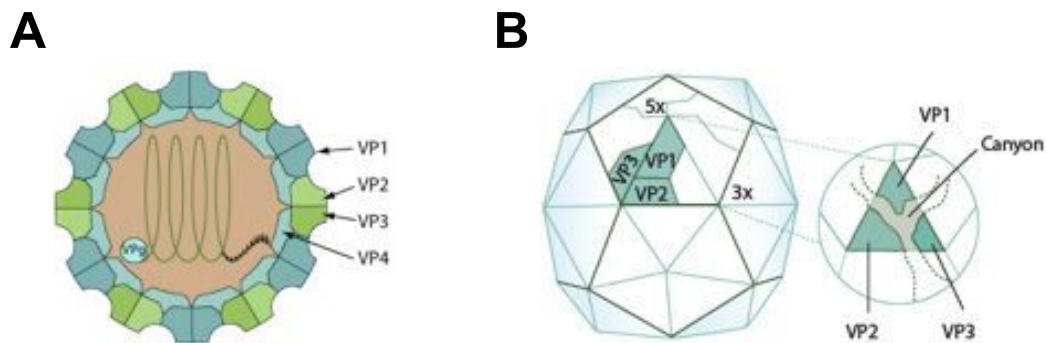


Figure 2.13: Virion structure of picornaviruses. (A) Cross sectional image showing the non-enveloped, 28 nm in diameter, icosahedral capsid surrounding the RNA genome. The capsid consists of a densely-packed icosahedral arrangement of 60 protomers, each consisting of 4 polypeptides, VP1, VP2, VP3 and VP4. VP4 is located on the internal side of the capsid. (B) The 3- and 5-fold axes are shown. The canyon, where receptor binding occurs (shaded in grey), surrounds the 5-fold axis. Source: Adapted from Arnold, E. *et. al.* (1987). Implications of the picornavirus capsid structure for polyprotein processing. *Proceedings of the National Academy of Sciences of the United States of America*, 84(1):21–25 [26].

Table 2.6: Common diseases caused by Coxsackieviruses.

Virus	Serotype	Disease
Coxsackievirus A (A1 - A22, A24)	1 - 2, 4 - 7, 9, 10, 14, 16, 22	Aseptic meningitis
	10	Lymphonodular pharyngitis
	18, 20, 21, 22, 24	Infantile diarrhoea
	2 - 6, 8, 10, 22	Herpangina
	24	Acute hemorrhagic conjunctivitis
	4, 5, 6, 9, 16	Exanthem
	4, 9	Hepatitis
	5, 10, 16	Hand-foot-mouth disease
	9, 10, 16, 21, 24	Upper and lower respiratory illnesses
	occasional types 4, 7, 9, 10	Paralysis and encephalitic diseases
Coxsackievirus B (B1 - B6)	1 - 6	Aseptic meningitis
	5	Diarrhea, exanthem, hepatitis
	occasional types 1 - 5	Paralysis and encephalitic diseases
	1 - 5	Pericarditis, myocarditis
	1 - 5	Pleurodynia
	1 - 5	Severe systemic infection in infants, meningoencephalitis and myocarditis
	1 - 6	Undifferentiated febrile illnesses
	4, 5	Upper and lower respiratory illnesses

Source: Adapted from Baron, S., Yin-Murphy, M. & Almond, J. W. Picornaviruses. (University of Texas Medical Branch at Galveston, 1996) [52].

destruction in all melanoma cultures tested, with the characteristic cytopathology associated with enterovirus infection. Data from co-culture experiments showed that CVA21 infection induced lysis in malignant cells only, leaving normal cell unharmed. In addition, efficient systemic spread of CVA21 was observed with regression of tumours also occurring at sites distant to the primary site of viral administration. Subsequent *in vivo* studies demonstrated the capacity of CVA21 to target and destroy mouse xenograft tumours via intratumoural, intravenous, and intraperitoneal administration [35].

Similar to melanoma, examination of surface markers on metastatic breast cancer has revealed over-expression of ICAM-1. A study conducted by Skelding *et al.* showed that human breast cancer cell lines expressed significantly elevated levels of surface ICAM-1 and DAF compared to normal breast cell lines, and that all malignant cell lines were more susceptible to lytic infection by CVA21 [684]. Treatment of pre-established T47D subcutaneous tumour xenografts with a single intravenous injection of CVA21 (5×10^7 TCID₅₀) resulted in significant regression compared to control mice. Furthermore, using bioluminescence to detect tumour metastases, all CVA21 treated mice were free of detectable lymph node metastases.

CVA21 also displays oncolytic efficacy in multiple myeloma [34]. Au *et al.* showed that ICAM-1 expression was upregulated in all multiple melanoma cell lines studied, and CVA21 exhibited a potent cytopathic effect against these cells, with reduced cytotoxicity against normal peripheral blood mononuclear cells. One major finding of this study was the effectiveness of CVA21 at purging clinical bone marrow biopsies with minimal effects on non-malignant cells, suggesting CVA21 could be used as a purging agent prior to autologous stem cell transplantation [34].

More recently, CVA21 oncolytic activity has been demonstrated in lung cancer [801, 802]. Immunohistochemical staining showed high levels of ICAM-1 in numerous lung cancer biopsies and high ICAM-1 expressing NSCLC cell lines displayed significant levels of cell death upon CVA21 infection [802]. Intratumoural injection of a single dose of CVA21 (1×10^8 TCID₅₀) in subcutaneous xenografts of the NSCLC cell line H157 in immunodeficient animals led to rapid cancer cell destruction and reductions in tumour burden. Furthermore, using an orthotopic model of NSCLC, Wong *et al.* presented evidence that systemic administration of CVA21 (2 doses at 1×10^8 TCID₅₀ 21 days apart) led to com-

plete tumour regression in four out of eight animals, and that this effect could be enhanced with the use of docetaxel (6/8 animals), a second-line treatment for NSCLC [802].

2.4 Study aims and hypothesis

Once melanoma has metastasised, no treatment currently available reliably controls the course of disease. At this stage of disease, malignant melanoma is highly refractory to conventional treatment modalities and is fatal, due to resistance of melanoma cells to the current conventional therapies. Therefore, novel therapeutics, such as oncolytic virotherapy are worthy of investigation. Although many believe that OVs have the potential to be used as frontline therapies, immediate clinical applications will require that they are at least compatible with current chemotherapeutics. The rationale for this combinatorial strategy is that the combination of various therapies may have a greater anticancer effect than either of these therapies alone. Secondly, combination of OVs with traditional chemotherapeutics may be synergistic, lowering the initial chemotherapy dose, thus decreasing any adverse side effects while still achieving the same or a greater therapeutic index than single agent therapies. Lastly, there should be little overlapping resistance between OVs and other therapies as OVs are biological entities that naturally infect cells triggering alternate death pathways to chemotherapy. As with other emerging therapeutics for cancer, the combined regimen of CVA21 and current treatment modalities is expected to play a significant role in future clinical applications. However it is currently unknown whether these agents augment or interfere with the oncolytic activity of CVA21. Therefore, this PhD project investigates the effects of CVA21 in combination with clinically relevant therapeutic agents for the treatment of melanoma.

The aims of this project are:

1. To investigate the *in vitro* combinatory effects of CVA21 and conventional chemotherapeutic agents (DTIC, P + C) against melanoma cell lines;
2. To determine the intracellular mechanism by which CVA21, conventional chemotherapy, and both in combination mediate their anticancer effects;
3. To assess oncolytic virotherapy in conjunction with chemotherapy *in vivo* in both immunodeficient and immunocompetent animal models of malignant melanoma;

4. To establish a fully immunocompetent CVA21-susceptible mouse model of malignant melanoma;
5. To determine whether oncolysates produced as a result of the lysis of melanoma cells by CVA21 were able to induce anti-tumour immunity in an immunocompetent setting;
6. To investigate the use of the immunostimulatory antibodies anti-PD-1 and anti-CTLA-4 in combination with intratumoural CVA21 virotherapy.

Chapter 3

Materials & Methods

3.1 Cell lines

3.1.1 Melanoma cells lines

Four human melanoma cell lines, SK-Mel-28, Mel-RM, ME4405 and MV3, and the murine melanoma cell line B16 were used in this study. SK-Mel-28 was obtained from the American Type Culture Collection (ATCC). Mel-RM was a gift by Dr. P. Hersey (University of Newcastle, New South Wales, Australia). ME4405 cells were established from primary melanoma lesions provided by Dr. G. Parmiani (National Cancer Institute, Milan, Italy). MV3 was kindly provided by Dr. R. Thorne (Cancer Research Unit, University of Newcastle, New South Wales, Australia). B16 murine melanoma cells were originally obtained from Dr. A. Shurbier (Queensland Institute for Medical Research, Brisbane, Queensland, Australia). All cell lines were maintained in Dulbecco's Modified Eagle's Medium (DMEM) (Thermo Scientific, Australia) containing 10% foetal calf serum (FCS) (SAFC Biosciences™, Australia), 10 mM sterile 4-(2-Hydroxyethyl)piperazine-1-ethanesulfonic acid (HEPES) (Thermo Scientific, Australia), 2mM L-glutamine (Thermo Scientific, Australia), sodium pyruvate (Invitrogen, Australia) and 100 IU/mL penicillin-streptomycin (Invitrogen, Australia) at 37°C with a 5% CO₂ humidified environment. Cell lines were subculture every three to four days using trypsin and were routinely tested for the absence of Mycoplasma using the MycoSensor™ QPCR Assay Kit (Stratagene, Mount Waverly, Victoria, Australia).

3.1.2 Luciferase-expressing cells

Human melanoma cell line SK-Mel-28-luc was established using a lentivirus vector encoding the firefly luciferase gene (driven by a ubiquitin promoter) that was provided by

Professor J. Shay (University of Texas Southwestern, Dallas, Texas, USA) [189]. The SK-Mel-28 cells were transduced with the lentivirus-containing medium supplemented with 10 mg/mL of Diethylaminoethyl-Dextran (DEAE-Dextran). After transduction, the lentivirus-containing medium was replaced with fresh medium to allow the cells to recover for 24 h. The cells (now termed SK-Mel-28-luc) were then subcultured, and examined for luciferase activity as described in Section 3.6.1.2.

3.1.3 ICAM-1-transfected murine melanoma cells

The murine B16 melanoma cells were transfected with human ICAM-1 cDNA using a pEF-BOS expression vector [519] to confer sensitivity to CVA21 infection [672]. Briefly, a DNA solution containing pEF-BOS encoding the human ICAM-1 cDNA was combined with 10 μ L of Lipofectamine (Invitrogen, Carlsbad, California, USA). After incubating at room temperature for 45 min, this solution was then overlaid on a 50% confluent monolayer of B16 cells grown in 6-well plate. Human ICAM-1 expressing transfected cells (now termed B-16-ICAM-1) were selected in DMEM containing G-418 (400 μ g/mL) and further enriched by fluorescence activated cell sorting (FACS Vantage, Becton Dickinson, Sydney, Australia) using the anti-ICAM-1 IH4 WEHI mAb.

3.2 Virus and drugs

3.2.1 Virus

The prototype strain of Coxsackievirus A21 (CVA21) Kuykendall strain was obtained from Dr. M. Kennett (Entero-respiratory Laboratory, Fairfield Hospital, Melbourne, Victoria, Australia). The virus was double-plaque purified and propagated in SK-Mel-28 cells. The proprietary formulation of CVA21 suitable for clinical use (CAVATAK™) was used for *in vivo* experiments and provided by Viralytics Ltd. (Newcastle, New South Wales, Australia). CVA21 was purified from stock preparations by velocity centrifugation in 5-30% sucrose gradients, as previously described [481, 671]. Peak infectious fractions were pooled, dialysed against phosphate buffered saline (PBS), and stored as single use aliquots at -80°C.

3.2.2 Chemotherapies

Dacarbazine (DTIC), paclitaxel (P), and carboplatin (C) were obtained from the Department of Clinical Toxicology & Pharmacology (Calvary Mater Newcastle, Newcastle, New South Wales, Australia). Dacarbazine was reconstituted to a concentration of 10 mg/mL

by adding 19.7 mL of sterile water for injections. Dacarbazine was activated by exposure to light for 1 h before use. Paclitaxel and carboplatin were obtained in its soluble form. The combination of paclitaxel and carboplatin was set at a constant molar ratio of 1 (paclitaxel) : 27 (carboplatin) μM .

3.2.3 Vaccine preparation

To generate oncolytic CVA21-induced lysis (oncolysate), B16-ICAM-1 tumour cells (1×10^7 cells) were infected with at a MOI of 100 TCID₅₀/cell and incubated at 37°C in a 5% CO₂ environment for 72 h. These titres resulted in 100% cell death. After 72 h, cells were subjected to three consecutive freeze-thaw cycles and the lysed cellular debris was harvested by centrifugation at $425 \times g$ for 5 min. The supernatant was discarded and the pellet was then resuspended with cold sterile PBS to a concentration of approximately $\sim 1 \times 10^6$ CVA21-lysed tumour cells/mL. This final concentration was the CVA21 oncolysate used for vaccination. In parallel, a non-viable cell lysate was produced as a control vaccine for any tumour antigens that may be released following the mechanical processing of the lysate, rather than resulting from a direct CVA21 lytic infection. The control vaccine was made by mechanically lysing 1×10^7 B16-ICAM-1 tumour cells through three freeze-thaw cycles. Cellular debris was centrifuged at $425 \times g$ for 5 min and the pellet resuspended with cold sterile PBS to a concentration of approximately $\sim 1 \times 10^6$ lysed tumour cells/mL.

3.3 Antibodies and flow cytometry

3.3.1 Antibodies

The anti-ICAM-1 (CD54) IH4 WEHI monoclonal antibody (mAb), which specifically binds to the N-terminal domain 1 of ICAM-1 was supplied by Dr. A. Boyd (Queensland Institute for Medical Research, Brisbane, Queensland, Australia) [95]. A commercially available anti-ICAM-1 mAb conjugated with phycoerythrin (PE) (Abcam #ab18222) was purchased from Abcam (Sapphire Bioscience Pty Ltd., New South Wales, Australia).

For immune checkpoint blockade studies, the following antibodies (BioXCell) were diluted in sterile PBS: mouse anti-PD-1 (clone RMP1-14) and mouse anti-CTLA-4 (clone 9D9). The following were used as isotype control antibodies: rat IgG2a (clone 2A3) and mouse IgG2b (clone MPC-11).

3.3.2 Flow cytometry

The surface expression of ICAM-1 in cell lines were analysed by flow cytometry. Phycoerythrin-labeled anti-ICAM-1 mAb were specific for the N-terminal domain of ICAM-1 (Abcam #ab18222). Sub-confluent monolayers of cells were dispersed by treatment with versene. Dispersed cells (1×10^6) were then pelleted by centrifugation at $425 \times g$ for 5 min at 4°C and resuspended in 100 μL of the appropriate mAb solution. All cells were incubated on ice for 30 min, washed with PBS, pelleted at $425 \times g$ for 5 min and resuspended in 100 μL of PBS before flow cytometry analysis using the BD FACSCanto™ II flow cytometer (Becton Dickinson, Sydney, New South Wales, Australia). Data was analysed using Weasel v2.1 software (WEHI Biotechnology Centre, Melbourne, Victoria, Australia). Results were presented as histograms.

3.4 Cell viability and synergy assay

3.4.1 Viral infectivity assay (TCID₅₀ assay)

Confluent monolayers of SK-Mel-28, Mel-RM, ME4404 and MV3 cells (1×10^4 cells seeded per well overnight) in 96-well tissue culture plates were inoculated with 10-fold serial dilutions (100 μL /well in triplicate) of CVA21 and incubated at 37°C in a 5% CO_2 environment for 72 h. Each virus stock was diluted to approximately 1×10^8 TCID₅₀/mL prior to making the 10-fold serial viral dilutions ranging from 1:10¹ to 1:10¹¹ in DMEM containing 2% FCS. Negative control wells comprising of untreated cells and positive control (100% lysis) wells comprising of cells treated with 1x lysis buffer (Promega, Sydney, New South Wales, Australia) were included in each plate. Wells were scored for cytopathic effects (CPE) visually under an inverted microscope. Wells that had detectable CPE were scored positive and the 50% viral endpoint titre was calculated using the Spearman-Kärber method [197]. The formula was defined as,

$$\text{Log}_{10}\text{TCID}_{50}/\text{mL} = 10^{1+L+d(s-0.5)}$$

where L represents the log of the lowest dilution; d being the log difference between the dilution steps (which is 1 for a 10-fold dilution); and s is the sum of the ratios of the positive tests. In parallel, photomicrographs of CPE were taken of cultured monolayers at 8, 24, 48 and 72 h post-infection using an Olympus IX70 inverted microscope with a DP72 digital camera (Olympus) at 100 \times magnification. Cell viability was also assessed using an

MTT viability assay as described in Section 3.4.4.

3.4.2 Chemosensitivity assay

The sensitivity of SK-Mel-28, Mel-RM, ME4404 and MV3 cells to dacarbazine (DTIC), paclitaxel (P) and carboplatin (C) in combination were tested. Cells were plated in 96-well plates at a density of 1×10^4 cells per well. After 24 h, they were treated with 2-fold serial dilutions of DTIC and P + C. DTIC was diluted to a final concentration of 800 $\mu\text{g}/\text{mL}$ (4.4 mM), P to 30 $\mu\text{g}/\text{mL}$ (35 μM) and C to 0.35 mg/ml (0.95 mM), prior to making the 2-fold serial dilutions ranging from 1:2¹ to 1:2¹¹, in DMEM containing 2% FCS. Negative control wells comprising of untreated cells and positive control (100% lysis) wells comprising of cells treated with 1 \times lysis buffer (Promega, Sydney, New South Wales, Australia) were included in each plate. Plates were then incubated at 37°C in a 5% CO₂ environment for 72 h before cell viability was assessed by an MTT assay (Section 3.4.4). Photomicrographs of cell morphology were captured at 8, 24, 48 and 72 h post-infection using an Olympus IX70 inverted microscope with a DP72 digital camera (Olympus) at 100 \times magnification.

3.4.3 *In vitro* synergy assay

Firstly, the concentrations inducing 50% viability decrease (EC₅₀) of all single drugs were determined. Confluent monolayers of SK-Mel-28, Mel-RM, ME4404 and MV3 cells (1×10^4 cells seeded per well overnight) were exposed in quadruplicate to 2-fold serial dilutions of each agent or both in combination using the ‘constant-ratio combination design’ [144, 145]. The drugs were combined in the same concentration ratio based on their corresponding EC₅₀ values of the respective agent, and cells were exposed to seven dilutions ranging from $0.0625 \times \text{EC}_{50}$ to $4 \times \text{EC}_{50}$ (serial dilution factor = 2) of each drug in combination plus a negative control (media only). Cells were incubated for 72 h at 37°C, 5% CO₂ after which cell monolayers were microscopically examined and cell viability was determined by MTT assay. The effect of the combination of CVA21 and chemotherapy on cell viability was assessed by calculating combination index (CI) values using the CompuSyn software (Biosoft, Cambridge, UK). Derived from the median-effect principle of Chou and Talalay [147], the CI was defined as,

$$CI = \frac{(D)_1}{(D_x)_1} + \frac{(D)_2}{(D_x)_2}$$

Where $(D)_1$ and $(D)_2$ are the doses of drugs used in combination, whereas $(D_x)_1$ and $(D_x)_2$ are the isoeffective doses. The CI provides a quantitative measure of the degree of

interaction between two or more agents. A CI of 0.9 - 1.1 denotes an additive interaction, > 1.1 antagonism and < 0.9 synergy (Table 3.1). The CI values for each dose and corresponding effect level, referred to as the fraction affected (Fa), ranging from 5% to 95%, were generated. Fa is the fraction of cell death induced by drug treatment and ranges from 0 - 1, with 0 meaning no cell killing and 1 representing 100% of cell killing. These data were then used to generate Fa-CI plots, which is an effect-orientated means of presenting synergism or antagonism. Data was also analysed by the isobologram technique, which is dose-oriented. The axes on an isobologram represent the doses of each drug, Two points on the x and y axes are chosen that correspond to the doses of each drug necessary to generate the given Fa value. The hypotenuse drawn between these two points corresponds to the possible combination of doses that would be required to generate the same Fa value indicating that the interaction between the two drugs is strictly additive. If the point lies to the lower left of the hypotenuse, then the effect is synergistic, and conversely, if the the point lies to the upper right of the hypotenuse, then the effect is antagonistic at that Fa value.

Table 3.1: Description of the combination index (CI) method. CI values of between 0.9 and 1.1 represents additivity, CI values less than 0.9 represent synergism, while values above 1.1 indicate antagonism.

Combination index (CI) range	Description
< 0.1	very strong synergism
0.1 - 0.3	strong synergism
0.3 - 0.7	synergism
0.7 - 0.85	moderate synergism
0.85 - 0.90	slight synergism
0.90 - 1.10	additive
1.10 - 1.20	slight antagonism
1.20 - 1.45	moderate antagonism
1.45 - 3.3	antagonism
3.3 - 10	strong antagonism
>10	very strong antagonism

3.4.4 Cell viability assay

A modified 3-(4,5-dimethylthiazol-2-yl)-2,5-diphenyltetrazoliumbromide (Methyl Thiazolyl Tetrazolium/MTT) (Sigma-Aldrich Pty Ltd, Australia) cell viability assay was performed to assess the viability of SK-Mel-28, Mel-RM, ME4404 and MV3 cells when treated with CVA21 and chemotherapy, either as single agents or in combination. Briefly, 20 μ L of MTT

(5 mg/mL) was added to all wells and incubated at 37°C in a 5% CO₂ environment for 3 h. Appropriate media only controls, and 100% lysis controls were included. After treatment, the supernatant from all wells was carefully removed by aspiration with a syringe and the MTT crystals redissolved by adding 50 µL of dimethyl sulphoxide (DMSO) to all wells. Optical density (OD) of the soluble MTT was then measured using an enzyme-linked immunosorbent assay plate reader (Flow Laboratories, McLean, Virginia, USA) at $\lambda = 550$ nm, subtracting the $\lambda = 620$ nm background. The percentage viability was calculated by normalising the OD readings of the treatment wells against the media control and 100% lysis control wells. The EC₅₀ for CVA21 was defined as the virus dose (MOI expressed in TCID₅₀/cell) that resulted in 50% cell viability at 72 h post inoculation as compared to untreated controls. Sensitivity of the cell lines to chemotherapeutic agents were expressed as the respective drug concentrations that effectively inhibited cell growth by 50% (EC₅₀), compared to untreated controls 72 h post treatment. Both EC₅₀ values were calculated using the graphing software GraphPad Prism v6.0 software (GraphPad Software, Inc., California, USA). Each drug or combination was tested at least in quadruplicate.

3.4.5 One-step viral growth curve assay

The ability of CVA21 to replicate within the panel of melanoma cells in the presence of chemotherapy was evaluated by one-step viral growth curves. SK-Mel-28, Mel-RM, ME4405 and MV3 cells were plated in 24-well plates at a density of 1×10^5 cells per well. Cells were then infected with either CVA21 at an MOI of 10 TCID₅₀/cell alone or with CVA21 in combination with DTIC and P + C at their respective EC₅₀ values. The infected cells were incubated for 1 h at 37°C in a 5% CO₂ environment before being washed three times with PBS to remove any unbound virus. An overlay of fresh media containing the respective drugs was then added to the cell monolayers. CVA21 alone treated wells were replenished with fresh media containing no drugs. Cells and media were harvested at 0, 8, 24, 48, and 72 h. Three freeze-thaw cycles were performed to release intracellular virus. Cell lysates were pelleted by centrifugation at $425 \times g$ for 5 mins. Using the supernatant only, a standard TCID₅₀ infectivity assay was performed on SK-Mel-28 cells to evaluate the levels of infectious CVA21 particles as previously described (Section 3.4.1). All samples were performed in triplicate. The results were then analysed and graphed using GraphPad Prism v6.0 software (GraphPad Software, Inc., California, USA).

3.4.6 Fluorescence-activated cell scanning analysis of cell cycle distribution

Melanoma cells were plated at 1×10^5 cells per well of a 24-well plate overnight. CVA21 (MOI = 10 TCID₅₀/cell), DTIC (1 mM), and P (1 μ M) + C (27 μ M) was added. After 24 h, floating cells were collected and combined with trypsinised, adherent cells. Cells were centrifuged at $425 \times g$, washed in PBS and suspended in a small amount of PBS supplemented with 0.1% glucose. Then, ice-cold 70% ethanol was added drop-wise, and the cells were fixed at -20°C. After fixation (24 h later), residual ethanol was removed by centrifugation and treated with PBS supplemented with RNase (100 μ g/mL) (Sigma-Aldrich Pty Ltd, Australia) and propidium iodide (PI) (5 μ g/mL) at room temperature for 30 min. Finally, cells were analysed on a FACSCanto™ II cytometer (Becton Dickinson, Sydney, New South Wales, Australia), where PI was excited at 488 nm and fluorescence analysed at 695 nm (PerCP-Cy5-5). Ten thousand events were collected per analysis. Cell cycle analysis was evaluated by FlowJo vX.0.7 (TreeStar, Ashland, USA) and dead cells were characterised by subdiploid DNA content as detected by flow cytometry.

3.4.7 Caspase 3/7 analysis by caspase-glo assay

The activities of caspase 3/7, were determined using a commercially available kit (Caspase-Glo™3/7 Assay, Promega, Sydney, New South Wales, Australia) based on the ability of caspases to cleave specific amino acid sequences present in a substrate for luciferase. SK-Mel-28, Mel-RM, ME4405 and MV3 cells were plated at 1×10^4 cells per well in 96-well plates and treated the next day with CVA21 (MOI = 10 TCID₅₀/cell) and P + C ($1 \times EC_{50}$). Control cells were left untreated (media only). The Caspase-Glo™ 3/7 luminescence-based report assay lyophilised substrate (DEVD-aminoluciferin powder) was resuspended in Caspase-Glo™ 3/7 lysis buffer and thawed to room temperature. At 24 and 48 h post-treatment, the Caspase-Glo™ 3/7 reagent was added in a 1:1 volume ration to each well. Immediately following the addition of the reagent, the contents of the wells were gently mixed with a plate shaker. After a 1 h incubation, the luminescence was measured with a SpectraMax M5e plate reader (Molecular Devices, Camberwell, Victoria, Australia).

3.5 Animals

3.5.1 Ethics statement and housing conditions

All animal procedures performed were approved by the University of Newcastle Animal Care and Ethics Committee (ACEC) in compliance with the “Guide for the Care and Use of Laboratory Animals, 8th Edition”, under protocol number A-2008-113, A-2008-120, and A-2013-327. Animals were housed in groups of four within HEPA-filtered Techni-Plast Cages (1145 IVC) connected to a Techni-Plast Slim Line air handling system. Cages are held in a humidity- and temperature-regulated animal holding facility under specific-pathogen-free (SPF) conditions with a 12/12 hr light/dark cycle. Animals have free access to food and water *ad libitum*. Animals were allowed to acclimatise to their environment for one week prior to the commencement of the experimental protocol. To limit suffering and for ethical reasons, animals from all studies were humanely euthanised via carbon dioxide (CO₂) asphyxiation when the total tumour mean volume exceeded 2500 mm³ or when the tumour had ulcerated.

3.5.2 Tumour inoculation

In all experiments, the respective cells were harvested with trypsin, washed twice with PBS and resuspended in sterile PBS. The viability of the prepared cells were assessed by trypan blue staining using a TC-10 Automated Cell Counter (Biorad, Hercules, California, USA) and only cell preparations with a viability greater than 95% were used for tumour implantation. Cells were kept on ice to maintain viability. Prior to cell injection, mice were anaesthetised via isoflurane inhalation (4 L/min; induction at 5% and maintenance of general anaesthesia at 2%). At recovery, all animals received 100% oxygen until the gain of righting reflex. In all studies, a group of four mice did not receive tumour cells in order to serve as a no tumour control (NTC) group.

3.5.3 Animal monitoring and tumour measurement

Animals were weighed and examined for tumour development up to three times per week. Two tumour diameters (A , B) were measured using digital callipers and tumour volumes were calculated by using the formula of a spheroid:

$$V = \frac{1}{6} \times \Pi \times A \times B^2$$

where A is the polar diameter and B is the equatorial diameter. Animals were judged to have failed treatment if tumour volume exceeded 2500 mm^3 or had ulcerated resulting in the loss of body fluid (humane survival end point).

3.6 *In vivo* investigations of CVA21 in combination with conventional chemotherapeutic agents for the treatment of melanoma

The primary research objective was to assess the efficacy of CVA21 in melanoma *in vivo* when combined with chemotherapeutic agents DTIC and P + C doublet therapy. Two murine models of melanoma were developed. The first model was performed using severe combined immunodeficient (SCID) mice bearing SK-Mel-28-luc cell xenografts. The second model was performed in immunocompetent C57BL/6 mice using B16- ICAM-1 cells.

3.6.1 Immunodeficient mouse melanoma model study design

3.6.1.1 Animals and treatment schedule

To establish subcutaneous tumours, 2×10^6 SK-Mel-28-luc cells in $100 \mu\text{L}$ of PBS were injected into the flank of female BALB/c SCID mice (Animal Resource Centre, Perth, Western Australia, Australia) aged between six to eight weeks (Section 3.5.2). When subcutaneous tumours reached a volume of approximately $\sim 300 \text{ mm}^3$, intratumoural (i.t.) injections of CVA21 (1×10^8 TCID₅₀/injection) were followed by intraperitoneal (i.p.) injections of DTIC (8 mg/kg), or P (15 mg/kg) in combination with C (50 mg/kg). Animals receiving combination therapy were treated with their respective chemotherapeutics 30 min after receiving CVA21 treatment. All injections were administered in a volume of $100 \mu\text{L}$ per injection. Control animals received an equivalent volume of saline alone. Ten days later, a second dose of chemotherapy was injected intraperitoneally in all mice, according to their respective treatment group. Bloods from mice treated with CVA21 were collected on a weekly basis by venipuncture of the saphenous vein and centrifuged at $10,621 \times g$ for 5 min at room temperature to collect the serum. Serum samples were stored at -80°C for further analysis (Section 3.10). All animals were euthanised at day 77.

3.6.1.2 *In vitro* bioluminescent imaging

Prior to melanoma cell transplantation into mice, cells transduced with the luciferase gene, SK-Mel-28-luc cells were examined for luciferase expression *in vitro* via bioluminescent ima-

ging, using the IVIS™ Imaging System (Xenogen, California, USA). Cells were diluted in a 2-fold serial dilution from 100,000 to 3,125 cells in PBS in a black 96-well tissue culture plate. Twenty microlitres of 1× cell lysis buffer (Promega, Sydney, New South Wales, Australia) was added to lyse cells, releasing their cellular contents. Fifty microlitres of D-luciferin reagent (Xenogen, California, USA) was then added to each well, and bioluminescent intensity (BLI) was immediately examined using the IVIS™ Imaging System. BLI data was then acquired and analysed using Living Image® software v2.50 (Xenogen, California, USA) to quantitate the luminescent output for each well. A standard curve was constructed using the linear regression model from GraphPad Prism v6.0 software (GraphPad Software, Inc., California, USA) to determine the BLI output per cell.

3.6.1.3 Bioluminescent imaging of tumours *in vivo*

Tumour development was also monitored weekly via bioluminescent imaging using the IVIS™ Imaging System 100 (Xenogen, California, USA). A single intraperitoneal injection of luciferase substrate, *d*-luciferin (250 mg/kg in a volume of 50 µL/mouse) (PerkinElmer Inc., USA) was delivered approximately 5 min prior to *in vivo* bioluminescent imaging to allow the development of bioluminescent signals. Animals were anaesthetised using isoflurane at 5% induction via gaseous inhalation. Mice were maintained under anaesthesia (2 - 3% isoflurane) while images were taken in a dorsal position using the sequential acquisition mode of the Living Image® software v2.50 (Xenogen, California, USA). Acquisition was standardised with a 60 s exposure, a 20 cm field of view (Stage position C), and use of the high resolution setting (small binning). Bioluminescent measurements were acquired and analysed using Living Image® software (Xenogen, California, USA). Regions of interest (ROIs) were selected for each mouse and the average radiance of tumours (photons/s/sr/cm²) were quantitated. Bioluminescent images were presented as bioluminescence data overlaid on photographic images.

3.6.2 Immunocompetent mouse melanoma model study design

To establish subcutaneous tumours, 2×10^6 B16-ICAM-1 cells (described in Section 3.1.3) in 100 µL of PBS were injected into the flank of female C57BL/6 mice (Animal Resource Centre, Perth, Western Australia, Australia) aged between six to eight weeks. Animals were housed in the same conditions described previously (Section 3.5.1). Two days prior to tumour implantation, fur at the injection site was removed with a pair of electric clippers. Treatment was initiated four days post tumour cell injection. Animals received i.t.

injections of CVA21 (1×10^8 TCID₅₀/injection), followed by i.p. injections of DTIC (8 mg/kg) or P (15 mg/kg) in combination with C (50 mg/kg). Animals receiving combination therapy were treated with their respective chemotherapeutics 30 min after receiving CVA21 treatment. All injections were administered in a volume of 100 μ L per injection. Control animals received an equivalent volume of saline alone. Mice treated with CVA21 alone or in combination with chemotherapy received three additional injections of CVA21 intraperitoneally on a three day cycle. Two weeks after initiation of the first treatment, mice were treated with a second dose of chemotherapy. Monitoring of animals and tumour development was previously described in Section 3.5.3. Blood samples were collected from all mice on a weekly basis by venipuncture of the saphenous vein and centrifuged at $10,621 \times g$ for 5 min at room temperature to collect the serum. Serum samples were stored at -80°C for further analysis (Section 3.10). All animals were euthanised at day 28.

3.7 Optimisation of the immunocompetent B16-ICAM-1 mouse melanoma model

3.7.1 Animals and treatment schedule

Female C57BL/6 mice (Animal Resource Centre, Perth, Western Australia, Australia) aged between 6 to 8 weeks were housed in the same conditions described previously (Section 3.5.1). Two days prior to tumour implantation, fur at the injection site was removed with a pair of electric clippers. To establish cutaneous tumours, 2×10^5 B16 and B16-ICAM-1 tumour cells in 50 μ L of PBS were injected subcutaneously or intradermally into the flank of animals on day 0 (Section 3.5.2). Successful intradermal (i.d.) injection induced a bleb at the site of inoculation. Animal monitoring was previously described in Section 3.5.3. All animals were euthanised at day 30.

3.7.2 Histological evaluation of tumours using H&E staining method

Tumours harvested during necropsy were preserved in 10% neutral buffered formalin (Sigma-Aldrich Pty Ltd, Australia) solution at 4°C . After fixation and embedding in paraffin, tissue sections were cut to 5 μ m thick sections. To visualise the growth and dissemination of tumour cells in the lungs of mice, haematoxylin and eosin (H&E) staining was performed on the sectioned slides. Briefly, the sections were deparaffinised and rehydrated by immersing the slides in a series of histolene (Fronine Laboratory Supplies, Australia), absolute ethanol (100%), 70% ethanol and water for 1-2 min each. Slides were then stained with

Carazzi's hematoxylin (Fronine Laboratory Supplies, Australia) before being differentiated with a brief immersion into acid alcohol (97% ethanol with 3% hydrochloric acid) (Fronine Laboratory Supplies, Australia). Nuclei were stained blue when slides were immersed in Scott's tap water substitute (Sigma-Aldrich Pty Ltd, Australia). To counterstain the connective tissues pink, sectioned slides were then immersed in eosin (Sigma-Aldrich Pty Ltd, Australia) before being dehydrated in a series of absolute ethanol (100%) and histolene. Stained tissue sections were then mounted with resin-based Entellan[®] New Mounting media (ProSciTech Pty Ltd., Australia) and cover-slipped before being left to air-dry overnight. Photomicrographs of sections were taken at 20 \times magnification using the ScanScope Spectrum[™] slide scanner v11.2.0.780 (Aperio Technologies Inc., California, USA).

3.7.3 Tumour cell isolation and primary culture

Immediately following resection, tumours were placed in 4°C normal saline and transported to the laboratory. Using aseptic technique, excess fat and normal tissue were removed and the tumours washed with sterile PBS. The trimmed tumours were placed in a petri dish filled with 10 mL of trypsin. Using sharp dissection scissors, tumours were minced into 1 - 3 mm³ chunks and homogenised. The tumour homogenates were then filtered through a sterile 70 μ m nylon cell strainer (BD Falcon, Australia), washed with PBS and centrifuged at 425 $\times g$ for 5 min at 4°C. Cells were re-suspended using DMEM supplemented with 10% FCS, 10 mM sterile HEPES (ThermoScientific, Australia), 2mM L-glutamine (ThermoScientific, Australia), sodium pyruvate (Invitrogen, Australia) and 100 IU/mL penicillin-streptomycin (Invitrogen, Australia). Cell counts and viability were determined by trypan blue staining and the use of a TC-10 Automated Cell Counter (Biorad, Hercules, California, USA).

3.8 Animal immunisation with oncolysates and tumour challenge

Preparation of oncolysates and the control vaccine were described in Section 3.2.3. Female C57BL/6 mice (Animal Resource Centre, Perth, Western Australia, Australia) aged between six to eight weeks were immunised intraperitoneally with CVA21 alone (2×10^8 TCID₅₀/injection), control vaccine ($\sim 2 \times 10^5$ lysed tumour cells/injection), control vaccine + CVA21, or CVA21 oncolysate ($\sim 2 \times 10^5$ lysed tumour cells/injection). All injections

were administered in a volume of 200 μL per injection. Control animals received an equivalent volume of saline alone. Animals were housed in the same conditions described previously (Section 3.5.1). Fourteen days later, all animals were challenged with 2×10^5 B16 cells intradermally and development of flank tumour was recorded (Section 3.5.2). Animals were monitored regularly as described in Section 3.5.3 and survival was defined as the time to euthanasia. All animals were euthanised at day 31.

3.9 CVA21 in combination with immune checkpoint inhibitors for the treatment of melanoma *in vivo*

The primary research objective was to evaluate combinatorial strategies of oncolytic CVA21 with PD-1 and CTLA-4 systemic blockade. The overall study design was focused on therapeutic efficacy in reducing primary tumour burden, prolonging survival, and protection from a secondary tumour challenge, as described in the sections below.

3.9.1 CVA21 and PD-1 blockade in an immunocompetent murine model of melanoma

Female C57BL/6 mice (Animal Resource Centre, Perth, Western Australia, Australia) aged between four to six weeks were housed in the same conditions described previously (Section 3.5.1). Fur at the injection site was removed with a pair of electric clippers two days prior to tumour implantation to allow sufficient recovery of any inflammation generated from the shaving. To establish cutaneous tumours, 2×10^5 B16-ICAM-1 cells in 50 μL of PBS were injected intradermally into the right flank of animals (Section 3.5.2). On days 6, 9, 12, and 15, animals were treated with i.t. injections of CVA21 (1×10^8 TCID₅₀/injection), followed by i.p. injections of anti-PD-1 murine antibody (12.5 mg/kg). Control groups received a corresponding dose of i.p. isotype antibody (12.5mg/kg; clone: 2A3) and i.t. PBS. All i.t. injections were administered in a volume of 100 μL per injection whereas i.p. injections were administered in a volume of 200 μL per injection. Mice treated with CVA21 alone or in combination with immunotherapy received four additional weekly injections of CVA21 (1×10^8 TCID₅₀/injection) intratumourally. On day 31, 2×10^5 B16 cells in a volume of 50 μL were injected intradermally into the left flank of remaining animals. Monitoring of animal's wellbeing and tumour development was previously described in Section 3.5.3 and survival was defined as the time to euthanasia. Blood samples were collected from all mice on a weekly basis by venipuncture of the saphenous vein and centrifuged at $10,621 \times g$ for

5 min at room temperature to collect the serum. Serum samples were stored at -80°C for further analysis (Section 3.10). All animals were euthanised at day 66.

3.9.2 CVA21 and CTLA-4 blockade in an immunocompetent murine model of melanoma

Female C57BL/6 mice (Animal Resource Centre, Perth, Western Australia, Australia) aged between four to six weeks were housed in the same conditions described previously (Section 3.5.1). The hind flanks of mice were shaved using electric clippers three days prior to the injection of tumour cells to allow sufficient recovery time. To establish cutaneous tumours, 2×10^5 B16-ICAM-1 cells in 50 μL of PBS were injected intradermally into the right flank of animals (Section 3.5.2). On days 7, 10, 13, and 16, animals were treated with i.t. injections of CVA21 (1×10^8 TCID₅₀/injection), followed by i.p. injections of anti-CTLA-4 murine antibody (12.5 mg/kg). Control groups received a corresponding dose of i.p. isotype antibody (12.5mg/kg; clone: 2A3) and i.t. PBS. All i.t. injections were administered in a volume of 100 μL per injection whereas i.p. injections were administered in a volume of 200 μL per injection. No additional CVA21 injections were administered thereafter. On day 37, 2×10^5 B16 cells in a volume of 50 μL were injected intradermally into the left flank of remaining animals. Monitoring of animal's wellbeing and tumour development was previously described in Section 3.5.3 and survival was defined as the time to euthanasia. Blood samples were collected from all mice on a weekly basis by venipuncture of the saphenous vein and centrifuged at $10,621 \times g$ for 5 min at room temperature to collect the serum. Serum samples were stored at -80°C for further analysis (Section 3.10). All animals were euthanised at day 77.

3.10 Serum analysis

3.10.1 Quantitative RT-PCR detection of CVA21 viral genomes in sera

Serum samples of all animals were analysed to determine the levels of CVA21 RNA using realtime quantitative RT-PCR. One step RT-PCR was carried out using the SuperScript III Platinum One-Step qRT-PCR Kit (Invitrogen, Australia). The primers and probe were specific for the VP3 region of the CVA21 (Kuykendall) genome and were designed using Primer Express 1.5 Software (Applied Biosystems, Foster City, CA). The sequence for the forward primer (KKVP3fwd) was 5'-GAGCTAA ACCACCAACCAATCG-3' and the reverse primer (KKVP3rev) was 5'-CGGTGCAA CCATGGAACAA-3'. The FAM labelled

probe (KKVP3) used was 6FAM- CACACACAT CATCT GGGGA-MGB. In a volume of 25 mL, the reaction mixture comprised 1× SuperScript reaction mix, 500 nM forward primer, 500 nM reverse primer, 250 nM probe, 500 nM ROX, 0.5 mL SuperScript III RT/Platinum Taq Mix and 5 µL of extracted RNA. Quantitative RT-PCR reactions were carried out using the ABI Prism 7000 Sequence Detection System (Applied Biosystems). Cycling conditions consisted of 30 min at 60°C followed by 5 min at 95°C and then 50 cycles of 15 s at 95°C and 1 min at 60°C. Samples were quantitated against pre-validated CVA21 RNA standards of known concentration. Results were reported as TCID₅₀ equivalents/ml for viraemia positive serum.

3.10.2 Detection of CVA21 viraemia levels

Viral infectivity assays were conducted to determine CVA21 viraemia levels in serum of mice. Confluent monolayers of SK-Mel-28 cells grown in 2% FCS supplemented DMEM in 96-well tissue culture plates were inoculated with serum samples prepared as 10-fold serial dilutions (100 µL/well in quadruplicate). Negative control (untreated cells) wells were included in each plate. Following incubation of cells at 37°C in a 5% CO₂ environment for 72 h, cells were microscopically examined for cellular lysis (viral-induced CPE). Cell survival was quantitated by visual scoring of CPE and the 50% viral endpoint titres were calculated using the Karber method [197]. The viraemia results were then graphed and analysed using the GraphPad Prism v6.0 software (GraphPad Software, Inc., California, USA).

3.10.3 Anti-CVA21 neutralising antibody assay

To test for presence of anti-CVA21 neutralising antibodies, serum samples were briefly heat inactivated by incubation at 56°C for 30 min and were diluted in 2% FBS supplemented DMEM at 2-fold serial dilutions from 1:32 to 1:2048. One hundred microlitres of each serum dilution was incubated with 100 µL of CVA21 virus stock (containing 100 TCID₅₀) at 37°C for 1 h. Fifty microlitres of this serum/virus mixture was then titrated in triplicate on SK-Mel-28 cells grown in a 384-well tissue culture plate. A +IgG control (positive control) was commercially obtained from the Commonwealth Serum Laboratories (Sandoglobulin[®] NF Liquid; Batch number: 43228-00002) and was included on each plate. Plates were then incubated at 37°C in a 5% CO₂ environment for 72 h, before being examined microscopically for the development of CPE, and stained with crystal violet/formalin solution (0.1% crystal violet, 20% methanol, and 4% formaldehyde in PBS)

for 24 h. Intact cells stain purple when incubated with crystal violet. Neutralisation titres were calculated using the Karber method [197], whereby serum neutralising titres $> 1:32$ were considered positive. The neutralising titre values were then analysed and graphed using the GraphPad Prism v6.0 software (GraphPad Software, Inc., California, USA).

3.10.4 Cell viability assay with serum *ex vivo*

Cytotoxic activity was assessed in serum of animals (day 42) that received anti-CTLA-4 administration. SK-Mel-28 cells were seeded onto 96-well plates and incubated overnight. Cells were then incubated with media only (containing 2% FCS), CVA21 (containing 100 TCID₅₀), and the serum samples (1:100) at 37°C for 72 h. Photomicrographs of cells were taken at 72 h post-incubation using an Olympus IX70 inverted microscope with a DP72 digital camera (Olympus) at 40× and 100× magnification.

3.11 Statistical analysis

All data were expressed as mean \pm standard error mean (SEM) and obtained from at least three independent experiments unless otherwise stated. Comparisons between groups were done using the two-tailed Student's *t*-tests or the one-way ANOVA tests where appropriate. For synergy analysis, all median dose-effect parameters, CI values, isobolograms, and Fa-CI plots were calculated by CompuSyn software (Biosoft, Cambridge, UK) and re-graphed with GraphPad Prism v6.0 software (GraphPad Software, Inc., California, USA). For analysis of animal data, statistical analysis between treatment groups was conducted with the two-way ANOVA test corrected for multiple comparison with Tukey's method. Log-rank (Mantel-Cox) test and log-rank test for trend was used for determining the statistical significance of the difference in Kaplan-Meier survival between the treatments. All data analyses were carried out using GraphPad Prism v6.0 software (GraphPad Software, Inc., California, USA). *P*-values below 0.05 were considered statistically significant, where $*P = < 0.05$, $**P = < 0.01$, $***P = < 0.001$, $****P = < 0.0001$.

Chapter 4

Combination of CVA21 with conventional chemotherapy drugs *in vitro*

Coxsackievirus A21 (CVA21) Kuykendall strain, is a naturally occurring common-cold virus that has the inherent capacity to preferentially target, infect and destroy malignant cells. The oncolytic properties of CVA21 as an anticancer agent have been demonstrated in both *in vitro* and *in vivo* studies, against different types of cancers, including breast and prostate cancer, malignant glioma, multiple myeloma, NSCLC, and melanoma. The patient tolerance profile to multiple administration of CVA21 and potential efficacy are currently being investigated in phase I/II clinical trials. Within a clinical setting, increased potency and a low toxicity profile are requirements for the successful control of cancer, and one current trend to achieve this target is the use of combination of virotherapy with mainstream therapies such as chemotherapy. A fundamental requirement of this strategy is that the combination chemotherapy does not interfere with the life cycle of the oncolytic virus from the point of viral entry to the release of viral progeny.

In this chapter, we assessed the effectiveness of CVA21 oncolysis in combination with dacarbazine (DTIC) or with the doublet chemotherapy regimen of paclitaxel and carboplatin (P + C). The goal was to investigate whether melanoma cell destruction could be improved by combining oncolytic CVA21 with the conventional chemotherapies compared to the respective monotherapies and whether these chemotherapeutic agents would inhibit CVA21 oncolysis. The combinatorial effects were assessed in a panel of human melanoma cell lines via the combination index (CI) method. The mechanism of synergy was elucid-

ated using viral yield assays and cell cycle analysis. These results were further translated into *in vivo* animal models and are presented in the later chapters.

4.1 Oncolytic activity of CVA21 in a panel of human melanoma cells

The *in vitro* susceptibility of melanoma cell lines to CVA21 was first determined. Cell monolayers of four human melanoma cell lines (SK-Mel-28, Mel-RM, ME4405 and MV3) were infected with serially diluted CVA21 and incubated at 37°C, 5% CO₂, for 72 h. Cells were then observed under a microscope for any detectable CPE. Within 72 h, quantification of CVA21 mediated cell lysis using MTT cell viability assays revealed that CVA21 induced significant levels of cell death in all four melanoma cell lines in a dose-dependent manner (Figure 4.1). The 50% effective concentration (EC₅₀) of CVA21, defined as the initial virus dose (multiplicity of infection [MOI], expressed as 50% tissue culture infectious dose per cell [TCID₅₀/cell]) that resulted in 50% cell viability at 72 h post-infection as compared to untreated controls, ranged from $1.48 \times 10^{-5} \pm 9.38 \times 10^{-6}$ to 3.68 ± 2.31 (mean \pm SD from three separate experiments) TCID₅₀/cell (Table 4.1). Dose response curves from all four cell lines infected with CVA21 revealed that viability was reduced in a dose-dependent manner. SK-Mel-28 was found to be most sensitive to CVA21 infection, followed by Mel-RM, ME4405 then MV3 in descending order respectively.

Table 4.1: EC₅₀ values of CVA21 in four melanoma cell lines. EC₅₀: 50% effective concentration defined by the initial MOI (TCID₅₀/cell) to achieve 50% cell death at 72 h post-infection. Data is presented as mean \pm SD from three independent experiments. The SK-Mel-28 cell line was most susceptible to CVA21 infection, followed by Mel-RM, ME4405 and MV3.

Melanoma cell line	EC ₅₀ (TCID ₅₀ /cell: mean \pm SD)
SK-Mel-28	$1.48 \times 10^{-5} \pm 9.38 \times 10^{-6}$
Mel-RM	$1.11 \times 10^{-3} \pm 1.15 \times 10^{-3}$
ME4405	$4.59 \times 10^{-2} \pm 4.02 \times 10^{-2}$
MV3	3.68 ± 2.31

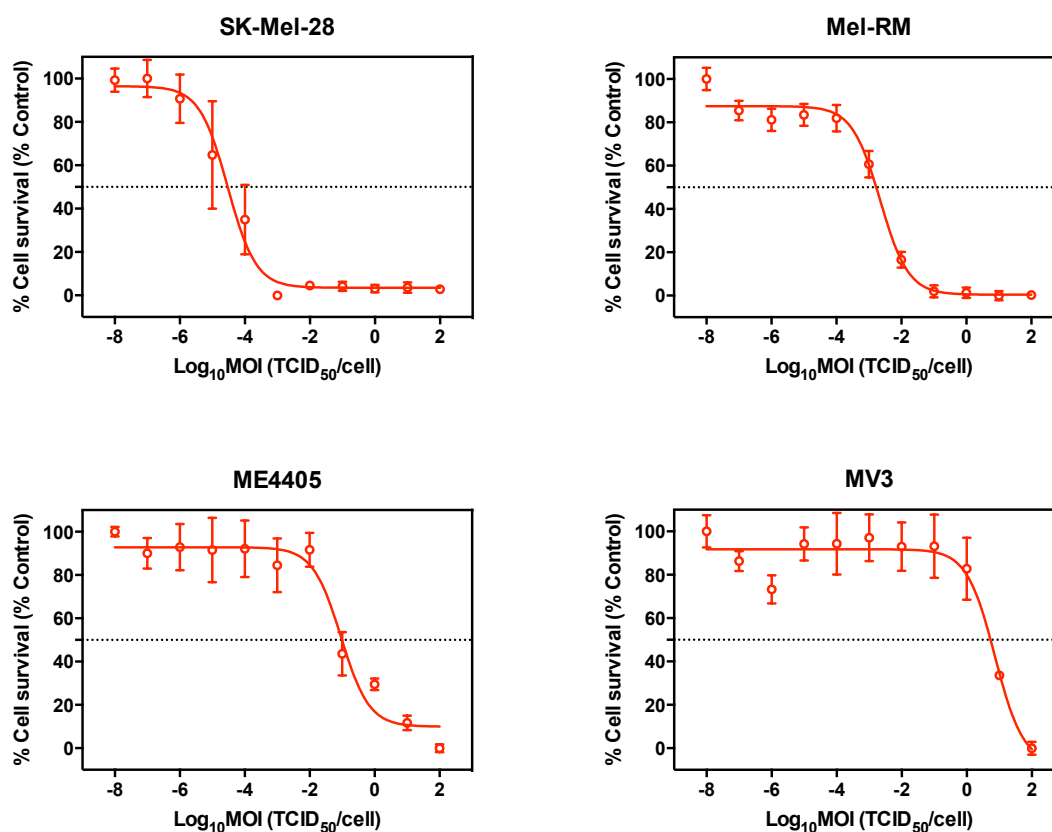


Figure 4.1: Oncolytic effect of CVA21 in melanoma cells. Dose-dependent cell death expressed as % cell survival induced by CVA21 in four melanoma cell lines evaluated by the MTT viability assay at 72 h post-infection. CVA21 dose is defined as MOI expressed in TCID₅₀/cell. The curves were fitted by non-linear regression (sigmoidal dose-response) using GraphPad Prism v6.0 (GraphPad Software, Inc., California, USA) for all four cell lines. Data points indicate the mean of quadruplicate values \pm SEM and are representative of three independent experiments.

Cells were also infected with an MOI of 10 TCID₅₀/cell and photomicrographs were taken at 8, 24, 48 and 72 h post-infection (Figure 4.2). CPE was noticeable as early as 24 h post-infection in the SK-Mel-28 and Mel-RM cell line, showing that the infected cells became circular and detached from the cell monolayer. Oncolytic virus-mediated cell lysis was observed in all cell lines 72 h post-infection.

4.2 *In vitro* chemosensitivity assay of DTIC and P + C on a panel of melanoma cell lines

In parallel, the cytotoxic effects of chemotherapeutic agents, DTIC and P + C doublet chemotherapy was investigated. Confluent monolayers of SK-Mel-28, Mel-RM, ME4405

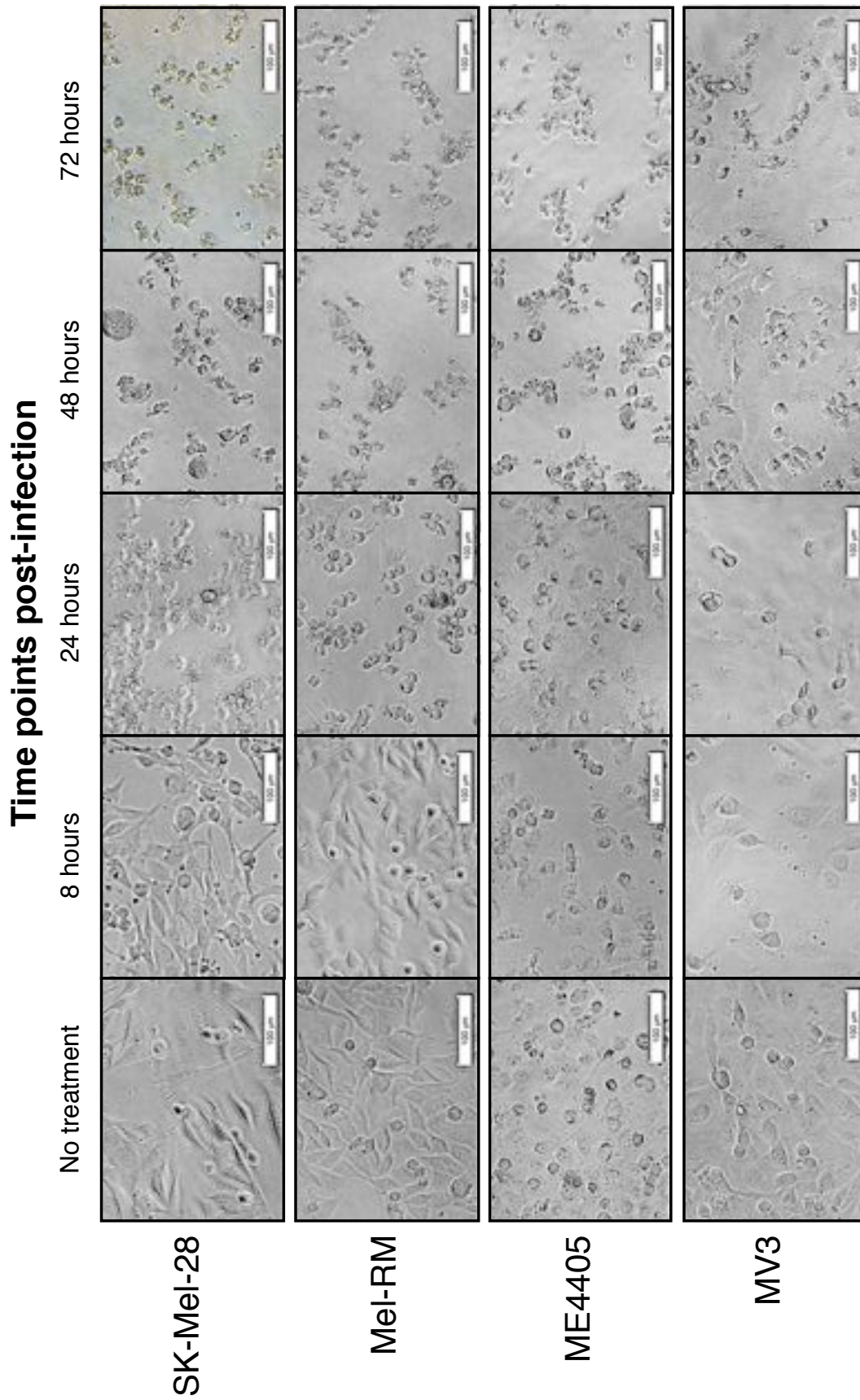


Figure 4.2: Cytopathic effects of CVA21 in melanoma cells. Photomicrographs show CPE in all melanoma cell lines infected at an MOI of 10 TCID₅₀/cell. All images were taken at 8, 24, 48, and 72 h post-CVA21 infection using an Olympus IX70 inverted microscope with a DP72 digital camera at 100× magnification. Complete cell destruction was observed in all cell lines 72 h post-infection.

and MV3 cells were incubated with increasing concentrations of DTIC (4 to 4,400 μM) and P (0.55 to 35.13 μM) + C (14.78 to 946.05 μM). After 72 h, cytotoxic effects were determined in each cell line by the MTT viability assay, and results expressed as the drug concentration that inhibited cell viability by 50% compared to the untreated control cells (EC_{50}).

DTIC treatment showed a dose-dependent anti-tumour effect in all cell lines tested (Figure 4.3). At a concentration of 2,200 μM , a 72 h exposure to DTIC suppressed the proliferation of Mel-RM ($67.24 \pm 1.32\%$) and ME4405 ($58.70 \pm 2.92\%$) cells by up to 50% or higher, whereas SK-Mel-28 ($37.34 \pm 1.32\%$) and MV3 ($31.06 \pm 13.65\%$) showed only partial responses to the chemotherapy treatment. SK-Mel-28 showed the highest resistance to DTIC treatment and the EC_{50} value could not be determined. Not surprisingly, DTIC treatment was not successful in completely destroying any of the studied cell lines even at very high concentrations.

All cell lines were also exposed to doses of P and C as single agents and in combination. Dose optimisation studies were carried out (data not shown) and the combination molar ratio of 1 : 27 μM (P : C) was used for all further studies. For example, data from the ME4405 cell line showed that combination of P + C doublet chemotherapy was more potent than single-agent therapies over a range of concentrations (Figure 4.4A). After determining the optimum ratio of P and C, the EC_{50} value of P together with C as a combination agent was determined (P + C). All four melanoma cell lines also showed dose-dependent cytotoxicity after exposure to P + C doublet chemotherapy (Figure 4.4B). ME4405 had the best cytotoxic response with an EC_{50} value of 3.163 ± 0.523 (mean \pm SD) μM . In contrast, SK-Mel-28 was more resistant to the P + C doublet therapy with an EC_{50} value of 8.344 ± 5.788 μM . This is consistent with previous reports that characterised SK-Mel-28 as a multi-drug resistant cell line [530]. A summary of the EC_{50} values obtained for both DTIC and P + C against the four melanoma cell lines are presented in the table below (Table 4.2).

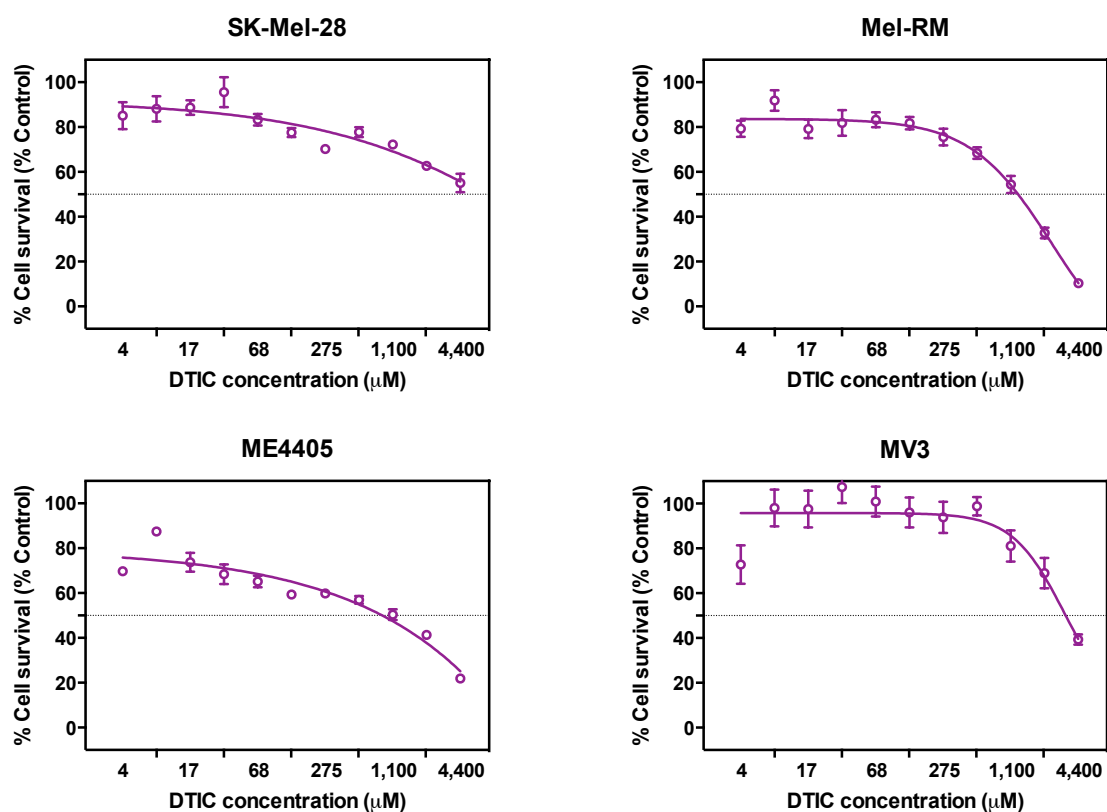
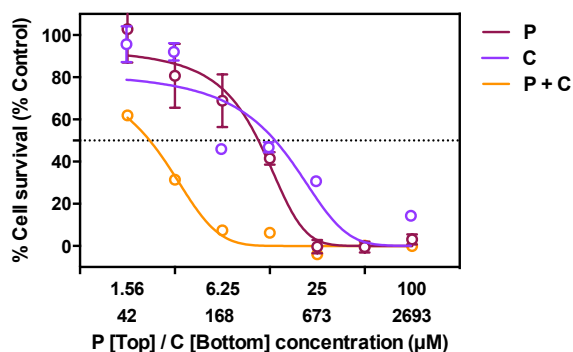


Figure 4.3: Dose response curve of DTIC in melanoma cells. Dose-dependent cell death expressed as % cell survival induced by DTIC in four melanoma cell lines at 72 h post-treatment. SK-Mel-28 showed high levels of resistance to DTIC treatment. The curves were fitted by non-linear regression [log(inhibitor) *vs* response - variable slope (four parameters)] using GraphPad Prism v6.0 software (GraphPad Software, Inc., California, USA) for all four cell lines. Data points indicate the mean of quadruplicate values \pm SEM and are representative of three independent experiments.

A



B

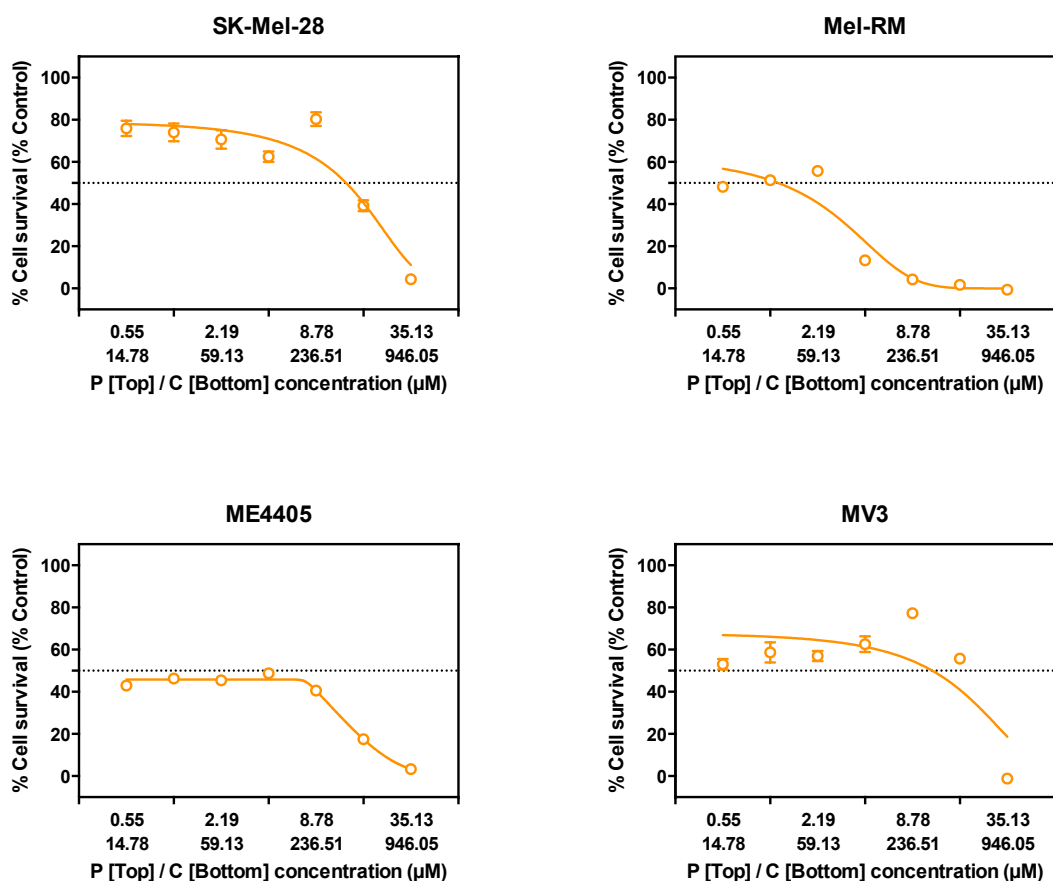


Figure 4.4: Dose response curve of P + C doublet chemotherapy in melanoma cells. (A) The combination of P + C was synergistic. ME4405 melanoma cells were exposed to 2-fold serial dilutions of P + C at a ratio of 1 : 27 μM (P : C) and incubated at 37°C, 5% CO₂ for 72 h. (B) Dose-dependent cell death shown as % cell survival induced by P + C in four melanoma cell lines evaluated by MTT assay at 72 h post-treatment. The curves were fitted by non-linear regression [log(inhibitor) *vs* response - variable slope (four parameters)] using GraphPad Prism v6.0 software (GraphPad Software, Inc., California, USA) for all four cell lines. Data points indicate the mean of quadruplicate values \pm SEM and are representative of three independent experiments.

Table 4.2: EC₅₀ values of DTIC and P + C in four melanoma cell lines. EC₅₀ values were obtained from the dose response curve. Concentrations of DTIC and P + C were expressed as mM and μ M respectively. Only the concentration of P was shown for the doublet chemotherapy. The ratio of P : C was maintained at 1 : 27 μ M. Data is presented as mean \pm SD from three independent experiments. SK-Mel-28 was not sensitive to DTIC treatment (>100 mM indicates that a maximum value was not found and that extremely high doses of DTIC still had little effect). Similarly, SK-Mel-28 was relatively resistant to the combination of P + C as well.

Drug & cell lines	Drug sensitivity EC ₅₀ (mM/ μ M: mean \pm SD)
DTIC	
SK-Mel-28	>100 (mM)
Mel-RM	2.589 ± 0.617 (mM)
ME4405	5.084 ± 1.213 (mM)
MV3	3.325 ± 1.115 (mM)
P + C	
SK-Mel-28	8.344 ± 5.788 (μ M)
Mel-RM	4.101 ± 3.615 (μ M)
ME4405	3.163 ± 0.523 (μ M)
MV3	4.210 ± 1.800 (μ M)

Confluent monolayers of SK-Mel-28, Mel-RM, ME4405 and MV3 were then exposed to DTIC and P + C at their respective EC₅₀ concentrations. Photomicrographs of each cell line were taken at 8, 24, 48, and 72 h post-treatment using an Olympus IX70 inverted microscope with a DP72 digital camera at 100 \times magnification. Cells treated with DTIC showed minimal changes to the cell's structure and morphology (Figure 4.5). These photos reflect the poor efficacy of DTIC in treating melanoma as seen in the dose response curves presented earlier.

In contrast, photomicrographs of cells treated with P + C revealed changes in morphology and cell membrane blebbing, which are characteristic of apoptosis (Figure 4.6). These changes were most evident in the ME4405 cell line where membrane blebbing was observed 8 h post-treatment. Interestingly, despite significant changes to the morphology of the SK-Mel-28 line, no signs of cell death were observed even after 72 h exposure. This implies that even higher concentrations would be needed to completely eradicate multi-drug resistant cell lines, though these concentrations may not be practical in a clinical setting without generating undesirable adverse effects.

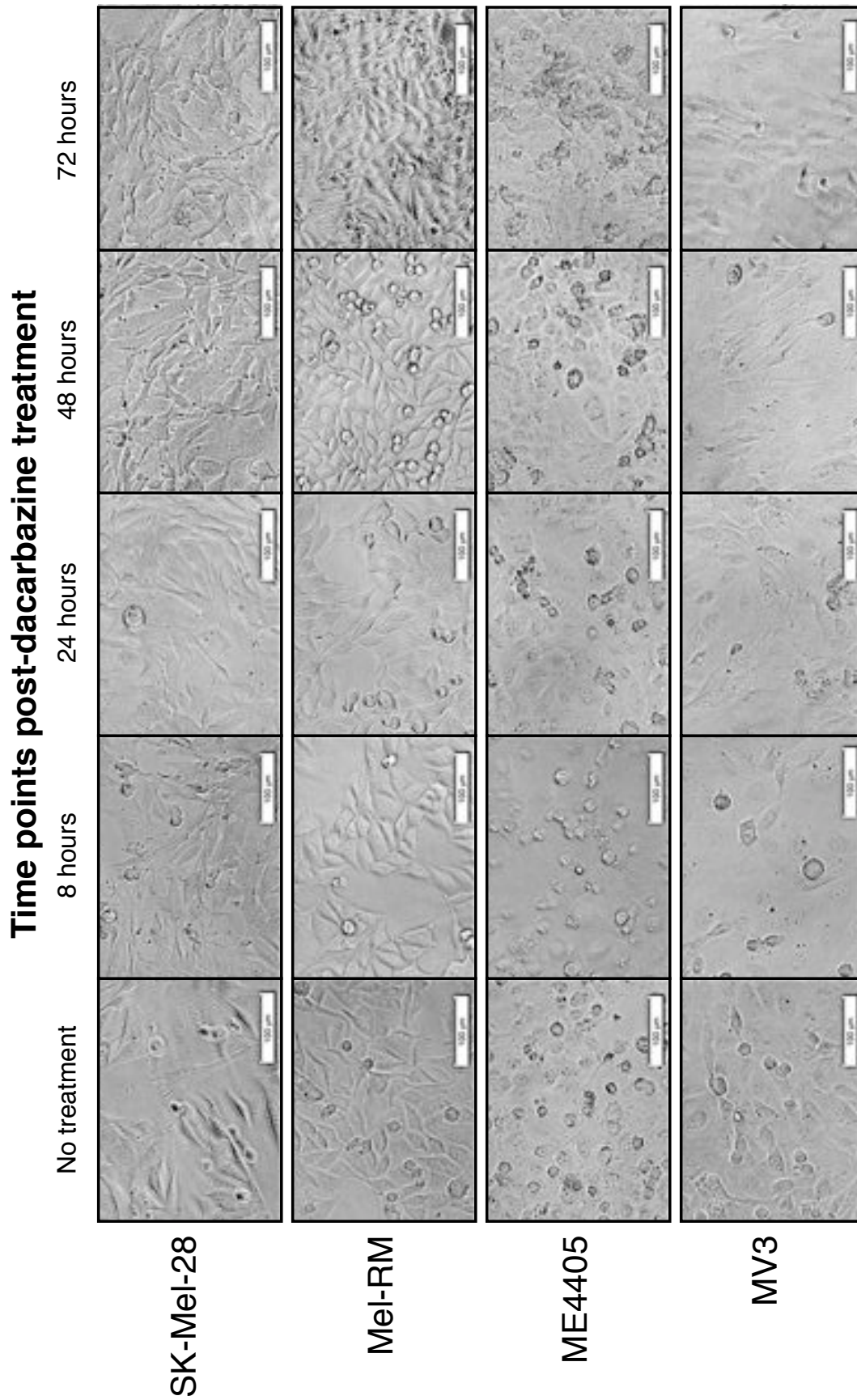


Figure 4.5: Cytotoxic effect of DTIC on melanoma cells. Photomicrographs show a panel of melanoma cells exposed to DTIC at their respective $1 \times EC_{50}$ concentration (Table 4.2). Minimal changes to the cell's structure or morphology were observed in any of the cell lines. No changes were observed in the highly resistant SK-Mel-28 cell line. All images were taken at 8, 24, 48, and 72 h post-treatment using an Olympus IX70 inverted microscope with a DP72 digital camera at $100\times$ magnification.

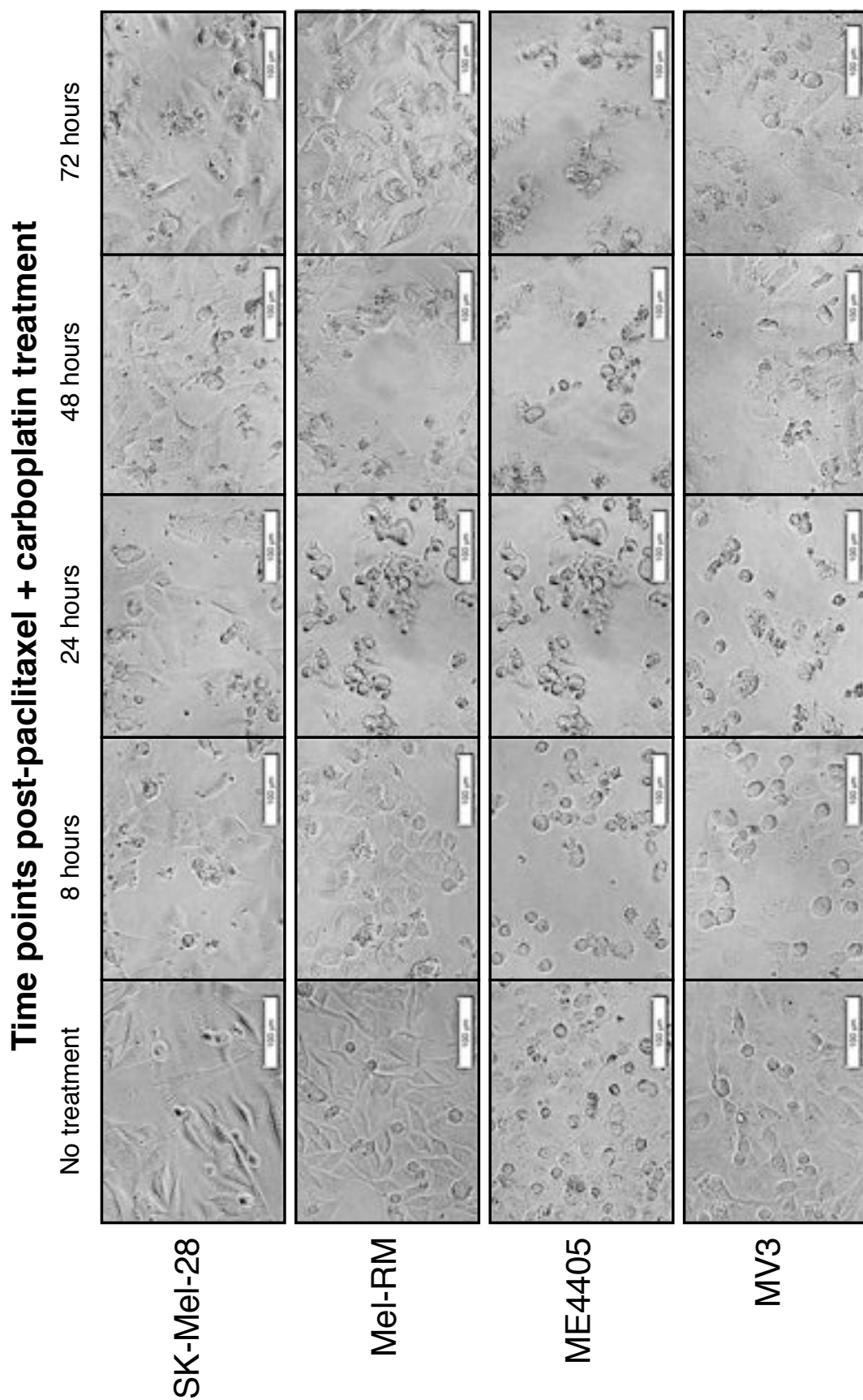


Figure 4.6: Cytotoxic effect of P + C doublet chemotherapy on melanoma cells. Photomicrographs show a panel of melanoma cells exposed to P + C at their respective $1 \times EC_{50}$ concentration (Table 4.2). Extensive cytotoxicity can be clearly seen in the ME4405 cell line with morphological changes starting as early as 8 h post-treatment. Cellular changes were most prominent 72 h post-treatment. All images were taken at 8, 24, 48, and 72 h post-treatment using an Olympus IX70 inverted microscope with a DP72 digital camera at $100\times$ magnification.

4.3 *In vitro* combination studies with CVA21

The drug DTIC and more recently P + C doublet chemotherapy are typically the first-line chemotherapeutic agents used for the treatment of malignant melanoma. To assess whether these chemotherapies interfere with CVA21 oncolysis of melanoma cells, and to explore potential synergism, SK-Mel-28, Mel-RM, ME4405 and MV3 were treated with a combination of CVA21 and DTIC or P + C doublet chemotherapy. The cytotoxicity of CVA21, DTIC and P + C as single agents or in combination was measured using the MTT viability assay across a range of the individual EC_{50} doses determined previously (Table 4.1 and 4.2). Data for Mel-RM, ME4405 and MV3 show that combination of CVA21 with DTIC is more potent than single agent therapies at all EC_{50} ratios (Figure 4.7A). Similarly, a better response was achieved with the combination of CVA21 and P + C doublet therapy and CVA21 oncolysis was not inhibited in these three cell lines (Figure 4.7B). Improved cell death in the SK-Mel-28 line was only observed at the higher concentrations of both DTIC and P + C doublet therapy in combination with CVA21.

The type of interaction between CVA21 and the chemotherapy drugs was formally evaluated using Chou-Talalay's equations. Table 4.3 shows the dose-effect parameters (Dm , m , and r) as well as the CI values of all the combinations tested. Concordant with the results shown in Figure 4.7, the CVA21 and DTIC combination caused significant levels of cell death and these translated to synergistic activity from EC_{50} to EC_{95} in Mel-RM, ME4405 and MV3 (Figure 4.3). For the SK-Mel-28 cell line, the CVA21 and DTIC combination was antagonistic across all EC ranges. Interestingly, the level of synergism between CVA21 and P + C therapy was concentration driven and cell line dependent. This combination was synergistic at lower concentrations for SK-Mel-28, Mel-RM and MV3, while stronger synergism was observed at higher combination ratios in the ME4405 cell line. SK-Mel-28 cells which are typically highly sensitive to CVA21 infection, were not as sensitive when treated with CVA21 and P + C in combination. Most combination ratios of CVA21 and P + C were highly antagonistic with only the CI value at EC_{50} being slightly synergistic.

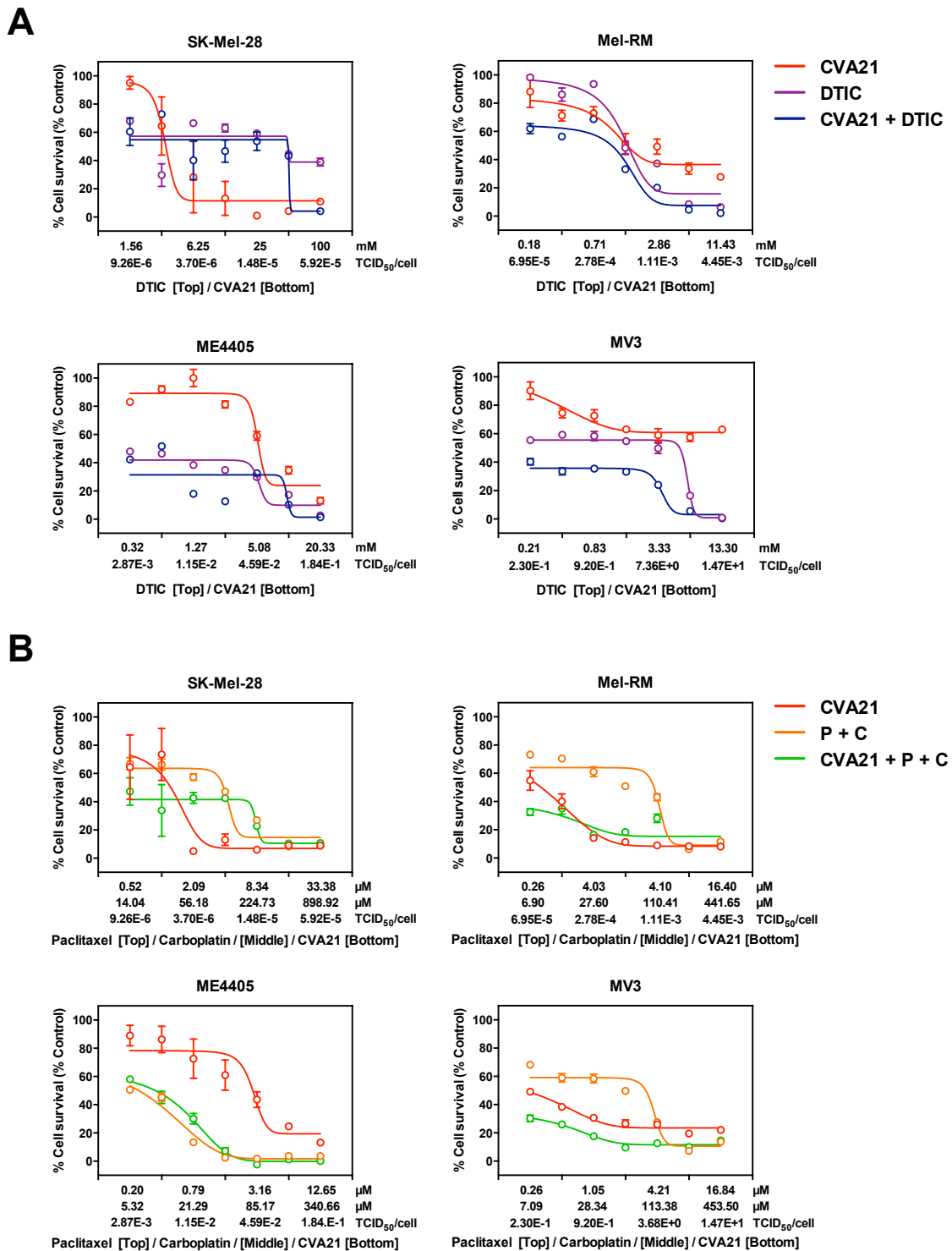


Figure 4.7: Dose response curves of CVA21 in combination with chemotherapy in SK-Mel-28, Mel-RM, ME4404 and MV3 cells. (A) The effects of combining CVA21 with DTIC. The following combination resulted in enhanced cell death in Mel-RM, ME4405 and MV3. DTIC and CVA21 in combination was shown to be antagonistic in the treatment of SK-Mel-28 cells. **(B)** The combination effects of CVA21 with P + C. The following combinations were generally synergistic on all cell lines at low concentrations except SK-Mel-28. The curves were fitted by non-linear regression (sigmoidal dose-response) using GraphPad Prism v6.0 software (GraphPad Software, Inc., California, USA) for all four cell lines. Data points indicate the mean of quadruplicate values \pm SEM and are representative of three independent experiments.

Table 4.3: Combination index (CI) values of each cell line treated with CVA21 and chemotherapy. Evaluation of drug-drug interaction in a panel of melanoma cell lines at 50%, 75%, 90% and 95% inhibition.

Drugs & Cell lines	Combination Index (CI) values						
	EC ₅₀	EC ₇₅	EC ₉₀	EC ₉₅	Dm^1	m^2	r^3
DTIC + CVA21							
SK-Mel-28	>10	>10	>10	>10	7.435	0.651	0.739
Mel-RM	0.477	0.500	0.605	0.720	0.555	1.119	0.932
ME4405	0.663	0.560	0.474	0.423	0.372	0.805	0.824
MV3	0.427	0.407	0.398	0.394	0.667	1.000	0.839
P + C + CVA21							
SK-Mel-28	0.868	2.115	5.160	9.466	0.615	0.511	0.882
Mel-RM	0.202	0.792	3.170	8.234	0.046	0.381	0.765
ME4405	2.585	1.543	0.921	0.648	0.334	1.677	0.980
MV3	0.038	0.121	0.889	4.409	0.011	0.282	0.773

¹ Dm : The median-effect dose, usually depicted at the EC₅₀ value of the dose-effect curve

² m value: a measurement of sigmoidicity of the dose-effect curve; $m = 1, > 1, < 1$ indicates hyperbolic, sigmoidal, and negative sigmoidal

³ r value: correlation coefficient; $r = 1$ perfect conformity, poor r value may be a result of biological variability

To further illustrate this complex relationship, isobolograms at EC₅₀, EC₇₅ and EC₉₀ were generated. Since CVA21 and both drugs have entirely independent modes of action, the conservative isobologram method was applied [147]. The effective concentration (EC₅₀, EC₇₅ and EC₉₀) refers to the concentration of a drug or the combination of the two drugs that induces 50%, 75% and 90% inhibition of cell viability [144]. Figure 4.8 and 4.9 shows the conservative isobologram plots of EC₅₀, EC₇₅ and EC₉₀ for the DTIC and P + C doublet combination separately. In the conservative isobologram plot, the diagonal connecting each axis indicates the simulated additive effect for EC₅₀, EC₇₅ and EC₉₀. The experimental EC₅₀, EC₇₅ and EC₉₀ doses of the combination treatment groups are displayed as the single point labelled with the respective CI value. Point values for the combination treatment that fall below the diagonal are considered synergistic, while those that are above the diagonal are antagonistic.

For example, in the EC₅₀ isobologram (Figure 4.8A, far right), from the simulated diagonal of the additive effect, it shows that to reach 50% inhibition of MV3 cell viability requires approximately 17 MOI CVA21 or 0.8 μ M DTIC. However, with the combination of CVA21 and DTIC, it takes a lower dose (1 MOI CVA21 plus 0.3 μ M DTIC) to achieve the same efficacy, suggesting that the combination treatment elicits a greater effect than an

additive effect. The results in Figure 4.8A - C have demonstrated that the combination of CVA21 and DTIC at EC_{50} , EC_{75} and EC_{90} elicits a synergistic anti-tumour effect in Mel-RM, ME4405 and MV3 cell lines at most of the tested concentrations. However, combining CVA21 and DTIC at all combination ratios resulted in high levels of antagonism in the SK-Mel-28 line.

Similarly, point values of the CVA21 and P + C combination in Mel-RM, ME4405 and MV3 cell lines were to the lower left of the hypotenuse, indicating synergistic effects (Figure 4.9A - C). The CVA21 and P + C combination was also antagonistic when tested in the SK-Mel-28 cell line. Interestingly, combining CVA21 with P + C doublet therapy at increasing concentrations resulted in CI values that fell far to the right of the diagonal in the SK-Mel-28 and Mel-RM cell lines. In contrast, synergistic interactions were improved at higher combination ratios in the ME4405 line. Taken together, interaction of CVA21 with chemotherapy is likely to be cell line and concentration-dependent.

Additionally, as the drug-drug interactions may change as a function of concentration or activity, the combination data for each cell lines were evaluated using representative plots of the CI values over a range of affected fractions (F_a) (Figure 4.10). In most instances, the combination of CVA21 + DTIC was found to exert moderate to strong synergistic effects in the Mel-RM, ME4405 and MV3 cell lines, as shown by the CI values that were consistently lower than 1 (Figure 4.10A). The combination was highly antagonistic for the SK-Mel-28 cell line and CI values were beyond the limit of the F_a -CI representative plot. For CVA21 in combination with P + C, very strong synergism was observed at lower concentration ratios but became increasingly antagonistic at higher concentrations in the SK-Mel-28, Mel-RM and MV3 cell lines (Figure 4.10B). Combination data from the ME4405 cell line was only synergistic at higher concentrations. In summary, combination studies suggest that CVA21 and DTIC were synergistic in three out of the four cell lines tested at most concentrations, and that the combination of CVA21 with P + C exhibited mild to strong synergism depending on the dosage and cell line employed.

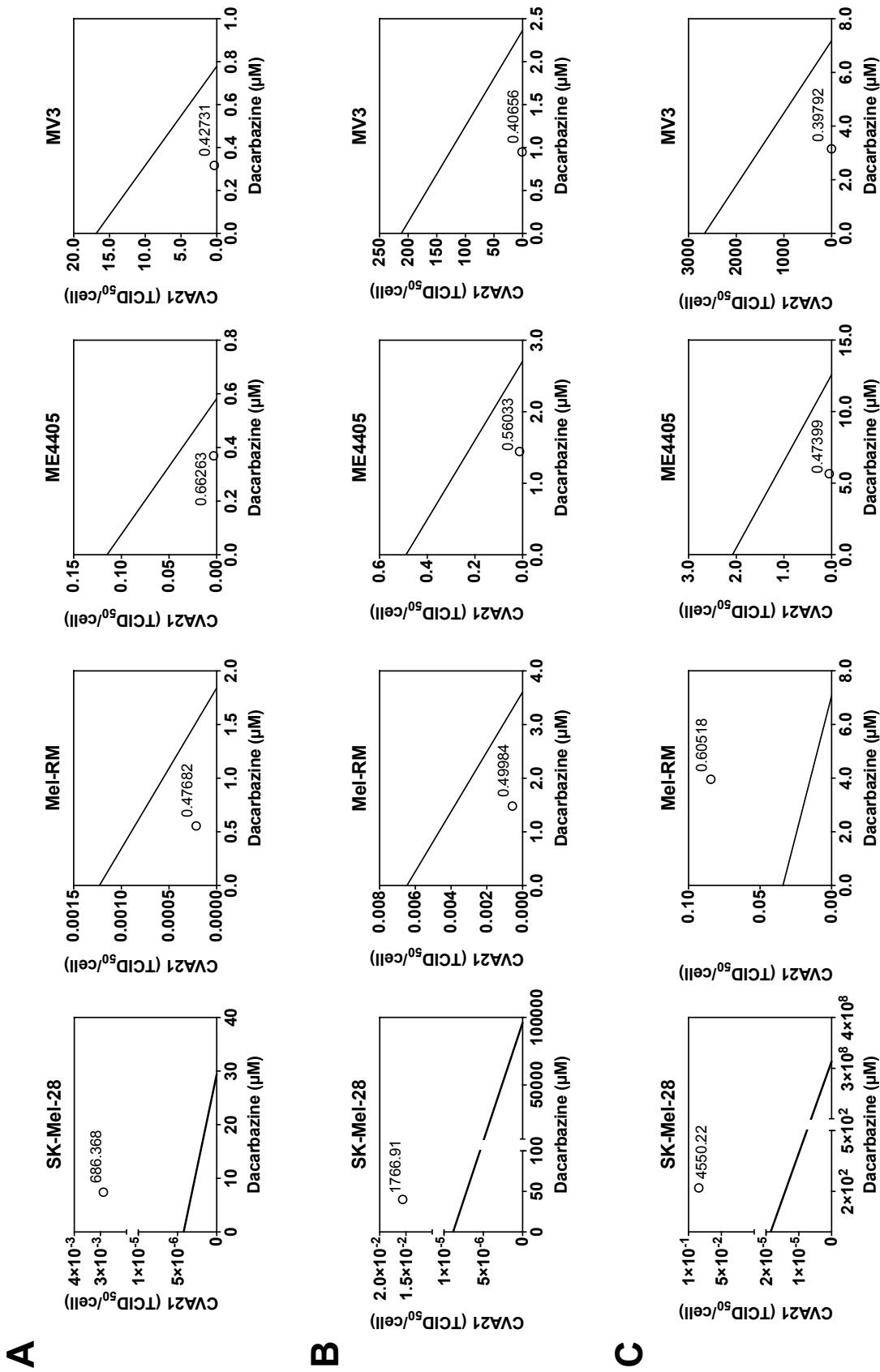


Figure 4.8: Isobolograms showing the interaction between CVA21 and DTIC at EC_{50} , EC_{75} and EC_{90} . The doses of CVA21 and DTIC necessary to achieve (A) 50% cell kill, (B) 75% cell kill, and (C) 90% cell kill are plotted on the y- and x- axis respectively, and the connecting solid line represent the expected additive effects for combination therapy. Synergism is indicated by the EC points located on the lower left of the diagonal. Antagonism is implied by the EC points located on the upper right above the diagonal. Experimental combination doses required to generate the respective level of cell killing is indicated by the circle. CVA21 concentration is expressed as $TCID_{50}/cell$ and DTIC as μM . The results are representative of three independent experiments.

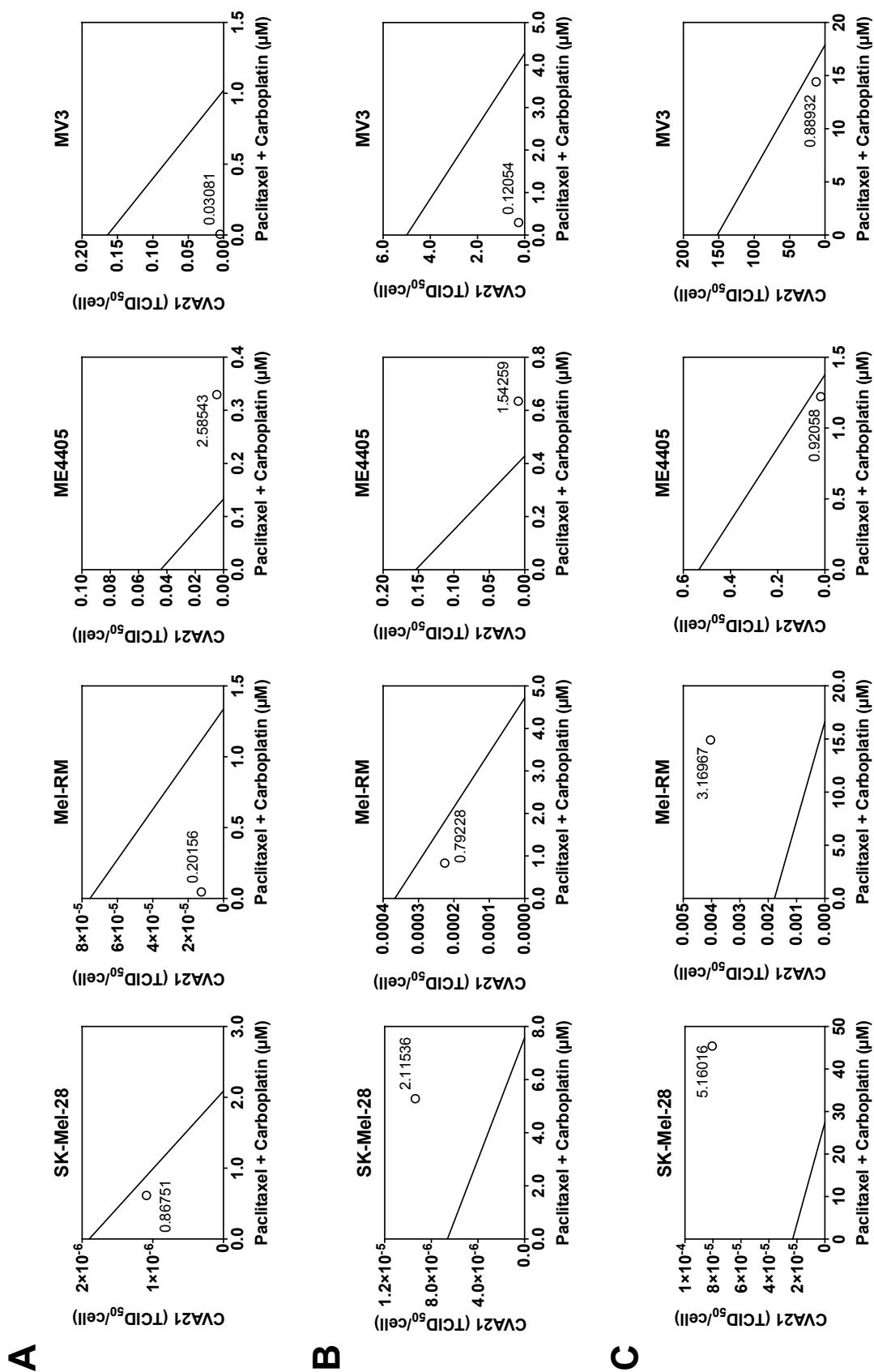


Figure 4.9: Isobolograms showing the interaction between CVA21 and P + C at EC₅₀, EC₇₅ and EC₉₀. The doses of CVA21 and P + C necessary to achieve (A) 50% cell kill, (B) 75% cell kill, and (C) 90% cell kill are plotted on the y- and x- axis respectively, and the connecting solid line represent the expected additive effects for combination therapy. Synergism is indicated by the EC points located on the lower left of the diagonal. Antagonism is implied by the EC points located on the upper right above the diagonal. Experimental combination doses required to generate the respective level of cell killing is indicated by the circle. CVA21 concentration is expressed as TCID₅₀/cell. The combination of P + C is expressed as the concentration of P (µM) at the ratio of 1 : 27, P : C. The results are representative of three independent experiments.

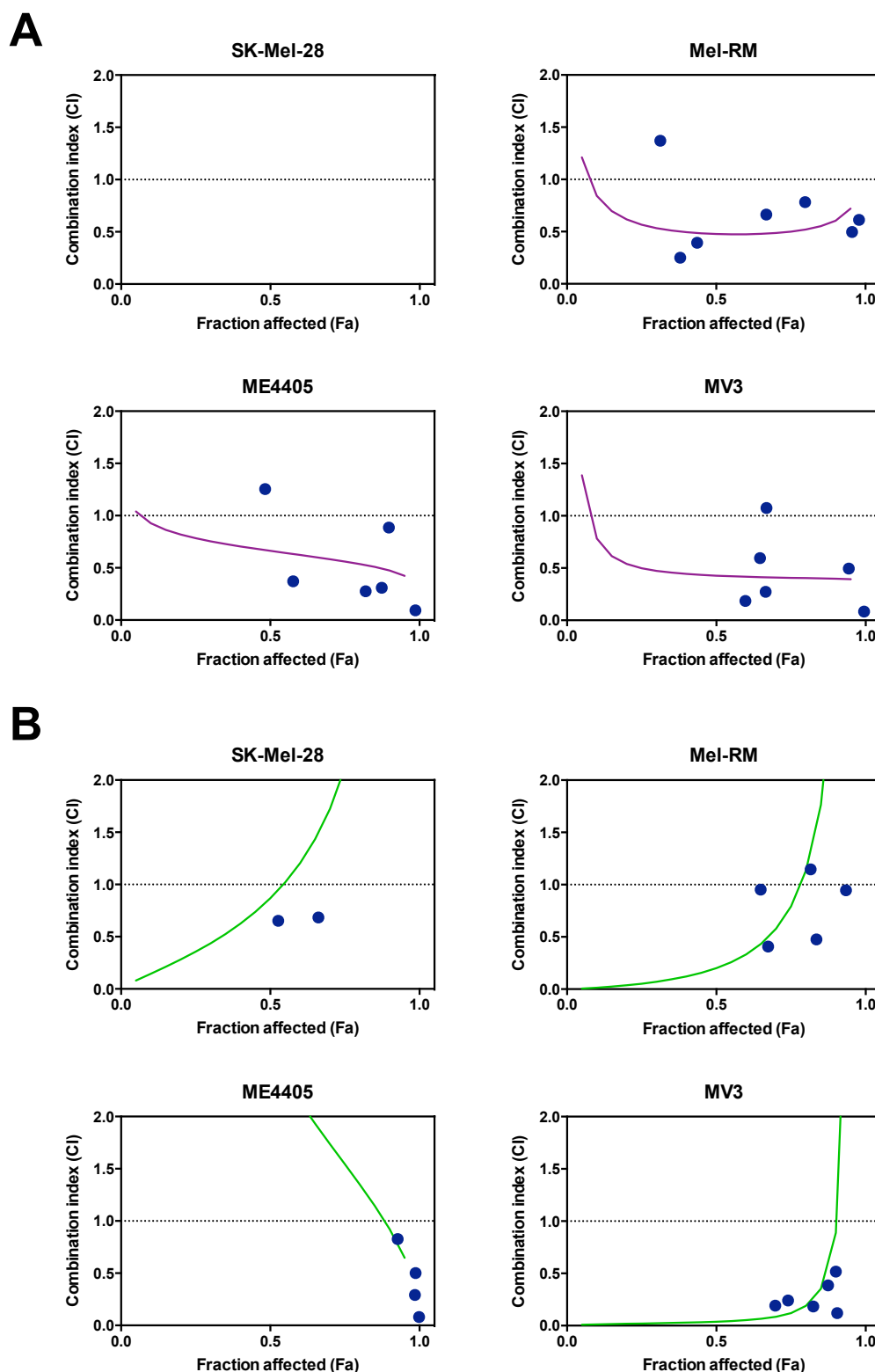


Figure 4.10: Fraction affected (Fa) - combination index (CI) plot. Cells were treated with CVA21 in combination with (A) DTIC or (B) P + C at concentrations corresponding to their EC_{50} values in multiples of $0.0625\times$, $0.125\times$, $0.25\times$, $0.5\times$, $1\times$, $2\times$ or $4\times$. The additive effect of CVA21 with the respective chemotherapy is represented at $CI = 1$ (dotted line), $CI < 1$ indicates synergism, while $CI > 1$ indicates antagonism. The Fa-CI plot was constructed using experimental data points (circles) and by simulating CI values over the entire range of Fa values from 5% to 95% (solid line) using CompuSyn software (Biosoft, Cambridge, UK).

4.4 Examination of viral replication within cells in the presence of chemotherapy

To determine whether the increased cytotoxicity of cells treated with the various drugs was supported by enhanced viral replication, or inhibited in the SK-Mel-28 cell line, CVA21 viral replication in the presence of chemotherapy exposure in all cells was assessed. Cell monolayers were infected with CVA21 at a MOI of 10 TCID₅₀/cell. After 1 h of incubation in a 37°C and 5% CO₂ environment, cell monolayers were then washed three times to remove unbound virus particles. Infected cell monolayers were then replenished with standard growth media supplemented with 2% FCS for the virus only treatment wells. For the combination treatment, infected cells were treated with standard growth media containing either the DTIC or P + C at 1× the respective EC₅₀ value. Samples were harvested at 0, 8, 24, 48 and 72 h following infection. One-step growth curves were generated for all cells as described previously [Section 3.4.5].

In all four cell lines, CVA21 viral titres in cells infected with virus alone, increased up to 48 h and decreased at 72 h post-infection (Figure 4.11). CVA21 replication kinetics was quickest in the SK-Mel-28 and Mel-RM cell line, peaking at 24 h post-infection with a viral titre of 2.51×10^8 TCID₅₀/mL and 2.32×10^8 TCID₅₀/mL respectively. For ME4405 and MV3 cells, peak viral titres were 1.74×10^8 TCID₅₀/mL and 2.32×10^6 TCID₅₀/mL respectively, at 48 h post-infection. CVA21 titres were decreasing at 72 h post-infection in all four cell lines. SK-Mel-28 cells which were highly sensitive to CVA21 supported the highest levels of replication with 1.36×10^8 TCID₅₀/mL after 72 h. In contrast, MV3 cells which were least susceptible to CVA21 infection supported the lowest levels of viral replication, with viral titres of 8.93×10^5 TCID₅₀/mL at 72 h.

The results of the one-step growth curve show that CVA21 viral yields were slightly lower in the presence of DTIC, compared to virus alone (Figure 4.11A). The difference was most pronounced in the Mel-RM cell line, where viral titres of cell treated with DTIC were consistently lower than cell treated with the virus alone. Though not statistically significant for any time points ($P > 0.05$), these data suggest CVA21 viral replication could be slightly suppressed when used together with DTIC.

On the other hand, there were minimal alterations in the kinetics of CVA21 replication

in all cell lines in the presence of P + C, which suggests that viral replication was not affected by the doublet chemotherapy treatment (Figure 4.11B). Interestingly, with the exception of the SK-Mel-28 cell line, viral titres in all other cell lines treated with P + C were increased at 72 h post-infection. The increase in viral titre was not statistically significant in all cell lines ($P > 0.05$) but the data suggest that the total virus production may still increase 72 h later. Surprisingly, CVA21 replication in the SK-Mel-28 cell line was not affected by the addition of DTIC or P + C, suggesting that the antagonism observed was not related to viral yield.

4.5 Cytotoxic activity of CVA21 with DTIC or P + C at clinically relevant concentrations

To ensure the oncolytic ability of CVA21 was not compromised at clinically relevant concentrations of DTIC and P + C, confluent SK-Mel-28 cells were treated with serial dilutions of CVA21 but fixed concentrations of chemotherapy. SK-Mel-28 cells were selected as they were the most susceptible cell line to a CVA21 infection and any inhibition would be easily detected. The cells were treated with different MOIs of CVA21 (from 0.0001 - 10 TCID₅₀/cell). Media supplemented with 55 μ M and 274 μ M DTIC; 0.19 μ M P / 27 μ M C, 0.94 μ M P / 135 μ M C and 1.87 μ M P / 673 μ M C were added simultaneously and cell morphology was observed 72 h later with crystal violet staining. The percentage of cell death was assessed with MTT cell viability assays and used to construct dose-response curves.

Infection of SK-Mel-28 cells at 0.01 TCID₅₀/cell resulted in 82% survival where as 55 μ M DTIC and 0.94/135 μ M P/C showed 76% and 75% survival respectively (Figure 4.12A & B). However, when CVA21 and DTIC or P + C were administered simultaneously at these concentrations, cell survival decreased significantly to 31% and 37% respectively ($P < 0.0001$). Our finding suggests that the combination of CVA21 with either DTIC or P + C significantly reduced cell viability in the multi-drug resistant SK-Mel-28 at clinically relevant concentrations. Furthermore, the combination with DTIC did not appear to have a negative influence on the viability of SK-Mel-28, in contrast to the combination data shown earlier.

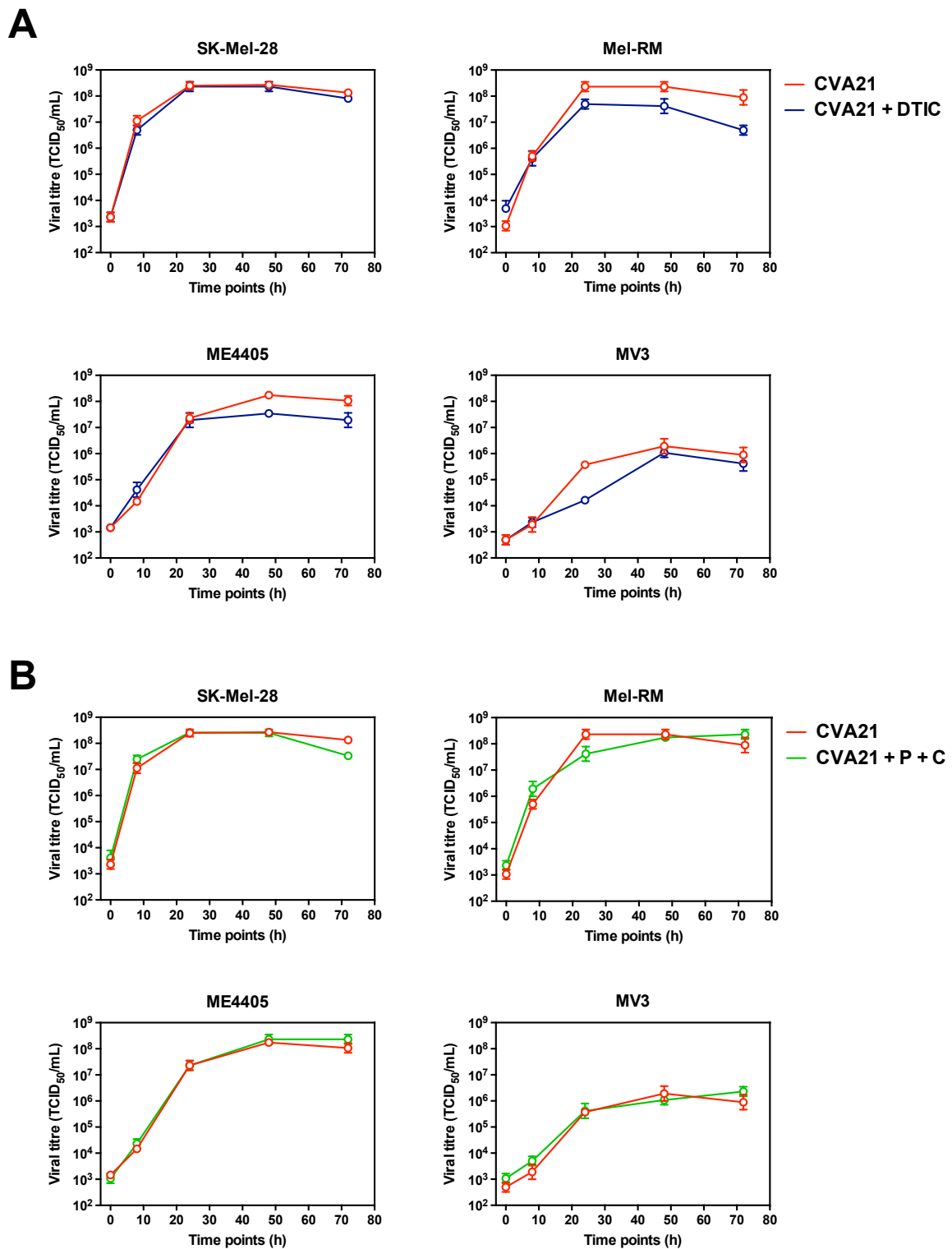


Figure 4.11: Effect of DTIC and P + C on CVA21 one step replication kinetics over time. A panel of melanoma cells were infected with CVA21 at MOI 10 TCID₅₀/cell alone or in combination with 1× EC₅₀ concentrations of either (A) DTIC or (B) P + C. Cell monolayers were challenged with CVA21 for 1 h, and samples were collected at 0, 8, 24, 48, 72 h. Viral titres were determined by end-point titrations in SK-Mel-28 cells. Data are presented as the mean ± SD from two independent experiments. *P*-values were derived from the two-way ANOVA with Bonferroni's correction for multiple comparison, where **P* < 0.05. Treatment groups were each tested for significance against single agent CVA21 treatment.

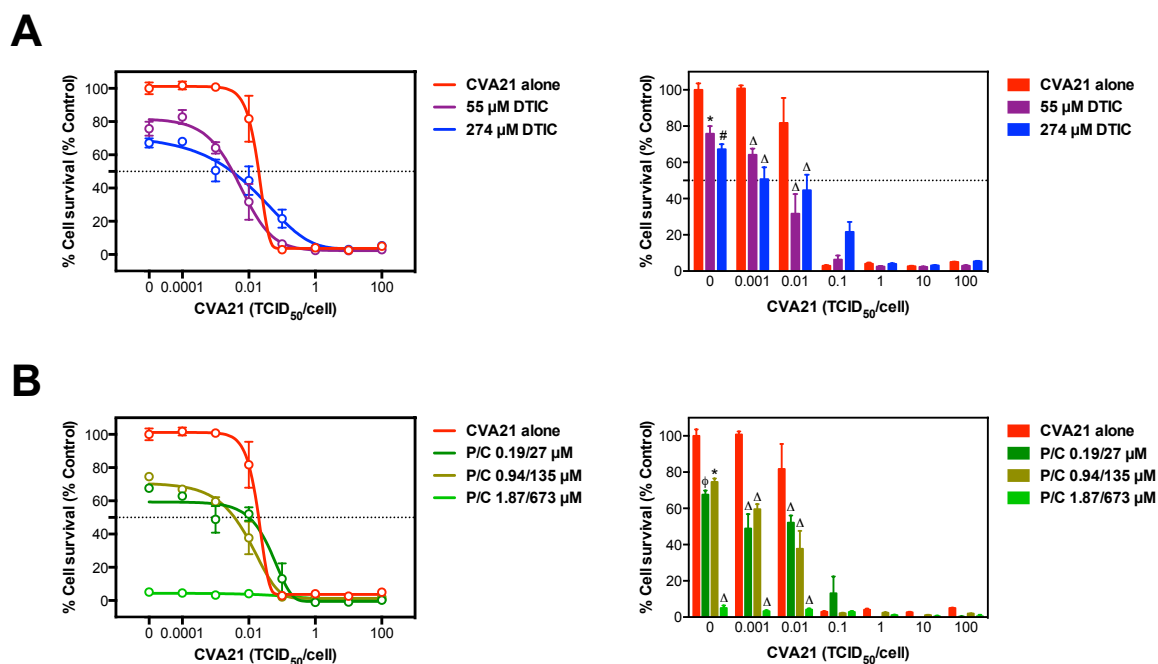


Figure 4.12: Dose-dependent cytotoxicity of CVA21 in combination with DTIC and P + C on SK-Mel-28 cells. SK-Mel-28 cells were treated with 0.0001 - 10 TCID₅₀/cell CVA21 alone or in combination with fixed concentrations of (A) DTIC and (B) P + C. The results were quantitated into cell viability %. Data points indicate the mean of quadruplicate values \pm SEM and are representative of three separate experiments. Combination treatments were compared with controls using the two-way ANOVA analysis with Bonferroni's correction for multiple comparison, where $*P < 0.05$, $\#P < 0.01$, $\phi P < 0.001$, $\Delta P < 0.0001$). Only comparisons that show significance were indicated.

Morphological changes in SK-Mel-28 cells were assessed by crystal violet staining, in parallel with the cytotoxic assays. DTIC alone had minimal effects on SK-Mel-28's morphology even after 72 h (Figure 4.13A). Decreased cell numbers and cell shrinkage were indicative of apoptosis as observed in cells treated with P + C alone as early as 8 h post-treatment (Figure 4.13B). Importantly, the oncolytic effects of CVA21 was not inhibited by either DTIC or P + C, and increased cell death was achieved. These data demonstrated that while the combinatory interaction was highly antagonistic (with DTIC) or mildly synergistic (with P + C) using Chou-Talalay's 'constant ratio model', improved efficacy was achieved with clinically relevant concentrations.

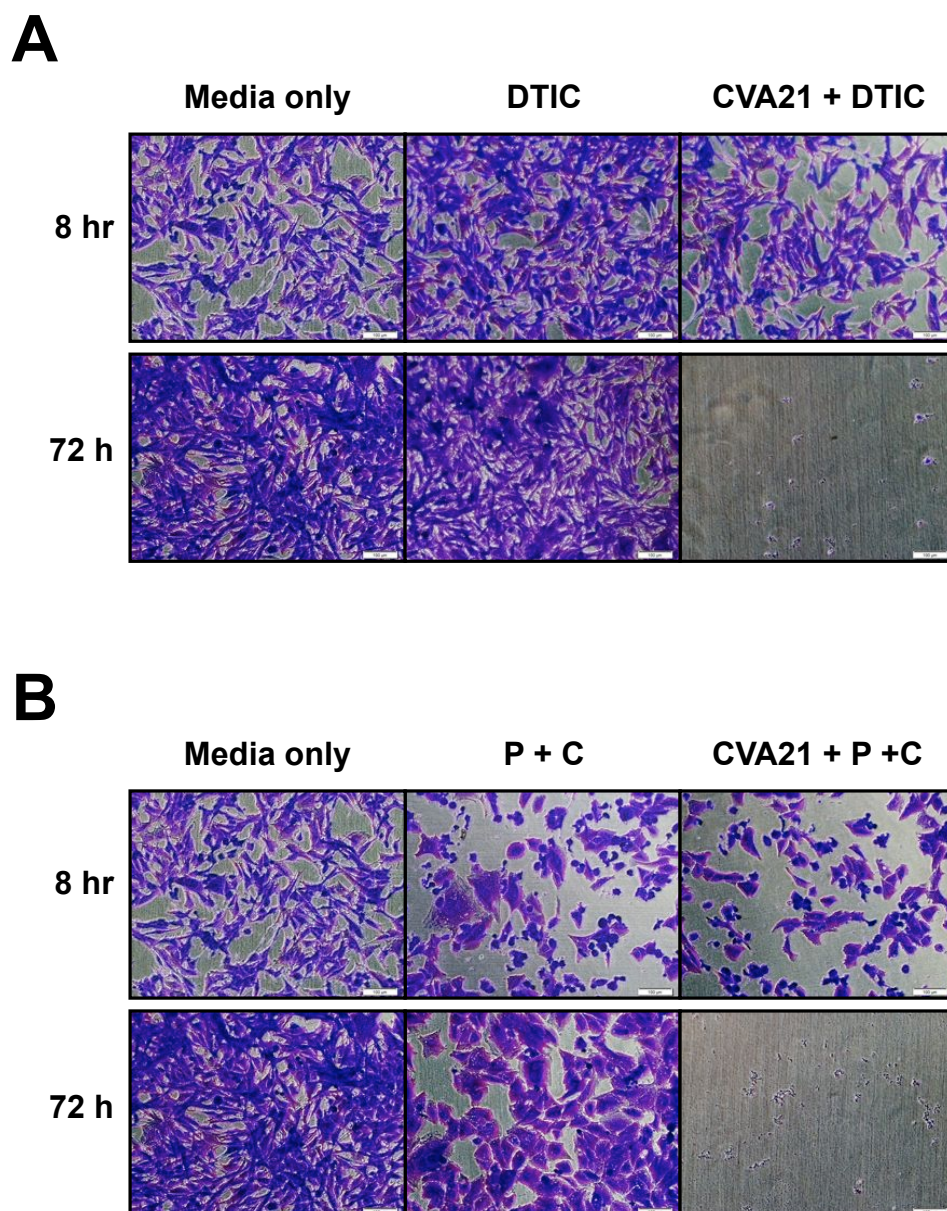


Figure 4.13: Morphological changes in SK-Mel-28 cells observed using crystal violet stain. Photomicrographs show SK-Mel-28 cells exposed to (A) DTIC (55 μ M) and (B) P (0.19 μ M) + C (27 μ M) in combination with CVA21 (MOI = 10 TCID₅₀/cell). All images were taken at 8 and 72 h post-treatment using an Olympus IX70 inverted microscope with a DP72 digital camera at 100 \times magnification. Cells were stained with 0.1% crystal violet/formalin for 24 h before photos were taken.

4.6 Effects of CVA21 with DTIC and P + C on the cell cycle

Whilst relatively little is known concerning the effect of CVA21 infection on the cell cycle, the mechanism of action of DTIC and P + C is proposed to be cell-cycle dependent. To further investigate the effects of CVA21 in combination with DTIC and P + C, cell cycle distribution was determined by fluorescence-activated cell scanning analysis for all four cell lines. Cells were treated with: CVA21 (MOI of 10 TCID₅₀/cell); DTIC (1 mM); P (1 μ M) + C (27 μ M) or the combination therapy of CVA21 with either DTIC or P + C for 24 h. The percentage of cells in each phase of the cell cycle was calculated. The cell cycle distribution of untreated control cells did not change significantly, consisting of \sim 70% in G1 phase, \sim 12% of cells in S phase and \sim 18% of cells in G2/M phase of the cell cycle. Similar to untreated control cells, data from all four melanoma cell lines after 24 h incubation with CVA21 alone did not show major alterations in the cell cycle, though some accumulation of cells in the S-phase was noted (Figure 4.14). The effects of DTIC on the cell cycle was minimum. The treatment appears to have induced an accumulation of cells in the G1 phase in the ME4405 and MV3 cell line, a S-phase accumulation in the Mel-RM cell line, but was largely ineffective in SK-Mel-28 cells. Interestingly, higher levels of accumulation in the S-phase were observed in the Mel-RM cell line when treated with the combination treatment, largely at the expense of the G1 population, with the G2/M fraction remaining relatively stable.

On the other hand, P + C treatment triggered a G2/M arrest in all cell lines at varying degrees, with the accumulation most noticeable in the MV3 cell line. As expected, the accumulation observed was largely at the expense of the G1 population with the S phase fraction remaining unaffected. The most striking feature of the experiment was the emergence of the sub-G1/G₀ population indicative of DNA degradation as a result of cell death. Detection of the sub-G1/G₀ population was present in all cell lines except SK-Mel-28, but was substantially more pronounced in the ME4405 and MV3 cell line. Moreover, the combination of CVA21 with either chemotherapy increased the percentage of sub-G1/G₀ cells in the ME4405 and MV3 cell line. This was accompanied by a decrease in G2/M cells while G1 and S-phase cell population remain relatively unaltered, suggesting that the addition of the virus could have accelerated the cell death process.

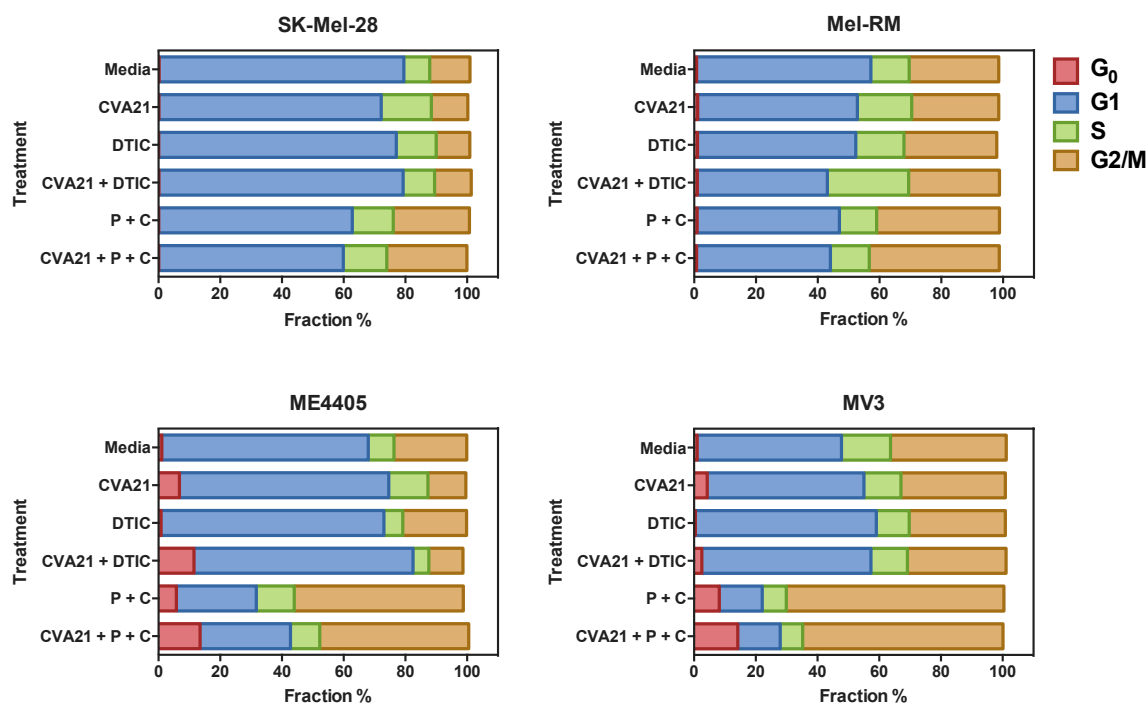


Figure 4.14: Effects of CVA21 and chemotherapy individually and in combination on the cell cycle. Cell monolayers were treated with: CVA21 (MOI of 10 TCID₅₀/cell); P (1 μ M); DTIC (1 mM); P (1 μ M) + C (27 μ M) and the combination therapy (same concentrations as above) for 24 h. Cells were then harvested, washed once in PBS, and resuspended in a 0.1% glucose/PBS and ice-cold 70% ethanol solution. After fixation, cells were rinsed and resuspended in a PI staining solution supplemented with RNase. Cell cycle status was assessed by fluorescence-activated cell scanning. Results were presented as percentage of cells in each phase of the cell cycle and are representative data from two independent experiments.

4.7 Effects of combination therapy with CVA21 and P + C on caspase-3/7 activation

To gain a mechanistic insight into the enhanced sub-G₁/G₀ population induced by the CVA21 and P + C combination, activation of caspase-3/7 using the caspase-glo assay was studied. Data from all cell lines confirmed that CVA21 infection had minimal effect on the activation of caspase-3/7 (with the exception of the MV3 cell line 48 h post-treatment), suggesting that it is unlikely the activation of caspase-3/7 is involved with CVA21-mediated cell death (Figure 4.15). As expected, treatment of all cell lines with the doublet therapy of P + C at their respective EC₅₀ concentrations significantly increased caspase-3/7 activity. The increase in caspase-3/7 activity peaked at 24 h post-treatment and was slightly depressed 24 hours later (48 h time point). Consistent with the resistance of SK-Mel-28 to P + C treatment, caspase-3/7 activity only peaked 48 h post-treatment and did not

translate to cell death (Figure 4.14). For most time points, the combination of CVA21 with P + C induced slightly higher levels of caspase-3/7 activity. However, this difference was not significant ($P > 0.05$), strongly suggesting that the mechanism of synergy may be influenced by caspase-3/7 but was not completely driven by these molecules.

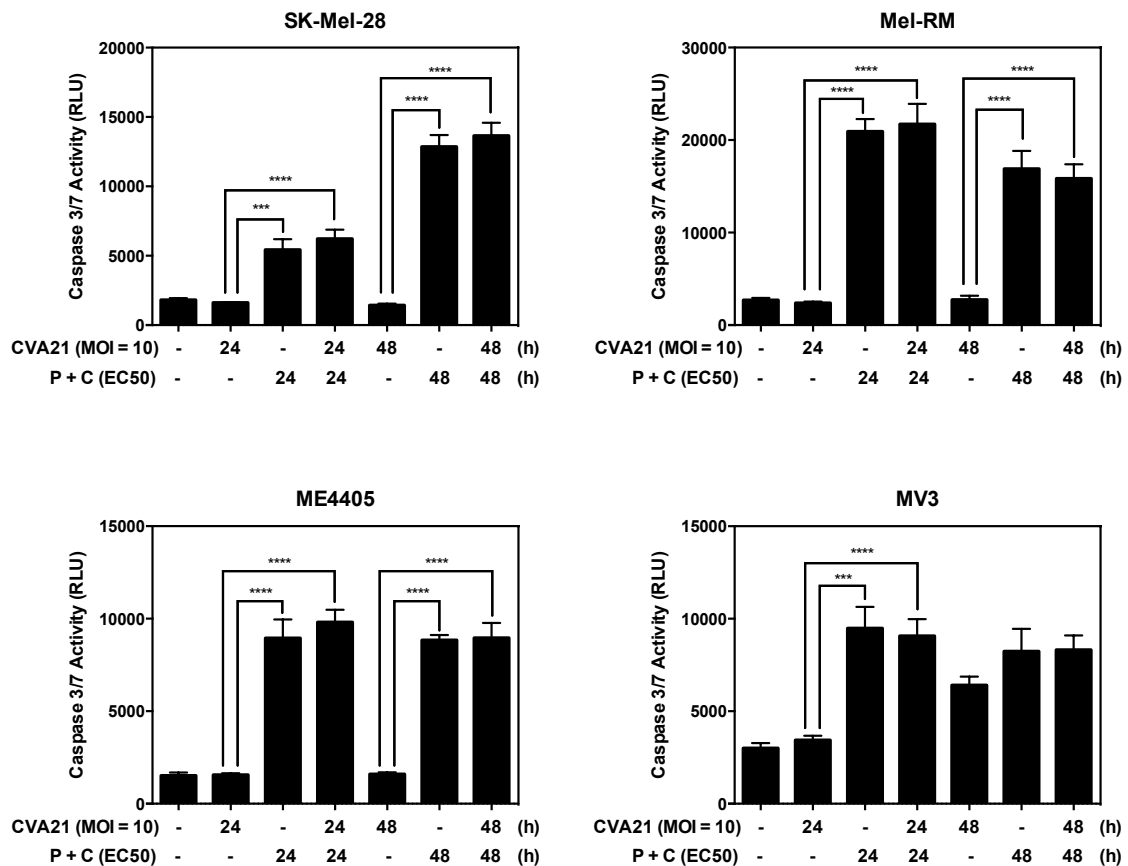


Figure 4.15: Caspase-3/7 activation in a panel of melanoma cells by caspase glo-assay. SK-Mel-28, Mel-RM, ME4405 and MV3 cells were treated with CVA21 at an MOI of 10 TCID₅₀/cell, P + C, both at $1 \times EC_{50}$, as single agents or in combination as indicated, and were assessed for caspase-3/7 activity via the caspase glo-assay at 24 and 48 h. Data represents the mean relative light units (RLU) \pm SD of at least two independent experiments. P values were derived from the one-way ANOVA with Tukey's correction for multiple comparisons where *** $P < 0.001$ and **** $P < 0.0001$. Treatment groups were each tested for significance against single agent CVA21 treatment. Only comparisons that showed statistical significance are indicated.

Chapter 5

In vivo evidence for CVA21 as a monotherapy and in combination with DTIC and P + C for the treatment of melanoma

As highlighted previously, many tumour microenvironmental factors exist which may potentially limit the efficacy of oncolytic virotherapy. Moreover, with an increasing knowledge that oncolytic viruses act to initiate therapeutic anti-tumour immune responses, the study of CVA21 interaction with the tumour microenvironment is of great significance. Hence, while our *in vitro* results highlight CVA21 as a promising therapy for melanoma, *in vivo* studies validating these results are necessary for translational success. Animal studies outlined in this chapter were performed to provide preclinical evidence that CVA21 has therapeutic activity against melanoma *in vivo* and is capable of acting synergistically with mainstream chemotherapies DTIC and P + C.

To determine whether the synergistic cancer cell death was reproducible *in vivo*, two melanoma animal models were designed; an immunodeficient melanoma xenograft model and a syngeneic immunocompetent mouse model. Our findings revealed that there was no statistical difference between single agent CVA21 and CVA21 in combination with chemotherapy in our immunodeficient mouse model. Such a result was not unexpected, as the absence of neutralising antibodies in the immunodeficient model allows the virus to replicate indefinitely until all tumour cells are destroyed. Having proven that chemotherapy

fails to interfere with the replication cycle of CVA21 *in vivo*, we developed a syngeneic immunocompetent mouse model and treated the animals with the same combinations as per the immunodeficient study. Overall we observed a good level of treatment tolerance and tumour clearance in both single agent/combination therapy treatment groups, however there were no statistically significant differences between the groups. These findings may provide further insight to the application of CVA21 in combination with chemotherapeutic agents in the clinic.

5.1 Immunodeficient xenograft mouse model of melanoma

To assess whether the *in vitro* susceptibility of human melanoma cell lines is predictive of the effectiveness of CVA21 as an anticancer agent *in vivo*, the therapeutic effects of intratumoural CVA21 infection on subcutaneous melanoma tumour xenografts were investigated. The main objective was to determine the safety of utilising CVA21 in combination with conventional chemotherapy *in vivo*; as well as to examine the anti-tumour efficacy of this combination.

5.1.1 Development of SK-Mel-28 human melanoma cells stably expressing the firefly luciferase gene

SK-Mel-28-luc cells stably expressing the firefly luciferase gene were established for *in vivo* bioluminescent intensity (BLI) detection. SK-Mel-28 cells were transduced with a non-replicative lentivirus vector encoding the firefly luciferase gene and cultured under normal conditions. Prior to xenotransplantation, the BLI of SK-Mel-28-luc cells was first quantified *in vitro* using the IVIS™ Imaging System (Xenogen IVIS 100, California, USA). Cells in suspension were serially diluted in a black 96-well tissue culture plate to prevent ‘spill-over’ of light and minimise BLI emission scattering between wells. Images captured showed stable expression of the luciferase gene in the SK-Mel-28-luc cells (Figure 5.1A). The measured total flux for 3,130 to 100,000 cells ranged between 4.19×10^3 p/s to 2.78×10^7 p/s. Data from the linear regression model showed a strong correlation between total flux and cell numbers, evident by an r^2 value of 0.9936 (Figure 5.1B). Next, to ensure SK-Mel-28-luc cells were still susceptible to CVA21, confluent monolayers were infected with the virus at increasing MOIs. Cytopathic effects over 72 h at an MOI of 100 down to 1×10^{-7} TCID₅₀/cell were assessed. Data from the infectivity assay showed little difference between SK-Mel-28-luc from its parental line in terms of sensitivity to CVA21 (Figure 5.1C).

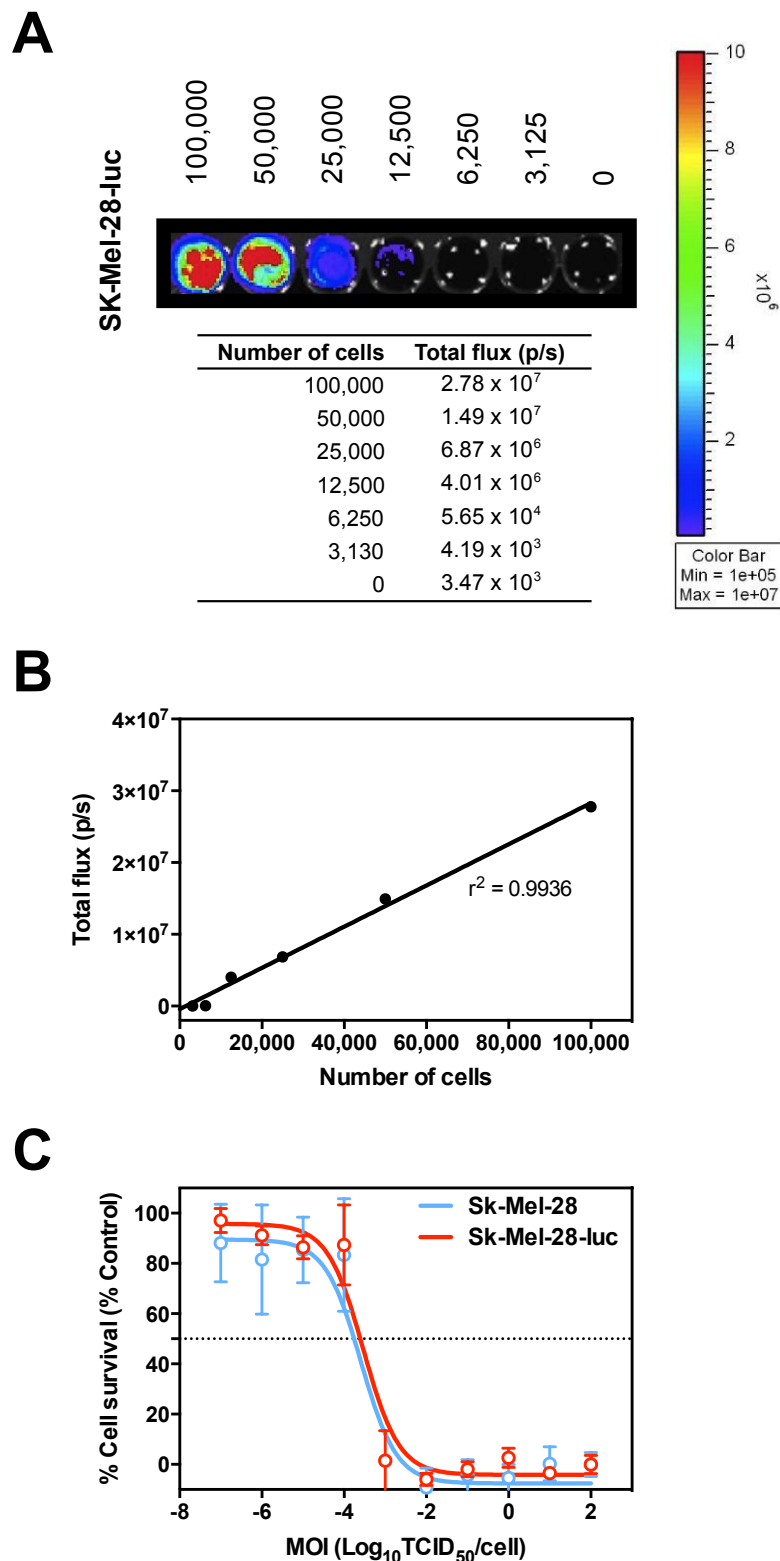


Figure 5.1: Establishment of SK-Mel-28-luc cells using a lentiviral vector. (A) Bioluminescent intensity (BLI) of serially diluted SK-Mel-28-luc cells. (B) Linear regression analysis of BLI *vs* number of cells seeded per well. BLI was measured as total photons per second (p/s). (C) Oncolytic activity of CVA21 in SK-Mel-28-luc cells. CVA21 dose is defined as multiplicity of infection (MOI) expressed in logarithmic 50% tissue culture infectious dose per cell (TCID₅₀/cell). TCID₅₀ data are plotted as mean values \pm SEM, representative of three independent experiments.

5.1.2 Establishment of a subcutaneous murine model of melanoma for combination therapy

SK-Mel-28-luc tumour cells (2×10^6 in a volume of 100 μ L) were implanted subcutaneously into the hind flanks of SCID mice. Tumours were allowed to establish before commencement of treatment Cycle 1 at day 35 and Cycle 2 at day 45 post-tumour inoculation (Figure 5.2). Mice were weighed and tumour volumes measured by electronic callipers up to three times a week. Xenogen bioluminescent imaging together with blood sampling from the saphenous vein were carried out at weekly intervals. The study was terminated at Day 77.

5.1.3 Animal weights throughout the course of study

Animal body weights were obtained to monitor the wellbeing of tumour bearing mice during the course of the study. Changes in body weight over time in the DTIC and P + C combination therapy were shown in Figure 5.3A & B respectively. Both combination therapies were well tolerated by animals, indicated by the increasing average weights during the course of the study. Rapid weight gain was observed in the saline treated mice relative to all other groups from day 60 onwards which was likely due to the increasing tumour mass. At day 67, all saline treated animals were euthanised as a result of increasing tumour burden. The mean body weight of the saline treated animals was 25.06 ± 2.08 g. The mean weight was 22.10 ± 17.30 g for the no tumour control group, 21.75 ± 1.24 g for the CVA21 group, 22.97 ± 0.66 g for the DTIC group, 22.91 ± 1.36 g for the P + C group, 22.52 ± 1.11 g for the CVA21 + DTIC group, and 21.97 ± 1.76 g for the CVA21 + P + C group. Using the two-way ANOVA test with Tukey's correction for multiple comparison, there were no statistical differences between any of the treatment groups at each time point.

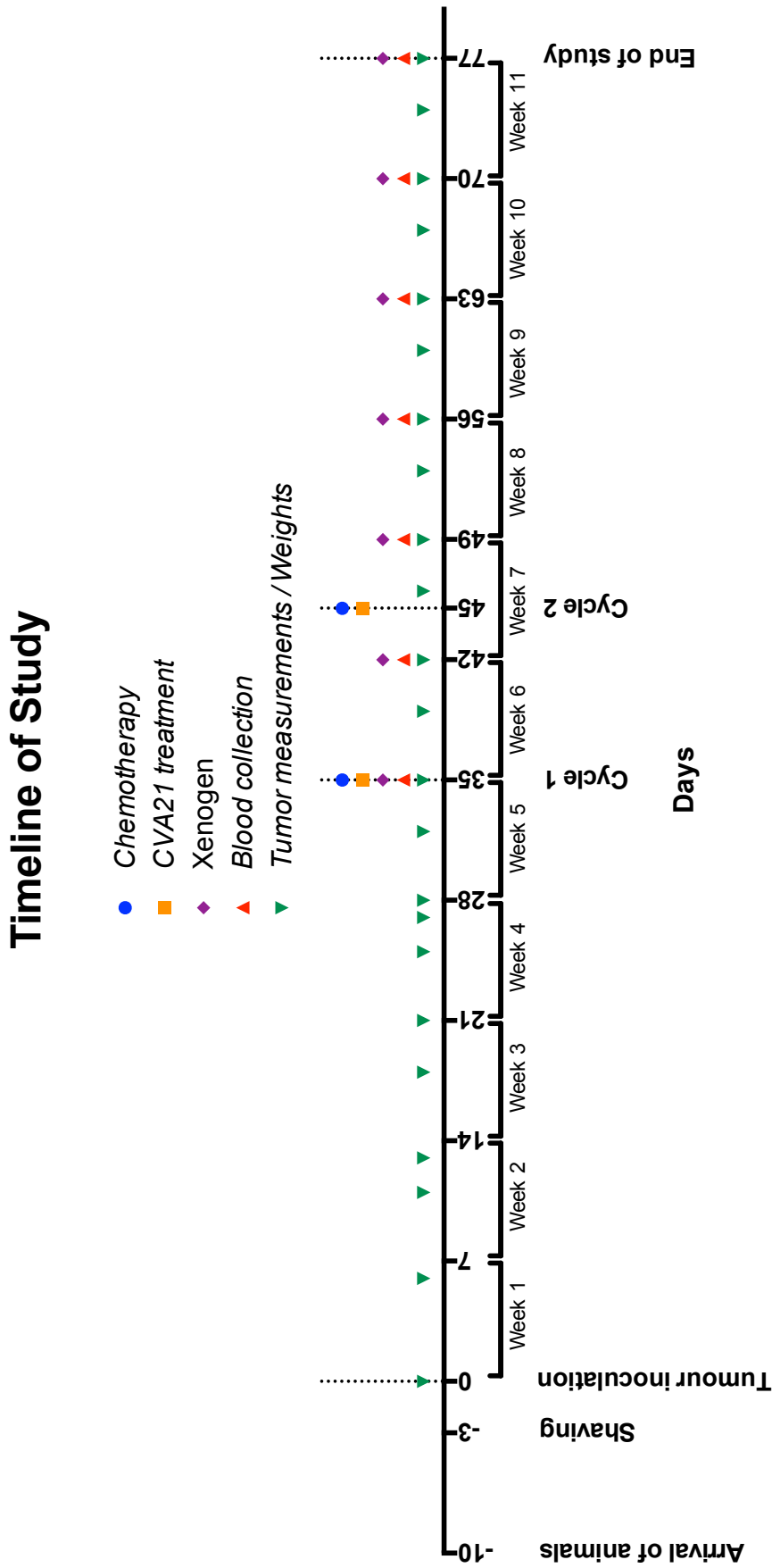


Figure 5.2: Overview of experimental protocol for immunodeficient murine melanoma model. Animals in each group ($n = 8$) received two cycles of therapy spaced ten days apart. Each cycle consisted of a single intratumoural (i.t.) injection of saline (0.1 mL) or CVA21 ($1 \times 10^8 \text{ TCID}_{50}$ in 0.1 mL) followed by the respective chemotherapeutic agent [DTIC (8 mg/kg), P (15 mg/kg) in combination with C (50 mg/kg) in a volume of $100 \text{ }\mu\text{L}$ /injection] intraperitoneally (i.p.) 30 min later.

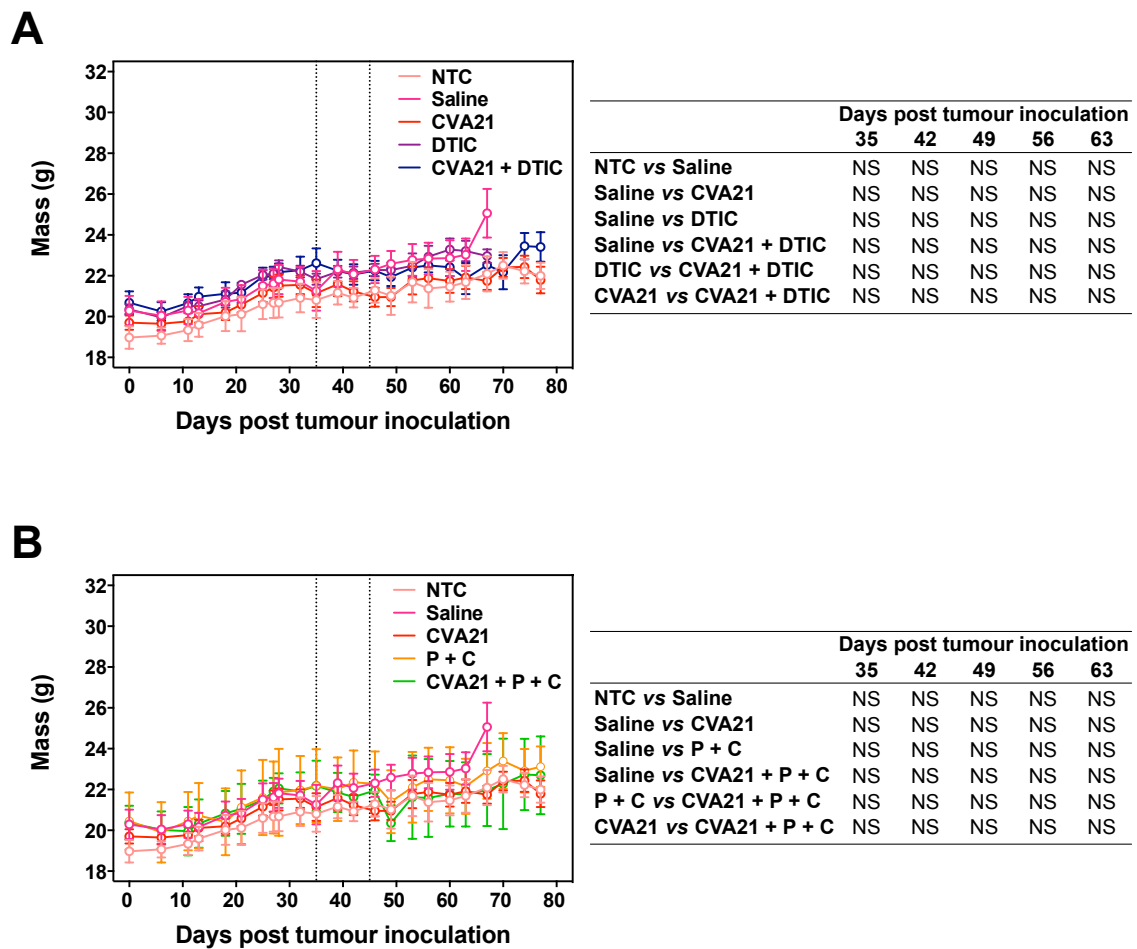


Figure 5.3: Mean body weights of mice (g) over time (days). Mass of (A) DTIC experimental treatment groups and (B) P + C experimental treatment groups were expressed as grams (g) with error bars indicating SEM ($n = 8$). The dotted lines at day 35 and day 45 indicate the start of cycle 1 and 2 respectively. The same NTC, saline and CVA21 data are plotted in panel A and B for comparison. The inset displays a summary of P values calculated using the two-way ANOVA corrected for multiple comparison with Bonferonni's method.

5.1.4 Tumour volume data

Having established the compatibility of CVA21 and both DTIC and P + C doublet chemotherapy *in vitro* (Chapter 4), the efficacy of these combinations was investigated *in vivo* using a xenograft tumour model of SK-Mel-28-luc cells. The six to eight week old female BALB/c SCID mice were used for this animal study. The treatment protocols were summarised in (Figure 5.2) and tumour volume was calculated using the formula of a spheroid. At 35 days post-tumour implantation (mean tumour volume $313.55 \pm 135.62 \text{ mm}^3$), animals were treated either with CVA21 alone, chemotherapy alone or CVA21 in combination with chemotherapy. Control animals were given intratumoural injections of saline. Results demonstrated that the tumour volumes in the saline and DTIC treated groups continued to escalate up until day 66 (at which point animals were euthanised due to excessive tumour burden) (Figure 5.4A). Transient tumour reduction was observed in DTIC treated animals but regrowth occurred a week after treatment. This was in contrast to animals receiving DTIC with a single intratumoural injection of CVA21, where tumour volumes had regressed to the point they were non-palpable from day 45 onwards (Figure 5.4B Table).

On the other hand, SK-Mel-28-luc flank tumours treated with P + C doublet chemotherapy showed considerable levels of tumour growth inhibition. However, the doublet therapy alone was unable to completely eradicate the disease, evident by the regrowth eleven days after treatment cycle 2 (Figure 5.4B). Importantly, tumours in animals receiving the combination treatment of CVA21 and P + C were completely eradicated by day 66. Using the two-way ANOVA accompanied by Tukey's correction for multiple comparison, the average tumour volumes of each treatment group was assessed for statistically significant differences. The table from Figure 5.4A showed that tumours treated with DTIC alone at day 66 had slightly smaller mean volumes than the control group ($1138.63 \pm 566.35 \text{ mm}^3$ compared to $1442.12 \pm 502.90 \text{ mm}^3$), but was without statistical significance for most measurements ($P > 0.05$). Tumours treated with P + C showed a significant reduction in tumour size ($503.05 \pm 205.63 \text{ mm}^3$, $P < 0.0001$) at day 66.

A major finding of this study was that tumour reductions were most dramatic approximately 10 days post-cycle 1 treatment in the single agent CVA21, CVA21 + DTIC and CVA21 + P + C group. Mean tumour volumes of these animals were significantly lower when compared to animals receiving the P + C doublet therapy alone ($P < 0.0001$)

and were maintained for the duration of the study. Taken together, these findings suggest a single treatment cycle of CVA21 together with conventional chemotherapy maybe sufficient in inhibiting tumour growth thus reducing the toxic sides effects of multiple treatment cycles. However, we did not observe a significant difference between single agent CVA21 and CVA21 + chemotherapy treated tumour volumes ($P > 0.05$).

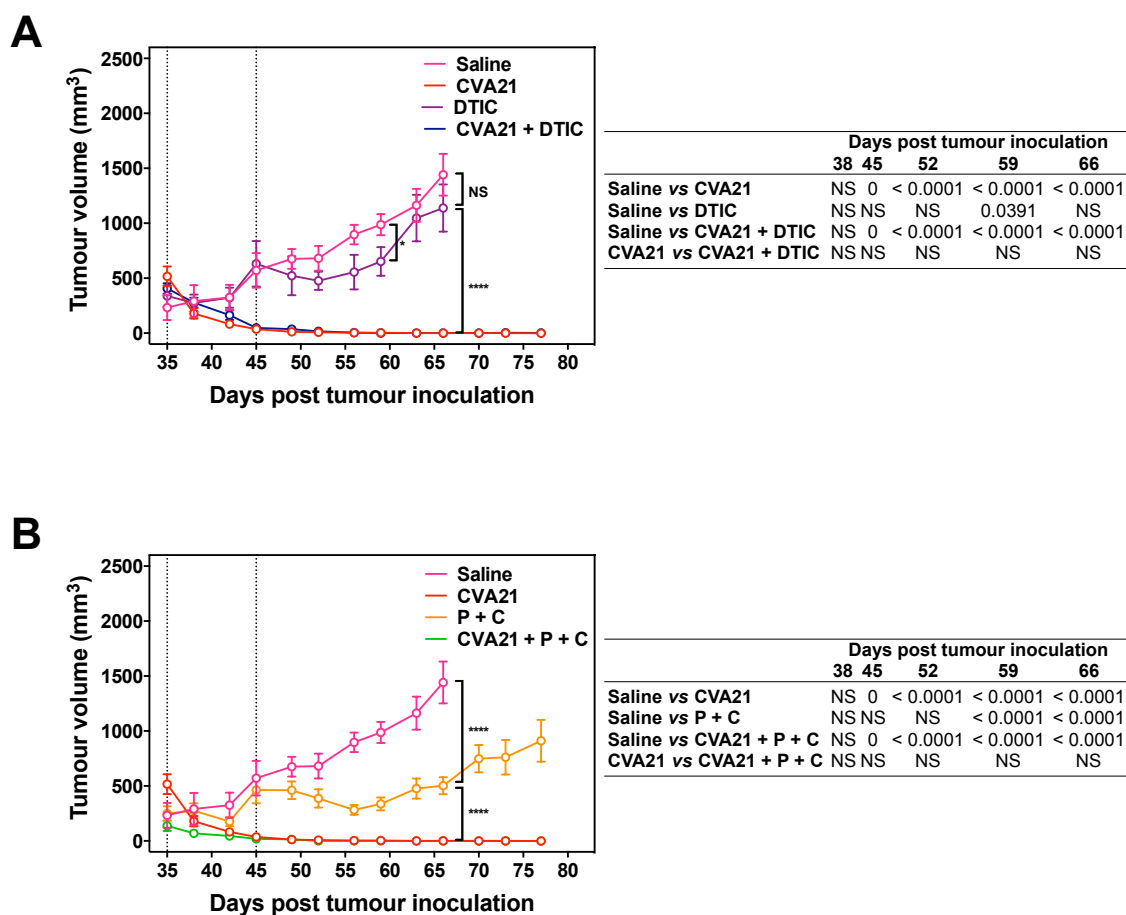


Figure 5.4: Combination of chemotherapy and CVA21 virotherapy on SK-Mel-28-luc melanoma xenografts in SCID mice. SCID mice were injected with SK-Mel-28-luc cells on the hind flank. Tumours were allowed to establish for 35 days, prior to treatment with either saline (i.t.), CVA21 (i.t., 1×10^8 TCID₅₀/mouse), DTIC (i.p., 8 mg/kg), P (i.p., 15 mg/kg) + C (i.p., 50 mg/kg) injection, or CVA21 in combination with DTIC or P + C. Mice received a second cycle of dosing at day 45. **(A)** Combination of DTIC with CVA21 on melanoma. **(B)** Combination of P + C with CVA21 on melanoma. All tumour volumes are expressed as the average tumour burdens \pm SEM mm³ (n = 8). The inset displays a summary of P values calculated using the two-way ANOVA corrected for multiple comparison with Tukey's method.

5.1.5 Bioluminescent imaging *in vivo*

Mice were first imaged using bioluminescent imaging initially at day 28 post-tumour inoculation (7 days prior to treatment). Animals were then routinely imaged once a week for the

duration of the study. Figure 5.5 shows detection of SK-Mel-28-luc flank tumours pre- and post-treatment by *in vivo* imaging. Bioluminescent signal were detectable seven days pre-treatment (Day 28) exclusively from the flank tumours in all mice. Bioluminescent signal was highest in the control group 31 days post-treatment (Day 66), indicated by the colour intensity emitted. The amount of signal detected in the flank tumours of mice treated with either DTIC or P + C alone increased over the course of treatment, with no signs of regression. Tumour shrinkage was most evident in the animals that received CVA21 or CVA21 + chemotherapy, see Figure 5.5 (pre-treatment *vs* 31 days post-treatment).

Quantitative bioluminescence data were acquired and analysed using the Living Image software v2.5 (Xenogen), and presented in graphical form (Figure 5.6A & B). Using the two-way ANOVA followed by the Tukey's correction for multiple comparison test, the average radiance of each treatment group was assessed for statistically significant differences (Figure 5.6A & B [table inset]). Xenogen data showed a significant reduction in tumour burden in all treatment groups after day 52 (7 days after completion of 2nd treatment cycle) when compared to the control group ($P < 0.05$). Furthermore, tumours treated with the combination of CVA21 and either chemotherapy showed enhanced anti-tumour activity in comparison to DTIC and P + C alone treatment groups ($P < 0.01$). Xenogen data did not report a statistically significant difference between CVA21 and CVA21 + chemotherapy treatment groups as well.

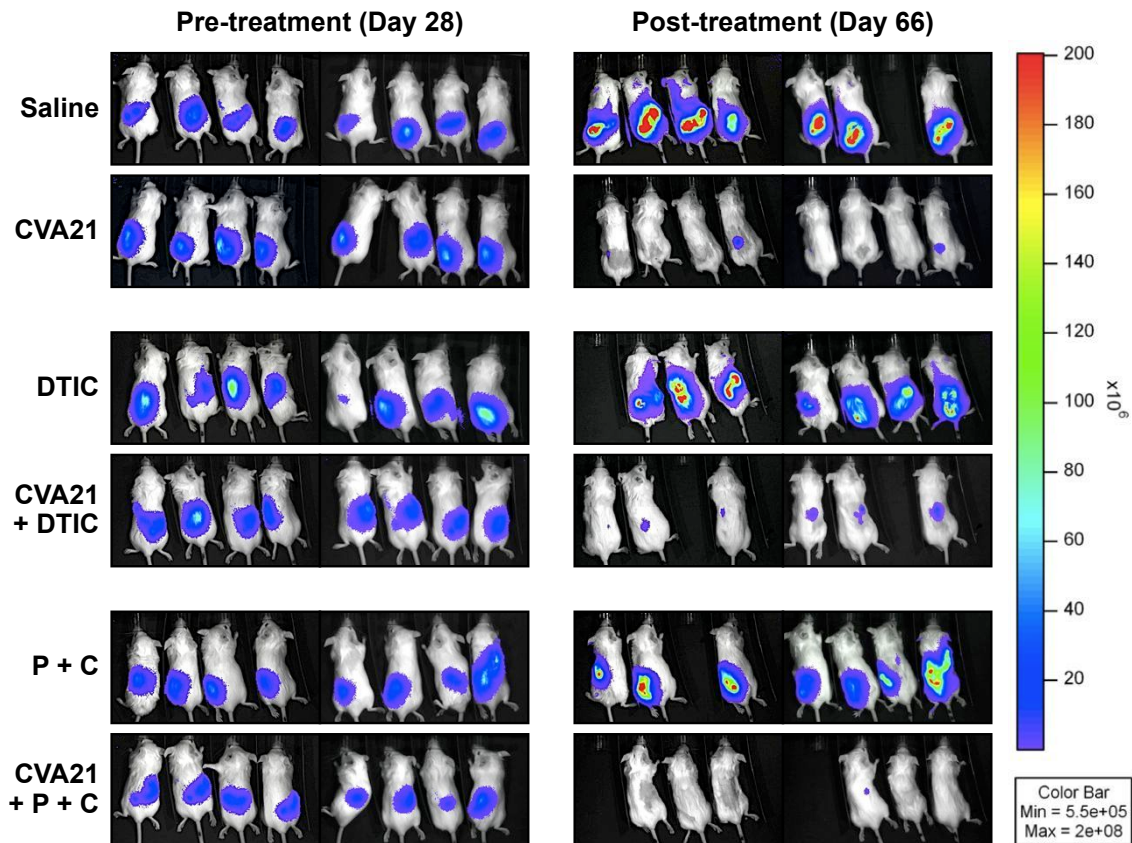


Figure 5.5: Bioluminescent imaging of BALB/c SCID mice transplanted with luciferase expressing SK-Mel-28 cells. Tumour development can be seen by the coloured-contour overlay showing luminescent intensity (measured in photons/cm²/s/sr) ($n = 8$). Bioluminescent imaging was performed under a high resolution setting following i.p. injection of the luciferase substrate d-luciferin. Images were captured once the BLI reached its peak levels. For all images shown, the colour scale ranges from blue (just greater than the background noise; set to 5.5×10^5 photons/cm²/s/sr) to red (at least 2×10^8 photons/cm²/s/sr). Images in the left column were taken 7 days before treatment (28 days post-tumour inoculation), with the right column showing the anti-tumoural responses 38 days later (66 days post-tumour inoculation). Dramatic levels of regression were observed in mice treated with CVA21, or CVA21 in combination with chemotherapy. Animals that were treated with chemotherapy alone showed limited or no response to therapy.

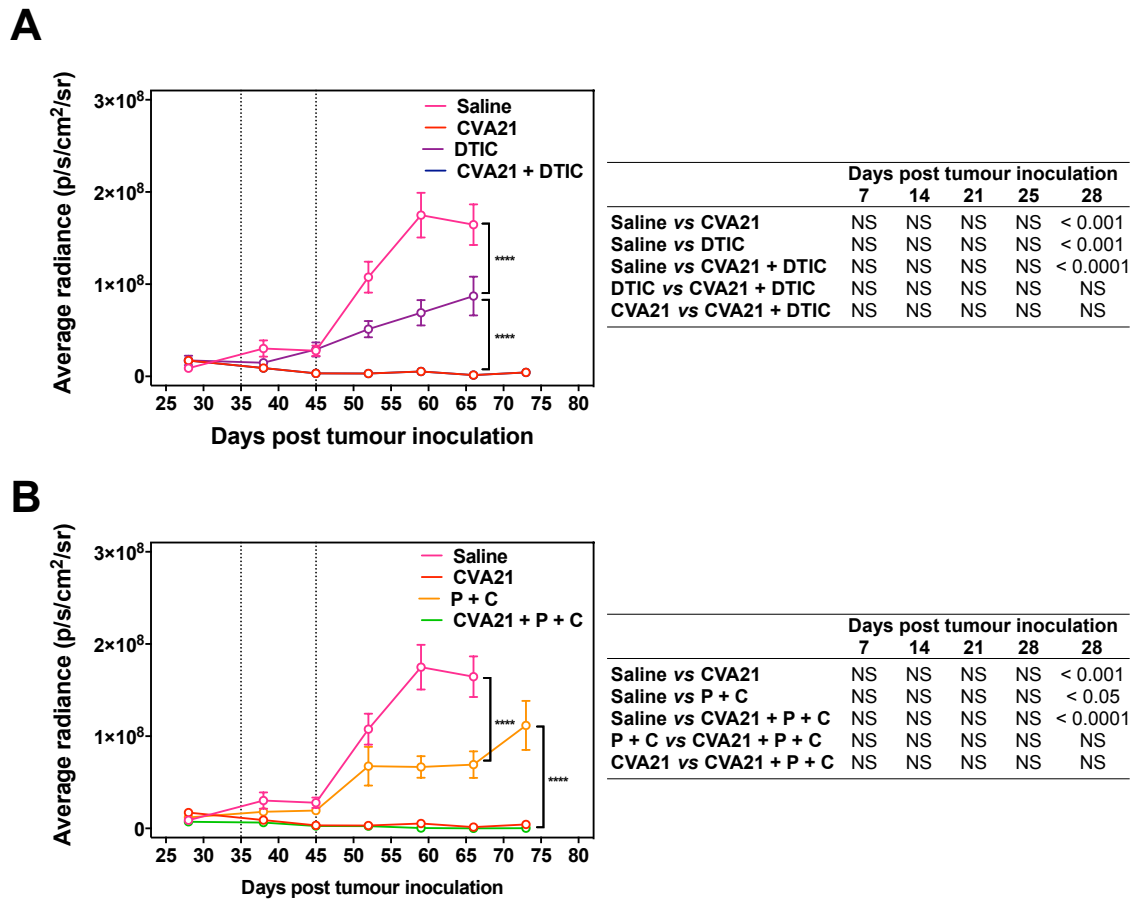


Figure 5.6: *In vivo* response monitoring in SK-Mel-28-luc melanoma model with BLI. Serial monitoring of BLI flux changes in (A) DTIC combinations and (B) P + C combinations, expressed as average radiance \pm SEM (photons/s/sr/cm²) over the study (n = 8). Data from saline alone and CVA21 alone were plotted in panel A and B for comparison. Dotted lines indicate treatment cycles. Two-way ANOVA (corrected for multiple comparisons with Tukey’s method) demonstrates statistical significance between treatment groups, denoted by asterisks ($P < 0.0001$).

5.1.6 CVA21 viraemia

We have previously shown that the presence of DTIC and P + C did not inhibit CVA21 replication *in vitro*. We therefore collected weekly serum samples from all CVA21 treated mice in order to observe if virus was produced. Serum samples were analysed by quantitative reverse transcriptase polymerase chain reaction (qRT-PCR) to determine the levels of CVA21 RNA present. One-step qRT-PCR was carried out using the SuperScript III Platinum One-Step qRT-PCR Kit (Invitrogen). Initial serum samples were taken 1 h after treatment was completed.

Viraemia levels increased progressively over the duration of the study indicating successful infection and replication of CVA21 in the host (Figure 5.7A). Furthermore, animals treated with CVA21, with or without chemotherapy had serum viraemia in excess of 10^6 TCID₅₀ equivalents/mL at the time of euthanasia (Figure 5.7B). This finding supports our tumour burden results showing that successive replication of CVA21 leads to the destruction of tumour cells over time. There were no statistical differences between single agent CVA21 treatment and combination treatments ($P > 0.05$; two-way ANOVA with Tukey's correction for multiple comparisons).

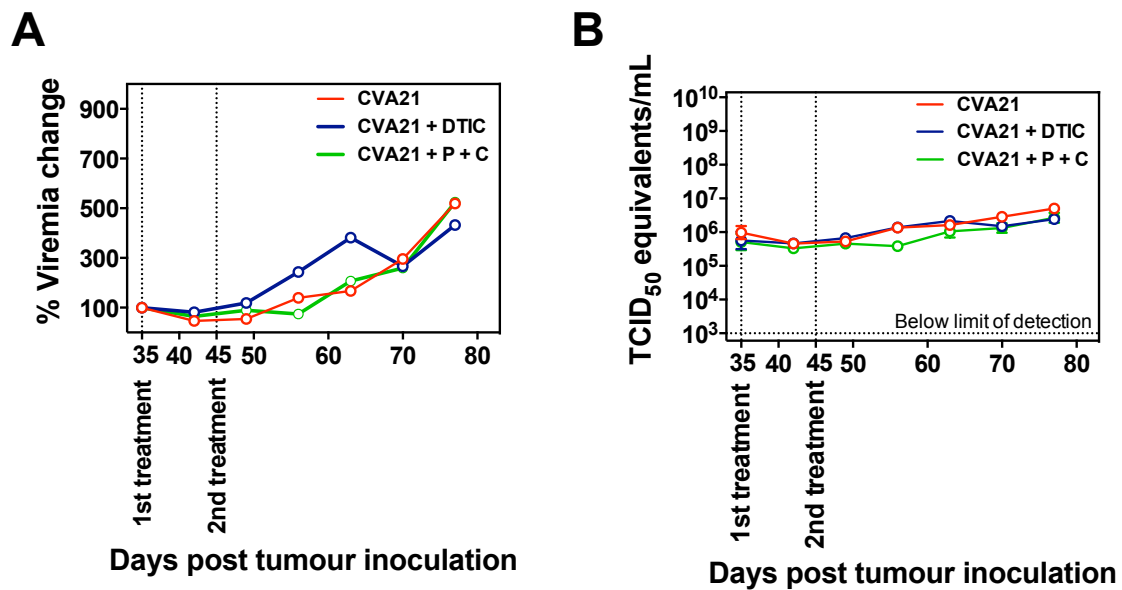


Figure 5.7: Detection of viraemia using one-step qRT-PCR. (A) Percentage viraemia change compared to the start of treatment (Day 35). (B) Viraemia levels during the duration of the study. Viraemia levels were expressed as average TCID₅₀ equivalents/mL \pm SEM ($n = 8$). One TCID₅₀ equivalents/mL represents approximately 1×10^3 viral copies/mL. Horizontal dotted line represents the limit of detection. Viraemia levels continued to escalate over time with no signs of clearance in this immune deficient model. No statistically significant differences in viraemia were observed between the treatment groups.

5.2 Development of a syngeneic model of B16-ICAM-1 murine melanoma

Due to poor infectivity and replication in mouse tumour cell types compared with human tumour cell lines, the use of CVA21 in syngeneic animal model systems was limited. Surface expression of ICAM-1 is one of the most critical determinants of CVA21 tissue tropism and lytic infection. Although CVA21 can bind and interact with an alternate attachment receptor (DAF), CVA21 is dependent on ICAM-1 for high affinity attachment, and subsequent induction of capsid conformational changes leading to successful cell entry and infection. Mouse melanoma B16 cells lack the human form of ICAM-1 (h-ICAM-1) and thus, not susceptible to CVA21 infection. In efforts to develop a syngeneic immunocompetent mouse model of melanoma, B16 mouse melanoma cells were transfected with the human ICAM-1 receptor.

5.2.1 Establishing B16-ICAM-1 cells for tumour development

B16 mouse melanoma cells were stably transfected with the human ICAM-1 gene using Lipofectamine to confer susceptibility to CVA21. A population of high h-ICAM-1 expressing B16 cells (B16-ICAM-1) were isolated by fluorescent activated cell sorting. Following expansion of this cell population *in vitro*, h-ICAM-1 levels were assessed by flow cytometry. No surface h-ICAM-1 was detected on the surface of the non-transfected B16 cells compared to the B16-ICAM-1 cell line which showed a distinct shift to the right in the histogram (Figure 5.8A). To show that only B16-ICAM-1 cells support CVA21 viral replication, one-step growth curve assays were generated. CVA21 viral titres peaked at 24 h post-infection with a viral titre of 1.47×10^8 TCID₅₀/mL (Figure 5.8B). In contrast, data from the B16 cells show that without the expression of the h-ICAM-1 surface receptor, viral titres never exceeded the initial input inoculum and decreased over time.

Having shown that h-ICAM-1 surface receptor was detectable on B16-ICAM-1 cells and these cells supported CVA21 viral replication, the cytopathic effect of CVA21 on B16-ICAM-1 cells was addressed. Confluent monolayers of B16 and B16-ICAM-1 cells were infected with serial dilutions of CVA21 (0.001 - 100 TCID₅₀/cell) and stained with crystal violet 72 h later. CVA21 induced lytic destruction of the B16-ICAM-1 monolayers at viral concentrations as low as 0.1 TCID₅₀/cell (Figure 5.8C). In contrast, B16 cells were not permissive to the lytic infection as indicated by the intact monolayer and absence of CPE 72

h post-infection. Cell viability data performed in parallel reinforces that CVA21 mediates B16-ICAM-1 cell death in a dose-dependent manner but not in the native B16 cells (Figure 5.8D). The EC_{50} value of CVA21 against B16-ICAM-1 was 8.51×10^{-3} $TCID_{50}/cell$.

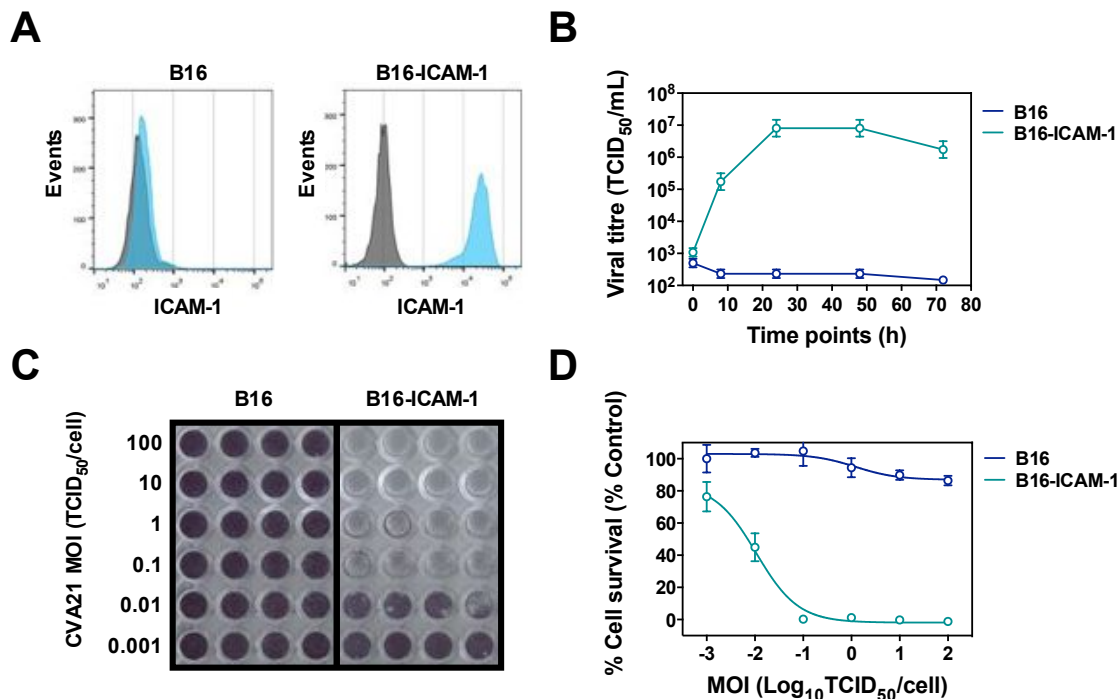


Figure 5.8: Characterisation of B16-ICAM-1 melanoma cells. (A) Flow cytometric analysis of ICAM-1 levels on B16 cells stably transfected with h-ICAM-1 cDNA. ICAM-1 positive cells (blue histogram) and control staining (grey histogram) are shown. (B) One-step viral replication kinetics of CVA21 in B16 and B16-ICAM-1 cells. Cells were infected with an MOI of 10 $TCID_{50}/cell$. Samples were collected at 0, 8, 24, 48, 72 h and viral titres determined by $TCID_{50}$ assays (C) Cytopathic effect of CVA21 on B16-ICAM-1 cells. Cells were infected with 0.001 - 100 $TCID_{50}/cell$ of virus for 72 h and stained with crystal violet. (D) Oncolytic effects of CVA21 on B16-ICAM-1 cells. Cell viability was assessed using the MTT cell viability assay 72 h post-infection. Error bars indicate SEM. All results displayed are representation of two independent experiments.

5.2.2 Assessment of tumour growth and survival analysis

Next, we sought to determine the most suitable route for the development of a syngeneic murine model of B16-ICAM-1. The hind flank of naive syngeneic C57BL/6 mice were injected subcutaneously (s.c.) or intradermally (i.d.) with 2×10^5 B16-ICAM-1 tumour cells established earlier. The native B16 murine cells were used as controls. Tumour volumes were measured twice a week using electronic vernier callipers. Animals with tumours that appear ulcerated or greater than 2500 mm³ in volume were euthanised. Any remaining animals were terminated 30 days post-tumour inoculation.

Our study shows that the growth of B16 flank tumour was not dependent on the route of administration (Figure 5.9A). B16 cells invariably yielded a tumour that continued to grow progressively. Maximum allowed tumour volume for B16 i.d. and B16 s.c. cells was reached 23 and 25 days post-tumour inoculation, respectively. On the other hand, volumes of B16-ICAM-1 flank tumours injected intradermally showed a significantly higher mean tumour volume ($827 \pm 220 \text{ mm}^3$) compared with tumour injected subcutaneously ($496 \pm 210 \text{ mm}^3$) by day 28 ($P < 0.05$) (Figure 5.9B).

Apart from measuring tumour dimensions with digital callipers, we investigated if the route of administration had an effect on tissue necrosis or ulceration of the skin overlying the developing tumour. The number of animals euthanised due to tumour ulceration from each group and their corresponding tumour volume is shown in Figures 5.9C & D. Irrespective of the cell line, flank tumours inoculated intradermally were more likely to ulcerate. The percentage of animals with ulcerated tumours for B16 i.d. (92%), B16 s.c. (75%), B16-ICAM-1 i.d. (66.7%) and B16-ICAM-1 s.c. (50%) was recorded.

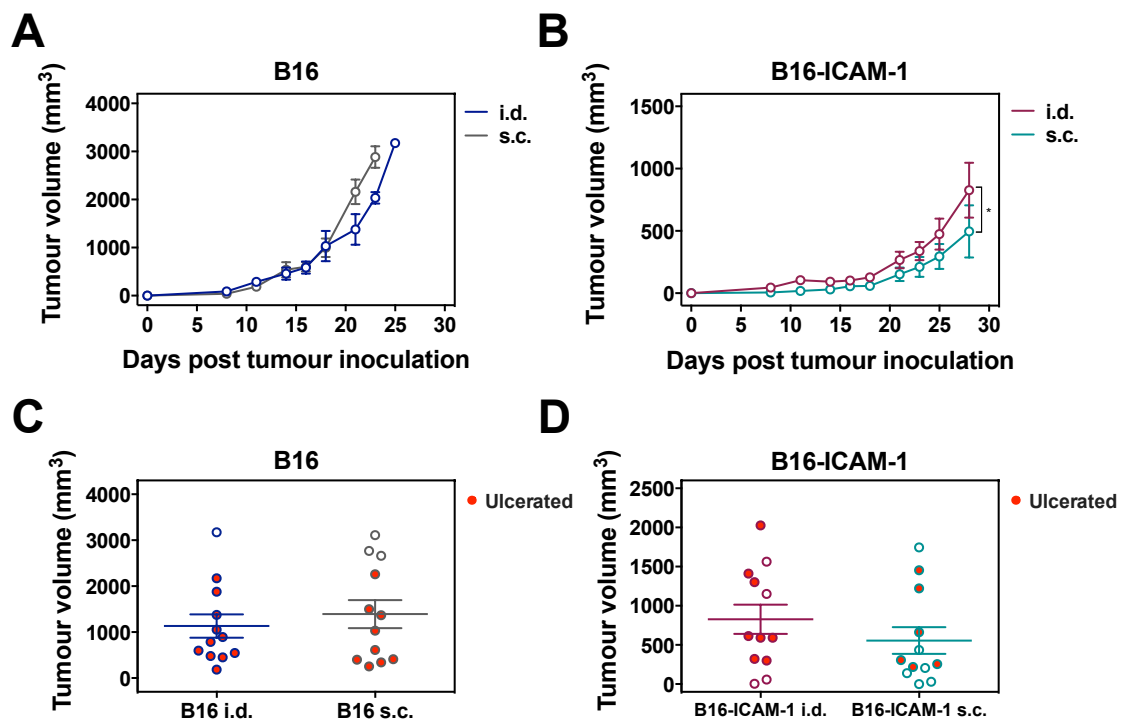


Figure 5.9: Growth of B16 and B16-ICAM-1 flank tumours. Tumour volumes of (A) B16 and (B) B16-ICAM-1 cells inoculated either intradermally or subcutaneously. Data points indicate the mean tumour volume \pm SEM ($n = 12$). *B16-ICAM-1 i.d. *vs* B16-ICAM-1 s.c. ($P < 0.05$; two-way ANOVA with Bonferroni's correction for multiple comparisons). Distribution of the maximum tumour volume for (C) B16 and (D) B16-ICAM-1 cells over the course of the experiment. Red circles represents the volume animals were euthanised as a result of an ulcerated tumour.

B16 flank tumours developed in all animal regardless of the route of inoculation (Figure 5.10A). On the other hand, not all animals developed palpable B16-ICAM-1 flank tumours at the end of the study. 92% of animals (11/12) receiving B16-ICAM-1 intradermally developed palpable tumours as compared to 83% (10/12) of animals from the subcutaneous group. Interestingly, a delay in tumour growth was observed in animals inoculated with B16-ICAM-1 cells subcutaneously, but not when delivered intradermally (Figure 5.10A). The median time to a palpable B16-ICAM-1 tumour delivered subcutaneously (19.0 days) was noticeably longer than B16 tumours delivered intradermally (6.5 days), subcutaneously (8.6 days) and B16-ICAM-1 delivered intradermally (10.8 days).

Next, animals were followed for 30 days for survival. The route of administration of either tumours did not have an impact on the animal's survival (B16 i.d. *vs* B16 s.c., B16-ICAM-1 i.d. *vs* B16-ICAM-1 s.c.; $P > 0.05$; log-rank test) . Animals bearing B16 flank tumours (Figure 5.10B) had a median survival of 14 days (i.d. delivery) and 15.5 days (s.c. delivery); while B16-ICAM-1 (Figure 5.10C) flank tumours was recorded at 28.5 days (i.d. delivery) and 29 days (s.c. delivery). However, survival data suggests that the B16 flank tumours were more lethal than B16-ICAM-1 tumour. All animals bearing B16 flank tumours were euthanised by day 25.

5.2.3 Haematoxylin and eosin analysis

To validate the location in which the tumour cells were actually deposited, tumour histological features were shown by haematoxylin and eosin (H&E) staining. Examination of normal skin sections revealed four layers of organisation, the epidermis, dermis, adipose tissue and skeletal muscles (Figure 5.11A). H&E staining confirmed the location B16-ICAM-1 tumours cells were deposited. Subcutaneous injection led to the development of B16-ICAM-1 tumour beneath the layers of the skin (Figure 5.11B), while B16-ICAM-1 cells injected intradermally developed between the dermis and skeletal muscle layer, occupying majority of the adipose layer (Figure 5.11C). B16 melanomas are known to grow rapidly and some are prone to developing haemorrhagic necrotic areas, which can cause superficial erosion and ulceration. The dermis surrounding the site of ulceration revealed a predominantly mononuclear rich inflammatory cell infiltrates.

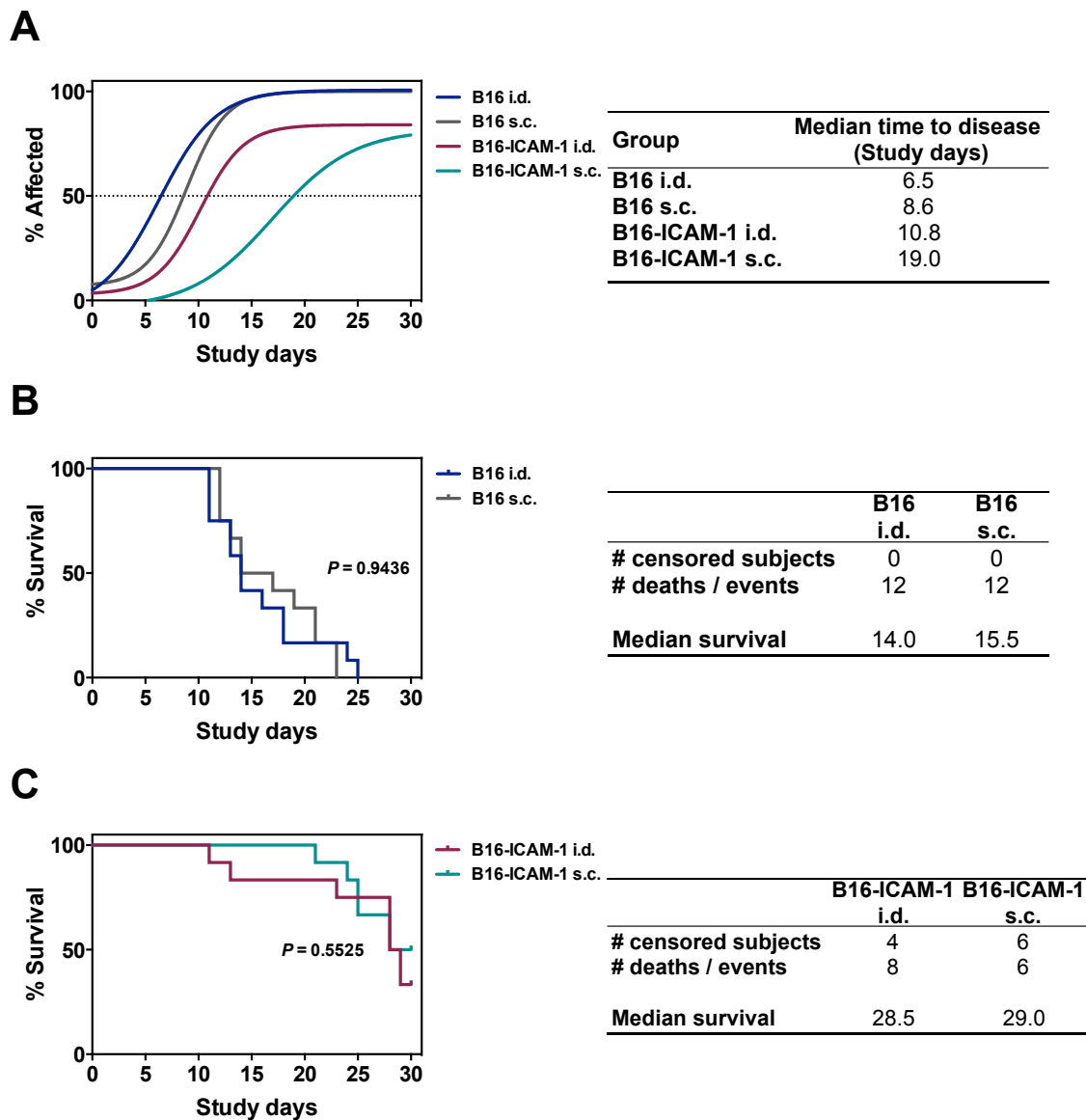


Figure 5.10: Growth rate and survival analysis for tumour bearing animals. (A) The percentage of animals that developed palpable flank tumours. An animal that developed a palpable flank tumour was counted as a positive subject. The data were fitted using a locally weighted scatterplot smoothing (LOWESS) method. Median time to disease was extrapolated from the four Parameter Logistic (4PL) nonlinear regression model [inset table]. B16-ICAM-1 tumours did not develop in all animals and cells that were implanted subcutaneously developed slower when compared to cells implanted intradermally. Kaplan-Meier survival plot demonstrating survival of animals bearing (B) B16 and (C) B16-ICAM-1 flank tumours. The inset table shows the median survival of each group. The route of administration has no statistically significant impact on overall animal survival. Data was analysed using the log-rank test ($n = 12$).

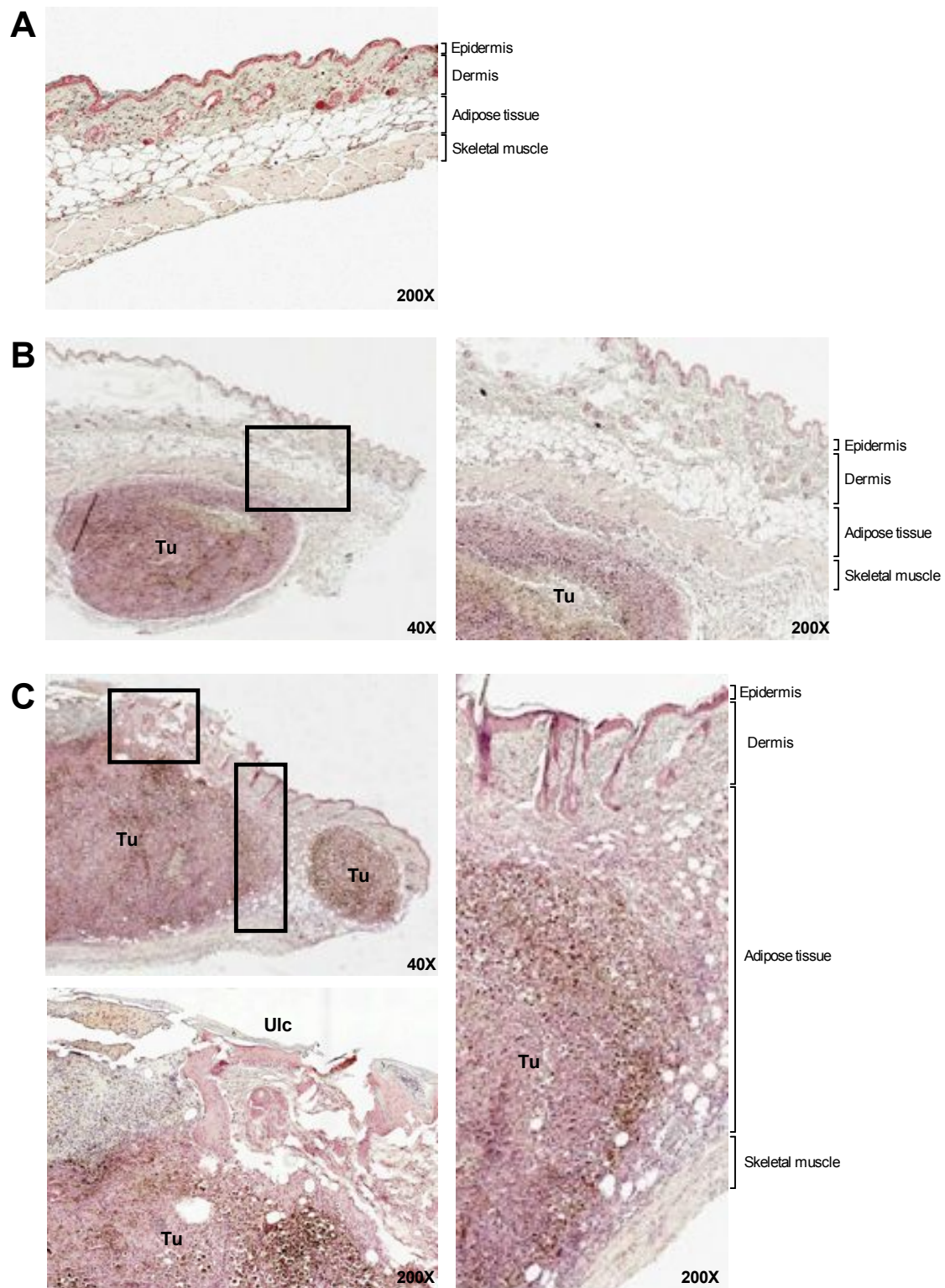


Figure 5.11: Histological analysis of tumour deposits using H&E staining. Representative section of (A) normal skin, B16-ICAM-1 tumour implanted (B) subcutaneously and (C) intradermally photographed at a scanning resolution of 20 \times with a 2 \times and 10 \times magnification. Normal skin shows distinct organisation delineated by the epidermis, dermis, adipose tissue, and skeletal muscle. Tumour mass implanted subcutaneously was present below the skeletal muscle layer. Intradermal tumour mass developed in the adipose layer, below the dermis, resulting in frequent tumour ulceration. Abbreviations: Tu, tumour; Ulc, ulceration.

5.2.4 Isolation and *in vitro* expansion of murine cells from tumour explants

To further characterise the difference between, B16 and B16-ICAM-1 murine melanoma tumours generated from both i.d. and s.c. route, primary cells were isolated and grown *in vitro*, as described previously [Section 3.7.3]. Approximately 30 - 50% of viable cell were recovered during the first passage. After 4 - 5 passages, cell viability fully recovered and were propagated as adherent cell lines. Following expansion of these cell lines *in vitro*, flow cytometric analysis was used to detect h-ICAM-1 receptor level.

As expected, no surface h-ICAM-1 was detected on the surface of the B16 primary cultures (Figure 5.12A, top panel). Interestingly, the expression of h-ICAM-1 on the surface was substantially reduced in B16-ICAM-1 cells implanted subcutaneously only (Figure 5.8A, bottom right panel). In direct contrast, there was little difference in the levels of h-ICAM-1 between B16-ICAM-1 cells isolated after intradermal transplantation and the parental line (Figure 5.8A, bottom left panel). These data strongly suggested that B16-ICAM-1 cells transplanted intradermally could retain h-ICAM-1 expression but not after s.c. injection.

To determine if the decrease in surface h-ICAM-1 receptor had an effect on CVA21 infectivity, confluent monolayers of B16 and B16-ICAM-1 explants were exposed to serial dilutions of the virus. Cells were stained with crystal violet 72 h post-treatment and scored for CPE. As expected, B16 cells were not susceptible to lytic infection, indicated by the intact monolayer and absence of CPE (Figure 5.12B). However, B16-ICAM-1 cells recovered from the i.d. transplantation were permissive to CVA21 infection, resulting in the lytic destruction characteristic of the CVA21 CPE. In contrast, B16 cells were not susceptible to lytic infection, indicated by the intact monolayer and absence of CPE.

In parallel, cell viability data demonstrates the reduced sensitivity of B16-ICAM-1 cells transplanted subcutaneously to CVA21 infection (Figure 5.12C). Intradermally injected B16-ICAM-1 cells remain sensitive to CVA21 infection. In summary, significant levels of ICAM-1 was detectable in B16-ICAM-1 primary cultures implanted intradermally and these cells were still susceptible to CVA21 infection. Based on the collection of these findings, cells were injected intradermally in all studies employing the B16-ICAM-1 immunocompetent model.

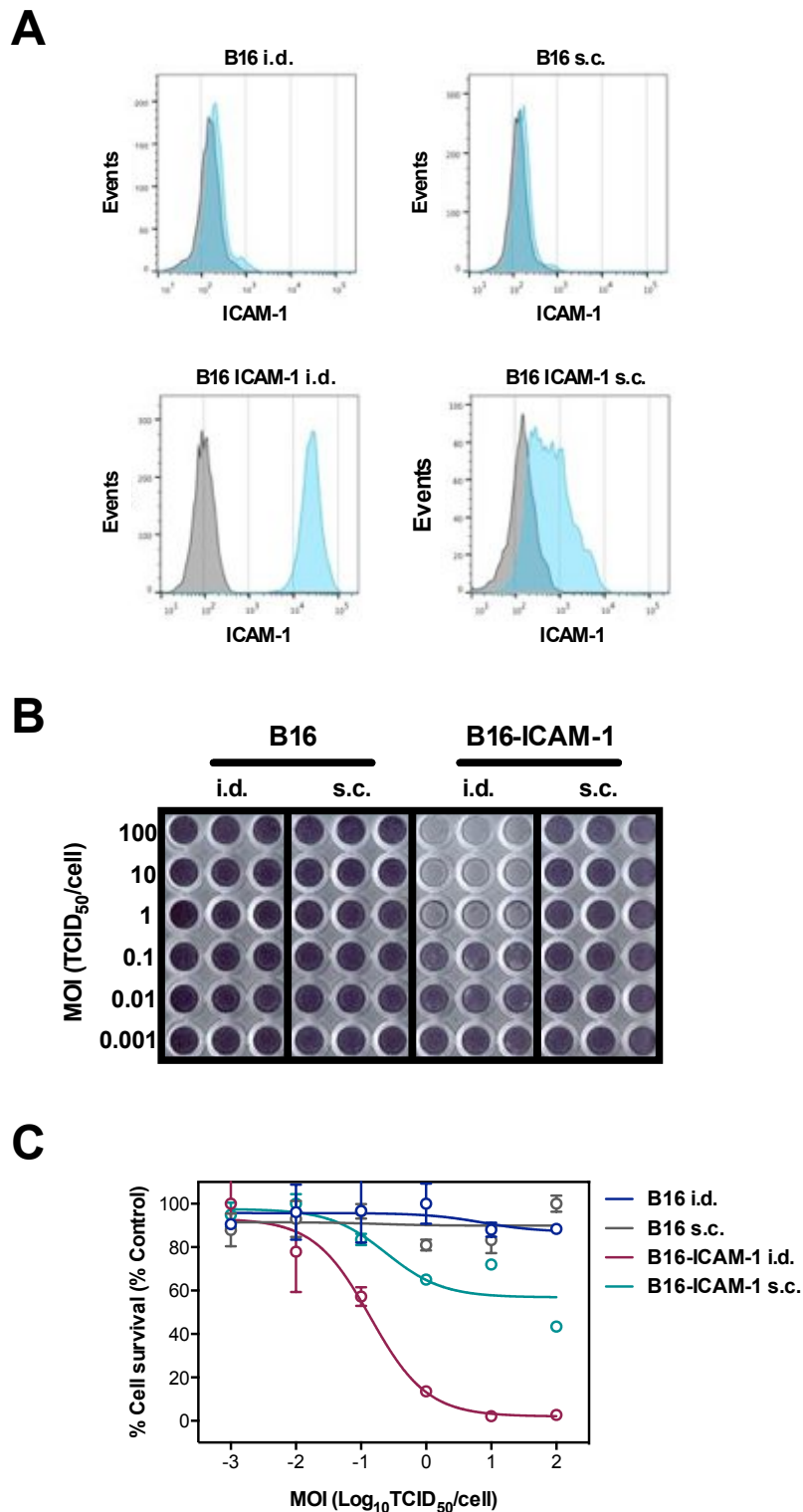


Figure 5.12: Lytic infection of primary B16 and B16-ICAM-1 culture from *in vivo* tumour explants. (A) Flow cytometric analysis of ICAM-1 levels on B16 and B16-ICAM-1 explants. ICAM-1 positive cells (blue histogram) and control staining (grey histogram) are shown. (B) Crystal violet stained B16 and B16-ICAM-1 explants. Monolayers were infected with 0.001 - 100 TCID₅₀/cell of CVA21 and stained with crystal violet 72 h post-treatment. (C) Cytotoxicity assay of B16 and B16-ICAM-1 explants infected with CVA21 at increasing MOI. Viability was assessed 72 h later by MTT assay. Data was presented as percentage to untreated control with bars indicating SEM.

5.3 Combinatory effects of CVA21 and DTIC and P + C on B16-ICAM-1 cells

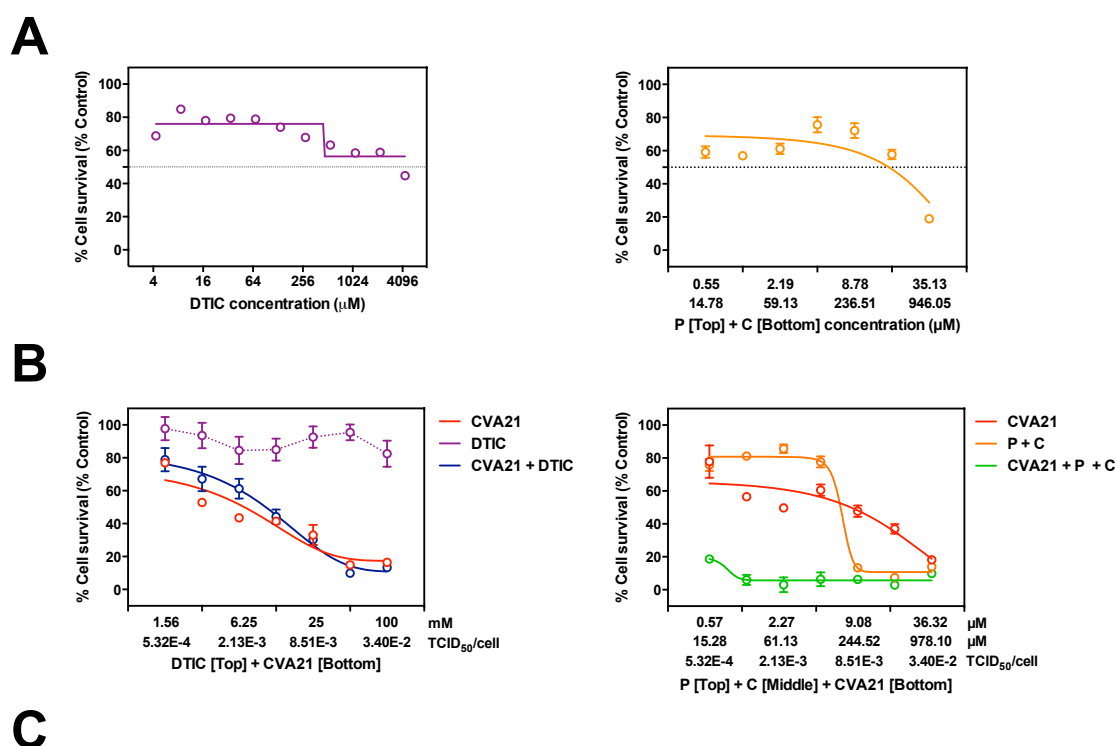
The purpose of this study was to evaluate the anti-tumour efficacy of the combined treatment of CVA21 with dacarbazine or paclitaxel and carboplatin in a mouse cell line *in vitro* before commencing *in vivo* experiments. To determine whether the commonly used chemotherapeutic agents in melanoma enhances the efficacy of CVA21, combination dose response data were analysed using the Chou-Talalay median-effect equations. Additionally, viral replication which is required for oncolytic success was also investigated in the presence of paclitaxel and carboplatin.

5.3.1 Dose response of B16-ICAM-1 cells to CVA21 in combination with DTIC and P + C

To explore potential interactions between oncolytic CVA21 and chemotherapy for the treatment of melanoma before proceeding into *in vivo* studies, cytotoxicity of CVA21 in combination with DTIC or P + C was assessed in B16-ICAM-1 cell lines *in vitro*. B16-ICAM-1 cells showed dose-dependent cytotoxicity over a three day time course after exposure to DTIC or P + C (Figure 5.13A). Dose response data revealed that B16-ICAM-1 cells were resistant to DTIC treatment even at the highest tested dose (4 mM), and the EC_{50} value could not be determined. B16-ICAM-1 cells were slightly more sensitive to P + C chemotherapy but still showed moderate levels of resistance, with approximately 20% of cells still alive at the highest concentration tested. The EC_{50} value of P + C was found to be 9.08 μ M for P and 0.24 mM for C.

Using results from these initial chemosensitivity experiments, combination experiments using 0.06 \times , 0.13 \times , 0.25 \times , 0.5 \times , 1 \times , 2 \times and 4 \times , the EC_{50} dose for the individual agents were combined at constant ratios. Sensitivity of B16-ICAM-1 to CVA21 infection was described earlier (Section 5.2.1). Dose response curves were evaluated 72 h post-treatment. The combination of CVA21 with DTIC does not appear to significantly improve efficacy in the B16-ICAM-1 cell line (Figure 5.13B, left). However, a significant increase in cytotoxicity was identified for the combination of CVA21 and P + C, at all doses tested (Figure 5.13B, right). Furthermore, at the lowest concentration tested, the combination treatment resulted in approximately 82% cell killing while single agent CVA21 and P + C treatment resulted in only 23% and 25% cell killing, respectively.

Data from this experiment was subjected to the Chou-Talalay equations. The analysis revealed that the combination of CVA21 and DTIC yields slight to moderate synergy at higher concentrations but was mostly antagonistic at lower concentrations (Figure 5.13C). CI values ranged from 0.5 to 1.0 from EC₇₅ to EC₉₅ but increased dramatically after EC₅₀. On the other hand, the CVA21 and P + C combination which induced the greatest levels of cell death translated into extremely high synergism across all combination ratios tested. The CI values ranged from 5.09×10^{-8} to 3.36×10^{-1} indicating that the combination interaction was highly synergistic.



Drug	Drug Sensitivity	Combination index values				Dm	m	r
		EC ₅₀	EC ₇₅	EC ₉₀	EC ₉₅			
Dacarbazine	> 100	1.455	0.986	0.669	0.5	8.039	0.862	0.971
Paclitaxel + Carboplatin	9.08 ± 5.37	5.09×10^{-8}	1.50×10^{-5}	5.66×10^{-3}	0.336	1.31×10^{-7}	0.155	0.326

Figure 5.13: Cytotoxicity of combination CVA21 and chemotherapy on B16-ICAM-1 murine cell line. (A) Dose-dependent cell death expressed as % cell survival induced by DTIC and P + C in B16-ICAM-1 at 72 hours post-treatment. (B) Dose response curves of CVA21 in combination with DTIC (left panel) and P + C (right panel). (C) Summary of B16-ICAM-1 combination assay. Sensitivity of B16-ICAM-1 to DTIC and P + C as single agent (mean \pm SD from three independent experiments). B16-ICAM-1 was not sensitive to DTIC treatment (>100 is an arbitrary figure stating extremely high dose of DTIC still had minimal effects). All data points indicate mean \pm SEM and are representative of three separate experiments. Abbreviations: Dm, median-effect dose; m, sigmoidicity of the dose-effect curve; r, correlation coefficient.

The results were also presented as isobolograms and Fa-CI plots. As mentioned previously, CVA21 and both drugs have entirely independent modes of action, thus the conservative isobologram method was applied [147]. The EC_{50} isobolograms showed a point value above the hypotenuse for the CVA21-DTIC combination (antagonistic), but was below the hypotenuse for the CVA21-P + C combination (highly synergistic) (Figure 5.14A). Additionally, drug-drug interaction over a range of concentrations were analysed using Fa-CI plots. The combination of CVA21 + DTIC was found to exert moderate synergistic effects only at higher concentration (Figure 5.14B, left). Interestingly, combining CVA21 with P + C resulted in CIs < 1 for the majority of the concentrations tested, strongly highlighting the synergistic anti-tumour effect of this combination across the broad range of Fa (5 - 95% cell death) (Figure 5.14B, right).

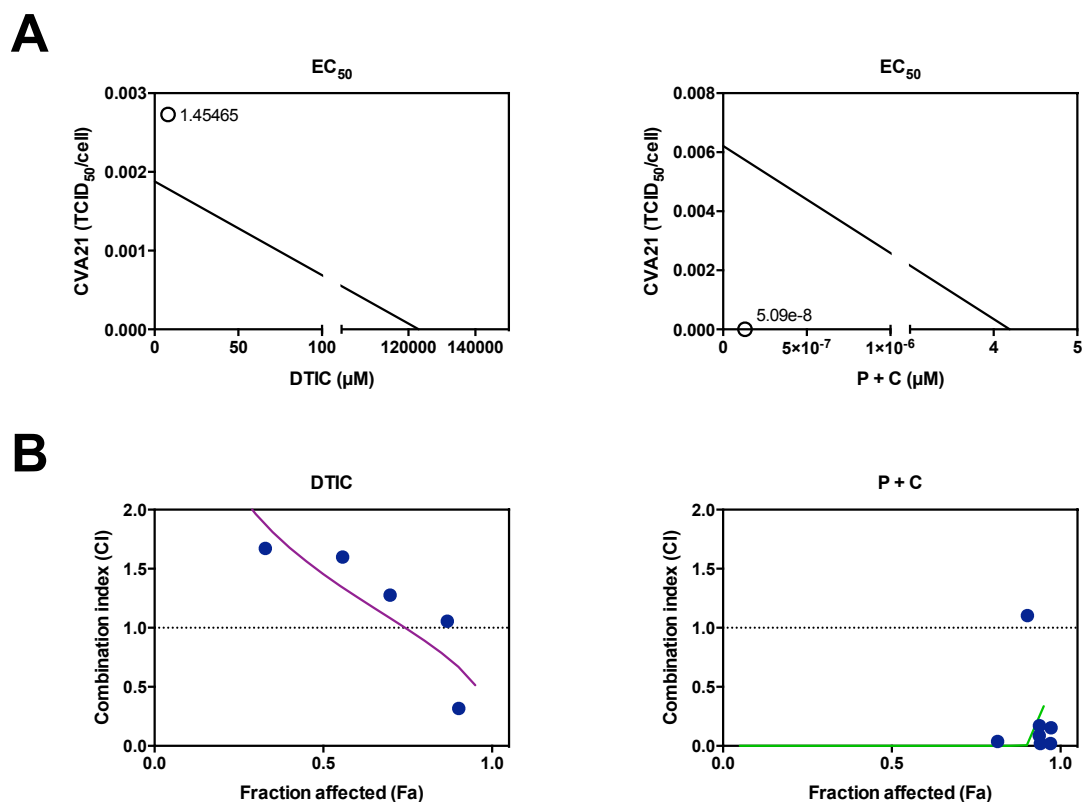


Figure 5.14: Synergistic activity of CVA21 and chemotherapy in B16-ICAM-1 cells. (A) Isobologram analysis showing the interaction between CVA21 and the respective chemotherapy at EC_{50} . Experimental combination doses required to generate 50% cell killing is indicated by the circle and labelled with the respective CI value. CVA21 is expressed as $TCID_{50}/cell$ and chemotherapeutics as μM . (B) Fa-CI plot. The additive effect of the combination is represented at $CI = 1$ (dotted line), $CI < 1$ indicates synergism, while $CI > 1$ indicates antagonism. Fa-CI plots were constructed using experimental data points (circles) and simulating CI values over the entire range of Fa values from 5% to 95% (solid line). Data shown are representative of three independent experiments.

5.3.2 Effects of P + C on CVA21 viral replication in B16-ICAM-1 cells

To explore the synergistic oncolytic effects of CVA21 and P + C combination in the B16-ICAM-1 cells, CVA21 viral replication was investigated. To capture changes in viral production levels, B16-ICAM-1 cells were inoculated with CVA21 (MOI = 1 TCID₅₀/cell). After 1 h of incubation in a 37°C and 5% CO₂ environment, unbound virus particles were washed off and cells were treated with P (0.01 - 100 µM) + C (0.27 - 2700 µM). Both supernatant and cell pellet samples were then harvested at 12, 24, and 48 h post-infection. Samples underwent three freeze-thaw cycles, centrifuged at 860 × *g* for 5 min to remove cellular debris before titrating them on confluent SK-Mel-28 cell monolayers.

Data from TCID₅₀ assays suggested that the addition of the doublet chemotherapy significantly increased viral production as early as 12 h post-treatment (Figure 5.15A). Presence of the doublet chemotherapy led to a significant increase in viral yield in a dose-dependent manner, although the response appeared less robust after 24 h. Cells treated with 100:2700 µM of P:C at 12 h had significantly higher CVA21 viral titre at 12 h with 2.3×10^4 TCID₅₀/mL, when compared to cells without the doublet chemotherapy (3.2×10^2 TCID₅₀/mL). At 24 h, the viral yield of cells treated with 100:2700 µM of P:C further increased to 1.9×10^5 TCID₅₀/mL, while viral load of cells treated with only CVA21 still maintained at 3.2×10^2 TCID₅₀/mL (Figure 5.15B). However, there was a significant decrease in viral load of cells exposed to 100:2700 µM of P:C after 48 h [2.3×10^3 TCID₅₀/mL (with P + C) *vs* 6.8×10^5 TCID₅₀/mL (without P + C) (Figure 5.15C). It is very likely that the reduction in viral yield was caused by the rapid killing induced by the chemotherapeutics at earlier time points. Without a viable host cell to replicate in, viral replication and production significantly decreases.

In parallel, to determine if the increase in viral load translates into increased cell death, B16-ICAM-1 cells were inoculated with serial dilutions of CVA21 ranging from an MOI of 0.001 - 10 TCID₅₀/cell in the absence or presence of P (1 µM) and C (27 µM). Cytotoxic effects of CVA21 with P + C were assessed at 12, 24 and 48 h post-treatment by MTT assays. In general, there was minimal difference between the two treatment options at 12 h and 24 h post-treatment (Figure 5.16A). However, significant enhancement of growth inhibition by the combination of CVA21 with P + C after 48 h of exposure. Furthermore, CVA21 mediated B16-ICAM-1 cell death in a dose dependent manner with or without P + C (Figure 5.16B). The combination of CVA21 at MOI 0.1 TCID₅₀/cell with the doublet

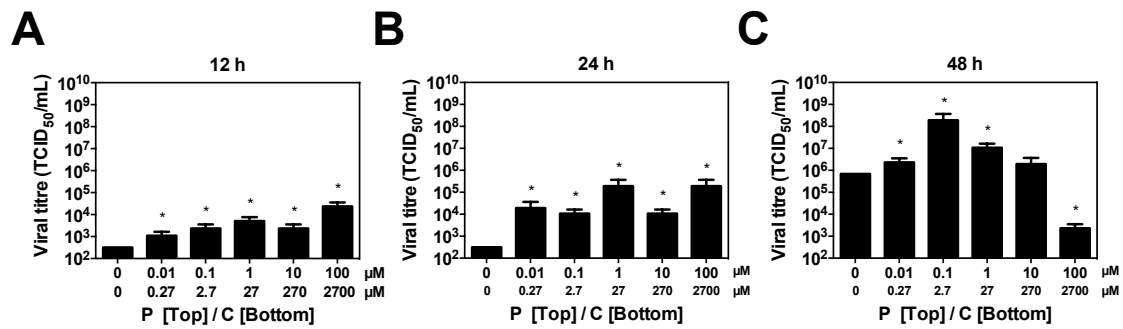


Figure 5.15: Effects of P + C on CVA21 viral production. B16-ICAM-1 cells were treated with CVA21 (1 TCID₅₀/cell) over a range of P + C concentrations over (A) 12, (B) 24, and (C) 48 h. Infectious viral titres were determined using the Karber method. Data are presented as the mean ± SD from two independent experiments. *P* values were derived from the Student’s t-test where **P* < 0.05. Treatment groups were each tested for significance against single agent CVA21 treatment.

chemotherapy inhibited more than 95% of B16-ICAM-1 cell growth 48 h post-treatment, an effect only achievable by single agent CVA21 when the initial virus inoculum was increased by 100-fold. In summary, *in vitro* experiments suggested that CVA21 and P + C interacted in a synergistic fashion resulting in enhanced B16-ICAM-1 cell killing, associated with a significant increase in viral production.

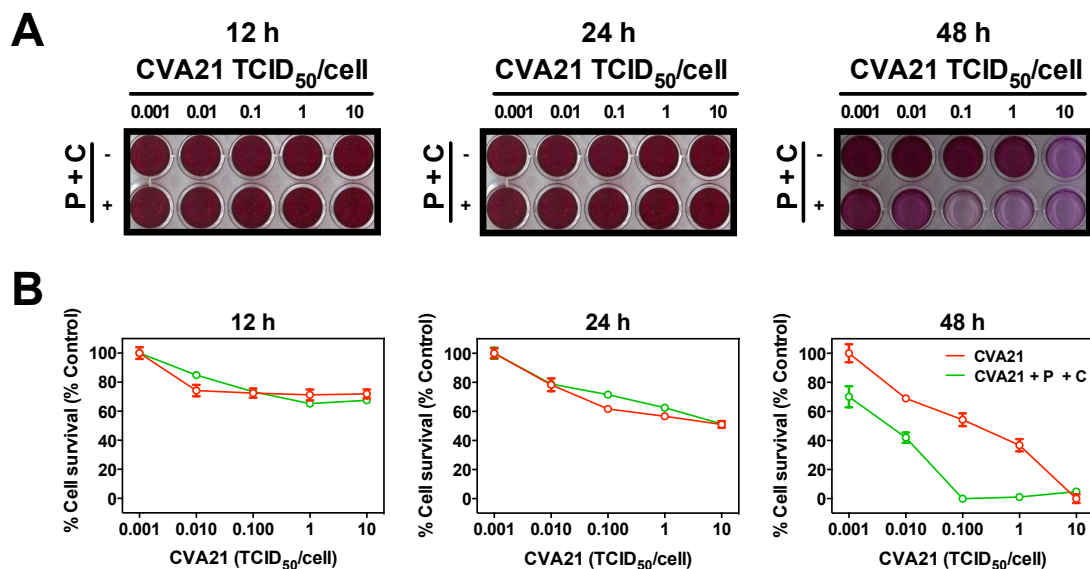


Figure 5.16: Dose-dependent cytotoxicity of CVA21 in combination with P + C on B16-ICAM-1 cells. (A) A MTT colorimetric cell viability assay was performed 12, 24, and 48 h post-treatment. Conversion of MTT into formazan crystals by living cells determined by mitochondrial activity. Cell viability correlates directly with colour intensity. (B) Dose response curves of CVA21 with or without P + C. B16-ICAM-1 cells were treated with 0.001 - 10 TCID₅₀/cell CVA21 alone or in combination with P (1 μM) + C (27 μM). The results were quantitated into cell viability %. Data points indicate the mean of duplicate values ± SEM and are representative of two separate experiments.

5.4 *In vivo* assessment of combination oncolytic CVA21 and chemotherapy in an immunocompetent mouse model

To assess whether this combination therapy approach was effective in an immunocompetent melanoma mouse model, C57BL/6 mice were implanted with murine B16-ICAM-1 tumour cells (2×10^6) intradermally on the hind flanks. Tumour were allowed to establish before commencement of chemotherapy treatment cycle 1 at day 4 and cycle 2 at day 18 post-tumour inoculation (Figure 5.17). Mice were treated with intratumoural saline or CVA21 (1×10^8 TCID₅₀/mouse), intraperitoneal DTIC (8 mg/kg), P (15 mg/kg) + C (50 mg/kg) or both on day 4. Three additional CVA21 injections (1×10^8 TCID₅₀/mouse/injection) was administered intraperitoneally at day 7, 10 and 13. Each mouse received a total of 4×10^8 TCID₅₀ virus particles during study. On day 18, animals received a second treatment of chemotherapy intraperitoneally. Mice were monitored daily and weigh up to three times a week and tumour volumes measured by electronic callipers twice a week. Blood sampling from the saphenous vein was carried out at weekly intervals. The study was terminated at day 28 post-tumour inoculation.

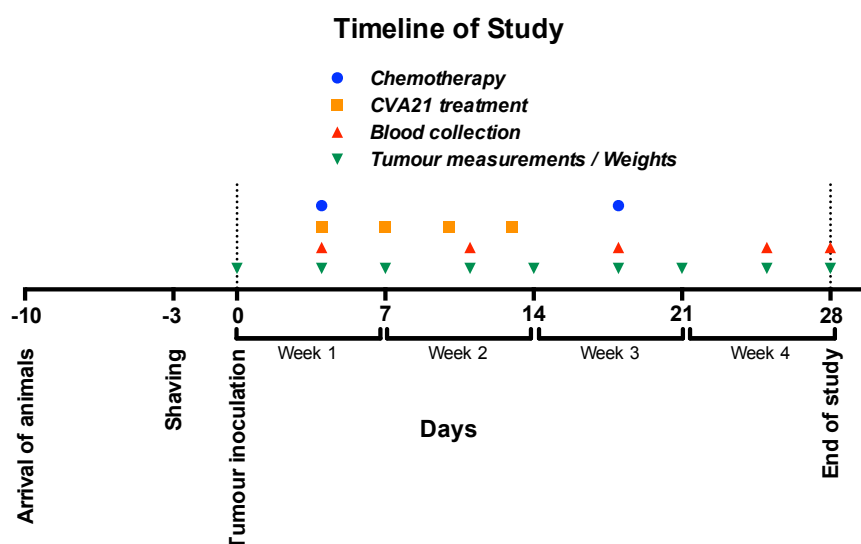
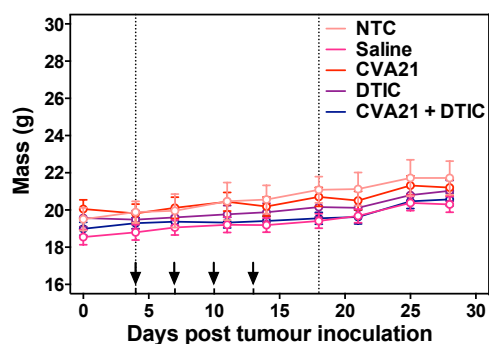


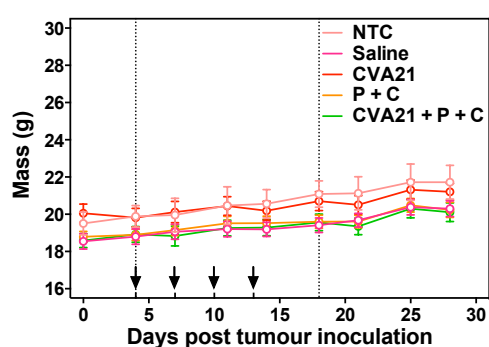
Figure 5.17: Overview of experimental protocol for immunocompetent murine melanoma model. Animals ($n = 8$) bearing B16-ICAM-1 flank tumours were treated with CVA21 (1×10^8 TCID₅₀), DTIC (8 mg/kg), P (15 mg/kg) and C (50 mg/kg), or in combination four days post-tumour cell inoculation. Animals treated with CVA21 received three additional doses of virus intraperitoneally every three days. On day 18, animals received a second treatment of chemotherapy intraperitoneally. The experiment was terminated on day 28.

5.4.1 Animal weights throughout the course of study

Animal body weights were obtained to monitor the wellbeing of tumour bearing mice during the course of the study. Changes in body weight over time in the DTIC and P + C combination were shown in Figures 5.18A & B. Both combination treatments were well tolerated by animals, indicated by the increasing average weights during the course of the study. At the end of the study, the mean body weight was 21.72 ± 1.82 for the no tumour control group, 21.21 ± 1.25 g for the CVA21 group, 21.03 ± 1.58 g for the DTIC group, 20.24 ± 1.15 g for the P + C group, 20.57 ± 1.97 for the CVA21 + DTIC group, and 20.11 ± 1.42 g for the CVA21 + P + C group. Using the two-way ANOVA test with Tukey's correction for multiple comparison, there were no statistical differences between any of the treatment groups at each time point (Figure 5.18A & B, inset). No deaths of unknown causes or signs of adverse toxicity in any mouse in the investigation were observed.

A

	Days post tumour inoculation			
	7	14	21	28
NTC vs Saline	NS	NS	NS	NS
Saline vs CVA21	NS	NS	NS	NS
Saline vs DTIC	NS	NS	NS	NS
Saline vs CVA21 + DTIC	NS	NS	NS	NS
DTIC vs CVA21 + DTIC	NS	NS	NS	NS
CVA21 vs CVA21 + DTIC	NS	NS	NS	NS

B

	Days post tumour inoculation			
	7	14	21	28
NTC vs Saline	NS	NS	NS	NS
Saline vs CVA21	NS	NS	NS	NS
Saline vs P + C	NS	NS	NS	NS
Saline vs CVA21 + P + C	NS	NS	NS	NS
P + C vs CVA21 + P + C	NS	NS	NS	NS
CVA21 vs CVA21 + P + C	NS	NS	NS	NS

Figure 5.18: Mean body weights of mice (g) over time (days). Mass of (A) DTIC experimental treatment groups and (B) P + C experimental treatment groups were expressed as grams (g) with error bars indicating SEM ($n = 8$). The dotted lines at day 4 and day 18 indicate the start of chemotherapy treatment cycles 1 and 2 respectively. The arrows indicate treatment with CVA21 at days 4, 7, 10, and 13. The same NTC, saline and CVA21 data are plotted in panel A and B for comparison. The inset displays a summary of P values calculated using the two-way ANOVA corrected for multiple comparison with Tukey's method.

5.4.2 Tumour volume data

The therapeutic efficacy of CVA21, DTIC, P + C, or the combination of virus with chemotherapy was compared in B16-ICAM-1 flank tumours in C57BL/6 mice. Tumour volumes were measured twice a week using electronic vernier callipers and calculated using the formula of a spheroid. At four days post-tumour implantation, animals were treated either with CVA21 alone, chemotherapy alone or CVA21 in combination with chemotherapy. By day 28, the study was terminated and all treatment groups showed reduced average tumour volumes compared to saline treated control mice (Figure 5.19A & B). The mean B16-ICAM-1 flank tumour volume of animals treated with saline was $268.91 \pm 344.54 \text{ mm}^3$, $84.49 \pm 111.74 \text{ mm}^3$ for CVA21, $78.18 \pm 151.66 \text{ mm}^3$ for DTIC, and $113.70 \pm 255.29 \text{ mm}^3$ for P + C.

Statistical analysis performed using the two-way ANOVA with Tukey's correction for multiple comparison revealed that single agent CVA21 and DTIC had a strong effect ($P < 0.001$) in reducing tumour burden while the doublet P + C treatment had a moderate effect ($P < 0.05$) when compared to saline treated animals (5.19A & B, inset). However, the combination of CVA21 with either DTIC ($42.87 \pm 66.87 \text{ mm}^3$) or P + C ($9.70 \pm 20.22 \text{ mm}^3$) produced the greatest anti-tumour effect ($P < 0.0001$), strongly suggesting a synergistic interaction between CVA21 and either chemotherapy in an immunocompetent setting. Furthermore, tumours treated with CVA21 and P + C had slightly smaller mean volumes than either single agent treatment but without statistical significance further suggesting that the synergistic cytotoxicity in B16-ICAM-1 cells seen *in vitro* may translate to the clinic.

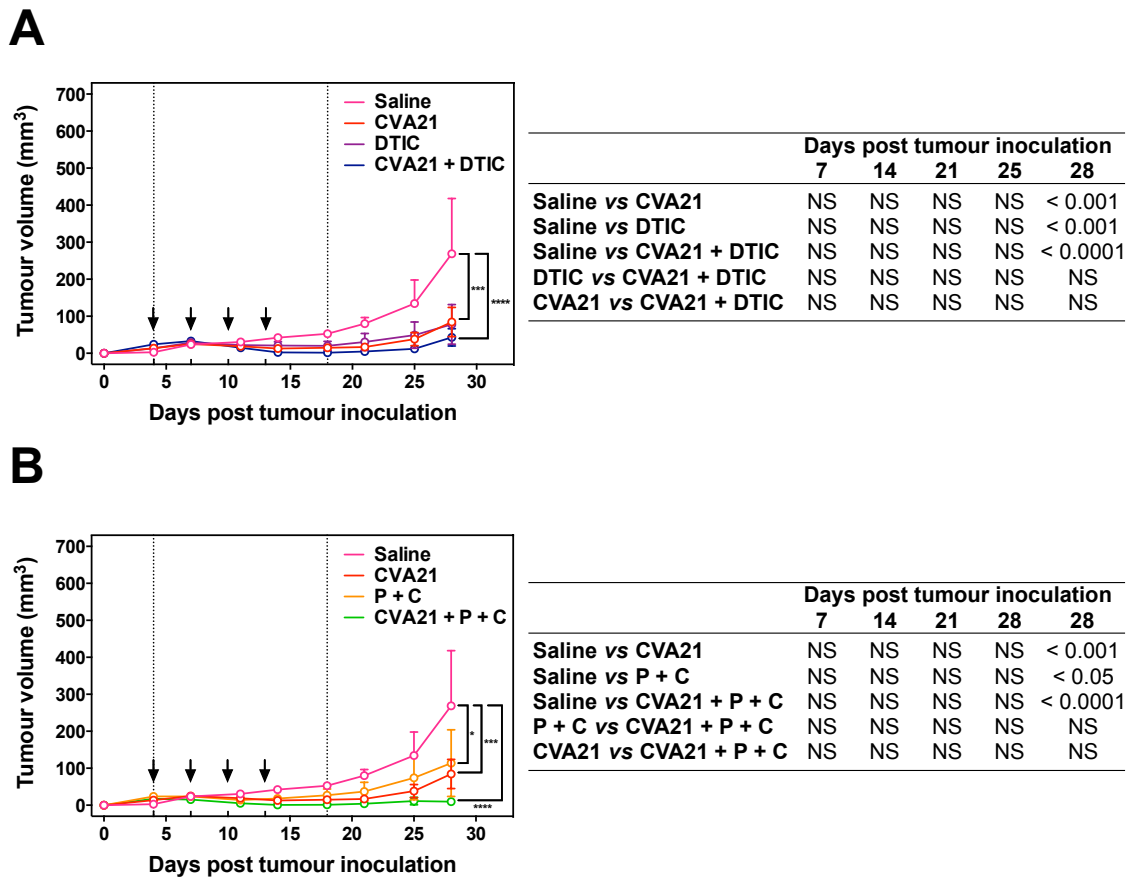


Figure 5.19: Combination of chemotherapy and CVA21 virotherapy on B16-ICAM-1 murine flank tumours. C57BL/6 mice were injected with B16-ICAM-1 melanoma cells on the hind flank. Tumours were allowed to establish for four days, prior to treatment with either saline (i.t.), CVA21 (i.t., 1×10^8 TCID₅₀), DTIC (i.p., 8 mg/kg), P (i.p., 15 mg/kg) + C (i.p., 50 mg/kg) injection, or in combination with DTIC of P + C. The arrows indicate treatment with CVA21 at days 4 (i.t.), 7 (i.p.), 10 (i.p.) and 13 (i.p.). Mice received a second cycle of chemotherapy dosing at day 18 (dotted lines indicate days of chemotherapy administration). Tumour volumes of (A) DTIC combination and (B) P + C combination were measured twice weekly. All tumour volumes are expressed as average tumour volume \pm SEM mm³ (n = 8). The inset displays a summary of P values calculated using the two-way ANOVA corrected for multiple comparison with Tukey's method.

5.4.3 CVA21 viraemia

To examine whether either chemotherapy affected levels of circulating viraemia, weekly serum samples were collected and assessed by one-step qRT-PCR for CVA21 virus particles. Infectious CVA21 was detected in the serum of virus treated animals approximately 45 min post-i.t. injection of virus on day four. Interestingly, the mean virus titre of animals receiving the combination therapy of DTIC (5.66×10^4 TCID₅₀ equivalent/mL; 2.3-fold higher) or P + C (9.08×10^4 TCID₅₀ equivalent/mL; 3.7-fold higher) was higher than animals receiving the virus alone (2.43×10^4 TCID₅₀ equivalent/mL) (Figure 5.20A). However, this difference was not statistically significant ($P > 0.05$, one-way ANOVA). Furthermore, the levels of virus in the blood were eliminated within the first week, by day 11 despite additional treatments with CVA21 intraperitoneally (Figure 5.20B). Given these mice have a fully intact immune system, the clearance of CVA21 from the blood stream is not surprising.

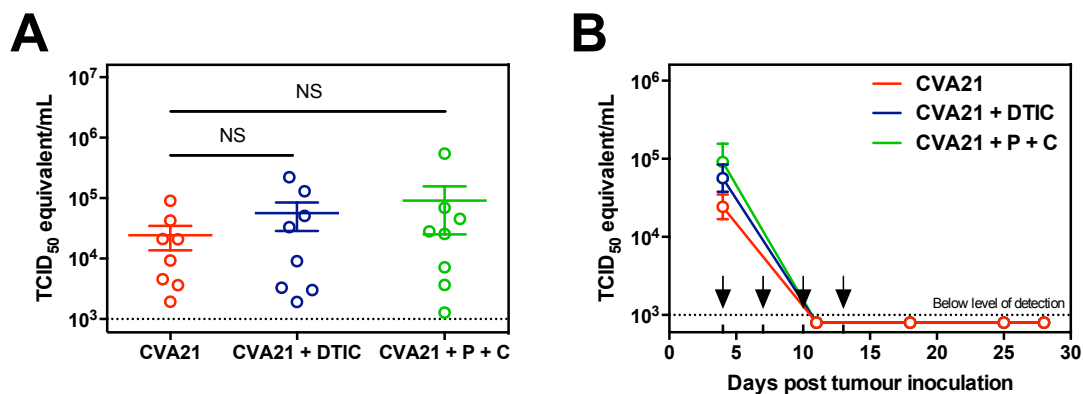


Figure 5.20: Detection of viraemia following CVA21 oncolytic virotherapy with and without chemotherapy. Viraemia levels were determined one-step qRT-PCR ($n = 8$). One TCID₅₀ equivalent/mL represents approximately 1×10^3 viral copies/mL. Arrows indicate administration of the virus intratumourally at day 4 and then intraperitoneally at days 7, 10 and 13. The horizontal dotted line represents the detection limit of the assay at 1,000 TCID₅₀equivalent/mL.

5.4.4 CVA21 neutralising antibodies

One of the hallmarks of anti-viral immunity is the production of neutralising antibodies against the virus. The previous immunodeficient model using SCID mice failed to address this aspect of the therapy. To evaluate this, terminal blood samples collected at the conclusion of the study via cardiac puncture were assessed for anti-CVA21 neutralising antibody (nAb) levels. In both treatment groups, clear signs of tumour regression were observed even in the presence of anti-CVA21 nAb levels as seen in Figure 5.19A & B. Animals treated with CVA21 alone showed higher levels of nAbs (a titre of 1:724) *vs* CVA21 in combination with DTIC (1:326) or P + C (1:326). No anti-CVA nAb were detected from all animals that did not received CVA21 injections (Figure 5.21).

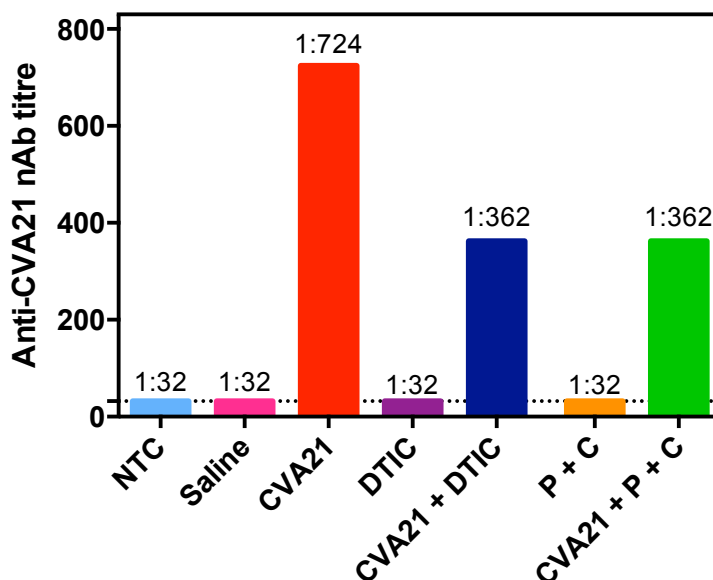


Figure 5.21: Presence of nAbs in serum following treatment with CVA21 and CVA21 in combination with DTIC or P + C. Evidence for circulating neutralising antibodies in immunocompetent mice ($n = 8$). Detectable neutralising antibodies in the bloodstream of CVA21 (red bar), CVA21 + DTIC (blue bar), and CVA21 + P + C (green bar) treated animals on day 28. The neutralising titre was defined as the reciprocal of the serum dilution required to reduce viral infectivity by 50% and expressed as the geometric mean from two independent experiments. 1:32 denotes baseline neutralisation .

Chapter 6

Combining oncolytic CVA21 with immune checkpoint inhibitors for the treatment of melanoma

Oncolytic virus immunotherapy is a new form of melanoma therapy that uses native or genetically modified viruses to selectively enter, replicate, and lyse tumour cells. Oncolytic viruses mediate anti-tumour activity through primary lysis of tumour cells, potent bystander effects on uninfected tumour cells, induction of local antiviral immunity, and priming of systemic tumour-specific immunity that can mediate tumour regression at distant, uninfected lesions [60, 88, 141, 442]. Numerous preclinical tumour models have demonstrated the therapeutic effectiveness of oncolytic immunotherapy [88]. In addition, the clinical success of several OVs in stimulating an effective anti-tumour immune response has been observed in early-phase and now late-phases clinical trials [81, 316, 340, 455].

Previously, we successfully demonstrated the efficacy of CVA21 as a single agent and in combination with several conventional chemotherapeutic agents in a range of melanoma mouse models. In this chapter, using the same animal models we previously have developed, we sought to investigate the role of CVA21 as an potential immunotherapeutic agent for the treatment of melanoma. Our hypothesis is that CVA21 infection and subsequent lysis of tumour cells, results in the release of cellular debris containing melanoma antigens that stimulate anti-tumoural immunity, thereby acting as a personalised *in situ* cancer vaccine. In the first section of this chapter, findings are presented on tumour immunity evoked by immunising animals with cell lysates produced following *in vitro* infection by CVA21. In the following sections, we explored the immunotherapeutic potential of CVA21

in combination with systemic CTLA-4 and PD-1 blockade. Our findings from this chapter provide a strong rationale for investigation of such combination therapies in the clinic.

6.1 Induction of anti-tumour immune response by CVA21 oncolysates

Triggering systemic and prolonged anti-tumour immunity by oncolysis represents a promising strategy for an effective and durable response. Tumour destruction by an OV can release a wide range of tumour-associated antigens (TAAs) that will be taken up by infiltrating APCs for cross-presentation to T cells for priming of antigen specific immune response. Based on this premise, the main aim of this study is to investigate if immunisation with an *in vitro* CVA21-infected melanoma cell lysate could prime an effective immune response against tumour cells and subsequently hinder melanoma growth. A schematic presentation of the immunisation model is showed in Figure 6.1. Briefly, C57BL/6 mice were immunised intraperitoneally with different laboratory made vaccines (described in Materials and Method, Section 3.2.3). Fourteen days after vaccination, 2×10^5 B16 cells were injected into the hind flank of animals intradermally. Mice were monitored daily and weigh up to three times a week and tumour volumes measured by electronic callipers twice a week. The study was terminated at 17 days post-tumour inoculation.

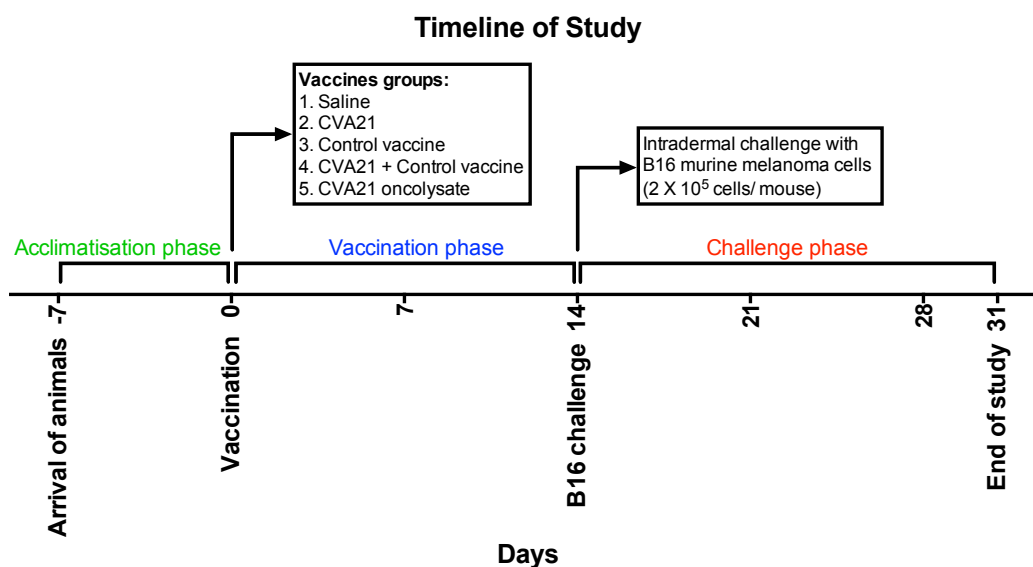


Figure 6.1: Overview of experimental protocol for CVA21-oncolysate immunisation murine melanoma model. After a seven day acclimatisation period, animals from each group ($n = 8$) were immunised intraperitoneally with five different vaccines, saline alone, CVA21 (2×10^8 TCID₅₀/mouse), control vaccine (2×10^6 mechanically lysed B16-ICAM-1 cells), CVA21 + control vaccine, and CVA21 oncolysate (CVA21 lysed B16-ICAM-1 cells). Fourteen days after vaccination, animals were challenged with 2×10^5 B16 cells injected intradermally into the hind flank. Study was terminated at day 31.

6.1.1 Animal weights throughout the course of study

Animal body weights were obtained to monitor the wellbeing of tumour bearing mice during the course of the study. Changes in body weight over time in the DTIC and P + C combination are shown in Figures 6.2. All laboratory made vaccines were well tolerated by animals, indicated by the increasing average weights during the vaccination phase of the study. The mean body weight was 21.35 ± 1.54 for the no tumour control group, $20.17.21 \pm 1.18$ g for the saline group, 20.30 ± 1.04 g for the CVA21 group, 20.59 ± 0.71 g for the control vaccine group, 20.47 ± 0.94 for the CVA21 + control vaccine group, and 20.58 ± 0.71 g for the CVA21 oncolysate group. During the live tumour challenge phase, animals with ulcerated tumours experienced significant weight loss and were euthanised immediately. No deaths of unknown causes or signs of adverse toxicity in any mouse were observed during the investigation.

6.1.2 Anti-tumour effect of CVA21 oncolysate

The therapeutic efficacy of the various laboratory vaccines were compared in B16 flank tumours in C57BL/6 mice. Animals were challenged with 2×10^5 live B16 cells after which tumours were measured using electronic vernier callipers and tumour volumes were

calculated using the formula of a spheroid. During the entire duration of the study, no signs of tumour regression were observed in any treatment group. All animals developed palpable tumours, some of which had begun to ulcerate and the study was terminated 17 days after tumour inoculation. The mean B16 flank tumour volume of animals immunised with saline was $813.91 \pm 669.69 \text{ mm}^3$, $603.91 \pm 259.01 \text{ mm}^3$ for CVA21, $719.59 \pm 565.28 \text{ mm}^3$ for control vaccine, $616.60 \pm 683.06 \text{ mm}^3$ for CVA21 + control vaccine, and 314.43

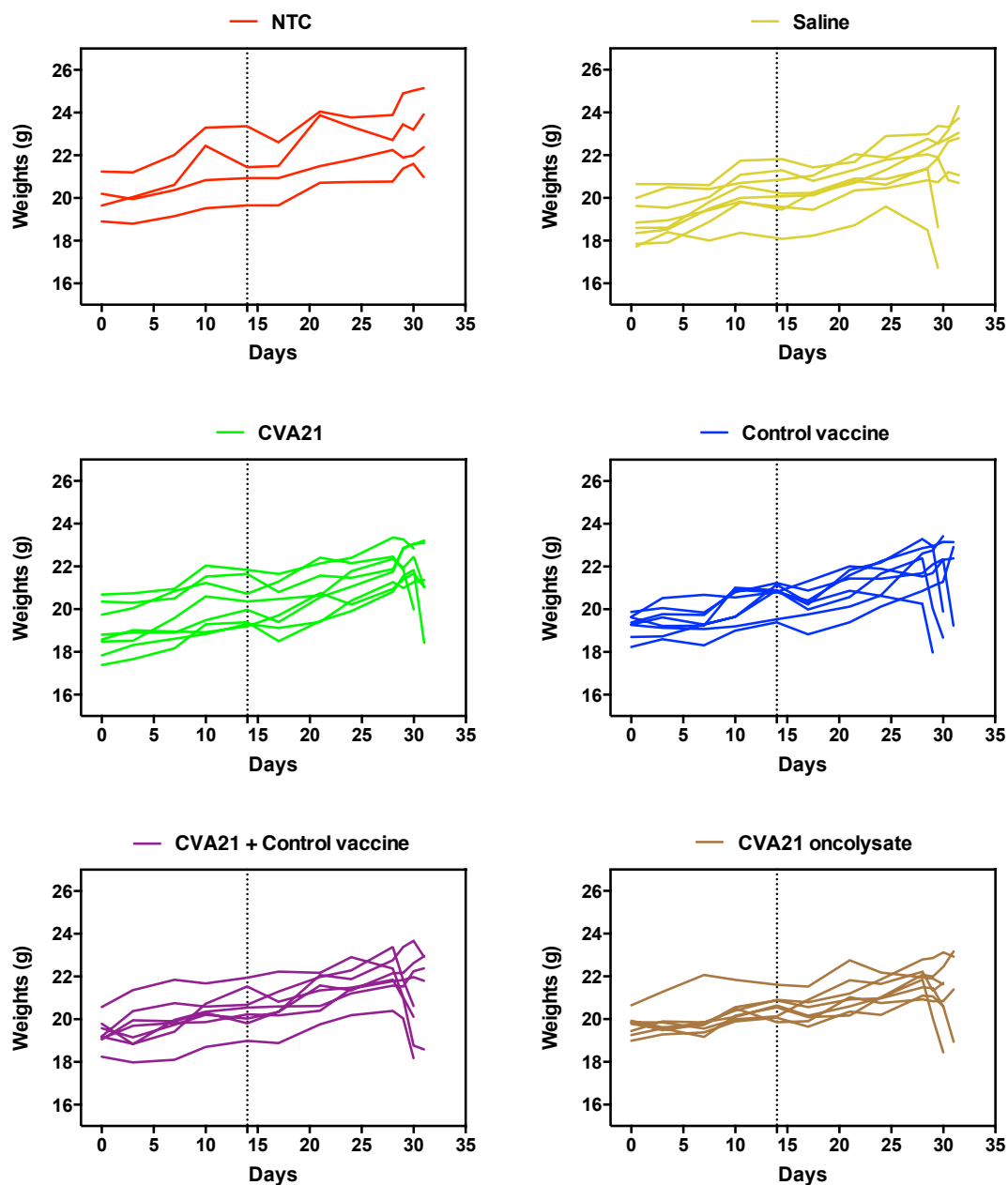


Figure 6.2: Individual body weights of mice (g) over time (days). The dotted line at day 14 indicates the start of the B16 live tumour challenge. Animals ($n = 8$) were weighed at least twice weekly during the entire duration of the study. Animals experiencing a weight loss of more than 10% from the previous measurement were euthanised immediately.

$\pm 91.84 \text{ mm}^3$ for CVA21 oncolysate (Figure 6.3A).

Statistical analysis performed using the two-way ANOVA with Tukey's correction for multiple comparisons did not indicate any significant inhibition of tumour growth for any of the treatment groups when compared to the saline treated animals ($P > 0.05$). Though not statistically significant, animals immunised with the CVA21 oncolysate did experienced a modest tumour growth inhibition (mean flank tumour volumes were approximately 2.5-fold lower than saline treated animals). Interestingly, when studying the tumour response of individual animals, 6 out of 8 animals from the CVA21 + control vaccine group experienced modest tumour growth inhibition (Figure 6.3B). These results, suggest that the lysis of B16-ICAM-1 cells by CVA21 or the interaction of CVA21 with B16-ICAM-1 cell debris may stimulate an anti-tumour response against B16 melanoma cells.

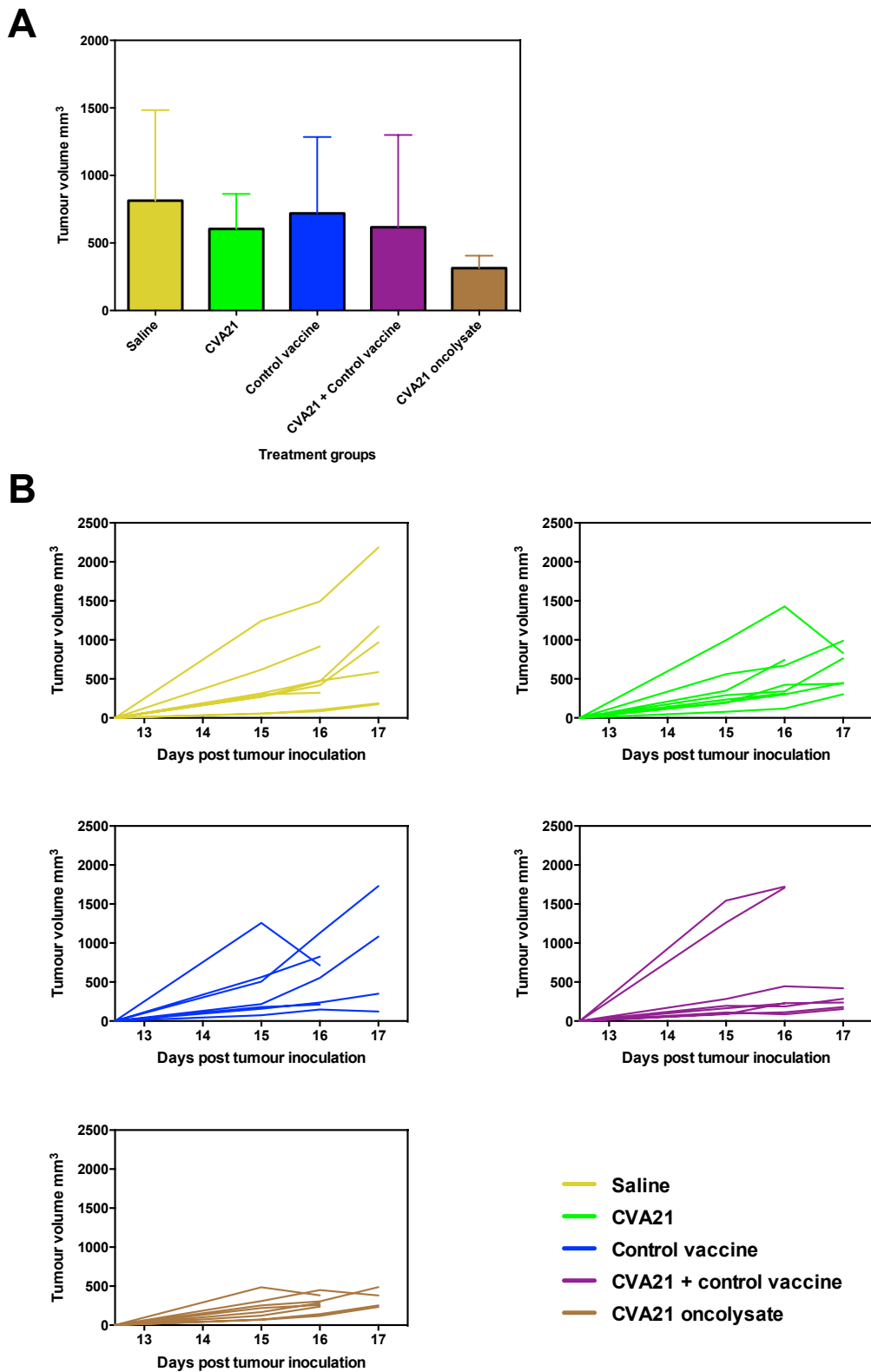
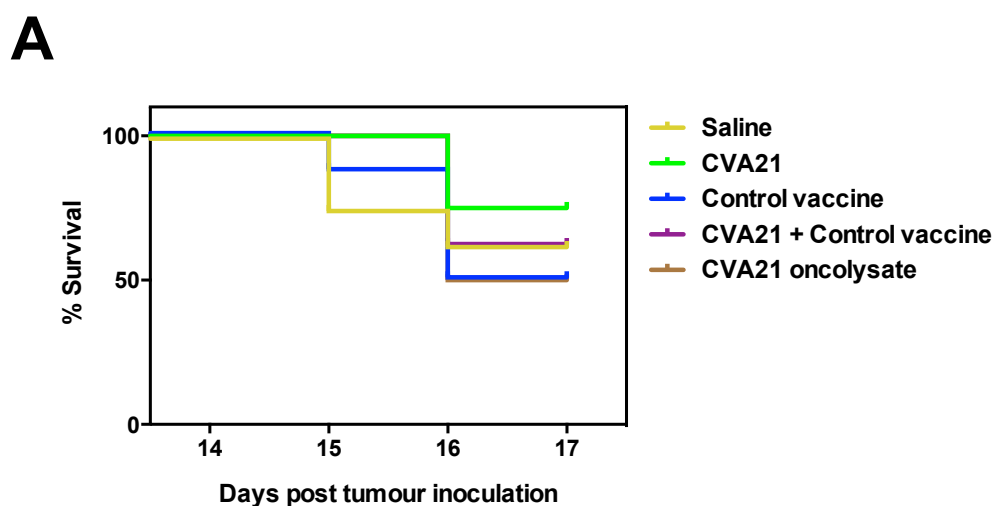


Figure 6.3: B16 tumour growth following immunisation with saline, CVA21, control vaccine, CVA21 + control vaccine, or CVA21 oncolysate. Animals were challenged with B16 tumours 14 days after immunisation. Tumour volumes were measured twice weekly. **(A)** Average tumour volume of each treatment group at the end of study with error bars indicating SEM ($n = 8$). Using the two-way ANOVA corrected for multiple comparison with Tukey's method, no significant difference was observed ($P > 0.05$). **(B)** Tumour response of individual animals. Several animals were euthanised due to tumour ulceration.

6.1.3 Survival data of animals treated with CVA21 oncolysate

As described previously, intradermal injection of B16 tumour cells produces a solid tumour which may ulcerate. Ulcerated/necrotic tissue may result in a loss of body fluid and/or severe weight loss, thus, was used as an endpoint for the study. The study was terminated 17 days post-tumour inoculation due to an observed onset of ulceration in all treatment groups. Analysis of Kaplan-Meier curves using log-rank tests showed no significant differences in the survival kinetics for all treatment groups (Figure 6.4A). The study did not provide any meaningful survival data as the study was terminated before the median survival could be determined for several groups (Figure 6.4B).



B

	Saline	CVA21	Control vaccine	CVA21 + Control vaccine	CVA21 oncolysate
# censored subjects	5	6	4	5	4
# deaths / events	3	2	4	3	4
Median survival	N/A	N/A	16.5	N/A	16.5

Figure 6.4: Survival of C57BL/6 mice following immunisation with CVA21 oncolysates. (A) Kaplan-Meier plot demonstrating survival rates of animals ($n = 8$) following immunisation with CVA21, control vaccine, CVA21 + control vaccine, and CVA21 oncolysate. A log-rank (Mantel-Cox) test was used to compare groups to the combination therapy. (B) Table showing median survival of mice from each treatment group. No significant survival benefit was observed.

6.2 *In vivo* assessment of combination oncolytic virotherapy and anti-PD-1 immunotherapy in an immunocompetent mouse model

The discovery of T cell regulatory receptors have provided targets for immunotherapies aiming to enhance activation of antitumour immune responses or to reverse immunosuppressive mechanisms governing tumour resistance. Targeting of the latter with antibodies to immunologic checkpoints such as PD-1 has demonstrated therapeutic efficacy for some cancers. To assess whether the combination CVA21 and anti-PD-1 therapy approach was effective in an immune-competent mouse model of melanoma, C57BL/6 mice were implanted with murine B16- ICAM-1 tumour cells (2×10^5 cells/mouse) intradermally on the left hind flank. Tumours were allowed to establish before commencement of therapy at 6, 9, 12 and 15 days post-tumour inoculation (Figure 6.5). CVA21-treated animals were given up to four additional intratumoural injections of CVA21 at weekly intervals. Saline or CVA21 was administered intratumourally at the indicated time points, while the control antibody or anti-PD-1 antibody were administered intraperitoneally. Mice were challenged with live B16 cells (1×10^5 cells/mouse) intradermally on the right hind flank. Mice were monitored daily and weighed up to three times a week and tumour volumes measured by electronic callipers three times a week. Blood sampling from the saphenous vein was carried out at weekly intervals. The study was terminated at day 66 post-tumour inoculation.

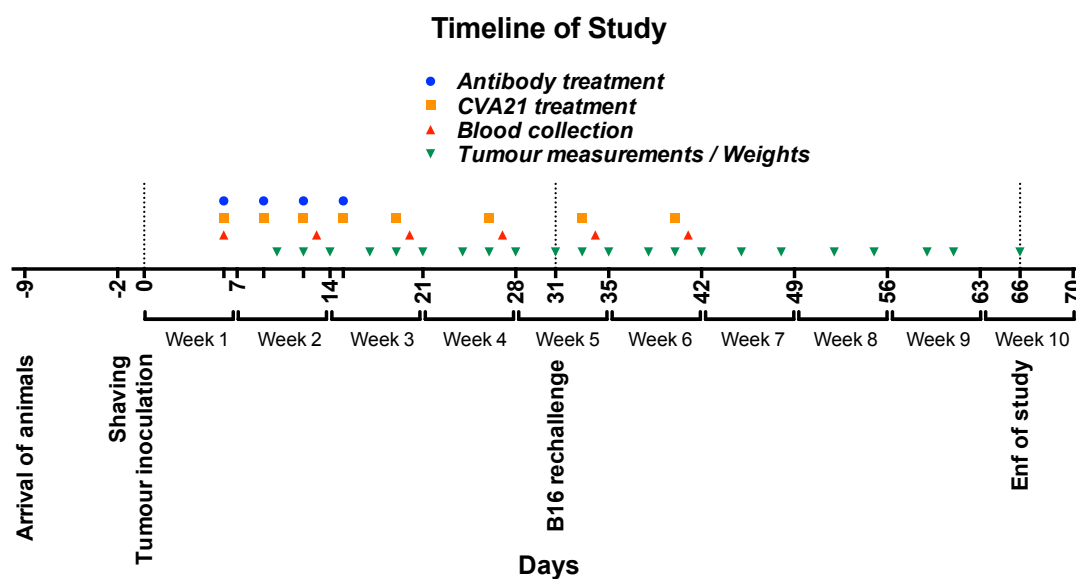


Figure 6.5: Treatment scheme of anti-PD-1 combination immune-competent murine melanoma protocol. Time line showing the schedule of treatments (blue circles [anti-PD-1 antibody], orange squares [CVA21]) and monitoring procedures (red triangles [blood collection] and green triangles [tumour measurements and body weight measurements]). Animals ($n = 12$) were first treated with either i.t. saline or CVA21 (1×10^8 TCID₅₀/injection), followed by i.p. injections with the murine isotype control antibody or the anti-PD-1 antibody (12.5 mg/kg). The experiment was terminated on day 66.

6.2.1 Body weights following treatment with either saline or CVA21 in combination with anti-PD-1 or control antibody

Body weights of animals were recorded up to three times a week as an indicator of the animal's wellbeing. The average changes in body weight over time were shown in Figure 6.6A, and individual changes were shown in Figure 6.6B. Animals that received the combination treatment generally exhibited steady weight gain or maintenance compared to control animals whose rapid weight gain/loss were likely to be due to the uncontrolled growth of large tumours resulting in ulceration. The combination treatment was well tolerated by animals evident by the increasing average weights during the course of the study. No statistically significant differences in the mean body weights were observed between the treatment groups and NTC mice at any of the time points (two-way ANOVA corrected for multiple comparisons using the Tukey's method). Furthermore, no deaths of unknown causes or signs of adverse toxicity were observed in any mouse during the investigation.

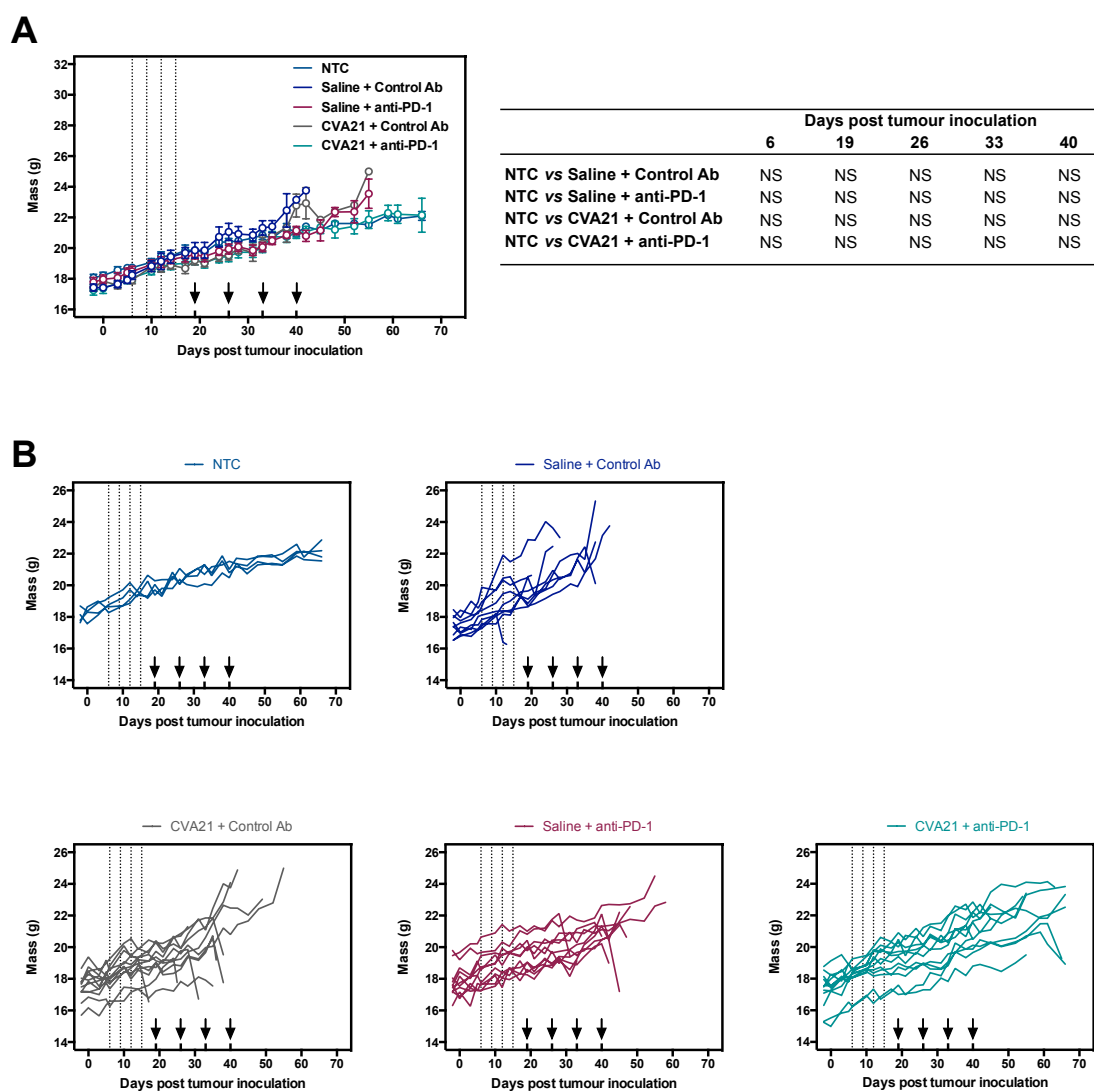


Figure 6.6: Body weights of mice (g) vs time (days). (A) Average mass of animals on study were expressed as grams (g) with error bars indicating SEM ($n = 12$). The inset displays a summary of P values calculated using the two-way ANOVA corrected for multiple comparison with Tukey's method. Some fluctuations in mean weights were observed due to the euthanasia of mice over the duration of the study. (B) Individual body weights of mice. The dotted lines at day 6, 9, 12 and 15 show each cycle of therapy. The arrows indicate additional treated with CVA21 at days 19, 26, 33, and 40.

6.2.2 Tumour volume data

The bilateral flank B16-ICAM-1/B16 tumour model was used to determine CVA21 efficacy in combination with anti-PD-1. Primary melanoma tumours were implanted by injecting 2×10^5 B16-ICAM-1 cells in the left hind flank intradermally on day 0. Secondary tumours were established by injecting 1×10^5 B16 cells in the right hind flank intradermally on day 31. Tumours were measured three times a week using digital callipers and animals were euthanised when tumour ulceration was observed.

6.2.2.1 Tumour volumes of primary B16-ICAM-1 nodules

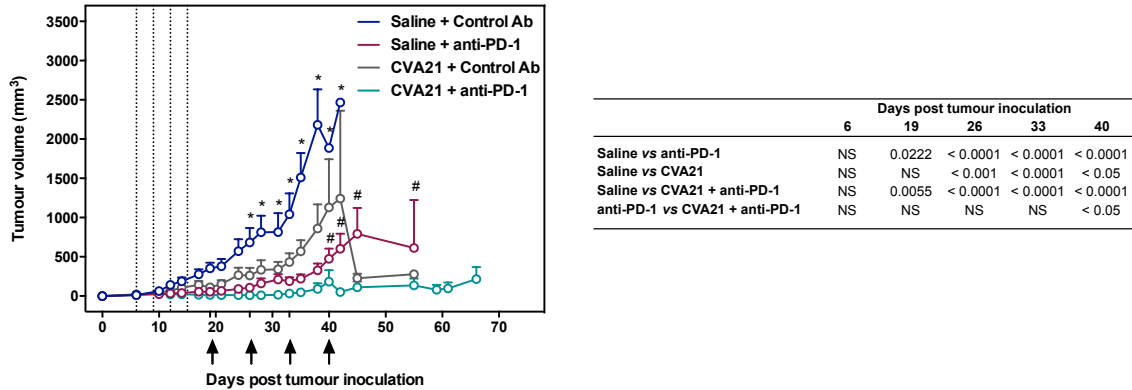
The *in vivo* data presented in the earlier section (Section 6.1) indicated that *in vitro* CVA21 cell lysis might be able to enhance the immunogenicity of B16-ICAM-1 cells, possibly delaying the growth of B16 melanoma tumour rechallenge. To determine if the lysis of CVA21-injected tumours could stimulate an anti-tumour immune response and whether the combination with anti-PD-1 could augment this response, the experiment was performed with B16-ICAM-1 and B16 melanoma tumours implanted on opposite flanks. The treatment protocol was summarised in Figure 6.5 and tumour volume was calculated using the formula of a spheroid.

All control animals developed tumours and were euthanised by day 42 due to progressive disease (Figure 6.7A & B, top left). Tumours had either ulcerated or had escalated reaching the maximal ethical endpoint ($> 2500 \text{ mm}^3$), necessitating euthanasia. Unsurprisingly, treatment with CVA21 alone was not curative and only resulted in the delay of primary tumour growth. A further delay in tumour growth was observed in animals treated with the anti-PD-1 antibody alone, but failed to result in the long-term inhibition (Figure 6.7B, top right). Remarkably, the combination of CVA21 with anti-PD-1 antibody showed the best tumour response with a notable delay in tumour onset and only six animals showing signs of primary tumour growth towards the latter half of the study, an effect that was not seen with either treatment alone.

Given that the last of the tumour-bearing animals in the saline + control antibody group were euthanised at day 42, a two-way ANOVA analysis was carried out using the tumour volume data of all mice collected up until this day, to compare the efficacy of each treatment groups. Using Tukey's method for multiple comparison, all treatments significantly inhibited tumour growth by day 26 when compared to the saline + control antibody treatment group ($P < 0.001$) (Figure 6.7A, inset). Furthermore, tumour growth inhibition was greater with the combination of intratumourally administered CVA21 and i.p. anti-PD-1 antibody and this was statistically significant ($P < 0.0001$). More importantly, a separate two-way ANOVA analysis was used to analyse the tumour volume data from both the saline + anti-PD-1 and CVA21 + anti-PD-1 treatment groups. The analysis revealed that mean tumour volumes of animals receiving the combination therapy were significantly lower when compared to animals receiving the anti-PD-1 antibody alone after day 40 ($P < 0.05$), suggesting that the combination treatment produces a more lasting anti-tumour

response.

A



B

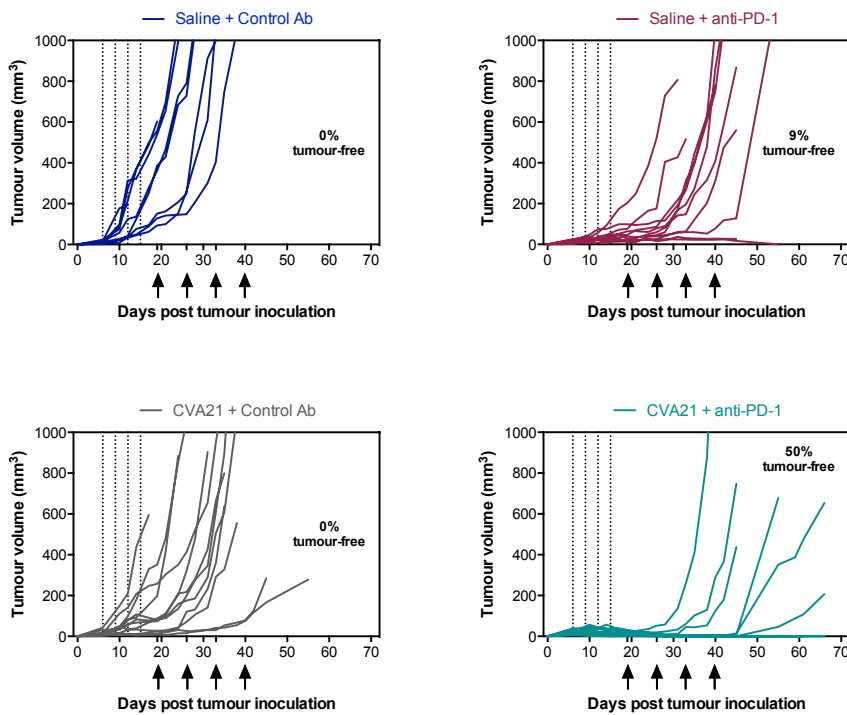


Figure 6.7: Tumour volumes following combination anti-PD-1 antibody and CVA21 virotherapy on primary B16-ICAM-1 murine melanoma tumours. C57BL/6 mice were injected with B16-ICAM-1 cells intradermally on the left hind flank. Animals were treated with either saline (i.t.), CVA21 (i.t., 1×10^8 TCID₅₀/injection), control or anti-PD-1 antibody (i.p., 12.5 mg/kg), or CVA21 in combination with anti-PD-1 antibody. **(A)** Tumour volumes (mm³) expressed as the average with the upper limit of the SEM (n = 12). The inset displays a summary of P values calculated using the two-way ANOVA corrected for multiple comparison with Tukey’s method. * Saline + control antibody vs all treatment groups (P < 0.05); # Saline + anti-PD-1 vs CVA21 + anti-PD-1 (P < 0.05). **(B)** Individual tumour volumes from each mouse. Treatment days are indicated by the dotted lines and additional i.t. virus injections (1×10^8 TCID₅₀/injection) were administered at days 19, 26, 33, and 40 (solid arrow).

6.2.2.2 Tumour volumes of secondary B16 nodules

To determine if a robust anti-tumour response had developed following treatment and whether durable anti-tumour protection was possible, remaining animals were rechallenged with 1×10^5 B16 cells into the right hind flank intradermally on day 31. Animals received B16 cells which lacked the human ICAM-1 receptor and were therefore resistant to CVA21 therapy, ruling out the possibility of oncolysis by residual CVA21. These cells are antigenically similar to the B16 cells used to generate the B16-ICAM-1 cell line and were used to identify the presence of a specific anti-tumoural immune response that may have resulted following oncolysis of the primary tumour.

As seen in Figure 6.8A, bilateral tumours eventually developed in all of the mice rechallenged with B16 cells. Although the combination therapy resulted in 50% tumour remission of the primary B16-ICAM-1 left flank tumour, it failed to result in long-term protection and tumour rejection in bilateral B16 tumours. Interestingly, only animals receiving the combination treatment demonstrated a significant delay in the incidence rate of a palpable B16 flank tumours (defined using Kaplan-Meier survival curves) ($P < 0.01$) (Figure 6.8B). It can be seen from the data in Table 6.8C that the median time to palpable B16 tumours in saline, single agent anti-PD-1, and CVA21 treated animals was significantly earlier when compared to the combination group (38 days *vs* 49.5 days, respectively). Overall, the above results suggest that in this study, intratumourally injected CVA21 was not sufficient in inducing an effective anti-tumour immune response against B16 tumours, but when combined with anti-PD-1 antibodies could illicit an immune response capable of significantly delaying the onset of palpable tumour nodules.

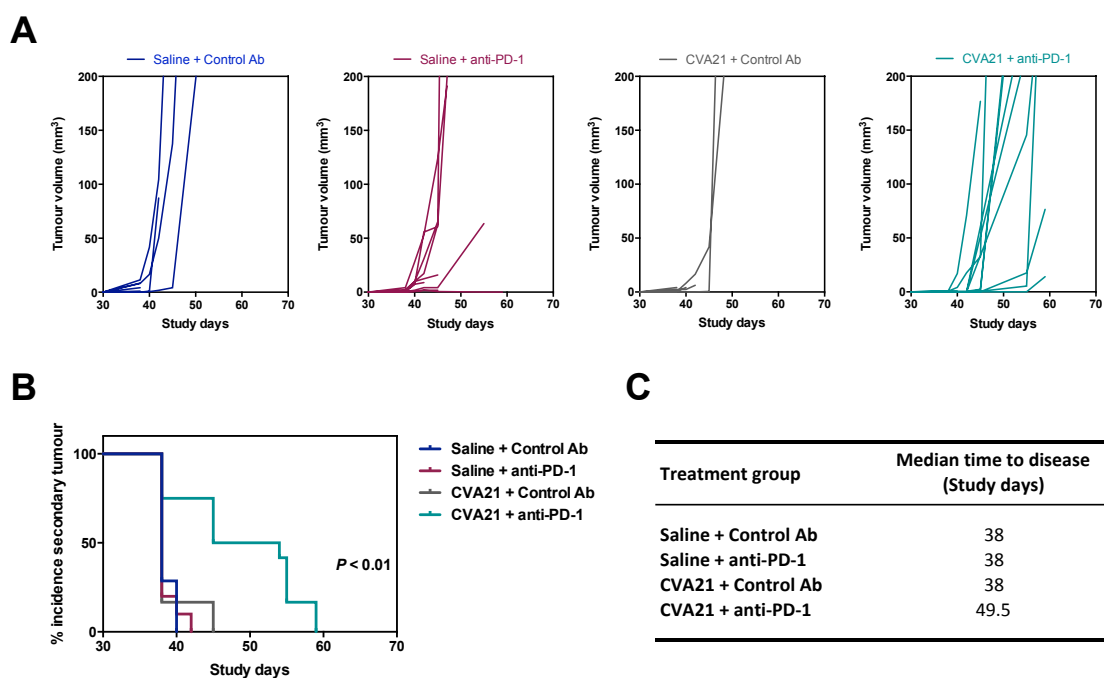
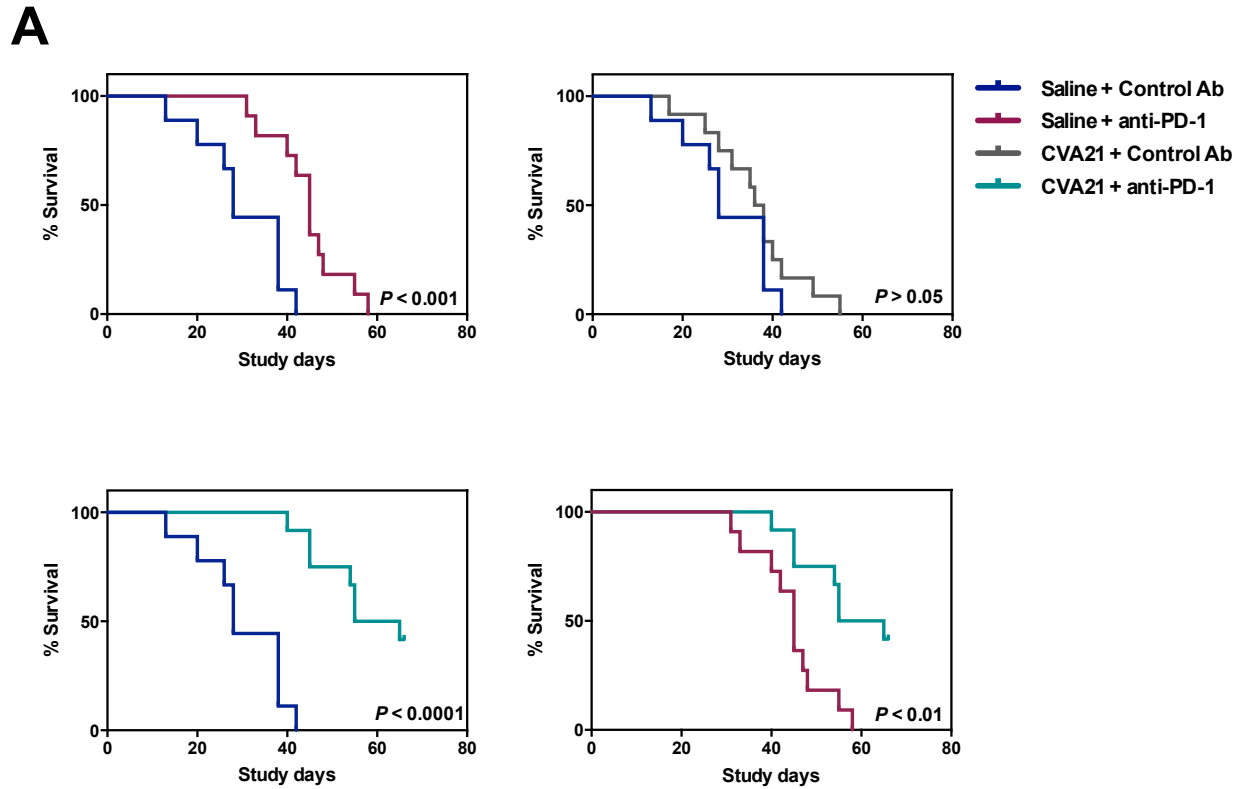


Figure 6.8: Tumour development of secondary B16 tumour nodules. (A) Individual tumour volumes from each mouse ($n = 12$) following rechallenge with B16 tumour cells (1×10^5 cells/mouse) on the right hind flank at day 31. (B) Kaplan-Meier survival plot demonstrating the development of secondary B16 tumour nodules. (C) Median time to a palpable B16 tumour nodule. All animals eventually developed palpable tumours, however, there was a trend indicating that the onset of B16 tumour growth was delayed by CVA21 + anti-PD-1 therapy.

6.2.3 Survival in mice treated with CVA21 in combination with anti-PD-1 or a control antibody

CVA21 in combination with the anti-PD-1 antibody demonstrated a statistically significant improvement in overall survival compared to the saline + control antibody group ($P < 0.0001$, Log-rank [Mantel-Cox] test) (Figure 6.9A). Comparing the CVA21 + control antibody and the saline + control antibody group, there was no statistically significant difference. When the saline + anti-PD-1 survival curve was compared with the CVA21 + anti-PD-1 treatment group there was a statistical difference ($P < 0.01$, Log-rank [Mantel-Cox] test) (Figure 6). Overall, these findings suggest that CVA21 used in combination with the anti-PD-1 antibody gave a significant survival advantage (median survival of 45 *vs* 60 days for saline + anti-PD-1 and CVA21 + anti-PD-1 respectively) (Figure 6.9B).



B

	Saline + Control Ab	Saline + anti-PD-1	CVA21 + Control Ab	CVA21 + anti-PD-1
# censored subjects	0	0	0	5
# deaths / events	9	11	12	7
Median survival	28.0	45.0	37.0	60.0

Figure 6.9: Survival of C57BL/6 mice following treatment with saline or CVA21 in combination with the control antibody or anti-PD-1. (A) Kaplan-Meier plot demonstrating survival rates. A log-rank (Mantel-Cox) test was used to compare groups to the combination therapy ($n = 12$). (B) Table showing median survival of mice from each treatment group. Animals receiving the combination treatment demonstrated a significantly longer overall survival when compared to animals treated with single agent anti-PD-1 or CVA21.

6.2.4 Serum analysis

Studies were undertaken to characterise the anti-viral immune responses generated against CVA21 following i.t. viral administration in the absence or presence of the immune check-point inhibitor anti-PD-1 antibody in the C57BL/6 mouse model. Serum was collected from mice starting 1 h post-treatment, and weekly thereafter.

6.2.4.1 CVA21 viraemia

To examine whether blocking PD-1 affected levels of circulating viraemia, weekly serum samples were collected and titrated against SK-Mel-28 cells. Virus titration from the serum of infected mice revealed a high level of viraemia 45 min post-treatment, with a subsequent drop a week later (Figure 6.10A & B). The average viral load of mice treated with CVA21 + control Ab and CVA21 + anti-PD-1 was an average titre of 3.85×10^5 TCID₅₀/mL and 2.36×10^5 TCID₅₀/mL respectively. (Figure 6.10B). Importantly, i.p. injection of anti-PD-1 antibody did not result in a significant difference of viraemia levels ($P > 0.05$, student t-test) indicating that blocking PD-1 did not adversely affect CVA21 viral replication. Interestingly, despite the administration of multiple weekly i.t. CVA21 treatments after the initial injection, viraemia levels in serum (with or without anti-PD-1) were not sustained and fell below the assay's limit of detection. These results suggest that sustained viral load is unlikely even with repeated doses of CVA21 at high titres, and that the antiviral immune response may pose as a very significant barrier to CVA21 virotherapy.

6.2.4.2 CVA21 neutralising antibodies

Next, to investigate the antiviral immune response of these animals, serum samples from animals treated with CVA21 were tested for the presence of CVA21-specific nAbs. Neutralisation assays were performed in which 2-fold serial dilution of the serum samples were incubated with 100 TCID₅₀ of CVA21 for 1 h before titrating them against SK-Mel-28 cells. As expected, the increase in serum CVA21 nAb titres corresponded to the clearance of virus from the serum of these mice (Figure 6.11A & B). No nAbs were detected prior to treatment. Somewhat surprisingly, animals receiving the anti-PD-1 antibody had approximately 2-fold lower levels of nAb than mice in the CVA21 only group, but this difference was not statistically significant ($P > 0.05$, two-way ANOVA corrected with Bonferroni's method for multiple comparison).

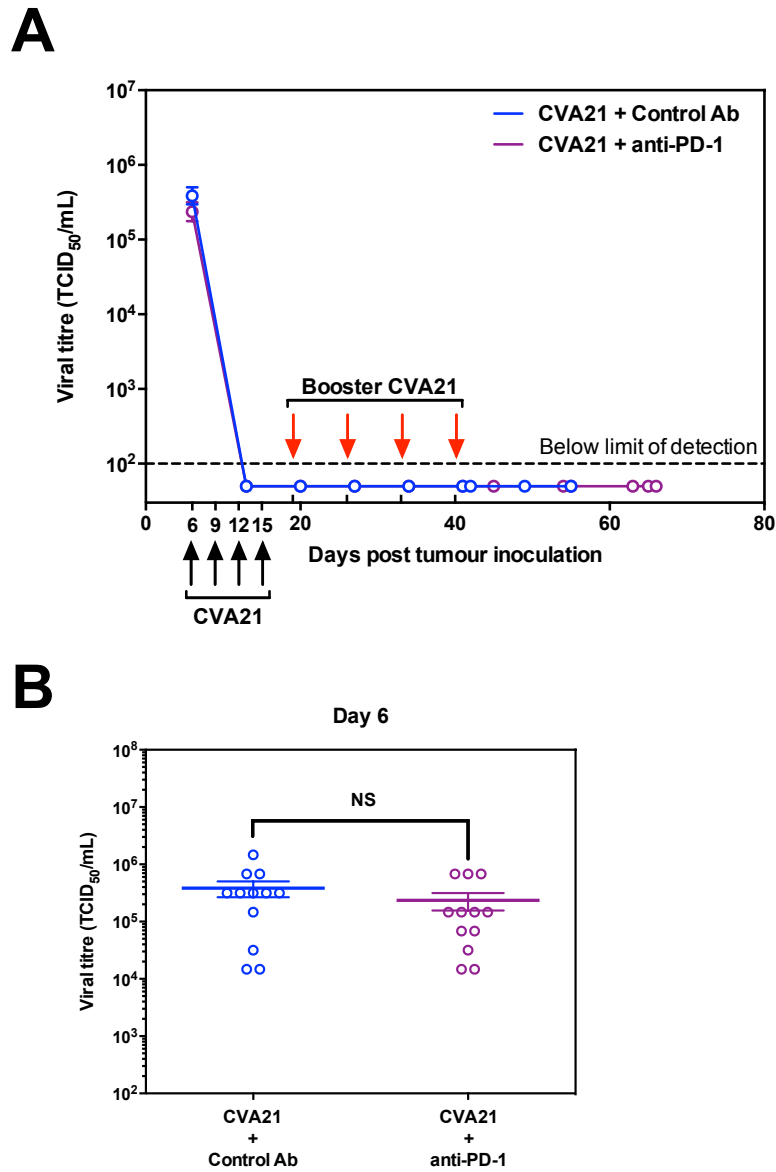


Figure 6.10: Detection of viraemia following CVA21 administration with and without anti-PD-1 immunotherapy. (A) Levels of infectious CVA21 in the serum of C57BL/6 mice following treatment with i.t. CVA21 (1×10^8 TCID₅₀/injection) with or without i.p. anti-PD-1 (12.5 mg/kg). The black arrows indicate administration of the virus intratumourally at day 6, 9, 12, and 15, while the red arrows indicate four additional CVA21 weekly injections at day 19, 26, 33, and 40. (B) Viral titres of each individual mouse 1 h post-i.t. administration as determined by viral infectivity assays. Viraemia levels were calculated using the Spearman-Kärber method and expressed as average viral titre \pm SEM TCID₅₀/mL ($n = 12$). The horizontal dotted line represents the detection limit of the assay at 100 TCID₅₀/mL. Despite repeated dosing, viraemia was only detected 1 h post-infection.

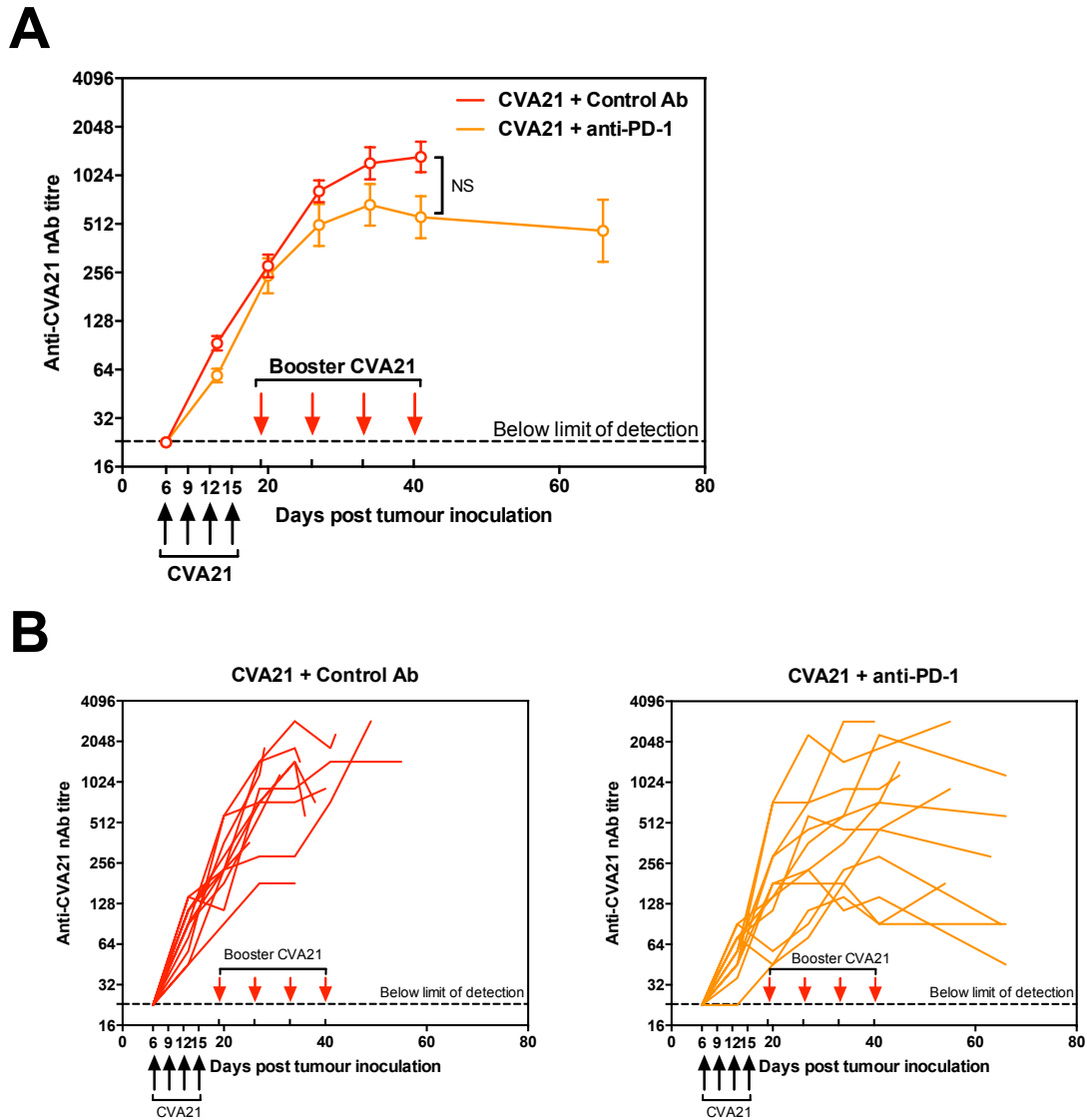


Figure 6.11: Detection of CVA21-specific neutralising antibodies (nAbs) following CVA21 administration with and without anti-PD-1 immunotherapy. (A) Anti-CVA21 nAb levels during study in serum of mice following CVA21 treatment, as determined by viral neutralisation assay. CVA21 + control antibody *vs* CVA21 + anti-PD-1 ($P > 0.05$). **(B)** Neutralising antibody levels of individual animals. The black arrows indicate administration of the virus intratumourally at day 6, 9, 12, and 15, while the red arrows indicate four additional CVA21 weekly injections at day 19, 26, 33, and 40. The neutralising titre was defined as the reciprocal of the serum dilution required to reduce viral infectivity by 50% and expressed as the mean \pm SEM neutralising units (NUs) ($n = 12$). The horizontal dotted line represents the detection limit of the assay at 23 NUs.

6.3 *In vivo* assessment of combination oncolytic virotherapy and anti-CTLA-4 immunotherapy in an immunocompetent mouse model

Next, the combination effect of CVA21 was explored with a further immune checkpoint inhibitor, anti-CTLA-4. To address this question, the recently established fully immunocompetent CVA21-susceptible mouse model of malignant melanoma, B16-ICAM-1 was used [5.2]. C57BL/6 mice were implanted with murine B16-ICAM-1 tumour cells (2×10^5 cells/mouse) intradermally on the left hind flank. Tumours were allowed to establish before commencement of therapy at 7, 10, 13 and 16 days post-tumour inoculation (see Figure 6.12). Saline or CVA21 was administered intratumourally at the indicated time points, while the control antibody or anti-CTLA-4 antibody were administered intraperitoneally. The presence of a robust anti-tumour immunity was examined by rechallenging animals with live B16 cells (1×10^5 cells/mouse) intradermally on the right hind flank. Mice were monitored daily and weighed up to three times a week and tumour volumes measured by electronic callipers three times a week. Blood sampling from the saphenous vein was carried out at weekly intervals. The study was terminated at day 77 post-tumour inoculation.

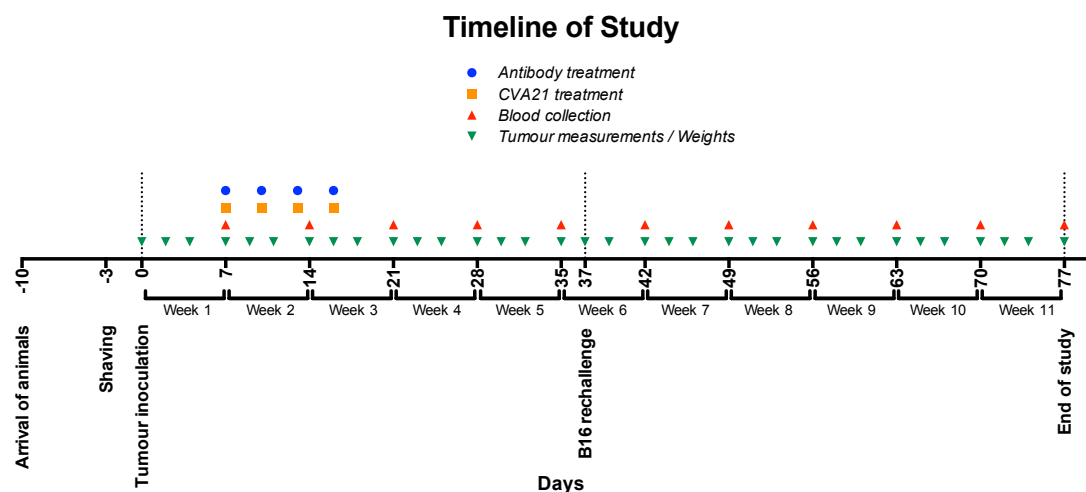


Figure 6.12: Treatment scheme of anti-CTLA-4 combination immunocompetent murine melanoma protocol. Time line showing the schedule of treatments (blue circles [anti-CTLA-4 antibody], orange squares [CVA21]) and monitoring procedures (red triangles [blood collection] and green triangles [tumour measurements and body weight measurements]). Animals ($n = 10$) were first treated with either saline or CVA21 (1×10^8 TCID₅₀/injection), followed by intraperitoneal injections with the murine isotype control antibody or the anti-PD-1 antibody (12.5 mg/kg). No additional treatment was administered after the initial four injections. The experiment was terminated on day 77.

6.3.1 Body weights following treatment with either saline or CVA21 in combination with anti-CTLA-4 or control antibody

Animals were weighed up to three times a week to monitor the wellbeing of tumour bearing mice during the course of the study. The average changes in body weight of animals on study were shown in Figure 6.13A, and individual changes were shown in Figure 6.13B. Animals responding to treatment generally exhibited steady weight gain or maintenance compared to control animals whose rapid weight gain/loss were likely linked to the associated tumour burden and tumour ulceration. The combination treatment was well tolerated by animals and is evidenced by the increasing average weight during the course of the study. No statistically significant differences in mean body weights were observed between the treatment groups and NTC mice at most time points (two-way ANOVA corrected for multiple comparison using Tukey's method) (Figure 6.13A, inset). Furthermore, no acute weight loss of unknown causes or signs of treatment-related adverse toxicity were observed during the course of the study.

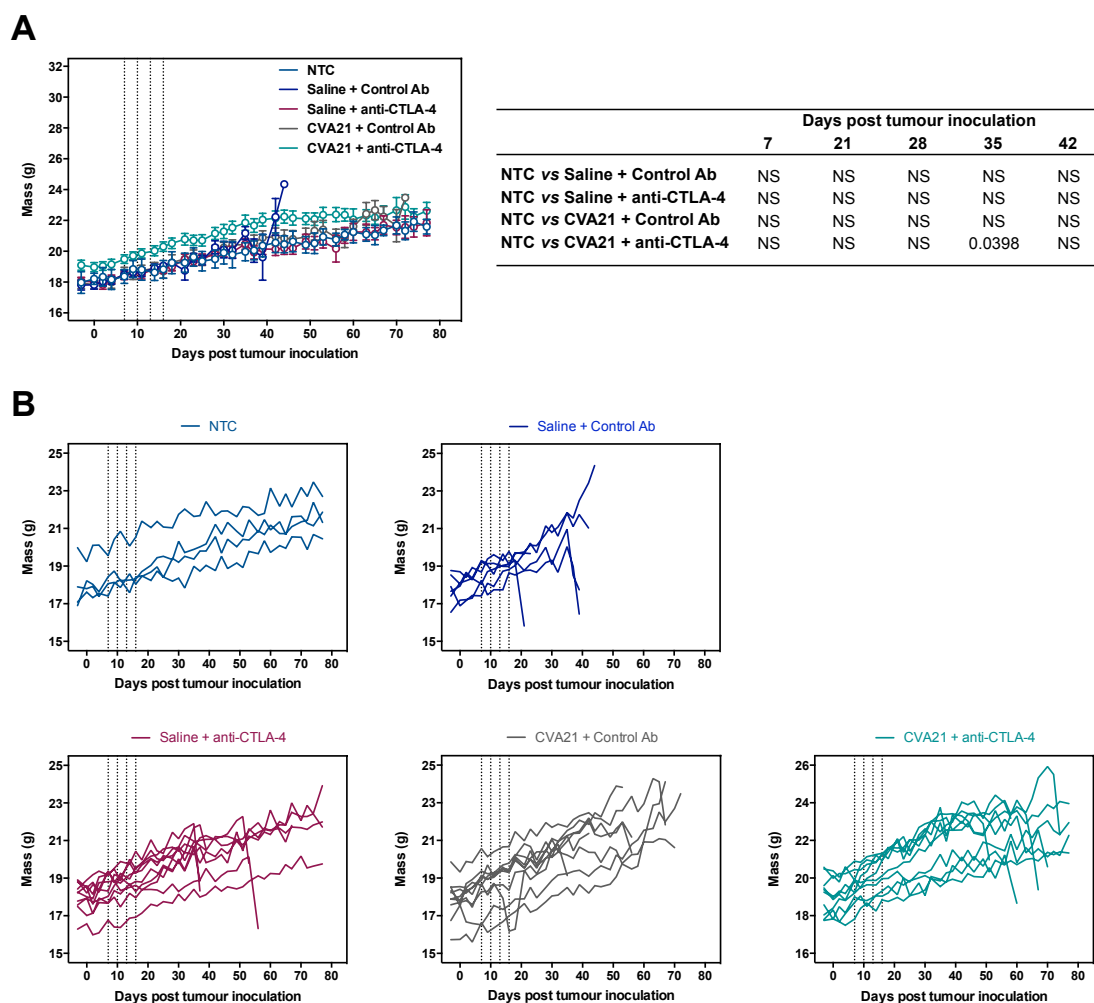


Figure 6.13: Body weights of mice (g) vs time (days). (A) Average mass of animals on study were expressed as grams (g) with error bars indicating SEM ($n = 10$). The inset displays a summary of P values calculated using the two-way ANOVA corrected for multiple comparison with Tukey's method. Some fluctuations in mean weights were observed due to the euthanasia of mice over the duration of the study. (B) Individual body weights of mice. The dotted lines at day 7, 10, 13 and 16 show each cycle of therapy. No unexpected weight changes were observed.

6.3.2 Tumour volume data

The bilateral flank B16-ICAM-1/B16 tumour model was used to determine CVA21 efficacy in combination with anti-CTLA-4. Primary melanoma tumours were implanted by injecting 2×10^5 B16-ICAM-1 cells in the left hind flank intradermally on day 0. At least thirty days after the first treatment was administered, secondary tumours were established by injecting 1×10^5 B16 cells in the right hind flank intradermally. Tumours were measured three times a week using digital callipers and animals were euthanised when tumour ulceration was observed or if weight loss was $> 10\%$.

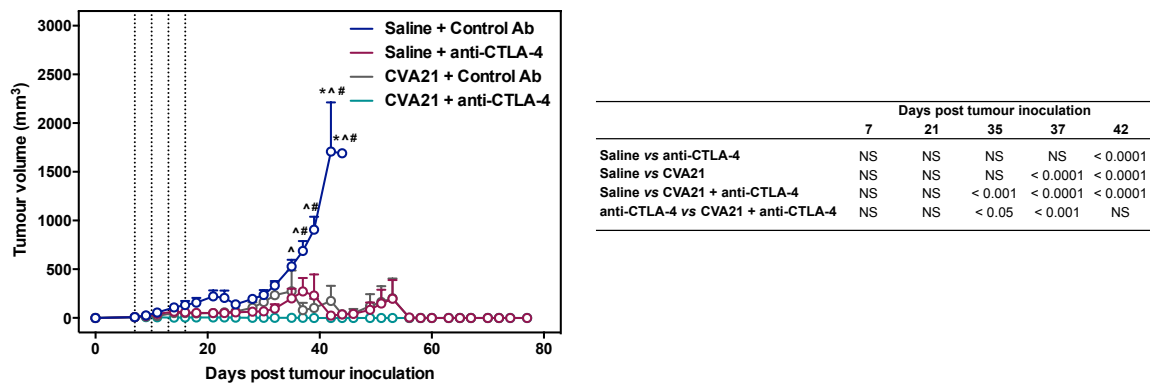
6.3.2.1 Tumour volumes of primary B16-ICAM-1 nodules

Results from Section 6.2 have demonstrated that CVA21 induced anti-tumour immunity can be augmented by systemically blocking PD-1. To determine whether this treatment strategy could be extended to other immune checkpoint inhibitors, combination treatment with anti-CTLA-4 was evaluated in the B16-ICAM-1/B16 bilateral tumour model. The treatment protocol was summarised in Figure 6.12 and tumour volume was calculated using the formula of a spheroid.

As shown in Figure 6.14A, little anti-tumour activity was observed in the saline + control antibody treated B16-ICAM-1 tumours. All control animals developed primary tumours evidenced by the increasing tumour volume and tumour ulceration. By day 45, all saline + control antibody treated mice were euthanised due to progressive disease, with tumour volumes reaching the maximal humane endpoint. Complete tumour regression followed by a durable response was observed in 60% of animals treated with either monotherapies (Figure 6.14B). Remarkably, all animals treated with CVA21 and anti-CTLA-4 combination therapy demonstrated complete tumour growth inhibition and this response was maintained until the end of the study.

Given that the last animals in the saline + control antibody group were euthanised at day 45, a two-way ANOVA was carried out using the primary tumour volume data of all mice collected up until this day, to compare the efficacy of different treatment groups. Using Tukey's method to compare all treatment groups to control animals, a significant difference in tumour volume was first observed in animals treated with the combination of i.t. CVA21 and i.p. anti-CTLA-4 antibody at day 35 ($P < 0.001$) (Figure 6.14A, inset). By day 42, all treatments significantly inhibited tumour growth ($P < 0.0001$). More importantly, a separate two-way ANOVA analysis used to analyse the tumour volumes of saline + anti-CTLA-4 and CVA21 + CTLA-4 treatment groups revealed a significant difference at day 35 and 37 ($P < 0.05$). However due to the termination of several animals that did not respond to treatment, the differences for the remainder of the study were no longer statistically significant. Overall, tumour volume data presented here strongly suggests that combination therapy with localised CVA21 therapy with systemic CTLA-4 blockade led to a more favourable therapeutic effect than either agents can achieve alone.

A



B

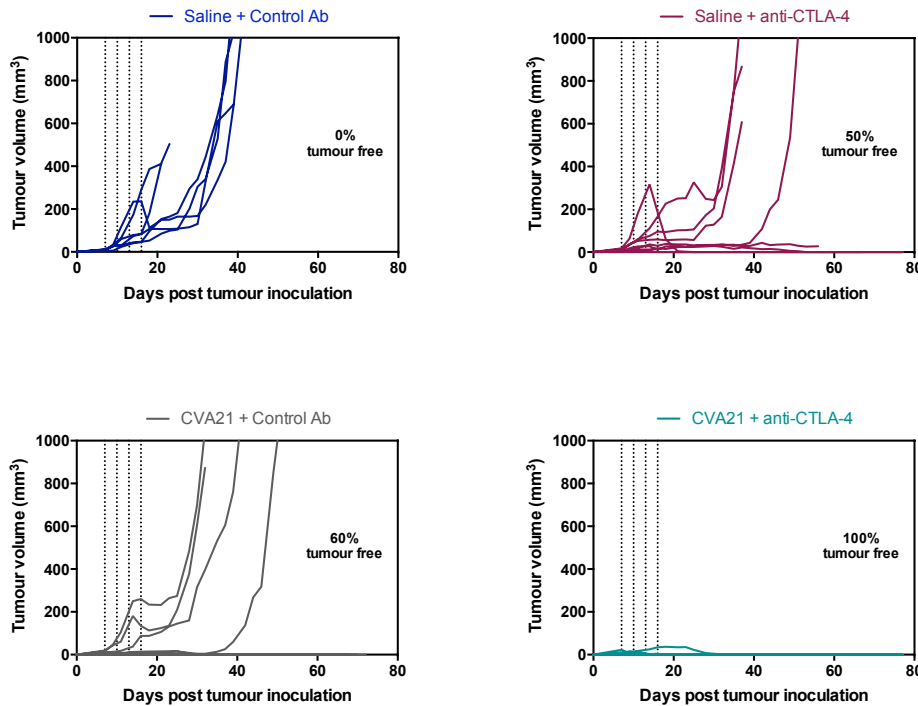


Figure 6.14: Tumour volumes following CVA21 virotherapy and CTLA-4 blockade on B16-ICAM-1 primary tumours. C57BL/6 mice were injected with B16-ICAM-1 cells intradermally on the left hind flank. Animals were treated with either saline (i.t.), CVA21 (i.t., 1×10^8 TCID₅₀/injection), control or anti-CTLA-4 antibody (i.p., 12.5 mg/kg), or CVA21 in combination with anti-CTLA-4 antibody. (A) Tumour volumes (mm³) expressed as the average with the upper limit of the SEM (n = 10). The inset displays a summary of P values calculated using the two-way ANOVA corrected for multiple comparison with Tukey’s method. *Saline + control antibody vs saline + anti-CTLA-4 ($P < 0.0001$); #Saline + control antibody vs CVA21 + control Ab ($P < 0.0001$); ^Saline + control antibody vs CVA21 + anti-CTLA-4 ($P < 0.0001$). (B) Individual tumour volumes from each mouse. Treatment days are indicated by the dotted lines. All animals treated with CVA21 + anti-CTLA-4 combination therapy demonstrated complete rejection against the primary tumour.

6.3.2.2 Tumour volumes of secondary B16 nodules

To establish whether a robust anti-tumoural immune response had developed following CVA21 therapy in combination with anti-CTLA-4 treatment, remaining animals were re-challenged with 1×10^5 B16 murine melanoma cells on day 37. B16 cells lack the human ICAM-1 receptor and are therefore resistant to CVA21 therapy. However, these cells are antigenically similar to the B16 cells used to generate the B16-ICAM-1 cell line and were used to identify the presence of anti-tumoural immune responses that may have resulted following oncolysis of the primary tumour.

The rechallenge of mice with B16 cells resulted in the development of heavy secondary tumour burdens in all control animals (Figure 6.15A). Similarly, animals treated with CVA21 + control antibody were not protected against the secondary tumour challenge. In contrast, animals treated with anti-PD-1 were resistant to B16 cells and this effect was greater in animals receiving the combination of the anti-CTLA-4 antibody and CVA21 virotherapy. The incidence of secondary B16 tumour formation was studied and presented in Figure 6.15B. Interestingly, while tumour protection was observed animals receiving the anti-CTLA-4 antibody alone, only animals receiving the combination treatment demonstrated a significant delay in the formation of the bilateral tumour ($P < 0.001$, log-rank [Mantel-Cox] analysis). The median time to a palpable B16 tumour was summarised in Table 6.15C.

As expected, evaluation of the primary and secondary tumour data revealed that all control animals developed primary flank tumours and were completely susceptible to the B16 tumour challenge (Figure 6.16A). Several animals treated with CVA21 alone were cured from the primary tumour (60% tumour free), but all of the remaining animals failed to develop resistance to the B16 tumour rechallenge (Figure 6.16B). Compared to the single agent CVA21 treatment group, the anti-CTLA-4 antibody treatment group achieved a similar primary tumour cure rate (60% tumour free), and showed long-term secondary tumour protection in two out of eight animals (25% tumour free) (Figure 6.16C). The most striking result to emerge from the data was that the CVA21 + anti-CTLA-4 treatment group produced a 100% primary tumour cure rate, and demonstrated protection against new tumour development in 40% of mice (Figure 6.16D). Collectively, these results indicate that CVA21 + anti-CTLA-4 treatment elicits a therapeutic and long-lasting protective anti-tumour immune response.

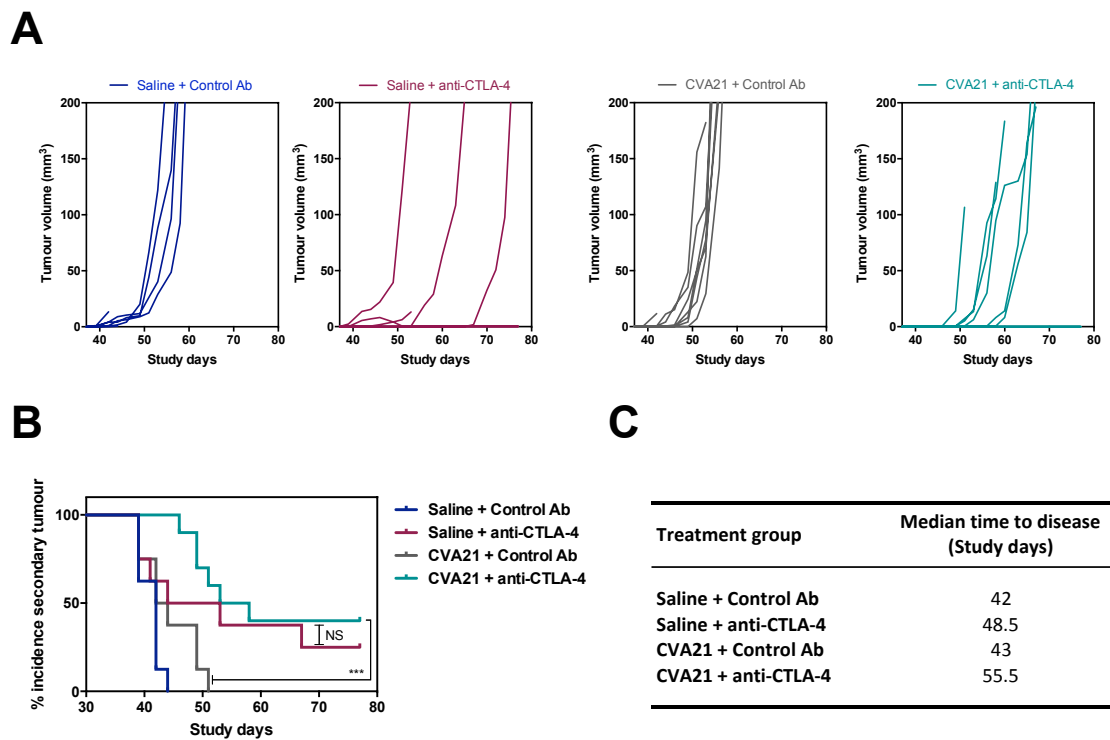


Figure 6.15: Tumour volumes of secondary B16 murine melanoma tumours. (A) Individual tumour volumes from each mouse ($n = 10$) following rechallenge with B16 tumour cells (1×10^5 cells/mouse) on the right hind flank at day 37. (B) Percentage incidence of secondary B16 tumour formation over time defined using Kaplan-Meier curves, examined by long-rank test. ***Saline + control antibody vs CVA21 + anti-CTLA-4 ($P < 0.001$). (C) Median time to the formation of palpable secondary tumours expressed as study days.

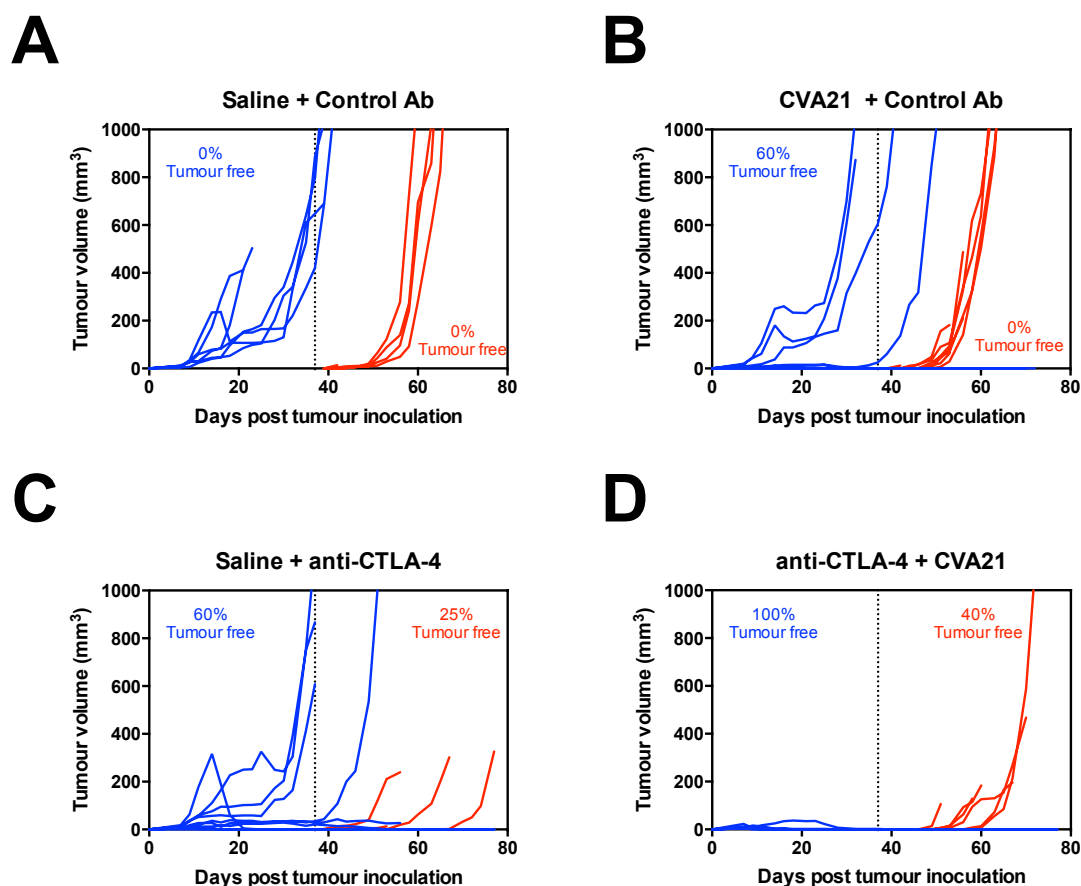
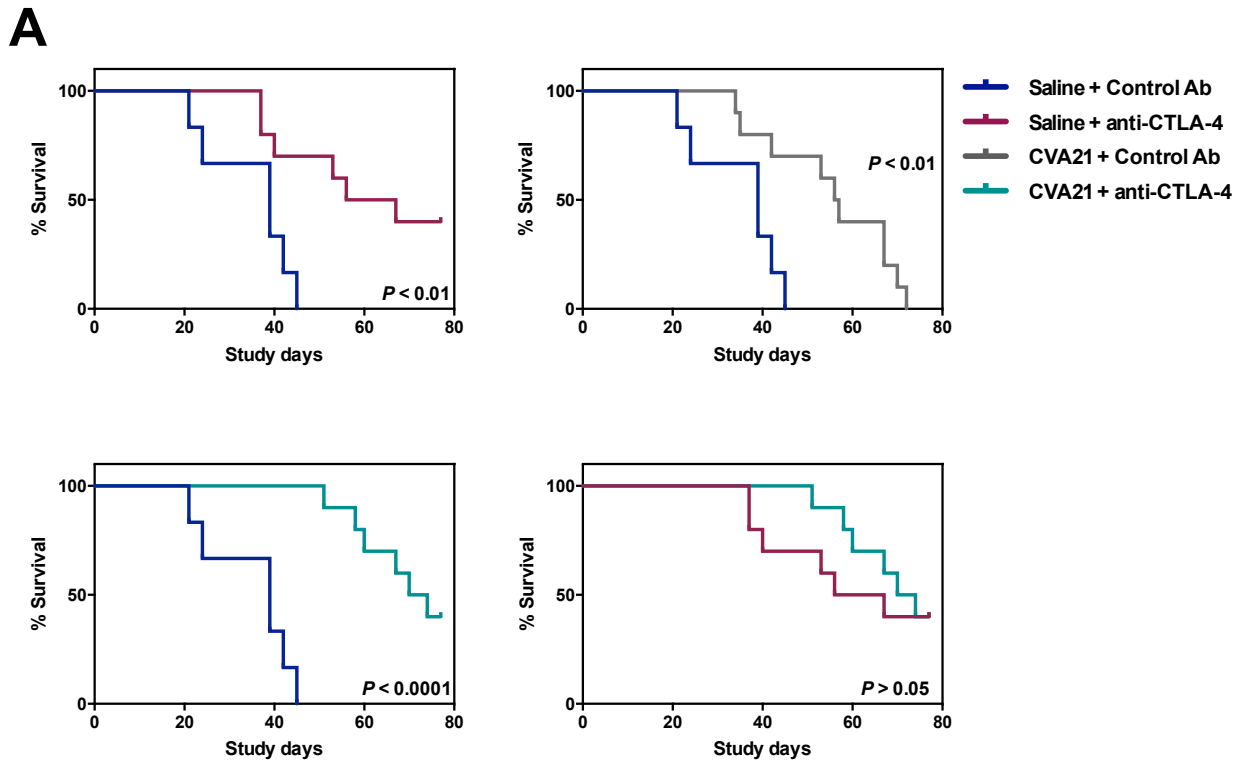


Figure 6.16: Analysis of primary and secondary with cure rate. Development of individual primary and secondary tumours of (A) saline + control antibody, (B) saline + anti-CTLA-4, (C) CVA21 + control antibody, and (D) CVA21 + anti-CTLA-4 treated animals at the conclusion of the study (day 77) ($n = 10$). Tumour volumes of B16-ICAM-1 (left flank, 2×10^5 cells) and bilateral B16 (right flank, 1×10^5 cells) tumours were calculated using the formula of a spheroid and expressed as mm³.

6.3.3 Survival in mice treated with CVA21 in combination with anti-CTLA-4 or a control antibody

Having demonstrated that combination treatment could deliver superior therapeutic benefit, the survival of these animals was examined (Figure 6.17). Once animals had lost 10% of their body weight, tumour burden exceeded 2500 mm³ or tumours had ulcerated, mice were euthanised and survival data was evaluated. By day 45, all animals from the control group were terminated and an overall median survival of 39 days was calculated (6.17A & B). Compared to the control group, both i.t. CVA21 and i.p. anti-CTLA-4 monotherapies significantly improved overall survival ($P < 0.01$, log-rank [Mantel-Cox] test), extending median overall survival to 56.5 and 61.5 days respectively, but only animals treated with the antibody exhibited a complete tumour response translating into a long-term survival

benefit. This difference was even larger when compared with the CVA21 + anti-CTLA-4 combination ($P < 0.0001$) and had a median survival rate of 72 days (Figure 6.17B). Animals receiving the combination treatment had prolonged survival compared to treatment with CVA21 only ($P = 0.01$), but not when compared with single agent anti-CTLA-4 treatment ($P = 0.60$).



B

	Saline + Control Ab	Saline + anti-CTLA-4	CVA21 + Control Ab	CVA21 + anti-CTLA-4
# censored subjects	0	4	0	4
# deaths / events	6	6	10	6
Median survival	39.0	61.5	56.5	72.0

Figure 6.17: Kaplan-Meier survival analysis for CVA21 virotherapy with CTLA-4 blockade. (A) Survival of animals following treatment with saline + control antibody, saline + anti-CTLA-4, CVA21 + control antibody, and CVA21 + anti-CTLA-4. A log-rank (Mantel-Cox) test was used to compare groups to the combination therapy ($n = 10$). (B) Table showing median survival of mice from each treatment group. The experiment was terminated on day 77.

6.3.4 Serum analysis

Next, the immunomodulatory effects of CTLA-4 blockade on CVA21 viral replication and anti-viral immunity was examined in the immunocompetent C57BL/6 mouse model. Serum was collected from mice starting 1 h post-treatment, and weekly thereafter.

6.3.4.1 Viraemia analysis

To examine whether blocking CTLA-4 affected levels of circulating virus particles, weekly serum samples were collected and titrated against SK-Mel-28 cells. At 45 min post-treatment, serum viral load for the CVA21-treated mice, with or without the anti-CTLA-4 antibody, ranged from approximately 10^3 to 10^5 TCID₅₀/mL, as determined by viral infectivity assays (Figure 6.18A, left). Importantly, there was no significant difference in the average viraemia levels of animals receiving CVA21 alone (8.71×10^4 TCID₅₀/mL) when compared to animals receiving the virus in the presence of the anti-CTLA-4 antibody (5.64×10^4 TCID₅₀/mL) ($P > 0.05$, student t-test), indicating that blocking PD-1 did not adversely affect CVA21 viral replication. Despite the administration of another three i.t. CVA21 injections (1×10^8 TCID₅₀/injection), viraemia levels fell below detection levels a week later and this was maintained for the duration of the study (Figure 6.18B). Interestingly, viraemia persisted in two animals at day 14, though the significance of this finding remains to be elucidated. The results presented here are consistent with earlier work using the anti-PD-1 antibody, whereby the anti-viral immune response prevented the circulation of infectious CVA21 progeny in the blood stream for longer than a week despite repeated dosing of CVA21.

6.3.4.2 Neutralising antibodies

Humoural immunity, rather than T cell-mediated immune responses, appears to be of primary importance in the protection against enterovirus infections, which may have contributed to the drop in viraemia beyond day 14. As such, the anti-CVA21 antibody immune response generated in CVA21-treated animals was examined (Figure 6.19). As expected, the increase in serum CVA21 nAb titres corresponded to the clearance of virus from the serum of these mice. Rapid nAb development was observed in all CVA21-treated animals with or without anti-CTLA-4 antibody a week after infection (Figure 6.19A). No nAbs were detected prior to treatment. CVA21-treated animals receiving i.p. anti-PD-1 antibody produced significantly higher levels of nAbs by day 42 ($P < 0.05$, multiple t-test), and the difference was maintained until the end of the study (Figure 6.19B). To further

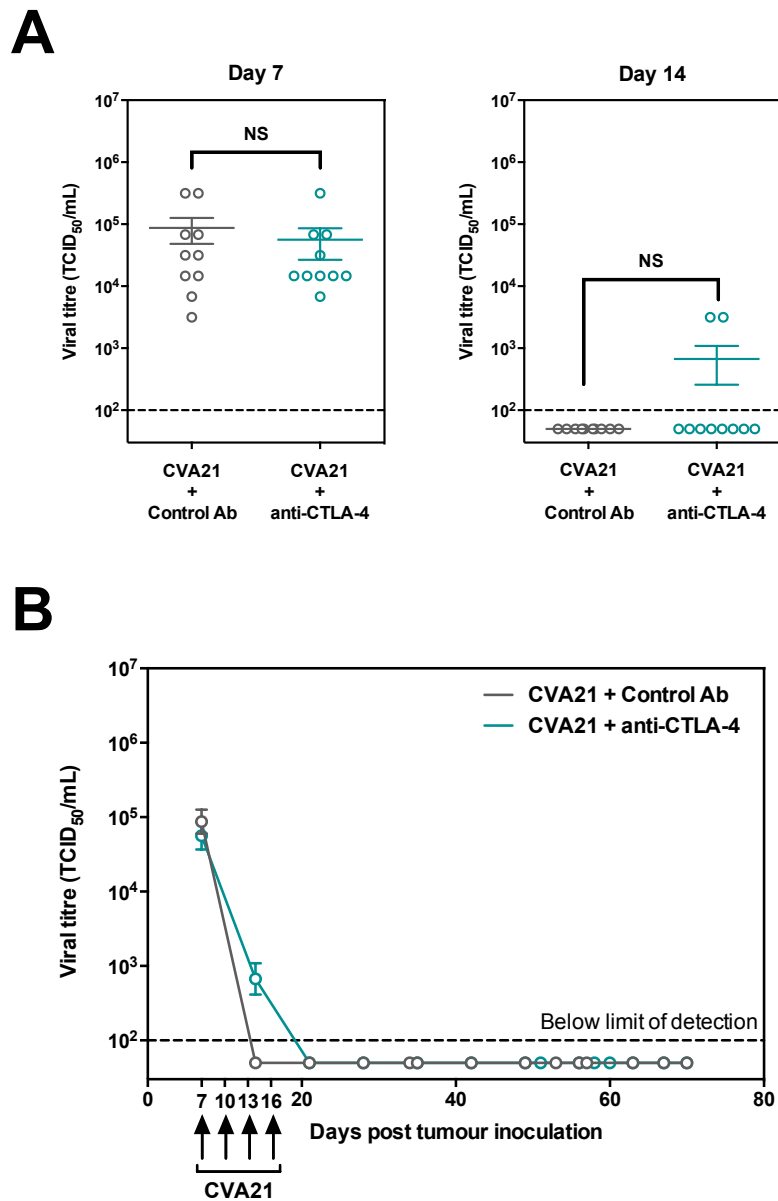


Figure 6.18: Detection of viraemia following CVA21 administration with and without anti-CTLA-4 immunotherapy. (A) Viral titres of each individual mouse 45 min post-i.t. CVA21 administration (1×10^8 TCID₅₀/injection) with or without i.p. anti-CTLA-4 (12.5 mg/kg) (day 7) and a week after (day 14) as determined by viral infectivity assays. Statistical significance between viral titres were analysed using a student's t-test. (B) Levels of infectious CVA21 in the serum of all animals on study. The black arrows indicate administration of the virus intratumourally at day 7, 10, 13, and 16. Circulating infectious virus was not detected in saline and anti-CTLA-4 serum samples. Viraemia levels were calculated using the Spearman-Kärber method and expressed as average viral titre \pm SEM TCID₅₀/mL ($n = 10$). The horizontal dotted line represents the detection limit of the assay at 100 TCID₅₀/mL.

study the kinetics of nAb development, the experimental data was fitted to a non-linear regression model (Figure 6.19C). Neutralising antibody production in animals treated with CVA21 and the control antibody peaked two weeks after the initial infection, but decreased over the duration of the experiment. Interestingly, nAb production in animals receiving CVA21 with the anti-CTLA-4 antibody was delayed, but maximum titres reached were higher than the CVA21 treatment group, peaking at day 42. This striking observation suggests that the addition of anti-CTLA-4 may condition the host immune system by transiently blunting antiviral immunity to provide a ‘window of opportunity’ for CVA21 oncolysis before evoking a more robust immune response.

6.3.4.3 *Ex vivo* cytotoxicity of serum-mediated cell death

Several mechanisms of tumour killing during antibody immunotherapy such as antibody-dependent cellular cytotoxicity (ADCC) and complement-dependent cytotoxicity (CDC) have been suggested in several models . In an attempt to investigate these mechanisms, serum samples (day 42) from animals receiving the anti-CTLA-4 antibody were incubated with SK-Mel-28 cells at 37°C, 5% CO₂, for 72 h. Photomicrographs of cells were taken and observed for cytotoxic activity (Figure 6.20). Reduced cell numbers without any noticeable cell death was observed in cells incubated with serum originating from animals treated with anti-CTLA-4 antibody alone. Only serum from animals treated with the combination led to the successful destruction of SK-Mel-28 cells. A significant decrease in cell density, changes in morphology and an increased amount of cellular debris was observed. The current study highlights a potential role of CVA21 in the induction of anti-tumour ADCC and future studies will need to investigate the underlying mechanism observed.

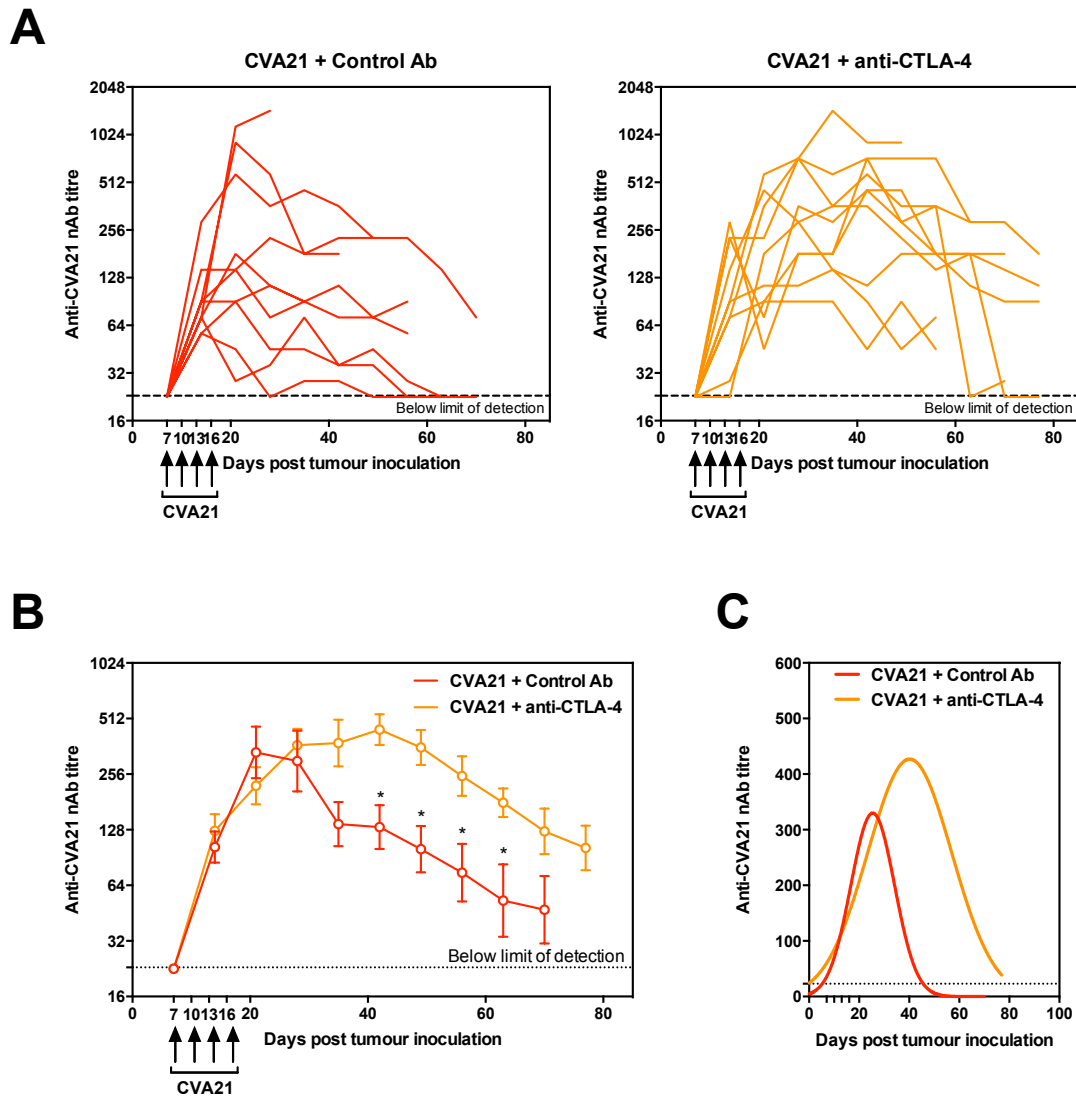


Figure 6.19: Serum neutralising antibodies against CVA21 in animals following CVA21 administration with or without anti-CTLA-4 immunotherapy. (A) Neutralising antibody levels of individual animals. **(B)** Anti-CVA21 nAb levels during study in serum of mice following CVA21 treatment, as determined by viral neutralisation assay. $*P < 0.05$, multiple t-test. **(C)** Neutralising antibody data fitted to a non-linear regression model. The black arrows indicate administration of the virus intratumourally at day 7, 10, 13, and 16. The neutralising titre was defined as the reciprocal of the serum dilution required to reduce viral infectivity by 50% and expressed as the mean \pm SEM NUs ($n = 10$). The horizontal dotted line represents the detection limit of the assay at 23 NUs.

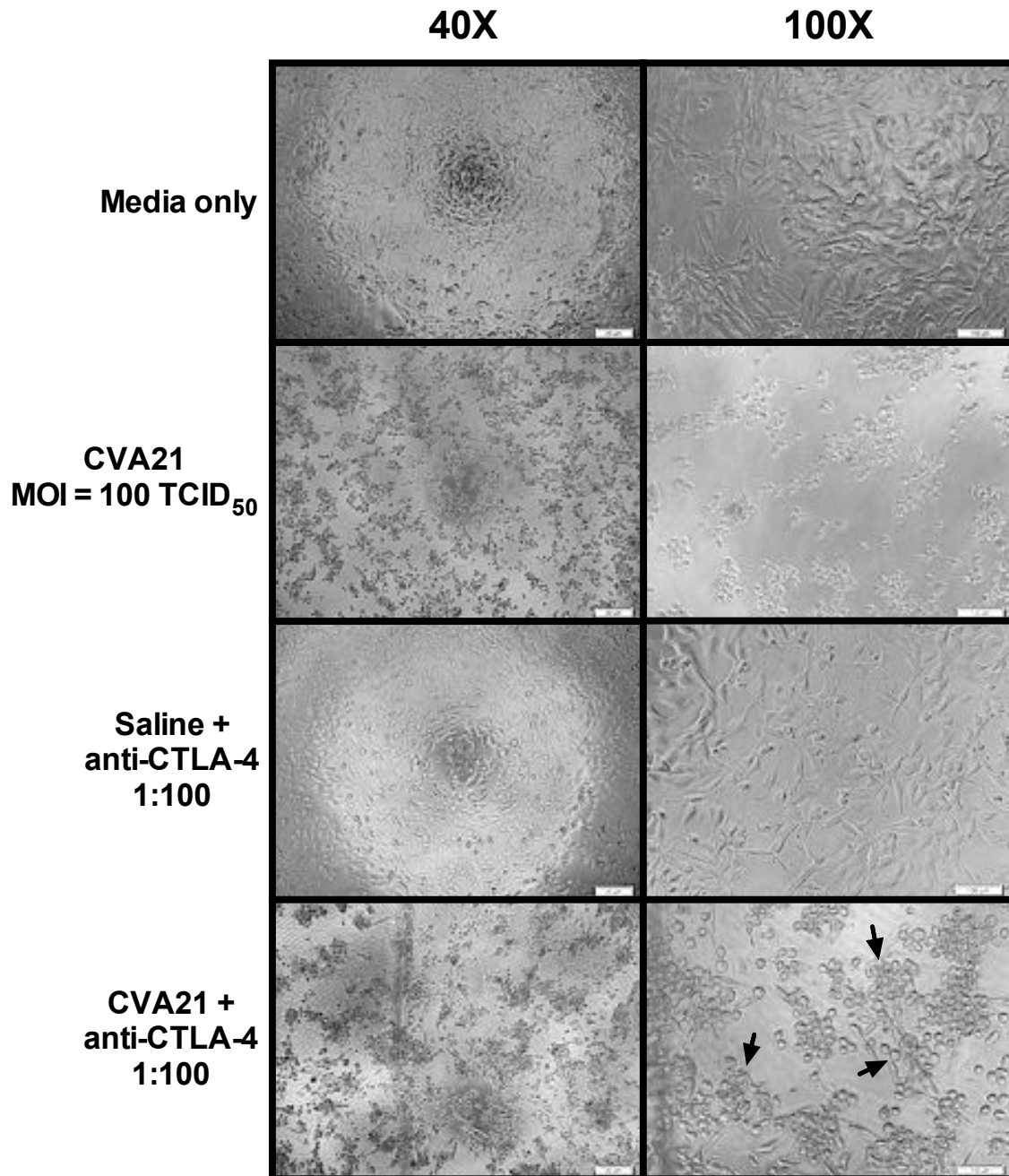


Figure 6.20: *Ex vivo* cytopathic effects of serum collected from animals treated with anti-CTLA-4. Representative photomicrographs showing the changes in morphology in SK-Mel-28 human melanoma cells incubated with animal serum (1:100). All images were taken 72 h post-incubation using an Olympus IX70 inverted microscope with a DP72 digital camera at 40× or 100× magnification. Black arrows are indicative of the cytopathic effects observed.

Chapter 7

Discussion and Conclusion

The incidence of metastatic melanoma has been steadily increasing over the past few decades. Metastatic melanoma remains as one of the leading causes of cancer mortality in Australia [36] and in the world [351]. Despite the tremendous progress in melanoma research, treatment outcomes remain poor. The field of oncolytic virotherapy has also progressed considerably and is now gaining acceptance as a viable therapeutic strategy. Aside from direct cytopathic effect and lysis of tumour cells, interactions of OV with the immune system can trigger systemic cellular immunity. Oncolysis leads to the release of TAAs, DAMPs, and PAMPs, which may facilitate the induction of a specific anti-tumour immune response [60, 88, 141, 442, 505]. However, it is becoming increasingly clear that OVs cannot be viewed as monotherapies for the sole cure of cancer. Instead they should be regarded as powerful tools to be used in combination with the current standard-of-care therapeutics, and will likely function best with immunotherapies that improve the adaptive anti-tumour immune response.

7.1 Discussion of research findings

Chapter 4

Preclinical studies have confirmed that oncolytic CVA21 is active *in vitro* and *in vivo* as a highly selective anticancer agent with significant potential for clinical translation in a broad range of tumour types [98]. Indeed, this agent has already been assessed in single-agent phase I studies in patients with advanced melanoma [668] and its success has led to its efficacy evaluation in a phase II study [20]. However, as OVs move toward clinical application, it is likely that in order to be successful, some type of combination therapy will need to be employed. Rather than simply combining CVA21 with a broad

range of chemotherapeutics, we first postulated that the combination with mainstream chemotherapeutics should not interfere with the oncolytic action of CVA21. Hence, we sought to determine the activity of CVA21 in the treatment of malignant melanoma cells when administered in combination with three chemotherapeutic drugs (DTIC and P + C doublet chemotherapy) used routinely in the clinic for the control of melanoma.

Dacarbazine was approved by the FDA for the treatment of metastatic melanoma and has been used in the clinic for the last four decades [206]. However, clinical studies have shown that the drug alone exhibits a response rate of only 10 - 25%, a complete response rate of less than 5%, and no distinguishable survival benefits. Moreover, combination cocktails of DTIC with other agents that kill tumour cells by alkylation, cross-linking, ribonucleotide depletion, microtubule destabilisation, or topoisomerase inhibition, have all failed to significantly improve long term survival rates in patients with metastatic melanoma [206, 666]. Thus, there is an urgent need to develop new therapeutic agents that can provide enhanced anti-tumour effects to overcome this disease.

Paclitaxel is a broad-spectrum anticancer agent used in the treatment of various cancers such as lung cancers, head and neck cancers, prostate cancers, gastric carcinoma, ovarian carcinoma and glioma [235]. In 2006, a study measured a small but significant tumour response in 45% of patients when it was used in combination with the platinum agent, carboplatin [612]. The rationale for combining these agents is 3-fold. Firstly, both platinum-alkylating agents and taxanes have demonstrated some activity in melanoma [132, 431]; secondly, *in vitro* and clinical data suggest synergy between these drugs when used in combination in a variety of malignancies [211, 317, 365, 806]; and thirdly, the toxicity profiles of these agents do not overlap [322, 612]. Against this background, we were interested in administering paclitaxel and carboplatin in combination with CVA21, as several studies have reported that the combination of a taxane and a platinum agent with virotherapy resulted in lower toxicity profiles, higher levels of synergy, and increased therapeutic index in comparison to when either agent was administered alone [335, 346, 445, 643].

In the current study, we demonstrated that not only does the co-administration of DTIC, paclitaxel and carboplatin not interfere with the replication cycle of CVA21, enhanced killing of melanoma cells was observed when both oncolytic agent and chemotherapy were combined, depending on the cell line treated. Comparison of the dose-response curves

of the virus with the chemotherapeutic combinations to their respective agents as monotherapies, demonstrated improved killing in three of the four cell lines tested (Figure 4.12A & B). Formal quantitative analysis of the experimental data was evaluated using the CI and isobologram method of Chou-Talalay, based on multiple drug effect analysis [144, 145]. This type of analysis is one of the few methods available that determines synergy based on derived equations to preclude unintended observer biases.

Firstly, the EC_{50} values (the concentration of the drug which induces a response halfway between the baseline and maximum response), were evaluated for CVA21 and the individual chemotherapeutic agents using four human melanoma cell lines. Oncolytic data showed that the cell viability of melanoma cells infected with CVA21 was greatly reduced in a dose dependent manner (Figure 4.1). SK-Mel-28 cells were most sensitive to CVA21 infection, followed by Mel-RM, ME4405 and MV3 cell lines. Previous work has demonstrated that the degree of sensitivity is positively correlated with the expression of the viral surface receptor ICAM-1 [35], though exceptions have been noted (unpublished data). Next, we found that DTIC treatment, despite being the gold standard chemotherapy for the treatment of melanoma, was not effective in killing melanoma cells at the tested concentrations (Figure 4.3). The combination of P + C doublet chemotherapy was synergistic itself (Figure 4.4A), and achieved better cell killing than DTIC, with 95% - 100% cell death achieved at the highest concentration tested (Figure 4.4B). Both chemotherapeutics reduced melanoma cell viability in a dose dependent manner.

Having established the EC_{50} values for each drug (Table 4.1 & 4.2), we sought to quantify the combination effects of CVA21 with DTIC and P + C using Chou-Talalay's method. The same panel of melanoma cell lines were challenged with CVA21 in the absence or presence of DTIC and P + C, using concentrations serially diluted either side of the drug's EC_{50} value ($0.0625 \times EC_{50}$ to $4 \times EC_{50}$; dilution factor = 2) to maintain a constant ratio (constant ratio combination design). Combination index values were generated using Combosyn after assessing the viability of treated cells, where a CI value of 0.9 - 1.1 was considered additive; above 1.1, antagonistic; and if below 0.9, synergistic. As expected, Chou-Talalay's method indicated significant levels of synergy between CVA21 with each of the chemotherapeutic agents in three out of the four tested melanoma cell lines (Table 4.3).

A major finding of the study was the high level of synergism achieved in the relatively CVA21-resistant melanoma cell line, MV3, whereas SK-Mel-28 cells, which are extremely susceptible to CVA21 infection demonstrated antagonism when treated in combination with either chemotherapeutic agent (Figure 4.8 & 4.9). Considering the rapid oncolysis of SK-Mel-28 cells by CVA21, it was unsurprising that combination with either chemotherapeutic did not lead to enhanced cell death, and was antagonistic. In contrast, co-administration of CVA21 with either chemotherapeutic agent led to increased cell death in the relatively CVA21-resistant MV3 cell line. Given this finding, our data suggest that the sensitivity of each of the cell lines to CVA21 infection was an important determinant for the *in vitro* synergistic effects of CVA21-chemotherapeutic combination regimens. Furthermore, CI values and isobolograms revealed that the addition of chemotherapeutics could potentiate the anticancer effects in cell lines that were less sensitive to CVA21. As such, it is conceivable that certain molecular changes induced by the administration of chemotherapeutic agents can enhance the susceptibility of CVA21 lytic infection.

The enhancement of viral replication by chemotherapeutics, leading to increased virus-induced cell death, could be a possible explanation for the detected synergistic effects. To study the replication kinetics of CVA21 together with DTIC and P + C, one-step viral growth curves were used. The results showed that in all cell lines except SK-Mel-28, treatment with CVA21 and DTIC gave marginally lower levels of viral replication (Figure 4.11A), while co-treatment with P + C appears to increase viral titres at 72 h post infection (Figure 4.11B). Despite the conflicting effects on viral replication, increased cell death was still observed in these cell lines. Similarly, others have also described synergistic interactions between OV_s and chemotherapy drugs in the absence of enhanced viral production [289, 335, 643]. A study using reovirus in combination with P + C doublet chemotherapy for the treatment of head and neck cancer showed a marginal reduction in viral yield, but the highest levels of cell kill [643]. These findings together with ours suggest that the synergistic cytotoxicity between CVA21 and the chemotherapeutic agents in three of the four melanoma cell lines tested, do not involve the enhancement of CVA21 replication and is unlikely to be solely dependent on viral replication.

Alternatively, drug-mediated viral inhibition could result in the antagonistic effects observed in the SK-Mel-28 cell line when treated simultaneously with either chemotherapeutic agent. On the basis that antagonism occurred consistently with two different drugs with

entirely different mechanisms of action, we speculated that CVA21 replication cycle might have been compromised in the SK-Mel-28 cell line when treated in combination. However, surprisingly, one-step growth curves in SK-Mel-28 cells showed that there was minimal alteration in the replication kinetics of CVA21 in the presence of either chemotherapy. More specifically, the use of DTIC or P + C doublet chemotherapy did not compromise viral replication in infected SK-Mel-28 cells.

Having established that neither DTIC nor P + C affects CVA21 replication, we reevaluated the EC_{50} values used in the constant-ratio study design. It is noteworthy that the high susceptibility of SK-Mel-28 cells to CVA21 and their multi-chemoresistant profile, resulted in a low EC_{50} value for CVA21 and very high EC_{50} values for the chemotherapies. As a result, a very low MOI (<0.0001 TCID₅₀/cell) of the virus was used in the presence of high concentrations of chemotherapy to treat SK-Mel-28 cells in the constant-ratio study experiments. Unlike the one-step growth curve assay which uses a high MOI (10 TCID₅₀/cell) to study viral replication, cells infected at a low MOI would have required several rounds of viral multiplication before cell lysis occurred [234]. Taken together, we hypothesise that while CVA21 is still undergoing multi-step replication, the chemotherapy combination could have damaged the infected cells, curtailing viral replication prematurely, thus resulting in the overall decrease of cell death observed in our constant-ratio study design.

To further study the antagonistic effects of CVA21 with chemotherapy in SK-Mel-28 cells, we infected SK-Mel-28 cells with serial dilutions of CVA21 beginning at an MOI of 100 TCID₅₀/cell in the presence of chemotherapy at clinically relevant concentrations. Cell viability data indicated that the combination was not antagonistic but increased cell death was observed with both chemotherapeutic drugs (Figure 4.12). This finding is particularly important because it excludes the possibility that chemotherapy would have antagonised CVA21 entirely and it highlights the increased efficacy of the combination at clinically relevant doses. Furthermore, significantly enhanced tumouricidal effects were observed when low dose chemotherapy was administered in combination with CVA21, thereby indicating that lower doses of drugs could be administered to patients in combination with CVA21, resulting in enhanced efficacy and reduced toxicity.

It is also well established that although DTIC and P + C utilise completely different pathways to exhibit their anticancer activity, all of them mediate cell death through cell

cycle arrest. [653, 770]. DTIC exerts its anticancer activity by methylation of nucleic acids resulting in non-specific cell cycle growth arrest (affecting more than one cell cycle phase), subsequently leading to cell death [103, 260]. On the other hand, paclitaxel mediates its cytotoxicity through kinetic suppression or stabilisation of microtubules in cells, leading to cell cycle arrest at G2M and ultimately cell death through apoptosis [371, 770]. Carboplatin is a second-generation platinum alkylating agent derived from cisplatin, possessing a milder toxicity profile and proven to synergistically enhance apoptosis levels when used in combination with paclitaxel [257]. Whilst not much is not known about the effects of CVA21 on the cell cycle, our data are consistent with previous work [685], which suggested that the virus triggers cell death early on in the cell cycle G1/S-phase reducing the population of cells reaching G2M. This is not the first time such an effect has been reported for Coxsackieviruses, with work from Feuer's group demonstrating high levels of Coxsackievirus B3 viral proteins in cells arrested in the G1/S phase [222, 223]. As DTIC and P + C mediate growth arrest in various stages of the cell cycle, this prompted us to examine the possibility that CVA21 may mediate synergy by enhancing cell cycle arrest.

The precise underlying mechanism of the combination treatment of DTIC and CVA21 is not well understood. One study found that DTIC when used together with an adenovirus, enhanced anti-tumour activity by more effectively inducing apoptosis in melanoma cells [361]. Conversely, Cun *et al.* reported that the combination of oncolytic adenovirus H101 with DTIC exerted a synergistic anti-tumour effect primarily through cell arrest in the G1 phase rather than by the induction of apoptosis [162]. In our study, DTIC as a single agent had minimal effects on the cell cycle and did not lead to an induction of the subG1/G₀ population. However, we found that each cell line responded very differently to the CVA21+ DTIC combination treatment. The combination increased the S phase population in Mel-RM cells, increased subG1/G₀ cells in ME4405 cells, but to our surprise, had no significant effect on the cell cycle of MV3 cell cells which demonstrated the strongest synergy with the DTIC combination (Figure 4.14). Nevertheless, the difference in action of DTIC from our experiments strongly suggests a dependency on the cell line used. In line with our study, recent work by Arozarena *et al.* on alkylating agents highlights the impact of the mutational status of melanoma cells and their influence on the chemosensitivity of cells [28]. One of their key findings was that NRAS mutant melanoma cells were less responsive to DTIC than BRAF mutant cells.

In addition, another possible explanation for the inconsistencies observed in published DTIC work, is the method of *in vitro* activation. In patients, studies have found that 5-(3,3-dimethyl-1-triazeno)imidazole-4-carboxamide (DTIC) needs to be metabolised by CYP450 isoforms in the microsomes of hepatocytes into methyl-triazeno-imidazole-carboxamide (MTIC), before undergoing spontaneous transformation into a cytotoxic DNA methylating agent [482, 618, 652]. Meer *et al.* also points out that DTIC activation is governed by other activation enzymes localised at a renal and pulmonary level [502]. It was proposed that an alternative approach to activate DTIC *in vitro* was to expose the drug to white light for 1 h prior to administration [435, 509]. Indeed, several studies together with ours (data not shown) have observed an increase in DTIC's inhibitory effect after exposure to white light [28, 61]. It must be pointed out that light activated DTIC (spontaneous activation) does not produce MTIC (enzymatic activation), but yields 5-diazoimidazole-4-carboxamide (diazo-ICA) and 2-azahypoxanthine (2-AH) [61, 677]. These molecules, however, have shown cytotoxic activity *in vitro* but not *in vivo* [61, 656]. Furthermore, through DNA alkylation assays and combinatorial treatments using DTIC and DNA repair inhibitors, Arozarena *et al.* provides clear evidence that light exposure does not transform DTIC into a DNA methylating agent, but rather an inhibitor of DNA synthesis [28]. In light of this, Tentori *et al.* put forward the view that investigation of MTIC-induced DNA methylation rather than the effects of photodecomposition products of DTIC would have been a more substantial representation of the anti-tumour effects of DTIC in the clinic [723].

One possible process underlying the increased activity of the CVA21 and P + C combination is the enhancement of apoptosis of cells exposed to the drug-virus combination therapy (Figure 4.14). During mitosis, the duplicated chromatids of a cell are separated to opposing poles by microtubules before cell cleavage. Dynamic changes in microtubule structure at mitotic spindles are critical for successful mitosis [646]. Paclitaxel is known to stabilise microtubules, impairing such dynamic changes, impeding chromatid separation, blocking cell mitosis, and promoting apoptosis in malignant cells [371]. We found that melanoma cells treated with CVA21 in combination with P + C exhibited significant increases in apoptosis. For the combination treatment, we detected increased sub-G1/G₀ cells compared to either single agents alone or untreated control samples. These findings suggest that CVA21 might enhance the mechanisms of P + C activity rather than vice versa, as originally hypothesised with enhanced viral replication. To gain more insight

into the mechanistic basis of accelerated apoptosis associated with the CVA21 and P + C combination, we examined the combination effects on caspase-3/7 activation in relation to cell cycle progression. We found that CVA21 together with P + C appears to slightly increase caspase-3/7 activity (Figure 4.15).

Although DTIC and P + C are among the few chemotherapeutic agents with some biological activity against melanoma, as single-agent therapies, they have continually failed to make a significant impact on improving patient survival. While there is growing evidence that CVA21 alone has some activity against melanoma in the clinic, this study shows that the combination of CVA21 with chemotherapy has synergistic cytotoxic effects. We failed to identify the exact mechanism by which the combinations exert their synergistic effect, but we did identify an increase in subG1/G₀ cells in some cell lines treated with CVA21 and P + C. This work offers a novel finding in which the combination of CVA21 does interact synergistically and may enhance mechanisms of chemotherapy activity.

In summary, the preclinical analysis presented here provides proof of principle for combining CVA21 with mainstream chemotherapies for the treatment of melanoma. CVA21 together with DTIC or P + C doublet chemotherapy is potent and synergistically active against melanoma cell lines and this data supports the further development of this approach *in vivo*.

Chapter 5

Having successfully highlighted the potential application of this combinatorial therapy as a potent treatment for melanoma in tissue culture models, future clinical translation warranted additional investigations in an *in vivo* setting. **Chapter 5** presents our results on the anti-melanoma effects of the combination of CVA21 with DTIC and P + C in the context of the host environment. We described two mouse melanoma models used in our investigations, an immunodeficient xenograft and a syngeneic immunocompetent model of melanoma.

The combination of CVA21 and chemotherapy was firstly assessed using immunodeficient SCID mice bearing SK-Mel-28-luc cell xenografts. SK-Mel-28 cell were chosen based on their high susceptibility to CVA21 infection and the combination of the virus with either chemotherapeutic drug was synergistic in this cell line at clinically relevant concen-

trations. Herein, SK-Mel-28-luc cells were developed as they express the luciferase gene which provides the means to capturing real time *in vivo* bioluminescent images of tumour development, as well as detecting metastasis in various organs which may not be palpable. Bioluminescent imaging of serially diluted SK-Mel-28-luc cells *in vitro* found the minimum number of detectable cells to be 12,500 cells (Figure 5.1A & B) and when challenged with CVA21, maintained their susceptibility to the virus as per the parental SK-Mel-28 cell line (Figure 5.1C).

We showed that when CVA21 was combined with either DTIC or P + C in a SCID mouse model of human melanoma, rapid reductions in tumour volumes were observed (Figure 5.4A & B). This tumour reduction was found to be significantly greater than observed for either of the chemotherapeutic agents alone. The quantitative bioluminescence data presented was highly consistent with the tumour volume data measured by digital callipers (Figure 5.6A & B). Tumour burdens of mice treated with CVA21 as a single agent and in combination with chemotherapy were no longer palpable. More interestingly, bioluminescent imaging revealed that six out of the eight mice from the CVA21 and P + C treatment group experienced complete tumour remission, whereas only four out of eight of the mice receiving single agent CVA21 were tumour free at the end of the study (Figure 5.5). Although not significant, this observation suggests that combination therapy may be beneficial in generating complete tumour regression in melanoma therapy.

Our data did not show any significant statistical difference between groups that received CVA21 as a single agent or in combination with chemotherapy in this immune deficient model. Such a finding was not surprising and could be attributed to the fact that SK-Mel-28 cells were highly sensitive to CVA21 viral challenge. It would be of interest to use a CVA21-resistant cell line in future work to better delineate any potential synergy. Furthermore, in an immunodeficient setting, the absence of antiviral neutralising antibodies allows for the indefinite replication of viral progeny until all tumour cells have been completely eradicated, thus over-shadowing any possible synergistic relationship between the combination therapy. This was evident in our immunocompromised mouse data, with sustained viraemia in all animals injected with CVA21 (Figure 5.7A & B).

Herein, we have shown that two intratumourally injected doses of CVA21 (total of 2×10^8 TICD₅₀/animal) can mediate the complete regression of melanoma xenografts in

a SCID mouse model. After being internalised into host cells, the injected virus initiates a productive infection that spreads rapidly through the tumour and spills into the bloodstream causing sustained viraemia. However, the viraemic animals later developed myositis, leading to hind limb paralysis, thus necessitating euthanasia. Hind limb paralysis was observed in a total of four animals, two in the CVA21 alone treated group (at day 73 and 78) and two from the CVA21 and DTIC combination treatment group (at day 63 and 73). It was noted that these animals experienced significant tumour regression as well but had to be euthanised as a result of hind limb paralysis. This side effect is likely an artefact specific to the SCID mouse model as immunocompetent animals are known to be resistant to CVA21 myositis [341]. In fact, experimental CVA21 infections in humans cause little more than a short lived upper respiratory tract infection [107, 475], and only one human case of localised CVA21 myositis has been reported [175].

In light of our results, along with other published data [792, 814, 821], it is clear that the efficacy of an OV *in vitro* may differ significantly from its anti-tumour effect *in vivo*. Although our *in vitro* data using Chou-Talalay's method showed antagonism between CVA21 and both chemotherapeutic drugs in SK-Mel-28 cells, enhanced tumour reduction was achieved *in vivo* with these chemotherapeutic agents in combination with CVA21, compared to mice treated with chemotherapy alone. These findings draw parallels with the *in vitro* data presented by Yarde *et al.*, who found that the combination of VSV and bertezomib was antagonistic *in vitro*, but significantly reduced tumour size when administered *in vivo* [814]. In direct contrast, Vile's group have reported that oncolytic VSV had no therapeutic effect on established mesothelioma tumours *in vivo* despite demonstrating potent oncolytic activity *in vitro* [792]. Taken together, results from these papers show that treatment with OVs can induce a variety of immune-mediated consequences *in vivo*, with positive or negative outcomes on anti-tumour therapy. These unexplored immune mechanisms may have significant, and possibly unexpected impacts on how oncolytic virotherapy interacts in combination with other immune modulating anti-tumour agents, an aspect not present when cells are grown in isolation *in vitro*.

One of the current requirements for the study of oncolytic virotherapy is the establishment of an optimal mouse model system other than using immunodeficient mice bearing human xenograft tumours. As mentioned previously, subcutaneously-growing human tumours in immunodeficient mice do not accurately represent cancer growth in patients,

especially with regard to metastasis and drug sensitivity [325]. Addressing the effects of the immune system on the combination therapy and establishing an immunocompetent melanoma model that would support CVA21 replication to answer this question represented a key challenge in our studies.

In order to obtain a clinically relevant model of melanoma, we have developed a syngeneic melanoma model using intradermally implanted B16 murine melanoma cells expressing the human-intracellular adhesion molecule-1 (h-ICAM-1) viral receptor. Mouse cells are known to be resistant to CVA21 infection because they lack the h-ICAM-1 surface receptor [672], thus limiting the use of CVA21 in a syngeneic mouse model. Here, we demonstrate enhanced infectivity and productive replication of CVA21 in B16 mouse melanoma cells following introduction of h-ICAM-1 surface receptor (Figure 5.8A & B). Introduction of ICAM-1 into B16 cells increased their sensitivity to CVA21 and these cells were supportive of viral replication (Figure 5.8C & D). These results reveal that oncolytic CVA21 can be applied to an immunocompetent mouse model with the introduction of ICAM-1 to a syngeneic mouse cell line.

Having ascertained the *in vitro* susceptibility of B16-ICAM-1 to CVA21 infection, we continued with the development of a syngeneic melanoma animal model. It is well established that most experimental mouse tumour models use s.c. injection of tumour cells to induce tumours on the hind flank of an animal. In the course of developing syngeneic immunocompetent murine melanoma model using B16 cells expressing h-ICAM-1, we became aware that there was a consistent pattern of differential growth and the rate of incidence for the B16-ICAM-1 cells when compared to parental B16 cell line (data not shown). The differences were sufficiently profound to compel us to investigate the route of administration on tumour growth in a more systematic manner.

We took great care to standardise the experimental procedures by using B16 and B16-ICAM-1 cells of the same passage, which were regularly checked for viability and mycoplasma. After harvesting from *in vitro* cultures, melanoma cells were kept at 4°C and were injected within 2 hours after cell collection to minimise changes in cell quality. Our studies showed that the route of administration had relatively little effect on B16 tumour growth but this was markedly different for the B16-ICAM-1 tumours. B16-ICAM-1 cells injected intradermally had a significantly larger tumour volume by day 28 and 50% of animals de-

veloped palpable tumours by day 11 as opposed to day 19 for cells injected subcutaneously and had a slightly better rate of incidence. The results, shown in Figures 5.10A - C reflects the mean time of appearance of palpable tumours, the tumour growth rate and the average survival time of the host animal. Apparent from the histological examination of the skin is the location of the tumour, where B16-ICAM-1 cells injected intradermally were deposited in the dermis within the dermal layer, above the skeletal muscles (Figure 5.11). Moreover, ICAM-1 expression levels and CVA21 susceptibility remained unaltered in intradermal tumour explants, but not in those inoculated subcutaneously (Figure 5.12A - C). Taken together, we present evidence that the site of B16-ICAM-1 cell inoculation significantly influences the tumourigenicity of the experimental tumour model and that intradermal inoculation of B16-ICAM-1 cells was more consistent with the widely accepted B16 melanoma model.

However, while our research findings are in agreement with several groups who have suggested administering melanoma cells intradermally [277, 499], others have shown decreased tumourigenicity when cells were implanted into the dermis. Specifically, Bonnotte *et al.* argues that i.d. injection as opposed to s.c. injection enhances immunogenicity and suppresses tumourigenicity of tumour cells [90]. Their experiments demonstrated that all rats that rejected the tumour cells after i.d. injection were vaccinated against subsequent s.c. tumour cell rechallenge. Similarly, there is mounting evidence that a high concentration of dendritic cells in the dermis may facilitate the capture of tumour-associated antigens when tumour cells are injected intradermally, leading to anti-tumour immunity [271, 441]. However, we would like to point out that these studies were designed around the concept of vaccine development using compounds such as attenuated viruses, tumour fragments and various peptides of interest, not live cells for tumour development. While Bonnotte's approach uses active progressive variant (PRO) murine tumour cells which give rise to lethal tumours after s.c. injection in rats, these cells were established from a rat colon adenocarcinoma [484]. The study would have been far more convincing if the author had included syngeneic mouse malignant cell lines inoculated in an orthotopic manner.

Another critical finding of this study was that the route of administration had little to no effect on B16 development but had a pronounced effect on the B16-ICAM-1 cells. This finding, while preliminary, suggests that transfecting B16 cells with h-ICAM-1 surface receptor may play a critical role in tumour development in the dermal environment. Vari-

ous published data have shown that surface expressed ICAM-1 receptor is a fundamental molecule in leukocyte-endothelial cell adhesion function and is upregulated on endothelial cells in response to inflammatory cytokines such as IL-1 and TNF- α [125, 642]. Using orthotopic human skin graft models, Mehta *et al.* have demonstrated that intradermal injection of TNF- α promoted a marked regulation of ICAM-1 expression, particularly in keratinocytes and dermal fibroblasts [503]. Against this background, we hypothesise that the dermal layer of the mouse's skin provides a suitable environment for the development of B16-ICAM-1 tumours when compared to the subcutaneous layer. Herein, we selected the i.d. route of cancer cell delivery for the remaining animal studies.

In the next part of the study, we sought to determine the interaction of CVA21 with DTIC and P + C in the newly established B16-ICAM-1 cell line using the Chou-Talalay method before progressing into *in vivo* application. Over a wide range of concentrations, P + C exerted a dose-dependent anti-tumour effect and its combination with CVA21 yielded a significantly greater anti-tumour effect than that of either agent alone (Figure 5.13B). Cell cytotoxic data was subjected to Chou-Talaly's method and extremely high levels of synergy were observed between the combination of CVA21 and P + C, but was predominantly antagonistic for the DTIC combination (Figure 5.13C & 5.14). The varied responses between these different combinations are an indicator of the complex interaction between host cell machinery for viral replication and the effects of chemotherapy drugs that induce cellular DNA damage (DTIC) or mitotic arrest (P + C).

In focusing on the synergistic interactions between CVA21 and P + C, we sought to determine if CVA21 replication is affected by P + C in the B16-ICAM-1 cells. Drawing on our viral replication data using human melanoma cell lines, we did not anticipate an increase in viral production in the B16-ICAM-1 cell line. Contrary to expectations, we found that the presence of P + C significantly enhances viral replication (Figure 5.15A-C). Furthermore, growth inhibition by the combination of CVA21 with P + C was most pronounced at MOI 0.1 and 1 TCID₅₀/cell where enhanced viral production was observed (Figure 5.16A & B), strongly suggesting synergistic cytotoxicity was related to an increase in CVA21 viral replication in the murine cell line.

We suspect that the observed increase in viral production could be linked to the activation of the RAS-RAF-MEK-ERK pathway (also known as the MAPK pathway) mediated

by the paclitaxel component of the drug-combination. Several studies have revealed that the activation of the MAPK pathway in cancer cells appears to be favourable for RNA virus replication and cytotoxicity [592]. Existing evidence also points to a mechanism of resistance induced by paclitaxel treatment mediating prolonged activation the MAPK pathway in various malignancies [43, 373, 352, 810]. Our observed P + C chemosensitivity data clearly demonstrate that the B16-ICAM-1 cell line was most resistant to the P + C doublet therapy (Figure 5.13A) and would theoretically provide a favourable environment for CVA21-induced replication. It can therefore be hypothesised that a synergistic interaction might occur in the B16-ICAM-1 cell line, through paclitaxel-mediated activation of MAPK signalling with consequent enhancement of CVA21 replication and cytotoxicity. This finding suggests that the P + C doublet chemotherapy might sensitise cells to CVA21 infection.

However, the increased progeny virion production is probably a unique outcome of CVA21 and P + C combination in the B16-ICAM-1 cell line, as we did not observe a significant increase in viral production in the other human cell lines tested. It remains unclear as to why CVA21 and P + C exhibit such strong synergistic effects in the murine cell line but not in our panel of human cells. Molecular pathways of taxol-induced cytotoxicity in different cells are far from being fully understood. Prior studies have noted that the activation of MAPK, especially in the c-jun-NH₂ terminal kinase (JNK) pathway as a crucial event of the programmed cell death in most cancer cells [603, 678]. In some tumour cells, however, JNK signalling is not known not to play a pronounced role, conceding the apoptotic effects of taxol to p38 and ERK [43, 174]. Furthermore, in other cell systems, MAPK has been shown not to be involved in potentiating taxol-effects [82, 352]. Thus, it is likely that a central role for MAPK as a key factor in enhancing the effects of taxols is cell line specific. Further studies, which take these variables into account, will need to be undertaken, as identification of these biomarkers will provide valuable information supporting future clinical design.

Having established that the synergistic effect of the combined treatment was due to increased viral replication, we examined the therapeutic efficacy of CVA21 in combination with chemotherapeutic drug in B16-ICAM-1 syngeneic melanoma tumours in C57BL/6 mice. As discussed previously, a critical aspect of CVA21 virotherapy that was not addressed in the SK-Mel-28 melanoma xenograft model was the role of the immune system.

Here we compared combination therapies of CVA21 and DTIC or CVA21 and P + C in C57BL/6 mice with an intact immune system. This model recapitulates important immune factors observed in human melanoma development over a highly unpredictable course [608]. Unlike xenograft models, the C57BL/6 syngeneic model retains an intact immune system and a host-derived tumour microenvironment that accurately models that present in human cancers. Therefore, this approach has significant advantages over xenograft models, which have been criticised over their failure to provide accurate predictions of drug efficacy in clinical trials.

The application of CVA21 and either chemotherapy combination therapy was corroborated *in vivo* in a murine flank tumour model of melanoma (Figure 5.19A & B). Combination therapy was more effective than either monotherapy treatment alone, and significant inhibition of tumour volume progression was noted in the combination-treated animals for the study duration. Furthermore, we did not observe any toxicity in any of the treatment groups (Figure 5.18A & B). These findings suggest that the combined application of CVA21 with chemotherapy would have significant clinical relevance. In summary, our data support the feasibility of a combination therapy for melanoma using oncolytic CVA21 with DTIC or P + C. Despite increased therapeutic efficacy in tumours treated with the combination therapy, serum viral titres were similar to those treated with CVA21 alone at all time points (Figure 5.20A & B). It was also observed that the production of antiviral neutralising antibodies was reduced in animals that received the combination treatment (Figure 5.21). We speculate that the combination of chemotherapy is able to illicit some form of antiviral protection allowing CVA21 to exert its oncolytic effects in an immunocompetent setting. In summary, our findings imply that DTIC or P + C treatment regimens, which have been the standard treatment of melanoma for decades, will not need to be interrupted for concurrent clinical investigations of oncolytic CVA21.

Chapter 6

Melanoma has been generally considered an immunogenic malignancy. The description of spontaneous regression in melanoma patients, the identification of common immunogenic melanoma antigens, infiltration of lymphocytes within tumour masses, *in vitro* demonstration of melanoma-specific cytolytic T-cell responses, and recent evidence of responsiveness to immunomodulators are all links between immune function and melanoma outcome [409, 477, 606]. Furthermore, the observation that patients with immunosuppression were

more likely to succumb to melanoma suggest that immunosuppressive therapy is associated with a more aggressive disease course in patients, indicating that melanoma may be susceptible to surveillance by the immune system [240]. Thus, strategies to augment the immunogenicity of melanoma cells are of potential benefit.

Inducing anti-tumour immunity by viral oncolysis is a promising strategy to enhance therapeutic efficacy of oncolytic virotherapy in patients. The success of active anti-tumour immune activation depends on the presentation of tumour antigens for stimulation of T cells. Pioneering work by Lindenmann noted that several animals that experienced spontaneous tumour remission from an OV infection were resistant to re-challenge with the same tumour cells [446]. Lindenmann and Klein went on to report that the resistance could not be directly attributed to oncolysis as no infectious virus particles were recovered and high levels of antiviral antibodies were present at the time of re-challenge [447]. Moreover, they showed that lysates prepared from virus-infected tumours were highly immunogenic while lysates prepared by mechanical disruption were not, suggesting that the induction of tumour-specific immunity was enhanced with an oncolytic agent [447]. These findings were further confirmed by Wallack *et al.*, who prepared oncolysates from vaccinia-infected GMMSVI tumour cells and used this preparation to immunise syngeneic BALB/c mice [765]. No vaccine-associated mouse deaths were reported and mice pre-vaccinated with the vaccinia oncolysates prior to receiving tumour cells did not develop tumours at the injection site compared to control animals. These findings together, encouraged our laboratory to initiate preclinical research with CVA21-induced oncolysates.

To study immune effects in the context of oncolytic virotherapy, immunocompetent models are mandatory. The B16-ICAM-1 melanoma model was used in fully immunocompetent C57BL/6 mice. In this study, we were able to demonstrate that CVA21 oncolysate administered intraperitoneally induces anti-tumour immunity in an immunocompetent mouse model of melanoma. Animals treated with the CVA21-induced oncolysate had a modest effect on inhibiting tumour growth. Although not significant, these animals had lower tumour volumes than saline treated animals (Figure 6.3). In direct contrast, immunisation with non-viable cells in the absence of CVA21 failed to elicit any protective immune responses. The above finding suggests that melanoma tumour antigens were released as a direct result of CVA21 lysis, and were not present in the non-viable cell lysate, therefore priming an anti-tumour response. Unfortunately, all animals developed palpable tumour

and no signs of tumour remission were observed from any treatment group, resulting in the early termination of the study. The Kaplan-Meier survival curves were almost identical for all parts of the curves and no survival benefit was observed in animals vaccinated with the CVA21 oncolysate (Figure 6.4A & B). However, all mice treated with the CVA21 oncolysate showed delayed tumour growth and we anticipate that there would have been an improvement in survival if the experiment was extended.

Our finding that the inoculation of CVA21 oncolysate reduces live tumour challenge in an immunocompetent setting clearly suggests that CVA21 is an *in vivo* inducer of immunogenic cell death (ICD). Until now, most of the identified inducers of ICD of tumour cells have been chemotherapeutics [347]. However, recent breakthroughs in cancer immunology have seen several other groups presenting compelling data indicating some OV's may induce ICD, allowing them to be a plausible agent of immunotherapy [657, 803, 804]. A study using lysates generated with PV, a picornavirus related to CVA21, showed that immunised animals survived beyond 100 days after tumour challenge while control animals died before 90 days of tumour challenge [735]. In another study, two other picornaviruses, the encephalomyocarditis virus (EMCV) and Semliki Forest virus (SFV) were also shown to be effective at presenting antigens for cross-priming of DCs *in vivo* [660]. The authors showed that the two OV's did not induce CD8 α^+ DCs activation when added as free viral particles, but when CD8 α^+ DCs were co-cultured with either EMCV or SFV infected-Vero cells, DC activation was observed. The activation was largely due to the recognition of viral RNA by TLR3, flagging tumour cells for phagocytosis. In line with studies using other picornaviruses, we postulate that CVA21's lytic cycle has the capacity to trigger the release of danger signals from tumour cells, which in turn induce an anti-tumour response.

The discovery of T cell regulatory receptors has provided a repertoire of immunotherapies, aiming to reverse the immunosuppressive mechanisms governing tumour resistance to immune surveillance and destruction. In humans, treatment with immunologic checkpoint inhibitors such as CTLA-4 and PD-1 has demonstrated durable tumour regressions, though the therapeutic efficacy has not been entirely universal [321, 734]. From our work with CVA21-induced oncolysates, we postulate that CVA21 is capable of acting as an adjuvant, by increasing the attraction of immune cells to infected cancer cells displaying viral proteins. Conversion of tumours to an inflammatory phenotype may make them more susceptible to therapy with systemic CTLA-4 and PD-1 blockade, leading to tumour rejection

and long-term survival with the combination approach. Furthermore, several authors have put forward the notion that the release of TAAs in an inflammatory milieu *in situ* may facilitate a more robust cellular immunity compared to traditional vaccination strategies [505, 537]. These data provide a strong rationale for testing CVA21 with these immune modulators in the hope of increasing therapeutic efficacy.

Here, we introduce the B16-ICAM-1/B16 bilateral flank melanoma model which is syngeneic to fully immunocompetent C57BL/6 mice. B16 cells expressing the ICAM-1 viral entry receptor were used for establishing the primary tumour. These cells are antigenically similar to B16 cells and we postulate that oncolysis of these cells would lead to the release of similar TAAs facilitating the induction of cellular immunity. The secondary tumour was established using the parental B16 cells. We chose to use the B16 cells because CVA21 infection is not supported in these cells, thus tumour reduction by CVA21 would not be possible, making it suitable to study the immune-mediated mechanisms exclusively. Herein, this model of melanoma will be used in our investigation of the effects of CVA21 oncolysis and systemic PD-1 and CTLA-4 blockade on melanoma immunotherapy.

When developing a suitable treatment regime for the study, an important consideration was the effect of blocking an immune checkpoint on CVA21 viral replication. Suppressing the acquired immune response may increase intratumoural spread of the OV in the short term, but it also diminishes the cross-priming of TAAs needed for the most effective anti-cancer immune response. Conversely, enhancing the anti-tumour immunity may improve cross-priming at the early stage, but suppresses the oncolytic effect of the OV needed for TAA release and tumour debulking. In reviewing the literature, *in vivo* work performed by Zamarin *et al.* successfully combined NDV virotherapy with immune checkpoint blockade to demonstrate an enhanced immunostimulatory effect with minimal levels of toxicity [820]. Hence, using Zamarin and colleague's work as a starting point, tumour bearing animals received four i.t. injections of CVA21 and i.p. injections of either anti-PD-1 or anti-CTLA-4 antibody (three days apart). In the anti-PD-1 study, animals received weekly booster injections of CVA21 (up to four weeks), but in the anti-CTLA-4 study, the additional booster injections were not administered.

Initial studies were conducted with CVA21 in combination with anti-PD-1 inhibitory antibody. In this study, we showed therapeutic benefits in terms of delayed tumour pro-

gression for animals treated with CVA21 or anti-PD-1 alone after intradermal injection of B16-ICAM-1 melanomas in C57BL/6 mice (Figure 6.7). The delay though significant, was only transient, with only one animal from the anti-PD-1 treatment group experiencing a complete response. In direct contrast, combined treatment with PD-1 blockade immunotherapy and CVA21 oncolysis could inhibit tumour formation in 50% of animals and was durable for the course of the study.

The secondary objective of this study was to determine whether the combination would be therapeutically beneficial in protecting animals against tumour rechallenge and prolong survival. Following treatment of the primary cutaneous B16-ICAM-1 tumour with eight cycles of CVA21 injections and four cycles of anti-PD-1 antibody, mice were challenged with an additional subcutaneous administration of B16 cells. Due to the euthanasia of several animals as a result of the primary tumour, the two-way ANOVA analysis was not used to determine the difference in tumour volumes. Instead, the incidence of secondary tumour was defined using Kaplan-Meier curves and statistical significance was tested using the log-rank test. By the end of the study, we found that only animals receiving the combination treatment demonstrated a significant delay in the incidence rate of the B16 tumour (Figure 6.8), leading to an increase in survival (Figure 6.9). These data suggest that PD-1 blockade with CVA21 virotherapy could slow down tumour growth but not completely reject the formation of the B16 tumour.

In the next section of the study, we demonstrate that CVA21 virotherapy was further enhanced by immune checkpoint modulation of CTLA-4. In all treatment groups, significant tumour regression was observed by day 42 when compared to control animals (Figure 6.14). Animals receiving the combination therapy had significantly lower B16-ICAM-1 tumour volumes when compared to animals treated with the anti-CTLA-4 antibody alone by day 35. However, as a result of the euthanasia of several animals with heavy tumour burdens, the significance was lost a week later (day 42). More importantly, while complete remission was achieved in 50% and 60% of mice treated with i.t. CVA21 and i.p. anti-CTLA-4 antibody respectively, all animals from the combination group experienced a complete response. In terms of the primary tumour, these animals remained tumour-free for the duration of the study. However, not all patients suffering from advanced melanoma remain tumour-free and even in those without detectable lesions, residual tumour cells may be present. In these cases, systemic anti-tumour immunity could prevent relapse and also

destroy micrometastases at distant sites.

To establish whether a robust systemic anti-tumoural immune response had developed following intratumoural CVA21 therapy in combination with anti-CTLA-4 antibody treatment, mice were rechallenged with intradermal B16 murine melanoma cells. Consistent with our anti-PD-1 animal model, development of the secondary tumour was delayed in animals treated with the CVA21 alone with no signs of tumour protection (Figure 6.15 & 6.16). Remarkably, the combination protected 40% of mice against growth of the poorly immunogenic B16 for 40 days, whereas tumours developed in 75% of anti-CTLA-4 treated mice. Due to the euthanasia of several animals as a result of the primary tumour, the two-way ANOVA analysis was not used to determine the difference in tumour volumes. Instead, the incidence of secondary tumour was defined using Kaplan-Meier survival curves and statistical significance was tested using the log-rank test. In line with our tumour volume data, median time to tumour growth was significantly suppressed in the combination group when compared CVA21 alone, however, not when compared with anti-CTLA-4 antibody alone (Figure 6.15). This translated to a significant overall survival benefit (Figure 6.17). In summary, we demonstrated the effectiveness of the CTLA-4 blockade with CVA21 oncolysis in inhibiting primary tumour outgrowth and preventing a secondary rechallenge of B16 melanoma cells, suggesting that the combination may be a powerful tool for treatment and protection of melanoma.

As little is known about the immune response mounted against CVA21 following systemic immune checkpoint blockade, the anti-viral immune response generated against CVA21 was examined in both anti-PD-1 and anti-CTLA-4 mouse models. We analysed serum samples from weekly blood samples. In both mouse models, infectious CVA21 was cleared from the systemic circulation by day 14 post treatment (Figure 6.10 & 6.18). We expected an increase in viral load in our anti-PD-1 study but viraemia fell below detectable levels after day 14 and was maintained for the duration of the study. This is a very interesting finding as C57BL/6 mice received a total of eight injections of CVA21 at 1×10^7 TCID₅₀/injection and many of the blood samples from the C57BL/6 mice were collected 1 day post treatment. Such rapid viral clearance indicates that anti-viral antibodies or other host immune factors successfully neutralised the virus within approximately 1 day of administration. It is noteworthy to point out that repeated treatment may lead to the rapid development of neutralising antibodies, presenting a potential drawback of

oncolytic virotherapy. Indeed, neutralising data from the anti-PD-1 study confirmed this finding (Figure 6.10). Repeated dosing of CVA21 led to a significant increase in CVA21-specific nAbs and is likely to have limited viral efficacy. Interestingly, average nAb levels in animals receiving the anti-PD-1 antibody were approximately 2-fold lower than animals without the antibody, suggesting that systemic PD-1 signalling blockade may dampen the humoral antiviral response against CVA21, providing a possible explanation for the increased therapeutic effects observed. Taken together, we decided to maintain the first four intratumoural CVA21 injection but remove the booster injection in our anti-CTLA-4 model, as the additional virus does not appear to provide any therapeutic benefit. More importantly, at the end both animal studies, no signs of treatment-related adverse toxicity in any mouse were recorded, as indicated by the increasing weight (Figure 6.6 & 6.13). Both treatment regimes possess an excellent safety profile.

A major finding in our anti-CTLA-4 animal model was the discovery of a ‘window of opportunity’, where CTLA-4 blockade would allow CVA21 to persist longer in the circulatory system, enabling the virus to exert its oncolytic effect for a longer duration. We found that animals treated with the anti-CTLA-4 antibody two weeks after the initial i.t. injection had reduced CVA21-specific nAbs (Figure 6.19). Consistent with this observation, infectivity assays performed on weekly blood sampling resulted in an unexpected detection of infectious virus particles a week after treatment (Figure 6.18). This was the first time we have detected viraemia in a fully immunocompetent setting a week after the initial challenge. Taken together, these data suggest the exciting possibility that CTLA-4 blockade does not exclusively upregulate T cells, but modulates the immune response by inducing the production of regulatory cytokines. This theory is supported by our non-linear modelling of the nAb response against CVA21 showing that nAbs titres though initially delayed, achieved maximum titres two week later when compared to animals that did not receive the anti-CTLA-4 antibody. We propose that the initial dampening of the innate immune response creates a ‘window of opportunity’ for CVA21 to exert its oncolytic effects, and the enhanced recovery of the immune response loosely suggests an augmented immune response. Further studies to establish this are therefore highly recommended.

Another interesting discovery was the induction of cell death in human melanoma cells treated with the serum from mice ($n = 3$) administered CVA21 + anti-CTLA-4 group. Such activity was not observed from serum of the saline + anti-CTLA-4 group. As the serum

samples were taken 26 days following the last viral administration and in an environment of anti-CVA21 neutralising antibodies, the likelihood that the observed activity against the SK-Mel-28 cells was via direct viral lysis is unlikely. Furthermore, photomicrographs taken of cells treated with serum from the combination group revealed cytotoxic morphology that differs from those that were treated with CVA21 alone (Figure 6.20). While preliminary, this finding strongly suggests the presence of a different mechanism of cell death. The observation that serum concentrations of only 1% can exhibit cytotoxic activity *ex vivo* suggests that this activity is potent and potentially clinically relevant. Complement activation is an important antiviral mechanism and antibody-mediated complement-dependent cytotoxicity (CDC) arising from the complement pathway is a known mechanism of cell killing [766]. For instance, antibody-mediated CDC was detected in JX-549 treated rabbits and Kim *et al.* presents compelling evidence that serum from these animals resulted in tumour necrosis and improved survival [396]. Furthermore, in a majority of patients treated with JX-549 on a phase 1 trial, CDC developed within four to eight weeks, with the longer surviving patients demonstrating highest levels of CDC activity. Given that CDC can be an important determinant of therapeutic antibody-mediated efficacy in cancer, future studies will elucidate the effect of CVA21 on antibody-mediated CDC.

In summary, our current work has indicated that doublet therapies using either anti-PD-1 or anti-CTLA-4 show a synergistic retardation of tumour outgrowth *in vivo*. Furthermore, our results suggest that the CTLA-4 blockade may have a stronger therapeutic effect than the PD-1 blockade when combined with CVA21 virotherapy. This finding is based on a higher CR rate of the primary tumour, higher rejection rate of the secondary tumour, and a longer overall survival when both immune checkpoint inhibitor studies were analysed retrospectively. The molecular basis underlying the efficacy of this treatment protocol was not investigated but several mechanisms have been posited. The stronger inhibitory mechanism of both primary B16-ICAM-1 and secondary B16 tumour by the CTLA-4 + CVA21 doublet therapy are likely due to a combination of the following: (i) decrease in antiviral response at the early phase of treatment, (ii) an increase in the number of circulating effector cells, and (iii) increased homing of effector cells to tumour sites. These mechanisms allow effector T cells to accumulate and proliferate in tumour sites at an early stage and to reject tumour deposits before they establish.

In addition, several authors have suggested that the absence of a PD-1 inhibitory signal

can augment antiviral immunity, which may be detrimental when the virus is administered to patients as a therapeutic agent. Specifically, Iwai *et al.* found that the inhibition of PD-1 induced the proliferation of effector T cells in a adenovirus-infected liver, resulting in rapid clearance of the virus [350], and Zinselmeyer *et al.* reported that a persistent viral infection by lymphocytic choriomeningitis virus (LCMV) resulting in immune exhaustion can be reversed by blocking PD-1 with an antibody [829]. In contrast to work by these two authors, we found that animals treated with the anti-PD-1 antibody had lower anti-CVA21 nAb titres. This discrepancy may be due to the differences in quantifying the antiviral immunity. While their investigation compared T cell proliferation and function, drawing the conclusion that an increase in infiltrating lymphocytes suggested an increase in antiviral response, we were focused on determining CVA21-specific nAb titres produced by B cells, where the humoral system plays an essential role in viral clearance. These results therefore need to be interpreted with caution. Nevertheless, the fact that the absence of the PD-1 inhibitory signal can augment antiviral immunity has significant implications on the efficacy of oncolytic virotherapy. More research on this topic needs to be undertaken before the intrinsic interplay between oncolytic viruses and both humoral and cellular immune responses is clearly understood.

In contrast, CTLA-4 deficiency does not have this effect on viral replication [41, 42, 828]. Using adoptive transfer experiments, Bachmann *et al.* measured T cell responses in C57BL/6 mice after infection with LCMW [42]. They found that the absence of CTLA-4 signals did not interfere with T cell-activation, kinetics of T cell-expansion, or the exhaustion of T cell-responses following the viral challenge. Similarly, in a model of LCMW, Zimmermann *et al.* revealed that blocking CTLA-4 does not significantly alter cytotoxic T-cell response against the virus and the IgG antibody response were slightly diminished [828]. These factors might partly explain why we could detect circulating viruses a week later in two animals treated with the anti-CTLA-4 antibody (Figure 6.18). Taken together, we speculate that PD-1 blockade may have a stronger potency to augment host immune responses against virus than CTLA-4 blockade, supporting the concept that CTLA-4 in combination with CVA21 is more suitable for melanoma immunotherapy.

As indicated by the rechallenge experiments, bilateral tumours were rejected by anti-CTLA-4 while treatment with anti-PD-1 antibody suppressed/delayed tumour growth. This finding was consistent with the work done by Mangsbo and colleagues [480]. The

reason for this is not clear but the induction of T effectors cells and the detection of antinuclear antibodies in animals displaying signs of tumour remission are thought to be the contributing factors. In contrast to our findings, Engeland *et al.* showed that a MV expressing the checkpoint inhibitor anti-CTLA-4 delayed the progression of tumours, while the MV expressing anti-PD-L1 induced tumour remission in some mice and increased overall survival [212]. The therapeutic gains were associated with enhanced cytotoxic T cell and reduced regulatory T cell infiltration into the tumour microenvironment. Together, these models implied that recruitment of cytotoxic lymphocytes to the tumour is essential and that the particular choice of checkpoint inhibition to be used in combination with OVs could be important. It is also important to appreciate the kinetics of action of the co-stimulatory/co-inhibitory interactions associated with checkpoint inhibition. For example, CTLA-4 T-cell inhibition is involved in tolerance induction at the early activation phase, where as PD-1/PD-L1 inhibition mediates the later phases of T-cell activation in the periphery [573]. Thus, future experiments will concentrate on the kinetics and timing of T cell infiltrates and its association with CVA21 replication.

In conclusion, our findings suggest that localised therapy of oncolytic CVA21 may induce inflammatory immune infiltrates in the treated tumour in a poorly immunogenic tumour model, making them susceptible to systemic therapy with the immunomodulatory PD-1 and CTLA-4 antibody. Furthermore, we were particularly successful in demonstrating a durable anti-tumour effect in distant tumours, with a significant increase in overall survival, using the CVA21 and anti-CTLA-4 combination. Importantly, inhibition of either immune checkpoints with CVA21 oncolysis did not affect the body mass in all treated mice and no treatment-related adverse events were observed, suggesting that a feasible safety profile is achievable in patients. This provides a strong rationale for investigation of such combination therapies in the clinic.

7.2 Rationale of combination oncolytic virotherapy

The rationale for a multi-target approach can be especially applicable to oncology. Given the combination of cellular genetic defects and local immune system alterations necessary to allow a neoplastic cell to develop and proliferate, in conjunction with the high rate of mutations that occur in neoplastic cells, it is unlikely that any single treatment will be entirely effective at controlling cancer. There is a general consensus that oncolytic

virotherapy will be much more efficacious when combined with other modalities of cancer treatments [225, 547, 545, 728, 782].

Combination therapy with OV's typically has one or more of the following goals. Firstly, the majority of OV's induce oncolysis of the cancer cells via a unique death pathway. Cancer cells have evolved and have the ability to evade cell death by inhibiting one or more specific pathways of cell death. This provides a rationale for combining another therapeutic drug to destroy cancer cells through alternate death pathways. The combination could be functionally additive or synergistic, leading to the lowering of therapeutic drug doses with non-overlapping toxicities. Alternatively, if the both drugs have similar therapeutic profiles, lowering the drug dose may achieve similar efficacy with few side effects. In addition, pre-treatment of refractory cells with an OV may resensitise these cells to chemotherapy or radiotherapy and may reduce the frequency of acquired resistance. For instance, i.t. infection of T-VEC administered in combination with systemic cisplatin and radiotherapy to patients with previously untreated head and neck squamous cell carcinoma, resulted in an objective tumour response in 14 out of 17 patients (82.3%), of which 93% demonstrated complete pathological remission at subsequent neck dissection [303]. These complementary mechanisms of action of OV's and other conventional agents suggest exciting opportunities for therapeutic synergy.

While the promising activity of OV's has been demonstrated in a variety of *in vitro* and animal models, the clinical results have not been as impressive. The major limitation of OV's is their poor delivery to distant lesions and the rapid development of neutralising antibodies by the host. As such, a considerable amount of research has gone into combining OV's with drugs that may also act to remove barriers to successful oncolytic virotherapy. For example, the most common immunosuppressant drug used in the context of oncolytic virotherapy is cyclophosphamide (CPA). The immunosuppressive features of CPA have been shown to enhance viral oncolysis and improve anti-tumour efficacy in HSV [244], Ad [724], MV [535], reovirus [413, 605], and VV [468]. Another drug that can be used for immune suppression are histone-deacetylase inhibitors (HDACi), which markedly increased and prolonged the therapeutic effect of VSV virus therapy for a variety of refractory cancers [546]. These groups have reasoned that pretreating tumours an immunosuppressive drug can enhance the replication and spread of OV's within malignancies, leading to a synergistic effect.

However, it has been increasingly recognised that modification of tumour cells by OVs may promote their recognition by the immune system, with activation of the adaptive immune responses specific not only for viral, but also for endogenous tumour antigens [287, 505]. Recently, evidence has emerged from both preclinical and clinical studies demonstrating the immune therapeutic potential of OVs, suggesting the possibility that the immunostimulatory properties of OVs can be steered to improve the efficacy of the newly discovered immunomodulatory agents [60]. There is increasing evidence suggesting that patients with pre-existing tumour immune cell infiltration are more likely to respond to immunotherapies involving vaccines and immune checkpoint inhibitors [297, 359]. Direct infection of tumour cells by OVs may render them immunogenic through the activation of the innate immune response, potentially reversing the immune inhibition of inflammation in the tumour microenvironment. In addition, OVs kill tumour cells through several mechanisms, including immunogenic apoptosis, necrosis, and autophagy, all of which have been described to be associated with ICD [286]. As a result, tumour cell lysis results in the release of endogenous TAAs and DAMPs, which increase infiltration of T lymphocytes, facilitating the reactivation of the immune system with the aid of various immunotherapies.

A growing number of studies demonstrate that the integration of OVs with various drugs show synergistic effects that translate into improved anti-tumour responses. Consistent with this, emerging data from clinical trials seem to indicate improved clinical outcomes in such multimodal therapies. These findings provide a strong rationale for combining an OV with other therapeutic modalities for the treatment of melanoma. Optimisation is still required in order to obtain successful combinations and a comprehensive understanding of the interactions of multiple drug components are crucial for clinical success.

7.3 Challenges of combination therapy with OV

Novel combinatorial applications with OVs are continually being developed, and investigators have highlighted several hurdles that may influence the therapeutic index of the combination therapy. As previously mentioned, the biological pathways that OVs manipulate to support their replication (accounting for their oncolytic capacity) are similar to those utilised by malignant cells. In fact, targeting certain pathways with chemotherapy will also, by association, compromise the replicative capacity OVs. For example, viruses may require actively dividing cells to maximise their replicative efficiency, while many an-

anticancer agents are either cytotoxic or cytostatic with death-inducing or anti-proliferative effects, respectively [566]. Furthermore, studies suggest that the leaky vasculature of tumours could be exploited by OV's to successfully extravasate into the tumour site [217, 648]. In fact some OV's, can actually stimulate angiogenesis to increase vascular permeability in tumours [4]. Thus, anti-angiogenic therapy may adversely affect the localisation of OV's to the tumour microenvironment.

Modulation of the host immune response through chemotherapy may conflict with the therapeutic function of the oncolytic virus. For instance, low dose CPA may remove immunosuppressive cells such as T regulatory cells to improve the adaptive anti-tumour immune responses, however, it also promotes the antiviral immune response, leading to early viral clearance [54]. Conversely high dose CPA may enhance viral oncolysis through wide-spread immunosuppression of the innate and adaptive antiviral immune response, but also completely abrogate the anti-tumour immune response [505, 597, 598]. These conflicting mechanisms, cell death *vs* viral replication, anti-angiogenesis *vs* viral trafficking, and antiviral immune response *vs* anti-tumour immune response, will need to be thoroughly investigated when developing combinatorial strategies.

The use of relevant animal tumour models is a concern for all investigators, however it is of particular importance for those studying OV's. Recent studies that have focused on elucidating the role of the immune system in OV therapy found that both the innate and adaptive immune responses contribute significantly to the overall efficacy of the OV [599]. Furthermore, the host's immune response is implicated in hindering OV efficacy by inhibiting early infection, but is required for eventual clearance of the virus. Many studies using OV's were performed in xenograft models using immunocompromised mice. This is appealing because it allows testing in human tumours (as opposed to murine tumours) however this comes at a significant cost. Adding to the limitation of these models is the widespread use of tumour cell lines and the scarcity of data using fresh human tumour samples. Although use of human tumours in xenograft models is useful at first, it is perhaps more clinically relevant to demonstrate OV efficacy in immunocompetent hosts. It will be important to consider these factors when choosing the best combination therapy regimens to develop clinically.

Another significant challenge of combination therapy is the optimisation of the dose

ratio. As cells do not make a distinction between a single drug or a combination, two drugs combined at a given ratio could be considered a third agent with its own dose-effect relation. Therefore, rather than simply investigating whether a particular combination is synergistic, emphasis should be placed on what dose ratio optimises the synergy [388]. Ideally, the dose ratio should be optimised in preclinical studies before proceeding to clinical testing in humans.

7.4 Quantifying synergy in drug combination studies

For complex diseases such as cancer, combination therapies have the potential of having enhanced efficacy without increasing the risk of adverse effects. However, the development of combination drugs can also be costly and risky investment without a well thought out set of experimental strategies, which may vary from drug to drug. High-throughput screening of drug pairs has sought to systematise and extend the empirical approach as a means of identifying new combination drugs [91]. However, given the likelihood that many new multicomponent drugs must be developed and that screening is restricted to a few cell types, it would be very valuable to develop predictive models of pharmacology in which at least part of the work can be done *in silico*.

To characterise drug interaction, the first step is often defining an appropriate null (or additive) model. When the effect of a combination dose is greater or less than that predicted by the additivity model, the combination dose is synergistic or antagonistic. Historically, three additivity reference models are commonly used: 1) effect addition, 2) Bliss independence, and 3) Loewe additivity [272]. The effect addition model has a simple form: $E(d_1, d_2) = E(d_1) + E(d_2)$, where $E(d_1, d_2)$ is the effect at (d_1, d_2) , and $E(d_i)$ is the effect of drug i alone at dose d_i with $i = 1, 2$. However, this model is not generally correct and soon became obsolete. For example, when $E(d_1) = E(d_2) = 70\%$, clearly $E(d_1, d_2)$ can not be 140% when the effect is measured as a proportion of cells killed.

The Bliss independence model is also called effect multiplication or the fractional product [84], and has the form:

$$f_{12} = f_1 + f_2 - f_1 f_2$$

Here f_1 , f_2 , and f_{12} are the effects expressed as the fractions of the maximal effects for

drug 1, drug 2, and the combination. Combination doses with effects more than predicted are synergistic, and conversely, antagonistic. However, Bliss independence implies that two drugs do not physically, pharmacologically, or biologically cooperate, acting independently. As such, Bliss independence can only be expected to be valid for simple biological pathways such as single enzymes and basic biochemical pathways [84].

The Loewe additivity model to characterise drug interaction can be defined as:

$$\frac{d_1}{D_{y,1}} + \frac{d_2}{D_{y,2}} = 1$$

where d_1 , d_2 are doses of drug 1 and drug 2 in mixture, which produces an effect y , while $D_{y,1}$ and $D_{y,2}$ are the doses of drug 1 and drug 2 that produce the same effect y when given alone [460]. The term $\frac{d_1}{D_{y,1}} + \frac{d_2}{D_{y,2}}$ is also called the interaction index at the combination dose (d_1, d_2) .

The Bliss independence and Loewe additivity models are the two most cited reference models for defining drug interactions [230, 272]. Debate continues as to which method performs better with clinical translation of synergy observed *in vitro*. However, only Loewe additivity correctly predicts the trivial case in which the two inhibitors are actually the same compound ('sham' mixture simulation). Since then, Loewe additivity approach has since been popularised for enzyme inhibitor studies by Chou and Talalay, and is arguably the most widely used method in recent literature for analysing combination interactions [146, 145], including the field of oncolytic virotherapy. Chou-Talalay proposed the Combination Index (CI) theorem, serving as a general expression and quantification of drug interaction based on the mass-action law in biophysics and biochemistry [146, 147, 145]. The Chou-Talalay CI index equation can be defined as:

$$CI = \frac{(D)_1}{(D_x)_1} + \frac{(D)_2}{(D_x)_2}$$

for mutually exclusive drugs that have the same or similar modes of action, or:

$$CI = \frac{(D)_1}{(D_x)_1} + \frac{(D)_2}{(D_x)_2} + \frac{(D)_1(D)_2}{(D_x)_1(D_x)_2} \begin{cases} = 1, & \textit{Additivity}; \\ < 1, & \textit{Synergistic} \\ > 1, & \textit{Antagonistic} \end{cases}$$

for mutually non-exclusive drugs that have totally independent modes of action. $(D)_1$

and $(D)_2$ are drug concentrations in combination inhibiting $x\%$, and $(D_x)_1$ and $(D_x)_2$ are the individual drug concentrations. If the CI is equal to, less than, or greater than 1, the combination dose is claimed to be additive, synergistic, or antagonistic, respectively. The method assumes that two or more drugs alone, as well as the combination, will result in sigmoidal concentration-effect curves. The concentration-effect data are log-linearised and the linear regression is fitted to an equation in which the growth-inhibitory effect of each drug is used to calculate a CI.

While the Median-Effect method can provide useful analyses, several authors have pointed out its shortcomings [87, 272, 485, 826]. Only agents that alone and in combinations that have dose-response curves fitting the median-effect equation can be used, and many inhibitors show dose-response curves that cannot be fitted by the equation. More specifically, most response curves do not closely fit to idealised mass-action models. For instance, in our own work, we found that the majority of combinations interacted synergistically but only showed a modest model-fit value (Table 4.3 & 5.13C). This interpretation is misleading in the sense that should we report the combination as a true synergistic effect, or a false positive as a result of experimental error invariably carried by most biological systems despite convincing cell viability data? Even more importantly, the linear transformation proposed by Chou and Talalay as the best way to estimate combination parameters has been subjected to considerable criticism [68, 87, 826]. Others have proposed that applying a nonlinear regression is a superior mean of obtaining combination parameter values as it allows investigators direct inspection of the acquired data. Another significant drawback of the method is that it requires substantial data preprocessing [826]. Raw data are averaged, converted to Fa values, and must lie within the $0 \leq Fa \leq 1$ interval. At lower drug concentrations or if the drug possesses a paradoxical effect on the cell line tested, the Fa values are likely to exceed 1.0, necessitating data exclusion and as such may introduce bias to the analysis.

In line with all of the serious limitations mentioned methods as a metric of synergy, several authors have presented other alternatives. Peterson and Novick introduces the concept of ‘nonlinear blending’ in assessing the joint efficacy of compounds in combination [582]. For the first time, instead of using an index to measure synergy, the authors introduces the concept of ‘weak’ and ‘strong’ blending properties to show how strong blending is the key for determining whether the combination enhanced efficacy [582]. Unlike the typical

Loewe synergy, the concept of ‘nonlinear blending’ can be applied to any combination drug response, including varying relative potency, partial inhibitors, potentiation, and coalism. Hence, this method offers a general approach to synergy that is needed for the wide variety of combination responses that could occur with complex signalling networks with multiple redundant pathways, such as the MAPK and PTEN-PI3K-AKT pathway.

Recently, Boik *et al.* proposed the MixLow (Mixed-effects Loewe) method, which is an improvement over the Median-Effect method [87]. The MixLow method is formulated by three core components, the nonlinear mixed-effect model, the Loewe index, and a method to calculate confidence intervals for index, allowing for a more accurate estimation of concentration-response parameters. Boik *et al.*’s simulation studies computed by the MixLow method were more precise than those computed by the Median-Effect method and calculated confidence intervals were closer to the nominal confidence coefficient (0.95) for the MixLow method than for the Median-Effect method [87]. Furthermore, Boik points out that the use of a nonlinear component of the MixLow model eliminates the need for data preprocessing, preventing data trimming that may be a requisite when using the Median-Effect model [87].

In summary, many classical synergy measures were derived under somewhat limited or idealised pharmacological situations. Further development of methods that allow statistical differentiation between synergy, additivity, and antagonism is warranted and will still likely be an ongoing challenge. Subsequently, claims of synergy should be used appropriately when evaluating drug combination in preclinical studies, but more importantly should provide clear evidence of enhanced therapeutic index before proceeding to clinical evaluation.

7.5 Future directions and conclusion

Currently, the treatment and management of advanced melanoma is trending towards the effective combination of available drugs. Hence, in order for OV_s to be successful, some type of combination therapy will need to be employed. The findings from this thesis have provided a strong rationale for integrating CVA21 with, though not limited to, conventional chemotherapeutics and the more recently discovered immune checkpoint inhibitors. However, several challenges remain to be addressed before translating to the clinic and seeking regulatory approval.

It is critical to understand the interplay between the virus and the combination of choice. As we have described earlier, some treatment modalities may inhibit viral replication, and as such would impede oncolytic efficacy. Rather than simply combining OV's with existing modalities, the challenge going forward is to elucidate the mechanism of OV-drug interactions which are pertinent to the design of future clinical trials. More information on the mechanism of action of the drugs used in combination would help us establish better treatment strategies. However, the presented studies in this thesis were designed as proof-of-principle therapeutic experiments, and we have yet to elucidate the mechanism of action or the mode of cell death induced by CVA21 replication. As ICAM-1 is the sole determine of successful CVA21 infection, future studies would need to investigate the effects of various drugs on the levels of ICAM-1 expression. Furthermore, as the potential of OV's in enhancing cancer immunogenicity becomes increasingly clear, emphasis should also be placed on elucidating the mechanism of cell death mediated by CVA21 infection. These include apoptosis, necrosis, pyroptosis, and autophagic cell death, often with one of these pathways as the dominant form of death for a particular OV.

It is noteworthy to mention that a major issue with the majority of OV research is the over-reliance on *in vitro* cell culture systems. Use of *in vitro* cultures may allow us to focus on dissecting individual pathways and proteins involve in OV-drug interactions but caution must be applied as *in vitro* synergy might not be transferable *in vivo*. The data presented in this thesis uses *in vitro* cell culture models and several animal model as we have yet to acquire access to melanoma patient samples. However, our *in vitro* findings provide a strong rationale for collecting tumour samples from patients currently enrolling in clinical protocols for further analysis. It would be especially useful to obtain pre- and post-treatment tumour samples from CVA21-treated patients and compare them against normal tissue to identify useful biomarkers. We intend to adopt this approach across a broad panel of tumour cell types in the hopes that it may provide guidance in developing better treatment regimes.

Chapter 6 presents the first report of the oncolytic capacity of CVA21 being assessed in combination in a syngeneic model with immune checkpoint inhibitors. There are, however, several limitations present in our study model with both immune checkpoint inhibitors. Firstly, we started therapy in the first week after B16-ICAM-1 tumour inoculation, where

tumour volumes were still relatively small. Although we are optimistic that the current combination approach will translate into improved clinical efficacy, effectiveness against larger tumours is certainly warranted. Secondly, we were successful in demonstrating regression of the bilateral tumour with long-term survival benefits without evidence of disease relapse. Given the metastatic nature of advanced melanomas, it would be important to evaluate whether a similar effect is present in a spontaneous, highly metastatic, animal model of melanoma. The establishment of a B16.F10 model, which is known to have a natural propensity for early spontaneous metastases would be of particular interest [224]. Thirdly, while our study focused primarily on the safety and efficacy of the treatment regimen, it would be interesting to characterise the immune responses in the tumour microenvironment of both primary and metastatic lesions. We found that serum harvested from animals treated with the combination of CVA21 and anti-CTLA-4 had the capacity to induce some form of cell death in monolayers of SK-Mel-28 cells. Further experiments will be needed to elaborate on this observation.

Although our study was not designed to assess and characterise tumour infiltrating lymphocytes in the context of i.t. CVA21 treatment, the use of B16 cells which are not susceptible to a CVA21 infection provided us with a reasonable measure for the generation of an anti-tumour immune response. Consistent with other OV, a virus-mediated immune component in addition to direct oncolysis is warranted for successful virotherapy. Importantly, the induction of an anti-tumoural immune response during oncolysis has the potential to provide durable tumour control long after the the OV has been cleared. In this context, further studies that employs the use of immunosuppressants or chemotherapeutic agents with immunosuppressive properties will need to be carefully timed in order to exert a positive impact against humoral immune response, but still allow the triggering of anti-tumoural immune response induced by viral oncolysis. More importantly, future studies will need to further elucidate the role that the host immune system is playing in CVA21 therapy and the effects on drug combinations will need to be well defined.

Our data with the CTLA-4 antibody also raises the question of whether antibodies targeting other co-inhibitory and/or co-stimulatory receptors could potentiate both antiviral and anti-tumoural immune responses through modulation of T regulatory cells in the tumour microenvironment. We have suggested that CTLA-4 signalling may play an immunomodulatory role which may prove beneficial to CVA21 oncolytic virotherapy. Re-

cent studies have found that CTLA-4 blockade could significantly enhance the tumour-infiltrating T effector/T regulatory cell ratio, in part by selectively depleting T regulatory cells in a manner that is dependent on the tumour microenvironment [683, 798]. Such targeted activity may relieve immune suppression within the tumour while leaving systemic immunity largely intact as widespread depletion of T regulatory cells can induce multiple autoimmune pathologies [395]. Furthermore, the apparent dual function of the novel target OX40 which affects both the T effector and T regulatory compartment, may be a suitable alternative in cancer immunotherapy [587]. Considerably more work will need to be performed to determine whether there will be any potential toxicities, and to optimise the treatment schedules of oncolytic viruses with novel immune checkpoint inhibitors.

Melanoma is an aggressive disease that carries an extremely poor prognosis when local invasion, nodal spread or systemic metastasis has occurred. As a result, the current stand of care therapy for the treatment of metastasised solid tumours is administered systemically. Similarly, while OVs may be delivered locally to accessible tumours, systemic administration via the vasculature gives OVs access to all perfused regions of primary and metastatic tumours, tremendously expanding their clinical applicability. In this regard, intravenous delivery of oncolytic CVA21 is the favoured route of application. In the current project, we have only evaluated the combination effects of CVA21 intratumourally. Based on these exploratory findings, biodistribution studies involving i.v. delivery of CVA21 with clinically relevant drugs using the same experimental animals models are currently underway. We have however, previously demonstrated that a single i.v. injection of CVA21 in established melanoma xenografts in a SCID mouse model caused regression in contralateral tumours, thereby indicating the potential application of CVA21 as a systemic oncolytic agent [670]. In line with delivering an OV intravenously, one should consider the inactivation of the therapeutic virus by neutralising antibodies in the blood and the subsequent development of the cellular immunity. Research is actively being pursued to investigate if the pre-existing and induced anti-viral immune responses can be pharmacologically tempered to limit the neutralisation of therapeutic viruses.

To conclude, we have demonstrated that enhanced efficacy was achieved when CVA21 was combined with a variety of clinically relevant chemotherapeutic and immunotherapeutic agents in both *in vitro* and *in vivo* settings. In addition, all combination treatment

regimes produced excellent tolerability profiles with no obvious treatment-related adverse events observed in the relevant mouse models. Taken together, these findings outlined in this thesis highlight the exciting potential of integrating CVA21 virotherapy with current melanoma treatments and should facilitate the rapid translation towards clinical application.

References

- [1] Abdel-Malek, Z., Suzuki, I., Tada, A., Im, S., and Akcali, C. (1999). The melanocortin-1 receptor and human pigmentation. *Annals of the New York Academy of Sciences*, 885:117–133.
- [2] Adams, M. J., King, A. M. Q., and Carstens, E. B. (2013). Ratification vote on taxonomic proposals to the International Committee on Taxonomy of Viruses (2013). *Archives of virology*, 158(9):2023–2030.
- [3] Adams, M. J., Lefkowitz, E. J., King, A. M. Q., and Carstens, E. B. (2014). Ratification vote on taxonomic proposals to the International Committee on Taxonomy of Viruses (2014). *Archives of virology*, 159(10):2831–2841.
- [4] Aghi, M., Rabkin, S. D., and Martuza, R. L. (2007). Angiogenic response caused by oncolytic herpes simplex virus-induced reduced thrombospondin expression can be prevented by specific viral mutations or by administering a thrombospondin-derived peptide. *Cancer Research*, 67(2):440–444.
- [5] Aghi, M., Visted, T., Depinho, R. A., and Chiocca, E. A. (2008). Oncolytic herpes virus with defective ICP6 specifically replicates in quiescent cells with homozygous genetic mutations in p16. *Oncogene*, 27(30):4249–4254.
- [6] Ahmad, S. R., Lidington, E. A., Ohta, R., Okada, N., Robson, M. G., Davies, K. A., Leitges, M., Harris, C. L., Haskard, D. O., and Mason, J. C. (2003). Decay-accelerating factor induction by tumour necrosis factor- α , through a phosphatidylinositol-3 kinase and protein kinase C-dependent pathway, protects murine vascular endothelial cells against complement deposition. *Immunology*, 110(2):258–268.
- [7] Ahmann, D. L., Hahn, R. G., and Bisel, H. F. (1972). Clinical evaluation of 5-(3,3-dimethyl-1-triazeno)imidazole-4-carboxamide (NSC-45388), melphalan (NSC-8806), and hydroxyurea (NSC-32065) in the treatment of disseminated malignant melanoma. *Cancer chemotherapy reports. Part 1*, 56(3):369–372.
- [8] Alam, M. and Ratner, D. (2001). Cutaneous squamous-cell carcinoma. *New England Journal of Medicine*, 344(13):975–983.
- [9] Alegre, M. L., Shiels, H., Thompson, C. B., and Gajewski, T. F. (1998). Expression and function of CTLA-4 in Th1 and Th2 cells. *Journal of immunology (Baltimore, Md. : 1950)*, 161(7):3347–3356.
- [10] Alemany, R., Suzuki, K., and Curiel, D. T. (2000). Blood clearance rates of adenovirus type 5 in mice. *The Journal of general virology*, 81(Pt 11):2605–2609.
- [11] Alexander, H. E., Koch, G., Mountain, I. M., and van Damme, O. (1958). Infectivity of ribonucleic acid from poliovirus in human cell monolayers. *The Journal of experimental medicine*, 108(4):493–506.
- [12] Alexandrescu, D. T. (2009). Melanoma costs: a dynamic model comparing estimated overall costs of various clinical stages. *Dermatology online journal*, 15(11):1.
- [13] Amaravadi, R. K. and Flaherty, K. T. (2007). Targeted therapy for metastatic melanoma. *Clinical Advances in Hematology and Oncology*, 5(5):386.
- [14] Anderson, B. D., Nakamura, T., Russell, S. J., and Peng, K.-W. (2004). High CD46 receptor density determines preferential killing of tumor cells by oncolytic measles virus. *Cancer Research*, 64(14):4919–4926.
- [15] Andino, R., Rieckhof, G. E., and Baltimore, D. (1990). A functional ribonucleoprotein complex forms around the 5' end of poliovirus RNA. *Cell*, 63(2):369–380.
- [16] Andreasen, P. A., Egelund, R., and Petersen, H. H. (2000). The plasminogen activation system in tumor growth, invasion, and metastasis. *Cellular and Molecular Life Sciences*, 57(1):25–40.

- [17] Andreasen, P. A., Kjoller, L., Christensen, L., and Duffy, M. J. (1997). The urokinase-type plasminogen activator system in cancer metastasis: a review. *International Journal of Cancer*, 72(1):1–22.
- [18] Andrew, C. G., Drachman, D. B., Pestronk, A., and Narayan, O. (1984). Susceptibility of skeletal muscle to Cocksackie A2 virus infection: effects of botulinum toxin and denervation. *Science (New York, N. Y.)*, 223(4637):714–716.
- [19] Andtbacka, R. H. I., Collichio, F. A., Amatruda, T., Senzer, N. N., Chesney, J., Delman, K. A., Spitler, L. E., Puzanov, I., Doleman, S., Ye, Y., Vanderwalde, A. M., Coffin, R., and Kaufman, H. (2013). OPTiM: A randomized phase III trial of talimogene laherparepvec (T-VEC) versus subcutaneous (SC) granulocyte-macrophage colony-stimulating factor (GM-CSF) for the treatment (tx) of unresected stage IIIB/C and IV melanoma. *Journal of Clinical Oncology, 2013 ASCO Annual Meeting Abstracts*, 31(18suppl):LBA9008.
- [20] Andtbacka, R. H. I., Curti, B. D., Kaufman, H., Daniels, G. A., Nemunaitis, J. J., Spitler, L. E., Hallmeyer, S., Lutzky, J., Schultz, S., Whitman, E. D., Zhou, K., Weisberg, J. I., and Shafren, D. (2014). CALM study: A phase II study of an intratumorally delivered oncolytic immunotherapeutic agent, coxsackievirus A21, in patients with stage IIIC and stage IV malignant melanoma. *Journal of Clinical Oncology, 2014 ASCO Annual Meeting Abstracts*, 32(15suppl):3031.
- [21] Angarita, F. A., Acuna, S. A., Ottolino-Perry, K., Zerhouni, S., and McCart, J. A. (2013). Mounting a strategic offense: fighting tumor vasculature with oncolytic viruses. *Trends in molecular medicine*, 19(6):378–392.
- [22] Archambault, M., Yaar, M., and Gilchrist, B. A. (1995). Keratinocytes and fibroblasts in a human skin equivalent model enhance melanocyte survival and melanin synthesis after ultraviolet irradiation. *The Journal of investigative dermatology*, 104(5):859–867.
- [23] Argenziano, G., Albertini, G., Castagnetti, F., De Pace, B., Di Lernia, V., Longo, C., Pellacani, G., Piana, S., Ricci, C., and Zalaudek, I. (2012). Early diagnosis of melanoma: what is the impact of dermoscopy? *Dermatologic therapy*, 25(5):403–409.
- [24] Arits, A. H. M. M., Mosterd, K., Essers, B. A., Spoorenberg, E., Sommer, A., De Rooij, M. J. M., van Pelt, H. P. A., Quaedvlieg, P. J. F., Krekels, G. A. M., van Neer, P. A. F. A., Rijzewijk, J. J., van Geest, A. J., Steijlen, P. M., Nelemans, P. J., and Kelleners-Smeets, N. W. J. (2013). Photodynamic therapy versus topical imiquimod versus topical fluorouracil for treatment of superficial basal-cell carcinoma: a single blind, non-inferiority, randomised controlled trial. *The lancet oncology*, 14(7):647–654.
- [25] Armstrong, B. K. and Krickler, A. (2001). The epidemiology of UV induced skin cancer. *Journal of photochemistry and photobiology. B, Biology*, 63(1-3):8–18.
- [26] Arnold, E., Luo, M., Vriend, G., Rossmann, M. G., Palmenberg, A. C., Parks, G. D., Nicklin, M. J., and Wimmer, E. (1987). Implications of the picornavirus capsid structure for polyprotein processing. *Proceedings of the National Academy of Sciences of the United States of America*, 84(1):21–25.
- [27] Arora, T. and Jelinek, D. F. (1998). Differential myeloma cell responsiveness to interferon-alpha correlates with differential induction of p19(INK4d) and cyclin D2 expression. *The Journal of biological chemistry*, 273(19):11799–11805.
- [28] Arozarena, I., Goicoechea, I., Erice, O., Ferguson, J., Margison, G. P., and Wellbrock, C. (2014). Differential chemosensitivity to antifolate drugs between RAS and BRAF melanoma cells. *Molecular Cancer*, 13:154.
- [29] Asada, T. (1974). Treatment of human cancer with mumps virus. *Cancer*, 34(6):1907–1928.
- [30] Ascierto, P. A., Simeone, E., Sznol, M., Fu, Y.-X., and Melero, I. (2010). Clinical experiences with anti-CD137 and anti-PD1 therapeutic antibodies. *Seminars in oncology*, 37(5):508–516.
- [31] Atherton, M. J. and Lichty, B. D. (2013). Evolution of oncolytic viruses: novel strategies for cancer treatment. *Immunotherapy*, 5(11):1191–1206.
- [32] Atkins, M. B., Lotze, M. T., Dutcher, J. P., Fisher, R. I., Weiss, G., Margolin, K., Abrams, J., Sznol, M., Parkinson, D., Hawkins, M., Paradise, C., Kunkel, L., and Rosenberg, S. A. (1999). High-dose recombinant interleukin 2 therapy for patients with metastatic melanoma: analysis of 270 patients treated between 1985 and 1993. *Journal of clinical oncology : official journal of the American Society of Clinical Oncology*, 17(7):2105–2116.

- [33] Au, G. G., Beagley, L. G., Haley, E. S., Barry, R. D., and Shafren, D. R. (2011). Oncolysis of malignant human melanoma tumors by Coxsackieviruses A13, A15 and A18. *Virology Journal*, 8(1):22.
- [34] Au, G. G., Lincz, L. F., Enno, A., and Shafren, D. R. (2007). Oncolytic Coxsackievirus A21 as a novel therapy for multiple myeloma. *British Journal of Haematology*, 137(2):133–141.
- [35] Au, G. G., Lindberg, A. M., Barry, R. D., and Shafren, D. R. (2005). Oncolysis of vascular malignant human melanoma tumors by Coxsackievirus A21. *International journal of oncology*, 26(6):1471–1476.
- [36] Australian Institute of Health and Welfare (2012). Cancer in Australia: an overview. Technical Report Cancer series no. 74, Canberra.
- [37] Autier, P., Doré, J. F., Gefeller, O., Cesarini, J. P., Lejeune, F., Koelmel, K. F., Lienard, D., and Kleeborg, U. R. (1997). Melanoma risk and residence in sunny areas. EORTC Melanoma Co-operative Group. European Organization for Research and Treatment of Cancer. *British Journal of Cancer*, 76(11):1521–1524.
- [38] Averbook, B. J., Lee, S. J., Delman, K. A., Gow, K. W., Zager, J. S., Sondak, V. K., Messina, J. L., Sabel, M. S., Pittelkow, M. R., Ecker, P. M., Markovic, S. N., Swetter, S. M., Leachman, S. A., Testori, A., Curiel-Lewandrowski, C., Go, R. S., Jukic, D. M., and Kirkwood, J. M. (2013). Pediatric melanoma: analysis of an international registry. *Cancer*, 119(22):4012–4019.
- [39] Avril, M. F., Aamdal, S., Grob, J. J., Hauschild, A., Mohr, P., Bonerandi, J. J., Weichenthal, M., Neuber, K., Bieber, T., Gilde, K., Guillem Porta, V., Fra, J., Bonnetterre, J., Saiag, P., Kamanabrou, D., Pehamberger, H., Sufiarsky, J., Gonzalez Larriba, J. L., Scherrer, A., and Menu, Y. (2004). Fotemustine compared with dacarbazine in patients with disseminated malignant melanoma: a phase III study. *Journal of clinical oncology : official journal of the American Society of Clinical Oncology*, 22(6):1118–1125.
- [40] Azoury, S. C. and Lange, J. R. (2014). Epidemiology, risk factors, prevention, and early detection of melanoma. *The Surgical clinics of North America*, 94(5):945–62–vii.
- [41] Bachmann, M. F., Gallimore, A., Jones, E., Ecabert, B., Acha-Orbea, H., and Kopf, M. (2001). Normal pathogen-specific immune responses mounted by CTLA-4-deficient T cells: a paradigm reconsidered. *European journal of immunology*, 31(2):450–458.
- [42] Bachmann, M. F., Waterhouse, P., Speiser, D. E., McKall-Faienza, K., Mak, T. W., and Ohashi, P. S. (1998). Normal responsiveness of CTLA-4-deficient anti-viral cytotoxic T cells. *Journal of immunology (Baltimore, Md. : 1950)*, 160(1):95–100.
- [43] Bacus, S. S., Gudkov, A. V., Lowe, M., Lyass, L., Yung, Y., Komarov, A. P., Keyomarsi, K., Yarden, Y., and Seger, R. (2001). Taxol-induced apoptosis depends on MAP kinase pathways (ERK and p38) and is independent of p53. *Oncogene*, 20(2):147–155.
- [44] Baertsch, M. A., Leber, M. F., Bossow, S., Singh, M., Engeland, C. E., Albert, J., Grossardt, C., Jäger, D., von Kalle, C., and Ungerechts, G. (2014). MicroRNA-mediated multi-tissue detargeting of oncolytic measles virus. *Cancer gene therapy*, 21(9):373–380.
- [45] Balch, C. M., Buzaid, A. C., Soong, S. j., Atkins, M. B., Cascinelli, N., Coit, D. G., Fleming, I. D., Gershenwald, J. E., Houghton, A., Kirkwood, J. M., McMasters, K. M., Mihm, M. F., Morton, D. L., Reintgen, D. S., Ross, M. I., Sober, A., Thompson, J. A., and Thompson, J. F. (2001). Final version of the American Joint Committee on Cancer staging system for cutaneous melanoma. In *Journal of clinical oncology : official journal of the American Society of Clinical Oncology*, pages 3635–3648. Johns Hopkins Medical Institutions, Baltimore, MD, USA. balchc@asco.org.
- [46] Balch, C. M., Gershenwald, J. E., Soong, S.-J., Thompson, J. F., Atkins, M. B., Byrd, D. R., Buzaid, A. C., Cochran, A. J., Coit, D. G., Ding, S., Eggermont, A. M., Flaherty, K. T., Gimotty, P. A., Kirkwood, J. M., McMasters, K. M., Mihm, M. C., Morton, D. L., Ross, M. I., Sober, A. J., and Sondak, V. K. (2009). Final version of 2009 AJCC melanoma staging and classification. *Journal of clinical oncology : official journal of the American Society of Clinical Oncology*, 27(36):6199–6206.
- [47] Balch, C. M., Soong, S.-J., Gershenwald, J. E., Thompson, J. F., Coit, D. G., Atkins, M. B., Ding, S., Cochran, A. J., Eggermont, A. M. M., Flaherty, K. T., Gimotty, P. A., Johnson, T. M., Kirkwood, J. M., Leong, S. P., McMasters, K. M., Mihm, M. C., Morton, D. L., Ross, M. I., and Sondak, V. K. (2013). Age as a prognostic factor in patients with localized melanoma and regional metastases. *Annals of surgical oncology*, 20(12):3961–3968.

- [48] Balzi, D., Carli, P., and Geddes, M. (1997). Malignant melanoma in Europe: changes in mortality rates (1970-90) in European Community countries. *Cancer causes & control : CCC*, 8(1):85-92.
- [49] Baraz, L., Khazanov, E., Condiotti, R., Kotler, M., and Nagler, A. (1999). Natural killer (NK) cells prevent virus production in cell culture. *Bone marrow transplantation*, 24(2):179-189.
- [50] Barclay, W., Li, Q., Hutchinson, G., Moon, D., Richardson, A., Percy, N., Almond, J. W., and Evans, D. J. (1998). Encapsidation studies of poliovirus subgenomic replicons. *The Journal of general virology*, 79 (Pt 7):1725-1734.
- [51] Barnes, D., Kunitomi, M., Vignuzzi, M., Saksela, K., and Andino, R. (2008). Harnessing endogenous miRNAs to control virus tissue tropism as a strategy for developing attenuated virus vaccines. *Cell host & microbe*, 4(3):239-248.
- [52] Baron, S., Yin-Murphy, M., and Almond, J. W. (1996). *Picornaviruses*. Medical Microbiology. University of Texas Medical Branch at Galveston, Galveston (TX), 4th edition.
- [53] Bart, R. S., Porzio, N. R., Kopf, A. W., Vilcek, J. T., Cheng, E. H., and Farcet, Y. (1980). Inhibition of growth of B16 murine malignant melanoma by exogenous interferon. *Cancer Research*, 40(3):614-619.
- [54] Bartlett, D. L., Liu, Z., Sathaiah, M., Ravindranathan, R., Guo, Z., He, Y., and Guo, Z. S. (2013). Oncolytic viruses as therapeutic cancer vaccines. *Molecular Cancer*, 12(1):103.
- [55] Basavappa, R., Syed, R., Flore, O., Icenogle, J. P., Filman, D. J., and Hogle, J. M. (1994). Role and mechanism of the maturation cleavage of VP0 in poliovirus assembly: structure of the empty capsid assembly intermediate at 2.9 Å resolution. *Protein science : a publication of the Protein Society*, 3(10):1651-1669.
- [56] Bastiaens, M. T., Hoefnagel, J. J., Bruijn, J. A., Westendorp, R. G., Vermeer, B. J., and Bouwes Bavinck, J. N. (1998). Differences in age, site distribution, and sex between nodular and superficial basal cell carcinoma indicate different types of tumors. *The Journal of investigative dermatology*, 110(6):880-884.
- [57] Bastian, B. C. (2014). The molecular pathology of melanoma: an integrated taxonomy of melanocytic neoplasia. *Annual review of pathology*, 9:239-271.
- [58] Bataille, V., Grulich, A., Sasieni, P., Swerdlow, A., Newton Bishop, J., McCarthy, W., Hersey, P., and Cuzick, J. (1998). The association between naevi and melanoma in populations with different levels of sun exposure: a joint case-control study of melanoma in the UK and Australia. *British Journal of Cancer*, 77(3):505-510.
- [59] Batus, M., Waheed, S., Ruby, C., Petersen, L., Bines, S. D., and Kaufman, H. L. (2013). Optimal management of metastatic melanoma: current strategies and future directions. *American journal of clinical dermatology*, 14(3):179-194.
- [60] Bauzon, M. and Hermiston, T. (2014). Armed therapeutic viruses - a disruptive therapy on the horizon of cancer immunotherapy. *Frontiers in immunology*, 5:74.
- [61] Beal, D. D., Skibba, J. L., Whitnable, K. K., and Bryan, G. T. (1976). Effects of 5-(3,3-dimethyl-1-triazeno)imidazole-4-carboxamide and its metabolites on Novikoff hepatoma cells. *Cancer Research*, 36(8):2827-2831.
- [62] Beatty, G. L., Chiorean, E. G., Fishman, M. P., Saboury, B., Teitelbaum, U. R., Sun, W., Huhn, R. D., Song, W., Li, D., Sharp, L. L., Torigian, D. A., O'Dwyer, P. J., and Vonderheide, R. H. (2011). CD40 agonists alter tumor stroma and show efficacy against pancreatic carcinoma in mice and humans. *Science (New York, N.Y.)*, 331(6024):1612-1616.
- [63] Bedard, K. M. and Semler, B. L. (2004). Regulation of picornavirus gene expression. *Microbes and infection / Institut Pasteur*, 6(7):702-713.
- [64] Bella, J. and Rossmann, M. G. (1999). Review: rhinoviruses and their ICAM receptors. *Journal of structural biology*, 128(1):69-74.
- [65] Belnap, D. M., Filman, D. J., Trus, B. L., Cheng, N., Booy, F. P., Conway, J. F., Curry, S., Hiremath, C. N., Tsang, S. K., Steven, A. C., and Hogle, J. M. (2000). Molecular tectonic model of virus structural transitions: the putative cell entry states of poliovirus. *Journal of Virology*, 74(3):1342-1354.

- [66] Bennett, D. C. (2008). How to make a melanoma: what do we know of the primary clonal events? *Pigment Cell & Melanoma Research*, 21(1):27–38.
- [67] Bennett, J. J., Delman, K. A., Burt, B. M., Mariotti, A., Malhotra, S., Zager, J., Petrowsky, H., Mastorides, S., Federoff, H., and Fong, Y. (2002). Comparison of safety, delivery, and efficacy of two oncolytic herpes viruses (G207 and NV1020) for peritoneal cancer. *Cancer gene therapy*, 9(11):935–945.
- [68] Berenbaum, M. C. (1989). What is synergy? *Pharmacological reviews*, 41(2):93–141.
- [69] Berendt, A. R., Simmons, D. L., Tansey, J., Newbold, C. I., and Marsh, K. (1989). Intercellular adhesion molecule-1 is an endothelial cell adhesion receptor for Plasmodium falciparum. *Nature*, 341(6237):57–59.
- [70] Berking, C., Hauschild, A., Kölbl, O., Mast, G., and Gutzmer, R. (2014). Basal cell carcinoma-treatments for the commonest skin cancer. *Deutsches Ärzteblatt international*, 111(22):389–395.
- [71] Berry, L. J., Au, G. G., Barry, R. D., and Shafren, D. R. (2008). Potent Oncolytic activity of human enteroviruses against human prostate cancer. *The Prostate*, 68(6):577–587.
- [72] Besaratina, A. and Pfeifer, G. P. (2008). Sunlight ultraviolet irradiation and BRAF V600 mutagenesis in human melanoma. *Human mutation*, 29(8):983–991.
- [73] Bevona, C., Goggins, W., Quinn, T., Fullerton, J., and Tsao, H. (2003). Cutaneous melanomas associated with nevi. *Archives of Dermatology*, 139(12):1620–4– discussion 1624.
- [74] Beyer, I., Cao, H., Persson, J., Song, H., Richter, M., Feng, Q., Yumul, R., van Rensburg, R., Li, Z., Berenson, R., Carter, D., Roffler, S., Drescher, C., and Lieber, A. (2012). Coadministration of epithelial junction opener JO-1 improves the efficacy and safety of chemotherapeutic drugs. *Clinical cancer research : an official journal of the American Association for Cancer Research*, 18(12):3340–3351.
- [75] Bi, X., Hameed, M., Mirani, N., Pimenta, E. M., Anari, J., and Barnes, B. J. (2011). Loss of interferon regulatory factor 5 (IRF5) expression in human ductal carcinoma correlates with disease stage and contributes to metastasis. *Breast Cancer Research*, 13(6):R111.
- [76] Bierman, H. R., Crile, D. M., Dod, K. S., Kelly, K. H., Petrakis, N. L., White, L. P., and Shimkin, M. B. (1953). Remissions in leukemia of childhood following acute infectious disease: staphylococcus and streptococcus, varicella, and feline panleukopenia. *Cancer*, 6(3):591–605.
- [77] Bilbao, R., Bustos, M., Alzuguren, P., Pajares, M. J., Drozdziak, M., Qian, C., and Prieto, J. (2000). A blood-tumor barrier limits gene transfer to experimental liver cancer: the effect of vasoactive compounds. *Gene Therapy*, 7(21):1824–1832.
- [78] Birch-Johansen, F., Hvilsum, G., Kjaer, T., and Storm, H. (2008). Social inequality and incidence of and survival from malignant melanoma in a population-based study in Denmark, 1994-2003. *European journal of cancer (Oxford, England : 1990)*, 44(14):2043–2049.
- [79] Bischoff, J. R., Kirn, D. H., Williams, A., Heise, C., Horn, S., Muna, M., Ng, L., Nye, J. A., Sampson-Johannes, A., Fattaey, A., and McCormick, F. (1996). An adenovirus mutant that replicates selectively in p53-deficient human tumor cells. *Science (New York, N.Y.)*, 274(5286):373–376.
- [80] Bishop, J. A., Wachsmuth, R. C., Harland, M., Bataille, V., Pinney, E., MacK, P., Baglietto, L., Cuzick, J., and Bishop, D. T. (2000). Genotype/phenotype and penetrance studies in melanoma families with germline CDKN2A mutations. *The Journal of investigative dermatology*, 114(1):28–33.
- [81] Black, A. J. and Morris, D. G. (2012). Clinical trials involving the oncolytic virus, reovirus: ready for prime time? *Expert review of clinical pharmacology*, 5(5):517–520.
- [82] Blagosklonny, M. V., Chuman, Y., Bergan, R. C., and Fojo, T. (1999). Mitogen-activated protein kinase pathway is dispensable for microtubule-active drug-induced Raf-1/Bcl-2 phosphorylation and apoptosis in leukemia cells. *Leukemia*, 13(7):1028–1036.
- [83] Blehacz, B., Splinter, P. L., Greiner, S., Myers, R., Peng, K.-W., Federspiel, M. J., Russell, S. J., and LaRusso, N. F. (2006). Engineered measles virus as a novel oncolytic viral therapy system for hepatocellular carcinoma. *Hepatology (Baltimore, Md.)*, 44(6):1465–1477.
- [84] Bliss, C. I. (1937). The toxicity of poisons applied jointly. *Annals of Applied Biology*, 26(3):585–615.

- [85] Bloom, H. H., Johnson, K. M., Mufson, M. A., and CHANOCK, R. M. (1962). Acute respiratory disease associated with Coxsackie A-21 virus infection. II. Incidence in military personnel: observations in a nonrecruit population. *JAMA : the journal of the American Medical Association*, 179:120–125.
- [86] Bluming, A. Z. and Ziegler, J. L. (1971). Regression of Burkitt's lymphoma in association with measles infection. *The Lancet*, 2(7715):105–106.
- [87] Boik, J. C., Newman, R. A., and Boik, R. J. (2008). Quantifying synergism/antagonism using non-linear mixed-effects modeling: a simulation study. *Statistics in medicine*, 27(7):1040–1061.
- [88] Boisgerault, N., Tangy, F., and Gregoire, M. (2010). New perspectives in cancer virotherapy: bringing the immune system into play. *Immunotherapy*, 2(2):185–199.
- [89] Boniol, M., Autier, P., Boyle, P., and Gandini, S. (2012). Cutaneous melanoma attributable to sunbed use: systematic review and meta-analysis. *BMJ (Clinical research ed.)*, 345:e4757.
- [90] Bonnotte, B., Gough, M., Phan, V., Ahmed, A., Chong, H., Martin, F., and Vile, R. G. (2003). Intradermal injection, as opposed to subcutaneous injection, enhances immunogenicity and suppresses tumorigenicity of tumor cells. *Cancer Research*, 63(9):2145–2149.
- [91] Borisy, A. A., Elliott, P. J., Hurst, N. W., Lee, M. S., Lehár, J., Price, E. R., Serbedzija, G., Zimmermann, G. R., Foley, M. A., Stockwell, B. R., and Keith, C. T. (2003). Systematic discovery of multicomponent therapeutics. *Proceedings of the National Academy of Sciences of the United States of America*, 100(13):7977–7982.
- [92] Boussemart, L., Routier, E., Mateus, C., Opletalova, K., Sebille, G., Kamsu-Kom, N., Thomas, M., Vagner, S., Favre, M., Tomasic, G., Wechsler, J., Lacroix, L., and Robert, C. (2013). Prospective study of cutaneous side-effects associated with the BRAF inhibitor vemurafenib: a study of 42 patients. *Annals of oncology : official journal of the European Society for Medical Oncology / ESMO*, 24(6):1691–1697.
- [93] Bousoo, P. (2008). T-cell activation by dendritic cells in the lymph node: lessons from the movies. *Nature reviews. Immunology*, 8(9):675–684.
- [94] Box, N. F., Duffy, D. L., Chen, W., Stark, M., Martin, N. G., Sturm, R. A., and Hayward, N. K. (2001). MC1R genotype modifies risk of melanoma in families segregating CDKN2A mutations. *American journal of human genetics*, 69(4):765–773.
- [95] Boyd, A. W., Wawryk, S. O., Burns, G. F., and Fecondo, J. V. (1988). Intercellular adhesion molecule 1 (ICAM-1) has a central role in cell-cell contact-mediated immune mechanisms. *Proceedings of the National Academy of Sciences of the United States of America*, 85(9):3095–3099.
- [96] Bradford, P. T., Anderson, W. F., Purdue, M. P., Goldstein, A. M., and Tucker, M. A. (2010). Rising melanoma incidence rates of the trunk among younger women in the United States. *Cancer Epidemiology Biomarkers & Prevention*, 19(9):2401–2406.
- [97] Bradford, P. T., Goldstein, A. M., Tamura, D., Khan, S. G., Ueda, T., Boyle, J., Oh, K.-S., Imoto, K., Inui, H., Moriwaki, S.-I., Emmert, S., Pike, K. M., Raziuddin, A., Plona, T. M., DiGiovanna, J. J., Tucker, M. A., and Kraemer, K. H. (2011). Cancer and neurologic degeneration in xeroderma pigmentosum: long term follow-up characterises the role of DNA repair. *Journal of medical genetics*, 48(3):168–176.
- [98] Bradley, S., Jakes, A. D., Harrington, K., Pandha, H., Melcher, A., and Errington-Mais, F. (2014). Applications of coxsackievirus A21 in oncology. *Oncolytic Virotherapy*, 3:47–55.
- [99] Brahmer, J. R., Tykodi, S. S., Chow, L. Q. M., Hwu, W.-J., Topalian, S. L., Hwu, P., Drake, C. G., Camacho, L. H., Kauh, J., Odunsi, K., Pitot, H. C., Hamid, O., Bhatia, S., Martins, R., Eaton, K., Chen, S., Salay, T. M., Alaparthi, S., Grosso, J. F., Korman, A. J., Parker, S. M., Agrawal, S., Goldberg, S. M., Pardoll, D. M., Gupta, A., and Wigginton, J. M. (2012). Safety and activity of anti-PD-L1 antibody in patients with advanced cancer. *The New England journal of medicine*, 366(26):2455–2465.
- [100] Breitbach, C. J., Burke, J., Jonker, D., Stephenson, J., Haas, A. R., Chow, L. Q. M., Nieva, J., Hwang, T.-H., Moon, A., Patt, R., Pelusio, A., Le Boeuf, F., Burns, J., Evgin, L., De Silva, N., Cvancic, S., Robertson, T., Je, J.-E., Lee, Y.-S., Parato, K., Diallo, J.-S., Fenster, A., Daneshmand, M., Bell, J. C., and Kirn, D. H. (2011a). Intravenous delivery of a multi-mechanistic cancer-targeted oncolytic poxvirus in humans. *Nature*, 477(7362):99–102.

- [101] Breitbach, C. J., De Silva, N. S., Falls, T. J., Aladl, U., Evgin, L., Paterson, J., Sun, Y. Y., Roy, D. G., Rintoul, J. L., Daneshmand, M., Parato, K., Stanford, M. M., Lichty, B. D., Fenster, A., Kirn, D., Atkins, H., and Bell, J. C. (2011b). Targeting tumor vasculature with an oncolytic virus. *Molecular therapy : the journal of the American Society of Gene Therapy*, 19(5):886–894.
- [102] Brown, B. A., Maher, K., Flemister, M. R., Naraghi-Arani, P., Uddin, M., Oberste, M. S., and Pallansch, M. A. (2009). Resolving ambiguities in genetic typing of human enterovirus species C clinical isolates and identification of enterovirus 96, 99 and 102. *The Journal of general virology*, 90(Pt 7):1713–1723.
- [103] Brown, D., Edwards, H., Seaton, L., and Buckley, T. (2015). *Lewis's Medical-Surgical Nursing*. Elsevier Health Sciences APAC.
- [104] Brown, F., Sellers, R. F., and Stewart, D. L. (1958). Infectivity of ribonucleic acid from mice and tissue culture infected with the virus of foot-and-mouth disease. *Nature*, 182(4634):535–536.
- [105] Bryant, R. W., Granzow, C. A., Siegel, M. I., Egan, R. W., and Billah, M. M. (1990). Phorbol esters increase synthesis of decay-accelerating factor, a phosphatidylinositol-anchored surface protein, in human endothelial cells. *Journal of immunology (Baltimore, Md. : 1950)*, 144(2):593–598.
- [106] Bryant, R. W., Granzow, C. A., Siegel, M. I., Egan, R. W., and Billah, M. M. (1991). Wheat germ agglutinin and other selected lectins increase synthesis of decay-accelerating factor in human endothelial cells. *Journal of immunology (Baltimore, Md. : 1950)*, 147(6):1856–1862.
- [107] Buckland, F. E., Bynoe, M. L., and Tyrrell, D. A. (1965). Experiments on the spread of colds. II. Studies in volunteers with coxsackievirus A21. *The Journal of hygiene*, 63(3):327–343.
- [108] Buettner, P. G., Leiter, U., Eigentler, T. K., and Garbe, C. (2005). Development of prognostic factors and survival in cutaneous melanoma over 25 years: An analysis of the Central Malignant Melanoma Registry of the German Dermatological Society. *Cancer*, 103(3):616–624.
- [109] Buller, D. B., Cokkinides, V., Hall, H. I., Hartman, A. M., Saraiya, M., Miller, E., Paddock, L., and Glanz, K. (2011). Prevalence of sunburn, sun protection, and indoor tanning behaviors among Americans: review from national surveys and case studies of 3 states. *Journal of the American Academy of Dermatology*, 65(5 Suppl 1):S114–23.
- [110] Bulliard, J. L. and Cox, B. (2000). Cutaneous malignant melanoma in New Zealand: trends by anatomical site, 1969-1993. *International journal of epidemiology*, 29(3):416–423.
- [111] Bulliard, J. L., Cox, B., and Elwood, J. M. (1994). Latitude gradients in melanoma incidence and mortality in the non-Maori population of New Zealand. *Cancer causes & control : CCC*, 5(3):234–240.
- [112] Bulman, A. (1995). People are overusing sunbeds. *BMJ (Clinical research ed.)*, 310(6990):1327.
- [113] Cadet, J., Sage, E., and Douki, T. (2005). Ultraviolet radiation-mediated damage to cellular DNA. *Mutation research*, 571(1-2):3–17.
- [114] Caini, S., Gandini, S., Sera, F., Raimondi, S., Fargnoli, M. C., Boniol, M., and Armstrong, B. K. (2009). Meta-analysis of risk factors for cutaneous melanoma according to anatomical site and clinicopathological variant. *European journal of cancer (Oxford, England : 1990)*, 45(17):3054–3063.
- [115] Cairns, R., Papandreou, I., and Denko, N. (2006). Overcoming physiologic barriers to cancer treatment by molecularly targeting the tumor microenvironment. *Molecular cancer research : MCR*, 4(2):61–70.
- [116] Camacho, L. H., Antonia, S., Sosman, J., Kirkwood, J. M., Gajewski, T. F., Redman, B., Pavlov, D., Bulanhagui, C., Bozon, V. A., Gomez-Navarro, J., and Ribas, A. (2009). Phase I/II trial of tremelimumab in patients with metastatic melanoma. *Journal of clinical oncology : official journal of the American Society of Clinical Oncology*, 27(7):1075–1081.
- [117] Carpén, O., Pallai, P., Staunton, D. E., and Springer, T. A. (1992). Association of intercellular adhesion molecule-1 (ICAM-1) with actin-containing cytoskeleton and alpha-actinin. *The Journal of cell biology*, 118(5):1223–1234.
- [118] Carvajal, R. D., Antonescu, C. R., Wolchok, J. D., Chapman, P. B., Roman, R.-A., Teitcher, J., Panageas, K. S., Busam, K. J., Chmielowski, B., Lutzky, J., Pavlick, A. C., Fusco, A., Cane, L., Takebe, N., Vemula, S., Bouvier, N., Bastian, B. C., and Schwartz, G. K. (2011). KIT as a therapeutic target in metastatic melanoma. *JAMA : the journal of the American Medical Association*, 305(22):2327–2334.

- [119] Casasnovas, J. M., Stehle, T., Liu, J. H., Wang, J. H., and Springer, T. A. (1998). A dimeric crystal structure for the N-terminal two domains of intercellular adhesion molecule-1. *Proceedings of the National Academy of Sciences of the United States of America*, 95(8):4134–4139.
- [120] Cascallo, M., Alonso, M. M., Rojas, J. J., Perez-Gimenez, A., Fueyo, J., and Alemany, R. (2007). Systemic toxicity-efficacy profile of ICOVIR-5, a potent and selective oncolytic adenovirus based on the pRB pathway. *Molecular therapy : the journal of the American Society of Gene Therapy*, 15(9):1607–1615.
- [121] Cassady, K. A. and Parker, J. N. (2010). Herpesvirus vectors for therapy of brain tumors. *The open virology journal*, 4:103–108.
- [122] Cassel, W. A. and Garrett, R. E. (1965). Newcastle Disease Virus as an Antineoplastic Agent. *Cancer*, 18:863–868.
- [123] Cassileth, P. A. and Hyman, G. A. (1967). Treatment of malignant melanoma with hydroxyurea. *Cancer Research*, 27(10):1843–1845.
- [124] Cattaneo, R., Miest, T., Shashkova, E. V., and Barry, M. A. (2008). Reprogrammed viruses as cancer therapeutics: targeted, armed and shielded. *Nature Reviews Microbiology*, 6(7):529–540.
- [125] Caughman, S. W., Li, L. J., and Degitz, K. (1992). Human intercellular adhesion molecule-1 gene and its expression in the skin. *The Journal of investigative dermatology*, 98(6 Suppl):61S–65S.
- [126] Cawood, R., Chen, H. H., Carroll, F., Bazan-Peregrino, M., van Rooijen, N., and Seymour, L. W. (2009). Use of tissue-specific microRNA to control pathology of wild-type adenovirus without attenuation of its ability to kill cancer cells. *PLoS Pathogens*, 5(5):e1000440.
- [127] Celebi, J. T., Shendrik, I., Silvers, D. N., and Peacocke, M. (2000). Identification of PTEN mutations in metastatic melanoma specimens. *Journal of medical genetics*, 37(9):653–657.
- [128] Centers for Disease Control and Prevention (CDC) (2012). Use of indoor tanning devices by adults—United States, 2010. *MMWR. Morbidity and mortality weekly report*, 61(18):323–326.
- [129] Cervoni, F., Oglesby, T. J., Fénichel, P., Dohr, G., Rossi, B., Atkinson, J. P., and Hsi, B. L. (1993). Expression of decay-accelerating factor (CD55) of the complement system on human spermatozoa. *Journal of immunology (Baltimore, Md. : 1950)*, 151(2):939–948.
- [130] Chakrabarty, R., Tran, H., Selvaggi, G., Hagerman, A., Thompson, B., and Coffey, M. (2015). The oncolytic virus, pelareorep, as a novel anticancer agent: a review. *Investigational New Drugs*.
- [131] Chalikhonda, S., Kivlen, M. H., O'Malley, M. E., Eric Dong, X. D., McCart, J. A., Gorry, M. C., Yin, X.-Y., Brown, C. K., Zeh, H. J., Guo, Z. S., and Bartlett, D. L. (2008). Oncolytic virotherapy for ovarian carcinomatosis using a replication-selective vaccinia virus armed with a yeast cytosine deaminase gene. *Cancer gene therapy*, 15(2):115–125.
- [132] Chang, A., Hunt, M., Parkinson, D. R., Hochster, H., and Smith, T. J. (1993). Phase II trial of carboplatin in patients with metastatic malignant melanoma. A report from the Eastern Cooperative Oncology Group. *American journal of clinical oncology*, 16(2):152–155.
- [133] Chang, F., Syrjänen, S., and Syrjänen, K. (1995). Implications of the p53 tumor-suppressor gene in clinical oncology. *Journal of clinical oncology : official journal of the American Society of Clinical Oncology*, 13(4):1009–1022.
- [134] Chang, Y.-m., Barrett, J. H., Bishop, D. T., Armstrong, B. K., Bataille, V., Bergman, W., Berwick, M., Bracci, P. M., Elwood, J. M., Ernstoff, M. S., Gallagher, R. P., Green, A. C., Gruijs, N. A., Holly, E. A., Ingvar, C., Kanetsky, P. A., Karagas, M. R., Lee, T. K., Le Marchand, L., MacKie, R. M., Olsson, H., Østerlind, A., Rebbeck, T. R., Sasieni, P., Siskind, V., Swerdlow, A. J., Titus-Ernstoff, L., Zens, M. S., and Newton-Bishop, J. A. (2009). Sun exposure and melanoma risk at different latitudes: a pooled analysis of 5700 cases and 7216 controls. *International journal of epidemiology*, 38(3):814–830.
- [135] Chapman, P. B., Hauschild, A., Robert, C., Haanen, J. B., Ascierto, P., Larkin, J., Dummer, R., Garbe, C., Testori, A., Maio, M., Hogg, D., Lorigan, P., Lebbe, C., Jouary, T., Schadendorf, D., Ribas, A., O'Day, S. J., Sosman, J. A., Kirkwood, J. M., Eggermont, A. M. M., Dreno, B., Nolop, K., Li, J., Nelson, B., Hou, J., Lee, R. J., Flaherty, K. T., McArthur, G. A., and BRIM-3 Study Group (2011). Improved survival with vemurafenib in melanoma with BRAF V600E mutation. *The New England journal of medicine*, 364(26):2507–2516.

- [136] Chen, L. and Flies, D. B. (2013). Molecular mechanisms of T cell co-stimulation and co-inhibition. *Nature reviews. Immunology*, 13(4):227–242.
- [137] Chen, Q., Gong, B., Mahmoud-Ahmed, A. S., Zhou, A., Hsi, E. D., Hussein, M., and Almasan, A. (2001). Apo2L/TRAIL and Bcl-2-related proteins regulate type I interferon-induced apoptosis in multiple myeloma. *Blood*, 98(7):2183–2192.
- [138] Chen, Y., Yu, D. C., Charlton, D., and Henderson, D. R. (2000). Pre-existent adenovirus antibody inhibits systemic toxicity and antitumor activity of CN706 in the nude mouse LNCaP xenograft model: implications and proposals for human therapy. *Human gene therapy*, 11(11):1553–1567.
- [139] Cheung, N. K., Walter, E. I., Smith-Mensah, W. H., Ratnoff, W. D., Tykocinski, M. L., and Medof, M. E. (1988). Decay-accelerating factor protects human tumor cells from complement-mediated cytotoxicity in vitro. *Journal of Clinical Investigation*, 81(4):1122–1128.
- [140] Chevalier, J., Bonastre, J., and Avril, M.-F. (2008). The economic burden of melanoma in France: assessing healthcare use in a hospital setting. *Melanoma research*, 18(1):40–46.
- [141] Chiocca, E. A. and Rabkin, S. D. (2014). Oncolytic viruses and their application to cancer immunotherapy. *Cancer immunology research*, 2(4):295–300.
- [142] Cho, W.-K., Seong, Y. R., Lee, Y. H., Kim, M. J., Hwang, K.-S., Yoo, J., Choi, S., Jung, C.-R., and Im, D.-S. (2004). Oncolytic effects of adenovirus mutant capable of replicating in hypoxic and normoxic regions of solid tumor. *Molecular therapy : the journal of the American Society of Gene Therapy*, 10(5):938–949.
- [143] Choi, J.-W., Lee, J.-S., Kim, S. W., and Yun, C.-O. (2012). Evolution of oncolytic adenovirus for cancer treatment. *Advanced drug delivery reviews*, 64(8):720–729.
- [144] Chou, T.-C. (2006). Theoretical basis, experimental design, and computerized simulation of synergism and antagonism in drug combination studies. *Pharmacological reviews*, 58(3):621–681.
- [145] Chou, T. C. (2010). Drug Combination Studies and Their Synergy Quantification Using the Chou-Talalay Method. *Cancer Research*, 70(2):440–446.
- [146] Chou, T.-C. and Talalay, P. (1983). Analysis of Combined Drug Effects- a New Look at a Very Old Problem. *Trends in Pharmacological Sciences*, 4:450–454.
- [147] Chou, T. C. and Talalay, P. (1984). Quantitative analysis of dose-effect relationships: the combined effects of multiple drugs or enzyme inhibitors. *Advances in enzyme regulation*, 22:27–55.
- [148] Cifuentes, J. O., Lee, H., Yoder, J. D., Shingler, K. L., Carnegie, M. S., Yoder, J. L., Ashley, R. E., Makhov, A. M., Conway, J. F., and Hafenstein, S. (2013). Structures of the procapsid and mature virion of enterovirus 71 strain 1095. *Journal of Virology*, 87(13):7637–7645.
- [149] Clingen, P. H., Arlett, C. F., Roza, L., Mori, T., Nikaido, O., and Green, M. H. (1995). Induction of cyclobutane pyrimidine dimers, pyrimidine(6-4)pyrimidone photoproducts, and Dewar valence isomers by natural sunlight in normal human mononuclear cells. *Cancer Research*, 55(11):2245–2248.
- [150] Cocks, B. G., Chang, C. C., Carballido, J. M., Yssel, H., de Vries, J. E., and Aversa, G. (1995). A novel receptor involved in T-cell activation. *Nature*, 376(6537):260–263.
- [151] Cohen, Y., Goldenberg-Cohen, N., Parrella, P., Chowers, I., Merbs, S. L., Pe'er, J., and Sidransky, D. (2003). Lack of BRAF mutation in primary uveal melanoma. *Investigative ophthalmology & visual science*, 44(7):2876–2878.
- [152] Cole, W. H. and Everson, T. C. (1956). Spontaneous regression of cancer: preliminary report. *Annals of surgery*, 144(3):366–383.
- [153] Colonno, R. J., Condra, J. H., Mizutani, S., Callahan, P. L., Davies, M. E., and Murcko, M. A. (1988). Evidence for the direct involvement of the rhinovirus canyon in receptor binding. *Proceedings of the National Academy of Sciences of the United States of America*, 85(15):5449–5453.
- [154] Connor, J. H., Naczki, C., Koumenis, C., and Lyles, D. S. (2004). Replication and cytopathic effect of oncolytic vesicular stomatitis virus in hypoxic tumor cells in vitro and in vivo. *Journal of Virology*, 78(17):8960–8970.

- [155] Coory, M., Baade, P., Aitken, J., Smithers, M., McLeod, G. R. C., and Ring, I. (2006). Trends in situ and invasive melanoma in Queensland, Australia, 1982-2002. *Cancer causes & control : CCC*, 17(1):21–27.
- [156] Cormier, J. N., Xing, Y., Ding, M., Lee, J. E., Mansfield, P. F., Gershenwald, J. E., Ross, M. I., and Du, X. L. (2006). Ethnic differences among patients with cutaneous melanoma. *Archives of internal medicine*, 166(17):1907–1914.
- [157] Couch, R. B., Cate, T. R., Gerone, P. J., Fleet, W. F., Lang, D. J., Griffith, W. R., and Knight, V. (1965). Production of Illness with a Small-Particle Aerosol of Coxsackie A21. *Journal of Clinical Investigation*, 44:535–542.
- [158] Coyne, K. E., Hall, S. E., Thompson, S., Arce, M. A., Kinoshita, T., Fujita, T., Anstee, D. J., Rosse, W., and Lublin, D. M. (1992). Mapping of epitopes, glycosylation sites, and complement regulatory domains in human decay accelerating factor. *Journal of immunology (Baltimore, Md. : 1950)*, 149(9):2906–2913.
- [159] Cripe, T. P., Racadio, J. M., Conner, J., Towbin, A., Brunner, M. M., Stockman, B. A., Currier, M., and Geller, J. I. (2013). A phase I dose-escalation study of intratumoral herpes simplex virus-1 mutant HSV1716 in pediatric/young adult patients with refractory non-central nervous system solid tumors. *ASCO Meeting Abstracts*, 31(15suppl):10047.
- [160] Cui, R., Widlund, H. R., Feige, E., Lin, J. Y., Wilensky, D. L., Igras, V. E., D’Orazio, J., Fung, C. Y., Schanbacher, C. F., Granter, S. R., and Fisher, D. E. (2007). Central role of p53 in the suntan response and pathologic hyperpigmentation. *Cell*, 128(5):853–864.
- [161] Cully, M., You, H., Levine, A. J., and Mak, T. W. (2006). Beyond PTEN mutations: the PI3K pathway as an integrator of multiple inputs during tumorigenesis. *Nature Reviews Cancer*, 6(3):184–192.
- [162] Cun, B., Song, X., Jia, R., Zhao, X., Wang, H., Ge, S., and Fan, X. (2012). Combination of oncolytic adenovirus and dacarbazine attenuates antitumor ability against uveal melanoma cells via cell cycle block. *Cancer biology & therapy*, 13(2):77–84.
- [163] Curry, S., Chow, M., and Hogle, J. M. (1996). The poliovirus 135S particle is infectious. *Journal of Virology*, 70(10):7125–7131.
- [164] Curry, S., Fry, E., Blakemore, W., Abu-Ghazaleh, R., Jackson, T., King, A., Lea, S., Newman, J., and Stuart, D. (1997). Dissecting the roles of VP0 cleavage and RNA packaging in picornavirus capsid stabilization: the structure of empty capsids of foot-and-mouth disease virus. *Journal of Virology*, 71(12):9743–9752.
- [165] Curti, B. D., Kovacovics-Bankowski, M., Morris, N., Walker, E., Chisholm, L., Floyd, K., Walker, J., Gonzalez, I., Meeuwse, T., Fox, B. A., Moudgil, T., Miller, W., Haley, D., Coffey, T., Fisher, B., Delanty-Miller, L., Rymarchyk, N., Kelly, T., Crocenzi, T., Bernstein, E., Sanborn, R., Urba, W. J., and Weinberg, A. D. (2013). OX40 is a potent immune-stimulating target in late-stage cancer patients. *Cancer Research*, 73(24):7189–7198.
- [166] Curtin, J. A., Busam, K., Pinkel, D., and Bastian, B. C. (2006). Somatic activation of KIT in distinct subtypes of melanoma. *Journal of clinical oncology : official journal of the American Society of Clinical Oncology*, 24(26):4340–4346.
- [167] Curtin, J. A., Fridlyand, J., Kageshita, T., Patel, H. N., Busam, K. J., Kutzner, H., Cho, K.-H., Aiba, S., Bröcker, E.-B., LeBoit, P. E., Pinkel, D., and Bastian, B. C. (2005). Distinct sets of genetic alterations in melanoma. *The New England journal of medicine*, 353(20):2135–2147.
- [168] Dal, H., Boldemann, C., and Lindelöf, B. (2007). Does relative melanoma distribution by body site 1960-2004 reflect changes in intermittent exposure and intentional tanning in the Swedish population? *European journal of dermatology : EJD*, 17(5):428–434.
- [169] Davies, H., Bignell, G. R., Cox, C., Stephens, P., Edkins, S., Clegg, S., Teague, J., Woffendin, H., Garnett, M. J., Bottomley, W., Davis, N., Dicks, E., Ewing, R., Floyd, Y., Gray, K., Hall, S., Hawes, R., Hughes, J., Kosmidou, V., Menzies, A., Mould, C., Parker, A., Stevens, C., Watt, S., Hooper, S., Wilson, R., Jayatilake, H., Gusterson, B. A., Cooper, C., Shipley, J., Hargrave, D., Pritchard-Jones, K., Maitland, N., Chenevix-Trench, G., Riggins, G. J., Bigner, D. D., Palmieri, G., Cossu, A., Flanagan, A., Nicholson, A., Ho, J. W. C., Leung, S. Y., Yuen, S. T., Weber, B. L., Seigler, H. F., Darrow, T. L., Paterson, H., Marais, R., Marshall, C. J., Wooster, R., Stratton, M. R., and Futreal, P. A. (2002). Mutations of the BRAF gene in human cancer. *Nature*, 417(6892):949–954.

- [170] Davis, J. J. and Fang, B. (2005). Oncolytic virotherapy for cancer treatment: challenges and solutions. *The Journal of Gene Medicine*, 7(11):1380–1389.
- [171] Davitz, M. A., Low, M. G., and Nussenzweig, V. (1986). Release of decay-accelerating factor (DAF) from the cell membrane by phosphatidylinositol-specific phospholipase C (PIPLC). Selective modification of a complement regulatory protein. *The Journal of experimental medicine*, 163(5):1150–1161.
- [172] de Snoo, F. A. and Hayward, N. K. (2005). Cutaneous melanoma susceptibility and progression genes. *Cancer Letters*, 230(2):153–186.
- [173] de Vries, E., Bray, F. I., Coebergh, J. W. W., and Parkin, D. M. (2003). Changing epidemiology of malignant cutaneous melanoma in Europe 1953-1997: rising trends in incidence and mortality but recent stabilizations in western Europe and decreases in Scandinavia. *International Journal of Cancer*, 107(1):119–126.
- [174] Deacon, K., Mistry, P., Chernoff, J., Blank, J. L., and Patel, R. (2003). p38 Mitogen-activated protein kinase mediates cell death and p21-activated kinase mediates cell survival during chemotherapeutic drug-induced mitotic arrest. *Molecular biology of the cell*, 14(5):2071–2087.
- [175] Dekel, B., Yoeli, R., Shulman, L., Padeh, S., and Passwell, J. H. (2002). Localized thigh swelling mimicking a neoplastic process: involvement of coxsackie virus type A21. *Acta paediatrica (Oslo, Norway : 1992)*, 91(3):357–359.
- [176] Dellinger, R. W., Liu-Smith, F., and Meyskens, F. L. (2014). Continuing to illuminate the mechanisms underlying UV-mediated melanomagenesis. *Journal of photochemistry and photobiology. B, Biology*, 138C:317–323.
- [177] Demierre, M.-F. and Sondak, V. K. (2005). Cutaneous melanoma: pathogenesis and rationale for chemoprevention. *Critical Reviews in Oncology/Hematology*, 53(3):225–239.
- [178] den Boon, J. A., Diaz, A., and Ahlquist, P. (2010). Cytoplasmic viral replication complexes. *Cell host & microbe*, 8(1):77–85.
- [179] Dennis, L. K. (1999). Analysis of the melanoma epidemic, both apparent and real: data from the 1973 through 1994 surveillance, epidemiology, and end results program registry. *Archives of Dermatology*, 135(3):275–280.
- [180] Dennis, L. K., Vanbeek, M. J., Beane Freeman, L. E., Smith, B. J., Dawson, D. V., and Coughlin, J. A. (2008). Sunburns and risk of cutaneous melanoma: does age matter? A comprehensive meta-analysis. *Annals of epidemiology*, 18(8):614–627.
- [181] DePace, N. G. (1912). Sulla scomparsa di un enorme cancro vegetante del collo dell’utero senz cura chirurgica. *Ginecologia*, pages 82–89.
- [182] Devary, Y., Gottlieb, R. A., Smeal, T., and Karin, M. (1992). The mammalian ultraviolet response is triggered by activation of Src tyrosine kinases. *Cell*, 71(7):1081–1091.
- [183] Devaud, C., John, L. B., Westwood, J. A., Darcy, P. K., and Kershaw, M. H. (2013). Immune modulation of the tumor microenvironment for enhancing cancer immunotherapy. *Oncoimmunology*, 2(8):e25961.
- [184] Devitt, B., Liu, W., Salemi, R., Wolfe, R., Kelly, J., Tzen, C.-Y., Dobrovic, A., and McArthur, G. (2011). Clinical outcome and pathological features associated with NRAS mutation in cutaneous melanoma. *Pigment Cell & Melanoma Research*, 24(4):666–672.
- [185] Dhiman, N., Jacobson, R. M., and Poland, G. A. (2004). Measles virus receptors: SLAM and CD46. *Reviews in medical virology*, 14(4):217–229.
- [186] Dias, J. D., Liikanen, I., Guse, K., Foloppe, J., Sloniecka, M., Diaconu, I., Rantanen, V., Eriksson, M., Hakkarainen, T., Lusky, M., Erbs, P., Escutenaire, S., Kanerva, A., Pesonen, S., Cerullo, V., and Hemminki, A. (2010). Targeted chemotherapy for head and neck cancer with a chimeric oncolytic adenovirus coding for bifunctional suicide protein FCU1. *Clinical cancer research : an official journal of the American Association for Cancer Research*, 16(9):2540–2549.
- [187] Diaz, R. M., Galivo, F., Kottke, T., Wongthida, P., Qiao, J., Thompson, J., Valdes, M., Barber, G., and Vile, R. G. (2007). Oncolytic immunovirotherapy for melanoma using vesicular stomatitis virus. *Cancer Research*, 67(6):2840–2848.

- [188] DiFronzo, L. A., Wanek, L. A., Elashoff, R., and Morton, D. L. (1999). Increased incidence of second primary melanoma in patients with a previous cutaneous melanoma. *Annals of surgical oncology*, 6(7):705–711.
- [189] Dikmen, Z. G., Gellert, G., Dogan, P., Mason, R., Antich, P., Richer, E., Wright, W. E., and Shay, J. W. (2004). A New Diagnostic System in Cancer Research Bioluminescent Imaging (BLI). *Turkish Journal of Medical Science*, 32:65–70.
- [190] Dingli, D., Peng, K.-W., Harvey, M. E., Greipp, P. R., O'Connor, M. K., Cattaneo, R., Morris, J. C., and Russell, S. J. (2004). Image-guided radiotherapy for multiple myeloma using a recombinant measles virus expressing the thyroidal sodium iodide symporter. *Blood*, 103(5):1641–1646.
- [191] Dobrikova, E. Y., Broadt, T., Poiley-Nelson, J., Yang, X., Soman, G., Giardina, S., Harris, R., and Gromeier, M. (2008). Recombinant oncolytic poliovirus eliminates glioma in vivo without genetic adaptation to a pathogenic phenotype. *Molecular therapy : the journal of the American Society of Gene Therapy*, 16(11):1865–1872.
- [192] Dock, G. (1904). Influence of complicating diseases upon leukarmia. *American Journal of Medical Science*, pages 563–592.
- [193] Dong, H., Strome, S. E., Salomao, D. R., Tamura, H., Hirano, F., Flies, D. B., Roche, P. C., Lu, J., Zhu, G., Tamada, K., Lennon, V. A., Celis, E., and Chen, L. (2002). Tumor-associated B7-H1 promotes T-cell apoptosis: a potential mechanism of immune evasion. *Nature medicine*, 8(8):793–800.
- [194] Dorer, D. E. and Nettelbeck, D. M. (2009). Targeting cancer by transcriptional control in cancer gene therapy and viral oncolysis. *Advanced drug delivery reviews*, 61(7-8):554–571.
- [195] Dörig, R. E., Marcil, A., Chopra, A., and Richardson, C. D. (1993). The human CD46 molecule is a receptor for measles virus (Edmonston strain). *Cell*, 75(2):295–305.
- [196] Dougherty, G. J., Murdoch, S., and Hogg, N. (1988). The function of human intercellular adhesion molecule-1 (ICAM-1) in the generation of an immune response. *European journal of immunology*, 18(1):35–39.
- [197] Dougherty, R. M. (1964). *Animal virus titration techniques*. Techniques in experimental virology. Academic Press, New York.
- [198] Dresler, W. and Stein, R. (1869). Ueber den hydroxylharnstoff. *Justus Liebigs Annalen der Chemie*, 150(2):242–252.
- [199] Drobetsky, E. A., Grosovsky, A. J., and Glickman, B. W. (1987). The specificity of UV-induced mutations at an endogenous locus in mammalian cells. *Proceedings of the National Academy of Sciences of the United States of America*, 84(24):9103–9107.
- [200] Dufresne, A. T. and Gromeier, M. (2004). A nonpolio enterovirus with respiratory tropism causes poliomyelitis in intercellular adhesion molecule 1 transgenic mice. *Proceedings of the National Academy of Sciences of the United States of America*, 101(37):13636–13641.
- [201] Dunki-Jacobs, E. M., Callender, G. G., and McMasters, K. M. (2013). Current management of melanoma. *Current problems in surgery*, 50(8):351–382.
- [202] Dustin, M. L., Rothlein, R., Bhan, A. K., Dinarello, C. A., and Springer, T. A. (1986). Induction by IL 1 and interferon-gamma: tissue distribution, biochemistry, and function of a natural adherence molecule (ICAM-1). *Journal of immunology (Baltimore, Md. : 1950)*, 137(1):245–254.
- [203] Edge, R. E., Falls, T. J., Brown, C. W., Lichty, B. D., Atkins, H., and Bell, J. C. (2008). A let-7 MicroRNA-sensitive vesicular stomatitis virus demonstrates tumor-specific replication. *Molecular therapy : the journal of the American Society of Gene Therapy*, 16(8):1437–1443.
- [204] Edwards, R. H., Ward, M. R., Wu, H., Medina, C. A., Brose, M. S., Volpe, P., Nussen-Lee, S., Haupt, H. M., Martin, A. M., Herlyn, M., Lessin, S. R., and Weber, B. L. (2004). Absence of BRAF mutations in UV-protected mucosal melanomas. *Journal of medical genetics*, 41(4):270–272.
- [205] Egeblad, M. and Werb, Z. (2002). New functions for the matrix metalloproteinases in cancer progression. *Nature Reviews Cancer*, 2(3):161–174.

- [206] Eggermont, A. M. M. and Kirkwood, J. M. (2004). Re-evaluating the role of dacarbazine in metastatic melanoma: what have we learned in 30 years? *European journal of cancer (Oxford, England : 1990)*, 40(12):1825–1836.
- [207] Eggermont, A. M. M., Suciú, S., Santinami, M., Testori, A., Kruit, W. H. J., Marsden, J., Punt, C. J. A., Salès, F., Gore, M., MacKie, R., Kusic, Z., Dummer, R., Hauschild, A., Musat, E., Spatz, A., Keilholz, U., and EORTC Melanoma Group (2008). Adjuvant therapy with pegylated interferon alfa-2b versus observation alone in resected stage III melanoma: final results of EORTC 18991, a randomised phase III trial. *Lancet*, 372(9633):117–126.
- [208] Eiser, J. R., Pendry, L., Greaves, C. J., Melia, J., Harland, C., and Moss, S. (2000). Is targeted early detection for melanoma feasible? Self assessments of risk and attitudes to screening. *Journal of medical screening*, 7(4):199–202.
- [209] Elwood, J. M. and Jopson, J. (1997). Melanoma and sun exposure: an overview of published studies. *International Journal of Cancer*, 73(2):198–203.
- [210] Eng, C. (2003). PTEN: one gene, many syndromes. *Human mutation*, 22(3):183–198.
- [211] Engblom, P., Rantanen, V., Kulmala, J., and Grénman, S. (1999). Carboplatin-paclitaxel- and carboplatin-docetaxel-induced cytotoxic effect in epithelial ovarian carcinoma in vitro. *Cancer*, 86(10):2066–2073.
- [212] Engeland, C. E., Grossardt, C., Veinalde, R., Bossow, S., Lutz, D., Kaufmann, J. K., Shevchenko, I., Umansky, V., Nettelbeck, D. M., Weichert, W., Jäger, D., von Kalle, C., and Ungerechts, G. (2014). CTLA-4 and PD-L1 checkpoint blockade enhances oncolytic measles virus therapy. *Molecular therapy : the journal of the American Society of Gene Therapy*, 22(11):1949–1959.
- [213] Eriksson, T. and Tinghög, G. (2014). Societal Cost of Skin Cancer in Sweden in 2011. *Acta dermato-venereologica*.
- [214] Estes, D. M., Tuo, W., Brown, W. C., and Goin, J. (1998). Effects of type I/type II interferons and transforming growth factor-beta on B-cell differentiation and proliferation. Definition of costimulation and cytokine requirements for immunoglobulin synthesis and expression. *Immunology*, 95(4):604–611.
- [215] Etchison, D., Milburn, S. C., Edery, I., Sonenberg, N., and Hershey, J. W. (1982). Inhibition of HeLa cell protein synthesis following poliovirus infection correlates with the proteolysis of a 220,000-dalton polypeptide associated with eucaryotic initiation factor 3 and a cap binding protein complex. *The Journal of biological chemistry*, 257(24):14806–14810.
- [216] Euvrard, S., Kanitakis, J., and Claudy, A. (2003). Skin cancers after organ transplantation. *The New England journal of medicine*, 348(17):1681–1691.
- [217] Fang, J., Nakamura, H., and Maeda, H. (2011). The EPR effect: Unique features of tumor blood vessels for drug delivery, factors involved, and limitations and augmentation of the effect. *Advanced drug delivery reviews*, 63(3):136–151.
- [218] Ferguson, M. S., Lemoine, N. R., and Wang, Y. (2012). Systemic delivery of oncolytic viruses: hopes and hurdles. *Advances in virology*, 2012:805629.
- [219] Ferlay, J., Steliarova-Foucher, E., Lortet-Tieulent, J., Rosso, S., Coebergh, J. W. W., Comber, H., Forman, D., and Bray, F. (2013). Cancer incidence and mortality patterns in Europe: estimates for 40 countries in 2012. *European journal of cancer (Oxford, England : 1990)*, 49(6):1374–1403.
- [220] Ferris, R. L., Gross, N. D., Nemunaitis, J. J., Andtbacka, R. H. I., Argiris, A., Ohr, J., Vetto, J. T., Senzer, N. N., Bedell, C., Ungerleider, R. S., Tanaka, M., and Nishiyama, Y. (2014). Phase I trial of intratumoral therapy using HF10, an oncolytic HSV-1, demonstrates safety in HSV+/HSV- patients with refractory and superficial cancers. *ASCO Meeting Abstracts*, 32(15suppl):6082.
- [221] Ferrone, C. R., Ben Porat, L., Panageas, K. S., Berwick, M., Halpern, A. C., Patel, A., and Coit, D. G. (2005). Clinicopathological features of and risk factors for multiple primary melanomas. *JAMA : the journal of the American Medical Association*, 294(13):1647–1654.
- [222] Feuer, R., Mena, I., Pagarigan, R., Slifka, M. K., and Whitton, J. L. (2002). Cell cycle status affects coxsackievirus replication, persistence, and reactivation in vitro. *Journal of Virology*, 76(9):4430–4440.

- [223] Feuer, R., Mena, I., Pagarigan, R. R., Hassett, D. E., and Whitton, J. L. (2004). Coxsackievirus replication and the cell cycle: a potential regulatory mechanism for viral persistence/latency. *Medical microbiology and immunology*, 193(2-3):83–90.
- [224] Fidler, I. J. and Hart, I. R. (1982). Biological diversity in metastatic neoplasms: origins and implications. *Science (New York, N.Y.)*, 217(4564):998–1003.
- [225] Fillat, C., Maliandi, M. V., Mato-Berciano, A., and Alemany, R. (2014). Combining oncolytic virotherapy and cytotoxic therapies to fight cancer. *Current pharmaceutical design*, 20(42):6513–6521.
- [226] Filman, D. J., Syed, R., Chow, M., Macadam, A. J., Minor, P. D., and Hogle, J. M. (1989). Structural factors that control conformational transitions and serotype specificity in type 3 poliovirus. *The EMBO journal*, 8(5):1567–1579.
- [227] Filman, D. J., Wien, M. W., Cunningham, J. A., Bergelson, J. M., and Hogle, J. M. (1998). Structure determination of echovirus 1. *Acta crystallographica. Section D, Biological crystallography*, 54(Pt 6 Pt 2):1261–1272.
- [228] Finkelman, F. D., Svetic, A., Gresser, I., Snapper, C., Holmes, J., Trotta, P. P., Katona, I. M., and Gause, W. C. (1991). Regulation by interferon alpha of immunoglobulin isotype selection and lymphokine production in mice. *The Journal of experimental medicine*, 174(5):1179–1188.
- [229] Firnhaber, J. M. (2012). Diagnosis and treatment of Basal cell and squamous cell carcinoma. *American family physician*, 86(2):161–168.
- [230] Fitzgerald, J. B., Schoeberl, B., Nielsen, U. B., and Sorger, P. K. (2006). Systems biology and combination therapy in the quest for clinical efficacy. *Nature chemical biology*, 2(9):458–466.
- [231] Flaherty, K. T., Puzanov, I., Kim, K. B., Ribas, A., McArthur, G. A., Sosman, J. A., O'Dwyer, P. J., Lee, R. J., Grippo, J. F., Nolop, K., and Chapman, P. B. (2010). Inhibition of mutated, activated BRAF in metastatic melanoma. *The New England journal of medicine*, 363(9):809–819.
- [232] Flaherty, K. T., Robert, C., Hersey, P., Nathan, P., Garbe, C., Milhem, M., Demidov, L. V., Hassel, J. C., Rutkowski, P., Mohr, P., Dummer, R., Trefzer, U., Larkin, J. M. G., Utikal, J., Dreno, B., Nyakas, M., Middleton, M. R., Becker, J. C., Casey, M., Sherman, L. J., Wu, F. S., Ouellet, D., Martin, A.-M., Patel, K., Schadendorf, D., and METRIC Study Group (2012). Improved survival with MEK inhibition in BRAF-mutated melanoma. *The New England journal of medicine*, 367(2):107–114.
- [233] Flanagan, J. B., Petterson, R. F., Ambros, V., Hewlett, N. J., and Baltimore, D. (1977). Covalent linkage of a protein to a defined nucleotide sequence at the 5'-terminus of virion and replicative intermediate RNAs of poliovirus. *Proceedings of the National Academy of Sciences of the United States of America*, 74(3):961–965.
- [234] Flint, S. J. (2000). *Principles of Virology: Molecular Biology, Pathogenesis, and Control*. Principles of Virology: Molecular Biology, Pathogenesis, and Control. ASM Press.
- [235] Foa, R., Norton, L., and Seidman, A. D. (1994). Taxol (paclitaxel): a novel anti-microtubule agent with remarkable anti-neoplastic activity. *International journal of clinical & laboratory research*, 24(1):6–14.
- [236] Foloppe, J., Kintz, J., Futin, N., Findeli, A., Cordier, P., Schlesinger, Y., Hoffmann, C., Tosch, C., Balloul, J.-M., and Erbs, P. (2008). Targeted delivery of a suicide gene to human colorectal tumors by a conditionally replicating vaccinia virus. *Gene Therapy*, 15(20):1361–1371.
- [237] Ford, D., Bliss, J. M., Swerdlow, A. J., Armstrong, B. K., Franceschi, S., Green, A., Holly, E. A., Mack, T., MacKie, R. M., and Osterlind, A. (1995). Risk of cutaneous melanoma associated with a family history of the disease. The International Melanoma Analysis Group (IMAGE). *International Journal of Cancer*, 62(4):377–381.
- [238] Fox, M. P., Otto, M. J., and McKinlay, M. A. (1986). Prevention of rhinovirus and poliovirus uncoating by WIN 51711, a new antiviral drug. *Antimicrobial agents and chemotherapy*, 30(1):110–116.
- [239] Franciszkiewicz, K., Boissonnas, A., Boutet, M., Combadière, C., and Mami-Chouaib, F. (2012). Role of chemokines and chemokine receptors in shaping the effector phase of the antitumor immune response. *Cancer Research*, 72(24):6325–6332.

- [240] Frankenthaler, A., Sullivan, R. J., Wang, W., Renzi, S., Seery, V., Lee, M.-Y., and Atkins, M. B. (2010). Impact of concomitant immunosuppression on the presentation and prognosis of patients with melanoma. *Melanoma research*, 20(6):496–500.
- [241] Fransen, M., Karahalios, A., Sharma, N., English, D. R., Giles, G. G., and Sinclair, R. D. (2012). Non-melanoma skin cancer in Australia. *The Medical journal of Australia*, 197(10):565–568.
- [242] Friedman, R. J., Rigel, D. S., and Kopf, A. W. (1985). Early detection of malignant melanoma: the role of physician examination and self-examination of the skin. *CA: A Cancer Journal for Clinicians*, 35(3):130–151.
- [243] Fueyo, J., Gomez-Manzano, C., Alemany, R., Lee, P. S., McDonnell, T. J., Mitlianga, P., Shi, Y. X., Levin, V. A., Yung, W. K., and Kyritsis, A. P. (2000). A mutant oncolytic adenovirus targeting the Rb pathway produces anti-glioma effect in vivo. *Oncogene*, 19(1):2–12.
- [244] Fulci, G., Breyman, L., Gianni, D., Kurozumi, K., Rhee, S. S., Yu, J., Kaur, B., Louis, D. N., Weissleder, R., Caligiuri, M. A., and Chiocca, E. A. (2006). Cyclophosphamide enhances glioma virotherapy by inhibiting innate immune responses. *Proceedings of the National Academy of Sciences of the United States of America*, 103(34):12873–12878.
- [245] Gaffen, S. L. and Liu, K. D. (2004). Overview of interleukin-2 function, production and clinical applications. *Cytokine*, 28(3):109–123.
- [246] Galanis, E., Markovic, S. N., Suman, V. J., Nuovo, G. J., Vile, R. G., Kottke, T. J., Nevala, W. K., Thompson, M. A., Lewis, J. E., Rumilla, K. M., Roulstone, V., Harrington, K., Linette, G. P., Maples, W. J., Coffey, M., Zwiebel, J., and Kendra, K. (2012). Phase II trial of intravenous administration of Reolysin(®) (Reovirus Serotype-3-dearing Strain) in patients with metastatic melanoma. *Molecular therapy : the journal of the American Society of Gene Therapy*, 20(10):1998–2003.
- [247] Gandini, S., Sera, F., Cattaruzza, M. S., Pasquini, P., Abeni, D., Boyle, P., and Melchi, C. F. (2005a). Meta-analysis of risk factors for cutaneous melanoma: I. Common and atypical naevi. *European journal of cancer (Oxford, England : 1990)*, 41(1):28–44.
- [248] Gandini, S., Sera, F., Cattaruzza, M. S., Pasquini, P., Picconi, O., Boyle, P., and Melchi, C. F. (2005b). Meta-analysis of risk factors for cutaneous melanoma: II. Sun exposure. *European journal of cancer (Oxford, England : 1990)*, 41(1):45–60.
- [249] Gandini, S., Sera, F., Cattaruzza, M. S., Pasquini, P., Zanetti, R., Masini, C., Boyle, P., and Melchi, C. F. (2005c). Meta-analysis of risk factors for cutaneous melanoma: III. Family history, actinic damage and phenotypic factors. *European journal of cancer (Oxford, England : 1990)*, 41(14):2040–2059.
- [250] Garbe, C. and Leiter, U. (2009). Melanoma epidemiology and trends. *Clinics in dermatology*, 27(1):3–9.
- [251] Garbe, C., McLeod, G. R., and Buettner, P. G. (2000). Time trends of cutaneous melanoma in Queensland, Australia and Central Europe. *Cancer*, 89(6):1269–1278.
- [252] Garibyan, L. and Fisher, D. E. (2010). How sunlight causes melanoma. *Current oncology reports*, 12(5):319–326.
- [253] Garriga, D., Pickl-Herk, A., Luque, D., Wruss, J., Castón, J. R., Blaas, D., and Verdaguer, N. (2012). Insights into minor group rhinovirus uncoating: the X-ray structure of the HRV2 empty capsid. *PLoS Pathogens*, 8(1):e1002473.
- [254] Geller, A. C., Colditz, G., Oliveria, S., Emmons, K., Jorgensen, C., Aweh, G. N., and Frazier, A. L. (2002a). Use of sunscreen, sunburning rates, and tanning bed use among more than 10 000 US children and adolescents. *Pediatrics*, 109(6):1009–1014.
- [255] Geller, A. C., Miller, D. R., Annas, G. D., Demierre, M.-F., Gilchrest, B. A., and Koh, H. K. (2002b). Melanoma incidence and mortality among US whites, 1969–1999. *JAMA : the journal of the American Medical Association*, 288(14):1719–1720.
- [256] Ghendon, Y., Yakobson, E., and Mikhejeva, A. (1972). Study of some stages of poliovirus morphogenesis in MiO cells. *Journal of Virology*, 10(2):261–266.

- [257] Giatromanolaki, A., Stathopoulos, G. P., Koukourakis, M. I., Rigatos, S., Vrettou, E., Kittas, C., Fountzilas, G., and Sivridis, E. (2001). Angiogenesis and apoptosis-related protein (p53, bcl-2, and bax) expression versus response of gastric adenocarcinomas to paclitaxel and carboplatin chemotherapy. *American journal of clinical oncology*, 24(3):222–226.
- [258] Gifford, R. and Dalldorf, G. (1951). The morbid anatomy of experimental Coxsackie virus infection. *The American journal of pathology*, 27(6):1047–1063.
- [259] Gilchrist, B. A., Eller, M. S., Geller, A. C., and Yaar, M. (1999). The pathogenesis of melanoma induced by ultraviolet radiation. *New England Journal of Medicine*, 340(17):1341–1348.
- [260] Gilman, A. G. and Goodman, L. S. (1990). *Goodman and Gilman's The Pharmacological Basis of Therapeutics*. McGraw-Hill.
- [261] Giranda, V. L., Chapman, M. S., and Rossmann, M. G. (1990). Modeling of the human intercellular adhesion molecule-1, the human rhinovirus major group receptor. *Proteins*, 7(3):227–233.
- [262] Goetz, C., Dobrikova, E., Shveygert, M., Dobrikov, M., and Gromeier, M. (2011). Oncolytic poliovirus against malignant glioma. *Future virology*, 6(9):1045–1058.
- [263] Goetz, C. and Gromeier, M. (2010). Preparing an oncolytic poliovirus recombinant for clinical application against glioblastoma multiforme. *Cytokine and Growth Factor Reviews*, 21(2-3):197–203.
- [264] Goggins, W. B. and Tsao, H. (2003). A population-based analysis of risk factors for a second primary cutaneous melanoma among melanoma survivors. *Cancer*, 97(3):639–643.
- [265] Goldsmith, K., Chen, W., Johnson, D. C., and Hendricks, R. L. (1998). Infected cell protein (ICP)47 enhances herpes simplex virus neurovirulence by blocking the CD8⁺ T cell response. *The Journal of experimental medicine*, 187(3):341–348.
- [266] Goldstein, A. M., Chan, M., Harland, M., Hayward, N. K., Demenais, F., Bishop, D. T., Azizi, E., Bergman, W., Bianchi-Scarra, G., Bruno, W., Calista, D., Albright, L. A. C., Chaudru, V., Chompret, A., Cuellar, F., Elder, D. E., Ghiorzo, P., Gillanders, E. M., Gruis, N. A., Hansson, J., Hogg, D., Holland, E. A., Kanetsky, P. A., Kefford, R. F., Landi, M. T., Lang, J., Leachman, S. A., MacKie, R. M., Magnusson, V., Mann, G. J., Bishop, J. N., Palmer, J. M., Puig, S., Puig-Butille, J. A., Stark, M., Tsao, H., Tucker, M. A., Whitaker, L., Yakobson, E., Lund Melanoma Study Group, and Melanoma Genetics Consortium (GenoMEL) (2007). Features associated with germline CDKN2A mutations: a GenoMEL study of melanoma-prone families from three continents. *Journal of medical genetics*, 44(2):99–106.
- [267] Goldstein, A. M., Struewing, J. P., Chidambaram, A., Fraser, M. C., and Tucker, M. A. (2000). Genotype-phenotype relationships in U.S. melanoma-prone families with CDKN2A and CDK4 mutations. *Journal of the National Cancer Institute*, 92(12):1006–1010.
- [268] Goldstein, A. M. and Tucker, M. A. (1995). Genetic epidemiology of familial melanoma. *Dermatologic clinics*, 13(3):605–612.
- [269] Goldstein, D. J. and Weller, S. K. (1988). Herpes simplex virus type 1-induced ribonucleotide reductase activity is dispensable for virus growth and DNA synthesis: isolation and characterization of an ICP6 lacZ insertion mutant. *Journal of Virology*, 62(1):196–205.
- [270] Gordon, R. (2013). Skin cancer: an overview of epidemiology and risk factors. *Seminars in oncology nursing*, 29(3):160–169.
- [271] Grabbe, S., Bruvers, S., Gallo, R. L., Knisely, T. L., Nazareno, R., and Granstein, R. D. (1991). Tumor antigen presentation by murine epidermal cells. *Journal of immunology (Baltimore, Md. : 1950)*, 146(10):3656–3661.
- [272] Greco, W. R., Bravo, G., and Parsons, J. C. (1995). The search for synergy: a critical review from a response surface perspective. *Pharmacological reviews*, 47(2):331–385.
- [273] Greenlee, R. T. and Howe, H. L. (2009). County-level poverty and distant stage cancer in the United States. *Cancer causes & control : CCC*, 20(6):989–1000.
- [274] Gresser, I., Belardelli, F., Maury, C., Maunoury, M. T., and Tovey, M. G. (1983). Injection of mice with antibody to interferon enhances the growth of transplantable murine tumors. *The Journal of experimental medicine*, 158(6):2095–2107.

- [275] Gresser, I. and Bourali-Maury, C. (1972). Inhibition by interferon preparations of a solid malignant tumour and pulmonary metastasis in mice. *Nature: New biology*, 236(64):78–79.
- [276] Greve, J. M., Davis, G., Meyer, A. M., Forte, C. P., Yost, S. C., Marlor, C. W., Kamarck, M. E., and McClelland, A. (1989). The major human rhinovirus receptor is ICAM-1. *Cell*, 56(5):839–847.
- [277] Grinshtein, N., Ventresca, M., Margl, R., Bernard, D., Yang, T.-C., Millar, J. B., Hummel, J., Beermann, F., Wan, Y., and Bramson, J. L. (2008). High-dose chemotherapy augments the efficacy of recombinant adenovirus vaccines and improves the therapeutic outcome. *Cancer gene therapy*, 16(4):338–350.
- [278] Grob, J. J., Bastuji-Garin, S., Vaillant, L., Roujeau, J. C., Bernard, P., Sassolas, B., and Guillaume, J. C. (1996). Excess of nevi related to immunodeficiency: a study in HIV-infected patients and renal transplant recipients. *The Journal of investigative dermatology*, 107(5):694–697.
- [279] Gromeier, M., Alexander, L., and Wimmer, E. (1996). Internal ribosomal entry site substitution eliminates neurovirulence in intergeneric poliovirus recombinants. *Proceedings of the National Academy of Sciences of the United States of America*, 93(6):2370–2375.
- [280] Gromeier, M., Bossert, B., Arita, M., Nomoto, A., and Wimmer, E. (1999). Dual stem loops within the poliovirus internal ribosomal entry site control neurovirulence. *Journal of Virology*, 73(2):958–964.
- [281] Gromeier, M., Dobrikova, E., Dobrikov, M., Brown, M., Bryant, J., Threatt, S., Boulton, S., Carter, K., Herndon, J., Desjardins, A., Friedman, H., Sampson, J., Friedman, A., and Bigner, D. (2014). Oncolytic Poliovirus Immunotherapy of Glioblastoma. *Neuro-oncology*, 16:iii41.
- [282] Gromeier, M., Lachmann, S., Rosenfeld, M. R., Gutin, P. H., and Wimmer, E. (2000). Intergenic poliovirus recombinants for the treatment of malignant glioma. *Proceedings of the National Academy of Sciences of the United States of America*, 97(12):6803–6808.
- [283] Gross, S., Knebel, A., Tenev, T., Neininger, A., Gaestel, M., Herrlich, P., and Böhmer, F. D. (1999). Inactivation of protein-tyrosine phosphatases as mechanism of UV-induced signal transduction. *The Journal of biological chemistry*, 274(37):26378–26386.
- [284] Grote, D., Russell, S. J., Cornu, T. I., Cattaneo, R., Vile, R., Poland, G. A., and Fielding, A. K. (2001). Live attenuated measles virus induces regression of human lymphoma xenografts in immunodeficient mice. *Blood*, 97(12):3746–3754.
- [285] Guidotti, L. G. and Chisari, F. V. (2001). Noncytolytic control of viral infections by the innate and adaptive immune response. *Annual review of immunology*, 19:65–91.
- [286] Guo, Z. S. and Bartlett, D. L. (2014). Oncolytic viruses as platform for multimodal cancer therapeutics: a promising land. *Cancer gene therapy*, 21(7):261–263.
- [287] Guo, Z. S., Liu, Z., and Bartlett, D. L. (2014). Oncolytic Immunotherapy: Dying the Right Way is a Key to Eliciting Potent Antitumor Immunity. *Frontiers in oncology*, 4:74.
- [288] Gupta-Saraf, P. and Miller, C. L. (2014). HIF-1 α downregulation and apoptosis in hypoxic prostate tumor cells infected with oncolytic mammalian orthoreovirus. *Oncotarget*, 5(2):561–574.
- [289] Gutermann, A., Mayer, E., von Dehn-Rothfelser, K., Breidenstein, C., Weber, M., Muench, M., Gungor, D., Suehnel, J., Moebius, U., and Lechmann, M. (2006). Efficacy of oncolytic herpesvirus NV1020 can be enhanced by combination with chemotherapeutics in colon carcinoma cells. *Human gene therapy*, 17(12):1241–1253.
- [290] Haigh, P. I., DiFronzo, L. A., and McCready, D. R. (2003). Optimal excision margins for primary cutaneous melanoma: a systematic review and meta-analysis. *Canadian journal of surgery. Journal canadien de chirurgie*, 46(6):419–426.
- [291] Haley, E. S., Au, G. G., Carlton, B. R., Barry, R. D., and Shafren, D. R. (2009). Regional administration of oncolytic Echovirus 1 as a novel therapy for the peritoneal dissemination of gastric cancer. *Journal of Molecular Medicine*, 87(4):385–399.
- [292] Hallenbeck, P. L., Chang, Y. N., Hay, C., Golightly, D., Stewart, D., Lin, J., Phipps, S., and Chiang, Y. L. (1999). A novel tumor-specific replication-restricted adenoviral vector for gene therapy of hepatocellular carcinoma. *Human gene therapy*, 10(10):1721–1733.

- [293] Halpern, M. T., Ward, E. M., Pavluck, A. L., Schrag, N. M., Bian, J., and Chen, A. Y. (2008). Association of insurance status and ethnicity with cancer stage at diagnosis for 12 cancer sites: a retrospective analysis. *The lancet oncology*, 9(3):222–231.
- [294] Hamada, K., Kohno, S., Iwamoto, M., Yokota, H., Okada, M., Tagawa, M., Hirose, S., Yamasaki, K., Shirakata, Y., Hashimoto, K., and Ito, M. (2003). Identification of the human IAI.3B promoter element and its use in the construction of a replication-selective adenovirus for ovarian cancer therapy. *Cancer Research*, 63(10):2506–2512.
- [295] Hamid, O., Robert, C., Daud, A., Hodi, F. S., Hwu, W.-J., Kefford, R., Wolchok, J. D., Hersey, P., Joseph, R. W., Weber, J. S., Dronca, R., Gangadhar, T. C., Patnaik, A., Zarour, H., Joshua, A. M., Gergich, K., Ellassaiss-Schaap, J., Algazi, A., Mateus, C., Boasberg, P., Tume, P. C., Chmielowski, B., Ebbinghaus, S. W., Li, X. N., Kang, S. P., and Ribas, A. (2013). Safety and tumor responses with lambrolizumab (anti-PD-1) in melanoma. *The New England journal of medicine*, 369(2):134–144.
- [296] Hamid, O., Robert, C., Ribas, A., Wolchok, J. D., Hodi, F. S., Kefford, R., Joshua, A. M., Hwu, W.-J., Gangadhar, T. C., Patnaik, A., Hersey, P., Weber, J. S., Joseph, R. W., Gergich, K., Li, X. N., Chun, P., Ebbinghaus, S., Kang, S. P., and Daud, A. (2014). Randomized comparison of two doses of the anti-PD-1 monoclonal antibody MK-3475 for ipilimumab-refractory (IPI-R) and IPI-naive (IPI-N) melanoma (MEL). *ASCO Meeting Abstracts*, 32(15suppl):3000.
- [297] Hamid, O., Schmidt, H., Nissan, A., Ridolfi, L., Aamdal, S., Hansson, J., Guida, M., Hyams, D. M., Gómez, H., Bastholt, L., Chasalow, S. D., and Berman, D. (2011). A prospective phase II trial exploring the association between tumor microenvironment biomarkers and clinical activity of ipilimumab in advanced melanoma. *Journal of Translational Medicine*, 9:204.
- [298] Hammill, A. M., Conner, J., and Cripe, T. P. (2010). Oncolytic virotherapy reaches adolescence. *Pediatric blood & cancer*, 55(7):1253–1263.
- [299] Hanahan, D. and Weinberg, R. A. (2000). The hallmarks of cancer. *Cell*, 100(1):57–70.
- [300] Handolias, D., Salemi, R., Murray, W., Tan, A., Liu, W., Viros, A., Dobrovic, A., Kelly, J., and McArthur, G. A. (2010). Mutations in KIT occur at low frequency in melanomas arising from anatomical sites associated with chronic and intermittent sun exposure. *Pigment Cell & Melanoma Research*, 23(2):210–215.
- [301] Hansen, R. M. and Libnoch, J. A. (1978). Remission of chronic lymphocytic leukemia after smallpox vaccination. *Archives of internal medicine*, 138(7):1137–1138.
- [302] Harlin, H., Meng, Y., Peterson, A. C., Zha, Y., Tretiakova, M., Slingsluff, C., McKee, M., and Gajewski, T. F. (2009). Chemokine expression in melanoma metastases associated with CD8+ T-cell recruitment. *Cancer Research*, 69(7):3077–3085.
- [303] Harrington, K. J., Hingorani, M., Tanay, M. A., Hickey, J., Bhide, S. A., Clarke, P. M., Renouf, L. C., Thway, K., Sibtain, A., McNeish, I. A., Newbold, K. L., Goldsweig, H., Coffin, R., and Nutting, C. M. (2010). Phase I/II study of oncolytic HSV GM-CSF in combination with radiotherapy and cisplatin in untreated stage III/IV squamous cell cancer of the head and neck. *Clinical cancer research : an official journal of the American Association for Cancer Research*, 16(15):4005–4015.
- [304] Harris, N. L. and Ronchese, F. (1999). The role of B7 costimulation in T-cell immunity. *Immunology and cell biology*, 77(4):304–311.
- [305] Harrow, S., Papanastassiou, V., Harland, J., Mabbs, R., Petty, R., Fraser, M., Hadley, D., Patterson, J., Brown, S. M., and Rampling, R. (2004). HSV1716 injection into the brain adjacent to tumour following surgical resection of high-grade glioma: safety data and long-term survival. *Gene Therapy*, 11(22):1648–1658.
- [306] Hasegawa, K., Pham, L., O’Connor, M. K., Federspiel, M. J., Russell, S. J., and Peng, K.-W. (2006). Dual therapy of ovarian cancer using measles viruses expressing carcinoembryonic antigen and sodium iodide symporter. *Clinical cancer research : an official journal of the American Association for Cancer Research*, 12(6):1868–1875.
- [307] Hauschild, A., Grob, J.-J., Demidov, L. V., Jouary, T., Gutzmer, R., Millward, M., Rutkowski, P., Blank, C. U., Miller, W. H., Kaempgen, E., Martín-Algarra, S., Karaszewska, B., Mauch, C., Chiarion-Sileni, V., Martin, A.-M., Swann, S., Haney, P., Mirakhur, B., Guckert, M. E., Goodman, V., and Chapman, P. B. (2012). Dabrafenib in BRAF-mutated metastatic melanoma: a multicentre, open-label, phase 3 randomised controlled trial. *Lancet*, 380(9839):358–365.

- [308] Hauschild, A., Grob, J.-J., Demidov, L. V., Jouary, T., Gutzmer, R., Millward, M., Rutkowski, P., Blank, C. U., Miller, W. H., Kaempgen, E., Martín-Algarra, S., Karaszewska, B., Mauch, C., Chiarion-Sileni, V., Mirakhur, B., Guckert, M. E., Swann, R. S., Haney, P., Goodman, V. L., and Chapman, P. B. (2013). An update on BREAK-3, a phase III, randomized trial: Dabrafenib (DAB) versus dacarbazine (DTIC) in patients with BRAF V600E-positive mutation metastatic melanoma (MM). *ASCO Meeting Abstracts*, 31(15suppl):9013.
- [309] Hauschild, A., Rosien, F., and Lischner, S. (2003). Surgical standards in the primary care of melanoma patients. *Onkologie*, 26(3):218–222.
- [310] Hawkes, J. E., Campbell, J., Garvin, D., Cannon-Albright, L., Cassidy, P., and Leachman, S. A. (2013). Lack of GNAQ and GNA11 Germ-Line Mutations in Familial Melanoma Pedigrees with Uveal Melanoma or Blue Nevi. *Frontiers in oncology*, 3:160.
- [311] Hayward, N. K. (2003). Genetics of melanoma predisposition. *Oncogene*, 22(20):3053–3062.
- [312] He, Y., Lin, F., Chipman, P. R., Bator, C. M., Baker, T. S., Shoham, M., Kuhn, R. J., Medof, M. E., and Rossmann, M. G. (2002). Structure of decay-accelerating factor bound to echovirus 7: a virus-receptor complex. *Proceedings of the National Academy of Sciences of the United States of America*, 99(16):10325–10329.
- [313] Heise, C., Sampson-Johannes, A., Williams, A., McCormick, F., Von Hoff, D. D., and Kirn, D. H. (1997). ONYX-015, an E1B gene-attenuated adenovirus, causes tumor-specific cytolysis and antitumoral efficacy that can be augmented by standard chemotherapeutic agents. *Nature medicine*, 3(6):639–645.
- [314] Heise, C. C., Williams, A., Olesch, J., and Kirn, D. H. (1999). Efficacy of a replication-competent adenovirus (ONYX-015) following intratumoral injection: intratumoral spread and distribution effects. *Cancer gene therapy*, 6(6):499–504.
- [315] Hemminki, K., Zhang, H., and Czene, K. (2003). Familial and attributable risks in cutaneous melanoma: effects of proband and age. *The Journal of investigative dermatology*, 120(2):217–223.
- [316] Heo, J., Reid, T., Ruo, L., Breitbach, C. J., Rose, S., Bloomston, M., Cho, M., Lim, H. Y., Chung, H. C., Kim, C. W., Burke, J., Lencioni, R., Hickman, T., Moon, A., Lee, Y.-S., Kim, M. K., Daneshmand, M., Dubois, K., Longpre, L., Ngo, M., Rooney, C., Bell, J. C., Rhee, B. G., Patt, R., Hwang, T.-H., and Kirn, D. H. (2013). Randomized dose-finding clinical trial of oncolytic immunotherapeutic vaccinia JX-594 in liver cancer. *Nature medicine*, 19(3):329–336.
- [317] Herbst, R. S., Takeuchi, H., and Teicher, B. A. (1998). Paclitaxel/carboplatin administration along with antiangiogenic therapy in non-small-cell lung and breast carcinoma models. *Cancer chemotherapy and pharmacology*, 41(6):497–504.
- [318] Hernandez-Alcoceba, R., Pihalja, M., Qian, D., and Clarke, M. F. (2002). New oncolytic adenoviruses with hypoxia- and estrogen receptor-regulated replication. *Human gene therapy*, 13(14):1737–1750.
- [319] Hernandez-Alcoceba, R., Pihalja, M., Wicha, M. S., and Clarke, M. F. (2000). A novel, conditionally replicative adenovirus for the treatment of breast cancer that allows controlled replication of E1a-deleted adenoviral vectors. *Human gene therapy*, 11(14):2009–2024.
- [320] Hikichi, M., Kidokoro, M., Haraguchi, T., Iba, H., Shida, H., Tahara, H., and Nakamura, T. (2011). MicroRNA regulation of glycoprotein B5R in oncolytic vaccinia virus reduces viral pathogenicity without impairing its antitumor efficacy. *Molecular therapy : the journal of the American Society of Gene Therapy*, 19(6):1107–1115.
- [321] Hodi, F. S., O’Day, S. J., McDermott, D. F., Weber, R. W., Sosman, J. A., Haanen, J. B., Gonzalez, R., Robert, C., Schadendorf, D., Hassel, J. C., Akerley, W., van den Eertwegh, A. J. M., Lutzky, J., Lorigan, P., Vaubel, J. M., Linette, G. P., Hogg, D., Ottensmeier, C. H., Lebbe, C., Peschel, C., Quirt, I., Clark, J. I., Wolchok, J. D., Weber, J. S., Tian, J., Yellin, M. J., Nichol, G. M., Hoos, A., and Urba, W. J. (2010). Improved survival with ipilimumab in patients with metastatic melanoma. *The New England journal of medicine*, 363(8):711–723.
- [322] Hodi, F. S., Soiffer, R. J., Clark, J., Finkelstein, D. M., and Haluska, F. G. (2002). Phase II study of paclitaxel and carboplatin for malignant melanoma. *American journal of clinical oncology*, 25(3):283–286.

- [323] Hodis, E., Watson, I. R., Kryukov, G. V., Arold, S. T., Imielinski, M., Theurillat, J.-P., Nickerson, E., Auclair, D., Li, L., Place, C., Dicara, D., Ramos, A. H., Lawrence, M. S., Cibulskis, K., Sivachenko, A., Voet, D., Saksena, G., Stransky, N., Onofrio, R. C., Winckler, W., Ardlie, K., Wagle, N., Wargo, J., Chong, K., Morton, D. L., Stenke-Hale, K., Chen, G., Noble, M., Meyerson, M., Ladbury, J. E., Davies, M. A., Gershenwald, J. E., Wagner, S. N., Hoon, D. S. B., Schadendorf, D., Lander, E. S., Gabriel, S. B., Getz, G., Garraway, L. A., and Chin, L. (2012). A landscape of driver mutations in melanoma. *Cell*, 150(2):251–263.
- [324] Hoeijmakers, J. H. (2001). Genome maintenance mechanisms for preventing cancer. *Nature*, 411(6835):366–374.
- [325] Hoffman, R. M. (1999). Orthotopic metastatic mouse models for anticancer drug discovery and evaluation: a bridge to the clinic. *Investigational New Drugs*, 17(4):343–359.
- [326] Hogle, J. M., Chow, M., and Filman, D. J. (1985). Three-dimensional structure of poliovirus at 2.9 Å resolution. *Science (New York, N.Y.)*, 229(4720):1358–1365.
- [327] Holland, J. J. and Kiehn, E. D. (1968). Specific cleavage of viral proteins as steps in the synthesis and maturation of enteroviruses. *Proceedings of the National Academy of Sciences of the United States of America*, 60(3):1015–1022.
- [328] Hollenbeak, C. S., Todd, M. M., Billingsley, E. M., Harper, G., Dyer, A.-M., and Lengerich, E. J. (2005). Increased incidence of melanoma in renal transplantation recipients. *Cancer*, 104(9):1962–1967.
- [329] Hong, C.-S., Fellows, W., Niranjana, A., Alber, S., Watkins, S., Cohen, J. B., Glorioso, J. C., and Grandi, P. (2010). Ectopic matrix metalloproteinase-9 expression in human brain tumor cells enhances oncolytic HSV vector infection. *Gene Therapy*, 17(10):1200–1205.
- [330] Horton, J., Hotchin, J. E., Olson, K. B., and Davies, J. N. (1971). The effects of MP virus infection in lymphoma. *Cancer Research*, 31(8):1066–1068.
- [331] Hoster, H. A., Zanes, R. P., and von Haam, E. (1949). Studies in Hodgkin’s syndrome; the association of viral hepatitis and Hodgkin’s disease; a preliminary report. *Cancer Research*, 9(8):473–480.
- [332] Howlander, N., Noone, A. M., Krapcho, M., Garshell, J., Miller, D., Altekruse, S. F., Kosary, C. L., Yu, M., Ruhl, J., Tatalovich, Z., Mariotto, A., Lewis, D. R., Chen, H. S., Feuer, E. J., and Cronin, K. A. (2014). SEER Cancer Statistics Review, 1975–2011. Technical Report based on November 2013 SEER data submission.
- [333] Hsu, E. C., Iorio, C., Sarangi, F., Khine, A. A., and Richardson, C. D. (2001). CDw150(SLAM) is a receptor for a lymphotropic strain of measles virus and may account for the immunosuppressive properties of this virus. *Virology*, 279(1):9–21.
- [334] Hu, J. C. C., Coffin, R. S., Davis, C. J., Graham, N. J., Groves, N., Guest, P. J., Harrington, K. J., James, N. D., Love, C. A., McNeish, I., Medley, L. C., Michael, A., Nutting, C. M., Pandha, H. S., Shorrock, C. A., Simpson, J., Steiner, J., Steven, N. M., Wright, D., and Coombes, R. C. (2006). A Phase I Study of OncoVEXGM-CSF, a Second-Generation Oncolytic Herpes Simplex Virus Expressing Granulocyte Macrophage Colony-Stimulating Factor. *Clinical Cancer Research*, 12(22):6737–6747.
- [335] Huang, B., Sikorski, R., Kirn, D. H., and Thorne, S. H. (2011). Synergistic anti-tumor effects between oncolytic vaccinia virus and paclitaxel are mediated by the IFN response and HMGB1. *Gene Therapy*, 18(2):164–172.
- [336] Huang, T.-G., Savontaus, M. J., Shinozaki, K., Sauter, B. V., and Woo, S. L. C. (2003). Telomerase-dependent oncolytic adenovirus for cancer treatment. *Gene Therapy*, 10(15):1241–1247.
- [337] Huber, B. E., Austin, E. A., Richards, C. A., Davis, S. T., and Good, S. S. (1994). Metabolism of 5-fluorocytosine to 5-fluorouracil in human colorectal tumor cells transduced with the cytosine deaminase gene: significant antitumor effects when only a small percentage of tumor cells express cytosine deaminase. *Proceedings of the National Academy of Sciences of the United States of America*, 91(17):8302–8306.
- [338] Huebner, R. J., Rowe, W. P., Schatten, W. E., Smith, R. R., and Thomas, L. B. (1956). Studies on the use of viruses in the treatment of carcinoma of the cervix. *Cancer*, 9(6):1211–1218.
- [339] Hunter-Craig, I., Newton, K. A., Westbury, G., and Lacey, B. W. (1970). Use of vaccinia virus in the treatment of metastatic malignant melanoma. *British medical journal*, 2(5708):512–515.

- [340] Hwang, T.-H., Moon, A., Burke, J., Ribas, A., Stephenson, J., Breitbart, C. J., Daneshmand, M., De Silva, N., Parato, K., Diallo, J.-S., Lee, Y.-S., Liu, T.-C., Bell, J. C., and Kirn, D. H. (2011). A mechanistic proof-of-concept clinical trial with JX-594, a targeted multi-mechanistic oncolytic poxvirus, in patients with metastatic melanoma. *Molecular therapy : the journal of the American Society of Gene Therapy*, 19(10):1913–1922.
- [341] Hyypia, T., Kallajoki, M., Maaronen, M., Stanway, G., Kandolf, R., Auvinen, P., and Kalimo, H. (1993). Pathogenetic differences between coxsackie A and B virus infections in newborn mice. *Virus Research*, 27:71–78.
- [342] Ibrahim, N. and Haluska, F. G. (2009). Molecular pathogenesis of cutaneous melanocytic neoplasms. *Annual review of pathology*, 4:551–579.
- [343] Ikeda, K., Ichikawa, T., Wakimoto, H., Silver, J. S., Deisboeck, T. S., Finkelstein, D., Harsh, G. R., Louis, D. N., Bartus, R. T., Hochberg, F. H., and Chiocca, E. A. (1999). Oncolytic virus therapy of multiple tumors in the brain requires suppression of innate and elicited antiviral responses. *Nature medicine*, 5(8):881–887.
- [344] Ikeda, K., Wakimoto, H., Ichikawa, T., Jung, S., Hochberg, F. H., Louis, D. N., and Chiocca, E. A. (2000). Complement depletion facilitates the infection of multiple brain tumors by an intravascular, replication-conditional herpes simplex virus mutant. *Journal of Virology*, 74(10):4765–4775.
- [345] Imko-Walczuk, B., Turner, R., and Wojnarowska, F. (2009). Malignant melanoma. *Cancer treatment and research*, 146:311–322.
- [346] Ingemarsdotter, C. K., Baird, S. K., Connell, C. M., Oberg, D., Halldén, G., and McNeish, I. A. (2010). Low-dose paclitaxel synergizes with oncolytic adenoviruses via mitotic slippage and apoptosis in ovarian cancer. *Oncogene*, 29(45):6051–6063.
- [347] Inoue, H. and Tani, K. (2014). Multimodal immunogenic cancer cell death as a consequence of anticancer cytotoxic treatments. *Cell death and differentiation*, 21(1):39–49.
- [348] International Agency for Research on Cancer Working Group on artificial ultraviolet (UV) light and skin cancer (2007). The association of use of sunbeds with cutaneous malignant melanoma and other skin cancers: A systematic review. *International Journal of Cancer*, 120(5):1116–1122.
- [349] Iwai, Y., Ishida, M., Tanaka, Y., Okazaki, T., Honjo, T., and Minato, N. (2002). Involvement of PD-L1 on tumor cells in the escape from host immune system and tumor immunotherapy by PD-L1 blockade. *Proceedings of the National Academy of Sciences of the United States of America*, 99(19):12293–12297.
- [350] Iwai, Y., Terawaki, S., Ikegawa, M., Okazaki, T., and Honjo, T. (2003). PD-1 inhibits antiviral immunity at the effector phase in the liver. *The Journal of experimental medicine*, 198(1):39–50.
- [351] J, F., I, S., M, E., r, D., S, E., C, M., M, R., DM, P., D, F., and F, B. (2013). GLOBOCAN 2012: Estimated Cancer Incidence, Mortality and Prevalence Worldwide in 2012. *IARC*.
- [352] J, O. and Rustgi, A. K. (2001). Paclitaxel induces prolonged activation of the Ras/MEK/ERK pathway independently of activating the programmed cell death machinery. *The Journal of biological chemistry*, 276(22):19555–19564.
- [353] Jacobson, M. F. and Baltimore, D. (1968). Polypeptide cleavages in the formation of poliovirus proteins. *Proceedings of the National Academy of Sciences of the United States of America*, 61(1):77–84.
- [354] Jakob, J. A., Bassett, R. L., Ng, C. S., Curry, J. L., Joseph, R. W., Alvarado, G. C., Rohlf, M. L., Richard, J., Gershenwald, J. E., Kim, K. B., Lazar, A. J., Hwu, P., and Davies, M. A. (2012). NRAS mutation status is an independent prognostic factor in metastatic melanoma. *Cancer*, 118(16):4014–4023.
- [355] Janeway, C. (2001). *Immunobiology Five*. Garland Publishing, 5 edition.
- [356] Jang, S. K., Kräusslich, H. G., Nicklin, M. J., Duke, G. M., Palmenberg, A. C., and Wimmer, E. (1988). A segment of the 5' nontranslated region of encephalomyocarditis virus RNA directs internal entry of ribosomes during in vitro translation. *Journal of Virology*, 62(8):2636–2643.
- [357] Jemal, A., Devesa, S. S., Hartge, P., and Tucker, M. A. (2001). Recent trends in cutaneous melanoma incidence among whites in the United States. *Journal of the National Cancer Institute*, 93(9):678–683.

- [358] Jhappan, C., Noonan, F. P., and Merlino, G. (2003). Ultraviolet radiation and cutaneous malignant melanoma. *Oncogene*, 22(20):3099–3112.
- [359] Ji, R.-R., Chasalow, S. D., Wang, L., Hamid, O., Schmidt, H., Cogswell, J., Alaparthi, S., Berman, D., Jure-Kunkel, M., Siemers, N. O., Jackson, J. R., and Shahabi, V. (2012). An immune-active tumor microenvironment favors clinical response to ipilimumab. *Cancer Immunology, Immunotherapy*, 61(7):1019–1031.
- [360] Jia, X. Y., Van Eden, M., Busch, M. G., Ehrenfeld, E., and Summers, D. F. (1998). trans-encapsidation of a poliovirus replicon by different picornavirus capsid proteins. *Journal of Virology*, 72(10):7972–7977.
- [361] Jiang, G., Liu, Y.-Q., Wei, Z.-P., Pei, D.-S., Mao, L.-J., and Zheng, J.-N. (2010). Enhanced anti-tumor activity by the combination of a conditionally replicating adenovirus mediated interleukin-24 and dacarbazine against melanoma cells via induction of apoptosis. *Cancer Letters*, 294(2):220–228.
- [362] Jiang, H., Gomez-Manzano, C., Alemany, R., Medrano, D., Alonso, M., Bekele, B. N., Lin, E., Conrad, C. C., Yung, W. K. A., and Fueyo, J. (2005). Comparative effect of oncolytic adenoviruses with E1A-55 kDa or E1B-55 kDa deletions in malignant gliomas. *Neoplasia (New York, N.Y.)*, 7(1):48–56.
- [363] Johansen, L. K. and Morrow, C. D. (2000). The RNA encompassing the internal ribosome entry site in the poliovirus 5' nontranslated region enhances the encapsidation of genomic RNA. *Virology*, 273(2):391–399.
- [364] Johansson, E. S., Xing, L., Cheng, R. H., and Shafren, D. R. (2004). Enhanced cellular receptor usage by a bioselected variant of coxsackievirus a21. *Journal of Virology*, 78(22):12603–12612.
- [365] Johnson, D. H. and Einhorn, L. H. (1995). Paclitaxel plus carboplatin: an effective combination chemotherapy for advanced non-small-cell lung cancer or just another Elvis sighting? *Journal of clinical oncology : official journal of the American Society of Clinical Oncology*, 13(8):1840–1842.
- [366] Johnson, J. P., Stade, B. G., Holzmann, B., Schwäble, W., and Riethmüller, G. (1989). De novo expression of intercellular-adhesion molecule 1 in melanoma correlates with increased risk of metastasis. *Proceedings of the National Academy of Sciences of the United States of America*, 86(2):641–644.
- [367] Johnson, K. M., Bloom, H. H., Mufson, M. A., and Chanockrm (1962). Acute respiratory disease associated with Coxsackie A-21 virus infection. I. Incidence in military personnel: observations in a recruit population. *JAMA : the journal of the American Medical Association*, 179:112–119.
- [368] Johnson, T. M. and Sondak, V. K. (2004). Melanoma margins: the importance and need for more evidence-based trials. *Archives of Dermatology*, 140(9):1148–1150.
- [369] Johnson, V. H. and Semler, B. L. (1988). Defined recombinants of poliovirus and coxsackievirus: sequence-specific deletions and functional substitutions in the 5'-noncoding regions of viral RNAs. *Virology*, 162(1):47–57.
- [370] Jonasch, E. and Haluska, F. G. (2001). Interferon in oncological practice: review of interferon biology, clinical applications, and toxicities. *The oncologist*, 6(1):34–55.
- [371] Jordan, M. A. and Wilson, L. (2004). Microtubules as a target for anticancer drugs. *Nature Reviews Cancer*, 4(4):253–265.
- [372] José, A., Rovira-Rigau, M., Luna, J., Giménez-Alejandre, M., Vaquero, E., García de la Torre, B., Andreu, D., Alemany, R., and Fillat, C. (2014). A genetic fiber modification to achieve matrix-metalloprotease-activated infectivity of oncolytic adenovirus. *Journal of controlled release : official journal of the Controlled Release Society*, 192:148–156.
- [373] Kalechman, Y., Longo, D. L., Catane, R., Shani, A., Albeck, M., and Sredni, B. (2000). Synergistic anti-tumoral effect of paclitaxel (Taxol)+AS101 in a murine model of B16 melanoma: association with ras-dependent signal-transduction pathways. *International Journal of Cancer*, 86(2):281–288.
- [374] Kambara, H., Okano, H., Chiocca, E. A., and Saeki, Y. (2005). An oncolytic HSV-1 mutant expressing ICP34.5 under control of a nestin promoter increases survival of animals even when symptomatic from a brain tumor. *Cancer Research*, 65(7):2832–2839.
- [375] Kamizono, J., Nagano, S., Murofushi, Y., Komiya, S., Fujiwara, H., Matsuishi, T., and Kosai, K.-i. (2005). Survivin-responsive conditionally replicating adenovirus exhibits cancer-specific and efficient viral replication. *Cancer Research*, 65(12):5284–5291.

- [376] Kanai, R., Tomita, H., Hirose, Y., Ohba, S., Goldman, S., Okano, H., Kawase, T., and Yazaki, T. (2007). Augmented therapeutic efficacy of an oncolytic herpes simplex virus type 1 mutant expressing ICP34.5 under the transcriptional control of musashi1 promoter in the treatment of malignant glioma. *Human gene therapy*, 18(1):63–73.
- [377] Kanai, R., Tomita, H., Shinoda, A., Takahashi, M., Goldman, S., Okano, H., Kawase, T., and Yazaki, T. (2006). Enhanced therapeutic efficacy of G207 for the treatment of glioma through Musashi1 promoter retargeting of gamma34.5-mediated virulence. *Gene Therapy*, 13(2):106–116.
- [378] Kanai, R., Zaupa, C., Sgubin, D., Antoszczyk, S. J., Martuza, R. L., Wakimoto, H., and Rabkin, S. D. (2012). Effect of γ 34.5 deletions on oncolytic herpes simplex virus activity in brain tumors. *Journal of Virology*, 86(8):4420–4431.
- [379] Kanavy, H. E. and Gerstenblith, M. R. (2011). Ultraviolet radiation and melanoma. *Seminars in cutaneous medicine and surgery*, 30(4):222–228.
- [380] Kao, C. C., Yew, P. R., and Berk, A. J. (1990). Domains required for in vitro association between the cellular p53 and the adenovirus 2 E1B 55K proteins. *Virology*, 179(2):806–814.
- [381] Karnachow, T. M., Dawe, S., Lublin, D. M., and Dimock, K. (1998). Short consensus repeat domain 1 of decay-accelerating factor is required for enterovirus 70 binding. *Journal of Virology*, 72(11):9380–9383.
- [382] Kato, A., Liu, Z., Minowa, A., Imai, T., Tanaka, M., Sugimoto, K., Nishiyama, Y., Arai, J., and Kawaguchi, Y. (2011). Herpes simplex virus 1 protein kinase Us3 and major tegument protein UL47 reciprocally regulate their subcellular localization in infected cells. *Journal of Virology*, 85(18):9599–9613.
- [383] Kaufman, H. L., Andtbacka, R. H. I., Collichio, F. A., Amatruda, T., Senzer, N. N., Chesney, J., Delman, K. A., Spitzer, L. E., Puzanov, I., Ye, Y., Li, A., Gansert, J. L., Coffin, R., and Ross, M. I. (2014). Primary overall survival (OS) from OPTiM, a randomized phase III trial of talimogene laherparepvec (T-VEC) versus subcutaneous (SC) granulocyte-macrophage colony-stimulating factor (GM-CSF) for the treatment (tx) of unresected stage IIIB/C and IV melanoma. *Journal of Clinical Oncology, 2014 ASCO Annual Meeting Abstracts*, 32(15suppl):9008a.
- [384] Kaufman, H. L., Kim, D. W., DeRaffele, G., Mitcham, J., Coffin, R. S., and Kim-Schulze, S. (2010). Local and distant immunity induced by intralesional vaccination with an oncolytic herpes virus encoding GM-CSF in patients with stage IIIC and IV melanoma. *Annals of surgical oncology*, 17(3):718–730.
- [385] Kaur, B., Chiocca, E. A., and Cripe, T. P. (2012). Oncolytic HSV-1 virotherapy: clinical experience and opportunities for progress. *Current pharmaceutical biotechnology*, 13(9):1842–1851.
- [386] Kaur, B., Cripe, T. P., and Chiocca, E. A. (2009). "Buy one get one free": armed viruses for the treatment of cancer cells and their microenvironment. *Current gene therapy*, 9(5):341–355.
- [387] Kefford, R. F. (2003). Adjuvant therapy of cutaneous melanoma: the interferon debate. *Annals of oncology : official journal of the European Society for Medical Oncology / ESMO*, 14(3):358–365.
- [388] Keith, C. T., Borisy, A. A., and Stockwell, B. R. (2005). Multicomponent therapeutics for networked systems. *Nature reviews. Drug discovery*, 4(1):71–78.
- [389] Kelly, E. and Russell, S. J. (2007). History of oncolytic viruses: genesis to genetic engineering. *Molecular therapy : the journal of the American Society of Gene Therapy*, 15(4):651–659.
- [390] Kelly, E. J., Hadac, E. M., Greiner, S., and Russell, S. J. (2008). Engineering microRNA responsiveness to decrease virus pathogenicity. *Nature medicine*, 14(11):1278–1283.
- [391] Kelly, E. J., Nace, R., Barber, G. N., and Russell, S. J. (2010). Attenuation of vesicular stomatitis virus encephalitis through microRNA targeting. *Journal of Virology*, 84(3):1550–1562.
- [392] Khuri, F. R., Nemunaitis, J., Ganly, I., Arseneau, J., Tannock, I. F., Romel, L., Gore, M., Ironside, J., MacDougall, R. H., Heise, C., Randlev, B., Gillenwater, A. M., Bruso, P., Kaye, S. B., Hong, W. K., and Kirn, D. H. (2000). A controlled trial of intratumoral ONYX-015, a selectively-replicating adenovirus, in combination with cisplatin and 5-fluorouracil in patients with recurrent head and neck cancer. *Nature medicine*, 6(8):879–885.

- [393] Kikuchi, E., Menendez, S., Ozu, C., Otori, M., Cordon-Cardo, C., Logg, C. R., Kasahara, N., and Bochner, B. H. (2007). Delivery of replication-competent retrovirus expressing *Escherichia coli* purine nucleoside phosphorylase increases the metabolism of the prodrug, fludarabine phosphate and suppresses the growth of bladder tumor xenografts. *Cancer gene therapy*, 14(3):279–286.
- [394] Kim, J., Kim, J.-H., Choi, K.-J., Kim, P.-H., and Yun, C.-O. (2007a). E1A- and E1B-Double mutant replicating adenovirus elicits enhanced oncolytic and antitumor effects. *Human gene therapy*, 18(9):773–786.
- [395] Kim, J. M., Rasmussen, J. P., and Rudensky, A. Y. (2007b). Regulatory T cells prevent catastrophic autoimmunity throughout the lifespan of mice. *Nature immunology*, 8(2):191–197.
- [396] Kim, M. K., Breitbach, C. J., Moon, A., Heo, J., Lee, Y. K., Cho, M., Lee, J. W., Kim, S.-G., Kang, D. H., Bell, J. C., Park, B.-H., Kirn, D. H., and Hwang, T.-H. (2013). Oncolytic and immunotherapeutic vaccinia induces antibody-mediated complement-dependent cancer cell lysis in humans. *Science translational medicine*, 5(185):185ra63.
- [397] Kim, N. W., Piatyszek, M. A., Prowse, K. R., Harley, C. B., West, M. D., Ho, P. L., Coviello, G. M., Wright, W. E., Weinrich, S. L., and Shay, J. W. (1994). Specific association of human telomerase activity with immortal cells and cancer. *Science (New York, N.Y.)*, 266(5193):2011–2015.
- [398] King, A. M. Q., Adams, M. J., and Lefkowitz, E. J. (2012). *Virus Taxonomy Classification and Nomenclature of Viruses*. Ninth Report of the International Committee on Taxonomy of Viruses. Elsevier, USA.
- [399] Kinoh, H., Inoue, M., Komaru, A., Ueda, Y., Hasegawa, M., and Yonemitsu, Y. (2009). Generation of optimized and urokinase-targeted oncolytic Sendai virus vectors applicable for various human malignancies. *Gene Therapy*, 16(3):392–403.
- [400] Kinoh, H., Inoue, M., Washizawa, K., Yamamoto, T., Fujikawa, S., Tokusumi, Y., Iida, A., Nagai, Y., and Hasegawa, M. (2004). Generation of a recombinant Sendai virus that is selectively activated and lyses human tumor cells expressing matrix metalloproteinases. *Gene Therapy*, 11(14):1137–1145.
- [401] Kirchhausen, T., Staunton, D. E., and Springer, T. A. (1993). Location of the domains of ICAM-1 by immunolabeling and single-molecule electron microscopy. *Journal of leukocyte biology*, 53(3):342–346.
- [402] Kirkwood, J. M., Ibrahim, J. G., Sondak, V. K., Richards, J., Flaherty, L. E., Ernstoff, M. S., Smith, T. J., Rao, U., Steele, M., and Blum, R. H. (2000). High- and low-dose interferon alfa-2b in high-risk melanoma: first analysis of intergroup trial E1690/S9111/C9190. *Journal of clinical oncology : official journal of the American Society of Clinical Oncology*, 18(12):2444–2458.
- [403] Kirkwood, J. M., Ibrahim, J. G., Sosman, J. A., Sondak, V. K., Agarwala, S. S., Ernstoff, M. S., and Rao, U. (2001). High-dose interferon alfa-2b significantly prolongs relapse-free and overall survival compared with the GM2-KLH/QS-21 vaccine in patients with resected stage IIB-III melanoma: results of intergroup trial E1694/S9512/C509801. *Journal of clinical oncology : official journal of the American Society of Clinical Oncology*, 19(9):2370–2380.
- [404] Kirkwood, J. M., Strawderman, M. H., Ernstoff, M. S., Smith, T. J., Borden, E. C., and Blum, R. H. (1996). Interferon alfa-2b adjuvant therapy of high-risk resected cutaneous melanoma: the Eastern Cooperative Oncology Group Trial EST 1684. *Journal of clinical oncology : official journal of the American Society of Clinical Oncology*, 14(1):7–17.
- [405] Kitamura, N., Adler, C., and Wimmer, E. (1980). Structure and expression of the picornavirus genome. *Annals of the New York Academy of Sciences*, 354:183–201.
- [406] Ko, D., Hawkins, L., and Yu, D.-C. (2005). Development of transcriptionally regulated oncolytic adenoviruses. *Oncogene*, 24(52):7763–7774.
- [407] Ko, J. M., Velez, N. F., and Tsao, H. (2010). Pathways to melanoma. *Seminars in cutaneous medicine and surgery*, 29(4):210–217.
- [408] Kogai, T. and Brent, G. A. (2012). The sodium iodide symporter (NIS): regulation and approaches to targeting for cancer therapeutics. *Pharmacology & therapeutics*, 135(3):355–370.
- [409] Komenaka, I., Hoerig, H., and Kaufman, H. L. (2004). Immunotherapy for melanoma. *Clinics in dermatology*, 22(3):251–265.

- [410] Kono, H. and Rock, K. L. (2008). How dying cells alert the immune system to danger. *Nature reviews. Immunology*, 8(4):279–289.
- [411] Koretz, K., Brüderlein, S., Henne, C., and Möller, P. (1992). Decay-accelerating factor (DAF, CD55) in normal colorectal mucosa, adenomas and carcinomas. *British Journal of Cancer*, 66(5):810–814.
- [412] Koski, A., Kangasniemi, L., Escutenaire, S., Pesonen, S., Cerullo, V., Diaconu, I., Nokisalmi, P., Raki, M., Rajecki, M., Guse, K., Ranki, T., Oksanen, M., Holm, S.-L., Haavisto, E., Karioja-Kallio, A., Laasonen, L., Partanen, K., Ugolini, M., Helminen, A., Karli, E., Hannuksela, P., Pesonen, S., Joensuu, T., Kanerva, A., and Hemminki, A. (2010). Treatment of cancer patients with a serotype 5/3 chimeric oncolytic adenovirus expressing GMCSF. *Molecular therapy : the journal of the American Society of Gene Therapy*, 18(10):1874–1884.
- [413] Kottke, T., Thompson, J., Diaz, R. M., Pulido, J., Willmon, C., Coffey, M., Selby, P., Melcher, A., Harrington, K., and Vile, R. G. (2009). Improved Systemic Delivery of Oncolytic Reovirus to Established Tumors Using Preconditioning with Cyclophosphamide-Mediated Treg Modulation and Interleukin-2. *Clinical Cancer Research*, 15(2):561–569.
- [414] KPMG (2014). Advanced Melanoma - The real cost of Australia’s national cancer. Technical report, Australia.
- [415] Kraemer, K. H., Lee, M. M., Andrews, A. D., and Lambert, W. C. (1994). The role of sunlight and DNA repair in melanoma and nonmelanoma skin cancer. The xeroderma pigmentosum paradigm. *Archives of Dermatology*, 130(8):1018–1021.
- [416] Krakoff, I. H., Brown, N. C., and Reichard, P. (1968). Inhibition of ribonucleoside diphosphate reductase by hydroxyurea. *Cancer Research*, 28(8):1559–1565.
- [417] Kräusslich, H. G., Nicklin, M. J., Toyoda, H., Etchison, D., and Wimmer, E. (1987). Poliovirus proteinase 2A induces cleavage of eucaryotic initiation factor 4F polypeptide p20. *Journal of Virology*, 61(9):2711–2718.
- [418] Krishnamurthy, S., Takimoto, T., Scroggs, R. A., and Portner, A. (2006). Differentially regulated interferon response determines the outcome of Newcastle disease virus infection in normal and tumor cell lines. *Journal of Virology*, 80(11):5145–5155.
- [419] Krutmann, J., Czech, W., Parlow, F., Trefzer, U., Kapp, A., Schöpf, E., and Luger, T. A. (1992). Ultraviolet radiation effects on human keratinocyte ICAM-1 expression: UV-induced inhibition of cytokine-induced ICAM-1 mRNA expression is transient, differentially restored for IFN gamma versus TNF alpha, and followed by ICAM-1 induction via a TNF alpha-like pathway. *The Journal of investigative dermatology*, 98(6):923–928.
- [420] Kuhns, M. S., Epshteyn, V., Sobel, R. A., and Allison, J. P. (2000). Cytotoxic T lymphocyte antigen-4 (CTLA-4) regulates the size, reactivity, and function of a primed pool of CD4+ T cells. *Proceedings of the National Academy of Sciences of the United States of America*, 97(23):12711–12716.
- [421] Kuphal, S. and Bosserhoff, A. (2009). Recent progress in understanding the pathology of malignant melanoma. *The Journal of pathology*, 219(4):400–409.
- [422] Kuttner-Kondo, L., Hourcade, D. E., Anderson, V. E., Muqim, N., Mitchell, L., Soares, D. C., Barlow, P. N., and Medof, M. E. (2007). Structure-based mapping of DAF active site residues that accelerate the decay of C3 convertases. *The Journal of biological chemistry*, 282(25):18552–18562.
- [423] Kwon, H. T., Mayer, J. A., Walker, K. K., Yu, H., Lewis, E. C., and Belch, G. E. (2002). Promotion of frequent tanning sessions by indoor tanning facilities: two studies. *Journal of the American Academy of Dermatology*, 46(5):700–705.
- [424] Kyo, S., Takakura, M., Fujiwara, T., and Inoue, M. (2008). Understanding and exploiting hTERT promoter regulation for diagnosis and treatment of human cancers. *Cancer science*, 99(8):1528–1538.
- [425] Lang, J., Boxer, M., and MacKie, R. (2003). Absence of exon 15 BRAF germline mutations in familial melanoma. *Human mutation*, 21(3):327–330.
- [426] Langer, E. (1964). Human Experimentation: Cancer Studies at Sloan-Kettering Stir Public Debate on Medical Ethics. *Science (New York, N.Y.)*, 143(3606):551–553.
- [427] Lazareth, V. (2013). Management of non-melanoma skin cancer. *Seminars in oncology nursing*, 29(3):182–194.

- [428] Leach, D. R., Krummel, M. F., and Allison, J. P. (1996). Enhancement of antitumor immunity by CTLA-4 blockade. *Science (New York, N.Y.)*, 271(5256):1734–1736.
- [429] Leber, M. F., Bossow, S., Leonard, V. H. J., Zaoui, K., Grossardt, C., Frenzke, M., Miest, T., Sawall, S., Cattaneo, R., von Kalle, C., and Ungerechts, G. (2011). MicroRNA-sensitive oncolytic measles viruses for cancer-specific vector tropism. *Molecular therapy : the journal of the American Society of Gene Therapy*, 19(6):1097–1106.
- [430] Lee, H., Kim, J., Lee, B., Chang, J. W., Ahn, J., Park, J. O., Choi, J., Yun, C. O., Kim, B. S., and Kim, J. H. (2000). Oncolytic potential of E1B 55 kDa-deleted YKL-1 recombinant adenovirus: correlation with p53 functional status. *International Journal of Cancer*, 88(3):454–463.
- [431] Legha, S. S., Ring, S., Papadopoulos, N., Raber, M., and Benjamin, R. S. (1990). A phase II trial of taxol in metastatic melanoma. *Cancer*, 65(11):2478–2481.
- [432] Lennette, E. H., Fox, V. L., Schmidt, N. J., and Culver, J. O. (1958). The Coe virus: an apparently new virus recovered from patients with mild respiratory disease. *American journal of hygiene*, 68(3):272–287.
- [433] Lens, M. B. and Dawes, M. (2002). Interferon alfa therapy for malignant melanoma: a systematic review of randomized controlled trials. *Journal of clinical oncology : official journal of the American Society of Clinical Oncology*, 20(7):1818–1825.
- [434] Lenschow, D. J., Walunas, T. L., and Bluestone, J. A. (1996). CD28/B7 system of T cell costimulation. *Annual review of immunology*, 14:233–258.
- [435] Lev, D. C., Ruiz, M., Mills, L., McGary, E. C., Price, J. E., and Bar-Eli, M. (2003). Dacarbazine causes transcriptional up-regulation of interleukin 8 and vascular endothelial growth factor in melanoma cells: a possible escape mechanism from chemotherapy. *Molecular Cancer Therapeutics*, 2(8):753–763.
- [436] Leveille, S., Samuel, S., Goulet, M.-L., and Hiscott, J. (2011). Enhancing VSV oncolytic activity with an improved cytosine deaminase suicide gene strategy. *Cancer gene therapy*, 18(6):435–443.
- [437] Levi, F., Randimbison, L., Te, V. C., and La Vecchia, C. (1996). Non-Hodgkin's lymphomas, chronic lymphocytic leukaemias and skin cancers. *British Journal of Cancer*, 74(11):1847–1850.
- [438] Li, H., Peng, K.-W., Dingli, D., Kratzke, R. A., and Russell, S. J. (2010). Oncolytic measles viruses encoding interferon beta and the thyroidal sodium iodide symporter gene for mesothelioma virotherapy. *Cancer gene therapy*, 17(8):550–558.
- [439] Li, J.-M., Kao, K.-C., Li, L.-F., Yang, T.-M., Wu, C.-P., Horng, Y.-M., Jia, W. W. G., and Yang, C.-T. (2013). MicroRNA-145 regulates oncolytic herpes simplex virus-1 for selective killing of human non-small cell lung cancer cells. *Virology Journal*, 10:241.
- [440] Li, L., Spendlove, I., Morgan, J., and Durrant, L. G. (2001). CD55 is over-expressed in the tumour environment. *British Journal of Cancer*, 84(1):80–86.
- [441] Liard, C., Munier, S., Joulin-Giet, A., Bonduelle, O., Hadam, S., Duffy, D., Vogt, A., Verrier, B., and Combadière, B. (2012). Intradermal immunization triggers epidermal Langerhans cell mobilization required for CD8 T-cell immune responses. *The Journal of investigative dermatology*, 132(3 Pt 1):615–625.
- [442] Lichty, B. D., Breitbach, C. J., Stojdl, D. F., and Bell, J. C. (2014). Going viral with cancer immunotherapy. *Nature Reviews Cancer*, 14(8):559–567.
- [443] Lin, J.-Y., Chen, T.-C., Weng, K.-F., Chang, S.-C., Chen, L.-L., and Shih, S.-R. (2009). Viral and host proteins involved in picornavirus life cycle. *Journal of biomedical science*, 16:103.
- [444] Lin, J. Y. and Fisher, D. E. (2007). Melanocyte biology and skin pigmentation. *Nature*, 445(7130):843–850.
- [445] Lin, S.-F., Gao, S. P., Price, D. L., Li, S., Chou, T.-C., Singh, P., Huang, Y.-Y., Fong, Y., and Wong, R. J. (2008). Synergy of a herpes oncolytic virus and paclitaxel for anaplastic thyroid cancer. *Clinical cancer research : an official journal of the American Association for Cancer Research*, 14(5):1519–1528.
- [446] Lindenmann, J. (1964). Immunity to Transplantable Tumors Following Viral Oncolysis. I. Mechanism of Immunity to Ehrlich Ascites Tumor. *Journal of immunology (Baltimore, Md. : 1950)*, 92:912–919.

- [447] Lindenmann, J. and Klein, P. A. (1967). Viral oncolysis: increased immunogenicity of host cell antigen associated with influenza virus. *The Journal of experimental medicine*, 126(1):93–108.
- [448] Linge, C., Gewert, D., Rossmann, C., Bishop, J. A., and Crowe, J. S. (1995). Interferon system defects in human malignant melanoma. *Cancer Research*, 55(18):4099–4104.
- [449] Linos, E., Swetter, S. M., Cockburn, M. G., Colditz, G. A., and Clarke, C. A. (2009). Increasing burden of melanoma in the United States. *The Journal of investigative dermatology*, 129(7):1666–1674.
- [450] Liu, B. L., Robinson, M., Han, Z.-Q., Branston, R. H., English, C., Reay, P., McGrath, Y., Thomas, S. K., Thornton, M., Bullock, P., Love, C. A., and Coffin, R. S. (2003). ICP34.5 deleted herpes simplex virus with enhanced oncolytic, immune stimulating, and anti-tumour properties. *Gene Therapy*, 10(4):292–303.
- [451] Liu, C.-C., Guo, M.-S., Lin, F. H.-Y., Hsiao, K.-N., Chang, K. H.-W., Chou, A.-H., Wang, Y.-C., Chen, Y.-C., Yang, C.-S., and Chong, P. C.-S. (2011). Purification and characterization of enterovirus 71 viral particles produced from vero cells grown in a serum-free microcarrier bioreactor system. *PLoS ONE*, 6(5):e20005.
- [452] Liu, H., Yuan, S.-J., Chen, Y.-T., Xie, Y.-B., Cui, L., Yang, W.-Z., Yang, D.-X., and Tian, Y.-T. (2013a). Preclinical evaluation of herpes simplex virus armed with granulocyte-macrophage colony-stimulating factor in pancreatic carcinoma. *World journal of gastroenterology : WJG*, 19(31):5138–5143.
- [453] Liu, J., Miwa, T., Hilliard, B., Chen, Y., Lambris, J. D., Wells, A. D., and Song, W.-C. (2005). The complement inhibitory protein DAF (CD55) suppresses T cell immunity in vivo. *The Journal of experimental medicine*, 201(4):567–577.
- [454] Liu, S., Dai, M., You, L., and Zhao, Y. (2013b). Advance in herpes simplex viruses for cancer therapy. *Science China. Life sciences*, 56(4):298–305.
- [455] Liu, T.-C., Galanis, E., and Kirn, D. (2007). Clinical trial results with oncolytic virotherapy: a century of promise, a decade of progress. *Nature Clinical Practice Oncology*, 4(2):101–117.
- [456] Liu, T.-C., Hwang, T., Park, B.-H., Bell, J., and Kirn, D. H. (2008). The targeted oncolytic poxvirus JX-594 demonstrates antitumoral, antivascular, and anti-HBV activities in patients with hepatocellular carcinoma. *Molecular therapy : the journal of the American Society of Gene Therapy*, 16(9):1637–1642.
- [457] Liu, Y., Wang, C., Mueller, S., Paul, A. V., Wimmer, E., and Jiang, P. (2010). Direct interaction between two viral proteins, the nonstructural protein 2C and the capsid protein VP3, is required for enterovirus morphogenesis. *PLoS Pathogens*, 6(8):e1001066.
- [458] Lloyd, R. E., Jense, H. G., and Ehrenfeld, E. (1987). Restriction of translation of capped mRNA in vitro as a model for poliovirus-induced inhibition of host cell protein synthesis: relationship to p220 cleavage. *Journal of Virology*, 61(8):2480–2488.
- [459] Lo, J. A. and Fisher, D. E. (2014). The melanoma revolution: from UV carcinogenesis to a new era in therapeutics. *Science (New York, N.Y.)*, 346(6212):945–949.
- [460] Loewe, S. (1953). The problem of synergism and antagonism of combined drugs. *Arzneimittel-Forschung*, 3(6):285–290.
- [461] London, R. E. (1955). Multiple myeloma: report of a case showing unusual remission lasting two years following severe hepatitis. *Annals of internal medicine*, 43(1):191–201.
- [462] Long, G. V., Menzies, A. M., Nagrial, A. M., Haydu, L. E., Hamilton, A. L., Mann, G. J., Hughes, T. M., Thompson, J. F., Scolyer, R. A., and Kefford, R. F. (2011). Prognostic and clinicopathologic associations of oncogenic BRAF in metastatic melanoma. *Journal of clinical oncology : official journal of the American Society of Clinical Oncology*, 29(10):1239–1246.
- [463] Long, G. V., Stroyakovskiy, D., Gogas, H., Levchenko, E., de Braud, F., Larkin, J., Garbe, C., Jouary, T., Hauschild, A., Grob, J.-J., Chiarion-Sileni, V., Lebbe, C., Mandalà, M., Millward, M., Arance, A., Bondarenko, I., Haanen, J. B. A. G., Hansson, J., Utikal, J., Ferraresi, V., Kovalenko, N., Mohr, P., Probachai, V., Schadendorf, D., Nathan, P., Robert, C., Ribas, A., DeMarini, D. J., Irani, J. G., Casey, M., Ouellet, D., Martin, A.-M., Le, N., Patel, K., and Flaherty, K. (2014). Combined BRAF and MEK inhibition versus BRAF inhibition alone in melanoma. *The New England journal of medicine*, 371(20):1877–1888.

- [464] Love, W. E., Bernhard, J. D., and Bordeaux, J. S. (2009). Topical imiquimod or fluorouracil therapy for basal and squamous cell carcinoma: a systematic review. *Archives of Dermatology*, 145(12):1431–1438.
- [465] Lublin, D. M. and Atkinson, J. P. (1989). Decay-accelerating factor: biochemistry, molecular biology, and function. *Annual review of immunology*, 7:35–58.
- [466] Lui, P., Cashin, R., Machado, M., Hemels, M., Corey-Lisle, P. K., and Einarson, T. R. (2007). Treatments for metastatic melanoma: synthesis of evidence from randomized trials. *Cancer Treatment Reviews*, 33(8):665–680.
- [467] Lukacik, P., Roversi, P., White, J., Esser, D., Smith, G. P., Billington, J., Williams, P. A., Rudd, P. M., Wormald, M. R., Harvey, D. J., Crispin, M. D. M., Radcliffe, C. M., Dwek, R. A., Evans, D. J., Morgan, B. P., Smith, R. A. G., and Lea, S. M. (2004). Complement regulation at the molecular level: the structure of decay-accelerating factor. *Proceedings of the National Academy of Sciences of the United States of America*, 101(5):1279–1284.
- [468] Lun, X. Q., Jang, J.-H., Tang, N., Deng, H., Head, R., Bell, J. C., Stojdl, D. F., Nutt, C. L., Senger, D. L., Forsyth, P. A., and McCart, J. A. (2009). Efficacy of systemically administered oncolytic vaccinia virotherapy for malignant gliomas is enhanced by combination therapy with rapamycin or cyclophosphamide. *Clinical cancer research : an official journal of the American Association for Cancer Research*, 15(8):2777–2788.
- [469] Lutz, M. B. and Schuler, G. (2002). Immature, semi-mature and fully mature dendritic cells: which signals induce tolerance or immunity? *Trends in immunology*, 23(9):445–449.
- [470] MacFarlane, M. P., Yang, J. C., Guleria, A. S., White, R. L., Seipp, C. A., Einhorn, J. H., White, D. E., and Rosenberg, S. A. (1995). The hematologic toxicity of interleukin-2 in patients with metastatic melanoma and renal cell carcinoma. *Cancer*, 75(4):1030–1037.
- [471] MacKie, R. M. (2002). Risk factors for the development of primary cutaneous malignant melanoma. *Dermatologic clinics*, 20(4):597–600.
- [472] MacKie, R. M. and Hole, D. J. (1996). Incidence and thickness of primary tumours and survival of patients with cutaneous malignant melanoma in relation to socioeconomic status. *BMJ (Clinical research ed.)*, 312(7039):1125–1128.
- [473] MacKie, R. M., Stewart, B., and Brown, S. M. (2001). Intralesional injection of herpes simplex virus 1716 in metastatic melanoma. *The Lancet*, 357(9255):525–526.
- [474] Madan, V., Lear, J. T., and Szeimies, R.-M. (2010). Non-melanoma skin cancer. *Lancet*, 375(9715):673–685.
- [475] Magee, W. E. and Miller, O. V. (1970). Individual variability in antibody response of human volunteers to infection of the upper respiratory tract by coxsackie A21 virus. *The Journal of infectious diseases*, 122(3):127–138.
- [476] Mahnke, K., Schmitt, E., Bonifaz, L., Enk, A. H., and Jonuleit, H. (2002). Immature, but not inactive: the tolerogenic function of immature dendritic cells. *Immunology and cell biology*, 80(5):477–483.
- [477] Maio, M. (2012). Melanoma as a model tumour for immuno-oncology. *Annals of oncology : official journal of the European Society for Medical Oncology / ESMO*, 23 Suppl 8:viii10–4.
- [478] Makgoba, M. W., Sanders, M. E., Ginther Luce, G. E., Dustin, M. L., Springer, T. A., Clark, E. A., Mannoni, P., and Shaw, S. (1988). ICAM-1 a ligand for LFA-1-dependent adhesion of B, T and myeloid cells. *Nature*, 331(6151):86–88.
- [479] Maldonado, J. L., Fridlyand, J., Patel, H., Jain, A. N., Busam, K., Kageshita, T., Ono, T., Albertson, D. G., Pinkel, D., and Bastian, B. C. (2003). Determinants of BRAF mutations in primary melanomas. *JNCI Journal of the National Cancer Institute*, 95(24):1878–1890.
- [480] Mangsbo, S. M., Sandin, L. C., Anger, K., Korman, A. J., Loskog, A., and Tötterman, T. H. (2010). Enhanced tumor eradication by combining CTLA-4 or PD-1 blockade with CpG therapy. *Journal of immunotherapy (Hagerstown, Md. : 1997)*, 33(3):225–235.
- [481] Mapoles, J. E., Krahn, D. L., and Crowell, R. L. (1985). Purification of a HeLa cell receptor protein for group B coxsackieviruses. *Journal of Virology*, 55(3):560–566.

- [482] Marchesi, F., Turriziani, M., Tortorelli, G., Avvisati, G., Torino, F., and De Vecchis, L. (2007). Triazene compounds: mechanism of action and related DNA repair systems. *Pharmacological research : the official journal of the Italian Pharmacological Society*, 56(4):275–287.
- [483] Marlin, S. D. and Springer, T. A. (1987). Purified intercellular adhesion molecule-1 (ICAM-1) is a ligand for lymphocyte function-associated antigen 1 (LFA-1). *Cell*, 51:813–819.
- [484] Martin, F., Caignard, A., Jeannin, J. F., Leclerc, A., and Martín, M. (1983). Selection by trypsin of two sublines of rat colon cancer cells forming progressive or regressive tumors. *International Journal of Cancer*, 32(5):623–627.
- [485] Martinez-Irujo, J. J., Villahermosa, M. L., Alberdi, E., and Santiago, E. (1996). A checkerboard method to evaluate interactions between drugs. *Biochemical pharmacology*, 51(5):635–644.
- [486] Martuza, R. L., Malick, A., Markert, J. M., Ruffner, K. L., and Coen, D. M. (1991). Experimental therapy of human glioma by means of a genetically engineered virus mutant. *Science (New York, N. Y.)*, 252(5007):854–856.
- [487] Mason, J. C., Yarwood, H., Sugars, K., Morgan, B. P., Davies, K. A., and Haskard, D. O. (1999). Induction of decay-accelerating factor by cytokines or the membrane-attack complex protects vascular endothelial cells against complement deposition. *Blood*, 94(5):1673–1682.
- [488] Mastrangelo, M. J., Maguire, H. C., Eisenlohr, L. C., Laughlin, C. E., Monken, C. E., McCue, P. A., Kovatich, A. J., and Lattime, E. C. (1999). Intratumoral recombinant GM-CSF-encoding virus as gene therapy in patients with cutaneous melanoma. *Cancer gene therapy*, 6(5):409–422.
- [489] Mathis, J. M., Stoff-Khalili, M. A., and Curiel, D. T. (2005). Oncolytic adenoviruses - selective retargeting to tumor cells. *Oncogene*, 24(52):7775–7791.
- [490] McArthur, G. A., Chapman, P. B., Robert, C., Larkin, J., Haanen, J. B., Dummer, R., Ribas, A., Hogg, D., Hamid, O., Ascierto, P. A., Garbe, C., Testori, A., Maio, M., Lorigan, P., Lebbe, C., Jouary, T., Schadendorf, D., O'Day, S. J., Kirkwood, J. M., Eggermont, A. M., Dreno, B., Sosman, J. A., Flaherty, K. T., Yin, M., Caro, I., Cheng, S., Trunzer, K., and Hauschild, A. (2014). Safety and efficacy of vemurafenib in BRAF(V600E) and BRAF(V600K) mutation-positive melanoma (BRIM-3): extended follow-up of a phase 3, randomised, open-label study. *The lancet oncology*, 15(3):323–332.
- [491] McCart, J. A., Mehta, N., Scollard, D., Reilly, R. M., Carrasquillo, J. A., Tang, N., Deng, H., Miller, M., Xu, H., Libutti, S. K., Alexander, H. R., and Bartlett, D. L. (2004). Oncolytic vaccinia virus expressing the human somatostatin receptor SSTR2: molecular imaging after systemic delivery using ¹¹¹In-pentetreotide. *Molecular therapy : the journal of the American Society of Gene Therapy*, 10(3):553–561.
- [492] McCart, J. A., Ward, J. M., Lee, J., Hu, Y., Alexander, H. R., Libutti, S. K., Moss, B., and Bartlett, D. L. (2001). Systemic cancer therapy with a tumor-selective vaccinia virus mutant lacking thymidine kinase and vaccinia growth factor genes. *Cancer Research*, 61(24):8751–8757.
- [493] McCourt, P. A., Ek, B., Forsberg, N., and Gustafson, S. (1994). Intercellular adhesion molecule-1 is a cell surface receptor for hyaluronan. *The Journal of biological chemistry*, 269(48):30081–30084.
- [494] McCubrey, J. A., Steelman, L. S., Chappell, W. H., Abrams, S. L., Wong, E. W. T., Chang, F., Lehmann, B., Terrian, D. M., Milella, M., Tafuri, A., Stivala, F., Libra, M., Basecke, J., Evangelisti, C., Martelli, A. M., and Franklin, R. A. (2007). Roles of the Raf/MEK/ERK pathway in cell growth, malignant transformation and drug resistance. *Biochimica et biophysica acta*, 1773(8):1263–1284.
- [495] McCusker, M., Basset-Seguín, N., Dummer, R., Lewis, K., Schadendorf, D., Sekulic, A., Hou, J., Wang, L., Yue, H., and Hauschild, A. (2014). Metastatic basal cell carcinoma: prognosis dependent on anatomic site and spread of disease. *European journal of cancer (Oxford, England : 1990)*, 50(4):774–783.
- [496] McDonald, J. C., Miller, D. L., Zuckerman, A. J., and Pereira, M. S. (1962). Coe (Coxsackie A 21) virus, para-influenza virus and other respiratory virus infections in the R.A.F., 1958-60. *The Journal of hygiene*, 60(2):235–248.
- [497] McGann, P. T. and Ware, R. E. (2011). Hydroxyurea for sickle cell anemia: what have we learned and what questions still remain? *Current opinion in hematology*, 18(3):158–165.

- [498] McKee, T. D. (2006). Degradation of Fibrillar Collagen in a Human Melanoma Xenograft Improves the Efficacy of an Oncolytic Herpes Simplex Virus Vector. *Cancer Research*, 66(5):2509–2513.
- [499] McWilliams, J. A., McGurran, S. M., Dow, S. W., Slansky, J. E., and Kedl, R. M. (2006). A modified tyrosinase-related protein 2 epitope generates high-affinity tumor-specific T cells but does not mediate therapeutic efficacy in an intradermal tumor model. *Journal of immunology (Baltimore, Md. : 1950)*, 177(1):155–161.
- [500] Meckbach, D., Bauer, J., Pflugfelder, A., Meier, F., Busch, C., Eigentler, T. K., Capper, D., von Deimling, A., Mittelbronn, M., Perner, S., Ikenberg, K., Hantschke, M., Büttner, P., Garbe, C., and Weide, B. (2014). Survival according to BRAF-V600 tumor mutations—an analysis of 437 patients with primary melanoma. *PLoS ONE*, 9(1):e86194.
- [501] Medof, M. E., Kinoshita, T., and Nussenzweig, V. (1984). Inhibition of complement activation on the surface of cells after incorporation of decay-accelerating factor (DAF) into their membranes. *The Journal of experimental medicine*, 160(5):1558–1578.
- [502] Meer, L., Janzer, R. C., Kleihues, P., and Kolar, G. F. (1986). In vivo metabolism and reaction with DNA of the cytostatic agent, 5-(3,3-dimethyl-1-triazeno)imidazole-4-carboxamide (DTIC). *Biochemical pharmacology*, 35(19):3243–3247.
- [503] Mehta, R. C., Stecker, K. K., Cooper, S. R., Templin, M. V., Tsai, Y. J., Condon, T. P., Bennett, C. F., and Hardee, G. E. (2000). Intercellular adhesion molecule-1 suppression in skin by topical delivery of anti-sense oligonucleotides. *The Journal of investigative dermatology*, 115(5):805–812.
- [504] Meignier, B., Longnecker, R., and Roizman, B. (1988). In vivo behavior of genetically engineered herpes simplex viruses R7017 and R7020: construction and evaluation in rodents. *The Journal of infectious diseases*, 158(3):602–614.
- [505] Melcher, A., Parato, K., Rooney, C. M., and Bell, J. C. (2011). Thunder and lightning: immunotherapy and oncolytic viruses collide. *Molecular therapy : the journal of the American Society of Gene Therapy*, 19(6):1008–1016.
- [506] Menzies, A. M., Haydu, L. E., Visintin, L., Carlino, M. S., Howle, J. R., Thompson, J. F., Kefford, R. F., Scolyer, R. A., and Long, G. V. (2012). Distinguishing clinicopathologic features of patients with V600E and V600K BRAF-mutant metastatic melanoma. *Clinical cancer research : an official journal of the American Association for Cancer Research*, 18(12):3242–3249.
- [507] Merrill, M. K., Bernhardt, G., Sampson, J. H., Wikstrand, C. J., Bigner, D. D., and Gromeier, M. (2004). Poliovirus receptor CD155-targeted oncolysis of glioma. *Neuro-oncology*, 6(3):208–217.
- [508] Mesnil, M. and Yamasaki, H. (2000). Bystander effect in herpes simplex virus-thymidine kinase/ganciclovir cancer gene therapy: role of gap-junctional intercellular communication. *Cancer Research*, 60(15):3989–3999.
- [509] Metelmann, H. R. and Von Hoff, D. D. (1983). In vitro activation of dacarbazine (DTIC) for a human tumor cloning system. *International journal of cell cloning*, 1(1):24–32.
- [510] Meyskens, F. L., Farmer, P. J., and Anton-Culver, H. (2004). Etiologic pathogenesis of melanoma: a unifying hypothesis for the missing attributable risk. *Clinical cancer research : an official journal of the American Association for Cancer Research*, 10(8):2581–2583.
- [511] Miest, T. S. and Cattaneo, R. (2014). New viruses for cancer therapy: meeting clinical needs. *Nature Reviews Microbiology*, 12(1):23–34.
- [512] Mildner, M., Eckhart, L., Lengauer, B., and Tschachler, E. (2002). Hepatocyte growth factor/scatter factor inhibits UVB-induced apoptosis of human keratinocytes but not of keratinocyte-derived cell lines via the phosphatidylinositol 3-kinase/AKT pathway. *The Journal of biological chemistry*, 277(16):14146–14152.
- [513] Miller, A. J. and Mihm, M. C. (2006). Melanoma. *The New England journal of medicine*, 355(1):51–65.
- [514] Minagawa, H., Tanaka, K., Ono, N., Tatsuo, H., and Yanagi, Y. (2001). Induction of the measles virus receptor SLAM (CD150) on monocytes. *The Journal of general virology*, 82(Pt 12):2913–2917.

- [515] Mineta, T., Rabkin, S. D., and Martuza, R. L. (1994). Treatment of malignant gliomas using ganciclovir-hypersensitive, ribonucleotide reductase-deficient herpes simplex viral mutant. *Cancer Research*, 54(15):3963–3966.
- [516] Mineta, T., Rabkin, S. D., Yazaki, T., Hunter, W. D., and Martuza, R. L. (1995). Attenuated multi-mutated herpes simplex virus-1 for the treatment of malignant gliomas. *Nature medicine*, 1(9):938–943.
- [517] Miwa, T., Maldonado, M. A., Zhou, L., Sun, X., Luo, H. Y., Cai, D., Werth, V. P., Madaio, M. P., Eisenberg, R. A., and Song, W.-C. (2002). Deletion of decay-accelerating factor (CD55) exacerbates autoimmune disease development in MRL/lpr mice. *The American journal of pathology*, 161(3):1077–1086.
- [518] Miyatake, S., Iyer, A., Martuza, R. L., and Rabkin, S. D. (1997). Transcriptional targeting of herpes simplex virus for cell-specific replication. *Journal of Virology*, 71(7):5124–5132.
- [519] Mizushima, S. and Nagata, S. (1990). pEF-BOS, a powerful mammalian expression vector. *Nucleic acids research*, 18(17):5322.
- [520] Moan, J. and Dahlback, A. (1992). The relationship between skin cancers, solar radiation and ozone depletion. *British Journal of Cancer*, 65(6):916–921.
- [521] Moehler, M., Goepfert, K., Heinrich, B., Breitbach, C. J., Delic, M., Galle, P. R., and Rommelaere, J. (2014). Oncolytic Virotherapy as Emerging Immunotherapeutic Modality: Potential of Parvovirus H-1. *Frontiers in oncology*, 4:92.
- [522] Mok, W., Boucher, Y., and Jain, R. K. (2007). Matrix metalloproteinases-1 and -8 improve the distribution and efficacy of an oncolytic virus. *Cancer Research*, 67(22):10664–10668.
- [523] Moran, P., Beasley, H., Gorrell, A., Martin, E., Gribbling, P., Fuchs, H., Gillett, N., Burton, L. E., and Caras, I. W. (1992). Human recombinant soluble decay accelerating factor inhibits complement activation in vitro and in vivo. *Journal of immunology (Baltimore, Md. : 1950)*, 149(5):1736–1743.
- [524] Moreau, S., Saiag, P., Aegerter, P., Bosset, D., Longvert, C., Hélias-Rodzewicz, Z., Marin, C., Peschaud, F., Chagnon, S., Zimmermann, U., Clerici, T., and Emile, J.-F. (2012). Prognostic value of BRAF(V600) mutations in melanoma patients after resection of metastatic lymph nodes. *Annals of surgical oncology*, 19(13):4314–4321.
- [525] Morgan, A. M., Lo, J., and Fisher, D. E. (2013). How does pheomelanin synthesis contribute to melanomagenesis?: Two distinct mechanisms could explain the carcinogenicity of pheomelanin synthesis. *BioEssays : news and reviews in molecular, cellular and developmental biology*, 35(8):672–676.
- [526] Morodomi, Y., Yano, T., Kinoh, H., Harada, Y., Saito, S., Kyuragi, R., Yoshida, K., Onimaru, M., Shoji, F., Yoshida, T., Ito, K., Shikada, Y., Maruyama, R., Hasegawa, M., Maehara, Y., and Yonemitsu, Y. (2012). BioKnife, a uPA activity-dependent oncolytic Sendai virus, eliminates pleural spread of malignant mesothelioma via simultaneous stimulation of uPA expression. *Molecular therapy : the journal of the American Society of Gene Therapy*, 20(4):769–777.
- [527] Morris, S., Cox, B., and Bosanquet, N. (2009). Cost of skin cancer in England. *The European journal of health economics : HEPAC : health economics in prevention and care*, 10(3):267–273.
- [528] Motley, R., Kersey, P., Lawrence, C., British Association of Dermatologists, and British Association of Plastic Surgeons (2003). Multiprofessional guidelines for the management of the patient with primary cutaneous squamous cell carcinoma.
- [529] Motz, G. T. and Coukos, G. (2013). Deciphering and reversing tumor immune suppression. *Immunity*, 39(1):61–73.
- [530] Mousavi-Shafaei, P., Ziaee, A.-A., and Zangemeister-Wittke, U. (2009). Increased cytotoxicity of cisplatin in SK-MEL 28 melanoma cells upon down-regulation of melanoma inhibitor of apoptosis protein. *Iranian biomedical journal*, 13(1):27–34.
- [531] Moutabarrik, A., Nakanishi, I., Namiki, M., Hara, T., Matsumoto, M., Ishibashi, M., Okuyama, A., Zaid, D., and Seya, T. (1993). Cytokine-mediated regulation of the surface expression of complement regulatory proteins, CD46(MCP), CD55(DAF), and CD59 on human vascular endothelial cells. *Lymphokine and cytokine research*, 12(3):167–172.
- [532] Mowbray, M., Stockton, D. L., and Doherty, V. R. (2007). Changes in the site distribution of malignant melanoma in South East Scotland (1979-2002). *British Journal of Cancer*, 96(5):832–835.

- [533] Moyal, D. D. and Fourtanier, A. M. (2008). Broad-spectrum sunscreens provide better protection from solar ultraviolet-simulated radiation and natural sunlight-induced immunosuppression in human beings. *Journal of the American Academy of Dermatology*, 58(5 Suppl 2):S149–54.
- [534] Myers, R., Greiner, S., Harvey, M., Soeffker, D., Frenzke, M., Abraham, K., Shaw, A., Rozenblatt, S., Federspiel, M. J., Russell, S. J., and Peng, K.-W. (2005). Oncolytic activities of approved mumps and measles vaccines for therapy of ovarian cancer. *Cancer gene therapy*, 12(7):593–599.
- [535] Myers, R. M., Greiner, S. M., Harvey, M. E., Griesmann, G., Kuffel, M. J., Buhrow, S. A., Reid, J. M., Federspiel, M., Ames, M. M., Dingli, D., Schweikart, K., Welch, A., Dispenzieri, A., Peng, K.-W., and Russell, S. J. (2007). Preclinical pharmacology and toxicology of intravenous MV-NIS, an oncolytic measles virus administered with or without cyclophosphamide. *Clinical pharmacology and therapeutics*, 82(6):700–710.
- [536] Nagore, E., Requena, C., Traves, V., Guillen, C., Hayward, N. K., Whiteman, D. C., and Hacker, E. (2014). Prognostic value of BRAF mutations in localized cutaneous melanoma. *Journal of the American Academy of Dermatology*, 70(5):858–62.e1–2.
- [537] Naik, J. D., Twelves, C. J., Selby, P. J., Vile, R. G., and Chester, J. D. (2011). Immune recruitment and therapeutic synergy: keys to optimizing oncolytic viral therapy? *Clinical cancer research : an official journal of the American Association for Cancer Research*, 17(13):4214–4224.
- [538] Nakamura, T., Peng, K.-W., Harvey, M., Greiner, S., Lorimer, I. A. J., James, C. D., and Russell, S. J. (2005). Rescue and propagation of fully retargeted oncolytic measles viruses. *Nature biotechnology*, 23(2):209–214.
- [539] Nakamura, T. and Russell, S. (2008). Engineering Oncolytic Measles Viruses for Targeted Cancer Therapy. In Kaufman, H., Wadler, S., and Antman, K., editors, *Molecular Targeting in Oncology*, pages 431–445. Humana Press, Totowa, NJ.
- [540] National Institute of Health (2014). Report on Carcinogens, Thirteenth Edition. *Department of Health and Human Services*.
- [541] Naylor, M. F., Boyd, A., Smith, D. W., Cameron, G. S., Hubbard, D., and Neldner, K. H. (1995). High sun protection factor sunscreens in the suppression of actinic neoplasia. *Archives of Dermatology*, 131(2):170–175.
- [542] Netti, P. A., Berk, D. A., Swartz, M. A., Grodzinsky, A. J., and Jain, R. K. (2000). Role of extracellular matrix assembly in interstitial transport in solid tumors. *Cancer Research*, 60(9):2497–2503.
- [543] Newcombe, N. G. (2003). Cellular receptor interactions of C-cluster human group A coxsackieviruses. *Journal of General Virology*, 84(11):3041–3050.
- [544] Newcombe, N. G., Beagley, L. G., Christiansen, D., Loveland, B. E., Johansson, E. S., Beagley, K. W., Barry, R. D., and Shafren, D. R. (2004). Novel role for decay-accelerating factor in coxsackievirus A21-mediated cell infectivity. *Journal of Virology*, 78(22):12677–12682.
- [545] Nguyen, A., Ho, L., and Wan, Y. (2014). Chemotherapy and Oncolytic Virotherapy: Advanced Tactics in the War against Cancer. *Frontiers in oncology*, 4:145.
- [546] Nguyen, T. L.-A., Abdelbary, H., Arguello, M., Breitbach, C., Leveille, S., Diallo, J.-S., Yasmeeen, A., Bismar, T. A., Kirn, D., Falls, T., Snoulten, V. E., Vanderhyden, B. C., Werier, J., Atkins, H., Vähä-Koskela, M. J. V., Stojdl, D. F., Bell, J. C., and Hiscott, J. (2008). Chemical targeting of the innate antiviral response by histone deacetylase inhibitors renders refractory cancers sensitive to viral oncolysis. *Proceedings of the National Academy of Sciences of the United States of America*, 105(39):14981–14986.
- [547] Nguyen, T. L.-A., Tumilasci, V. F., Singhroy, D., Arguello, M., and Hiscott, J. (2009). The emergence of combinatorial strategies in the development of RNA oncolytic virus therapies. *Cellular microbiology*, 11(6):889–897.
- [548] Nicholson-Weller, A., March, J. P., Rosen, C. E., Spicer, D. B., and Austen, K. F. (1985). Surface membrane expression by human blood leukocytes and platelets of decay-accelerating factor, a regulatory protein of the complement system. *Blood*, 65(5):1237–1244.
- [549] Nicholson-Weller, A. and Wang, C. E. (1994). Structure and function of decay accelerating factor CD55. *The Journal of laboratory and clinical medicine*, 123(4):485–491.

- [550] Niehans, G. A., Cherwitz, D. L., Staley, N. A., Knapp, D. J., and Dalmasso, A. P. (1996). Human carcinomas variably express the complement inhibitory proteins CD46 (membrane cofactor protein), CD55 (decay-accelerating factor), and CD59 (protectin). *The American journal of pathology*, 149(1):129–142.
- [551] Nikolaou, V. and Stratigos, A. J. (2014). Emerging trends in the epidemiology of melanoma. *The British journal of dermatology*, 170(1):11–19.
- [552] Norris, D. A., Lyons, M. B., Middleton, M. H., Yohn, J. J., and Kashihara-Sawami, M. (1990). Ultraviolet radiation can either suppress or induce expression of intercellular adhesion molecule 1 (ICAM-1) on the surface of cultured human keratinocytes. *The Journal of investigative dermatology*, 95(2):132–138.
- [553] Nugent, C. I., Johnson, K. L., Sarnow, P., and Kirkegaard, K. (1999). Functional coupling between replication and packaging of poliovirus replicon RNA. *Journal of Virology*, 73(1):427–435.
- [554] Nugent, C. I. and Kirkegaard, K. (1995). RNA binding properties of poliovirus subviral particles. *Journal of Virology*, 69(1):13–22.
- [555] Ochiai, H., Moore, S. A., Archer, G. E., Okamura, T., Chewning, T. A., Marks, J. R., Sampson, J. H., and Gromeier, M. (2004). Treatment of intracerebral neoplasia and neoplastic meningitis with regional delivery of oncolytic recombinant poliovirus. *Clinical cancer research : an official journal of the American Association for Cancer Research*, 10(14):4831–4838.
- [556] Ockenhouse, C. F., Betageri, R., Springer, T. A., and Staunton, D. E. (1992). Plasmodium falciparum-infected erythrocytes bind ICAM-1 at a site distinct from LFA-1, Mac-1, and human rhinovirus. *Cell*, 68(1):63–69.
- [557] O’Day, S. J., Maio, M., Chiarion-Sileni, V., Gajewski, T. F., Pehamberger, H., Bondarenko, I. N., Queirolo, P., Lundgren, L., Mikhailov, S., Roman, L., Verschraegen, C., Humphrey, R., Ibrahim, R., de Pril, V., Hoos, A., and Wolchok, J. D. (2010). Efficacy and safety of ipilimumab monotherapy in patients with pretreated advanced melanoma: a multicenter single-arm phase II study. *Annals of oncology : official journal of the European Society for Medical Oncology / ESMO*, 21(8):1712–1717.
- [558] O’Dea, D. (2009). The costs of skin cancer to New Zealand. *A Report to the cancer Society of New Zealand*.
- [559] Ohsie, S. J., Sarantopoulos, G. P., Cochran, A. J., and Binder, S. W. (2008). Immunohistochemical characteristics of melanoma. *Journal of cutaneous pathology*, 35(5):433–444.
- [560] Ohtani, N., Yamakoshi, K., Takahashi, A., and Hara, E. (2004). The p16INK4a-RB pathway: molecular link between cellular senescence and tumor suppression. *The journal of medical investigation : JMI*, 51(3-4):146–153.
- [561] Ollila, D. W., Hsueh, E. C., Stern, S. L., and Morton, D. L. (1999). Metastasectomy for recurrent stage IV melanoma. *Journal of surgical oncology*, 71(4):209–213.
- [562] Olsen, C. M., Carroll, H. J., and Whiteman, D. C. (2010). Estimating the attributable fraction for melanoma: a meta-analysis of pigmentary characteristics and freckling. *International Journal of Cancer*, 127(10):2430–2445.
- [563] Olsen, C. M., Knight, L. L., and Green, A. C. (2014). Risk of melanoma in people with HIV/AIDS in the pre- and post-HAART eras: a systematic review and meta-analysis of cohort studies. *PLoS ONE*, 9(4):e95096.
- [564] Oncolytics Biotech Inc. (2013). Oncolytics Biotech® Inc. Meets Primary Endpoint for First Stage of U.S. Phase 2 Metastatic Melanoma Trial.
- [565] Organtini, L. J., Makhov, A. M., Conway, J. F., Hafenstein, S., and Carson, S. D. (2014). Kinetic and structural analysis of coxsackievirus B3 receptor interactions and formation of the A-particle. *Journal of Virology*, 88(10):5755–5765.
- [566] Ottolino-Perry, K., Diallo, J.-S., Lichty, B. D., Bell, J. C., and McCart, J. A. (2010). Intelligent design: combination therapy with oncolytic viruses. *Molecular therapy : the journal of the American Society of Gene Therapy*, 18(2):251–263.
- [567] Palmenberg, A. C. (1982). In vitro synthesis and assembly of picornaviral capsid intermediate structures. *Journal of Virology*, 44(3):900–906.

- [568] Palmer, J. S., Duffy, D. L., Box, N. F., Aitken, J. F., O’Gorman, L. E., Green, A. C., Hayward, N. K., Martin, N. G., and Sturm, R. A. (2000). Melanocortin-1 receptor polymorphisms and risk of melanoma: is the association explained solely by pigmentation phenotype? *American journal of human genetics*, 66(1):176–186.
- [569] Papanastassiou, V., Rampling, R., Fraser, M., Petty, R., Hadley, D., Nicoll, J., Harland, J., Mabbs, R., and Brown, M. (2002). The potential for efficacy of the modified (ICP 34.5(-)) herpes simplex virus HSV1716 following intratumoural injection into human malignant glioma: a proof of principle study. *Gene Therapy*, 9(6):398–406.
- [570] Papi, A. and Johnston, S. L. (1999). Rhinovirus infection induces expression of its own receptor intercellular adhesion molecule 1 (ICAM-1) via increased NF-kappaB-mediated transcription. *The Journal of biological chemistry*, 274(14):9707–9720.
- [571] Parato, K. A., Breitbach, C. J., Le Boeuf, F., Wang, J., Storbeck, C., Ilkow, C., Diallo, J.-S., Falls, T., Burns, J., Garcia, V., Kanji, F., Evgin, L., Hu, K., Paradis, F., Knowles, S., Hwang, T.-H., Vanderhyden, B. C., Auer, R., Kirn, D. H., and Bell, J. C. (2012). The oncolytic poxvirus JX-594 selectively replicates in and destroys cancer cells driven by genetic pathways commonly activated in cancers. *Molecular therapy : the journal of the American Society of Gene Therapy*, 20(4):749–758.
- [572] Parato, K. A., Senger, D., Forsyth, P. A. J., and Bell, J. C. (2005). Recent progress in the battle between oncolytic viruses and tumours. *Nature Reviews Cancer*, 5(12):965–976.
- [573] Pardoll, D. M. (2012). The blockade of immune checkpoints in cancer immunotherapy. *Nature Reviews Cancer*, 12(4):252–264.
- [574] Park, B.-H., Hwang, T., Liu, T.-C., Sze, D. Y., Kim, J.-S., Kwon, H.-C., Oh, S. Y., Han, S.-Y., Yoon, J.-H., Hong, S.-H., Moon, A., Speth, K., Park, C., Ahn, Y.-J., Daneshmand, M., Rhee, B. G., Pinedo, H. M., Bell, J. C., and Kirn, D. H. (2008). Use of a targeted oncolytic poxvirus, JX-594, in patients with refractory primary or metastatic liver cancer: a phase I trial. *The lancet oncology*, 9(6):533–542.
- [575] Patel, N., Buthala, D. A., and Walker, J. S. (1964). Controlled Studies of Coxsackie a-21 (Coe) Virus in Volunteers. *The Journal of infectious diseases*, 114:87–94.
- [576] Paul, A. V., van Boom, J. H., Filippov, D., and Wimmer, E. (1998). Protein-primed RNA synthesis by purified poliovirus RNA polymerase. *Nature*, 393(6682):280–284.
- [577] Pawlik, T. M., Nakamura, H., Yoon, S. S., Mullen, J. T., Chandrasekhar, S., Chiocca, E. A., and Tanabe, K. K. (2000). Oncolysis of diffuse hepatocellular carcinoma by intravascular administration of a replication-competent, genetically engineered herpesvirus. *Cancer Research*, 60(11):2790–2795.
- [578] Pelletier, J. and Sonenberg, N. (1988). Internal initiation of translation of eukaryotic mRNA directed by a sequence derived from poliovirus RNA. *Nature*, 334(6180):320–325.
- [579] Peng, K.-W., Ahmann, G. J., Pham, L., Greipp, P. R., Cattaneo, R., and Russell, S. J. (2001). Systemic therapy of myeloma xenografts by an attenuated measles virus. *Blood*, 98(7):2002–2007.
- [580] Peng, K.-W., TenEyck, C. J., Galanis, E., Kalli, K. R., Hartmann, L. C., and Russell, S. J. (2002). Intraperitoneal therapy of ovarian cancer using an engineered measles virus. *Cancer Research*, 62(16):4656–4662.
- [581] Perez, O. D., Logg, C. R., Hiraoka, K., Diago, O., Burnett, R., Inagaki, A., Jolson, D., Amundson, K., Buckley, T., Lohse, D., Lin, A., Burrascano, C., Ibanez, C., Kasahara, N., Gruber, H. E., and Jolly, D. J. (2012). Design and selection of Toca 511 for clinical use: modified retroviral replicating vector with improved stability and gene expression. *Molecular therapy : the journal of the American Society of Gene Therapy*, 20(9):1689–1698.
- [582] Peterson, J. J. and Novick, S. J. (2007). Nonlinear blending: a useful general concept for the assessment of combination drug synergy. *Journal of receptor and signal transduction research*, 27(2-3):125–146.
- [583] Pevear, D. C., Fancher, M. J., Felock, P. J., Rossmann, M. G., Miller, M. S., Diana, G., Treasurywala, A. M., McKinlay, M. A., and Dutko, F. J. (1989). Conformational change in the floor of the human rhinovirus canyon blocks adsorption to HeLa cell receptors. *Journal of Virology*, 63(5):2002–2007.
- [584] Phillips, B. A. and Fennell, R. (1973). Polypeptide composition of poliovirions, naturally occurring empty capsids, and 14S precursor particles. *Journal of Virology*, 12(2):291–299.

- [585] Phillips, B. A., Summers, D. F., and Maizel, J. V. (1968). In vitro assembly of poliovirus-related particles. *Virology*, 35(2):216–226.
- [586] Phillips, R. A. and Tolmach, L. J. (1966). Repair of potentially lethal damage in x-irradiated HeLa cells. *Radiation research*, 29(3):413–432.
- [587] Piconese, S., Valzasina, B., and Colombo, M. P. (2008). OX40 triggering blocks suppression by regulatory T cells and facilitates tumor rejection. *The Journal of experimental medicine*, 205(4):825–839.
- [588] Piepkorn, M. (2000). Melanoma genetics: an update with focus on the CDKN2A(p16)/ARF tumor suppressors. *Journal of the American Academy of Dermatology*, 42(5 Pt 1):705–22– quiz 723–6.
- [589] Piepkorn, M. W. (1994). Genetic basis of susceptibility to melanoma. *Journal of the American Academy of Dermatology*, 31(6):1022–1039.
- [590] Pin, R. H., Reinblatt, M., and Fong, Y. (2004). Utilizing alpha-fetoprotein expression to enhance oncolytic viral therapy in hepatocellular carcinoma. *Annals of surgery*, 240(4):659–65– discussion 665–6.
- [591] Pleasance, E. D., Cheetham, R. K., Stephens, P. J., McBride, D. J., Humphray, S. J., Greenman, C. D., Varella, I., Lin, M.-L., Ordóñez, G. R., Bignell, G. R., Ye, K., Alipaz, J., Bauer, M. J., Beare, D., Butler, A., Carter, R. J., Chen, L., Cox, A. J., Edkins, S., Kokko-Gonzales, P. I., Gormley, N. A., Grocock, R. J., Haudenschild, C. D., Hims, M. M., James, T., Jia, M., Kingsbury, Z., Leroy, C., Marshall, J., Menzies, A., Mudie, L. J., Ning, Z., Royce, T., Schulz-Trieglaff, O. B., Spiridou, A., Stebbings, L. A., Szajkowski, L., Teague, J., Williamson, D., Chin, L., Ross, M. T., Campbell, P. J., Bentley, D. R., Futreal, P. A., and Stratton, M. R. (2010). A comprehensive catalogue of somatic mutations from a human cancer genome. *Nature*, 463(7278):191–196.
- [592] Pleschka, S. (2008). RNA viruses and the mitogenic Raf/MEK/ERK signal transduction cascade. *Biological chemistry*, 389(10):1273–1282.
- [593] Plevka, P., Hafenstein, S., Harris, K. G., Cifuentes, J. O., Zhang, Y., Bowman, V. D., Chipman, P. R., Bator, C. M., Lin, F., Medof, M. E., and Rossmann, M. G. (2010). Interaction of decay-accelerating factor with echovirus 7. *Journal of Virology*, 84(24):12665–12674.
- [594] Pober, J. S., Gimbrone, M. A., Lapierre, L. A., Mendrick, D. L., Fiers, W., Rothlein, R., and Springer, T. A. (1986). Overlapping patterns of activation of human endothelial cells by interleukin 1, tumor necrosis factor, and immune interferon. *Journal of immunology (Baltimore, Md. : 1950)*, 137(6):1893–1896.
- [595] Pollock, P. M., Harper, U. L., Hansen, K. S., Yudt, L. M., Stark, M., Robbins, C. M., Moses, T. Y., Hostetter, G., Wagner, U., Kakareka, J., Salem, G., Pohida, T., Heenan, P., Duray, P., Kallioniemi, O., Hayward, N. K., Trent, J. M., and Meltzer, P. S. (2003). High frequency of BRAF mutations in nevi. *Nature genetics*, 33(1):19–20.
- [596] Post, D. E. and Van Meir, E. G. (2003). A novel hypoxia-inducible factor (HIF) activated oncolytic adenovirus for cancer therapy. *Oncogene*, 22(14):2065–2072.
- [597] Prestwich, R. J., Errington, F., Diaz, R. M., Pandha, H. S., Harrington, K. J., Melcher, A. A., and Vile, R. G. (2009a). The case of oncolytic viruses versus the immune system: waiting on the judgment of Solomon. *Human gene therapy*, 20(10):1119–1132.
- [598] Prestwich, R. J., Harrington, K. J., Pandha, H. S., Vile, R. G., Melcher, A. A., and Errington, F. (2008). Oncolytic viruses: a novel form of immunotherapy. *Expert Review of Anticancer Therapy*, 8(10):1581–1588.
- [599] Prestwich, R. J., Ilett, E. J., Errington, F., Diaz, R. M., Steele, L. P., Kottke, T., Thompson, J., Galivo, F., Harrington, K. J., Pandha, H. S., Selby, P. J., Vile, R. G., and Melcher, A. A. (2009b). Immune-mediated antitumor activity of reovirus is required for therapy and is independent of direct viral oncolysis and replication. *Clinical cancer research : an official journal of the American Association for Cancer Research*, 15(13):4374–4381.
- [600] Psaty, E. L., Scope, A., Halpern, A. C., and Marghoob, A. A. (2010). Defining the patient at high risk for melanoma. *International journal of dermatology*, 49(4):362–376.
- [601] Pulkkanen, K. J. and Yla-Herttuala, S. (2005). Gene therapy for malignant glioma: current clinical status. *Molecular therapy : the journal of the American Society of Gene Therapy*, 12(4):585–598.

- [602] Purdue, M. P., Freeman, L. E. B., Anderson, W. F., and Tucker, M. A. (2008). Recent trends in incidence of cutaneous melanoma among US Caucasian young adults. *The Journal of investigative dermatology*, 128(12):2905–2908.
- [603] Pushkarev, V. M., Starenki, D. V., Saenko, V. A., Namba, H., Kurebayashi, J., Tronko, M. D., and Yamashita, S. (2004). Molecular mechanisms of the effects of low concentrations of taxol in anaplastic thyroid cancer cells. *Endocrinology*, 145(7):3143–3152.
- [604] Putnak, J. R. and Phillips, B. A. (1981). Differences between poliovirus empty capsids formed in vivo and those formed in vitro: a role for the morphopoietic factor. *Journal of Virology*, 40(1):173–183.
- [605] Qiao, J., Wang, H., Kottke, T., White, C., Twigger, K., Diaz, R. M., Thompson, J., Selby, P., de Bono, J., Melcher, A., Pandha, H., Coffey, M., Vile, R., and Harrington, K. (2008). Cyclophosphamide Facilitates Antitumor Efficacy against Subcutaneous Tumors following Intravenous Delivery of Reovirus. *Clinical Cancer Research*, 14(1):259–269.
- [606] Raaijmakers, M. I. G., Rozati, S., Goldinger, S. M., Widmer, D. S., Dummer, R., and Levesque, M. P. (2013). Melanoma immunotherapy: historical precedents, recent successes and future prospects. *Immunotherapy*, 5(2):169–182.
- [607] Racaniello, V. R. and Baltimore, D. (1981). Cloned poliovirus complementary DNA is infectious in mammalian cells. *Science (New York, N.Y.)*, 214(4523):916–919.
- [608] Radloff, D. R., Rinella, E. S., and Threadgill, D. W. (2008). Modeling cancer patient populations in mice: complex genetic and environmental factors. *Drug discovery today. Disease models*, 4(2):83–88.
- [609] Raimondi, S., Sera, F., Gandini, S., Iodice, S., Caini, S., Maisonneuve, P., and Fargnoli, M. C. (2008). MC1R variants, melanoma and red hair color phenotype: a meta-analysis. *International Journal of Cancer*, 122(12):2753–2760.
- [610] Ram, Z., Culver, K. W., Oshiro, E. M., Viola, J. J., DeVroom, H. L., Otto, E., Long, Z., Chiang, Y., McGarrity, G. J., Muul, L. M., Katz, D., Blaese, R. M., and Oldfield, E. H. (1997). Therapy of malignant brain tumors by intratumoral implantation of retroviral vector-producing cells. *Nature medicine*, 3(12):1354–1361.
- [611] Randazzo, B. P., Kucharczuk, J. C., Litzky, L. A., Kaiser, L. R., Brown, S. M., MacLean, A., Albelda, S. M., and Fraser, N. W. (1996). Herpes simplex 1716—an ICP 34.5 mutant—is severely replication restricted in human skin xenografts in vivo. *Virology*, 223(2):392–395.
- [612] Rao, R. D., Holtan, S. G., Ingle, J. N., Croghan, G. A., Kottschade, L. A., Creagan, E. T., Kaur, J. S., Pitot, H. C., and Markovic, S. N. (2006). Combination of paclitaxel and carboplatin as second-line therapy for patients with metastatic melanoma. *Cancer*, 106(2):375–382.
- [613] Ravanat, J. L., Douki, T., and Cadet, J. (2001). Direct and indirect effects of UV radiation on DNA and its components. *Journal of photochemistry and photobiology. B, Biology*, 63(1-3):88–102.
- [614] Redente, E. F., Dwyer-Nield, L. D., Barrett, B. S., Riches, D. W. H., and Malkinson, A. M. (2009). Lung tumor growth is stimulated in IFN-gamma-/- mice and inhibited in IL-4Ralpha-/- mice. *Anticancer research*, 29(12):5095–5101.
- [615] Reed, K. B., Brewer, J. D., Lohse, C. M., Bringe, K. E., Pruitt, C. N., and Gibson, L. E. (2012). Increasing incidence of melanoma among young adults: an epidemiological study in Olmsted County, Minnesota. *Mayo Clinic proceedings*, 87(4):328–334.
- [616] Rees, J. R., Zens, M. S., Gui, J., Celaya, M. O., Riddle, B. L., and Karagas, M. R. (2014). Non melanoma skin cancer and subsequent cancer risk. *PLoS ONE*, 9(6):e99674.
- [617] Reichard, K. W., Lorence, R. M., Cascino, C. J., Peeples, M. E., Walter, R. J., Fernando, M. B., Reyes, H. M., and Greager, J. A. (1992). Newcastle disease virus selectively kills human tumor cells. *The Journal of surgical research*, 52(5):448–453.
- [618] Reid, J. M., Kuffel, M. J., Miller, J. K., Rios, R., and Ames, M. M. (1999). Metabolic activation of dacarbazine by human cytochromes P450: the role of CYP1A1, CYP1A2, and CYP2E1. *Clinical cancer research : an official journal of the American Association for Cancer Research*, 5(8):2192–2197.
- [619] Reinblatt, M., Pin, R. H., and Fong, Y. (2004). Carcinoembryonic antigen directed herpes viral oncolysis improves selectivity and activity in colorectal cancer. *Surgery*, 136(3):579–584.

- [620] Reyes-Ortiz, C. A., Goodwin, J. S., Freeman, J. L., and Kuo, Y.-F. (2006). Socioeconomic status and survival in older patients with melanoma. *Journal of the American Geriatrics Society*, 54(11):1758–1764.
- [621] Ribas, A., Hodi, F. S., Kefford, R., Hamid, O., Daud, A., Wolchok, J. D., Hwu, W.-J., Gangadhar, T. C., Patnaik, A., Joshua, A. M., Hersey, P., Weber, J. S., Dronca, R. S., Zarour, H. M., Gergich, K., Li, X. N., Iannone, R., Kang, S. P., Ebbinghaus, S., and Robert, C. (2014). Efficacy and safety of the anti-PD-1 monoclonal antibody MK-3475 in 411 patients (pts) with melanoma (MEL). *ASCO Meeting Abstracts*, 32(18suppl):LBA9000.
- [622] Ribas, A., Kefford, R., Marshall, M. A., Punt, C. J. A., Haanen, J. B., Marmol, M., Garbe, C., Gogas, H., Schachter, J., Linette, G., Lorigan, P., Kendra, K. L., Maio, M., Trefzer, U., Smylie, M., McArthur, G. A., Dreno, B., Nathan, P. D., Mackiewicz, J., Kirkwood, J. M., Gomez-Navarro, J., Huang, B., Pavlov, D., and Hauschild, A. (2013). Phase III randomized clinical trial comparing tremelimumab with standard-of-care chemotherapy in patients with advanced melanoma. *Journal of clinical oncology : official journal of the American Society of Clinical Oncology*, 31(5):616–622.
- [623] Ribas, A., Kim, K. B., Schuchter, L. M., Gonzalez, R., Pavlick, A. C., Weber, J. S., McArthur, G. A., Hutson, T. E., Flaherty, K. T., Moschos, S. J., Lawrence, D. P., Hersey, P., Kefford, R. F., Chmielowski, B., Puzanov, I., Li, J., Nolop, K. B., Lee, R. J., Joe, A. K., and Sosman, J. A. (2011). BRIM-2: An open-label, multicenter phase II study of vemurafenib in previously treated patients with BRAF V600E mutation-positive metastatic melanoma. *ASCO Meeting Abstracts*, 29(15suppl):8509.
- [624] Rice, C. M., Levis, R., Strauss, J. H., and Huang, H. V. (1987). Production of infectious RNA transcripts from Sindbis virus cDNA clones: mapping of lethal mutations, rescue of a temperature-sensitive marker, and in vitro mutagenesis to generate defined mutants. *Journal of Virology*, 61(12):3809–3819.
- [625] Richardson, A., Fletcher, L., Sneyd, M., Cox, B., and Reeder, A. I. (2008). The incidence and thickness of cutaneous malignant melanoma in New Zealand 1994-2004. *The New Zealand medical journal*, 121(1279):18–26.
- [626] Rigel, D. S., Russak, J., and Friedman, R. (2010). The Evolution of Melanoma Diagnosis: 25 Years Beyond the ABCDs. *CA: A Cancer Journal for Clinicians*, 60(5):301–316.
- [627] Rimoldi, D., Salvi, S., Liénard, D., Lejeune, F. J., Speiser, D., Zografos, L., and Cerottini, J.-C. (2003). Lack of BRAF mutations in uveal melanoma. *Cancer Research*, 63(18):5712–5715.
- [628] Robert, C., Karaszewska, B., Schachter, J., Rutkowski, P., Mackiewicz, A., Stroiakovski, D., Lichinitser, M., Dummer, R., Grange, F., Mortier, L., Chiarion-Sileni, V., Drucis, K., Krajsova, I., Hauschild, A., Lorigan, P., Wolter, P., Long, G. V., Flaherty, K., Nathan, P., Ribas, A., Martin, A.-M., Sun, P., Crist, W., Legos, J., Rubin, S. D., Little, S. M., and Schadendorf, D. (2015). Improved overall survival in melanoma with combined dabrafenib and trametinib. *The New England journal of medicine*, 372(1):30–39.
- [629] Robert, C., Ribas, A., Wolchok, J. D., Hodi, F. S., Hamid, O., Kefford, R., Weber, J. S., Joshua, A. M., Hwu, W.-J., Gangadhar, T. C., Patnaik, A., Dronca, R., Zarour, H., Joseph, R. W., Boasberg, P., Chmielowski, B., Mateus, C., Postow, M. A., Gergich, K., Ellassais-Schaap, J., Li, X. N., Iannone, R., Ebbinghaus, S. W., Kang, S. P., and Daud, A. (2014). Anti-programmed-death-receptor-1 treatment with pembrolizumab in ipilimumab-refractory advanced melanoma: a randomised dose-comparison cohort of a phase 1 trial. *Lancet*, 384(9948):1109–1117.
- [630] Robert, C., Thomas, L., Bondarenko, I., O’Day, S., M D, J. W., Garbe, C., Lebbe, C., Baurain, J.-F., Testori, A., Grob, J.-J., Davidson, N., Richards, J., Maio, M., Hauschild, A., Miller, W. H., Gascon, P., Lotem, M., Harmankaya, K., Ibrahim, R., Francis, S., Chen, T.-T., Humphrey, R., Hoos, A., and Wolchok, J. D. (2011). Ipilimumab plus dacarbazine for previously untreated metastatic melanoma. *The New England journal of medicine*, 364(26):2517–2526.
- [631] Rodriguez, R., Schuur, E. R., Lim, H. Y., Henderson, G. A., Simons, J. W., and Henderson, D. R. (1997). Prostate attenuated replication competent adenovirus (ARCA) CN706: a selective cytotoxic for prostate-specific antigen-positive prostate cancer cells. *Cancer Research*, 57(13):2559–2563.
- [632] Roebuck, K. A. and Finnegan, A. (1999). Regulation of intercellular adhesion molecule-1 (CD54) gene expression. *Journal of leukocyte biology*, 66(6):876–888.
- [633] Rohll, J. B., Moon, D. H., Evans, D. J., and Almond, J. W. (1995). The 3’ untranslated region of picornavirus RNA: features required for efficient genome replication. *Journal of Virology*, 69(12):7835–7844.

- [634] Roland, C. L., Harken, A. H., Sarr, M. G., and Barnett, C. C. (2007). ICAM-1 expression determines malignant potential of cancer. *Surgery*, 141(6):705–707.
- [635] Rosenstein, Y., Park, J. K., Hahn, W. C., Rosen, F. S., Bierer, B. E., and Burakoff, S. J. (1991). CD43, a molecule defective in Wiskott-Aldrich syndrome, binds ICAM-1. *Nature*, 354(6350):233–235.
- [636] Rossmann, M. G., Arnold, E., Erickson, J. W., Frankenberger, E. A., Griffith, J. P., Hecht, H. J., Johnson, J. E., Kamer, G., Luo, M., and Mosser, A. G. (1985). Structure of a human common cold virus and functional relationship to other picornaviruses. *Nature*, 317(6033):145–153.
- [637] Rossmann, M. G., He, Y., and Kuhn, R. J. (2002). Picornavirus-receptor interactions. *Trends in microbiology*, 10(7):324–331.
- [638] Rossmann, M. G. and Johnson, J. E. (1989). Icosahedral RNA virus structure. *Annual review of biochemistry*, 58:533–573.
- [639] Rosso, S., Zanetti, R., Martinez, C., Tormo, M. J., Schraub, S., Sancho-Garnier, H., Franceschi, S., Gafà, L., Perea, E., Navarro, C., Laurent, R., Schrameck, C., Talamini, R., Tumino, R., and Wechsler, J. (1996). The multicentre south European study ‘Helios’. II: Different sun exposure patterns in the aetiology of basal cell and squamous cell carcinomas of the skin. *British Journal of Cancer*, 73(11):1447–1454.
- [640] Rotbart, H. A. (1995). *Human Enterovirus Infections*. American Society Mic Series. ASM Press.
- [641] Rothlein, R., Dustin, M. L., Marlin, S. D., and Springer, T. A. (1986). A human intercellular adhesion molecule (ICAM-1) distinct from LFA-1. *Journal of immunology (Baltimore, Md. : 1950)*, 137(4):1270–1274.
- [642] Rothlein, R. and Wegner, C. (1992). Role of intercellular adhesion molecule-1 in the inflammatory response. *Kidney international*, 41(3):617–619.
- [643] Roulstone, V., Twigger, K., Zaidi, S., Pencavel, T., Kyula, J. N., White, C., McLaughlin, M., Seth, R., Karapanagiotou, E. M., Mansfield, D., Coffey, M., Nuovo, G., Vile, R. G., Pandha, H. S., Melcher, A. A., and Harrington, K. J. (2012). Synergistic cytotoxicity of oncolytic reovirus in combination with cisplatin-paclitaxel doublet chemotherapy. *Gene Therapy*.
- [644] Rubinstein, J. C., Sznol, M., Pavlick, A. C., Ariyan, S., Cheng, E., Bacchiocchi, A., Kluger, H. M., Narayan, D., and Halaban, R. (2010). Incidence of the V600K mutation among melanoma patients with BRAF mutations, and potential therapeutic response to the specific BRAF inhibitor PLX4032. *Journal of Translational Medicine*, 8:67.
- [645] Rueckert, R. R. and Wimmer, E. (1984). Systematic nomenclature of picornavirus proteins. *Journal of Virology*, 50(3):957–959.
- [646] Rusan, N. M., Fagerstrom, C. J., Yvon, A. M., and Wadsworth, P. (2001). Cell cycle-dependent changes in microtubule dynamics in living cells expressing green fluorescent protein-alpha tubulin. *Molecular biology of the cell*, 12(4):971–980.
- [647] Russell, S. J. and Peng, K.-W. (2007). Viruses as anticancer drugs. *Trends in Pharmacological Sciences*, 28(7):326–333.
- [648] Russell, S. J., Peng, K.-W., and Bell, J. C. (2012). Oncolytic virotherapy. *Gene Therapy*, 30(7):658–670.
- [649] Russo, A. E., Torrisi, E., Bevelacqua, Y., Perrotta, R., Libra, M., McCubrey, J. A., Spandidos, D. A., Stivala, F., and Malaponte, G. (2009). Melanoma: molecular pathogenesis and emerging target therapies (Review). *International journal of oncology*, 34(6):1481–1489.
- [650] Saito, Y., Sunamura, M., Motoi, F., Abe, H., Egawa, S., Duda, D. G., Hoshida, T., Fukuyama, S., Hamada, H., and Matsuno, S. (2006). Oncolytic replication-competent adenovirus suppresses tumor angiogenesis through preserved E1A region. *Cancer gene therapy*, 13(3):242–252.
- [651] Salfeld, J. G. (2007). Isotype selection in antibody engineering. *Nature biotechnology*, 25(12):1369–1372.
- [652] Sanada, M., Hidaka, M., Takagi, Y., Takano, T. Y., Nakatsu, Y., Tsuzuki, T., and Sekiguchi, M. (2007). Modes of actions of two types of anti-neoplastic drugs, dacarbazine and ACNU, to induce apoptosis. *Carcinogenesis*, 28(12):2657–2663.

- [653] Sanada, M., Takagi, Y., Ito, R., and Sekiguchi, M. (2004). Killing and mutagenic actions of dacarbazine, a chemotherapeutic alkylating agent, on human and mouse cells: effects of Mgmt and Mlh1 mutations. *DNA Repair*, 3(4):413–420.
- [654] Sanchez, J. A. and Robinson, W. A. (1993). Malignant melanoma. *Annual review of medicine*, 44:335–342.
- [655] Sangfelt, O., Erickson, S., Castro, J., Heiden, T., Gustafsson, A., Einhorn, S., and Grandér, D. (1999). Molecular mechanisms underlying interferon-alpha-induced G0/G1 arrest: CKI-mediated regulation of G1 Cdk-complexes and activation of pocket proteins. *Oncogene*, 18(18):2798–2810.
- [656] Saunders, P. P. and Chao, L. Y. (1974). Fate of the ring moiety of 5-(3,3-dimethyl-1-triazeno)imidazole-4-carboxamide in mammalian cells. *Cancer Research*, 34(10):2464–2469.
- [657] Schierer, S., Hesse, A., Knippertz, I., Kaempgen, E., Baur, A. S., Schuler, G., Steinkasserer, A., and Nettelbeck, D. M. (2012). Human dendritic cells efficiently phagocytose adenoviral oncolysate but require additional stimulation to mature. *International Journal of Cancer*, 130(7):1682–1694.
- [658] Schmidt, C. W. (2012). UV radiation and skin cancer: the science behind age restrictions for tanning beds. *Environmental health perspectives*, 120(8):a308–13.
- [659] Schmidt, N. J., Fox, V. L., and Lennette, E. H. (1961). Immunologic identification of Coxsackie A21 virus with Coe virus. *Proceedings of the Society for Experimental Biology and Medicine. Society for Experimental Biology and Medicine (New York, N. Y.)*, 107:63–65.
- [660] Schulz, O., Diebold, S. S., Chen, M., Näslund, T. I., Nolte, M. A., Alexopoulou, L., Azuma, Y.-T., Flavell, R. A., Liljeström, P., and Reis e Sousa, C. (2005). Toll-like receptor 3 promotes cross-priming to virus-infected cells. *Nature*, 433(7028):887–892.
- [661] Schwartzentruber, D. J., Lawson, D. H., Richards, J. M., Conry, R. M., Miller, D. M., Treisman, J., Gailani, F., Riley, L., Conlon, K., Pockaj, B., Kendra, K. L., White, R. L., Gonzalez, R., Kuzel, T. M., Curti, B., Leming, P. D., Whitman, E. D., Balkissoon, J., Reintgen, D. S., Kaufman, H., Marincola, F. M., Merino, M. J., Rosenberg, S. A., Choyke, P., Vena, D., and Hwu, P. (2011). gp100 peptide vaccine and interleukin-2 in patients with advanced melanoma. *The New England journal of medicine*, 364(22):2119–2127.
- [662] Seidler, A. M., Pennie, M. L., Veledar, E., Culler, S. D., and Chen, S. C. (2010). Economic burden of melanoma in the elderly population: population-based analysis of the Surveillance, Epidemiology, and End Results (SEER)–Medicare data. *Archives of Dermatology*, 146(3):249–256.
- [663] Sekulic, A., Migden, M. R., Oro, A. E., Dirix, L., Lewis, K. D., Hainsworth, J. D., Solomon, J. A., Yoo, S., Arron, S. T., Friedlander, P. A., Marmur, E., Rudin, C. M., Chang, A. L. S., Low, J. A., Mackey, H. M., Yauch, R. L., Graham, R. A., Reddy, J. C., and Hauschild, A. (2012). Efficacy and safety of vemurafenib in advanced basal-cell carcinoma. *The New England journal of medicine*, 366(23):2171–2179.
- [664] Semler, B. L. and Wimmer, E. (2002). *Molecular Biology of Picornaviruses*. Amer Society for Microbiology.
- [665] Senzer, N. N., Kaufman, H. L., Amatruda, T., Nemunaitis, M., Reid, T., Daniels, G., Gonzalez, R., Glaspy, J., Whitman, E., Harrington, K., Goldsweig, H., Marshall, T., Love, C., Coffin, R., and Nemunaitis, J. J. (2009). Phase II clinical trial of a granulocyte-macrophage colony-stimulating factor-encoding, second-generation oncolytic herpesvirus in patients with unresectable metastatic melanoma. *Journal of clinical oncology : official journal of the American Society of Clinical Oncology*, 27(34):5763–5771.
- [666] Serrone, L., Zeuli, M., Sega, F. M., and Cognetti, F. (2000). Dacarbazine-based chemotherapy for metastatic melanoma: thirty-year experience overview. *Journal of experimental & clinical cancer research : CR*, 19(1):21–34.
- [667] Sgubin, D., Wakimoto, H., Kanai, R., Rabkin, S. D., and Martuza, R. L. (2012). Oncolytic herpes simplex virus counteracts the hypoxia-induced modulation of glioblastoma stem-like cells. *Stem cells translational medicine*, 1(4):322–332.
- [668] Shafren, D., Smithers, B. M., and Formby, M. (2011). A phase I, open-label, cohort study of two doses of coxsackievirus A21 given intratumorally in stage IV melanoma. *ASCO Meeting Abstracts*, 29(15suppl):8573.

- [669] Shafren, D. R. (1998). Viral cell entry induced by cross-linked decay-accelerating factor. *Journal of Virology*, 72(11):9407–9412.
- [670] Shafren, D. R., Au, G. G., Nguyen, T., Newcombe, N. G., Haley, E. S., Beagley, L., Johansson, E. S., Hersey, P., and Barry, R. D. (2004). Systemic therapy of malignant human melanoma tumors by a common cold-producing enterovirus, coxsackievirus a21. *Clinical cancer research : an official journal of the American Association for Cancer Research*, 10(1 Pt 1):53–60.
- [671] Shafren, D. R., Bates, R. C., Agrez, M. V., Herd, R. L., Burns, G. F., and Barry, R. D. (1995). Coxsackieviruses B1, B3, and B5 use decay accelerating factor as a receptor for cell attachment. *Journal of Virology*, 69(6):3873–3877.
- [672] Shafren, D. R., Dorahy, D. J., Greive, S. J., Burns, G. F., and Barry, R. D. (1997a). Mouse cells expressing human intercellular adhesion molecule-1 are susceptible to infection by coxsackievirus A21. *Journal of Virology*, 71(1):785–789.
- [673] Shafren, D. R., Dorahy, D. J., Ingham, R. A., Burns, G. F., and Barry, R. D. (1997b). Coxsackievirus A21 binds to decay-accelerating factor but requires intercellular adhesion molecule 1 for cell entry. *Journal of Virology*, 71(6):4736–4743.
- [674] Shafren, D. R., Dorahy, D. J., Thorne, R. F., and Barry, R. D. (2000). Cytoplasmic interactions between decay-accelerating factor and intercellular adhesion molecule-1 are not required for coxsackievirus A21 cell infection. *Journal of General Virology*, 81(Pt 4):889–894.
- [675] Shafren, D. R., Sylvester, D., Johansson, E. S., Campbell, I. G., and Barry, R. D. (2005). Oncolysis of human ovarian cancers by echovirus type 1. *International Journal of Cancer*, 115(2):320–328.
- [676] Sherr, C. J. and McCormick, F. (2002). The RB and p53 pathways in cancer. *Cancer Cell*, 2(2):103–112.
- [677] Shetty, B. V., Schowen, R. L., Slavik, M., and Riley, C. M. (1992). Degradation of dacarbazine in aqueous solution. *Journal of pharmaceutical and biomedical analysis*, 10(9):675–683.
- [678] Shiah, S. G., Chuang, S. E., and Kuo, M. L. (2001). Involvement of Asp-Glu-Val-Asp-directed, caspase-mediated mitogen-activated protein kinase kinase 1 Cleavage, c-Jun N-terminal kinase activation, and subsequent Bcl-2 phosphorylation for paclitaxel-induced apoptosis in HL-60 cells. *Molecular pharmacology*, 59(2):254–262.
- [679] Shingler, K. L., Yoder, J. L., Carnegie, M. S., Ashley, R. E., Makhov, A. M., Conway, J. F., and Hafenstein, S. (2013). The enterovirus 71 A-particle forms a gateway to allow genome release: a cryoEM study of picornavirus uncoating. *PLoS Pathogens*, 9(3):e1003240.
- [680] Shinozaki, K. (2004). Oncolysis of Multifocal Hepatocellular Carcinoma in the Rat Liver by Hepatic Artery Infusion of Vesicular Stomatitis Virus. *Molecular Therapy*, 9(3):368–376.
- [681] Shtrichman, R. and Kleinberger, T. (1998). Adenovirus type 5 E4 open reading frame 4 protein induces apoptosis in transformed cells. *Journal of Virology*, 72(4):2975–2982.
- [682] Siegel, R. L., Miller, K. D., and Jemal, A. (2015). Cancer statistics, 2015. *CA: A Cancer Journal for Clinicians*, 65(1):5–29.
- [683] Simpson, T. R., Li, F., Montalvo-Ortiz, W., Sepulveda, M. A., Bergerhoff, K., Arce, F., Roddie, C., Henry, J. Y., Yagita, H., Wolchok, J. D., Peggs, K. S., Ravetch, J. V., Allison, J. P., and Quezada, S. A. (2013). Fc-dependent depletion of tumor-infiltrating regulatory T cells co-defines the efficacy of anti-CTLA-4 therapy against melanoma. *The Journal of experimental medicine*, 210(9):1695–1710.
- [684] Skelding, K. A., Barry, R. D., and Shafren, D. R. (2009). Systemic targeting of metastatic human breast tumor xenografts by Coxsackievirus A21. *Breast Cancer Research and Treatment*, 113(1):21–30.
- [685] Skelding, K. A., Barry, R. D., and Shafren, D. R. (2012). Enhanced oncolysis mediated by Coxsackievirus A21 in combination with doxorubicin hydrochloride. *Investigational New Drugs*, 30(2):568–581.
- [686] Smith, C. H., McGregor, J. M., Barker, J. N., Morris, R. W., Rigden, S. P., and MacDonald, D. M. (1993). Excess melanocytic nevi in children with renal allografts. *Journal of the American Academy of Dermatology*, 28(1):51–55.

- [687] Smith, C. W., Marlin, S. D., Rothlein, R., Toman, C., and Anderson, D. C. (1989). Cooperative interactions of LFA-1 and Mac-1 with intercellular adhesion molecule-1 in facilitating adherence and transendothelial migration of human neutrophils in vitro. *Journal of Clinical Investigation*, 83(6):2008–2017.
- [688] Smith, T. J., Kremer, M. J., Luo, M., Vriend, G., Arnold, E., Kamer, G., Rossmann, M. G., McKinlay, M. A., Diana, G. D., and Otto, M. J. (1986). The site of attachment in human rhinovirus 14 for antiviral agents that inhibit uncoating. *Science (New York, N.Y.)*, 233(4770):1286–1293.
- [689] Smyth, M., Pettitt, T., Symonds, A., and Martin, J. (2003). Identification of the pocket factors in a picornavirus. *Archives of virology*, 148(6):1225–1233.
- [690] Snels, D. G., Hille, E. T., Gruis, N. A., and Bergman, W. (1999). Risk of cutaneous malignant melanoma in patients with nonfamilial atypical nevi from a pigmented lesions clinic. *Journal of the American Academy of Dermatology*, 40(5 Pt 1):686–693.
- [691] Soehnge, H., Ouhitit, A., and Ananthaswamy, O. N. (1997). Mechanisms of induction of skin cancer by UV radiation. *Frontiers in bioscience : a journal and virtual library*, 2:d538–51.
- [692] Soufir, N., Avril, M. F., Chompret, A., Demenais, F., Bombléd, J., Spatz, A., Stoppa-Lyonnet, D., Bénard, J., and Bressac-de Paillerets, B. (1998). Prevalence of p16 and CDK4 germline mutations in 48 melanoma-prone families in France. The French Familial Melanoma Study Group. *Human molecular genetics*, 7(2):209–216.
- [693] Spector, D. H. and Baltimore, D. (1975). Polyadenylic acid on poliovirus RNA. II. poly(A) on intracellular RNAs. *Journal of Virology*, 15(6):1418–1431.
- [694] Spendlove, I., Ramage, J. M., Bradley, R., Harris, C., and Durrant, L. G. (2006). Complement decay accelerating factor (DAF)/CD55 in cancer. *Cancer Immunology, Immunotherapy*, 55(8):987–995.
- [695] Spets, H., Georgii-Hemming, P., Siljason, J., Nilsson, K., and Jernberg-Wiklund, H. (1998). Fas/APO-1 (CD95)-mediated apoptosis is activated by interferon-gamma and interferon- in interleukin-6 (IL-6)-dependent and IL-6-independent multiple myeloma cell lines. *Blood*, 92(8):2914–2923.
- [696] Spickard, A., Evans, H., Knight, V., and Johnson, K. (1963). Acute respiratory disease in normal volunteers associated with Coxsackie A-21 viral infection. III. Response to nasopharyngeal and enteric inoculation. *Journal of Clinical Investigation*, 42:840–852.
- [697] Springfield, C., von Messling, V., Frenzke, M., Ungerechts, G., Buchholz, C. J., and Cattaneo, R. (2006). Oncolytic efficacy and enhanced safety of measles virus activated by tumor-secreted matrix metalloproteinases. *Cancer Research*, 66(15):7694–7700.
- [698] Stam-Posthuma, J. J., van Duinen, C., Scheffer, E., Vink, J., and Bergman, W. (2001). Multiple primary melanomas. *Journal of the American Academy of Dermatology*, 44(1):22–27.
- [699] Stanford, M. M., Breitbach, C. J., Bell, J. C., and McFadden, G. (2008). Innate immunity, tumor microenvironment and oncolytic virus therapy: friends or foes? *Current opinion in molecular therapeutics*, 10(1):32–37.
- [700] Staunton, D. E., Dustin, M. L., Erickson, H. P., and Springer, T. A. (1990). The arrangement of the immunoglobulin-like domains of ICAM-1 and the binding sites for LFA-1 and rhinovirus. *Cell*, 61(2):243–254.
- [701] Staunton, D. E., Marlin, S. D., Stratowa, C., Dustin, M. L., and Springer, T. A. (1988). Primary structure of ICAM-1 demonstrates interaction between members of the immunoglobulin and integrin supergene families. *Cell*, 52(6):925–933.
- [702] Staunton, D. E., Merluzzi, V. J., Rothlein, R., Barton, R., Marlin, S. D., and Springer, T. A. (1989). A cell adhesion molecule, ICAM-1, is the major surface receptor for rhinoviruses. *Cell*, 56(5):849–853.
- [703] Steck, M. B. (2014). The role of melanocortin 1 receptor in cutaneous malignant melanoma: along the mitogen-activated protein kinase pathway. *Biological research for nursing*, 16(4):421–428.
- [704] Steinman, R. M., Turley, S., Mellman, I., and Inaba, K. (2000). The induction of tolerance by dendritic cells that have captured apoptotic cells. *The Journal of experimental medicine*, 191(3):411–416.

- [705] Stevens, M. R. (1999). Hydroxyurea: an overview. *Journal of biological regulators and homeostatic agents*, 13(3):172–175.
- [706] Stoermer, K. A. and Morrison, T. E. (2011). Complement and viral pathogenesis. *Virology*, 411(2):362–373.
- [707] Stohrer, M., Boucher, Y., Stangassinger, M., and Jain, R. K. (2000). Oncotic pressure in solid tumors is elevated. *Cancer Research*, 60(15):4251–4255.
- [708] Stojdl, D. F., Lichty, B., Knowles, S., Marius, R., Atkins, H., Sonenberg, N., and Bell, J. C. (2000). Exploiting tumor-specific defects in the interferon pathway with a previously unknown oncolytic virus. *Nature medicine*, 6(7):821–825.
- [709] Stojdl, D. F., Lichty, B. D., tenOever, B. R., Paterson, J. M., Power, A. T., Knowles, S., Marius, R., Reynard, J., Poliquin, L., Atkins, H., Brown, E. G., Durbin, R. K., Durbin, J. E., Hiscott, J., and Bell, J. C. (2003). VSV strains with defects in their ability to shutdown innate immunity are potent systemic anti-cancer agents. *Cancer Cell*, 4(4):263–275.
- [710] Strauss, R., Sova, P., Liu, Y., Li, Z.-Y., Tuve, S., Pritchard, D., Brinkkoetter, P., Möller, T., Wildner, O., Pesonen, S., Hemminki, A., Urban, N., Drescher, C., and Lieber, A. (2009). Epithelial phenotype confers resistance of ovarian cancer cells to oncolytic adenoviruses. *Cancer Research*, 69(12):5115–5125.
- [711] Sullivan, R. J. and Flaherty, K. (2013). MAP kinase signaling and inhibition in melanoma. *Oncogene*, 32(19):2373–2379.
- [712] Summers, D. F. and Maizel, J. V. (1968). Evidence for large precursor proteins in poliovirus synthesis. *Proceedings of the National Academy of Sciences of the United States of America*, 59(3):966–971.
- [713] Suzuki, I., Cone, R. D., Im, S., Nordlund, J., and Abdel-Malek, Z. A. (1996). Binding of melanotropic hormones to the melanocortin receptor MC1R on human melanocytes stimulates proliferation and melanogenesis. *Endocrinology*, 137(5):1627–1633.
- [714] Swartz, M. A. and Lund, A. W. (2012). Lymphatic and interstitial flow in the tumour microenvironment: linking mechanobiology with immunity. *Nature Reviews Cancer*, 12(3):210–219.
- [715] Swerdlow, A. J., English, J., MacKie, R. M., O’Doherty, C. J., Hunter, J. A., Clark, J., and Hole, D. J. (1986). Benign melanocytic naevi as a risk factor for malignant melanoma. *British medical journal (Clinical research ed.)*, 292(6535):1555–1559.
- [716] Swerdlow, A. J. and Weinstock, M. A. (1998). Do tanning lamps cause melanoma? An epidemiologic assessment. *Journal of the American Academy of Dermatology*, 38(1):89–98.
- [717] Tada, A., Suzuki, I., Im, S., Davis, M. B., Cornelius, J., Babcock, G., Nordlund, J. J., and Abdel-Malek, Z. A. (1998). Endothelin-1 is a paracrine growth factor that modulates melanogenesis of human melanocytes and participates in their responses to ultraviolet radiation. *Cell growth & differentiation : the molecular biology journal of the American Association for Cancer Research*, 9(7):575–584.
- [718] Tahir, S. M., Cheng, O., Shaulov, A., Koezuka, Y., Buble, G. J., Wilson, S. B., Balk, S. P., and Exley, M. A. (2001). Loss of IFN-gamma production by invariant NK T cells in advanced cancer. *Journal of immunology (Baltimore, Md. : 1950)*, 167(7):4046–4050.
- [719] Taqi, A. M., Abdurrahman, M. B., Yakubu, A. M., and Fleming, A. F. (1981). Regression of Hodgkin’s disease after measles. *The Lancet*, 1(8229):1112.
- [720] Tatsuo, H., Ono, N., Tanaka, K., and Yanagi, Y. (2000). SLAM (CDw150) is a cellular receptor for measles virus. *Nature*, 406(6798):893–897.
- [721] Tauceri, F., Mura, G., Roseano, M., Framarini, M., Ridolfi, L., and Verdecchia, G. M. (2009). Surgery and adjuvant therapies in the treatment of stage IV melanoma: our experience in 84 patients. *Langenbeck’s archives of surgery / Deutsche Gesellschaft für Chirurgie*, 394(6):1079–1084.
- [722] Taylor, C. T. and Johnson, P. M. (1996). Complement-binding proteins are strongly expressed by human preimplantation blastocysts and cumulus cells as well as gametes. *Molecular human reproduction*, 2(1):52–59.

- [723] Tentori, L. and Graziani, G. (2004). Correspondence re: DC Lev et al., Dacarbazine causes transcriptional up-regulation of interleukin 8 and vascular endothelial growth factor in melanoma cells: a possible escape mechanism from chemotherapy. *Mol Cancer Ther*, 2003;2(8):753-63. *Molecular Cancer Therapeutics*, 3(3):383–author reply 383–4.
- [724] Thomas, M. A., Spencer, J. F., Toth, K., Sagartz, J. E., Phillips, N. J., and Wold, W. S. M. (2008). Immunosuppression enhances oncolytic adenovirus replication and antitumor efficacy in the Syrian hamster model. *Molecular therapy : the journal of the American Society of Gene Therapy*, 16(10):1665–1673.
- [725] Thomas, N. E., Edmiston, S. N., Alexander, A., Millikan, R. C., Groben, P. A., Hao, H., Tolbert, D., Berwick, M., Busam, K., Begg, C. B., Mattingly, D., Ollila, D. W., Tse, C. K., Hummer, A., Lee-Taylor, J., and Conway, K. (2007). Number of nevi and early-life ambient UV exposure are associated with BRAF-mutant melanoma. *Cancer epidemiology, biomarkers & prevention : a publication of the American Association for Cancer Research, cosponsored by the American Society of Preventive Oncology*, 16(5):991–997.
- [726] Thompson, J. F., Scolyer, R. A., and Kefford, R. F. (2005). Cutaneous melanoma. *Lancet*, 365(9460):687–701.
- [727] Thompson, J. F., Soong, S.-J., Balch, C. M., Gershenwald, J. E., Ding, S., Coit, D. G., Flaherty, K. T., Gimotty, P. A., Johnson, T., Johnson, M. M., Leong, S. P., Ross, M. I., Byrd, D. R., Cascinelli, N., Cochran, A. J., Eggermont, A. M., McMasters, K. M., Mihm, M. C., Morton, D. L., and Sondak, V. K. (2011). Prognostic significance of mitotic rate in localized primary cutaneous melanoma: an analysis of patients in the multi-institutional American Joint Committee on Cancer melanoma staging database. *Journal of clinical oncology : official journal of the American Society of Clinical Oncology*, 29(16):2199–2205.
- [728] Thorne, S. H. and Contag, C. H. (2007). Combining immune cell and viral therapy for the treatment of cancer. *Cellular and Molecular Life Sciences*, 64(12):1449–1451.
- [729] Tinghög, G., Carlsson, P., Synnerstad, I., and Rosdahl, I. (2008). Societal cost of skin cancer in Sweden in 2005. *Acta dermato-venereologica*, 88(5):467–473.
- [730] Todd, S., Towner, J. S., Brown, D. M., and Semler, B. L. (1997). Replication-competent picornaviruses with complete genomic RNA 3' noncoding region deletions. *Journal of Virology*, 71(11):8868–8874.
- [731] Tollefson, A. E., Ryerse, J. S., Scaria, A., Hermiston, T. W., and Wold, W. S. (1996a). The E3-11.6-kDa adenovirus death protein (ADP) is required for efficient cell death: characterization of cells infected with adp mutants. *Virology*, 220(1):152–162.
- [732] Tollefson, A. E., Scaria, A., Hermiston, T. W., Ryerse, J. S., Wold, L. J., and Wold, W. S. (1996b). The adenovirus death protein (E3-11.6K) is required at very late stages of infection for efficient cell lysis and release of adenovirus from infected cells. *Journal of Virology*, 70(4):2296–2306.
- [733] Tollefson, A. E., Scaria, A., Ying, B., and Wold, W. S. M. (2003). Mutations within the ADP (E3-11.6K) protein alter processing and localization of ADP and the kinetics of cell lysis of adenovirus-infected cells. *Journal of Virology*, 77(14):7764–7778.
- [734] Topalian, S. L., Hodi, F. S., Brahmer, J. R., Gettinger, S. N., Smith, D. C., McDermott, D. F., Powderly, J. D., Carvajal, R. D., Sosman, J. A., Atkins, M. B., Leming, P. D., Spigel, D. R., Antonia, S. J., Horn, L., Drake, C. G., Pardoll, D. M., Chen, L., Sharfman, W. H., Anders, R. A., Taube, J. M., McMiller, T. L., Xu, H., Korman, A. J., Jure-Kunkel, M., Agrawal, S., McDonald, D., Kollia, G. D., Gupta, A., Wigginton, J. M., and Sznol, M. (2012). Safety, activity, and immune correlates of anti-PD-1 antibody in cancer. *The New England journal of medicine*, 366(26):2443–2454.
- [735] Toyoda, H., Wimmer, E., and Cello, J. (2011). Oncolytic poliovirus therapy and immunization with poliovirus-infected cell lysate induces potent antitumor immunity against neuroblastoma in vivo. *International journal of oncology*, 38(1):81–87.
- [736] Tryggvadóttir, L., Gislum, M., Hakulinen, T., Klint, A., Engholm, G., Storm, H. H., and Bray, F. (2010). Trends in the survival of patients diagnosed with malignant melanoma of the skin in the Nordic countries 1964-2003 followed up to the end of 2006. *Acta oncologica (Stockholm, Sweden)*, 49(5):665–672.
- [737] Tsai, V., Johnson, D. E., Rahman, A., Wen, S. F., LaFace, D., Philopena, J., Nery, J., Zepeda, M., Maneval, D. C., Demers, G. W., and Ralston, R. (2004). Impact of human neutralizing antibodies on antitumor efficacy of an oncolytic adenovirus in a murine model. *Clinical cancer research : an official journal of the American Association for Cancer Research*, 10(21):7199–7206.

- [738] Tsao, H., Benoit, E., Sober, A. J., Thiele, C., and Haluska, F. G. (1998a). Novel mutations in the p16/CDKN2A binding region of the cyclin-dependent kinase-4 gene. *Cancer Research*, 58(1):109–113.
- [739] Tsao, H., Rogers, G. S., and Sober, A. J. (1998b). An estimate of the annual direct cost of treating cutaneous melanoma. *Journal of the American Academy of Dermatology*, 38(5 Pt 1):669–680.
- [740] Tsao, H., Zhang, X., Benoit, E., and Haluska, F. G. (1998c). Identification of PTEN/MMAC1 alterations in uncultured melanomas and melanoma cell lines. *Oncogene*, 16(26):3397–3402.
- [741] Tseng, J.-C., Hurtado, A., Yee, H., Levin, B., Boivin, C., Benet, M., Blank, S. V., Pellicer, A., and Meruelo, D. (2004). Using sindbis viral vectors for specific detection and suppression of advanced ovarian cancer in animal models. *Cancer Research*, 64(18):6684–6692.
- [742] Tsuji, S., Kaji, K., and Nagasawa, S. (1994). Decay-accelerating factor on human umbilical vein endothelial cells. Its histamine-induced expression and spontaneous rapid shedding from the cell surface. *Journal of immunology (Baltimore, Md. : 1950)*, 152(3):1404–1410.
- [743] Tucker, M. A. (2009). Melanoma epidemiology. *Hematology/oncology clinics of North America*, 23(3):383–95–vii.
- [744] Tucker, M. A. and Goldstein, A. M. (2003). Melanoma etiology: where are we? *Oncogene*, 22(20):3042–3052.
- [745] Tucker, M. A., Halpern, A., Holly, E. A., Hartge, P., Elder, D. E., Sagebiel, R. W., Guerry, D., and Clark, W. H. (1997). Clinically recognized dysplastic nevi. A central risk factor for cutaneous melanoma. *JAMA : the journal of the American Medical Association*, 277(18):1439–1444.
- [746] Ungerechts, G., Springfeld, C., Frenzke, M. E., Lampe, J., Johnston, P. B., Parker, W. B., Sorscher, E. J., and Cattaneo, R. (2007). Lymphoma chemovirotherapy: CD20-targeted and convertase-armed measles virus can synergize with fludarabine. *Cancer Research*, 67(22):10939–10947.
- [747] Uribe, P., Wistuba, I. I., and González, S. (2003). BRAF mutation: a frequent event in benign, atypical, and malignant melanocytic lesions of the skin. *The American Journal of dermatopathology*, 25(5):365–370.
- [748] Ushijima, Y., Luo, C., Goshima, F., Yamauchi, Y., Kimura, H., and Nishiyama, Y. (2007). Determination and analysis of the DNA sequence of highly attenuated herpes simplex virus type 1 mutant HF10, a potential oncolytic virus. *Microbes and infection / Institut Pasteur*, 9(2):142–149.
- [749] Vajdic, C. M. and van Leeuwen, M. T. (2009). Cancer incidence and risk factors after solid organ transplantation. *International Journal of Cancer*, 125(8):1747–1754.
- [750] Vallejo-Torres, L., Morris, S., Kinge, J. M., Poirier, V., and Verne, J. (2014). Measuring current and future cost of skin cancer in England. *Journal of public health (Oxford, England)*, 36(1):140–148.
- [751] Valverde, P., Healy, E., Jackson, I., Rees, J. L., and Thody, A. J. (1995). Variants of the melanocyte-stimulating hormone receptor gene are associated with red hair and fair skin in humans. *Nature genetics*, 11(3):328–330.
- [752] van de Stolpe, A. and van der Saag, P. T. (1996). Intercellular adhesion molecule-1. *Journal of Molecular Medicine*, 74(1):13–33.
- [753] van der Velden, P. A., Sandkuijl, L. A., Bergman, W., Pavel, S., van Mourik, L., Frants, R. R., and Gruis, N. A. (2001). Melanocortin-1 receptor variant R151C modifies melanoma risk in Dutch families with melanoma. *American journal of human genetics*, 69(4):774–779.
- [754] Van Raamsdonk, C. D., Bezrookove, V., Green, G., Bauer, J., Gaugler, L., O’Brien, J. M., Simpson, E. M., Barsh, G. S., and Bastian, B. C. (2009). Frequent somatic mutations of GNAQ in uveal melanoma and blue naevi. *Nature*, 457(7229):599–602.
- [755] Van Regenmortel, M. H. V., Fauquet, C. M., Bishop, D. H. L., Carstens, E. B., Estes, M. K., Lemon, S. M., Maniloff, J., Mayo, M. A., McGeoch, D. J., Pringle, C. R., and Wickner, R. B. (2000). *Virus Taxonomy Classification and Nomenclature of Viruses*. Seventh Report of the International Committee on Taxonomy of Viruses. Academic Pr, San Diego.
- [756] Varghese, S. and Rabkin, S. D. (2002). Oncolytic herpes simplex virus vectors for cancer virotherapy. *Cancer gene therapy*, 9(12):967–978.

- [757] Venkataraman, S., Reddy, S. P., Loo, J., Idamakanti, N., Hallenbeck, P. L., and Reddy, V. S. (2008). Structure of Seneca Valley Virus-001: an oncolytic picornavirus representing a new genus. *Structure (London, England : 1993)*, 16(10):1555–1561.
- [758] Verheije, M. H. and Rottier, P. J. M. (2012). Retargeting of viruses to generate oncolytic agents. *Advances in virology*, 2012:798526.
- [759] Vile, R., Ando, D., and Kirn, D. (2002). The oncolytic virotherapy treatment platform for cancer: unique biological and biosafety points to consider. *Cancer gene therapy*, 9(12):1062–1067.
- [760] von Andrian, U. H. and Mempel, T. R. (2003). Homing and cellular traffic in lymph nodes. *Nature reviews. Immunology*, 3(11):867–878.
- [761] Vongpunsawad, S., Oezgun, N., Braun, W., and Cattaneo, R. (2004). Selectively receptor-blind measles viruses: Identification of residues necessary for SLAMF- or CD46-induced fusion and their localization on a new hemagglutinin structural model. *Journal of Virology*, 78(1):302–313.
- [762] Voraberger, G., Schäfer, R., and Stratowa, C. (1991). Cloning of the human gene for intercellular adhesion molecule 1 and analysis of its 5'-regulatory region. Induction by cytokines and phorbol ester. *Journal of immunology (Baltimore, Md. : 1950)*, 147(8):2777–2786.
- [763] Wakimoto, H., Ikeda, K., Abe, T., Ichikawa, T., Hochberg, F. H., Ezekowitz, R. A. B., Pasternack, M. S., and Chiocca, E. A. (2002). The complement response against an oncolytic virus is species-specific in its activation pathways. *Molecular therapy : the journal of the American Society of Gene Therapy*, 5(3):275–282.
- [764] Wakimoto, H., Johnson, P. R., Knipe, D. M., and Chiocca, E. A. (2003). Effects of innate immunity on herpes simplex virus and its ability to kill tumor cells. *Gene Therapy*, 10(11):983–990.
- [765] Wallack, M. K., Steplewski, Z., KOPROWSKI, H., Rosato, E., George, J., Hulihan, B., and Johnson, J. (1977). A new approach in specific, active immunotherapy. *Cancer*, 39(2):560–564.
- [766] Walport, M. J. (2001). Complement. First of two parts. *New England Journal of Medicine*, 344(14):1058–1066.
- [767] Wan, P. T. C., Garnett, M. J., Roe, S. M., Lee, S., Niculescu-Duvaz, D., Good, V. M., Jones, C. M., Marshall, C. J., Springer, C. J., Barford, D., Marais, R., and Cancer Genome Project (2004). Mechanism of activation of the RAF-ERK signaling pathway by oncogenic mutations of B-RAF. *Cell*, 116(6):855–867.
- [768] Wan, Y. S., Wang, Z. Q., Shao, Y., Voorhees, J. J., and Fisher, G. J. (2001). Ultraviolet irradiation activates PI 3-kinase/AKT survival pathway via EGF receptors in human skin in vivo. *International journal of oncology*, 18(3):461–466.
- [769] Wang, K. S., Kuhn, R. J., Strauss, E. G., Ou, S., and Strauss, J. H. (1992). High-affinity laminin receptor is a receptor for Sindbis virus in mammalian cells. *Journal of Virology*, 66(8):4992–5001.
- [770] Wang, T. H., Wang, H. S., and Soong, Y. K. (2000). Paclitaxel-induced cell death: where the cell cycle and apoptosis come together. *Cancer*, 88(11):2619–2628.
- [771] Wang, X., Peng, W., Ren, J., Hu, Z., Xu, J., Lou, Z., Li, X., Yin, W., Shen, X., Porta, C., Walter, T. S., Evans, G., Axford, D., Owen, R., Rowlands, D. J., Wang, J., Stuart, D. I., Fry, E. E., and Rao, Z. (2012). A sensor-adaptor mechanism for enterovirus uncoating from structures of EV71. *Nature structural & molecular biology*, 19(4):424–429.
- [772] Ward, C. D., Stokes, M. A., and Flanagan, J. B. (1988). Direct measurement of the poliovirus RNA polymerase error frequency in vitro. *Journal of Virology*, 62(2):558–562.
- [773] Ward, E., Jemal, A., Cokkinides, V., Singh, G. K., Cardinez, C., Ghafoor, A., and Thun, M. (2004). Cancer disparities by race/ethnicity and socioeconomic status. *CA: A Cancer Journal for Clinicians*, 54(2):78–93.
- [774] Ward, T., Powell, R. M., Chaudhry, Y., Meredith, J., Almond, J. W., Kraus, W., Nelsen-Salz, B., Eggers, H. J., and Evans, D. J. (2000). Fatty acid-depleted albumin induces the formation of echovirus A particles. *Journal of Virology*, 74(7):3410–3412.

- [775] Watanabe, D., Goshima, F., Mori, I., Tamada, Y., Matsumoto, Y., and Nishiyama, Y. (2008). Oncolytic virotherapy for malignant melanoma with herpes simplex virus type 1 mutant HF10. *Journal of Dermatological Science*, 50(3):185–196.
- [776] Watanabe, Y., Watanabe, K., Katagiri, S., and Hinuma, Y. (1965). Virus-specific proteins produced in HeLa cells infected with poliovirus: characterization of subunit-like protein. *Journal of biochemistry*, 57(6):733–741.
- [777] Weber, J. (2009). Ipilimumab: controversies in its development, utility and autoimmune adverse events. *Cancer Immunology, Immunotherapy*, 58(5):823–830.
- [778] Weber, J. S., D’Angelo, S. P., Minor, D., Hodi, F. S., Gutzmer, R., Neyns, B., Hoeller, C., Khushalani, N. I., Miller, W. H., Lao, C. D., Linette, G. P., Thomas, L., Lorigan, P., Grossmann, K. F., Hassel, J. C., Maio, M., Sznol, M., Ascierto, P. A., Mohr, P., Chmielowski, B., Bryce, A., Svane, I. M., Grob, J.-J., Krackhardt, A. M., Horak, C., Lambert, A., Yang, A. S., and Larkin, J. (2015). Nivolumab versus chemotherapy in patients with advanced melanoma who progressed after anti-CTLA-4 treatment (CheckMate 037): a randomised, controlled, open-label, phase 3 trial. *The lancet oncology*, 16(4):375–384.
- [779] Weber, J. S., Minor, D. R., D’Angelo, S., Hodi, F. S., Gutzmer, R., Neyns, B., Hoeller, C., Khushalani, N. I., Miller, W. H., Grob, J., Lao, C., Linette, G., Grossman, K., Hassel, J., Lorigan, P., Maio, M., Sznol, M., Lambert, A., Yang, A., and Larkin, J. (2014). Results of a Phase III Randomised Study of Nivolumab in Patients with Advanced Melanoma After Prior Anti-CTLA4 Therapy.
- [780] Weinstein, M. C., Brodell, R. T., Bordeaux, J., and Honda, K. (2012). The art and science of surgical margins for the dermatopathologist. *The American Journal of dermatopathology*, 34(7):737–745.
- [781] Weintraub, L. R. (1969). Lymphosarcoma: Remission associated with viral hepatitis. *JAMA : the journal of the American Medical Association*, pages 1590–1591.
- [782] Wennier, S. T., Liu, J., and McFadden, G. (2012). Bugs and drugs: oncolytic virotherapy in combination with chemotherapy. *Current pharmaceutical biotechnology*, 13(9):1817–1833.
- [783] Westerdahl, J., Olsson, H., Måsbäck, A., Ingvar, C., Jonsson, N., Brandt, L., Jönsson, P. E., and Möller, T. (1994). Use of sunbeds or sunlamps and malignant melanoma in southern Sweden. *American journal of epidemiology*, 140(8):691–699.
- [784] Whalen, J. and Leone, D. (2009). Mohs micrographic surgery for the treatment of malignant melanoma. *Clinics in dermatology*, 27(6):597–602.
- [785] Whiteman, D. C., Watt, P., Purdie, D. M., Hughes, M. C., Hayward, N. K., and Green, A. C. (2003a). Melanocytic nevi, solar keratoses, and divergent pathways to cutaneous melanoma. *JNCI Journal of the National Cancer Institute*, 95(11):806–812.
- [786] Whiteman, S. C., Bianco, A., Knight, R. A., and Spiteri, M. A. (2003b). Human rhinovirus selectively modulates membranous and soluble forms of its intercellular adhesion molecule-1 (ICAM-1) receptor to promote epithelial cell infectivity. *The Journal of biological chemistry*, 278(14):11954–11961.
- [787] Whitton, J. L., Cornell, C. T., and Feuer, R. (2005). Host and virus determinants of picornavirus pathogenesis and tropism. *Nature Reviews Microbiology*, 3(10):765–776.
- [788] Whyte, P., Williamson, N. M., and Harlow, E. (1989). Cellular targets for transformation by the adenovirus E1A proteins. *Cell*, 56(1):67–75.
- [789] Williams, A. F. and Barclay, A. N. (1988). The immunoglobulin superfamily—domains for cell surface recognition. *Annual review of immunology*, 6:381–405.
- [790] Williams, M. and Ouhtit, A. (2005). Towards a Better Understanding of the Molecular Mechanisms Involved in Sunlight-Induced Melanoma. *Journal of biomedicine & biotechnology*, 2005(1):57–61.
- [791] Williams, P., Chaudhry, Y., Goodfellow, I. G., Billington, J., Powell, R., Spiller, O. B., Evans, D. J., and Lea, S. (2003). Mapping CD55 function. The structure of two pathogen-binding domains at 1.7 Å. *The Journal of biological chemistry*, 278(12):10691–10696.
- [792] Willmon, C., Diaz, R. M., Wongthida, P., Galivo, F., Kottke, T., Thompson, J., Albelda, S., Harrington, K., Melcher, A., and Vile, R. (2011). Vesicular stomatitis virus-induced immune suppressor cells generate antagonism between intratumoral oncolytic virus and cyclophosphamide. *Molecular therapy : the journal of the American Society of Gene Therapy*, 19(1):140–149.

- [793] Wimmer, E., Kuhn, R. J., Pincus, S., Yang, C. F., Toyoda, H., Nicklin, M. J., and Takeda, N. (1987). Molecular events leading to picornavirus genome replication. *Journal of cell science. Supplement*, 7:251–276.
- [794] Wirth, T., Zender, L., Schulte, B., Mundt, B., Plentz, R., Rudolph, K. L., Manns, M., Kubicka, S., and Kühnel, F. (2003). A telomerase-dependent conditionally replicating adenovirus for selective treatment of cancer. *Cancer Research*, 63(12):3181–3188.
- [795] Wojton, J. and Kaur, B. (2010). Impact of tumor microenvironment on oncolytic viral therapy. *Cytokine and Growth Factor Reviews*, 21(2-3):127–134.
- [796] Wolchok, J. D., Kluger, H., Callahan, M. K., Postow, M. A., Rizvi, N. A., Lesokhin, A. M., Segal, N. H., Ariyan, C. E., Gordon, R.-A., Reed, K., Burke, M. M., Caldwell, A., Kronenberg, S. A., Agunwamba, B. U., Zhang, X., Lowy, I., Inzunza, H. D., Feely, W., Horak, C. E., Hong, Q., Korman, A. J., Wigginton, J. M., Gupta, A., and Sznol, M. (2013). Nivolumab plus ipilimumab in advanced melanoma. *The New England journal of medicine*, 369(2):122–133.
- [797] Wolchok, J. D., Neyns, B., Linette, G., Negrier, S., Lutzky, J., Thomas, L., Waterfield, W., Schadendorf, D., Smylie, M., Guthrie, T., Grob, J.-J., Chesney, J., Chin, K., Chen, K., Hoos, A., O’Day, S. J., and Lebbe, C. (2010). Ipilimumab monotherapy in patients with pretreated advanced melanoma: a randomised, double-blind, multicentre, phase 2, dose-ranging study. *The lancet oncology*, 11(2):155–164.
- [798] Wolchok, J. D. and Saenger, Y. (2008). The mechanism of anti-CTLA-4 activity and the negative regulation of T-cell activation. *The oncologist*, 13 Suppl 4:2–9.
- [799] Wolfson, L. J., Strebel, P. M., Gacic-Dobo, M., Hoekstra, E. J., McFarland, J. W., Hersh, B. S., and Measles Initiative (2007). Has the 2005 measles mortality reduction goal been achieved? A natural history modelling study. *Lancet*, 369(9557):191–200.
- [800] Wong, D. and Dorovini-Zis, K. (1992). Upregulation of intercellular adhesion molecule-1 (ICAM-1) expression in primary cultures of human brain microvessel endothelial cells by cytokines and lipopolysaccharide. *Journal of neuroimmunology*, 39(1-2):11–21.
- [801] Wong, Y., Chan, E., Quah, M. Y., Shafren, D., and Au, G. (2011). Oncolytic Activity of Coxsackievirus A21 (CAVATAKTM) in Human Lung Cancer. In *14th World Conference on Lung Cancer*, pages 3–7th July.
- [802] Wong, Y., Quah, M. Y., Shafren, D., and Au, G. (2014). Synergistic Activity of Coxsackievirus A21 (CVA21) and Docetaxel in Non-Small Cell Lung Cancer (NSCLC). In *The 8th International Conference on Oncolytic Virus Therapeutics*, pages 9–13th April, Oxford, UK.
- [803] Workenhe, S. T. and Mossman, K. L. (2014). Oncolytic virotherapy and immunogenic cancer cell death: sharpening the sword for improved cancer treatment strategies. *Molecular therapy : the journal of the American Society of Gene Therapy*, 22(2):251–256.
- [804] Workenhe, S. T., Pol, J. G., Lichty, B. D., Cummings, D. T., and Mossman, K. L. (2013). Combining Oncolytic HSV-1 with Immunogenic Cell Death-Inducing Drug Mitoxantrone Breaks Cancer Immune Tolerance and Improves Therapeutic Efficacy. *Cancer immunology research*, 1(5):309–319.
- [805] Workenhe, S. T., Simmons, G., Pol, J. G., Lichty, B. D., Halford, W. P., and Mossman, K. L. (2014). Immunogenic HSV-mediated oncolysis shapes the antitumor immune response and contributes to therapeutic efficacy. *Molecular therapy : the journal of the American Society of Gene Therapy*, 22(1):123–131.
- [806] Wu, X., Feng, Q.-M., Wang, Y., Shi, J., Ge, H.-L., and Di, W. (2009). The immunologic aspects in advanced ovarian cancer patients treated with paclitaxel and carboplatin chemotherapy. *Cancer Immunology, Immunotherapy*, 59(2):279–291.
- [807] Wu, X.-C., Eide, M. J., King, J., Saraiya, M., Huang, Y., Wiggins, C., Barnholtz-Sloan, J. S., Martin, N., Cokkinides, V., Miller, J., Patel, P., Ekwueme, D. U., and Kim, J. (2011). Racial and ethnic variations in incidence and survival of cutaneous melanoma in the United States, 1999-2006. *Journal of the American Academy of Dermatology*, 65(5 Suppl 1):S26–37.
- [808] XIAO, C., Bator, C. M., Bowman, V. D., RIEDER, E., He, Y., Hébert, B., Bella, J., Baker, T. S., Wimmer, E., Kuhn, R. J., and Rossmann, M. G. (2001). Interaction of coxsackievirus A21 with its cellular receptor, ICAM-1. *Journal of Virology*, 75(5):2444–2451.

- [809] Xiao, C., Bator-Kelly, C. M., Rieder, E., Chipman, P. R., Craig, A., Kuhn, R. J., Wimmer, E., and Rossmann, M. G. (2005). The crystal structure of coxsackievirus A21 and its interaction with ICAM-1. *Structure (London, England : 1993)*, 13(7):1019–1033.
- [810] Xu, R., Sato, N., Yanai, K., Akiyoshi, T., Nagai, S., Wada, J., Koga, K., Mibu, R., Nakamura, M., and Katano, M. (2009). Enhancement of paclitaxel-induced apoptosis by inhibition of mitogen-activated protein kinase pathway in colon cancer cells. *Anticancer research*, 29(1):261–270.
- [811] Xu, Y., Fang, F., Ludewig, G., Jones, G., and Jones, D. (2004). A mutation found in the promoter region of the human survivin gene is correlated to overexpression of survivin in cancer cells. *DNA and cell biology*, 23(7):419–429.
- [812] Yamamoto, H., Ngan, C. Y., and Monden, M. (2008). Cancer cells survive with survivin. *Cancer science*, 99(9):1709–1714.
- [813] Yang, Y., Jun, C.-D., Liu, J.-h., Zhang, R., Joachimiak, A., Springer, T. A., and Wang, J.-h. (2004). Structural basis for dimerization of ICAM-1 on the cell surface. *Molecular cell*, 14(2):269–276.
- [814] Yarde, D. N., Nace, R. A., and Russell, S. J. (2013). Oncolytic vesicular stomatitis virus and bortezomib are antagonistic against myeloma cells in vitro but have additive anti-myeloma activity in vivo. *Experimental hematology*, 41(12):1038–1049.
- [815] Ye, Z., Wang, X., Hao, S., Zhong, J., Xiang, J., and Yang, J. (2006). Oncolytic adenovirus-mediated E1A gene therapy induces tumor-cell apoptosis and reduces tumor angiogenesis leading to inhibition of hepatocellular carcinoma growth in animal model. *Cancer biotherapy & radiopharmaceuticals*, 21(3):225–234.
- [816] Yew, P. R. and Berk, A. J. (1992). Inhibition of p53 transactivation required for transformation by adenovirus early 1B protein. *Nature*, 357(6373):82–85.
- [817] Ylösmäki, E., Hakkarainen, T., Hemminki, A., Visakorpi, T., Andino, R., and Saksela, K. (2008). Generation of a conditionally replicating adenovirus based on targeted destruction of E1A mRNA by a cell type-specific MicroRNA. *Journal of Virology*, 82(22):11009–11015.
- [818] Ylösmäki, E., Martikainen, M., Hinkkanen, A., and Saksela, K. (2013). Attenuation of Semliki Forest virus neurovirulence by microRNA-mediated detargeting. *Journal of Virology*, 87(1):335–344.
- [819] Young, C. (2009). Solar ultraviolet radiation and skin cancer. *Occupational medicine (Oxford, England)*, 59(2):82–88.
- [820] Zamarin, D., Holmgaard, R. B., Subudhi, S. K., Park, J. S., Mansour, M., Palese, P., Merghoub, T., Wolchok, J. D., and Allison, J. P. (2014). Localized oncolytic virotherapy overcomes systemic tumor resistance to immune checkpoint blockade immunotherapy. *Science translational medicine*, 6(226):226ra32.
- [821] Zamarin, D., Martínez-Sobrido, L., Kelly, K., Mansour, M., Sheng, G., Vigil, A., García-Sastre, A., Palese, P., and Fong, Y. (2009). Enhancement of Oncolytic Properties of Recombinant Newcastle Disease Virus Through Antagonism of Cellular Innate Immune Responses. *Molecular Therapy*, 17(4):697–706.
- [822] Zhang, K. Z., Junnikkala, S., Erlander, M. G., Guo, H., Westberg, J. A., Meri, S., and Andersson, L. C. (1998). Up-regulated expression of decay-accelerating factor (CD55) confers increased complement resistance to sprouting neural cells. *European journal of immunology*, 28(4):1189–1196.
- [823] Zhang, M., Qureshi, A. A., Geller, A. C., Frazier, L., Hunter, D. J., and Han, J. (2012). Use of tanning beds and incidence of skin cancer. *Journal of clinical oncology : official journal of the American Society of Clinical Oncology*, 30(14):1588–1593.
- [824] Zhang, Q., Chen, G., Peng, L., Wang, X., Yang, Y., Liu, C., Shi, W., Su, C., Wu, H., Liu, X., Wu, M., and Qian, Q. (2006). Increased safety with preserved antitumoral efficacy on hepatocellular carcinoma with dual-regulated oncolytic adenovirus. *Clinical cancer research : an official journal of the American Association for Cancer Research*, 12(21):6523–6531.
- [825] Zhang, Q., Yu, Y. A., Wang, E., Chen, N., Danner, R. L., Munson, P. J., Marincola, F. M., and Szalay, A. A. (2007). Eradication of solid human breast tumors in nude mice with an intravenously injected light-emitting oncolytic vaccinia virus. *Cancer Research*, 67(20):10038–10046.
- [826] Zhao, L., Wientjes, M. G., and Au, J. L.-S. (2004). Evaluation of combination chemotherapy: integration of nonlinear regression, curve shift, isobologram, and combination index analyses. *Clinical cancer research : an official journal of the American Association for Cancer Research*, 10(23):7994–8004.

- [827] Zhu, Z. B., Makhija, S. K., Lu, B., Wang, M., Rivera, A. A., Kim-Park, S., Ulasov, I. V., Zhou, F., Alvarez, R. D., Siegal, G. P., and Curiel, D. T. (2005). Incorporating the survivin promoter in an infectivity enhanced CRAd-analysis of oncolysis and anti-tumor effects in vitro and in vivo. *International journal of oncology*, 27(1):237–246.
- [828] Zimmermann, C., Seiler, P., Lane, P., and Zinkernagel, R. M. (1997). Antiviral immune responses in CTLA4 transgenic mice. *Journal of Virology*, 71(3):1802–1807.
- [829] Zinselmeyer, B. H., Heydari, S., Sacristán, C., Nayak, D., Cammer, M., Herz, J., Cheng, X., Davis, S. J., Dustin, M. L., and McGavern, D. B. (2013). PD-1 promotes immune exhaustion by inducing antiviral T cell motility paralysis. *The Journal of experimental medicine*, 210(4):757–774.
- [830] Zitvogel, L., Tesniere, A., and Kroemer, G. (2006). Cancer despite immunosurveillance: immunoselection and immunosubversion. *Nature reviews. Immunology*, 6(10):715–727.
- [831] Zuo, L., Weger, J., Yang, Q., Goldstein, A. M., Tucker, M. A., Walker, G. J., HAYWARD, N., and Dracopoli, N. C. (1996). Germline mutations in the p16INK4a binding domain of CDK4 in familial melanoma. *Nature genetics*, 12(1):97–99.